UNIVERSIDAD POLITÉCNICA DE MADRID
Escuela Técnica Superior de Ingeniería Agronómica, Alimentaria y de Biosistemas

Leucine-Rich Repeat Malectin Receptor Kinases: a novel group of *Arabidopsis thaliana* Pattern Recognition Receptors required for cell wall-derived glycans perception and plant immunity activation

DOCTORAL THESIS

Submitted for the degree of Doctor by:

Marina Martín Dacal
BSc in Biology
MSc in Agricultural and Forestry Biotechnology

Madrid, 2024

UNIVERSIDAD POLITÉCNICA DE MADRID
Escuela Técnica Superior de Ingeniería Agronómica, Alimentaria y de Biosistemas

Doctoral Degree in Biotechnology and Genetic Resources of Plants and Associated Microorganisms

Leucine-Rich Repeat Malectin Receptor Kinases: a novel group of *Arabidopsis thaliana* Pattern Recognition Receptors required for cell wall-derived glycans perception and plant immunity activation

DOCTORAL THESIS

Submitted for the degree of Doctor by:

Marina Martín Dacal
BSc in Biology
MSc in Agricultural and Forestry Biotechnology

Under the supervision of:
Dr. Antonio Molina Fernández
Dr. Patricia Fernández Calvo

Madrid, 2024

Title: Leucine-Rich Repeat Malectin Receptor Kinases: a novel group of *Arabidopsis thaliana* Pattern Recognition Receptors required for cell wall-derived glycans perception and plant immunity activation

Author: Marina Martín Dacal

Doctoral Programme: Biotechnology and Genetic Resources of Plants and Associated Microorganisms

Thesis Supervision:

Dr. Antonio Molina Fernández, Professor, Escuela Técnica Superior de Ingeniería Agronómica, Alimentaria y de Biosistemas, Universidad Politécnica de Madrid. (Supervisor)

Dr. Patricia Fernández Calvo, Postdoctoral Researcher, Consejo Superior de Investigaciones Científicas. (Co-supervisor)

External Reviewers:

Thesis Defense Committee:

Thesis Defense Date:

"This thesis has been partially supported by RTI2018-096975-B-I00 grant to Antonio Molina and associated PRE2019-088120 fellow to Marina Martín Dacal from the Spanish Research Agency and by PID2021-126006OB-I00 to Antonio Molina and Lucía Jordá, funded by the Spanish Research Agency (Spanish Ministry of Science, Innovation and Universities)/ 10.13039/501100011033 and by "ERDF A way of making Europe". This work has been also financially supported by the "Severo Ochoa Program for Centres of Excellence in R&D" (2017-2021 and 2022-2025) from Spanish Research Agency (grants SEV-2016-0672 and CEX2020-000999-S to the Centro de Biotecnología y Genómica de Plantas) and by L´Oreal-FWIS Spanish edition 2019 grant "Inmunidad por azúcares en plantas" to Patricia Fernández-Calvo."

Con todo el amor del mundo, a mis padres y mi hermano.

"Un país sin investigación es un país sin desarrollo"

Acknowledgement

This Thesis has been carried out in Dr. Antonio Molina´s group at the Centro de Biotecnología y Genómica de Plantas (CBGP-UPM-INIA/CSIC). The doctorate program in which has been developed is the "Biotechnology and Genomics Resources of Plants and Associated Microorganisms" of the Department of Biotechnology and Plant Biology in the Escuela Técnica Superior de Ingeniería Agronómica, Alimentaria y de Biosistemas (ETSIAAB) of the Universidad Politécnica de Madrid.

Dr. Antonio Molina Fernández (UPM-CBGP) and Dr. Patricia Fernández Calvo (CBGP*) have supervised this Thesis, being great mentors and being involved in experiments designed, result discussion and correction of this document.

Dr. Julia Santiago Cuéllar (University of Lausanne (UNIL), Switzerland) kindly hosted me in her laboratory for three months allowing me to use her resources and technology, helping me planning experiments and discussing results. Dr. Julia Santiago and Dr. Pedro Jiménez Sandoval (UNIL) have also participated in results shown in this Thesis, as the ITC experiments of the IGPs with different glycans (Figure 4.18 and 4.19).

Dr. Luis Fernández Pacios (UPM-CBGP) and Dr. María Garrido Arandía (UPM-CBGP) have participated in this Thesis doing structural *in silico* analysis (Figures 4.16 and 4.17).

Dr. Miguel Ángel Torres (UPM-CBGP) performed ROS assays (Figures 4.10 and 4.13).

Dr. Diego Rebaque (UPM-CBGP**) has performed cross-elicitation assay (Figure 4.9).

Dr. Irene del Hierro (UPM-CBGP) and Dr. Jose María Jiménez-Gómez (CBGP) performed and helped in the SNPs sequencing and identification.

Gemma López (CBGP) and Patricia Fernández Calvo (CBGP*) helped along the Thesis with technical support and performed replicates of different experiments.

I also want to express my gratitude to all the people who have supported me all these years:

First of all, to my family, for the unconditional support, without it I could not have been able to take all the steps I have taken in the professional and personal level. Thank you for being an inspiration day by day.

To all the members of the lab 235, which whom I have shared so good moments and all the support given all these years.

To Antonio for teaching me not to lose hope, when you are convinced of something, you have to keep going.

To Piti, for being a friend and a great inspiration throughout these years, as a scientist and as a woman, demonstrating that, women were, are and will be great scientists.

To Gemma, without you these years would have been very hard, thank you for your advice, your kind words and your infinite affection, for being a friend and a confidant.

To all the friends I have made in the CBGP: Natalia, Klara, Guillem, Joselu, Ana, Sara and all the people with whom I have shared so many good moments during these years.

To Diego, which has been the person I have shared more laughs and tears with, friends for life, because what the Thesis joins, nothing can separate.

To Carlos, whose infinite patience has been essential these years, for being a kind and attentive friend every time I have needed it.

To Daniela, who has been my best company especially in the writing time, thank you for being a great friend and a great support.

To the founders of the AIJ-CBGP with whom, with minimal resources, we have managed to create a space for collaboration and fight for labor rights.

To my friends in Lausanne, Pedro, Owen, Francis, Emanuele and Caroline, for welcoming me as one of them and making my stay in Switzerland one of the best experiences of my life.

To my longtime friends, Raquel, Sofía, Rocío, Marta, Sandra, and María, for being a great support these years and always.

And last but not least, to Javi, you have believed in me more than myself, thank you for always being there for me, especially these last months.

*Present address: Stress signaling and plant development group, Misión Biológica, Centro Superior de Investigaciones Científicas (CSIC), Galicia, Spain.

**Present address: Área de Fisiología Vegetal, Departamento de Ingeniería y Ciencias Agrarias, Universidad de León, León, Spain.

Abstract

Plants are constantly challenged by environmental conditions and are exposed to different organisms. Plant cell walls, mainly composed of carbohydrates, are the first barrier that pathogens and other plant-interacting organisms encounter and must overcome to produce a successful infection/invasion. As a consequence of these interactions, a diverse bouquet of glycans, peptides and biocompounds from microorganisms ("Microbe-Associated Molecular Patterns", MAMPs) and plants ("Damage-Associated Molecular Patterns", DAMPs) are released and perceived by plant Pattern Recognition Receptors (PRRs) activating one of the first layers of immunity in plants, the Pattern-Triggered Immunity (PTI). However, most of the PRRs described perceive peptidic MAMPs and DAMPs, even though in recent years numerous glycans triggering immunity in plants have been characterized.

In this context, the main objective of this thesis is the identification and functional characterization of molecular components involved in the plant immune response mediated by cell wall-derived glycans, to expand the knowledge in this field. For this, a genetic screening of a chemically mutagenized *Arabidopsis thaliana* population was carried out to identify mutants *i*mpaired in *g*lycan *p*erception (*igp*). Using this strategy, *Arabidopsis thaliana igp*s impaired in perception of Mixed-Linked Glucans (such as MLG43) and cellulose-derived oligosaccharides, such as cellotriose (CEL3), were isolated.

The characterization of *igp*s resulted in the identification of mutations in the genes that encode three receptor kinases (RKs) - AT1G56145 (IGP1), AT1G56130 (IGP2/IGP3) and AT1G56140 (IGP4) - with Leucine-Rich-Repeats (LRR) and malectin (MAL) domains in their ectodomains. *igp1* and *igp2/3* mutant plants contain a point mutation E906K and G773E, respectively, in their kinase domains, while *igp4* is a loss-of-function mutant with a T-DNA insertion (identified in the laboratory in parallel in a Genome-Wide Association Study (GWAS)-type experimental approach). Notably, Isothermal Titration Calorimetry (ITC) assays showed that the ectodomain of IGP1 binds with high affinity CEL3 and cellopentaose (CEL5), but not MLG43, supporting its function as a PRR of cellulose-derived oligosaccharides. These data suggest that IGP1 is the main cellulose receptor, and that IGP3 and IGP4 can be considered molecular components that participate as co-receptors of CEL3 and MLG43 since mutations in their coding sequences render plants unable to perceive these compounds.

On the other hand, we have demonstrated that these LRR-MAL RKs also participate in the perception of additional glycans, since *igp* mutants are affected in different PTI hallmarks such as calcium influxes, Mitogen-Activated Protein Kinases (MAPKs) phosphorylation and upregulation of defence genes after treatments with xylotetraose (XYL4) and 3^3-α-L-arabinofuranosyl-xylotetraose (XA_3XX). These facts raise the relevance of IGPs in glycans perception and downstream signalling activation.

The results obtained in this Thesis highlight the importance of glycan in plant immunity and represent a step forward in the field of cell wall-derived immunity through the discovery of a new group of RKs that participate in glycan perception. The LRR-MAL RKs family opens new research opportunities that would allow to identify other PRRs involved in the perception of carbohydrates. A further understanding of these mechanisms of glycan perception by IGPs identified will help to develop bio-protection strategies for crop resistance.

Resumen

Las plantas se enfrentan a un desafío constante provocado por factores de estrés (a)bióticos procedentes del entorno que las rodea. Las paredes celulares de las plantas, compuestas principalmente por carbohidratos, son la primera barrera a la que se enfrentan los patógenos y otros organismos y tienen que superar para producir una infección/invasión exitosa. Como consecuencia de esta interacción, numerosos glicanos, péptidos y material genético tanto de los microorganismos ("Microbe-Associated Molecular Patterns" MAMPs) como de la planta ("Damage-Associated Molecular Patterns", DAMPs) son liberados y percibidos por los receptores de reconocimiento de patrones o PRRs ("Pattern Recognition Receptors") activando una de las primeras capas de inmunidad en las plantas mediada por patrones o PTI ("Pattern-Triggered Immunity"). Sin embargo, la mayor parte de PRRs descritos perciben MAMPs y DAMPs de naturaleza peptídica, a pesar de que en los últimos años se han caracterizado numerosos glicanos capaces de activar inmunidad en plantas.

En este contexto, el principal objetivo de esta Tesis es la identificación y caracterización funcional de componentes moleculares implicados en la respuesta inmune de las plantas mediada por glicanos derivados de la pared celular, con el fin de expandir el conocimiento en este campo. Para ello, se llevó a cabo un cribado genético de plantas mutadas químicamente. De esta manera, se aislaron y caracterizaron mutantes de *Arabidopsis thaliana* denominados *igp*s ("*i*mpaired in *g*lycan *p*erception"), incapaces de percibir ß-glicanos, debido a su falta de respuesta ante tratamientos con glucanos mixtos ("Mixed-Linked Glucans"; como el MLG43) y oligosacáridos derivados de celulosa como la celotriosa (CEL3).

La caracterización de estos mutantes nos permitió identificar mutaciones en genes que codifican para tres receptores de tipo kinasa (RKs) denominados- AT1G56145 (IGP1), AT1G56130 (IGP2/IGP3) y AT1G56140 (IGP4). Estas proteínas portan un ectodominio compuesto por una sección con repeticiones ricas en leucina (LRR) y un dominio malectina (MAL). *igp1* e *igp2/3* contienen una mutación puntual de tipo E906K y G773E, respectivamente, en sus dominios kinasa, mientras que *igp4* es un mutante de pérdida de función con una inserción de T-DNA (identificado paralelamente en una aproximación de asociación de genoma completo o GWAS). Cabe destacar que los ensayos de Calorimetría de Titración Isotérmica (ITC) mostraron que el ectodominio de IGP1 une con alta afinidad CEL3 y celopentaosa (CEL5), pero no MLG43, apoyando su función como un PRR de oligosacáridos

derivados de celulosa. Estos datos sugieren que, a pesar de ser IGP1 el principal receptor de celulosa, IGP3 e IGP4 pueden considerarse componentes moleculares que participan como co-receptores de CEL3 y MLG43 ya que los respectivos mutantes no son capaces de percibir estos compuestos.

Por otro lado, se comprobó que estas RKs participan en la percepción de glicanos adicionales derivados de xilosa como xilotetraosa (XYL4) y 3^3-α-L-arabinofuranosil-xilotetraosa (XA_3XX). Los mutantes *igp* están afectados en la PTI tras los tratamientos con estos glicanos, presentando una respuesta baja o nula de la activación de flujos de calcio, fosforilación de proteínas kinasa y transcripción de genes de defensa en respuesta a XYL4 y XA_3XX. Estos hechos elevan la relevancia de los IGPs en la percepción de glicanos.

Los resultados obtenidos en esta Tesis no solo apoyan la importancia de la percepción de glicanos en la inmunidad de las plantas, sino que también suponen un gran avance para el campo ya que se ha descrito un nuevo grupo de RKs que participan en la percepción de los mismos. La familia LRR-MAL RKs abre una nueva vía a futuras investigaciones que permitan encontrar nuevos PRRs implicados en la percepción de carbohidratos. Una mayor comprensión de estos mecanismos ayudará a desarrollar estrategias de bioprotección permitiendo una mayor resistencia de los cultivos.

Table of Contents

List of Figures

List of Tables

Abbreviations and Acronyms

ABA	Abscisic Acid
AF	Allele Frequency
AGP	Arabinogalactan Protein
ANX	ANXUR
APAP1	ARABINOXYLAN PECTIN ARABINOGALACTAN PROTEIN1
APBS	Adaptive Poisson Boltzmann Solver
AVR	Avirulence proteins
AX	Arabinoxylan
BAK1	BRI1-ASSOCIATED KINASE 1
BAP	Benzylamino Purine
BASTA	Glufosinate-ammonium
BBE	Berberine Bridge Enzyme
BIK1	BOTRYTIS-INDUCED KINASE 1
BR	Brassinosteroid
BRI1	BRASSINOSTEROID-INSENSITIVE 1
BSA	Bovine Serum Albumine
BSK	BRASSINOSTEROID-SIGNALING KINASE
BSR	BSK 3-INTERACTING RK
Ca^{2+}	Calcium
CaM	Calmodulin
CAZymes	Carbohydrate-Active enzymes
CDKC	Cyclin-Dependent Kinase C
cDNA	Complementary DNA
CDPK	Ca^{2+}-Dependent Protein Kinase
CEBiP	CHITIN OLIGOSACCHARIDE ELICITOR-BINDING PROTEINS

CEL	Cellulose
CEL2	Cellobiose
CEL3	Cellotriose
CEL4	Cellotetraose
CEL5	Cellopentaose
CEL6	Cellohoxaose
CELLOX	Cellodextrin oxidase
CERK1	CHITIN ELICITOR RECEPTOR KINASE 1
CESA	Cellulose Synthase A
CHI6	$(1,4\text{-}\beta\text{-N-acetylglucosamine})_6$
CNGC	Cyclic Nucleotide Gated Channels
CNI	Close-Neighbor-Interchange
CO	Chito-Oligosaccharide
Co-IP	Co-Immunoprecipitation
Col	Columbia
Col-0^{AEQ}	Col-0 transgenic plants carrying the *Apoaequorin* gene
CR4L	CRinkly-Like
CrRLK1L	*Catharanthus roseus* RECEPTOR LIKE
CSC	Cellulose Synthase Complex
CSCs/OSCAs	Calcium permeable stress/hyperosmolality-induced channel
CSI1	CELLULOSE SYNTHASE INTERACTIVE1
CSL	Cellulose Synthase-Like
CTAB	N-Cetyl-N-trimethyl-ammoniumbromid
CTD	Carboxyl-Terminal Domain
CW	Cell Wall
CWD	Cell Wall Damage
CWDE	Cell Wall Degrading Enzymes
CWI	Cell Wall Integrity

$_{cyt}Ca^{2+}$	Cytoplasmatic calcium
DAMP	Damage-associated molecular pattern
DET3	DE-ETIOLATED 3
DNA	Deoxyribonucleic acid
DP	Degree of Polymerization
DTT	Dithiotreitol 1,4-Dithiothreitol
ECD	Ectodomain
EDTA	Ethylenediaminetetraacetic Acid Disodium Salt 2-Hydrate
EFR	EF-Tu Receptor
EGF	Epidermal Growth Factor
Elf	Elongation factor
EMS	Ethyl methanesulfonate
EP	Electrostatic Potential
EPR3	EXOPOLYSACCHARIDE RECEPTOR 3
EPS	Exopolysaccharides
ER	Endoplasmic Reticulum
ESK1	ESKIMO
ET	Ethylene
ETI	Effector Triggered Immunity
F_1 and F_2	First and second generation
FAD	Flavin Adenine Dinucleotide
FER	FERONIA
Flg22	Flagellin epitope 22
FLS2	FLAGELLIN SENSITIVE2
GalA	1,4-D-galacturonic acid
GFP	Green Fluorescence Protein
GlA	Glucuronic Acid
GlcNAc	ß-(1,4)-linked N-acetyl-D glucosamine

GLR	Glutamate Receptor-Like
GPI	Glycosylphosphatidyl-inositol
GRP	Glycine-Rich Protein
GT2	Glycosyltransferase 2
GX	Glucuroarabinoxylans
GWAS	Genome-Wide Association Study
HA	Hemagglutinin
HG	Homogalacturonan
HPCA1	HYDROGEN-PEROXIDE-INDUCED Ca^{2+} INCREASES 1
HRGP	Hydroxyproline-Rich Glycoprotein
HRP	Horseradish Peroxidase
IGP	IMPAIRED IN GLYCAN PERCEPTION
IOS1	IMPAIRED OOMYCETE SUSCEPTIBILITY1
IP	Immunoprecipitation
IRX	IRREGULAR XYLEM
ITC	Isothermal Titration Calorimetry
JA	Jasmonic
KD	Kinase domain
K*d*	Dissociation constant
KDO	3-deoxy-D-manno-2- octulosonate
LAM6	Laminarinhexaose
LCO	Lipo-Chito-Oligosaccharide
LecRK1	LECTIN RECEPTOR KINASE1
LLG	LRE-LIKE GPI-ANCHORED PROTEINS
LPMOs	Lytic Polysaccharide Monooxygenases
LPS	Lipopolysaccharide
LRE	LORELEI
LRR	Leucine-Rich Repeat

LRRPK	LIGHT-REPRESSIBLE RECEPTOR PROTEIN KINASE
LRX8	LEUCINE-RICH REPEAT EXTENSIN 8
LYK	Lys MOTIF - CONTAINING RECEPTOR - LIKE KINASE
LYM	LysM DOMAIN-CONTAINING GPI-ANCHORED PROTEIN
LYR4	LysM RECEPTOR 4
LysM	Lysin motif
$M_{1, 2, 3}$	Mutagenized generation
MAL	Malectin
MAMP	Microbe-Associated Molecular Pattern
MAPK	Mitogen-Activated Protein Kinase
MC4	Metacaspase 4
ME	Minimum Evolution
MED	Mediator
Me-GlA	4-O-Methyl-Glucuronic Acid
MES	2-(Nmorpholine)-ethanesulphonic acid
MIK2	MALE DISCOVERER 1-INTERACTING RECEPTOR LIKE KINASE2
MLD	Malectin-Like Domain
MLG	Mixed Linkage Glucans
MPK	Mitogen-activated protein kinases
MPKK	Mitogen-activated protein kinase kinase
MP3K	Mitogen-activated protein kinase kinase kinase
MS	Murashige and Skoog
MST	Microscale Thermophoresis
MurNAc	N-acetylmuramic acid
MYC factor	Arbuscular mycorrhizal fungi factor
NADPH	Nicotinamide Adenine Dinucleotide Phosphate
NASC	Nottingham Arabidopsis Stock Centre
NFP	NOD FACTOR PERCEPTION

NFR	NOD FACTOR RECEPTOR
NLP	Necrotric Lytic Peptides
NMR	Nuclear Magnetic Resonance
Ogs	Oligogalacturonides
OGOX	Oligogalacturonide oxidase
PAD3	Phytoalexin Deficient 3
PB	Poisson–Boltzmann
PBS	Protein-Free Blocking Buffer
PCR	Polymerase Chain Reaction
PCW	Primary Cell Wall
PDB	Protein Data Bank
PEP	Plant Elicitor Peptide
Pep1	Plant elicitor peptide 1
PEPR	PLANT ELICITOR PEPTIDES RECEPTOR
PERK	Proline-rich extensin-like receptor kinase
PG	Endopolygalacturonase (BcPG1 from *Botrytis cinerea*)
PGN	Peptidoglycan
PIPs	MAMP-Induced Secreted Peptides
p*l*DDT	predicted *l*ocal Distance Difference Test
PM	Plasma Membrane
PME	Pectin Methyl Esterase
PMEI	Pectin Methyl Esterase Inhibitor
PMSF	Phenylmethanesulfonyl Fluoride
POPC	Phosphatidylcholine
PR1	Pathogenesis Related 1
PRP	Proline-Rich Protein
PRR	Pattern-Recognition Receptor
PTI	Pattern Triggered Immunity

qRT-PCR	Quantitative real-time PCR
QTL	Quantitative Trait Loci
RALF	Rapid Alkalinization Facto
R genes	Resistance genes
R protein	Resistance protein
RBOHD	Respiratory Burst Oxidase Homolog D
RGI	Rhamnogalacturonan I
RGII	Rhamnogalacturonan II
RK	Receptor kinase
RKF1	RECEPTOR-LIKE KINASE IN FLOWERS 1
RLP42	Receptor-Like Protein 42
RLU	Relative Luminescence Units
RNA	Ribonucleic Acid
RNAPII	RNA polymerase II
ROS	Reactive Oxygen Species
RP	Receptor-Like Proteins
RPe	Extracellular protein
RPg	(GPI)-anchor protein
RWA2	REDUCED WALL ACETYLATION 2
SCOOP	Serine Rich Endogenous Peptide
SCW	Secondary Cell Wall
SEC	Size Exclusion Chromatography
SERK	SOMATIC EMBRYOGENESIS RECEPTOR KINASE
SIF	STRESS INDUCED FACTOR
SNP	Single Nucleotide Polymorphism
SOD	Superoxide Dismutase
$T_{1, 2, 3}$	Transgenic lines
TAIR	The Arabidopsis Information Resource

T-DNA	Transfer-DNA
TF	Transcription Factors
TM	Transmembrane domain
VQP	VQ motif-containing Protein
WAK	WALL-ASSOCIATED RECEPTOR KINASE
WT	Wild-Type
XA_3XX	3^3-α-L-arabinofuranosyl-xylotetraose
XGA	Xylogalacturonan
XPS1	XANTHINE/URACIL PERMEASE SENSITIVE 1
XTH	Endo-transglycosylases/hydrolase
XYL2	Xylobiose
XYL4	Xylotetraose
XylG	Xyloglucans
YFP	Yellow Fluorescence Protein

1. Introduction

Plants are under continuous biotic stresses caused by their exposition to microbial populations (microbiota), pathogens and pests. Despite the diversity of biotic and environmental challenges to which plants are exposed, they can reprogram their physiological processes to respond to these conditions. This ability of plants is facilitated by a variety of complex and efficient mechanisms of resilience, which include diverse molecular monitoring systems that perceive stresses-derived signals and trigger specific adaptative responses (Alonso Baez & Bacete 2023; Atkinson & Urwin 2012; Engelsdorf & Hamann 2014).

One of these adaptative mechanisms is the activation of disease resistance against pathogens and pests, which is costly because implies the allocation of resources (e.g. signalling components and antimicrobial molecules) to invest in defence. This re-assignment of energy might compromise plants' development, reproduction, and generation of offspring. Accordingly, disease resistance activation generally impacts developmental plant traits, such as biomass and seed production, which are critical for agricultural outcomes (Denancé *et al.*, 2013; Karasov *et al.*, 2017; Lozano-Durán & Zipfel., 2015; Molina *et al.*, 2021; Monson *et al.*, 2022). To keep the balance between growth and defence, the activation of plant disease resistance mechanisms against pathogens and pests is tightly regulated by cell-autonomous monitoring systems that perceive pathogen/pest attacks and specific mechanisms that fine-tune the intensity and duration of the defensive response (Lozano-Durán & Zipfel 2015; Wolf *et al.*, 2012).

Disease resistance in plants relies both on constitutive and inducible elements. Interestingly, plant cell walls play a dual role as structural barriers that hinder stress-related challenges but also as sources of bioactive molecules that activate plant immunity (Wolf, 2022). Therefore, plant cell walls have gained attention due to their relevant function as a safeguard against both abiotic and biotic stresses (Benedetti *et al.*, 2018; Molina *et al.*, 2021; Wolf, 2022). Synthesis and remodelling of plant cell walls are complex processes involving a significant proportion of genes in plant genomes, which we are now starting to identify and functionally characterize (Yong *et al.*, 2005; Zhang *et al.*, 2021). Modifications of plant cell walls by chemical treatments of plants (e.g. by using inhibitors of enzymes involved in polysaccharides synthesis such as isoxaben) or genetically, by impairing or overexpressing cell wall-related genes in some species (e.g. *Arabidopsis thaliana*),

have contributed to gain knowledge and understand the impact of some plant cell wall modifications on plant development and fitness, but also on immunity and disease resistance (Denness *et al.*, 2011; Ogden *et al.*, 2023; Tateno *et al.*, 2016).

In addition to the cell wall monitoring system, plants have evolutionary acquired the capacity to detect conserved pathogen-derived ("non-self") ligands, known as Microbe-Associated Molecular Patterns (MAMPs), by plasma membrane-anchored Pattern-Recognition Receptors (PRRs), which are mainly Receptor Kinases (RKs) and Receptor-Like Proteins (RPs) (Bender & Zipfel, 2023). These types of receptors can also perceive "plant-self" derived Damage-Associated Molecular Patterns (DAMPs), that are released or synthesized upon plant tissue damage/infection by pathogens (De Lorenzo & Cervone, 2022). MAMPs/DAMPs recognition by PRRs activate Pattern Triggered Immunity (PTI) and disease resistance responses. The plant immune system also recognizes microbial effectors (avirulence (Avr) proteins, not conserved between microbial strains) through intracellular receptors that might be encoded by Resistance genes (R), activating Effector Triggered Immunity (ETI: Boutrot & Zipfel, 2017; DeFalco & Zipfel, 2021; Li, Yu *et al.*, 2016). PTI and ETI have recently been shown to function cooperatively in disease resistance (Yuan *et al.*, 2021).

1.1. Plant cell walls

The first plant defensive barriers that pathogens/pests must encounter are cuticle (composed of hydrophobic compounds; Arya *et al.*, 2021; Carpita & McCann, 2000) and cell walls. Cell Walls (CWs) are dynamic and complex structures surrounding all plant cells and providing a physical barrier and mechanical support, determining cell differentiation, shape, and control of growth processes (Wolf 2022; Carpita & McCann, 2000). The structure of the cell walls changes during cell differentiation after division. A dedicated Cell Wall Integrity (CWI) mechanism has been recently described that encompasses all the molecular events that modulate CW shape and function (Bacete *et al.*, 2020; Baez *et al.*, 2022; Vaahtera *et al.*, 2019). The composition and structure of the CW change during cell specialization. First, during cell division is formed the middle lamella (Figure 1.1), which is mainly composed of peptides/proteins and pectins and represents the outermost layer of cell wall (Zamil & Geitmann, 2017); later, Primary Cell Wall (PCW) is synthesized by the deposition of different carbohydrate polymers and additional proteins and metabolites (this is common to all plant cells) (Figure 1.1). Also, a Secondary Cell Wall (SCW), between the plasma membrane and PCW, is

deposited in those cells that have completed their cellular expansion or need a functional specialization to reinforce their walls, like in xylem cells (Figure 1.1) (Arya *et al.*, 2021; Carpita & McCann, 2000).

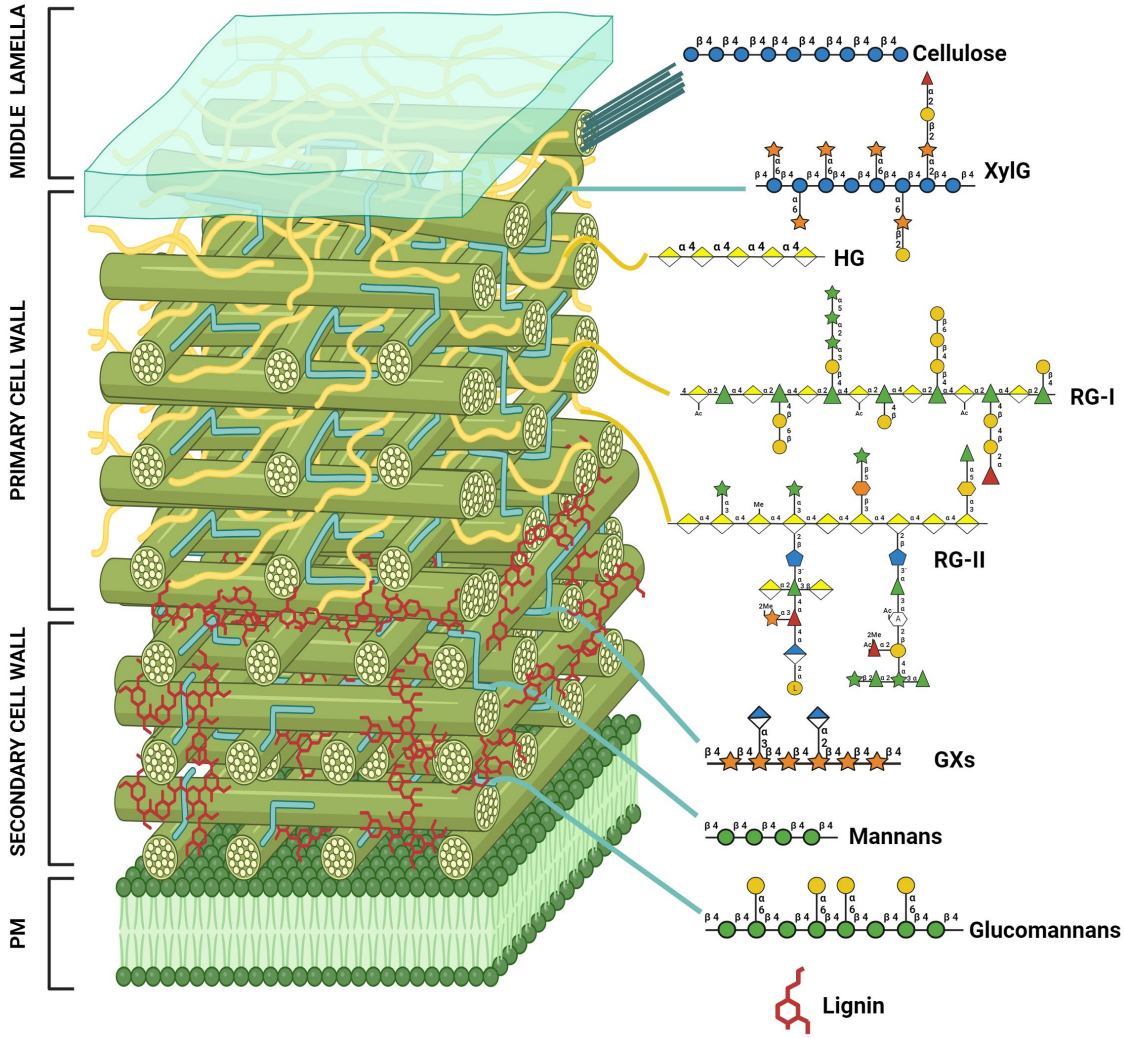

Figure 1.1: Plant cell wall and its main polymers simplify cartoon representation. Different parts of the cell wall are illustrated (as middle lamella, type I PCW and SCW) and the Plasma Membrane (PM). Main components of each layer are represented following the SNFG (Symbol Nomenclature for Glycans) (Neelamegham *et al.*, 2019; Varki *et al.*, 2016). PCW: XylG (xyloglucans), HG (homogalacturonan), RG-I (rhamnogalacturonan-I) and RG-II (rhamnogalacturonan-II); SCW: GXs (glucuronoxylans), mannans and glucomannans among other polysaccharides. In the SCW lignin is shown in red structures.

1.1.1. Plant cell wall structures

Plant cell walls have important differences in their structure and composition (Zhang *et al.*, 2021). Also, there are a lot of differences between monocotyledons and dicotyledons plant cell walls as well as between species (Addison *et al.*, 2024; Cosgrove, 2023; Zhao *et al.*, 2022). All these chemical differences have an obvious

impact on the three-dimensional architectures and physicochemical properties of plant walls, and the diversity of wall structures found in plants (Alonso Baez & Bacete, 2023).

All plant cells are surrounded by a PCW, whereas those cells that have completed their cellular expansion or reinforced their walls for functional specialization, such as xylem cells, have also SCW (Carpita & McCann, 2020). Although the plant cell wall is a continuum structure, the composition varies along cell development (Liu, Persson *et al.*, 2015).

The **middle lamella** is a thin layer that pastes together the primary cell walls of two adjacent cells (Figure 1.1) (Carpita & McCann, 2020).

1.1.1.1. Primary Cell Wall (PCW)

PCWs are mainly composed of carbohydrate-based polymers (cellulose, pectins and hemicelluloses) integrated by different monosaccharide moieties (e.g. glucose, xylose, arabinose, galacturonic acid) bound by diverse types of linkages and stabilized by cellulose microfibrils (Figure 1.1) (Carpita & McCann, 2000). These bounds determine the linearity or the degree of branching of the polysaccharides. Moreover, glycan moieties of the polysaccharides can have different types of biochemical decorations (acetylations, esterifications, methylations, aminations, etc.), undergo modifications (oxidation or reduction), or be bound to ions/cations (e.g. calcium, boron), making the structures of cell wall polysaccharides extremely diverse and complex (Burton *et al.*, 2010; Carpita & McCann 2020). Moreover, polysaccharide structures can be modified through linkages established among them and with other cell wall components like proteins, lignin and suberin (Carpita & McCann 2020).

We can differentiate two types of PCW (Type I and Type II) depending mainly on the phylogenetic relationships of two different groups of plants. PCW of eudicots are Type I and mainly consist of cellulose (CEL) arrays, composed of ß-1,4-D-glucan chains (Carpita & Gibeaut 1993). These chains are synthesized at the plasma membrane by Cellulose Synthase (CESA) complexes and are subsequently assembled into semi-crystalline microfibrils (Burton *et al.*, 2010). These microfibrils gain stability through their interaction with other ß-1,4 backbones, mainly xyloglucans (XylGs) in PCWs. These arrays of fibers are embedded in a matrix of pectins, primarily comprising α-1,4-D-galacturonic acid (GalA) chains that form the structural backbones of homogalacturonans (HGs) (Figure 1.1)

(Atmodjo *et al.*, 2013). These HGs are decorated with diverse sugar branches in rhamnogalacturonan I (RG-I) and rhamnogalacturonan II (RG-II) polymers (Figure 1.1) (Atmodjo *et al.*, 2013). Besides these glycan polymers, highly glycosylated Arabinogalactan Proteins (AGPs) are covalently linked to hemicelluloses and pectins (Tan *et al.*, 2013). These AGPs influence cell adhesion during growth and development by establishing glycosylphosphatidyl-inositol (GPI) links with the plasma membrane (Leszczuk *et al.*, 2023).

The composition of the PCW of grasses follows a Type II model and differs from that of dicots in the types and relative abundance of non-cellulosic polysaccharides, proteins and phenolic compounds (Carpita & Gibeaut, 1993; Vogel, 2008). The PCW of grasses is mainly composed of a structural framework of cellulose fibers interconnected with arabinoxylans and glucuronoarabinoxylans. Pectins and proteins are less prominent than in dicots, and their structural role is carried out by unbranched and unsubstituted chains of Mixed-Linked ß-1,3/ß-1,4-Glucans (MLGs; (Vogel, 2008). Moreover, these walls are characterized by the presence of significant quantities of phenylpropanoid molecules including lignin, ferulic acid and p-coumaric acid, and suberin in some cells, that are cross-linked to cell wall polysaccharides to provide rigidity and mechanical strength to cell walls (Hatfield *et al.*, 2017; Wolf, 2022).

1.1.1.2. Secondary Cell Wall (SCW)

SCWs are deposited in plant cells that have completed their expansion or need to reinforce their structure, especially important in those that provide mechanical support or are involved in water transport as xylem cells. SCWs are composed of robust matrixes primarily consisting of cellulose microfibrils, intertwined with various hemicelluloses, particularly xylans, glucomannans and mannans (Figure 1.1) (Kumar *et al.*, 2016; Sarkar *et al.*, 2009). This structural framework is further strengthened by crosslinking with lignin, resulting in a rigid and impermeable barrier that imparts durability to plant cells (Figure 1.1) (Kang *et al.* 2019).

SCW is composed by three main polymers which are cellulose (represents 40-80% of SCW composition), hemicellulose (10-40%), lignin (5-25%) and cell wall proteins (Figure 1.1) (Kumar *et al.*, 2016). Lignin is a key element in the SCW since creates an amorphous matrix, where cellulose and hemicelluloses are embedded (Hatfield *et al.*, 2017).

There is considerable variability in the fine structures of PCW or SCW polymers (e.g. degree of xylan/pectin acetylation or pectin methylation) within a given phylogenetic group of plants, and even plant species. Moreover, CW composition and structure vary significantly between different tissues (e.g. leaves vs. roots) and even between one cell and its adjacent ones. All these biochemical differences have an obvious impact on the physicochemical properties and diversity of plant cell walls (Alonso Baez & Bacete, 2023).

1.1.2. Plant cell wall components

Plant cell wall main components are carbohydrate-based polymers, cellulose, pectins (as homogalacturonan, rhamnogalacturonan I and rhamnogalacturonan II), two principal hemicellulose (xyloglucan and xylan) and other less presented polysaccharides (mannan and glucomannan) integrated by different monosaccharides units as glucose, xylose, arabinose or galacturonic acid, bounded by different linkages that determine the Degree of Polymerization (DP) (Zablackis *et al.*,1995).

1.1.2.1. Cellulose

Cellulose is a linear polymer of ß-1,4-glucosyl residues connected via O-glycosidic linkages between the C1 and C4 carbons of the glucopyranose rings (Kloareg *et al.*, 2021; McNamara *et al.*, 2015), forming microfibrils which are semi-crystalline structures constituting the main abundant compound of all plant cell walls (Burton *et al.*, 2010; Carpita & Gibeaut 1993; Guerriero *et al.*, 2010). Between each glucose monomer, two hydrogen bonds are established in a coplanar orientation allowing the aggregation into microfibrils stabilized by van der Waals interactions between the glucopyranose rings. Thus, the glucan chains have a hydrophilic and a hydrophobic face that allows for very strong interchain interaction, although each interaction is weak (Delmer *et al.*, 2024).

Cellulose is synthesized from intracellular uridine diphosphate-glucose at the plasma membrane by cellulose synthase enzymes, organized into multisubunit Cellulose Synthase Complexes (CSCs) (Burton *et al.*, 2010). As CSCs polymerize multiple glucose chains to form cellulose, they move along linear trajectories in the plasma membrane. A substantial proportion of CSCs in the plasma membrane are guided by microtubules via direct interactions between CESAs and microtubule-associated proteins, such as CELLULOSE SYNTHASE INTERACTIVE1 (CSI1) (Mohammad & McFarlane, 2024). Cellulose gains stability through its interaction

with other ß-1,4 backbones, mainly xyloglucans in primary cell walls. While CESA moves through the plasma membrane by interacting with the microtubules, it organizes multiple linear glucose polymers into microfibrils as load-bearing wall components (Purushotham *et al.,* 2020), synthesizing 18-24 glucan chains that form one microfibril in a specific orientation (Harris *et al.*, 2010; McNamara *et al.*, 2015; Taylor *et al.*, 2008; Turner & Kumar, 2018).

1.1.2.2. Pectins

Pectins are the most soluble and dynamic wall polysaccharides, forming a hydrated gel-like matrix in the space between cellulose microfibrils (Cosgrove, 2023). They primarily comprise covalently linked α-1,4-D-galacturonic acid (GalA) chains, also called homogalacturonan (HG), which are decorated with diverse sugar branches in rhamnogalacturonan I (RG-I) and rhamnogalacturonan II (RG-II) polymers (Atmodjo *et al.*, 2013; Mohnen, 2008). They account for the 35% of PCWs in dicots and non-graminaceous monocots, 2–10% of grass and other commelinids PCWs, and up to 5% of walls in woody tissues. The biosynthesis of pectins is estimated to require at least 67 transferases including glycosyl-, methyl-, and acetyltransferases (Mohnen, 2008). They are important determinants of wall thickness, hydration, porosity, ion exchange capacity and electrostatics. Although pectins are found throughout the wall, they are particularly concentrated in the middle lamella (Cosgrove 2023).

Homogalacturonan (HG)

HG, the most abundant pectic polysaccharide, comprises approximately 65% of pectins (Mohnen, 2008; Zablackis *et al.*, 1995). After their synthesis in the Golgi, the carboxyl group of most homogalacturonan residues typically becomes methyl-esterified. The methyl esters may be removed in the wall by Pectin Methyl Esterase (PME), increasing the negative charge of homogalacturonan and enabling cooperative ionic crosslinking by calcium between homogalacturonan chains. Processive de-esterification by PME can result in linear segments of six or more residues that can be ionically crosslinked by calcium ions to a neighbouring chain, conforming “egg-box junctions”. The degree and pattern of methyl esterification are important determinants of pectin physicochemical, mechanical and signalling properties (Cosgrove 2023). The frequency and length of these zones determine the cell wall porosity (Carpita & McCann, 2000).

Additionally, Pectin Methyl Esterase Inhibitors (PMEIs) regulate PME activity, loosening the pectin matrix to control cell adhesion and cell expansion (Wormit & Usadel, 2018). Moreover, HG demethylation can also affect the biomechanical properties of the cell wall by rendering pectin susceptible to enzymatic depolymerization by pectin lyases and polygalacturonases (Cosgrove 2023; De Lorenzo & Cervone, 2022; Wolf, 2022).

Rhamnogalacturonan I (RGI)

RGI has a backbone of the galacturonic acid-rhamnose disaccharide repeat [-α-D-galacturonyl-1,2-α-L-rhamnosyl-1-4-]$_n$ substituted by a lot of sugar moieties and branched oligosaccharides (e.g. galactans, arabinans and arabinogalactans). In some cases, they establish bottle brush-like appearance and may be covalently linked to HG and glycoproteins (Cosgrove, 2023; Ridley *et al.*, 2001). Between 20% and 80% of the rhamnosyl of RGI has α-L-arabinose and ß-D-galactose individual, linear or branched residues at the O-4 (Mohnen, 2008; Sun *et al.*, 2019). Besides these residues, α-L-arabinose can also appear branched by arabinose, arabinans and galactans, demonstrating the complexity of these polysaccharides (Nakamura *et al.*, 2001; O'Neill & York, 2018). RGI is the second most abundant pectin and represents about 20-35% of the total pectin (Mohnen, 2008). RG-I contributes to some wall properties like the adhesive features of the middle lamella and the hygroscopic properties of seed coat mucilage (the polysaccharide slime on the surface of many seeds) (Cosgrove, 2023).

Rhamnogalacturonan II (RGII)

The composition and structure of RGII, which accounts for 10% of total pectins, are even more complex than RGI (Mohnen, 2008; O'Neill *et al.*, 2004). Its structure is largely conserved across plant species and is based on an HG backbone of at least DP 8 1,4-linked α-D-GalA residues with side branches of 12 different types of sugars like D-apiose, D-xylose, L-fucose or L-rhamnose bounded by 20 types of different linkages (O'Neill *et al.*, 2004). RG-II can be dimerized by a borate diester bond that is required for normal pectin condensation in the wall. RGII is much less abundant than RG-I, and yet its specific functions remain unknown (Cosgrove, 2023).

Xylogalacturonan (XGA)

XGA are HG backbones with 25-75% of ß-1,3-xylosyl substitutions at O-3 that can be at the same time substituted by an additional ß-linked xylose at O-4 (Coenen *et al.*, 2007; Mohnen, 2008). It has been shown that XGA may contribute to preventing the degradation of HG by endopolygalacturonases from pathogens, since xylogalacturonan:xylosyltransferases implicated in XGA biosynthesis are upregulated in some plant-pathogen interactions (Jensen *et al.*, 2008; Mohnen, 2008).

1.1.2.3. Hemicelluloses

Hemicelluloses comprise a diverse group of non-cellulosic polysaccharides such as xyloglucans, xylans, mannans and ß-1,3/1,4-D-glucans. They interact with cellulose microfibrils by hydrogen bonds, covering or forming a network between them (Carpita & McCann, 2000). This heterogenous group of polysaccharides typically consists of a linear backbone of ß-1,4-linked sugars decorated with short side chains of 1-3 sugar residues. They are synthesized in the Golgi apparatus, sorted into vesicles, and delivered to the wall by exocytosis. PCWs typically contain xyloglucan and smaller amounts of arabinoxylan. However, in SCWs, other hemicelluloses as xylans are dominant, whereas mannans and ß-1,3/1,4-D-glucans are also prevalence molecules (Cosgrove, 2023).

Xyloglucans (XylGs)

XylGs are composed of a backbone of ß-1,4-D-glucans branched with xyloses through α-1,6-glycosidic linkages. Xylosyl units can be further substituted with α-L-arabinose or ß-D-galactose and galactosyl residues with α-L-fucose (Carpita & McCann, 2000). They are the most abundant hemicellulose polysaccharide in PCW type I, representing approximately 20% of cell wall polysaccharides (Liepman & Cavalier, 2012).

They are synthesized by Cellulose Synthase-Like (CSL) proteins belonging to the Glycosyltransferase 2 (GT2) family at the Golgi apparatus. Later they are transported to the plasma membrane via vesicle trafficking (Kim *et al.* 2020). XylGs synthesis requires at least four types of enzymatic activities, UDP-glucose-dependent 1,4-ß-glucan synthase to assemble the glucan backbone, UDP-xylose-dependent 1,6-α-xylosyltransferase to attach xylosyl residues to selected glucosyl residues of the glucan backbone, UDP-galactose-dependent 1,2-ß-

galactosyltransferase to attach galactosyl residues to specific xylosyl residues, and GDP-fucose-dependent 1,2-α-fucosyltransferase to join fucosyl residues with selected galactosyl residues (Faik *et al.*, 2002; Liepman & Cavalier, 2012). The interaction points between cellulose-hemicelluloses determine the biomechanical properties of the cell wall and serve as targets for expansins and other proteins for cell wall remodelling and cell expansion and to prevent self-association of cellulose microfibrils (Park & Cosgrove, 2012; Zhang, Chang, *et al.*, 2021). They can also be cleaved and reconnected by endo-transglycosylases/hydrolases (XTH) (Sechet *et al.*, 2016).

XylGs interact as well with other cell wall polymers mainly coating and cross-linking adjacent cellulose microfibrils by non-covalent association, having a big implication in the cell wall rigidity and cell wall loosening during cell wall elongation (Cosgrove 2023; Hayashi, 1989). The acetylation of XylGs impacts its functionality (Jia *et al.*, 2005). Acetylated XylGs can be found in most of the species in fucogalactoxyloglucans and arabinoxyloglucans forms (Carpita & McCann, 2000).

Xylans

Xylans are made of a ß-1,4-D-xylose backbone substituted with acetyl, α-1,2-Glucuronic Acid (GlcA) or 4-O-Methyl-Glucuronic Acid (Me-GlcA), and arabinose residues. There is variation in xylan structures between different species and even between different tissues in the same species. In dicots, xylan is the predominant hemicellulose in SCWs, but little is found in PCWs being the major non-cellulosic polysaccharide in the PCW of commelinids. In Arabidopsis, the ratio of Me-GlcA to GlcA substitutions is around two, and Me-GlcA substitutions are found, on average, on one out of every eight xylose residues (Rennie & Scheller, 2014).

A common modification of xylans is substitution with α-(1→2)-linked glucuronosyl and 4-O-methyl glucuronosyl residues. Xylans dominated by this type of substitution are often known as glucuronoxylans (GXs) and are the dominating non-cellulosic polysaccharide in the SCW of dicots (Scheller & Ulvskov, 2010). This polymer can appear O-acetylated in C-2 and C-3 of xylosyl residues, modulating the interaction with cellulose microfibrils (Busse-Wicher *et al.*, 2014; Mélida *et al.*, 2020). Monocot xylans usually contain many arabinose residues attached to the backbone and are known as arabinoxylans (AXs). Arabinofuranose substitutions

are, in principle, less frequent in dicot xylans, but exceptions are found (Darvill *et al.*, 1980; Fischer *et al.*, 2004; Naran *et al.*, 2008).

Mannans and glucomannans

This group is based on ß-1,4-linked polysaccharides containing mannose. The backbones may consist entirely of mannose, as in mannans and galactomannans (with galactose substituents), or with mannose and glucose in a non-repeating pattern as in glucomannans and galactoglucomannans (mannose and glucose backbone in a non-repeating manner with galactose substituents) and all of them often acetylated (Kumar et al., 2016; Scheller & Ulvskov, 2010). Mannans are found in variable amounts in all cell walls and have been widely studied/described as seed storage compounds. In gymnosperms, galactoglucomannans are major components of the secondary walls (Ebringerová *et al.*, 2005), but in Arabidopsis represent only a small percentage of hemicelluloses (Scheller and Ulvskov, 2010).

ß-1,3/1,4-D-glucans or Mixed Linked Glucans (MLGs)

Mixed-Linked Glucans (MLGs; ß-1,3/1,4-glucans; (1,3;1,4)-ß-D-glucans) consist of unbranched and unsubstituted chains of ß-1,4-glucosyl residues interspersed by ß-1,3 linkages. MLGs are widely distributed as matrix polysaccharides in the cell walls of plants from the *Poaceae* group. They are present in other species such *Equisetum* spp., other vascular plants outside the *Poaceae*, bryophytes and algae, and in other organisms such as lichen-forming ascomycete symbionts, in fungi and oomycetes (Rebaque *et al.*, 2021).

MLGs tend to self-aggregate and bind to other hemicelluloses and cellulose, therefore MLGs might have an architectural role in the cell wall (Fry *et al.*, 2008). MLG function in CW porosity regulation during active growth has been hypothesized (Harris & Fincher, 2009). These interactions differ from those found in other hemicelluloses which are mainly regulated by the degree of substitutions to prevent extensive alignments (Mohnen, 2008). In the case of MLGs (non-branched polymers) the cross-link regulation seems to be mediated by the irregular conformation of MLGs that prevents extensive alignments mediated by long ß-1,4 regions (up to 12). Other roles have been described for MLGs as storage polysaccharides in *Poaceae* endosperm (Lazaridou & Biliaderis, 2007; Sørensen *et al.*, 2008) and playing a role in cell expansion (Fry *et al.*, 2008).

MLGs are synthesized by members of the Cellulose Synthase - Like (CSL) subfamilies from Glycosyltransferase 2 (GT2) family, localized in the Golgi apparatus (Coutinho *et al.*, 2003; Kim *et al.*, 2018; Lombard *et al.*, 2014; Scheller & Ulvskov, 2010), which are very similar to CESA proteins (Little *et al.*, 2018).

1.1.2.4. Lignin

Lignin is only present in SCWs. Chemically, it is a heterogeneous and complex polymer largely derived from three hydroxycinnamyl alcohol precursors, p-coumaryl, coniferyl, and sinapyl alcohols. These precursors give rise to the p-hydroxylphenyl, guaiacyl and syringyl units of lignin, respectively, varying the proportion depending on the biological source. Guaiacyl and syringyl units are more abundant in monocots and dicots but the monocot lignin also contains significant amounts of p-hydroxylphenyl units (Kumar *et al.*, 2016). Lignin not only provides strength and compression to the walls but is also essential for cell wall integrity (Boerjan *et al.*, 2003) and provides a physical barrier avoiding the spread of pathogens, toxins and enzymes (Miedes *et al.*, 2014). The most recent advances on the biochemical and structural characterization of lignin have been described in the reviews Peracchi *et al.*, 2024 and Yadav & Chattopadhyay, 2023.

1.1.2.5. Cell wall proteins

They play important roles in the structural and biological processes of cell walls (Lee *et al.*, 2004). The synthesis of cell wall proteins occurs in the endoplasmic reticulum. Its regulation is tissular and developmental-dependent and can be altered in response to biotic and abiotic stresses (Albersheim *et al.*, 2010; Marowa *et al.*, 2016).

Most cell wall proteins, which have structural functions, are glycoproteins and can be placed into one of four classes based on the abundance of certain amino acids or glycan motifs in their sequence. These are Glycine-Rich Proteins (GRPs), Proline-Rich Proteins (PRPs), Arabinogalactan-rich Proteins (AGPs), and Hydroxyproline-Rich Glycoproteins (HRGPs or extensins) (Showalter, 1993). Additionally, some of these proteins influence cell adhesion during growth and development by establishing glycosylphosphatidyl-inositol (GPI) links with the plasma membrane forming a plasma membrane–cell wall continuum (Leszczuk *et al.* 2023). They can

be released into the cell wall when needed by the action of phospholipases (Kumar *et al*, 2016; Liu, Persson *et al.*, 2015).

In addition to these group of cell wall proteins, there are other group of soluble proteins associated to cell walls, like hydrolases, transglycosylases, kinases, extensins and extracellular peroxidases, which are involved in biological processes such as cell wall extension and assembly, molecular transport, cell recognition and pathogen resistance (Delmer *et al.*, 2024; Marowa *et al.*, 2016).

1.1.3. Plant cell wall modifications affect plant disease resistance

During plant-microbe interactions, microorganisms secrete Cell Wall Degrading/modifying Enzymes (CWDEs), like cellulases, polygalacturonases or xylanases, to break and overcome the barriers presented by the walls, by modifying their composition and structure (Zheng *et al.*, 2021). Altering the expression pattern of certain microbial CWDEs during plant colonization (achieved by impairing or miss-expressing CWDE genes in microbial strains) has been demonstrated to influence the outcome of plant disease resistance and pathogen colonization (Lorrai & Ferrari, 2021). CWDEs represent a significant proportion of the encoded proteins of plant-pathogenic fungal genomes, further indicating their relevance for breaching and modifying the walls and suggesting that microbial CWDE repertoire might determine plant-microbe specificity and colonization (Kubicek *et al.*, 2014).

The arsenal of CWDEs of microbes is quite diverse and is classified in different groups in CAZYme database (http://www.cazy.org) (Drula *et al.* 2022). CWDEs can either hydrolyze/break down linkages between glycan moieties, add/release groups to glycan moieties, or modify wall glycans/polysaccharides through oxidation or reduction. This diversity of activities of microbial CWDEs illustrates the complexity of plant wall structures that microorganisms encounter and must degrade to get into the cell or to release free glycans that they might use as energy sources or building blocks for the biosynthesis of new biomolecules (Delannoy-Bruno *et al.* 2022).

Notably, certain alterations in the expression patterns of CWDEs in genetically modified microbial strains result in contrasting and initially unexpected virulence phenotypes compared to wild-type strains. This observation further supports that the balance between plant cell wall degradation during pathogen colonization and

the perception by plants derived from CWDEs activity might determine the progression of colonization and disease resistance outcome (Dora *et al.*, 2022; Gámez-Arjona *et al.*, 2022; Yang *et al.*, 2021).

Accordingly, many wall modifications caused by mutations affecting plant genes encoding functions related to cell wall biosynthesis and structural composition might also be perceived by plant monitoring systems and have an impact on plant disease resistance outcome (Bacete *et al.*, 2018; Miedes *et al.*, 2014). These phenotypic alterations have been particularly documented in *Arabidopsis thaliana* mutants impaired in cell wall-related genes and support the relevant role of wall extracellular matrix on plant immunity (Bacete *et al.*, 2018; Molina *et al.*, 2021).

For example, mutants impaired in CESA complexes, required for the synthesis of cellulose, are usually associated with specific enhanced disease resistance phenotypes. Arabidopsis *cev1* and *rsw* mutants, affected in *CESA3* and *CESA1* genes, respectively, required for PCW cellulose biosynthesis, display enhanced resistance to several biotrophic powdery mildew fungi (*Golovinomyces cichoracearum*, *Golovinomyces orontii* and *Oidium lycopersicum*) (Ellis *et al.*, 2002; Ellis, Karafyllidis & Turner, 2002), but did not display altered susceptibility to the necrotrophic fungus *Plectosphaerella cucumerina* or the soil-borne bacterium *Ralstonia solanacearum* (Hernandez-Blanco *et al.*, 2007). In contrast, Arabidopsis *irregular xylem* mutants, *irx5-1/irx3-1/irx1-6*, affected, respectively, in *CESA4/CESA7/CESA8* required for SCW cellulose biosynthesis, are more resistant than wild-type plants to these *P. cucumerina*, *R. solanacearum* and other pathogens (Hernandez-Blanco *et al.*, 2007; Molina *et al.*, 2021).

Alteration of the biosynthesis and/or structure of wall pectins, like the degree of methyl-esterification and acetylation, can also affect pathogen resistance (Bethke *et al.*, 2016). Mutants with enhanced or reduced pectin content show alterations in disease resistance to different pathogens. For example, Arabidopsis *powdery mildew resistant* (*pmr*) mutants impaired either in a pectin acetyltransferase that transfers acetyl groups to GalA (*pmr5*; Chiniquy *et al.*, 2019), or in a pectate lyase–like protein (*pmr6-1*; Vogel *et al.*, 2002), exhibit cell walls with increased total pectins and enhanced resistance to powdery mildew fungi (*G. cichoracearum* and *Erysiphe orontii*; (Vogel *et al.*, 2002; Vogel *et al.*, 2004) and the hemibiotrophic fungus *Colletotricum higginsianum* (Engelsdorf *et al.*, 2017). In contrast, these mutants are highly susceptible to *Botrytis cinerea*, (Chiniquy *et al.*, 2019; Wang *et al.*, 2017) and are unaffected in their resistance to *P. cucumerina* (Hernandez-Blanco *et al.*, 2007; Molina *et al.*, 2021).

Similarly, Arabidopsis *gae1 gae6* double mutant, impaired in genes encoding glucuronate 4-epimerases required for pectin precursor UDP-D-galacturonic acid biosynthesis, that displays a strong reduction in GalA, total uronic acids and pectin in its cell walls, is slightly more susceptible to *Pseudomonas syringae pv. maculicola* ES4326 bacterium and shows enhanced susceptibility to *B. cinerea* isolates (Bethke *et al.*, 2016). In contrast, Arabidopsis plants expressing constitutively a fungal polygalacturonase that degrades HG, as well as loss-of-function mutants for *QUASIMODO2 (QUA2)*, encoding a putative pectin methyltransferase important for HG biosynthesis, show reduced growth and almost complete resistance to *B. cinerea*, probably explained by the accumulation of reactive oxygen species (Lorrai & Ferrari, 2021).

Immune-related phenotypes have been also documented for some plant mutants with reduced content and/or structural alterations in the composition of hemicelluloses. For example, alterations in some Arabidopsis cell wall-related genes result in an increase of xylose content, enhancing resistance to *P. cucumerina*, such as mutations in *xylosidase 1* (*XYL1*) gene (that affects xyloglucan structure), in the glycophosphatidyl-inositol (GPI)-linked IRREGULAR XYLEM 6 (IRX6), and in the component of the vacuolar H+-ATPase Arabidopsis DE-ETIOLATED 3 (DET3) (Delgado-Cerezo *et al.*, 2012). Moreover, mutations affecting the decorations (e.g. acetylations) and side chains of hemicelluloses have also an influence on immunity, as has been observed in *REDUCED WALL ACETYLATION 2* (*RWA2*) mutant impaired in an O-acetyltransferase that shows an overall reduction of acetylation on several polymers and enhanced resistance to the biotrophic oomycete *Hyaloperonospora arabidopsidis* and *B. cinerea*, but not to *P. syringae* and *P. cucumerina* (Manabe *et al.*, 2011; Pawar *et al.*, 2016). In contrast, mutations in the plant-specific polysaccharide O-acetyltransferase *ESKIMO1* (*ESK1*), involved in xylan acetylation, show enhanced resistance to *P. cucumerina* but not to the biotrophic pathogens tested (Escudero *et al.*, 2017).

Alteration of the biosynthesis of complex cell wall components like the AGPs also leads to modifications in plant disease resistance. Loss of function mutants of ARABINOXYLAN PECTIN ARABINOGALACTAN PROTEIN1 (APAP1), an AGP that is covalently attached to pectin and hemicellulose (Tan *et al.*, 2013) display increased susceptibility to *P. syringae* (Kim *et al.*, 2023). Conversely, *arabinokinase1* mutant, which displays reduced levels of arabinose (Sherson *et al.*, 1999), shows enhanced resistance to this pathogen (Kim *et al.*, 2023). Also, alterations of the cell wall lignin content lead to susceptibility phenotypes.

Arabidopsis mutants in lignin biosynthetic genes *phenylalanine ammonia-lyase* (Huang *et al.*, 2010), *caffeic acid o-methyltransferase* (Quentin *et al.*, 2009) and *cinnamyl alcohol dehydrogenase* (Tronchet *et al.*, 2010) display reduced lignin deposition and are more susceptible to various bacterial and fungal pathogens (Miedes *et al.*, 2014).

In summary, all these data clearly illustrate the relevance of plant cell walls in disease resistance and suggest some correlations between cell wall modification and modulation of disease resistance levels. However, with a few exceptions (Molina *et al.*, 2021), specific links between wall modification and immune activation must be established.

1.2.From plant cell wall to signalling activation

Cell wall modifications caused by pathogens during plant cell colonization can be perceived by plant cell wall monitoring systems to trigger defensive responses (Bacete *et al.*, 2018; Miedes *et al.*, 2014). Plants have evolved a complex immune system that comprises several defence layers and mechanisms for the recognition of pathogens and pests that cooperatively interact to restrict plant infection. One of these layers is PTI based on the detection of conserved Pathogen-derived ("non-self") MAMPs ligands by plasma membrane-anchored PRRs, which are mainly Receptor Kinases (RKs) and Receptor-Like Proteins (RPs) (Bender & Zipfel, 2023; Bigeard *et al.*, 2015). These types of receptors can also perceive "plant-self" derived DAMPs that are released or synthesized upon plant tissue damage/infection by pathogens. Among these DAMPs are oligosaccharides released from plant cell walls (Bacete *et al.*, 2018; De Lorenzo & Cervone, 2022).

1.2.1. Microbe-Associated Molecular Patterns (MAMPs)

MAMPs are fragments of proteins or molecules (e.g. glycans) that are essential for the biology of microbes (Buscaill & van der Hoorn, 2021). They comprise molecules well conserved in a group of microorganisms (e.g. bacteria), such as peptides (e.g. flagellin epitope 22 (flg22) from bacterial flagellum) and carbohydrates (chitin-derived oligosaccharides (e.g. $(1,4\text{-}\beta\text{-N-acetylglucosamine})_6$, or CHI6), 1,4-β-glucans and 1,3-β-glucans from fungal/oomycete cell walls) (Bacete *et al.*, 2018; Wolf, 2022). In addition, exogenous microbial DNA and RNA can be perceived as

MAMPs (Bhat & Ryu, 2016). Some of the most relevant MAMPs are described below but a complete list can be found in Buscaill & van der Hoorn (2021).

1.2.1.1. Peptidic MAMPs

This group comprises short peptide sequences derived from microbial pathogens proteins. Several types of peptidic MAMPs have been identified, each with distinct structures and functions.

Flagellin (Flg) is the main building block of bacterial flagella, and it is well-established as a major activator of innate immunity in animals (Ramos *et al.*, 2004). When bacteria interact with the surface of different parts of plants, several flagellin epitopes can be perceived, such as **flg22,** a 22-amino acids peptide located at the highly conserved N terminus of flagellin, that is the most studied MAMP because is widely recognized by plants (Felix *et al.*, 1999; Newman *et al.*, 2013). flg22 is perceived by FLAGELLIN SENSITIVE2 (FLS2), a PRR from the RK family, with Leucine-Rich Repeat (LRR) ectodomain (ECD). flg22 peptides from most ε-, δ-, and α-proteobacteria induce moderate, weak, or no response, respectively, in contrast to flg22 peptides from the majority of γ- and ß-proteobacteria, which trigger strong responses (Buscaill & van der Hoorn, 2021).

flg22-induced activation of FLS2 in Arabidopsis, involves a complex formation with the BRASSINOSTEROID-INSENSITIVE 1 (BRI1)- ASSOCIATED RECEPTOR KINASE 1 (BAK1) (Chinchilla *et al.*, 2007). BAK1 acts as a positive regulator of MAMP signalling in Arabidopsis, interacting with FSL2 in a ligand-dependent manner (Chinchilla *et al.*, 2007; Newman *et al.*, 2013). This interaction allows phosphorylation and activation of the receptor complex (Schulze *et al.*, 2010). Downstream of the FLS2-BAK1 receptor complex, there is a cytoplasmic receptor kinase BOTRYTIS-INDUCED KINASE 1 (BIK1), which is constitutively associated with FLS2. After FLS2-BAK1 dimerization, BIK1 dissociates from FLS2, possibly allowing BIK1 to phosphorylate downstream components, and thus linking the MAMP receptor complex to downstream intracellular signalling (Newman *et al.*, 2013).

Elongation factor thermo unstable (EF-Tu) is the most abundant protein in the bacterial cell (Jeppesen *et al.*, 2005). EF-Tu associates with ribosome during protein biosynthesis. Notably, the N-terminus of EF-Tu, either a 26 or 18 aa peptides, named elongation factor 26 or 18 (elf26 or elf18), are perceived as MAMP

by the plant immune system through EF-Tu Receptor (EFR) which belongs to the RK family and has an LRR-ECD (Newman *et al.*, 2013; Zipfel *et al.*,2006). Despite elf18 and flg22 have perceived by different receptors, they trigger the up-regulation of the same pool of genes, and a common set of responses in Arabidopsis. Also, a combined treatment with elf26/18 and flg22 induce the same kinases proteins without an additive effect (Zipfel *et al.*, 2006; Newman *et al.*, 2013).

In addition to flg22 and elf18, a high number of microbial MAMPs have been identified, and in most of the cases their corresponding PRR determined (see Buscaill & van der Hoorn, 2021). For example, the **xup25** peptide is a membrane protein derived from a xanthine/uracil permease family protein, very well conserved among the bacteria, that is bound by XANTHINE/URACIL PERMEASE SENSITIVE 1 (XPS1), an LRR-RK (Mott *et al.*, 2016). **The endopolygalacturonase 1 (BcPG1)** is a virulence factor participating in fungi pathogenicity such as that of *B. cinerea* (Ten Have *et al.*, 1998), but it has been described as an activator of plant defence responses (Poinssot *et al.*, 2003). BcPG1 is perceived by the LRR Receptor-Like Protein 42 (RLP42), that in Arabidopsis form part of the RLP family comprising 57 members (Wang *et al.*, 2008).

Other well-characterized MAMPs are **Necrotric Lytic Peptides (NLPs)** that form a superfamily of proteins that are produced and secreted by bacterial, fungal and oomycete species (Oome & Van den Ackerveken, 2014). NLPs have initially been discovered as cytotoxic proteins triggering leaf necrosis and plant defences in dicotyledonous, but not in monocotyledonous plants, destabilizing plant plasma membranes during infection thereby facilitating host cell death (Böhm *et al.*, 2014). Inspection of NLP protein sequences from the various lineages revealed the presence of a nlp20-motif that triggers plant immunity and reduced symptom development and microbial growth rates on infected plants (Böhm *et al.*, 2014). A complex of different proteins is implicated in nlp20 perception, including RLP23- and the LRR-SUPPRESSOR OF BAK1 INTERACTING RECEPTOR KINASE 1 (SOBIR1), that interact physically *in planta* (Albert *et al.*, 2015). At the same time, RLP23-mediated immune activation is dependent on SOMATIC EMBRYOGENESIS RECEPTOR KINASE 3 (SERK3)/BAK1 and possibly other members of the SERK protein family, such as SERK4. Altogether, RLP23, SOBIR1 and BAK1 build a signaling-competent array in which all three proteins are in close physical proximity, likely forming a tripartite PRR complex (Albert *et al.*, 2015).

1.2.1.2. Carbohydrate-based MAMPs

During infection, CWDEs are secreted by the pathogens to break the cell wall barrier, but plants are also able to secrete host CWDEs that can hydrolase microbes surfaces at the contact point with the plant cells. As a result of the activity of host CWDEs (e.g. chitinases and glucanases secrete into the apoplast), many glycan MAMPs are released on pathogen-host interface, such as fungal oligosaccharides derived from main fungal wall polysaccharides, like chitin or ß-1,3-glucans, (Dora *et al.*, 2022; Geoghegan *et al.*, 2017; Wanke *et al.*, 2021).

Although a lot of carbohydrate-based MAMPs are released during the plant-pathogen interaction, the knowledge about the specific mechanisms of plant defence activation by glycan patterns is very low compared to the animal field, where different types of receptors have been described to bind carbohydrate-based ligands (Erwig & Gow, 2016). Also, current knowledge of carbohydrate-based pattern recognition by plants is clearly behind that of peptidic-based MAMP perception by the plant immune system (Bacete *et al.*, 2018; Tang *et al.*, 2017).

Chitin

The best characterized MAMP of the carbohydrate-based group is fungal chitin. Chitin is a linear homopolymer of ß-(1,4)-linked N-acetyl-D glucosamine (GlcNAc) monomers, that is a highly abundant polysaccharide in nature. Chitin is an important structural component in the cell walls of fungi, in which chains of chitin associate in microfibrils covalently bound to the major component of fungal cell walls, ß-(1,3)-glucan, and form a network together with glycoproteins (Sánchez-Vallet *et al.*, 2015).

Perception of chitin requires LysM RKs, like Arabidopsis CHITIN ELICITOR RECEPTOR KINASE1 (CERK1) with a LysM ectodomain, transmembrane domain and a kinase intracellular domain. AtCERK1 can bind chitin, although its affinity for chitin binding appears to be rather low, up to 68 µM for chitin oligomers of eight units of GlcNAc (Iizasa *et al.*, 2010; Liu *et al.*, 2012; Petutschnig *et al.*, 2010). It was suggested that chitin oligomers are bound by the LysM domains of two CERK1 monomers, resulting in receptor dimerization and transphosphorylation of their cytoplasmic kinase domains. This dimerization is established by oligomers containing eight GlcNAc monomers (Liu *et al.*, 2012). Arabidopsis LysM-CONTAINING RECEPTOR-LIKE KINASE 5 (AtLYK5) is also essential, like CERK1, in chitin-derived oligosaccharides perception being its ECD-

CHI6 binding affinity in Isothermal Titration Calorimetry (ITC) experiments higher than that of CERK1 ECD (Cao *et al.*, 2014). In addition, it has been reported that the LysM RK AtLYK4 is required for chitin triggered immunity and may form part of the chitin receptor complex being, with AtLYK5, the true receptors, whereas CERK1 will function as co-receptor (Wan *et al.*, 2012), phosphorylating downstream signalling proteins, such as the mitogen-activated protein kinases (Sánchez-Vallet *et al.*, 2015).

Interestingly, Arabidopsis plasmodesmata possess an alternative CERK1-independent chitin perception mechanism which involves LysM DOMAIN GPI ANCHORED PROTEIN 2 (LYM2; LysM domain-containing glycosylphosphatidylinositol (GPI)-anchored domain) and LYK4 that form a complex (Cheval *et al.*, 2020; Faulkner *et al.*, 2013).

Chitin can suffer different alterations as deacetylations, generating chitosan. This conversion during host invasion may protect hyphae of pathogenic fungi from being hydrolysed by extracellular plant chitinases, since chitosan is a poor substrate for chitinases, and consequently will reduce the release of elicitors (Ride & Barber, 1990; Sánchez-Vallet *et al.*, 2015). Moreover, chitosan-derived oligosaccharides are poor ligands for LysM RKs (Iizasa *et al.*, 2010; Liu *et al.*, 2012; Petutschnig *et al.*, 2010).

β-glucans

Some chitin fibrils are covalently linked to β-glucan chains, the predominant component of the outer cell wall layer of many fungi (~65–90% of polysaccharide content) (Bowman & Free, 2006). β-glucans in this layer are mainly connected via β-1,3-linkages with regularly occurring β-1,6-side branches every 2–25 glucose units, thought to structurally interconnect the β-1,3-linked fibrils (Zekovic *et al.*, 2005). In some cases, additional β-1,4-linked moieties and mixed-linkage β-1,3/1,4-glucose polymers can be observed (Wanke *et al.*, 2021).

In fungi and some groups of algae, the main cell wall polymers are made of a β-1,3-D-glucan backbone that can be branched by β-1,6-D-glucan chains (Mélida *et al.*, 2018; Ramos *et al.*, 2013; Wanke *et al.*, 2021). β-1,6-glucan backbones have not been reported in fungal walls other than yeasts, and even there they are scarce compared with oomycetes (Latge & Calderone, 2006). However, Arabidopsis can perceive non-branched 1,3-β-glucans of various degrees of polymerization and this recognition is at least partially mediated by PRRs of LysM family (CERK1, LYK5

and LYK4), but in a different way as previously described for chitin (Liu *et al.*, 2012; Mélida *et al.*, 2018).

Notably, glucans containing ß-1,4 glycosidic linkages in their main backbones (cellulose) trigger PTI responses in plants (Claverie *et al.*, 2018; del Hierro *et al.*, 2021; Johnson *et al.*, 2018; Souza *et al.*, 2017). Cellulose has been described in several microorganisms. The shorter active ligand is cellobiose (CEL2), but cellotriose-cellopentaose (CEL3-CEL5) have been shown to be the most active molecules triggering PTI (Claverie *et al.*, 2018; Johnson *et al.*, 2018; Souza *et al.*, 2017).

Recently, Mixed Linked Glucans (MLGs; ß-1,3/1,4-glucans) consist of unbranched and unsubstituted chains of ß-1,4-glucosyl residues interspersed by ß-1,3 linkages have been described as good activators of PTI (Burton & Fincher, 2009). MLGs are present in some oomycetes and in cell walls of some plant families, as *Poaceae* (Rebaque *et al.*, 2021; Yang *et al.*, 2021). However, the PRR or molecular components implicated in their perception remain unknown. Plants also perceive ß-1,6 glucans, as shown recently in Arabidopsis (Álvarez-Martínez *et al.*, 2023; Fernández-Calvo *et al.*, 2024).

This field of ß-glucan perception by plants has regained momentum due to these recent discoveries which demonstrate that glucans containing different types of ß-glycosidic linkages in their main backbones trigger PTI responses in plants (Claverie *et al.*, 2018; del Hierro *et al.*, 2021; Johnson *et al.*, 2018; Melida *et al.*, 2018; Souza *et al.*, 2017; Wanke *et al.*, 2020; Wawra *et al.*, 2016).

Peptidoglycan (PGN)

PGN is an essential and unique membrane envelope component of all bacteria, providing rigidity and structure to Gram-positive and Gram-negative bacteria (Dziarski & Gupta 2006; McDonald *et al.*, 2005). PGN consists of numerous glycan chains that are cross-linked by oligo-peptides. These glycan chains are made of N-acetylglucosamine (GlcNAc) and N-acetylmuramic acid (MurNAc), with short peptides attached by anamide linkage to the lactyl group of MurNAc. PGN from both Gram-positive and Gram-negative bacteria acts as an elicitor of plant innate immunity in Arabidopsis (Erbs *et al*,. 2008; Gust *et al.*, 2007; Newman *et al.*, 2013). PGN is perceived in Arabidopsis by two of three Arabidopsis CHITIN OLIGOSACCHARIDE ELICITOR-BINDING PROTEINS (AtCEBiP), LYM1, and LYM3, involved in the perception/signalling of PGN with AtCERK1. Structurally,

CEBiPs contain extracellular LysM domains that are considered to generally mediate binding to GlcNAc-containing glycans, like those present in the backbone of PGN and fungal chitin (Gust *et al.*, 2012).

Lipopolysaccharides (LPSs)

LPSs are outer membrane glycolipids of Gram-negative bacteria known to induce the innate immune response in plants and mammals (Newman *et al.*, 2007). LPSs have a lipid A, which is embedded in the outer part of the phospholipid bilayer. Lipid A is linked to the core oligosaccharide, usually by the sugar 3-deoxy-D-manno-2- octulosonate (KDO). The core oligosaccharide consists of a short series of sugars and ends in the O-antigen, which is composed of repeating oligosaccharide units (Raetz & Whitfield, 2002). LPSs have been reported to induce immune responses in plants, such as the oxidative burst, cytoplasmatic calcium influx, the induction of pathogenesis-related gene expression and cell wall alterations that include the deposition of callose and pH changes (Erbs & Newman, 2012). LPS sensing has been described to be dependent on CERK1 presence in tomatoes but not in Arabidopsis, remaining the LPS-perception mechanism in Arabidopsis yet unknown (Desaki *et al.*, 2018).

1.2.2. Damage-Associated Molecular Patterns (DAMPs)

DAMPs comprise molecules released from plant cell walls, like oligosaccharides derived from wall polysaccharides such as cellulose, mixed-linked glucans, homogalacturonan, xyloglucans, xylans or arabinoxylan (Bacete *et al.*, 2018; Molina *et al.*, 2024; Wolf, 2022). DAMPs also include peptides that, upon plant infection by pathogens, are *de novo* synthesized or processed by specific proteases to produce mature active ligands (Abarca *et al.*, 2021; Bartels & Boller, 2015; Gully *et al.*, 2019; Peng *et al.*, 2018). Below are described some of the best-characterized DAMPs (Hou *et al.*, 2019).

1.2.2.1. Peptidic DAMPs

An array of small secretory peptides is involved in the control of growth, development, and stress responses. These peptides are typically expressed as a protein precursor, which upon certain stimuli is processed by proteolytic cleavage

to release the active signal. Some of these ligands act as immunomodulatory peptides formed upon cellular disruption and pathogen infection and are referred to phytocytokines (Rhodes *et al.*, 2021).

Plant elicitor Peptides (PEPs)

PEPs and their corresponding PRRs, PLANT ELICITOR PEPTIDES RECEPTORS (PEPRs) (LRR-RKs), are involved in plant immune responses to a broader range of pathogens and pests (Yamaguchi *et al.*, 2010). Expression of the PEP precursor proteins, proPEPs, is triggered by wounding, MAMP treatment, pathogen infection, herbivory, and treatment with PEPs themselves (Tanaka & Heil, 2021). Plant elicitor peptide 1 (Pep1) was the first peptide DAMP identified in Arabidopsis (Huffaker *et al.*, 2013). This 23-aa peptide is derived from a 92-aa precursor proPEP1 (Huffaker *et al.*, 2013; Yamaguchi *et al.*, 2006). Arabidopsis encodes eight different proPEP paralogs (proPEP1-8) that harbour conserved C-terminal epitopes (Hou *et al.*, 2019). proPEP1 is processed by metacaspase 4 (MC4) and released into the apoplastic region upon cellular damage, whereas MC4 undergoes sequestration at the vacuolar membrane if there are no stimuli (Hou *et al.*, 2019).

Serine Rich Endogenous Peptide (SCOOP)

SCOOP family consists of more than 40 genes in the Arabidopsis genome. Arabidopsis SCOOP12 is a 13-aa peptide which is the elicitor-active epitope in the C-terminal region of PROSCOOP12 (Gully *et al.*, 2019). It has been demonstrated that a treatment with a synthetic SCOOP12 peptide induces PTI, which results in enhanced defence responses against a hemi biotrophic pathogen. SCOOP12 perception occurs through MALE DISCOVERER 1-INTERACTING RECEPTOR LIKE KINASE 2 (MIK2), an LRR-RK (Rhodes *et al.*, 2021).

Rapid Alkalinization Factors (RALFs)

RALFs are secreted peptides that induce the rapid alkalinization of the extracellular compartment of plant cells. In Arabidopsis, RALF peptides belong to a family of 30 members (Yamaguchi & Kawasaki., 2021). Recently it has been demonstrated that the apoplastic extensin LEUCINE-RICH REPEAT EXTENSIN 8 protein (LRX8; with LRR domains) interacts with RALF4 peptide forming a

complex that specifically interacts with demethylesterified pectins in a charge-dependent manner through RALF4's polycationic surface (Moussu *et al.* 2023). Notably, RALF4 has a dual structural and signalling role by assembly of extracellular wall polymers in a complex that involves LRX8, FERONIA (FER) and LORELEI (LRE)/LORELEI-LIKE GLYCOSYLPHOSPHATIDYLINOSITOL-ANCHORED PROTEINS (LLGs). This complex regulates cell wall integrity during pollen growth and root growth in Arabidopsis (Moussu *et al.*, 2023; Schoenaers *et al.*, 2024).

1.2.2.2. Carbohydrate-based DAMPs

Plant cell walls are a source of potential carbohydrate-based defence signalling molecules (DAMPs) that can be released upon the breakdown or modification of wall polymers (Bacete *et al.*, 2018).

Oligogalacturonides (OGs)

The best-studied cell wall DAMPs are the oligogalacturonides (OGs), breakdown products of pectin. Pectin is a preferred target of many invading pathogens as it is much more susceptible to enzymatic degradation than cellulose. The strongest defence reactions has been described to be induced by OGs with a chain length of 10–15 galacturonic acid residues derived from demethylesterified pectin (Benedetti *et al.*, 2015). In addition, oligogalacturonide trimers and tetramers can also promote defence responses (Benedetti *et al.*, 2015; Ferrari *et al.*, 2013). Both kinds of OGs are also suspected to play a role in development, for example, by antagonizing auxin and inhibiting photomorphogenesis (Sinclair *et al.*, 2017). The production of the defence-active OGs requires the activity of pectin methylesterase (PME) to remove methyl groups, which renders the demethylesterified HG susceptible to the hydrolytic activity of polygalacturonases (Wolf, 2022). The activity of PMEs on pectins, which are upregulated upon mechanical damage, plant-herbivores interaction, or fungal infection, leads to the release of methanol, that activates some early defence responses including cytoplasmatic calcium ($_{cyt}Ca^{2+}$) influxes, Mitogen-Activated Protein Kinases (MAPKs) phosphorylation, ethylene (ET) production, and the expression of immune-related genes, and enhance resistance against pathogens or herbivorous insects (Dixit *et al.*, 2013;

Hann *et al.*, 2014; Körner *et al.*, 2009; Lionetti *et al.*, 2017; Tran *et al.*, 2018; von Dahl & Baldwin 2007).

OGs originated from the HG component of the cell wall pectins are the proposed ligands for WALL-ASSOCIATED RECEPTOR KINASES (WAKs) (Liu, Yu, *et al.*, 2023). OGs perception by WAKs has been implicated directly in immunity and might function during symbiotic interactions as well (Rui & Dinneny, 2020; Su, 2023). Shorter fragments of HG and OGs have been described to be perceived by WAKs, but not monomeric galacturonic acid or other types of pectin (Kohorn *et al.*, 2009). However, a recent quintuple mutant in Arabidopsis *WALL-ASSOCIATED KINASES* encoding genes questioned the role of WAKs as true OGs receptors (Herold *et al.*, 2024).

Cello-oligosaccharides

Cellulose, a linear polymer of ß-1,4-glucosyl residues, is present in all plant's extracellular matrixes or walls, and is the most abundant biomolecule on earth (Burton & Fincher, 2009; Kloareg *et al.*, 2021; Morgan *et al.*, 2013). Breakdown products of cellulose, cello-oligomers, trigger immune signals followed by upregulation of defence-related genes and callose deposition. Among cello-oligomers, CEL3 is the strongest inducer of cytoplasmatic calcium influx and seems to be the one able to trigger ROS production (Tanaka & Heil, 2021). Cellulose-derived oligosaccharides, e.g. β-1,4-D-(Glc)2 to β-1,4-D-(Glc)6 (cellobiose to cellohexaose or CEL2–CEL6), trigger PTI responses in Arabidopsis, rice and other plant species (Klarzynski *et al.*, 2000; Locci *et al.*, 2019; Rebaque *et al.*, 2021; Souza *et al.*, 2017; Yang *et al.*, 2021).

Mixed-Linked Glucans (MLGs)

Although MLGs have been previously described as MAMPs, they are widely distributed as matrix polysaccharides in the cell walls of plants from the *Poaceae* family but have also been reported in *Equisetum* spp. and other vascular plants (Fry *et al.*, 2008; Sørensen *et al.*, 2008). MLG-derived oligosaccharides, e.g. MLG43 (β-1,4-D-$(Glc)_2$- β-1,3-D-Glc), MLG443 (β-1,4-D-$(Glc)_3$- β-1,3-D-Glc) and MLG34 (β-1,3-D-Glc-β-1,4-D-Glc_2), are perceived with different degrees of specificity by the immune system of several plant species, e.g. Arabidopsis, *Capsicum annuum* (pepper), *Hordeum vulgare* (barley), *Oryza sativa* (rice), and *Solanum*

lycopersicum (tomato), with MLG43-mediated PTI responses being the best characterized (Barghahn *et al.*, 2021; Rebaque *et al.*, 2021; Yang *et al.*, 2021). MLG- and CEL-derived oligosaccharides can be released from plant cell walls by the activity of microbial endoglucanases, such as cellulases, secreted during plant colonization (Gámez- Arjona *et al.*, 2022; Yang *et al.*, 2021).

Xyloglucans (XylGs)

Xyloglucan oligosaccharides perceived as DAMPs are derived from the major components of hemicellulose of cell walls of dicotyledonous plants. Previous studies indicated that xyloglucans may play a role in the regulation of plant growth and development in different plant species (Fry *et al.*, 1993; Vargas-Rechia *et al.*, 1998). Moreover, it was shown that xyloglucans can increase plant resistance to abiotic stress, in particular cold or water stress, when used at low concentrations (Salvador & Lasserre, 2010). Some specific oligosaccharides derived from xyloglucans were found to trigger a broad range of defence responses in grapevine and Arabidopsis inducing MAPKs activation and defence genes Phytoalexin Deficient 3 (*PAD3*) and Pathogenesis Related 1 (*PR1*) expression in Arabidopsis (Claverie *et al.*, 2018).

Xylans and Arabinoxylans (AXs)

Xylans are main hemicelluloses of SCWs, with the common feature of a backbone of ß-1,4-linked xylose residues whose presence is essential for plant development (Brown *et al.*, 2007; Wu *et al.*, 2009). Recently xylose-derived glycans as xylobiose (XYL2; Dewang *et al.*, 2023) and xylotetraose (XYL4; Fernández-Calvo *et al.*, 2024) have been described as activators of PTI responses as $_{cyt}Ca^{2+}$ burst and MAPKs phosphorylation. Xylans usually contain many arabinose residues attached to the backbone forming the arabinoxylans (AXs). AXs can be perceived as molecular patterns by plants. Several active oligosaccharides structures from AXs have being described as the most active ones in Arabidopsis (Mélida *et al.*, 2020). In particular, XA_3XX (3^3-α-L-arabinofuranosyl-xylotetraose) triggers $_{cyt}Ca^{2+}$ influxes, ROS production, MAPKs phosphorylation, and a global gene reprogramming in Arabidopsis at micromolar concentrations (Mélida *et al.*, 2020). XA_3XX perception mechanism differs from that of chitin and ß-1,3-glucans, but the PRRs and molecular components implicated in their perception are still unknown (Cao *et al.*, 2014; Liu *et al.*, 2012; Mélida *et al.*, 2018).

1.2.3. Importance of glycans perception and PTI activation regulation

During plant-microbe interaction coevolution, pathogens have acquired a wide range of mechanisms to breach plant cell walls, that include an arsenal of Carbohydrate-Active enzymes (CAZymes), that specifically hydrolyze (CWDEs) or modify different cell wall components to break down wall structural barriers. The activity of these enzymes on plant cell wall polysaccharides leads to the release of active glycans triggering PTI (DAMPs), further confirming plant cell walls as vast sources of carbohydrate-based DAMPs that have not been characterized in detail (Mélida *et al.*, 2020; Pring *et al.*, 2023; Rebaque *et al.*, 2021).

In recent years, numerous studies have allowed to uncover novel plant cell wall bioactive fragments (DAMPs, see Table 1.1). These DAMPs comprise, ß-1,4-D-glucosyl cellulose-derived products or cellodextrins (DP of 3-5, CEL3-CEL5) (Aziz *et al.*, 2007; Johnson *et al.*, 2018; Locci *et al.*, 2019; Souza *et al.*, 2017), OGs (Ferrari *et al.*, 2007), ß-1,4-linked hemicellulose-derived DAMPs (ß-1,4-D-glucan backbone with xylosyl, galactosyl, and fucosyl-type branching, mainly of DP 7) (Claverie *et al.*, 2018), mannans (composed of ß-1,4-D-manose and of DP 2-6) (Zang *et al.*, 2019), arabinoxylans derived oligosaccharides (like the pentasaccharide 3^3-α-L-arabinofuranosylxylotetraose or XA_3XX) (Mélida *et al.*, 2020), and xylan based oligosaccharides (ß-1,4-D-xylose oligomer of DP 2-6), which are released by the action of endoglucanases and xyloglucanases (Dewangan *et al.*, 2023; Pring *et al.*, 2023) (Table 1.1).

Interestingly, some carbohydrate-based molecular patterns can be classified as DAMPs and MAMPs since are released from plant walls and microbial out layers. For example, non-branched 1,3-ß-D-Glc oligosaccharides (DP 6-12), like laminarinhexaose (LAM6; 1,3-ß-D-(Glc)6), that can be released during callose synthesis or pathogen degradation of callose, and unbranched Mixed-Linked ß-1,3/1,4-Glucans (MLGs, like ß-1,4-D-$(Glc)_2$-ß-1,3-D-Glc or MLG43), which are present in some groups of plants (e.g. grasses or *Equisetum* sp.), but also in oomycetes and microbial cell walls (Barghahn *et al.*, 2021; Chowdhury *et al.*, 2014; Mélida *et al.*, 2018; Rebaque *et al.*, 2021) (Table 1.1). These DAMPs, generated through the action of inherent plant CWDEs, accumulate in the extracellular matrix where they are perceived alongside MAMPs by plant receptors activating PTI (Bacete *et al.*, 2018; Bender & Zipfel, 2023).

Table 1.1: Glycan structures that induce PTI responses in plants.

Glycan	Representative oligosaccharide(s) DAMP/MAMP	Source	PRR[a] (co-PRR)[b]	PTI in plants	Reference
Cellulose	CEL2-CEL9: ß-1,4-D-$(Glc)_{2-9}$	Plants Oomycetes	nd	Arabidopsis, tomato, lettuce	Aziz *et al*., 2007 Souza *et al*., 2017 Johnson *et al*., 2018 Zarattini *et al*., 2021 He *et al*., 2023
Mixed-linked ß-1,3/ 1,4-glucans (MLGs)	MLG43: D-cellobiosyl-(1,3)-ß-D-Glc MLG34/MLG443	Plants (monocots) *Equisetum* sp. Oomycetes	OsLECRK1/OsCERK1 (OsCeBIP)	Rice, barley, tomato, pepper	Rebaque *et al*., 2021 Yang, Liu *et al*., 2021 Barghahn *et al*., 2021 Dai *et al*., 2023
Homogalacturonan (HG)	oligogalacturonides (OGs): α-1,4-D-$(GalA)_{9-15}$ $GalA_3$: α-1,4-D-$(GalA)_3$	Plants	LRX8-RALF4 (FER/LLGs) LRX1-RALF22 (FER/LLGs) (WAK1-WAK5) (RFO1/WAKL10, FER)[c]	Arabidopsis, tomato, grapevine, and several plant species	Benedetti *et al*., 2015 Voxeur *et al*., 2019 Liu, Yu *et al*., 2023 Moussu *et al*., 2023 Huerta *et al*., 2023 Schoenaers *et al*., 2024
Arabinoxylans	XA3XX: 3^3-α-L-arabinofuranosylxylotetraose	Plants	nd	Arabidopsis, tomato, pepper	Mélida *et al*., 2020 Fernández-Calvo *et al*., 2024
Xylans	β-1,4-D-$(Xyl)_{2-5}$	Plants	nd	Arabidopsis, tomato, wheat	Dewangan *et al*., 2023 Pring *et al*., 2023 Fernández-Calvo *et al*., 2024
Mannans	ß-1,4-D-$(Man)_{2-6}$	Plants	nd	Rice, tobacco	Zang *et al*., 2019
Xyloglucans	Heptamaloxyloglucan	Plants	nd	Arabidopsis, grapevine, wheat, soybean	Claverie *et al*., 2018
Linear ß-1,3-D-glucans	LAM6: 1,3- b-D-$(Glc)_6$ LAMINARIN: b-1,3-D-(Glc) > $_{10}$	Plants Fungi Oomycetes	(CERK1, LYK4, LYK5)	Arabidopsis, barley, *Brachypodium distachyon* *Nicotiana benthamiana*[d]	Mélida *et al*., 2018 Wanke *et al*., 2020
Branched ß-1,3-D-glucans	ß-1,3-D-$(Glc)_n$/ß-1,6-D-Glc_n branched (decasaccharide)	Fungi Oomycetes	LjEPR3/LjEPR3a (CERK1)	*Lotus japonica,* Arabidopsis, rice, barley, tobacco	Kelly *et al*., 2023 Wanke *et al*., 2020, 2023
Chitin	CHI6-CHI8: ß-1,4-D-$(GlcNAc)_{6-8}$ COs: chitin-oligosaccharides	Fungi Insectes	LYK5, LYK4 (CERK1) OsCEBIP (OsCERK1) (MtCERK1, MtLYR4) (LjCERK6) (VvLYK5-1, VvLYK1-1)	Grapevine, and several plant species	Cao *et al*., 2014 Liu *et al*., 2012 Liu, Wang *et al*., 2016 Xue *et al*., 2019 Khokhani *et al*., 2021 Roudaire *et al*., 2023
ß-1,6-D-Glucans	ß-1,6-D-$(Glc)_{2-9}$	Fungi Bacteria	(CERK1)	Arabidopsis	Chaube *et al*., 2022

[a]PRR has been identified by direct ECD/PRR-glycan binding assays (e.g., ITC, thermophoresis, crystal structure determined). Os, Mt, Lj, and Vv indicate the names of the plant species. The rest of the PRRs and co-PRRs indicated are from Arabidopsis thaliana.

[b]co-PRR has been identified genetically or not direct binding to DAMP/MAMP has been determined.

[c]Direct binding to DAMP/MAMP has been shown, but proof of the PRR function deserves further characterization.

[d]*Nicotiana benthamiana* only perceives long ß-1,3-D-glucans (LAMINARIN).

Cell walls and extracellular outer layers of microorganisms are also a source of carbohydrate-based ligands perceived as MAMPs (reviewed by Wanke *et al.*, 2021). The best-characterized MAMPs of this group are oligosaccharides (DP 4-8) derived from fungal chitin (Chito-Oligosaccharides (COs), like ß-1,4-D$(GlcNAc)_{6-8}$ or CHI6-CHI8) (Khokhani *et al.*, 2021) (Table 1.1). However, bacterial compounds derived

from lipopolysaccharide- and peptidoglycan, and 1,6-ß-D-glucans have been described to trigger immune responses in different plant species as well (Chaube *et al.*, 2022) (Table 1.1). In addition, 1,3-ß-D-Glc oligosaccharides with 1,6-ß-D-Glc branches have been reported to trigger immunity in different plant species (Wanke *et al.*, 2020; Wanke *et al.*, 2023) (Table 1.1). Notably, some complex exopolysaccharides from endophytic fungi, as well as Lipo-Chito-Oligosaccharides (LCOs) from symbiotic bacteria (Nod factor) and arbuscular mycorrhizal fungi factors (MYC factors), are also perceived by plants. However, these molecules activate symbiotic processes, instead of immune responses, through recognition mechanisms involving RKs with LysM ECDs (Chandrasekar *et al.*, 2022; Kelly *et al.*, 2023; Khokhani *et al.*, 2021).

Despite the relevance of glycan-based perception in the regulation of plant immunity, the mechanisms of recognition of these ligands are not as well characterized as that of peptidic/PRR pairs. Moreover, the turnover/metabolism of cell wall-derived signals during non-pathogenic (e.g. cell expansion) and pathogenic conditions is not well characterised, and these processes are essential for plant fitness and survival (Benedetti *et al.*, 2018).

In this context, some plant enzymes have been described in the modification of DAMPs released during plant-pathogen interaction, participating in the regulation of the eliciting capacity of these compounds and the defence responses activated in the plant (Benedetti *et al.*, 2018; Locci *et al.*, 2019). A family of Flavin Adenine Dinucleotide (FAD)-binding Berberine Bridge Enzyme like (AtBBE-like) has been studied for its role in the homeostasis of some DAMPs perception and PTI activation, as OGs and cellulose-derived oligosaccharides (Benedetti *et al.*, 2018). There have been described four OG-oxidases (OGOXs) and one cellodextrin oxidase (CELLOX) from the AtBBE-like family, which are able to oxidate the anomeric carbon of OGs and CEL3-CEL6, MLGs, respectively (Locci *et al.*, 2019). These oxidations not only regulate PTI activation in plants since they are biologically less active, but also, they are less accessible to fungal lytic enzymes, limiting pathogens proliferation (Locci *et al.*, 2019).

The structural mechanisms underlying glycans recognition by plant PRRs remain limited, being just a few PRRs characterized, despite the number of oligosaccharides DAMPs and MAMPs have been increasing in the last years.

1.3.Plant Pattern Recognition Receptors (PRRs)

Plasma membrane-anchored PRRs are mainly Receptor Kinases (RKs) and Receptor-Like Proteins (RPs) (Bender & Zipfel, 2023). These receptors have extracellular ectodomains (ECDs) attached to plasma membrane by a transmembrane (TM) domain. There are also Receptor-Proteins harboring ECDs that lack TM and can be either attached to the plasma membrane by a glycosylphosphatidyl-inositol (GPI)-anchor proteins (RPg) or be extracellular proteins (RPe) (Bellande *et al.*, 2017; Del Hierro *et al.*, 2021) (Figure 1.2a). The number of RK/RP/RPg/e proteins in plant genomes is larger than PRR-counterparts in animal genomes, supporting the relevance of these receptors in plant development and adaptation to environmental challenges (Bacete *et al.*, 2018; Zipfel, 2014).

Plant RK/RPs (PRRs) involved in PTI activation bind MAMPs/DAMPs through their ECDs. RKs, but not RPs, possess a cytoplasmic Kinase Domain (KD) that upon phosphorylation activates downstream signalling pathways (Bacete *et al.*, 2018; Del Hierro *et al.*, 2021) (Figure 1.2a). Often, a PRR co-receptor might be required to activate phosphorylation cascades (Bender & Zipfel, 2023).

On the other hand, RPs lack the KD and need to interact with a RK co-receptor for activation of downstream signalling. RK/RPs are classified into different groups based on their ECD features that are structurally diverse (Figure 1.2b). These receptor proteins (RKs and RPs) comprise more than 600 members in Arabidopsis, and in general represent 2-3% of genes of plants genomes (Del Hierro *et al.*, 2021).

RKs are the most numerous receptors and can be subdivided into nearly 60 subfamilies that are already present in liverworts and mosses, suggesting that during land plant evolution RK diversity was acquired early (Bowman *et al.*, 2017; Dievart *et al.*, 2020; Lehti-Shiu *et al.*, 2009). Indeed, this hypothesis is in line with the relatively few domain-gain events detected for RKs through evolution (Lehti-Shiu *et al.*, 2009; Man *et al.*, 2020).

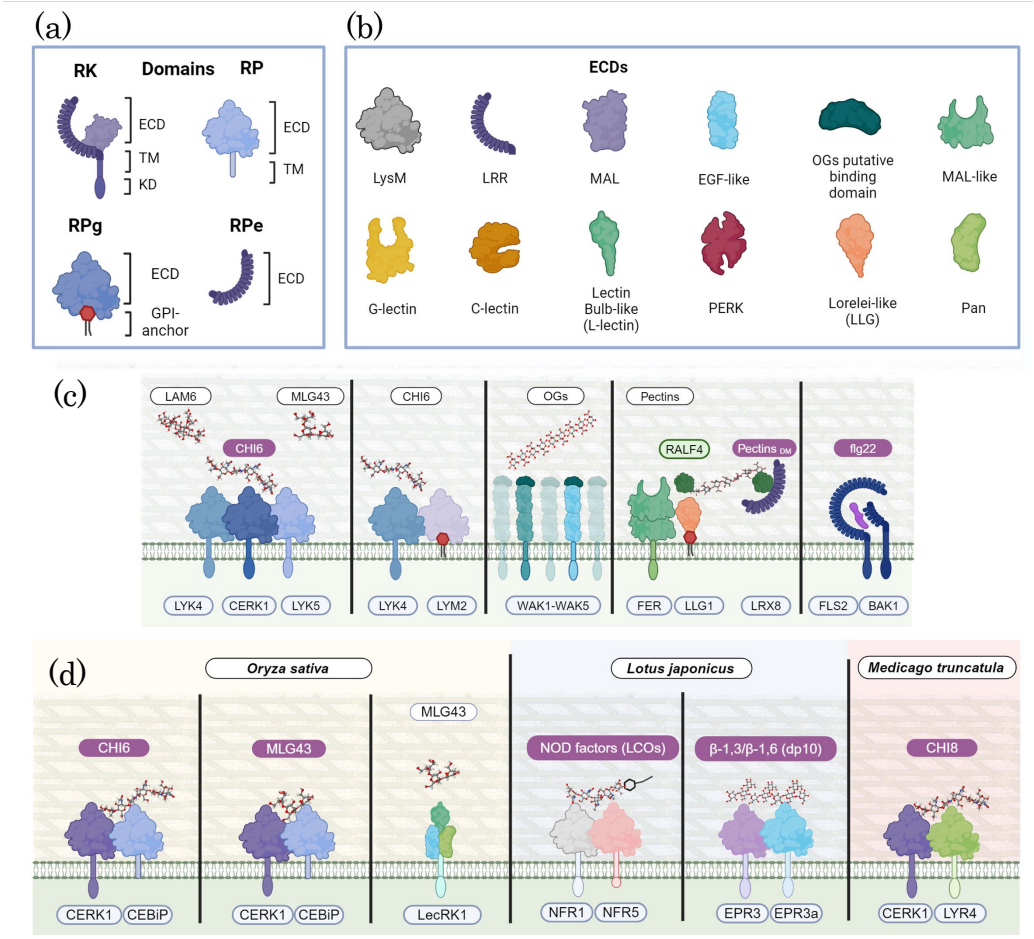

Figure 1.2: Types of plant receptor structures and examples of plant receptors involved in the perception of different glycans structures in plant immunity or symbiosis. The different structures of plant receptors (RK/RP/RPe/g) and the domains in their ECDs are represented in (a) and (b) respectively. (c) shows receptors (PRRs) and co-receptors (co-PRRs) from *Arabidopsis thaliana* and (d) from other plant species described to be required for different glycan perception. Glycan names indicated in purple correspond to DAMPs/MAMPs that have been demonstrated to be bound by the indicated PRRs, protein receptors (e.g., LRX8), or RALF peptides, either by in vitro binding experiments or by structural characterization, and are shown in close interaction with the corresponding receptor. The co-PRRs involved in glycan perception are also depicted. Glycans highlighted in white have been shown to require these PRR-co-PRRs complexes to trigger immune/symbiotic responses, but direct binding by PRR has not been demonstrated. FLS2-BAK1-flg22 recognition complex is included for comparison. Overlapping of RK domains indicates that PRR-coPRR interaction has been demonstrated. MtLYK3 and MtNFP from *M. truncatula* are the corresponding pair/orthologs of LjNFR1 and LjNFR5 from *L. japonicus* shown in (d). The structures of glycans represented have been obtained from different sources.

Plant RKs/RP/RPg/e are classified into different types based on their ECDs predicted structures, being the most abundant receptors those with Leucine-Rich Repeats (LRR) domains in their ECDs (Figure 1.2b). Other types of described structural domains in receptors ECDs are: Lysin Motif (LysM, generally containing 3 LysM domains), lectin domains (with either G, L and C type), Malectin (MAL), LRR-MAL, MAL-like domains (MLD; present in *Catharanthus roseus* RECEPTOR-LIKE KINASES 1-LIKE (CrRLK1L)), Proline-rich Extensin-like domain (in PERKs and extracellular proteins like extensins), Epidermal Growth Factor-like domain (in WALL-ASSOCIATED KINASES (WAK) and WAK-like receptors) (Figure 1.2b), and not well characterised domains present in CRinkly-Like (CR4L), pathogenic-related Thaumatin-like (ThaumatinL/PR5), and Cysteine-Rich Receptor Kinases (CRK/DUF26; (Del Hierro *et al.*, 2021; Zeiner *et al.*, 2023).

1.3.1. Leucine-Rich Repeats (LRR) receptors

LRRs are the largest family among the known PRRs and play central roles in sensing signals to regulate plant development, respond to the environment and defend against pathogens (Afzal *et al.*, 2008; Tang *et al.*, 2010). LRR-PRRs are classified into 15 to 20 classes depending on the phylogeny of their kinase domains (Chen, 2021). Their ECDs share a plant consensus sequence of leucine-rich repeats following the sequence patterns "LxxLxLxxNxL" (s/t) GxLPxxLxxLxx ("L" refers to a hydrophobic amino acid, "N" refers to an asparagine, threonine, serine or cysteine, and "x" refers to variable residue) (Matsushima *et al.*, 2007). N-glycosylations appear to be highly present in LRR-PRRs and would putatively help them to fold and function correctly (Hong *et al.*, 2012; Sun *et al.*, 2012).

FLS2 and EFR are the best characterized LRR-PRRs, receptors of flg22 and elf18, respectively (Gómez- Gómez & Boller, 2000; Zipfel *et al.*, 2006) (Figure 1.2c). These and other LRR-PRRs have the LRR-PRR BAK1 as a co-receptor mediating developmental and/or immune responses (Chinchilla *et al.*, 2007; Sun, Li *et al.*, 2013). Additional LRR receptors examples are PEPRs that recognize PEPs in a manner very similar to that of FLS2 with flg22, and RECEPTOR-LIKE KINASES 7 (RLK7) that recognizes MAMP-Induced Secreted Peptides or PIPs (Hou *et al.*, 2014; Yamaguchi *et al.*, 2006). Another subgroup of LRR-PRRs recently characterized is the LRXs (Figure 1.2c), that in addition to LRR domains harbours an extensin domain similar to that present in cell wall-associated extensin

proteins. LRX has been proposed to modulate plant cell wall immunity and to bind RALF peptides (Figure 1.2c) (Moussu *et al.*, 2020, 2023).

1.3.2. Lysin Motif (LysM) receptors

LysM domain containing RKs (LYKs) have ECDs with two or three LysM domains composed by 45 amino acids (Buist *et al.*, 2008). Arabidopsis LysM-PRRs subclass has 10 members, 5 of them are RKs (AtCERK1/LYK1, AtLYK2, AtLYK3, AtLYK4 and AtLYK5), 2 RPs (AT5G62150 and AT4G25433) and 3 putative RPg/e (AtLYM1, AtLYM2 and AtLYM3) (Bellande *et al.*, 2017; Faulkner *et al.*, 2013). In the Arabidopsis plasma membrane, AtLYK5 perceives chitin oligomers (DP 6-8, CHI6-CHI8) and then AtCERK1 associates with it to activate immune signalling (Figure 1.2c) (Cao *et al.*, 2014; Liu *et al.*, 2012; Petutschnig *et al.*, 2010; Wan *et al.*, 2012). AtLYK4 can additionally associate with AtCERK1 in a chitin-dependent manner, but this association requires AtLYK5 (Xue *et al.*, 2019). Since the kinase domains of AtLYK4 and AtLYK5 have negligible activity *in vitro* (Cao *et al.*, 2014; Wan *et al.*, 2012), it has been suggested that the active kinase AtCERK1 initiates signalling upon the recruitment of AtLYK4/AtLYK5 (Figure 1.2c). In the plasmodesmata, AtLYM2 forms a complex with AtLYK4 once chitin is perceived in a AtCERK1-independent manner (Figure 1.2c) (Cheval *et al.*, 2020; Faulkner *et al.*, 2013). In addition, the perception of bacterial peptidoglycans requires AtCERK1 and the contribution of AtLYM1 and AtLYM3, but the exact structure from peptidoglycan recognised by these receptors is unknown (Gust *et al.*, 2017; Willmann *et al.*, 2011).

In rice (*Oryza sativa*) chitin is perceived by the LysM-RP CHITIN ELICITOR BINDING PROTEIN (OsCEBiP), but immune signalling is activated by recruitment of OsCERK1 (Figure 1.2d) (Kouzai *et al.*, 2014; Shimizu *et al.*, 2010; Takagi *et al.*, 2022). Notably, OsCERK1, but not OsCEBiP, seems to bind MLGs (MLG43 and MLG443) based on Microscale Thermophoresis (MST) assays, but crystal structures of this complex have not been obtained (Figure 1.2d) (Yang *et al.*, 2021).

Another member of the LysM-RK family in *Lotus japonica* is EXOPOLYSACCHARIDE RECEPTOR 3 (EPR3) involved in the perception of bacterial carbohydrate-based exopolysaccharides (EPS) (Figure 1.2d) (Kelly *et al.*, 2013). Recently, the *Lotus japonicus* glycan RK EPR3a, which is closely related to the EPS receptor EPR3, has been also characterized. Notably, both EPR3a and

EPR3 bind a well-defined ß-1,3/ß-1,6-decasaccharide derived from exopolysaccharides of endophytic and pathogenic fungi (Figure 1.2d) (Kelly *et al.*, 2023).

Intriguingly, LysM receptors participate in both symbiotic and immune signalling in some plant species (e.g. legumes and rice) through distinct LysM receptor complexes as NOD FACTOR RECEPTOR 1 and 5 (NFR1 and NFR5), that recognize chitin from fungal cell walls or LCOs produced by mycorrhiza fungi (MYC-factors) and bacteria (Nod factor; (Khokhani *et al.*, 2021; Madsen *et al.*, 2003; Radutoiu *et al.*, 2003; Zhang *et al.*, 2015) (Figure 1.2d). In *Medicago truncatula*, MtCERK1 (also known as MtLYK9) and LysM RECEPTOR 4 (MtLYR4) form a receptor complex to directly bind CHI8 (Figure 1.2d), triggering immune responses, but they seem to be also needed to initiate symbiotic responses (Bozsoki *et al.*, 2017; Feng *et al.*, 2019).

1.3.3. G, L and C lectin receptors

C-lectins are a family of calcium-dependent proteins highly represented in mammals where they are involved in innate immunity (Brown, 2006). However, despite the high number of PRRs in plants, C-lectins are under-represented, in comparison to animals, in all plant species (Vaid *et al.*, 2013). Arabidopsis, rice (*Oryza sativa*) and tomato (*Solanum lycopersicum*) have one member each, and wheat has only two members.

G-lectins were thought to have specificity towards mannose, but later it was discovered that they have affinity towards oligomannosides and high-mannose N-glycans (Bellande *et al.*, 2017; Loris, 2002; Shiu & Bleecker, 2001; Van Damme *et al.*, 2008).

L-lectins, receive this name because their ECDs are similar to LEGUME-LECTIN PROTEIN-LIKE ISOLECTIN LoLI of *Lathyrus ochrus* (Bourne *et al.*, 1990). This protein family is clearly expanded in the plant kingdom. L-lectins have putative glucose and mannose affinity and their ECDs revealed in some analyses to have post-translational modifications like glycosylation (Hervé *et al.*, 1999; Navarro-Gochicoa *et al.*, 2003). The rice LECTIN RECEPTOR KINASE1 (OsLecRK1), but not the OsLecRK2, have been shown to bind different MLGs but not CEL4 in Microscale Thermophoresis (MST) assays (Figure 1.2d) (Dai *et al.* 2023).

1.3.4. Malectin/Malectin-like receptors

The first protein with a maltose-binding domain (called malectin) was initially found in the Endoplasmic Reticulum (ER) of the african frog *Xenopus laevis*. This protein is a type-I membrane-anchored ER protein with high similarity to glycosyl-hydrolases (Bellande *et al.*, 2017). In plants, proteins with malectin domains (MAL) or malectin-like domains (MLD) are typically linked to a kinase domain and/or to an LRR domain, grouped in the following subgroups of proteins: MLD PRR (*Catharanthus roseus* RECEPTOR-LIKE KINASE 1-LIKE or CrRLK1L), MLD-LRR PRR and LRR-MAL PRR.

CrRLK1L is an RK subfamily able to recognize small molecules with their ECDs consisting of one or two MLD domains (Boisson-Dernier *et al.*, 2011; Franck *et al.*, 2018; Zhang *et al.*, 2020). This subfamily has been involved in the regulation of multiple immune responses and development processes, like pollen tube germination, that is associated to cell wall remodeling (Goring, 2023; Lee & Goring, 2021). Several ECDs of CrRLK1 have been crystalized such as ANXUR1 and 2 (ANX1, ANX2) and FER; whose Protein Data Bank (PDB) accession codes are 6FIG, 6A5C and 6A5E, respectively (Moussu *et al.*, 2018; Xiao *et al.*, 2019). Some of these CrRLK1-ECD structures have been shown to bind RALF phytocytokine peptides (Moussu *et al.*, 2020; Xiao *et al.*, 2019) by the apoplastic extensin LRX8 protein (with LRR domains) (Moussu *et al.*, 2023). Notably, RALF4 has a dual structural and signalling role by assembly extracellular wall polymers in a complex that involves LRX8, FER and LLG (Figure 1.2c) (Moussu *et al.*, 2023).

MLD domains may also be followed by an LRR in the ECD of some PRRs, which are grouped into LRR-RK sub-family (Bellande *et al.*, 2017). LIGHT-REPRESSIBLE RECEPTOR PROTEIN KINASE (LRRPK) was the first member described of this subfamily (Decken & Kaldenhoff, 1997). IMPAIRED OOMYCETE SUSCEPTIBILITY1 (IOS1), another member of this subfamily, has roles modulating plant response to the infection by filamentous hemi/biotrophs and attenuating Abscisic Acid (ABA) responses in Arabidopsis (Hok *et al.*, 2011). Indeed, IOS1 is a global modulator of PTI responses and disease resistance to several pathogens by its association with different LRRs: FLS2, EFR, BAK1, FER and CERK1 (Stegmann *et al.*, 2017; Yeh *et al.*, 2016).

The LRR–MAL RKs have a LRR domain followed by a single malectin domain. Several LRR–MD RK genes, are named BRASSINOSTEROID (BR)-SIGNALING KINASE (BSK) 3-INTERACTING encoding RKs (BSRs), since they are

transcriptionally responsive to brassinosteroids (BRs) (Xu *et al.*, 2013) and could be involved in the signalling pathways regulated by this hormone. There are considerable cross-talks between BRs and immunity signalling (Lozano-Durán & Zipfel, 2015). The expression of several BSRs, including RECEPTOR-LIKE KINASE IN FLOWERS 1 (RKF1), BSR430, BSR840 and At1G56120, was triggered during immunity response (Hok *et al.*, 2011; Qutob *et al.*, 2006; Yang, Wang *et al.*, 2021). Since cross-talks between BRs and immunity signalling is feasible (Lozano-Durán and Zipfel, 2015), the involvement of LRR-MD RKs in the regulation of PTI should not be excluded.

1.3.5. Proline Extensin-like Receptor Kinase (PERK)/Extensins

The first member of this group, PERK1, was discovered in 2002 in *Brassica napus* (Silva & Goring, 2002) and its ECD is composed by a proline- rich sequence like those of the extension family. In Arabidopsis several PERKs can be found: i) PERK1 involved in viral infections (Nakhamchik *et al.*, 2004); ii) PERK4 participates in root growth control related with ABA (Bai *et al.*, 2009); iii) PERK8, 9 and 10 collaborate in primary root growth control (Humphrey *et al.*, 2015); iv) PERK12 is involved in apical dominance regulation (Hwang *et al.*, 2010); and v) PERK13 has an implication in radical root hair elongation (Humphrey *et al.*, 2015).

1.3.6. Wall-Associated Receptor Kinases (WAKs)

WAKs have Epidermal Growth Factor (EGF)-like domains in their ECDs (Figure 1.2c) (Liu, Yu, *et al.*, 2023). The EGF-like domain, which is also present in mammal receptors, is found exclusively in extracellular proteins or regions of transmembrane proteins and functions primarily in mediating protein-protein interactions (Haltom & Jafar-Nejad, 2015). OGs perception by WAKs has been implicated directly in immunity and is also speculated to function during symbiotic interactions (Figure 1.2c) (Rui & Dinneny, 2020; Su, 2023). WAK1 N-terminal part of its ECD has been proposed to associate with demethylesterified pectin or polygalacturonic acid (with a clear preference for pectate in the Ca^{2+}-cross-linked configuration) whereas EGF-like repeats are not involved in the binding with cell wall components (Brutus *et al.*, 2010; Decreux *et al.*, 2006; Decreux & Messiaen, 2005; Kohorn *et al.*, 2009). Shorter fragments of HG and OGs are also bound by WAK-ECDs, but not monomeric galacturonic acid or other types of pectin (Kohorn *et al.*, 2009). However, the crystal structure of WAK or WAK-Like ECD is missing and the potential ECD pocket(s) of WAK/WAKL involved in the binding of pectins

and OGs (e.g. GalA3) are unknown. Moreover, *wak1/wak5* quintuple mutant has been shown to be impaired not only in PTI triggered by pectin-derivatives but also by CHI6 and flg22, suggesting a role for these WAKs beyond OGs perception (Kohorn *et al.*, 2021).

1.4.Downstream events upon activation of plant immunity

Plants have different strategies to prevent pathogens infections in the early stages. These defence mechanisms are the innate basal first-line immune defence gadgets indigenously constitutive in the plant even before colonization by the pathogen as wax layers, cuticular lipids or the cell wall (Doughari, 2015). Other mechanisms can be changes in features that are normally in the plant, such as stomatal closure to limit the entry of bacteria, restriction of nutrient transfer from the cytosol to the apoplast and secretion of antimicrobial compounds (Bigeard *et al.*, 2015).

Although plants have all these arsenals of defence barriers, sometimes they are not enough to avoid pathogens attacks. For this reason, plants can also perceive pathogens in other ways as recognition of pathogen effectors, which are molecules synthesized by the pathogens and delivered in the extracellular matrix or into the plant cell to enhance pathogen fitness by, for example, counteracting the induction of Pattern Triggered Immunity (PTI) (Bigeard *et al.*, 2015). The plant immune system also recognizes microbial effectors (avirulence proteins, Avr), not conserved between microbial strains) through intracellular receptors called Resistance proteins (R proteins) that might be encoded by resistance genes, activating Effector Triggered Immunity (ETI: (Boutrot & Zipfel, 2017; DeFalco & Zipfel, 2021; Li, Yu *et al.*, 2016). The coevolution of pathogens and plants can have determined the repertoire of effectors of pathogens and R proteins from plants led to propose the so-called zigzag model to explain plant disease resistance (Jones & Dangl, 2006).

PTI and ETI have recently been shown to function cooperatively in the control of pathogen infection and disease resistance outcomes leading to mutual potentiation and interdependency, which is essential for a full immune response (Wang & Luan, 2024; Yuan *et al.*, 2021). In general, PTI contributes to plant basal resistance to diverse adapted and non-adapted microbes, whereas ETI plays a central role in defending against race-specific host-adapted pathogens. In addition, localized primary infection can signal the development of systemic acquired resistance, which manifests as enhanced resistance in distal tissues (Li, Yu *et al.*, 2016).

The initial perception of pathogens activates early PTI responses initiating largely overlapping signalling events, including cytoplasmatic calcium ($_{cyt}Ca^{2+}$) fluxes, Reactive Oxygen Species (ROS) burst, Mitogen-Activated Protein Kinases (MAPKs) phosphorylation and transcriptional reprograming (Wang & Luan, 2024) (Figure 1.3).

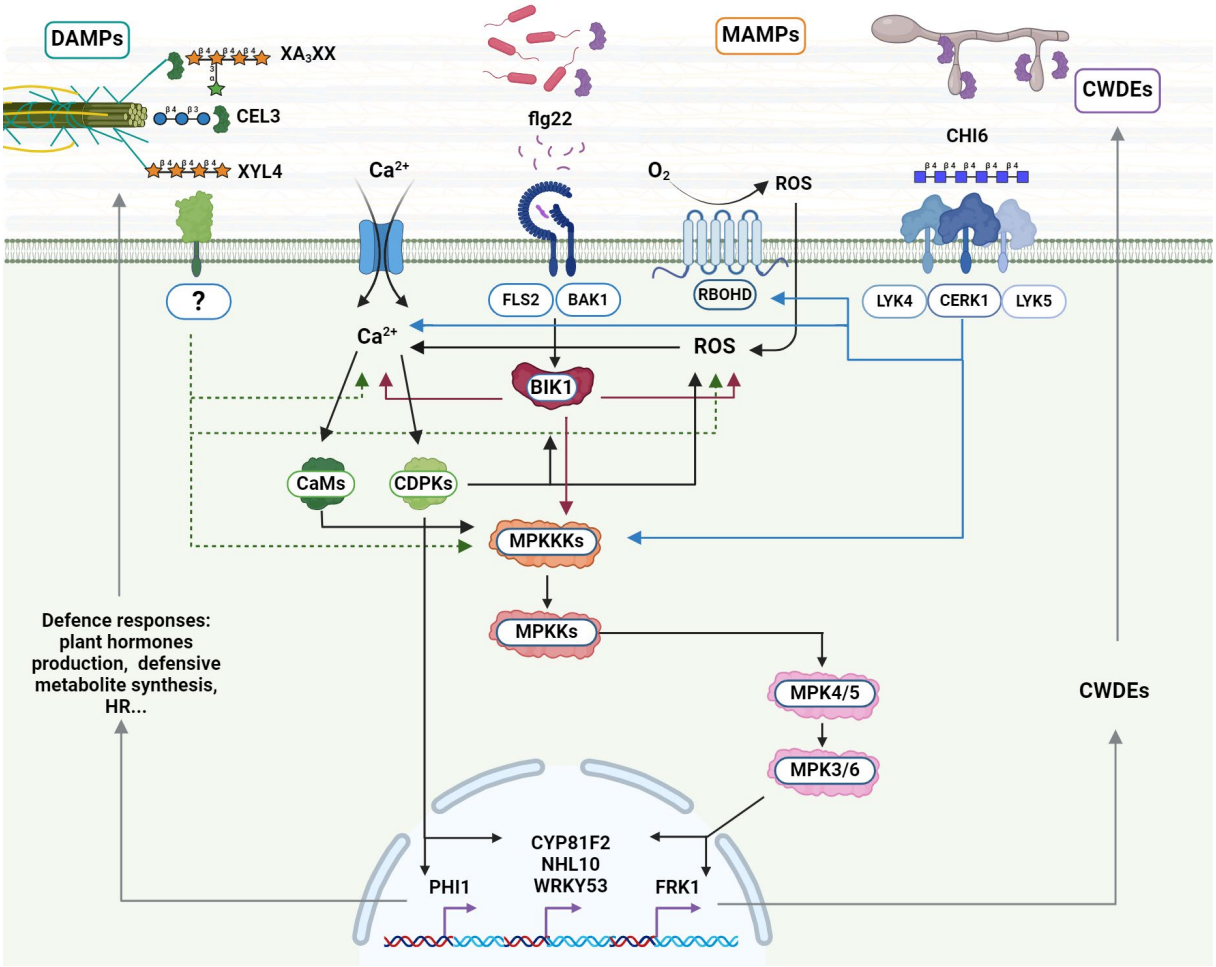

Figure 1.3: Simplify representation of Pattern Triggered Immunity (PTI) signalling and downstream events. PTI events triggered by ligand-PRR binding. After ligand perception, Ca^{2+} channels open leading $_{cyt}Ca^{2+}$ influxes in the cell, activating Ca^{2+} sensors as calmodulins (CaMs) and Ca^{2+}-Dependent Protein Kinases (CDPKs), which in turn activate Reactive Oxygen Species (ROS) production, MAPKs phosphorylation, and in last instance, transcriptional changes in defence genes. On the other hand, ligands perception can also activate RBOHD generating ROS production which, at the same time, stimulates more calcium influxes in surrounding cells promoting cell-to-cell communication. Transcriptional changes of defence genes end in different defence responses such as Cell Wall Degrading Enzymes (CWDEs) generation, defensive metabolite secretion as phytoalexins and hypersensitive response (HR) among others. These transcriptional changes also allow the cell to regulate PTI avoiding an over-activation of the immunity along time. In the figure, CWDEs produced by the plants appear in purple and those produced by the pathogens appear in green.

1.4.1. Cytoplasmatic calcium influxes

One of the earliest known physiological responses to MAMPs/ DAMPs perception is an influx of extracellular Ca^{2+} in the cytosol. $_{cyt}Ca^{2+}$ influx upon pathogen infection has long been acknowledged as a crucial step in the initiation of plant immune responses (Wang & Luan 2024). This $_{cyt}Ca^{2+}$ influx induces the opening of other membrane transporters (influx of H^+, efflux of K^+, Cl^-, and NO_3^-), which lead to an extracellular alkalinization and a depolarization of the plasma membrane (Bigeard *et al.*, 2015; Ranf *et al.*, 2011).

Cytoplasmatic Ca^{2+} is a central second messenger following the activation of receptors in immunity (Wang & Luan, 2024). To turn immune receptor-induced $_{cyt}Ca^{2+}$ elevations into immunity signalling, Ca^{2+}-binding proteins are first in charge of translating the Ca^{2+} signals. These proteins have different affinity to Ca^{2+}, allowing them to turn on and off in response to calcium concentration changes which initiate functional interactions with downstream effectors (Boudsocq *et al*, 2012; Gifford *et al.*, 2007; Wang & Luan, 2024).

Mainly, there are two types of Ca^{2+} sensors: calmodulin (CaM) and Ca^{2+}-Dependent Protein Kinases (CDPKs), which are linkers of $_{cyt}Ca^{2+}$ elevations to immune responses (Figure 1.3). In response to pathogens, MAMP-induced $_{cyt}Ca^{2+}$ elevation is believed to be perceived by CPK5 and other related CDPKs associated with the plasma membrane (Wang & Luan 2024). CPK5 exhibits a high Ca^{2+} binding affinity leading to autoimmunity (Guerra *et al.*, 2020). One of the target enzymes, is the Respiratory Burst Oxidase Homolog D (RBOHD), phosphorylated and activated by CPK5 and other kinases, driving to ROS production that further amplifies $_{cyt}Ca^{2+}$ influx (Figure 1.3). The $_{cyt}Ca^{2+}$/ROS activation and propagation might serve as a communication mechanism to propagate the defence responses to other parts of the plant or other tissues (Dubiella *et al.*, 2013; Wang & Luan, 2024). CPK5 can enhance immunity phosphorylating E3 ubiquitin ligase, that degrades CPK28, which is an immunity negative regulator, and stabilizes BIK1 (Figure 1.3) (Liu, Zhou *et al.*, 2023; Delormel, 2022). Moreover, CDPKs act downstream, carrying out changes in transcriptional levels of defence genes such as PHI1. This immunity regulation of the cytoplasmatic calcium response allows plants to precisely control their defence responses (Boudsocq *et al.*, 2010)

Ca^{2+} channels involved in PTI contain multiple transmembrane domains, and include Cyclic Nucleotide Gated Channels (CNGCs), calcium permeable stress/hyperosmolality-induced channels (CSCs/OSCAs), and Glutamate Receptor-

Like (GLRs) (Bjornson *et al.*, 2021; Thor *et al.,* 2020; Tian *et al.*, 2019; Wang & Luan, 2024).

In the resting state before plant-pathogen interaction takes place, these Ca^{2+} channels are involved in Ca^{2+} homeostasis or used in other signalling processes. Upon MAMP/DAMP-perception and the activation of the receptors involved in their perception at the cell surface, BIK1 (previously stabilized by CPK5) phosphorylates and, in consequence, activates CNGC2-CNGC4 channel which has also a role in the activation of immunity by other elicitors, such as the fungal elicitor chitin (Wang & Luan, 2024). This channel also has a basal level of activity important for introducing Ca^{2+} into the cell vacuole avoiding Ca^{2+} overaccumulation in the apoplast, which is a potential risk that can produce growth arrest. This data suggests that CNGC2-CNGC4 is key for initiating the immune response (Wang *et al.*, 2017; Zhao *et al.*, 2021).

1.4.2. Reactive Oxygen Species (ROS) production

In plants ROS have a double function, being very harmful and toxic but at the same time necessary for the regulation of biotic and abiotic stresses. High levels of ROS can lead to detrimental effects by causing lipid peroxidation in cellular membranes, protein denaturation, carbohydrate oxidation, pigment breakdown, and DNA damage (Møller *et al.*, 2007). In contrast, ROS play important roles as signalling molecules in plant development and growth, and in response to various abiotic and biotic stresses (Liu & He, 2016). ROS can be synthetized in chloroplasts, mitochondria, peroxisomes, and the apoplastic space by diverse pathways as the electron transport chain in photosynthesis and respiration, glycolate and xanthine oxidase, excited chlorophyll, fatty acid oxidation, and peroxidases (Bose *et al.*, 2014; Wrzaczek *et al.*, 2013). ROS include singlet oxygen ($^1O_2$), superoxide anion (O^{2-}), hydrogen peroxide (H_2O_2) and hydroxyl radicals ($OH^{\cdot}$) (Liu & He, 2016).

At the apoplast, ROS can be produced by respiratory burst oxidase homologue (RBOH) proteins, also known as plant Nicotinamide Adenine Dinucleotide Phosphate (NADPH) oxidases by donning electrons to the extracellular O_2 to generate superoxide (O_2-) (Sagi & Fluhr, 2006; Torres, 2010; Wrzaczek *et al.*, 2013). This O_2- can be dismutated to H_2O_2 spontaneously or catalytically by Superoxide Dismutase (SOD). H_2O_2 functions locally but can also activate long distance

signalling (Liu & He, 2016) triggering AtRBOHD-dependent ROS production in all adjacent cells producing a ROS wave (Mittler & Blumwald, 2015).

In *Arabidopsis thaliana* ROS production by RBOHD is a ubiquitous mechanism in response to DAMPs/MAMPs, defensive metabolites (as sphingobases) and pathogens attack (Figure 1.3) (Liu & He, 2016).

Cell Wall Damage (CWD)-induced ROS production is also dependent on AtRBOHD and may regulate lignin biosynthesis and callose deposition (Luna *et al.*, 2011; Poovaiah *et al.*, 2014). ROS production also participates in immunity responses co-ordinately with other early responses as calcium burst. In this context, AtRBOHD is a phosphorylation target of AtCPK5 (Figure 1.3) (Dubiella *et al.*, 2013). AtRBOHD is also a phosphorylation substrate of BIK1 in PTI for MAMP-induced ROS production on the plasma membrane (Figure 1.3) (Kadota *et al.*, 2014; Li, Li *et al.*, 2014). In this interaction, AtCPK28 negatively regulates AtRBOHD-dependent ROS production by the phosphorylation of BIK1 facilitating its degradation (Kadota *et al.*, 2014; Torres *et al.,* 2013; Torres & Dangl, 2005). PTI-induced ROS bursts have a positive feedback effect on $_{cyt}Ca^{2+}$ by inducing a second $_{cyt}Ca^{2+}$ elevation or prolonged plateau (Figure 1.3) (Ranf *et al.*, 2011). Furthermore, ROS production can also be regulated by MAPK signalling (Pitzschke & Hirt, 2006). Some MAPKs, as AtMPK6 and AtMPK8, may regulate gene expression of AtRBOHD. AtMPK4 is another MAPK that plays a role negatively regulating AtRBOHD-dependent ROS production (Liu & He, 2016).

In a global context, all immunity hallmarks are connected, AtMPK8 may link Ca^{2+} and AtRBOHD-dependent ROS signalling together in systemic wound response, as AtMPK8 could be activated by direct binding of CaMs in a Ca^{2+}-dependent manner and negatively regulates AtRBOHD-related ROS production (Figure 1.3) (Liu & He, 2016). However, it has been demonstrated that these signals are not linked in some PTI responses as the ROS burst triggered by OGs, cellobiose, or ß-1,3 glucans, triggering $_{cyt}Ca^{2+}$ burst but not strong ROS production (Davidsson *et al.*, 2017; Galletti *et al.*, 2011; Mélida *et al.*, 2018; Savatin *et al.*, 2014; Souza *et al.*, 2017).

1.4.3. Mitogen-Activated Protein Kinase (MAPKs) phosphorylation

MAPKs are conserved enzymes from the serine kinase family, important players in complex signalling networks (Xie *et al.*, 2023). They activate several cellular processes in response to different cellular stimuli as stress responses,

differentiation, apoptosis, metabolism, cell proliferation, gene expression, mitosis, and survival or cell death, by alternately acting kinases (Khan *et al.,* 2024; Shi *et al.*, 2023).

The MAPKs cascade pathway is one specific signal transduction mechanism relevant activating diverse signalling pathways in many plants. Three essential components make up the traditional MAPKs pathway: MAP KINASES (MPKs), MAP KINASE KINASES (MPKKs), and MAP KINASE KINASE KINASES (MPKKKs, MP3Ks) (Figure 1.3) (Khan *et al.,* 2024). To regulate many biological events, MP3Ks phosphorylate two serine and/or threonine residues located within the activation loop of the MPKKs, which subsequently phosphorylate conserved threonine and tyrosine residues in the T-X-Y activation motifs of the MPKs (Xie *et al.*, 2023). MPKs are serine/threonine kinases that subsequently phosphorylate a wide range of substrates, mainly Transcription Factors (TFs), to alter patterns of gene expression or modulate the activity of other proteins (Figure 1.3) (Colcombet & Hirt, 2008, Rasmussen *et al.*, 2012; Zheng *et al.*, 2006).

The MAPKs cascades activate different cell responses, such as gene expression and cell death (through the phosphorylation of certain target proteins, cytoplasmic kinases and transmembrane signalling molecules), plant defence hormones and Reactive Oxygen Species (ROS) production, defence genes up-regulation and hypersensitive response (HR) (Figure 1.3) (Kim & Choi, 2010; Meng & Zhang, 2013).

In *Arabidopsis thaliana*, MPK3, MPK4, and MPK6 are the MAPKs activated upon perception of pathogens. This pathway is triggered by MAMPs/DAMPs recognition, activating MPKK4 and MPKK5 to phosphorylate MPK3 and MPK6 (Figure 1.3). Downstream, WRKY22 and WRKY29 are activated by FRK1, which in turn is activated by MAPKs, to stimulate the plant defence response. Furthermore, MPK3 and MPK6 phosphorylate WRKY33, leading to camalexin biosynthesis (Figure 1.3) (Khan *et al.*, 2024; Mao *et al.*, 2011). MAPKs with CDPKs are also in charge of transcriptional changes of other genes as NHL10, CYP81F2 and WRKY53 (Boudsocq *et al.*, 2010).

Accurate regulation of these MAPK signalling modules allows plants to have appropriate defence responses for stopping pathogen infections, establishing a sophisticated signalling network (Khan *et al.*, 2024).

1.4.4. Transcriptional regulation in PTI defence-related genes

Genes encoding immunity components are often rapidly and transiently upregulated in response to MAMPs/DAMPs perception leading to the amplification of innate immune responses. Perception of different ligands by PRRs triggers profound transcriptional reprogramming of a set of largely overlapping genes with distinct temporal dynamics (Li, Yu *et al.*, 2016). Many genes are commonly upregulated by treatments with MAMPs (e.g. flg22, elf18, bacterial peptidoglycan, fungal chitin) and DAMPs (e.g. OGs, xylans, arabinoxylans) (Denoux *et al.*, 2008; Fernández-Calvo *et al.*, 2024; Gust *et al.*, 2007; Wan *et al.*, 2008; Zipfel *et al.*, 2006). Although both MAMPs and DAMPs activate convergent signalling pathways ending in similar transcriptional changes, the induction dynamics and amplitude of individual genes may differ in response to different MAMPs (Li, Meng *et al.*, 2016).

mRNA transcription is catalysed by the multi-subunit enzyme RNA polymerase II (RNAPII) that binds selectively to the promoters of target genes, not only modulating basal transcriptional activity but also controlling selectively activation of specific genes (Li, Cheng *et al.*, 2014). Rpb1 is the largest subunit of RNAPII, which contains a Carboxyl-Terminal Domain (CTD) made of conserved heptapeptide repeats with a consensus sequence. Phosphorylation of this domain regulates transcription cycles via recruiting different CTD binding proteins (Buratowski, 2009).

After the perception of MAMPs/DAMPs in the plant-pathogen interaction, all the machinery is activated, being MPK3/MPK6 directly phosphorylated, leading to the activation of Arabidopsis Cyclin-Dependent Kinase C (CDKC), which in turn phosphorylate the CTD of RNAPII being the link between MAPKs and transcriptional changes (Figure 1.3) (Cui *et al.*, 2007; Li, Cheng *et al.*, 2014).

The Mediator (MED) complex, which is an evolutionarily conserved multiunit protein complex, regulates RNAPII, contributing to transcriptional specificity via interaction with gene-specific transcription factors. The transcriptional responses to pathogen infections are specific and regulated by different sophisticated regulatory mechanisms (Li, Cheng *et al.*, 2016). There are different Mediator subunits implicated in defence, such as MED8, MED16, MED21, and MED25, involved in jasmonic acid/ethylene (JA/ET)-mediated resistance to the necrotrophic fungi *Botrytis* sp. and *Alternaria* sp. (Kidd *et al.*, 2011; Samanta & Thakur, 2015)

or MED18, also important for plant immunity against necrotrophic fungi, but in a JA/ET-independent manner (Lai *et al.*, 2014).

Members of the WRKY gene family of plant-specific transcription factors are often induced in response to diverse pathogens (Figure 1.3) (Tsuda & Somssich, 2015). WRKYs tend to form positive feedback regulatory loops via binding to their own promoters to amplify the signal. In other cases, VQ motif-containing Proteins (VQPs) act as bridges between MAPKs and WRKYs (Liu, Kracher *et al.*, 2015; Mao *et al.*, 2011).

Among the targets of WRKY TF are set of genes encoding enzymes required for the synthesis of antimicrobial compounds. For example, the CYP81F2 gene in Arabidopsis plays a crucial role in the plant's defence mechanisms against pathogens since it encodes a cytochrome P450 monooxygenase involved in the synthesis of specialized metabolites known as phytoalexins, activating defence signalling pathways, and providing broad-spectrum protection (Figure 1.3) (Tao *et al.*, 2022).

1.5.Opened questions in plant immunity mediated by plant cell walls

Though significant progresses have been made in the characterization of the function of plant cell wall on plant disease resistance and in the mechanisms of immunity triggered by carbohydrate-based DAMPs/MAMPs, there are still several fundamental questions that need to be addressed. Among these question we can remark the following: i) what is the biochemical composition of active DAMPs released from plant cell walls upon plant infection by pathogens?; ii) are glycans released from plant cell walls upon alteration of CWI caused by other biological processes, like abiotic stresses or development?; iii) if this is the case, are these glycans identical to DAMPs released upon pathogen infection and do they trigger signalling responses (e.g. PTI)?; iv) what are the main domains (ECDs) of plant receptors involved in the perception of glycans (DAMPs/MAMPs)?; v) what are the binding pockets of these plant ECDs-receptors involved in glycans recognition?; vi) what are the co-receptors (co-PRRs) involved in the formation of glycan-PRR complex required for downstream PTI activation apart from those already determined for CHI6-LysM-RK and RALF-LRX complexes characterized so far? Moreover, genetic screening and the use of genome editing to generate high order (multiple) mutants in putative glycan PRR gene families will be required to

overcome receptor redundancy in plants and to characterize PRR and co-PRR involved in glycan perception. These efforts will contribute to identify glycan/receptors pairs that would allow the development of novel sustainable agriculture solution for crop protection. Treating plants, harbouring the appropriate PRRs, with cell wall-derived glycans (pure or mixture of ligands) might trigger adaptative responses to biotic stresses and, probably, to abiotic stresses.

2. Objectives

In contrast to the extended knowledge of the perception of peptidic MAMPs/DAMPs, our understanding of the mechanisms of perception of carbohydrate-based DAMPs/MAMPs by the plant immune system and the activation of immune responses is scarce. However, carbohydrates are highly abundant molecules in plant and microbial extracellular layers, such as cell walls, and some of these glycan structures are known to be immunogenic since they trigger PTI responses. In this context, **the main aim of this Thesis is the identification and functional characterization of molecular components implicated in the plant immune response mediated by cell wall-derived glycans.** For this purpose, we propose the following objectives:

1. Identification by genetic screening of *Arabidosis thaliana* mutants defective in PRRs and signalling elements that regulate immune responses activated by cell wall-derived ß-glucans.
2. Characterization of the PRRs and additional molecular components identified and determination of their function in the signalling pathway(s) triggered by ß-glucans.
3. Structural characterization of the ligand (ß-glucans)/PRR complexes that regulate plant immune responses.

3. Materials and methods

3.1.Biological material

3.1.1. Plants

In this Thesis, *Arabidopsis thaliana* transgenic plants background Columbia-0 (Col-0) carrying the *Apoaequorin* gene (*35S::Apoaequo*$_{cyt}$; Col-0^{AEQ}) (Knight *et al.*, 1991; Ranf *et al.*, 2011) were used to evaluate the changes in cytoplasmatic Ca^{2+} concentration. These plants were used in the mutagenic process for the genetic screening and to obtain calcium sensor lines by crossing them with other T-DNA (from the Nottingham Arabidopsis Stock Centre (NASC) and Torres *et al.*, 2002) mutants of interest. All these lines used in this Thesis are summarized in Table 3.1.

Table 3.1: Arabidopsis mutant lines.

Mutant lines with a T-DNA insertion				
Name	**Locus**	**Line**	**Type of mutation**	**Background**
cerk1-2	*AT3G21630*	GABI-KAT _096F09	T-DNA insertion line	Col-0
lyk4 lyk5	*AT2G23770* *AT2G33580*	WiscDsLox_297300_01C SALK_131911C	T-DNA insertion line	Col-0
back1-4	*AT4G33430*	*SALK_116202*	T-DNA insertion line	Col-0
rbohD	*AT5G47910*	*(Torres et al., 2002)*	T-DNA insertion line	Col-0
igp1-3	*AT1G56145*	SALK_101924C	T-DNA insertion line	Col-0
igp1-4	*AT1G56145*	SALK_021490C	T-DNA insertion line	Col-0
igp4-1	*AT1G56140*	SALK_005808	T-DNA insertion line	Col-0
AT1G56120	*AT1G56120*	SALK_206246C	T-DNA insertion line	Col-0
Mutant lines with SNPs from the screening				
igp1-1	*AT1G56145*	from screening	SNP (E906K)	Col-0^{AEQ}
igp2/3-1	*AT1G56130*	from screening	SNP (G773E)	Col-0^{AEQ}

Other plant species used was *Nicotiana benthamiana* (tobacco) for heterologous expression.

3.1.1.1. Mutagenized population

Arabidopsis thaliana Col-0^{AEQ} seeds were mutagenized with 0,3% ethyl methanesulfonate (EMS) for 17 hours. EMS is a chemical compound that produces Single Nucleotide Polymorphisms (SNPs) in the DNA. After the incubation with the EMS, seeds were sown in 3:1 soil-vermiculite to obtain two next-generation seeds, M_1 and M_2 (Ranf *et al.*, 2012). The genetic screening was performed in M_2 and M_3 mutagenized seeds population. The selective pressure applied was a 50 µM MLG43 treatment (Rebaque *et al.*, 2021). Those seeds with impaired $_{cyt}Ca^{2+}$ burst were selected for further characterization.

3.1.1.2. Plant growth conditions

Arabidopsis seeds were used for *in vitro* and greenhouse assays.

Seeds for growing under *in vitro* conditions were surface sterilized in a laminar flow chamber with 75% ethanol 0,01% tween solution (Tween™ 20, Sigma-Aldrich) (v/v) for 5 minutes and 95% ethanol solution for other 5 minutes and dried in the tubes. Sterile and dried seeds were sown in different plates, 24-well plates for MAPKs and genes assays (around 10 seedlings per well) and 96-well plates for $_{cyt}Ca^{2+}$ influxes and ROS production assays (one seedling per well). The media in these plates was 0,5x Murashige and Skoog (MS) basal salt medium including vitamins (Duchefa Biochemie) (Murashige & Skoog, 1962), which is supplemented with 0,25% (w/v) sucrose (Merk) and 1mM 2-(Nmorpholine)-ethanesulphonic acid (MES; Serva) with a 5,7 pH in ultrapure Mili-Q water.

For protein assays and transgenic lines selection in BASTA, plants were sown in plates 0,5x MS media supplemented with 1% (w/v) sucrose, 2,5 mM MES monohydrate and 0,7% Plant Agar (Duchefa Biochemie).

Once plants were sown, they were stratified in dark conditions at 4 ºC for 72 hours. All *in vitro* plants were grown in a climatic chamber under 14 hours light/10 hours darkness photoperiod. For MAPKs, gene expression and proteins assays they were grown for 12 days (at day 10, media from MAPKs and gene assays plates was changed by 1 ml of new media per well). For $_{cyt}Ca^{2+}$ influxes and ROS production assays, they were grown for 8 days.

Arabidopsis plants for obtaining next-generation seeds were stratified for 48 hours at 4 ºC in the darkness and grown on 3:1 soil-vermiculite in a growth chamber with 10 hours of light/14 hours of darkness at 20-21ºC, light intensity 120 µE/m^{2}s and

65% of relative humidity. After three weeks growing they were moved to a greenhouse at 18-22 ºC.

N. benthamiana seedlings for heterologous protein expression were grown for three weeks at 20-21ºC in the greenhouse.

3.1.1.3. Microorganisms

In this Thesis microorganisms have been used for cloning and plants transformation.

For cloning the proteins used later in the transformation process, we have used *Escherichia coli* strain DH5.

For the transformation process, we used *Agrobacterium tumefaciens* GV3101 strain with gentamicin and rifampicin resistance.

3.1.1.4. Insect cells

For protein expression and purification, two types of insect cells were used: *Spodoptera frugiperda* Sf9 cells (Geneart, Thermo Fisher Scientific) and *Trichoplusia ni* Tnao38 cells (Hashimoto *et al.*, 2012). Sf9 cells were grown for 4 days at 28 ºC in HyClone SFX-Insect cell culture media (Cytiva) with 110 rpm shaking; Tnao38 cells were grown 1 day at 28 ºC and two days at 22 ºC with 110 rpm shaking.

3.2. DNA extraction

DNA extraction for genotyping was performed collecting tissue from Arabidopsis plants in 2 ml tubes with crystal beads and immediately frozen with liquid nitrogen. Using a MagNa Lyser (Roche) grinder machine and the crystal beads inside the tubes, the material was homogenized. The extraction was performed with an extraction buffer adding 316 µl/sample (0.35 M Sorbitol, 100 mM Tris (Duchefa Biochemie) pH 7.5, 5 mM Ethylenediaminetetraacetic Acid Disodium Salt 2-Hydrate (EDTA; Panreac), adjust pH 7,5), a lysis buffer adding 350 µl/sample (200 mM Tris, 50 mM EDTA, 2 M NaCl (Panreac), 2% N-Cetyl-N-trimethyl-ammoniumbromid (CTAB; Merk) and 20 µl of Sarcosyl 10% (Sodium lauroyl sarcosinate; Sigma) per sample.

Next the samples were incubated at 60 ºC for 30 minutes and 500 µl of chloroform were added to each sample. Samples were centrifuged at 8500 rpm for 10 minutes.

Supernatants were transferred to a new tube with 0,7 volume of isopropanol and tubes were centrifuged again at 13000 rpm 15 minutes. Pellets were washed with 500 µl of 70% ethanol. After a last centrifuge of 5 minutes at 15000 rpm, pellets were dried and resuspended in 50 µl of sterile Mili-Q water.

DNA samples were quantified using the spectrophotometer NanoDrop ND-1000 (NanoDrop Technologies INC).

3.3. Genes expression assays

3.3.1. RNA extraction

Col-0 seedlings and/or other genetic backgrounds were grown in 24 well plates as described in 3.1.1.2 for 12 days. Two days before the experiment (day 10) the 0,5x MS media was removed and replaced by 1 ml of new 0,5x MS media. Seedlings were treated for 30 minutes with water as a mock and different carbohydrate treatments. After the treatment period, samples were collected and frozen in liquid nitrogen. Plant material was grinded with a mortar cooled with liquid nitrogen. Total RNA was extracted using the RNeasy Mini Kit (Qiagen) following the protocol recommended by the provider and resuspended in 30 µl of RNase-Free Water. The concentration of the samples was quantified by the NanoDrop ND-1000 spectrophotometer (NanoDrop Technologies Inc.).

3.3.2. cDNA synthesis

The cDNA was synthetized from 2 µg of the total RNA extracted, previously treated with DNase (TURBO DNA-freeTM Kit, Invitrogen, Thermo Fisher Scientific) to hydrolase residual DNA from the extraction. The reverse-transcription reaction was carried out for 60 minutes at 50 ºC using the Transcriptor First Strand cDNA Synthesis Kit (Roche Applied Science) and oligo-dT oligonucleotides.

3.3.3. qRT-PCRs

Quantitativereal-time PCRs (qRT-PCRs) were performed in a 7300 Real-Time PCR System (Thermo Fisher Scientific). The final reaction volume was 20 µl with 10 µl of 2X SYBR Green Master Mix (Roche Applied Science), 1 µM of oligonucleotides, and 10ng of cDNA obtained as described before (3.3.2.). qRT-PCR conditions were 95 ºC for 10 minutes, 45 cycles of 95 ºC for 15 seconds and 60ºC for 1 minute. Finally, a dissociation stage was performed with three steps: 95 ºC for 15 seconds,

60 ºC for 30 seconds and 95 ºC for 15 seconds) (Rebaque *et al.*, 2021). All oligonucleotides used for qRT-PCRs are shown in Table 3.2.

Table 3.2: Oligonucleotides used for qRT-PCRs.

Name	Locus	Forward oligonucleotide	Reverse oligonucleotide
IGP1	*AT1G56145*	TTGGTTTGTGTTCATGTCTGGT	TATCTTGTTCAACGCCCGAG
IGP2/3	*AT1G56130*	TCTCTCAGCGGATTTCAAATCA	TTGGCTTAAAGTCGCTGTCTC
IGP4	*AT1G56140*	TCAATCAGCGGCTTTCCATT	CTAGCGTCGTTGTTTCTCGG
AT1G56120	*AT1G56120*	TGTTGAATGCTATTGACTGGTGT	CCGCGTCCTCCTTTTCAAAT
UBC21	*AT5G25769*	GCTCTTATCAAAGGACCTTCGG	CGAACTTGAGGAGGTTGCAAAG
CYP81F2	*AT5G57220*	TATTGTCCGCATGGTCACAGG	CCACTGTTGTCATTGATGTCCG
WRKY53	*AT4G23810*	CACCAGAGTCAAACCAGCCATTA	CTTTACCATCATCAAGCCCATCGG

3.4. Characterization of T-DNA insertion line mutants

All T-DNA insertion lines used in this Thesis were in Col-0 genetic background, the double and triple mutants generated from them and those lines ordered for the first time were checked for homozygosity by polymerase chain reaction methodology (PCR). PCRs were performed with the Dream Taq Polymerase (Thermo Fischer Scientific), under the conditions specified by the provider, using DNA extracted from each line as described in 3.2. section. For checking the T-DNA insertion in each line we used Lba1 oligonucleotide as forward one with the reverse oligonucleotide of the gene of interest. A list of the specific oligonucleotides used to check the mutants is shown in the Table 3.3.

Table 3.3: Oligonucleotides for T-DNA insertion lines genotyping.

Name	Locus	Line	Forward oligonucleotide	Reverse oligonucleotide
cerk1-2	AT3G21630	GABI-KAT_096F09	AGAATATATCCACGAGCACACGGTTCCAG	GACGAAAAGAGAGTGGATAAAGCAACCAC
lyk4 lyk5	*AT2G23770*	CS850683	CATTTTCATCCATCGATGGAC	TTCCCTTTCACAACAATCCTG
	AT2G33580	SALK_131911C	TTCTGGTCTCAACCACCGTAC	CAGAAACCTGAGAGACGGATG
igp1-3	*AT1G56145*	SALK_101924C	TGGAAATAACAGGCTGAATGG	ATTCGCCTTCCAAGACTTTTC
igp1-4	*AT1G56145*	SALK_021490C	TGCATCGTTTTAAGGCTCAAC	CTTTTCCTCTGCCACAGTCAC
igp4-1	*AT1G56140*	SALK_005808	AATGATACAGGTAATCCCCCG	GCCAGTGTTCTCGACTCAAAC
AT1G56120	*AT1G56120*	SALK_206246C	ATTCAACGTGTTGTTTCCCAG	AGTGTTCGTCGACCACAAAAG
Lba1			TGGTTCACGTAGTGGGCCATCG	

3.5.Elicitors

3.5.1. Carbohydrates

Carbohydrates used in all the experiments performed in this Thesis were bought to different companies with a purity guarantee. All of them appear in the Table 3.4.

For all the *in vitro* experiments with carbohydrate treatments, sugars were warmed at 80 ºC for 10 minutes and cooled at room temperature before their application.

Table 3.4: Oligosaccharides used as elicitors.

Code	Chemical name	Type of glycan	Provider
MLG43	ß-D-Cellobiosyl-1,3-ß-D-glucose	ß-1,3/1,4-D-glucans	Megazyme (O-BGTRIB)
MLG34	ß-D-Glucosyl-1,3-ß-D-cellobiose	ß-1,3/1,4-D-glucans	Megazyme (O-BGTRIA)
CEL2	Cellobiose	ß-1,4-D-glucans	Sigma (C7252)
CEL3	Cellotriose	ß-1,4-D-glucans	Megazyme (O-CTR-50 mg)
CEL4	Cellotetraose	ß-1,4-D-glucans	Megazyme (O-CTE-50 mg)
CEL5	Cellopentaose	ß-1,4-D-glucans	Megazyme (O-CPE-20 mg)
CHI6	Hexaacetyl-Chitohexaose	chito-oligosaccharides DP 6-8	Megazyme (O-CHI6)
OGs 10/15	galacturonan oligosaccharide DP10/DP15	[GalAα1-4]±10-15	ELICITYL (GAT114)
Xyl4	Xylotetraose	ß-1,4-D-$(xylose)_n$	Megazyme (O-XTE-30 mg)
XA_3XX	3^3-α-L-Arabinofuranosyl-xylotetraose	α-L-Arabinofuranosyl-[ß-1,4-D-$(xylose)_n$]	Megazyme (O-XA3XX-30 mg)

3.5.2. Peptides

Peptides were used in this Thesis as controls and for the specificity assays to confirm that our mutants were impaired in oligosaccharides perception and not in general signalling pathways. There were used two peptides, flg22 (1 mg) from EZBiolab and AtPep1 (1 mg) from Abyntek.

3.6. Analysis of PTI responses

3.6.1. Calcium influxes assays

Aequorin is a calcium binding photoprotein made up of an apoprotein, apoaequorin, and a luciferin molecule which is a prosthetic group, coelenterazine. Col-0^{AEQ} (Knight *et al.*, 1991; Ranf *et al.*, 2011) constitutively express the apoaequorin but the coelenterazine must be added exogenously. When there is oxygen in the media and coelenterazine is added, the functional holoprotein, aequorin, reconstitutes having three calcium binding sites. In presence of cytoplasmatic calcium, these calcium binding sides are occupied and aequorin suffers a conformational change behaving as an oxygenase, transforming coelenterazine into exited coelenteramide with carbon dioxide production and emitting blue light (λ = 469 nm) (Mithöfer & Mazars, 2002) that can be measured with a luminometer as the Varioskan Lux Reader luminometer (Thermo Fisher Scientific) (Figure 3.1).

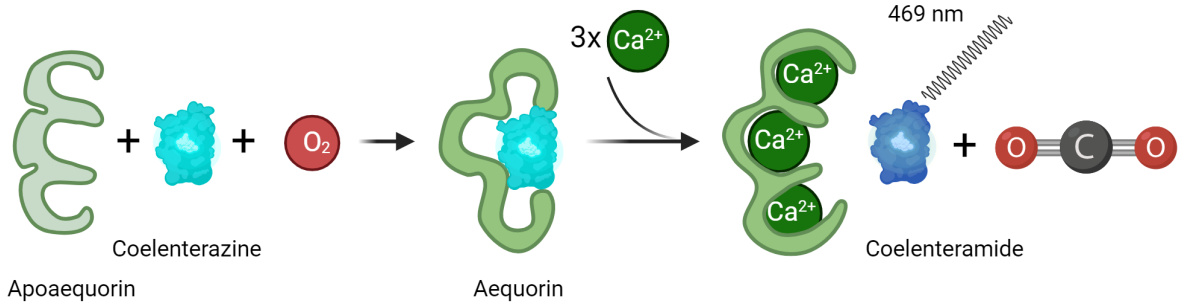

Figure 3.1: Cartoon representing apoaequorin as a calcium sensor. Aequorin in presence of oxygen and coelenterazine, reconstitutes showing three sites where cytoplasmatic calcium is going to bind, suffering a conformational change transforming coelenterazine into exited coelenteramide with carbon dioxide production and emitting blue light (λ = 469 nm).

Sterilized Col-0^{AEQ} (Knight *et al.*, 1991) seeds with different genotypes were sown in 96 well (1 seed per well) plates in 0,5x Murashige and Skoog (MS) basal salt

medium (Duchefa Holland) (Murashige & Skoog, 1962) were stratified and grown under the conditions described previously (3.1.1.2.) for 8 days. After this period, media was removed and 75 µl of 10 µM coelenterazine ((2-(p-hydroxybenzyl)-6-(p-hydroxyphenyl)-8-benzyl-imidazol[1,2-a]pyrazin-3-(7H)-one; PJK GmbH) were added per well and left overnight at room temperature in the darkness. The next day, plates were placed in the Varioskan and 75 µl of the ligand of interest at 2x concentration were added in each well. Luminescence was measured in each well after the treatment application (300 ms of integration time) (Bacete *et al.*, 2017).

3.6.1.1. Calcium discharge assays

To check seedlings were not affected in the *Apoaequorin* transgene, the total calcium of the seedlings was discharged by adding $CaCl_2$ being the final concentration per well of 1,5 M. Total relative luminescence units (RLU) were obtained by calculating the integral under the kinetic curve in each well and compared to the one of the control Col-0^{AEQ}.

3.6.2. ROS production assays

Reactive Oxygen Species (ROS) production assays are based on the chemiluminescence reaction between luminol and hydrogen peroxide (H_2O_2) catalysed by horseradish peroxidase (HRP). In the presence of H_2O_2, HRP oxidizes luminol which is transformed in excited aminophtalate producing light at a wavelength of 490 nm (Bisceglia *et al.*,2015). Using this chemical reaction, ROS production was determined in 10-day-old seedlings of Col-0 with different genotypes grown in 96-well plates under the growth conditions described below (3.1.1.2.) in 0,5x MS media. The day before the experiment, media was replaced by 100 µl of 0.3 µM luminol (L-012 FUJIFILM Wako Chemicals USA Corp) and 15 µg/ml of horseradish peroxidase (HRP, Sigma). Plates were placed in the Varioskan and the ligand of interest was applied at 2x concentration in each well. Luminiscence was measured in each well after the treatment application (300 ms of integration time) (Rebaque *et al.*, 2021).

3.6.3. MAPKs phosphorylation assays

The level of phosphorylation of the MAPKs after treatments with different carbohydrate ligands was analysed by Western Blot as described in Rebaque *et al.*, 2021 with some modifications. For theses assays, 12-day-old Col-0 seedlings and/or

other genetic backgrounds, were grown under the conditions already described (3.1.1.2.). Two days before the experiment (day 10) the 0,5x MS media was removed and replaced by 1 ml of new 0,5x MS media to avoid a differential evaporation of the media between the wells. Treatments were added with a mock solution (water) and seedlings were harvested after 0, 10 and 20 minutes in 2 ml tubes with ceramic beads and immediately frozen in liquid nitrogen. The material was grinded with a FastPrep Bead Beating System (MP Biomedicals) and 50 µl of Protein Extraction Buffer (25mM Tris-HCl pH 7.8; 75mM NaCl; 15mM Ethylene Glycol Tetraacetic Acid (EGTA; Serva); 10mM $MgCl_2$ (Merk); 15mM ß-glycerophosphate (Sigma-Aldrich); 15mM 4-nitrophenylphosphate bis; 1mM Dithiotreitol 1,4-Dithiothreitol (DTT); 1mM NaF (Acros Organic); 0.5 mM activated Na_3VO_4 pH 10; 0.5mM Phenylmethanesulfonyl Fluoride (PMSF; Sigma-Aldrich); 1% (v/v) protease inhibitor cocktail P9599 (Sigma-Aldrich); 0.1% (v/v) Tween-20).

Samples were centrifugated for 20 minutes at 4 ºC and the supernatant was collected to determine total protein concentration, measured by the Bradford assays (Bio-Rad). This assay allowed us to equilibrate protein concentration among samples. A total amount of 30 µg of protein per sample was analysed. Protein samples were separated in a 10% Mini-PROTEAN TGX Precast protein gels (Bio-Rad) and transferred to nitrocellulose membranes using the iBlot 3 Western Blot Transfer System (Thermo Fischer Scientific).

Membranes were blocked for 1 hour at room temperature with Pierce ™ Protein-Free Blocking Buffer (PBS, Thermo Fisher Scientific). After blocking, membranes were incubated overnight at 4 ºC with the primary antibody Phospho-p44/42 MAPK (Erk1/2) (Thr202/Tyr204) (Cell Signalling Technology; 1:1000) in PBS. After incubation, membranes were washed with home-made TBS-T (1,5 M NaCl, 100 mM Tris pH 7,6 and 0,1% Tween-20) and incubated for 2 hours at room temperature with horseradish peroxidase-conjugated α-rabbit secondary antibody (GE-Healthcare) (1:5000) in PBS.

After all incubations, membranes were developed with the ECL Western Blotting Substrate (Thermo Fisher Scientific; Pierce) for 4 minutes and imaged using the iBright FL1000 Image System (Thermo Fisher Scientific).

A loading control analysis with α-AtMPK3 (1:1000) (Sigma-Aldrich) was done in the same membranes after stripping (incubation for 5 minutes in a 50 mM glycine pH 2, 0,1% SDS and 0,05% Tween-20 solution), washing with TBS-T and blocking

again but this time with milk 5%. Next steps were the same as already mentioned changing the primary antibody.

3.6.4. Expression of defence marker genes

The gene expression analysis was performed carrying out qRT-PCRs in a 7300 Real-Time PCR System (Thermo Fisher Scientific) as described in section 3.3.

The expression level of each gene was relativized to the housekeeping gene *UBC21 (AT5G25769)* expression, and was determined using Pfaffl method (Pfaffl, 2001). Genes analysed in PTI responses assays were *CYP81F2 (AT5G57220)* and *WRKY53 (AT4G23810)*. Oligonucleotides used for these experiments are shown in Table 3.2.

3.7.Screening

3.7.1. Selection of the putative mutants

The main objective of the screening was to find putative mutants defective in MLG43 perception. For this purpose, EMS M_2 Col-0^{AEQ} seeds (3.1.1.1) were grown in vitro (3.1.1.2) for 8 days in a 96 well plate and the amount of cytoplasmatic calcium produced after 100 µM MLG43 treatment was measured for each seedling following the calcium influxes assay protocol described in 3.6.1. Based on the level of cytoplasmatic calcium released after the MLG43 treatment, seedlings with a low response (less than 50% the signal of the wild-type) comparing to the control Col-0^{AEQ}, were selected and transferred to soil to grow for obtaining next-generation seedlings. Total calcium burst was tested in the M_2 putative candidates taking 4 mm diameter leaf discs from the grown plant, using a cork borer and putting the discs in a 96 well plate, to confirm that the impaired response to MLG43 was due to a mutation in a certain gene and not in the Apoaequorin transgene (3.6.1.1.).

The selected M_2 candidates with low response to the treatment and good calcium burst discharge were backcrossed with Col-0^{AEQ}.

3.7.2. Specificity assays

To confirm that the selected putative mutants were not affected in a general perception pathway, we performed calcium influxes assays as described in 3.6.1. with different carbohydrates and peptides. Treatments were: 10 µM CEL2, 10 µM

CEL3, 10 µM CEL4, 10 µM CEL5, 100 µM MLG34, 0,5 mg/ml OGs (DP 10-15), 1 µM flg22, 1 µM AtPep1.

3.7.3. Mapping by whole-genome sequencing and SNPs analysis

Pooled tissues from 50 backcrossed M_2 plants of the validated mutants with impaired response to MLG43 and from parental Col-0^{AEQ} plants as a control, were harvested and gDNA was extracted (3.3.). 10 ng of total gDNA were send to Macrogen to perform whole genome sequencing.

Sequencing (150-bp paired-end reads) was performed on an Illumina platform (https://www.illumina.com) to reach a coverage of 30 million reads (Andrews, 2010). Reads were aligned with BWA-MEM 0.7.17 (Macrogen, https://dna.macrogen.com) against the *A. thaliana* TAIR10 (The Arabidopsis Information Resource) genome release (Li, 2013). BAM files were obtained with SAMTOOLS 1.15.1 (http://www.htslib.org). The variant caller 16GT DOCKER IMAGE was employed to obtain VCF files (Danecek *et al.*, 2021; Luo *et al.*, 2017). From these VCF files, chromosome, position, reference, alternate and allelic depth (AD) fields were extracted with BCFTOOLS 1.15.1, and SNPs were subtracted from the resulting files. Frequency was calculated from AD fields as follows: [AD-alternate allele/(AD-alternate allele + AD-reference allele)]. SNPs with frequency values higher than 0.99 were selected for further analysis.

3.7.4. Phylogenetic analysis

The evolutionary history of IMPAIRED IN GLYCAN PERCEPTION (IGP) proteins was inferred using the Minimum Evolution (ME) method (Rzhetsky & Nei, 1992). The bootstrap consensus tree inferred from 1000 replicates is taken to represent the evolutionary history of the taxa analysed (Felsenstein, 1985). Branches corresponding to partitions reproduced in less than 50% bootstrap replicates are collapsed. The percentage of replicate trees in which the associated taxa clustered together in the bootstrap test (1000 replicates) are shown next to the branches (Felsenstein, 1985). The evolutionary distances were computed using the p-distance method (Nei & Kumar, 2000). The ME tree was searched using the Close-Neighbor-Interchange (CNI) algorithm (Nei & Kumar, 2000) at a search level of 1. The neighbor-joining algorithm (Saitou & Nei, 1987) was used to generate the initial tree. The analysis involved 25 amino acid sequences. All ambiguous positions were removed for each sequence pair and a total of 709 positions were

present in the final data set. Evolutionary analyses were conducted in MEGA 6 (Tamura *et al.*, 2013).

3.8. Obtention of IGP gain-of-function and complementation lines

For carrying out different experiments with IGPs proteins to study more deeply their biochemistry we expressed them *in planta* (both Arabidopsis and *N. benthamiana*). Below we provide a detailed explanation of the steps we followed to express IGP proteins.

3.8.1. Cloning of IGP coding sequences

The coding region of *At1G56145* (*IGP1*), *At1G56140* (*IGP4*) and *AT1G56120* was synthesized by GeneScript and cloned in a pGenDONR entry vector (https://www.genscript.com). IGP coding sequences were recombined in pGWB destination vectors with diverse C-terminal tags: *35S*::pGWB614 carrying three units of tag HA; *35S*::pGWB611 carrying FLAG tag; *35S*::pGWB605 carrying GFP tag under the control of the CaMV-35S promoter (Earley *et al.*, 2006) (Figure 3.2). LR-Gateway technology was used in this step.

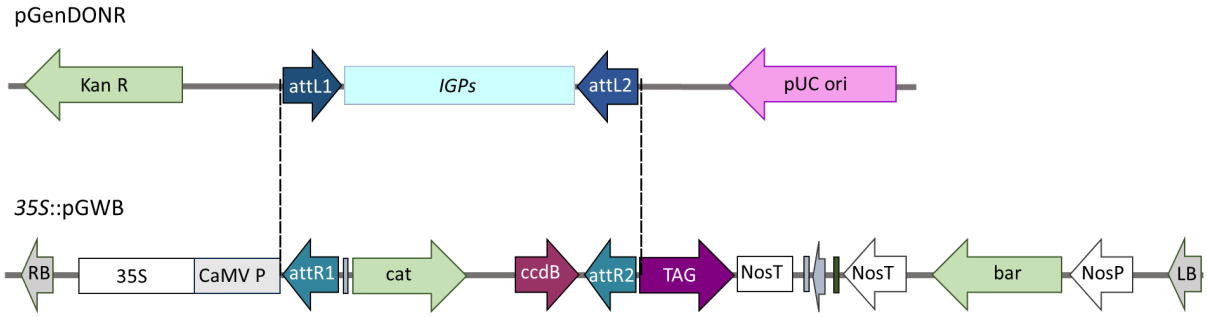

Figure 3.2: Constructs used for generating Arabidopsis complementation and overexpression lines of IGP1. IGP1 cDNA was inserted substituting the *attR1-(cat, ccdB)-attR2K* cassette by an LR reaction.

Briefly, the LR reaction was performed using LR Clonase II enzyme (Thermo Fisher Scientific) as following: in one tube were added 2 µl of TE buffer (Tris-EDTA), 3,5 µl (100-300 ng/reaction) of the pGenDONR with the gene of interest, 2,5 µl (300 ng/reaction) of the different destination vectors and 2 µl of LR Clonase II enzyme. The mix was left at 25 ºC overnight and the next morning 2 µl of

proteinase K were added to the tube and incubated at 37 ºC for 10 minutes to stop the reaction.

The LR product was transformed into electrocompetent *Escherichia coli* strain DH5α. 1 µl of the LR product was added to 50 µl of bacteria, mixed gently and introduced in an electroporation cuvette, and a pulse of 50 volts for 50 msec was passed through the cuvettes. After the pulse, they were put in ice for 2 minutes and let them recover in LB media (Tryptone 10 g/l (Pronadisa), yeast extract 5 g/l (Pronadisa), NaCl 10 g/l (Panreac), pH 7) at 37 ºC for 1 hour. At the end of the process, bacteria were plated in LB-agar media (plus 15 g/l of American bacteriological agar) supplemented with selective antibiotics: kanamycin 50 (sigma-Aldrich) for pGenDONR initial isolation, spectinomycin 50 for pGWB destination vectors selection.

Positive colonies for the presence of the insert were checked by colony PCR using Dream Taq Polymerase (Thermo Fischer Scientific) and following the protocols specified by the provider. Oligonucleotides specific for the insert and for the vector were combined in the PCR reaction (Table 3.5)

Table 3.5: Oligonucleotides for colony PCRs.

oligonucleotide name	oligonucleotide sequence
IGP1 Fw	CGTCGACGATGCTGAGATTA
IGP4 Fw	GAATGCGATGGATGACTTT
AT1G56120 Fw	CACAAGCTCCTCATTCAGCA
HA Rv	CGGGACGTCATAGGGATA
FLAG Rv	CTTGTCATCGTGATCCTTGTA
GFP Rv	CTGAACTTGTGGCCGTT

Plasmid DNA was extracted from positive *E. coli* using the QIAprep Spin Miniprep Kit (Qiagen) and transformed into *Agrobacterium tumefaciens* GV3101 strain that carry the Ti plasmid that allows plant transformation. Positive *A. thumefaciens* colonies for the presence of the insert were verified by PCR. Later they were used for two different purposes, transformation of *Arabidopsis thaliana* by the floral dip method (Clough & Bent, 1998), to obtain stable transgenic lines, and infiltration of *N. benthamiana* leaves for heterologous and transient expression of IGP proteins.

3.8.2. *Arabidopsis thaliana* transformation

Arabidopsis plants with different genotypes were transformed using the flower dip method (Clough & Bent, 1998) but with some modifications.

500 ml bacteria culture of each construct was prepared the day before letting the bacteria grow overnight, with rifampicin 50 (Duchefa Biochemie) and gentamicin 50. The next day, when the OD was around 0.5, every culture was centrifugated at 3500 rpm for 15 minutes. Pellets were resuspended in 250 ml 5% sucrose, and 44 µl of BAP 50 µg/ml and 60 µl of Silwet L-77 were added to the bottles. The flower dip method (Clough & Bent, 1998) is based on dipping the flowers of *Arabidopsis thaliana* in the different construct cultures but, to increase and improve the level of transformation, all the process was carried out in a vacuum chamber doing 2 steps of 1-minute vacuum with a resting minute step in between.

T1, T2 and T3 were grown *in vitro* in MS-plant agar as previously described (3.1.1.2.) and glufosinate-ammonium (BASTA) 50 µM was added to the plates for selecting transgenic plants.

3.8.3. Heterologous expression of IGPs in *N. benthamiana*

Agroinfiltration in *N. benthamiana* to perform transient expression of the proteins of interest was carried out following an agroinfiltration protocol but with some modifications (Li, 2011).

Two days before the infiltration, a 5 ml LB media with antibiotics pre-inoculum with the different constructs was prepared. Next day, 100 µl of the pre-inoculum were added to 50 ml LB media with antibiotics and let to grow to the required OD (around 1). Then, they were centrifuged in 50 ml Falcon tubes 10 minutes at 4000 rpm. Pellets were resuspended in the corresponding volume of infiltration buffer (10 mM MES supplemented with 10 mM $MgCl_2$ and 100 µM acetosyringone; Sigma Aldrich).

The silence suppressor *p19* plasmid was added to each construct to a final OD of 1. (Norkunas *et al.*, 2018).

Once the constructs were mixed with *p19*, 1 ml of the mix was infiltrated in the back side of three-weeks-old *N. benthamiana* leaves with a syringe. Infiltration zone was marked with a pen and, two days later, harvested, grinded and processed to check proteins' transient expression.

3.8.4. Protein expression and interaction assays

3.8.4.1. Fast protein extraction protocol

To quickly check protein expression both in Arabidopsis and in *N. benthamiana*, a fast protein extraction protocol in Laemmli buffer was carried out. Briefly, plant tissue was frozen with liquid nitrogen and grinded in a mortar. All frozen grinded tissue was collected, and 1,5 g were transferred to a 2 ml tube. 100 µl of 2x Laemmli buffer (65,8 mM Tris-HCl pH 4,6, 26,3% (w/v) glycerol (Panreac), 2,1% Sodium Dodecyl Sulfate (SDS; Merk) and 0,01% bromophenol blue (Sigma Aldrich)) were added to each sample. Samples were let in ice and shacking for 20 minutes and boiled at 85 ºC for 5 minutes and at 95 ºC for other five minutes. Tubes were centrifugated at 14000 rpm for 10 minutes at 4 ºC and supernatants were transferred to new tubes. Samples were loaded in a 7-15% Mini-PROTEAN TGX Precast protein gel (Bio-Rad) and transferred to nitrocellulose membranes. The rest of the protocol is the same as described previously for MAPKs assays (3.6.3.) but with some differences: for FLAG and GFP-tagged proteins membranes were blocked with 5% milk but for HA-tagged membranes 5% bovine serum albumin (BSA; Sigma Aldrich) solution was used for blocking the membranes; α-FLAG (1:2500), α-HA (1:1000) and α-GFP (1:2500) antibodies were used as primary antibodies and α-mouse (1:5000) as secondary antibody.

3.8.4.2. Immunoprecipitations and Co-Immunoprecipitations

Plant tissue was frozen with liquid nitrogen and grinded in a mortar. All the frozen grinded tissue was collected, and 1,5 g were transferred to a 2 ml tube. 500 µl of Protein Extraction buffer (100 mM Tris-HCl pH 4,6; 300 mM NaCl; 20% glycerol; 4 mM EDTA; 5 mM DTT; 0,5% (w/v) Polyvinyl pirrolidone (PVPP); 1% (v/v) protease inhibitor cocktail; 2% (v/v) IGEPAL (Sigma Aldrich); 2 mM Na_2MoO_4; 2,5 mM NaF; 1 mM PMSF; 1,5 mM $Na_3V\ O_4$; 50 µM MG132) were added to each tube. Samples were incubated in ice for 40 minutes and shaken for mixing the tissue with the buffer. Samples were sonicated at low energy with pulses of 30 seconds on/30 seconds off for 3 minutes in a bath cell disruptor (Diagenode). Tubes were centrifugated at 4ºC and 14000 rpm and supernatants were transferred to new tubes.

Protein concentration was measured using the Bradford protocol already described (3.6.3.). Samples with adjusted protein concentrations were prepared in triplicate (for immunoprecipitation, Co-Immunoprecipitation, and input) and 500 µl of

protein extraction buffer was added again to each sample for better homogenization of the proteins. 2,5 µl of the proper antibody for IP were added to each tube (except input samples). Samples were then incubated with the antibody at 4ºC for 2 hours in a rotatory wheel. Meanwhile, the incubation was going on, 10 µl Dynabeads™ Protein G (Thermo Fischer Scientific) were pipetted in LoBind tubes with LoBind tips and washed three times with 500 µl of protein extraction buffer. Washed beads were added to the mixture of extracted proteins + antibodies and incubated for 1 hour and a half, at 4 ºC and shacking. Later the supernatant was removed and magnetic beads bound to immunoprecipitated proteins were washed four times with 250 µl of protein extraction buffer (without detergents). Finally, proteins attached to the beads were eluted in 40 µl of 2x Laemmli buffer pH 4,6 (pH specific for IGPs). Samples were boiled, also input samples (not immunoprecipitated), for 10 minutes at 70 ºC. A protocol similar to the one described in 3.6.3. was followed to do the Western Blot assay using the corresponding antibodies for the tag present in the constructs.

3.9. Structure analyses *in silico*

Model structures of IGP1/CORK1/AT1G56145, IGP3/AT1G56130 and IGP4/AT1G56140 were downloaded from the AlphaFold Protein Structure Database (Tunyasuvunakool *et al.*, 2021). They present six identifiable domains: N-terminal containing a signal peptide annotated in PFAM (Mistry *et al.*, 2021), LRR, MAL, TM, KD and the C-terminal tail. The plDDT metric over most of LRR, MAL and KDs is ≥90% (Jumper *et al.*, 2021). To achieve the proper extracellular/TM/intracellular domain separation, and taking the IGP4 model as the benchmark, we proceeded as follows: (i) torsions were applied to backbone dihedral angles in the segment following MAL with CHIMERA 1.15 (Pettersen *et al.*, 2004); (ii) energy minimization of the extended segment joining the MAL and TM domains was performed with CHIMERA 1.15, keeping all the remaining structure fixed; (iii) the resulting structure was inserted in a pre-equilibrated model of a bilayer composed of 256 phosphatidylcholine (POPC) lipids with a pore of radius 8 Å, downloaded from the CHARMM-GUI archive (Jo *et al.*, 2007), and the protein-bilayer system was parametrized using the CHARMM 3.6 force field (Huang *et al.*, 2017) with CHARMMGUI (Jo *et al.*, 2008); (iv) the protein bilayer system was solvated with a 16-Å margins solvation box and NaCl 0.150 M salt ions with VMD 1.9.3 (Humphrey *et al.*, 1996), and the whole structure was optimized with 10 000 conjugated gradient minimization steps using NAMD 2.14 (Phillips *et*

al., 2020). The optimized final structure of IGP4 was then used as the input for modelling the corresponding structures of IGP1/CORK1 and IGP3 with SWISS-MODEL (Waterhouse *et al.*, 2018) in 'user template mode'. The structural comparisons of MAL and KD were analysed with the TM-Align web server (Zhang & Skolnick, 2005). The structural analysis of mutants IGP1-E906K and IGP3-G773E, and their corresponding wild-type KDs, was addressed by modelling them separately with AlphaFold 2 (Jumper *et al.*, 2021) using ColabFold (Mirdita *et al.*, 2022). Poisson–Boltzmann (PB) Electrostatic Potentials (EPs) were computed with the Adaptive Poisson Boltzmann Solver, APBS 3.0.0 (Jurrus *et al.*, 2018) through its plug-in in PYMOL 2.5.1 (Schrödinger, 2020), solving the nonlinear PB equation in sequential focusing multigrid mode at 3D grids of 1613 = 4 173 281 points (approx. 0.5-Å step size), with T = 298 K, ionic concentration of 0.150 M (NaCl), and dielectric constants of 4.00 for proteins and 78.54 for water. The PB EP was then mapped onto molecular surfaces computed and rendered with PYMOL 2.5.1 (Schrödinger, 2020).

3.10. Protein-ligand binding assays

3.10.1. Protein expression in insect cells

Codon-optimized synthetic genes corresponding to the ectodomains of AT1G56145 (residues 25–630), AT1G56140 (residues 29– 636) and AT1G56130 (residues 30–636) from Invitrogen GeneArt were cloned into a modified pFastBac donor vector (Geneva Biotech, https://geneva-biotech.com) harboring the *Drosophila BiP* (Smakowska-Luzan *et al.*, 2018) or the 30K Bombyx mori (Soejima *et al.*, 2013) secretion signal peptides, and with a TEV (tobacco etch virus protease) cleavable C-terminal StrepII-9xHis tag. Baculovirus vectors were generated in DH10MultiBac *E. coli* cells (Geneva Biotech). Briefly, virus amplification was carried out in *Spodoptera frugiperda* Sf9 cells (Geneart, Thermo Fisher Scientific) and was used to infect *Trichoplusia ni Tnao38* cells (Hashimoto *et al.*, 2012) for protein expression. The cells were grown for 1 day at 28°C and for 2 days at 22°C with gentle shaking.

3.10.2. Protein purification

3.10.2.1. Tandem affinity purification

The secreted proteins were subjected to tandem affinity purification, using Ni^{2+} (HisTrap excel, equilibrated in 25 mM KPi, pH 7.8, and 500 mM NaCl; GE Healthcare, https://www.gehealthcare.com) and Strep columns (Strep-Tactin Superflow high-capacity; IBA, https://www.iba.de) equilibrated in 25 mM Tris, pH 8.0, 250 mM NaCl, 1 mM EDTA. Affinity tags were removed using His-tagged TEV protease in a 1:50 ratio at 4°C overnight and performing the next morning a second step of Ni^{2+} His columns.

3.10.2.2. Analytical size-exclusion (SEC) chromatography

Separation of cleavage tags and aggregated proteins was performed using size-exclusion chromatography on a Superdex 200 Increase 10/300 GL column (GE Healthcare) equilibrated in 20 mM citric acid, pH 5.0, 150 mM NaCl. A 400-µg portion of protein (approx. 6 µM) was injected using a loop of 1 ml, and the sample was eluted with a flow of 0.5 ml min^{-1}. UV absorbance at 280 nm was used to monitor the elution of proteins. The peak fractions were analysed by SDS-PAGE followed by Coomassie blue staining.

3.10.3. Isothermal titration calorimetry (ITC)

Experiments were performed at 25°C using a MicroCal PEAQ-ITC (Malvern Instruments, https://www.malvernpanalytical.com) with a 200-lL standard cell and a 40-lL titration syringe. Briefly, for ITC experiments in MicroCal PEAQ-ITC, proteins were gel-filtrated into the ITC buffer (20 mM sodium citrate, pH 5.0, 150 mm NaCl). A 3-lL sample of potential ligand (CEL3, CEL5 or MLG43) was injected at a concentration range between 135 and 400 lM into the ITC cell containing ECDs of AT1G56145 or AT1G56140 protein at 9 lM. A total of 13 injections were performed at 150-s intervals with a 500-rpm stirring speed. Dilution heat was corrected using the thermograph of the titration of the ligand into the cell containing only buffer as a control. Experiments were performed in duplicate or triplicate, unless otherwise specified, and data were analysed using the MICROCAL PEAQ-ITC analysis software provided by the manufacturer. All ITC runs used for data analysis have an N ranging from 0.98 to 1.05. The N values were fitted to 1 in the analysis.

4. Results

4.1. A novel family of LRR-MAL RKs, IGPs, are key components for MLG- and cellulose-derived oligosaccharides perception

4.1.1. Forward genetic screening to discover new molecular components involved in glycan perception

Carbohydrates are highly abundant molecules in plant cell walls and microbial extracellular layers, and several of them are known to be perceived by the plant immune system as DAMPs /MAMPs and to trigger PTI (Mélida *et al.*, 2018; Mélida *et al.*, 2020; Versluys *et al.*, 2022; Voxeur *et al.*, 2019; Wanke *et al.*, 2020; Zang *et al.*, 2019).

Remarkably, about 50% of RKs/RP/RPg/e plant genomes have ECDs that are predicted to bind carbohydrate-based ligands, therefore, oligosaccharide–PRR pairs are expected to play a role in immune activation by carbohydrates in plants (Cosgrove, 2022; Wan *et al.*, 2021). However, our understanding of plant immunity activation by carbohydrate-based DAMPs and MAMPs is scarce.

To expand the knowledge of carbohydrate-based ligands/PRRs pairs, we chose a mutant genetic screening strategy since in the cell wall field, different examples of genetic screenings have been described that allowed the discovery of new components and molecular processes that mediate cell wall biosynthesis and cell wall integrity responses in plants (Brown *et al.*, 2005; Engelsdorf *et al.*, 2019; Farrokhi *et al.*, 2006; Gille *et al.*, 2009).

Alkylating agents such as Ethyl Methanesulfonate (EMS) induce chemical modifications of nucleotides resulting in one Single Nucleotide Polymorphisms (SNPs) in the DNA. In 99% of the cases, EMS induces C-to-T changes resulting in C/G to T/A substitutions. Chemical mutagenesis can be used to search for loss or gain function mutants and to identify specific amino acid residues in proteins that are essential for their function (Kim *et al.*, 2006).

In this PhD work, we generated an EMS-mutagenized population of an *A. thaliana* transgenic line that carries the jellyfish *Aequorine* transgene that has been

previously employed as a calcium sensor (Col-0^{AEQ}; Knight *et al.*, 1991; Ranf *et al.*, 2011). With the M_2 seed population resulting from the mutagenesis we performed a screening to identify new molecular components that participate in the perception of MLG43, recently described as an activator of PTI responses in *A. thaliana* (Barghahn *et al.*, 2021; Rebaque *et al.*, 2021; Yang *et al.*, 2021).

Briefly, eight-day-old seedlings of M_2 EMS-mutagenized Col-0^{AEQ} population were grown in microtiter plates together with the Col-0^{AEQ} control line. These seedlings were treated with 100 µM MLG43 and changes of cytoplasmatic Ca^{2+} concentration were then determined in a luminometer (Figure 4.1).

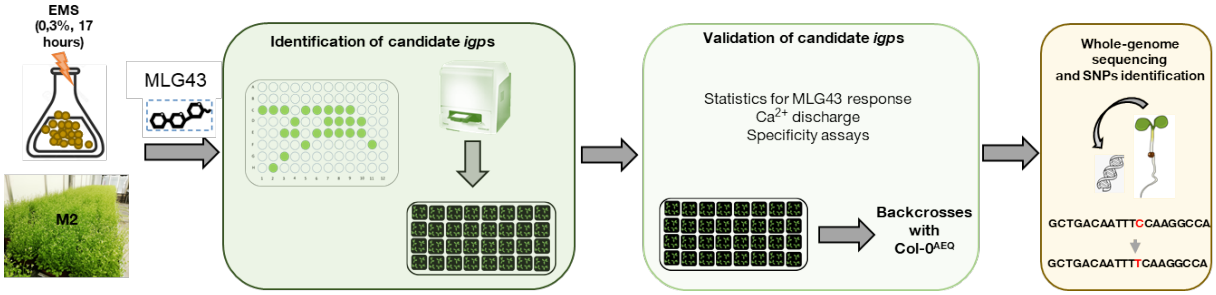

Figure 4.1: Forward genetic screening using EMS mutagenized Col-0^{AEQ} seedlings was used as a tool to discover new PRRs involved in oligosaccharide perception and PTI activation. *Arabidopsis thaliana* seeds carrying the *Apoaequorin* transgene (*35S::Apoaequo*$_{cyt,}$ Col-0^{AEQ}), encoding a calcium cytoplasmatic sensor, were mutagenized with 0.3% (v/v) EMS for 17 hours. M_2 seedlings were grown *in vitro* for 8 days, and calcium influxes were evaluated using a luminometer upon oligosaccharide treatment. Seedlings with a low response to the treatments were transferred to soil and backcrossed with Col-0^{AEQ}. Whole-genome sequencing of F_2 segregating plants for this backcross led to the identification of SNPs associated with the phenotype of each single mutant isolated.

Several mutants that showed a weaker $_{cyt}Ca^{2+}$ burst than that of Col-0^{AEQ} plants, were selected. These putative mutants were called *igp* because they were *i*mpaired in *g*lycan *p*erception (*igp1*^{AEQ}–*igp3*^{AEQ}). To assess the specificity of MLG43 perception impairment in *igp* mutants, they were also treated with CHI6 (50 µM) and we selected those *igp*s with similar $_{cyt}Ca^{2+}$ bursts as those observed in Col-0^{AEQ}

plants, which contrasted with *cerk1-2*^{AEQ} plants fully impaired in CHI6 perception, as previously reported (Mélida *et al.*, 2018; Rebaque *et al.*, 2021) (Figure 4.2).

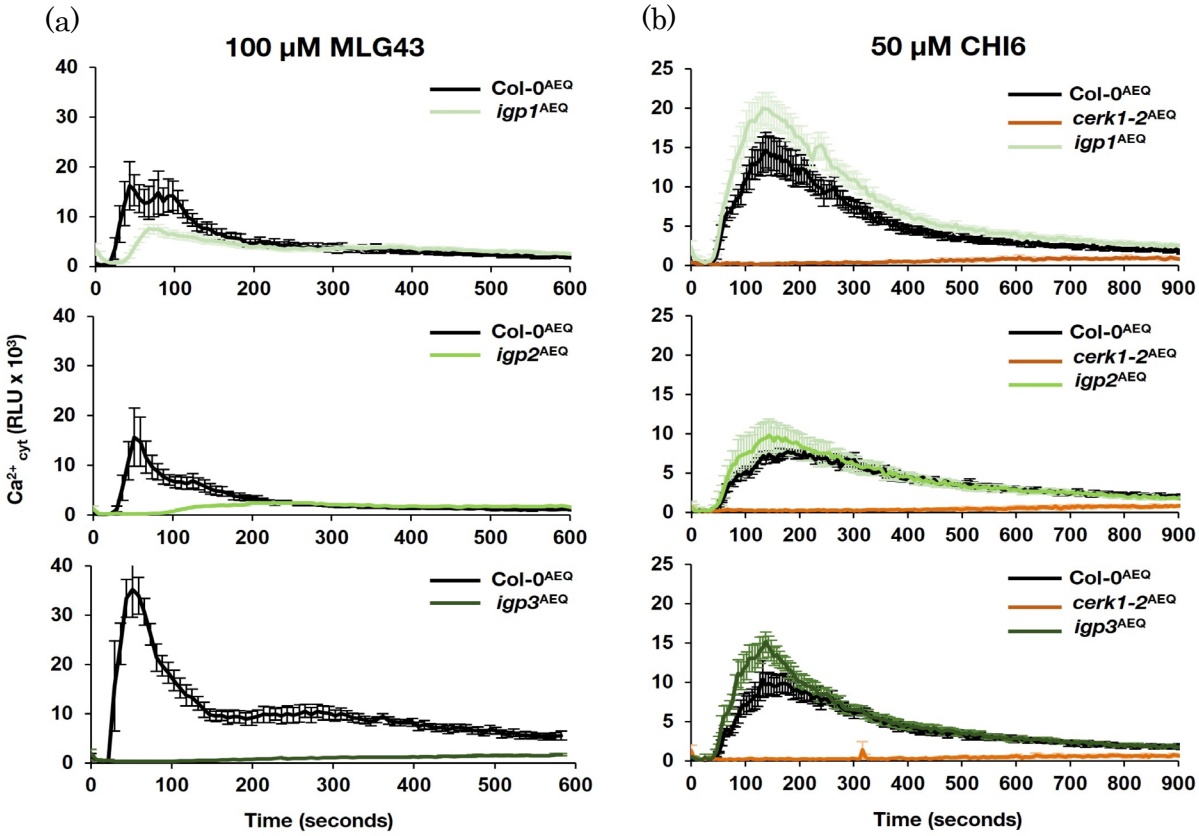

Figure 4.2: Identification of *Arabidopsis thaliana* mutants impaired in glycan perception (*igp*). $_{cyt}Ca^{2+}$ burst upon application of (a) 100 µM MLG43 and (b) 50 µM CHI6 was measured as Relative Luminescence Units (RLUs) over time in Col-0^{AEQ} and *igp*^{AEQ} mutants. The *cerk1-2*^{AEQ} line, impaired in CHI6 perception, was included for comparison. Data represent the mean ± standard error (n = 4 in Col-0^{AEQ} and *cerk1-2*^{AEQ}; n = 8 in *igp*^{AEQ}). Data are from one of the four experiments performed that gave similar results.

These data suggested that the mechanism of perception of CHI6 and MLG43 in Arabidopsis might not be identical, in contrast to what has been described in rice (Yang *et al.*, 2022). No mutations were found in the *Aequorin* transgene sequence in *igp1*^{AEQ}–*igp3*^{AEQ} (online data set A.1), and no differences were observed in endogenous Ca^{2+} levels between the *igp1*^{AEQ}–*igp3*^{AEQ} and Col-0^{AEQ} seedlings, based on Ca^{2+} discharge analyses (Figure 4.3a). These data supported that the lower $_{cyt}Ca^{2+}$ bursts observed in MLG43-treated *igp1*^{AEQ}–*igp3*^{AEQ} seedlings were the result of the defective perception of MLG43.

To check if the mutations were recessive or dominant, a chi-square test was performed with M_2 progeny of backcrosses of the mutants (Table 4.1), showing that

all the mutations were recessive. *igp* mutants were also crossed between them for an allelism test, and we found that *igp2* and *igp3* were allelic, meaning that they carry a mutation in the same gene (Table 4.1, Figure 4.3b).

Table 4.1: Chi-square test of the *igp*s and the allelism test.

	H_0	*p*- value	Result
igp1 ^{AEQ}	recessive mutation	0,7 > *P* > 0,5	H_0 accepted
igp2 ^{AEQ}	recessive mutation	0,5 > *P* > 0,3	H_0 accepted
igp3 ^{AEQ}	recessive mutation	0,8 > *P* > 0,7	H_0 accepted
Allelism test *igp2* ^{AEQ} **x *igp3*** ^{AEQ}	allelic mutations	*P* > 0,95	H_0 accepted

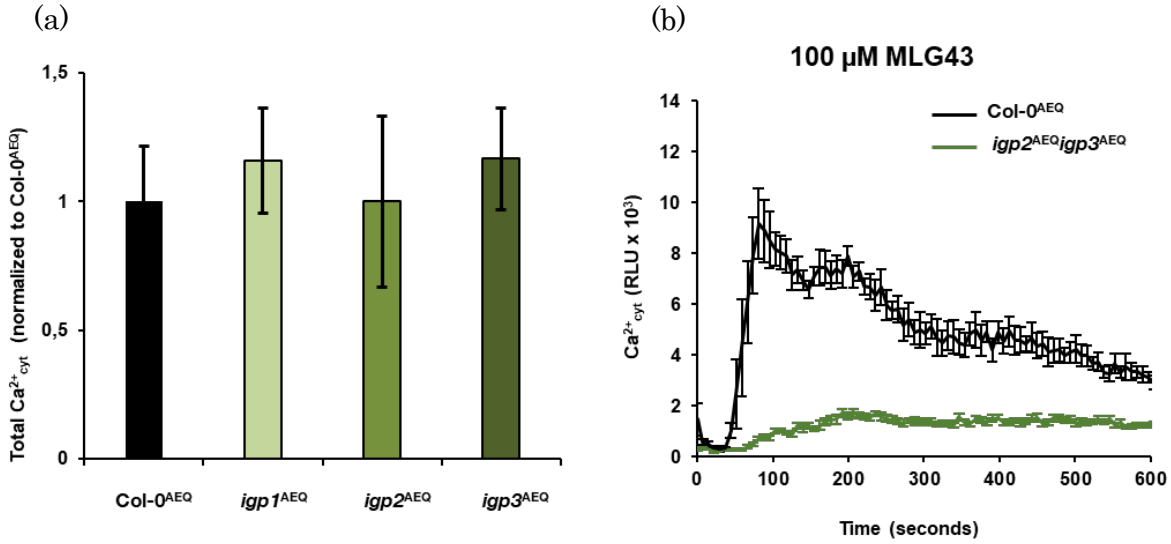

Figure 4.3: The allelism test showed that *igp2* and *igp3* are allelic. (a) Total calcium of the *igp1-igp3*^{AEQ} was discharged by the addition of 1,5 mM $CaCl_2$ to the seedlings. The kinetic areas were integrated, and their values were used for the calculation of the total Ca^{2+}% produced which was similar in all genotypes tested. (b) Elevation of cytoplasmatic calcium concentration over time, measured as Relative Luminescence Units (RLUs) after treatment with 100 µM of MLG43, of Col-0^{AEQ} and F_1 *igp2*^{AEQ}*igp3*^{AEQ} cross eight-day old seedlings. The lack of response to MLG43 in F_1 indicates that both mutations are allelic. Data represent the mean ± standard error (n = 6 in Col-0^{AEQ} and n = 12 in F_1 of *igp2*^{AEQ}*igp3*^{AEQ}). Data from one of the three experiments performed that gave similar results.

4.1.2. *igp* mutants are impaired in LRR-MAL RKs genes

Genomic DNA from 50 individuals selected from F_2 progeny of *igp1*^{AEQ}, *igp2*^{AEQ} and *igp3*^{AEQ} backcrosses with Col-0^{AEQ} was sequenced and assembled to identify putative mutations (frequency higher than 0.99 in alignments; Table 4.2; Online data set A.1).

Table 4.2: Chromosomal localization of SNPs mutations in *igp* mutants.

Only mutations with Allele Frequency (AF) equal or higher than 0.99 are shown.

Candidate	Locus	Position*	AF**	Protein	Change	Motif affected
igp1	***AT1G56145***	***21008701***	**0.99**	**LRR-MAL RLK**	**E to K (906)**	**Protein Kinase Domain**
igp2	***AT1G56130***	***20995970***	**1**	**LRR-MAL RLK**	**G to E (625)**	**Transferase(Phosphotransferase) domain1**
	AT1G56140	*21006273*	1	LRR-MAL RLK	6th intron	
	AT1G58050	*21482658*	1	RNA helicase family protein	silent mutation	
	AT1G57800	*21412060*	0.99	ORTH3	G to E (75)	Between zinc finger domains
igp3	***AT1G56130***	***20995970***	**1**	**LRR-MAL RLK**	**G to E (625)**	**Transferase(Phosphotransferase) domain1**
	AT1G56140	*21006273*	1	LRR-MAL RLK	6th intron	
	AT1G58050	*21482658*	0.99	RNA helicase family protein	silent mutation	
	AT1G58037	*21474508*	0.99	Cysteine/Histidine-rich C1 domain family protein	R to H (10)	Near N-terminal end
	AT1G58100	*21513013*	0.99	TCP DOMAIN PROTEIN 8	silent mutation	
	AT1G54610	*20394863*	0.99	Protein kinase superfamily protein	5th intron	

We found that *igp1*^{AEQ} carries a point mutation in the *AT1G56145* gene that encodes an RK with an LRR-MAL ECD. IGP1 was simultaneously described by Tseng *et al.*, 2022 who named the same gene as *CORK1; CELLO-OLIGOMER RECEPTOR KINASE 1*. The sequenced mutation in *igp1*^{AEQ} resulted in E906K amino acid change in its KD (Table 4.2, Figure 4.4, Online data set A.1). On the other hand, sequencing confirmed the results of the allelism test (Figure 4.3b) since *igp2*^{AEQ} and *igp3*^{AEQ} share the same point mutation in the *AT1G56130* gene, encoding an additional LRR-MAL RK, which resulted in G773E amino acid change in its KD (Table 4.2, Figure 4.4, Online data set A.1).

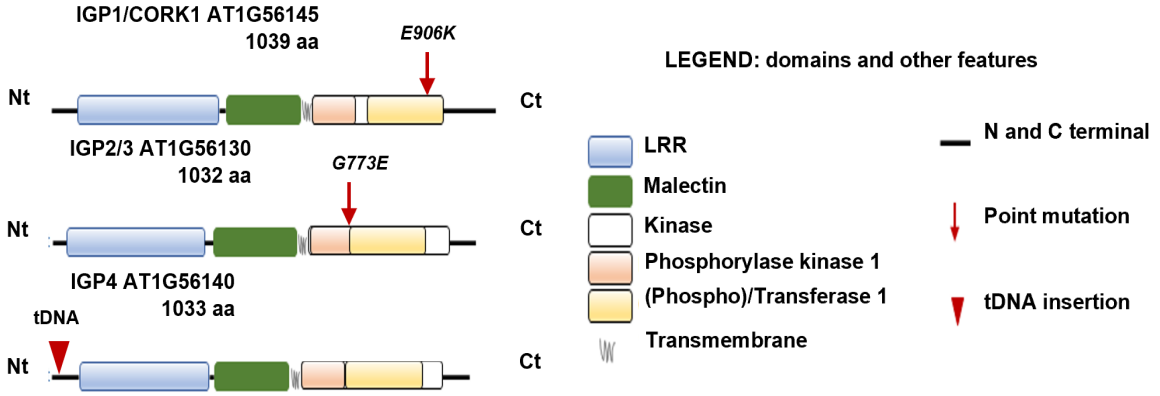

Figure 4.4: Representation of IGP1, IGP2/3 and IGP4 domains. Leucine-Rich Repeat (LRR; blue), Malectin (MAL; green), phosphorylase kinase (orange) and phosphotransferase (yellow) of Kinase Domain (KD; white), N- and C-terminal domains (black lines) and Transmembrane Domain (TM; gray). Red arrows indicate the position of the mutations in the coding regions of *igp1*^{AEQ}, *igp2*^{AEQ} and *igp3*^{AEQ}, and the red triangle indicates the insertion of the T-DNA sequence in *igp4*.

Notably, these two LRR-MAL RKs are in a genomic cluster with two additional genes, *AT1G56120* and *AT1G56140*, which encode two additional LRR-MAL RKs (Yang, Wang *et al.*, 2021). These RKs are members of a specific group of LRR-MAL proteins that comprise at least 13 genes in the *A. thaliana* genome, with *AT1G56120*, *AT1G56130*, *AT1G56140* and *AT1G56145* genes constituting a specific clade of the family (Figure 4.5a). This family has a few described members, such as RFK1 (*AT1G29720*), that promotes compatible pollen grain hydration and pollen tube growth (Lee & Goring, 2021) and the BRASSINOSTEROID (BR) KINASE (BSK) 3- INTERACTING RLK (BSR), however the majority of the members of this family are not well characterized (Yang, Wang, *et al.*, 2021).

To check whether IGPs were glycan-responsive genes we used reverse transcription quantitative Real-Time Polymerase Chain Reaction (qRT-PCR), to quantify their expression in response to MLG43, CHI6 and CEL3. Only the expression levels of *AT1G56140*, but not that of *AT1G56120, AT1G56130* and *AT1G56145*, were upregulated upon treatment of seedlings with those glucans (Figure 4.5b).

To understand the role of *AT1G56120* and *AT1G56140* genes in the perception of MLG43 and CHI6 we first obtained loss-of-function T-DNA insertion lines for both genes. Then we measured the upregulation of PTI marker genes, i.e., *WRKY53* and *CYP81F2,* using qRT-PCR 30 minutes after glucan treatment in *at1g56120* and *at1g56140* mutant lines (Figure 4.5c). The expression of both marker genes, *WRKY53* and *CYP81F2,* was compromised in the *at1g56140* knockout mutant, but not in *at1g56120* plants (Figure 4.5c). Both mutants displayed a similar

upregulation of *WRKY53* and *CYP81F2* expression to wild-type plants upon CHI6 treatment (Figure 4.5c). These analyses indicate that similar to *AT1G56145* and *AT1G56130*, *AT1G56140* plays a prominent role at least in MLG43 perception.

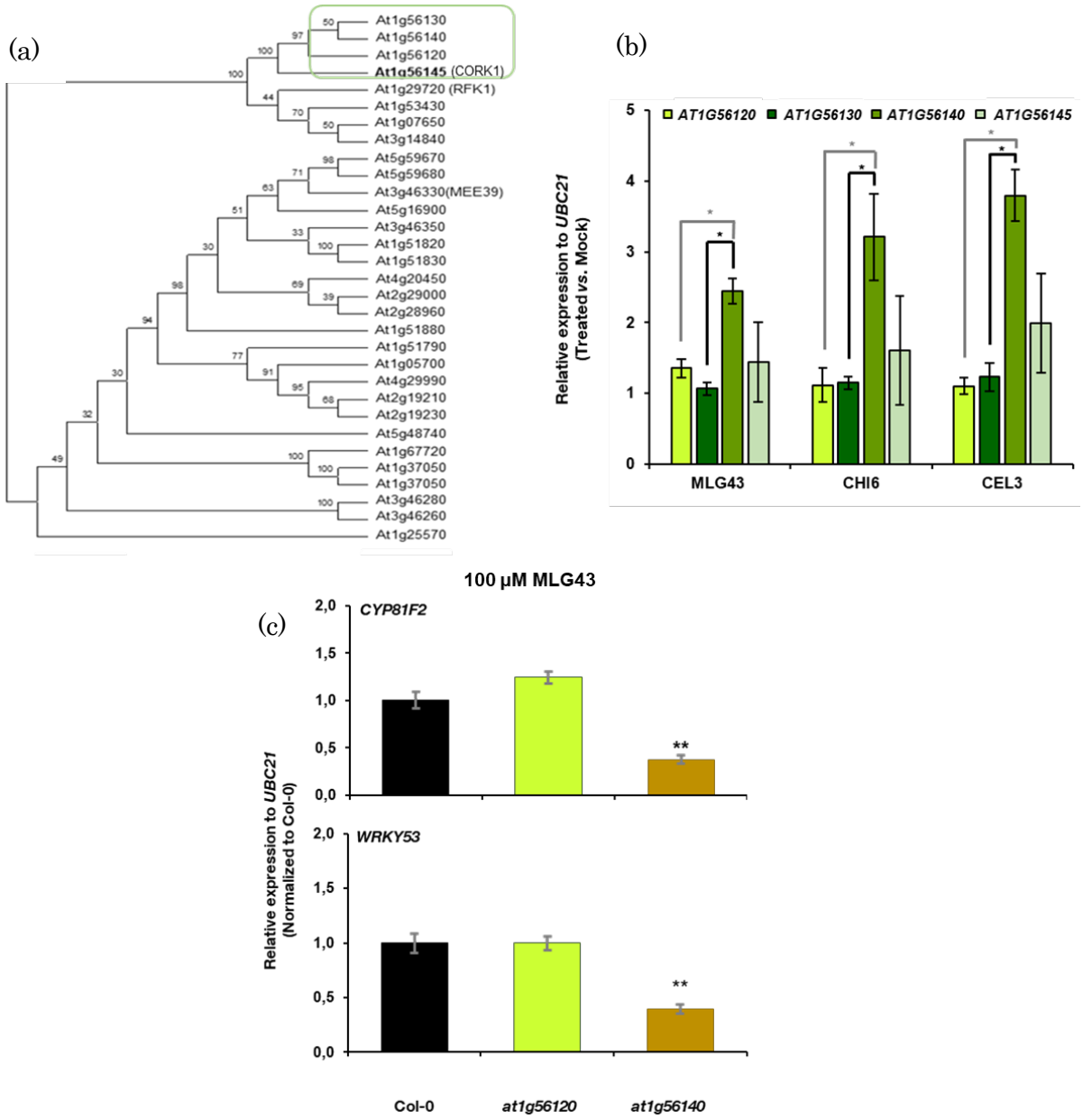

Figure 4.5: LRR-MAL RK family in *Arabidopsis thaliana* includes additional members, such as IGP4/AT1G56140, that is also required for MLG43 perception. (a) Phylogenetic tree of the *Arabidopsis thaliana* LRR-MAL RKs. The full-length sequence of *Arabidopsis thaliana* proteins predicted to contain a MAL domain in their ECDs (del Hierro *et al.*, 2021) were aligned using the ClustalW algorithm. The evolutionary history was inferred using the Minimum Evolution method. The analysis involved 25 protein sequences. All ambiguous positions were removed for each sequence pair. Evolutionary analyses were conducted in MEGA6. (b) Endogenous expression of the four genes (*AT1G56120*, *AT1G56130* (IGP2/3), *AT1G56140* (IGP4), *AT1G56145* (IGP1)) of the IGP

clade family members in Col-0 wild-type plants determined by qRT-PCR in seedling treated (30 minutes) with water (mock), MLG43 (100 µM), CEL3 (10 µM) or CHI6 (50 µM). Gene expression values are relative to the housekeeping gene *UBC21* (*AT5G25769*), and to the expression levels in mock treated. (c) qRT-PCR analysis of the immunity marker genes *CYP81F2* and *WRKY53* in T-DNA lines of LRR-MAL RKs members of the same clade (*at1g56120* and *at1g56140*) and Col-0 seedlings after treatment with MLG43 (100 µM). Gene expression values are relative to the housekeeping gene *UBC21* (*AT5G25769*) and are normalized to Col-0 (value of 1). Data represent the mean ± standard error of three technical replicates out of three independent biological replicates (n = 3). Statistically significant differences were calculated according to Student's t-test (*P <0.05, ** 0.01< P <0.001).

To further validate the phenotype of the *at1g56140* mutant, we crossed this line with Col-0^{AEQ} to generate a Ca^{2+} sensor in the mutant. The $_{cyt}Ca^{2+}$ burst upon MLG43 and CHI6 treatments was tested in the homozygous *at1g56140*^{AEQ} line. *at1g56140*^{AEQ} was impaired in MLG43 but not in CHI6 perception, like *igp1*^{AEQ}–*igp3*^{AEQ}, and such defective response was not caused by any alteration in the endogenous levels of Ca^{2+}, as revealed by Ca^{2+} discharge experiments (Figure 4.6). Accordingly, the *at1g56140* mutant was named *igp4* and selected for further analyses to determine the contribution of AT1G56140/IGP4 RK in the regulation of PTI responses mediated by MLG43 (Figure 4.6).

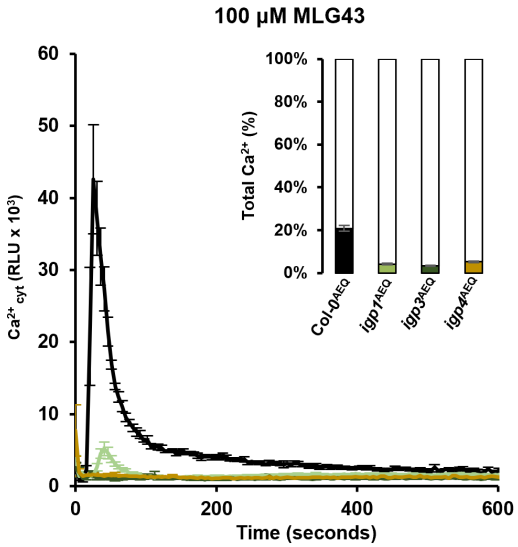

Figure 4.6: *igp4*^{AEQ} is also impaired in MLG43 perception. $_{cyt}Ca^{2+}$ burst measured as Relative Luminescence Units (RLUs) over time in Col-0^{AEQ}, *igp1*^{AEQ}, *igp3*^{AEQ} and *igp4/at1g56140*^{AEQ} seedlings upon treatment with 100 µM MLG43. Data represent the mean ± standard error (n = 4 in Col-0^{AEQ} and n = 8 in *igp*$_s^{AEQ}$). Total Ca^{2+} was discharged by the addition of 1 mM $CaCl_2$ to the wells and these values were used for the calculation of the total Ca^{2+} % induced by MLG43 treatment (graph at top right). This is one of three experiments performed that gave similar results.

4.1.3. IGPs are also required for the perception of additional cellulose- and MLGs-derived oligosaccharides

To assess the specificity of the IGPs in the perception of MLG43, we measured the $_{cyt}Ca^{2+}$ bursts in *igp1*^{AEQ}, *igp3*^{AEQ}, *igp4*^{AEQ} and Col-0^{AEQ} seedlings after treatment with different carbohydrate ligands such as CEL3 (Figure 4.7a) and OGs (DP10–DP12) (Figure 4.7c), the peptide AtPep1 (Figure 4.7e) and the MAMP flg22 (Figure 4.7d). Remarkably, the three *igp*^{AEQ} lines were almost fully impaired in CEL3-mediated $_{cyt}Ca^{2+}$ burst activation, suggesting that these RKs are also required for the perception of cellulose-derived oligosaccharides (Figure 4.7a). In contrast, the $_{cyt}Ca^{2+}$ responses induced by flg22, OGs and AtPep1 treatments in the mutants were similar to those observed in Col-0^{AEQ} (Figure 4.7d, c, e).

As other cellulose- and MLGs-derived oligosaccharides, such as cellobiose (CEL2), cellotetraose (CEL4), cellopentaose (CEL5) and MLG34, have been described as carbohydrates that trigger PTI in *A. thaliana* (Locci *et al.*, 2019; Rebaque *et al.*, 2021; Souza *et al.*, 2017), we also determined $_{cyt}Ca^{2+}$ burst activated by these glucans in *igp*^{AEQ} mutants and Col-0^{AEQ} (Figure 4.8). The three mutants showed reduced $_{cyt}Ca^{2+}$ influxes in comparison with Col-0^{AEQ} upon treatment with MLG34 (Figure 4.8b), CEL4 (Figure 4.8d) and CEL5 (Figure 4.8e), indicating that the three LRR-MAL RKs are required for the perception of these cellulose- and MLGs-derived oligosaccharides. By contrast, the $_{cyt}Ca^{2+}$ influxes triggered by CEL2 were, under our experimental conditions, very low, even in Col-0^{AEQ} (Figure 4.8f), suggesting that this disaccharide has low immunogenic activity in Arabidopsis, and that CEL3 is the cellulose-derived oligosaccharide with the lowest Degree of Polymerization (DP) perceived through the sensing mechanism involving these RKs (Figure 4.8).

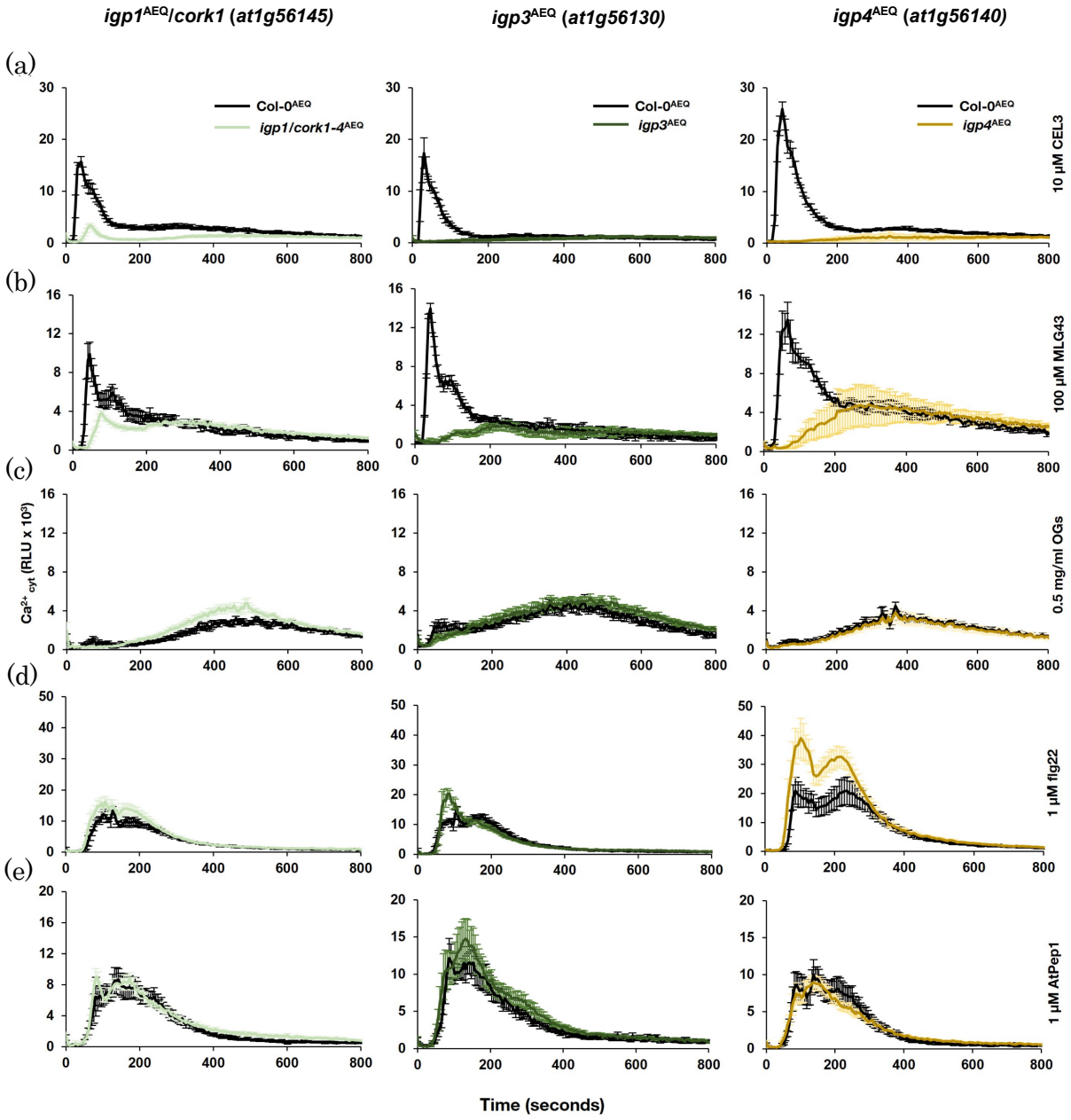

Figure 4.7: *igp*^{AEQ} mutants are also impaired in CEL3 perception. $_{cyt}Ca^{2+}$ burst measured as relative luminescence units (RLUs) over time in Col-0^{AEQ}, *igp1*^{AEQ}, *igp3*^{AEQ} and *igp4*^{AEQ} seedlings after treatment with: (a) 10 µM CEL3; (b) 100 µM MLG43; (c) 0.5 mg/ml OGs; (d) 1 µM flg22; and (e) 1 µM AtPep1. Data represent the mean ± standard error (n = 4 in Col-0^{AEQ} and n = 8 in *igp*s^{AEQ}). Data are from one of three experiments performed that gave similar results.

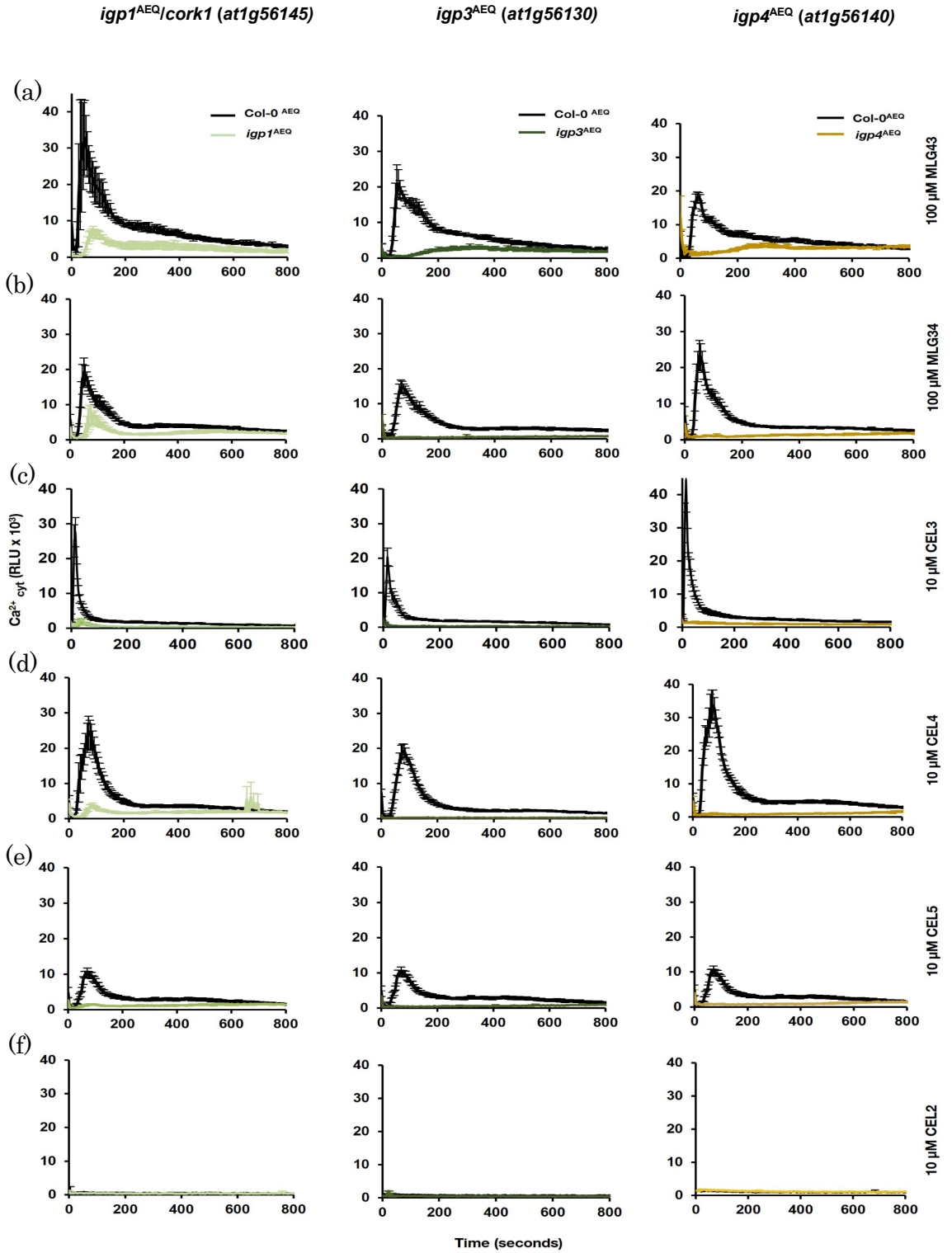

Figure 4.8: *igp* mutants are impaired in additional MLG- and cellulose-derived oligosaccharides. $_{cyt}Ca^{2+}$ burst measured as Relative Luminescence Units (RLUs) over time in 8-day-old Col-0^{AEQ}, *igp1*^{AEQ}, *igp3*^{AEQ} and *igp4*^{AEQ} seedlings after treatment with: (a) 100 µM MLG43; (b) 100 µM MLG34; (c) 10 µM CEL3; (d) 10 µM CEL4; (e) 10 µM CEL5; and (f) 10 µM CEL2. Data represent the mean ± standard error (n = 3 in the case of Col-0^{AEQ} and n = 12 in the case of *igps*^{AEQ}). The x-axis scale in (c) has been shortened for a better comparison of the enhanced response of seedlings to CEL3. Data are from one of three experiments performed that gave similar results.

To further validate whether the mechanism of perception of cellulose- and MLGs-derived oligosaccharides in *A. thaliana* share some PRRs and signalling components, we performed cross-elicitation experiments by treating 8-day old Col-0^{AEQ} seedlings, first with MLG43 or CEL3, and a few minutes later with either CEL3 or MLG43 (Figure 4.9). In Col-0^{AEQ} seedlings first treated with MLG43, $_{cyt}Ca^{2+}$ influxes were not observed upon the second application of CEL3 (MLG43 + CEL3) (Figure 4.9c), similarly to what was observed after treatments with CEL3 + CEL3 (Figure 4.9b) and MLG43 + MLG43 (Figure 4.9a), indicating that the mechanisms of perception of MLG43 and CEL3 share molecular components in Arabidopsis.

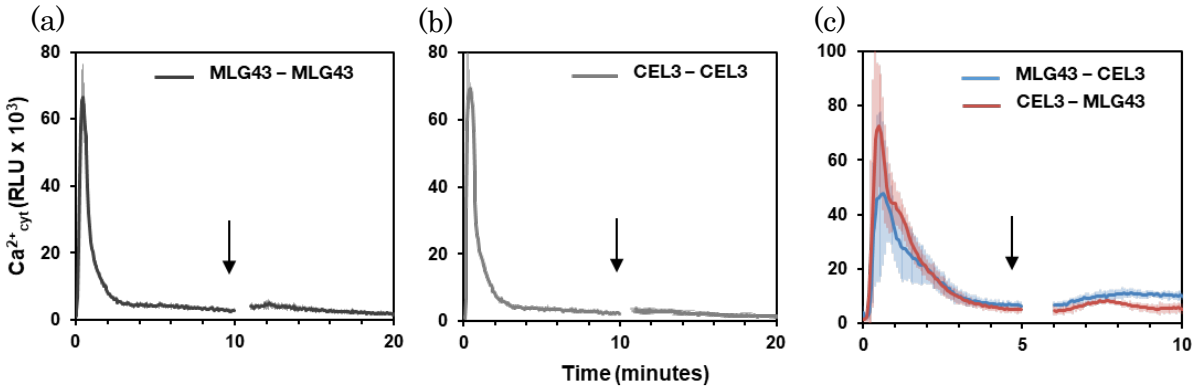

Figure 4.9: Cross-elicitation during the refractory period of calcium burst triggered by MLG43 or CEL3. Data show cytoplasmatic calcium burst measured as relative luminescence units (RLUs) over time in 8- day-old Col-0^{AEQ} seedlings after sequentially treatments with (a) 50 µM MLG43 and 50 µM MLG43, (b) 10 µM CEL3 and 10 µM CEL3, and (c) 50 µM MLG43 and 10 µM CEL3 (blue) and 10 µM CEL3 and 50 µM MLG43 (red). Arrow indicates the application time of the second elicitor within the refractory period of the first elicitation. Data represent the average RLU values of 4 seedlings (n = 4) ± standard deviation. Data are from one of the three experiments performed that gave similar results.

4.1.4. Additional PTI hallmarks in *igp* mutants

To confirm the role of this group of LRR-MAL receptors as potential RKs for cellulose- and MLGs-derived oligosaccharide perception and PTI activation, we checked additional PTI responses after MLG43 and CEL3 treatments, firstly monitoring ROS production in *igp1*^{AEQ}, *igp3*^{AEQ}, *igp4*, Col-0 and *rbohD* lines (this last one impaired in ROS production; Torres 2010; Morales *et al.*, 2016), upon treatment with MLG43, CEL3, CHI6 and flg22 (Figure 4.10). The ROS burst was partially impaired in the *igp* mutants compared with the Col-0 plants after treatment with MLG43, and was significantly reduced, even to a higher extent, after CEL3 treatment (Figure 4.10a, b). In both cases, the reduction in ROS was

not as noticeable as in *rbohD,* included as positive control of ROS impairment. Notably, the ROS burst in *igp* mutants upon treatment with CHI6 and flg22 was not altered in comparison with Col-0 plants (Figure 4.10d, c).

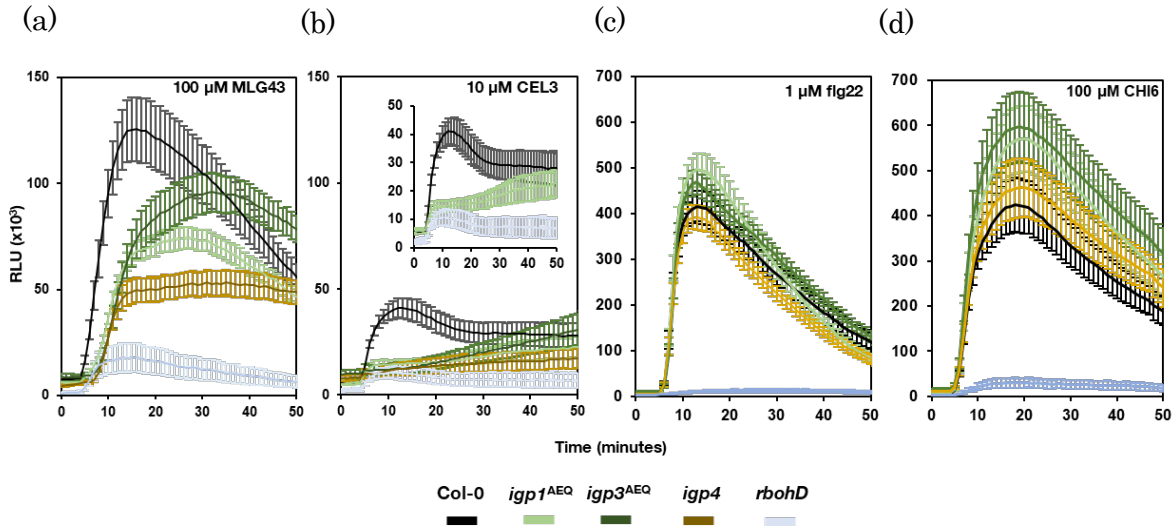

Figure 4.10: ROS production in *igp* mutants is also affected after MLG43 and CEL elicitations. Reactive Oxygen Species (ROS) production was monitored as H_2O_2 production over a period of 50 minutes by luminol assays and measured as Relative Luminescence Units (RLUs) in the indicated genotypes; (a) 100 µM MLG43 (b) and 10 µM CEL3 (c) 1µM flg22 and (d) 100 µM CHI6 were added 5 minutes after the experiment. Data represent mean ± standard error (n = 8). Comparison with Col-0 assessed by Student's t-test (n = 24) at the time of the Col-0 peak shows statistically significant differences for *igp1*^{AEQ} and *igp3*^{AEQ} ($P < 0.01$) and *igp4*^{AEQ} ($P < 0.001$) in response to MLG43. Likewise, all three mutants show statistical differences at $P < 0.001$, compared with Col-0, in response to CEL3. However, for flg22 and CHI6 there was no statically significant differences ($P < 0.001$) for *igp*s^{AEQ}. *rbohD* plants impaired in ROS production showed statistically significant differences ($P < 0.001$) with all treatments. These results are from one representative experiment out of three performed that gave similar results. The inset in (b) has been included in the graph to allow an easy comparison of the RLU data for *igp1*^{AEQ} and Col-0.

Next, we tested the phosphorylation of MAPKs by Western Blot (Figure 4.11). MPK3 and MPK6 phosphorylation triggered by MLG43 and CEL3 was significantly reduced in *igp1*^{AEQ}, *igp3*^{AEQ} and *igp4* plants compared with Col-0 plants, whereas MAPKs phosphorylation in the mutants was similar to Col-0 in response to CHI6 (Figure 4.11). MPK4/11 phosphorylation was almost undetectable in either CEL3-treated or MLG43-treated plants, as reported previously (Rebaque *et al.*, 2021).

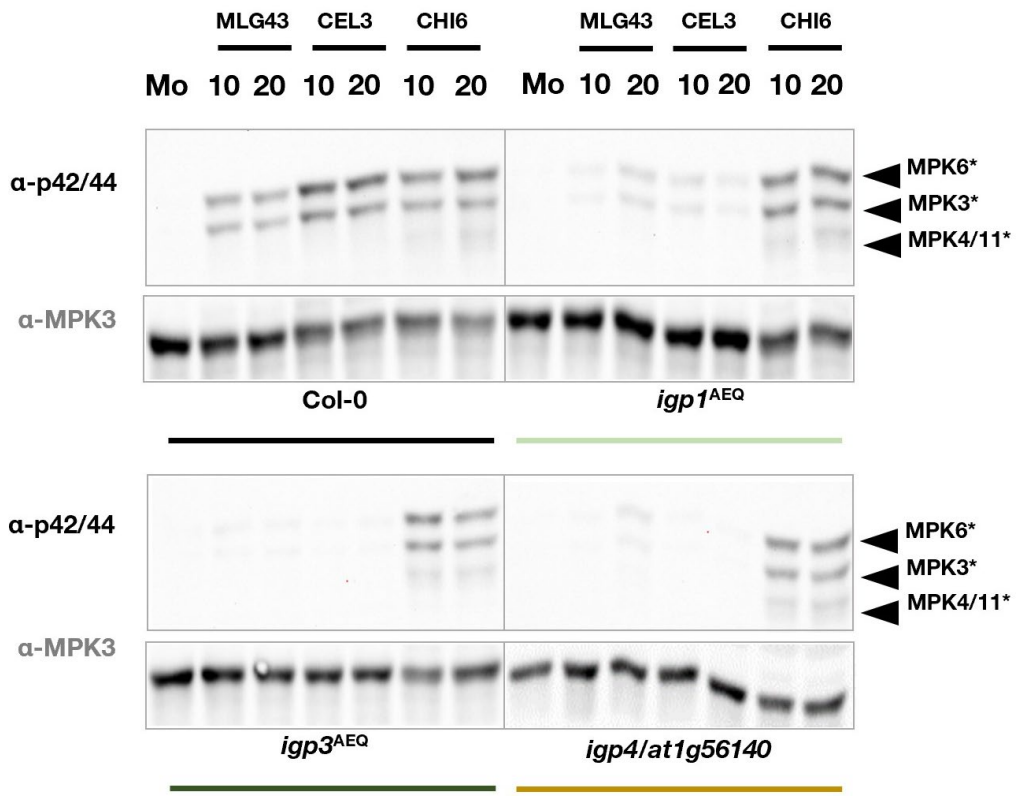

Figure 4.11: MAPKs phosphorylation in *igp* mutants is affected after MLG43 and CEL elicitations. MAPKs phosphorylation was analyzed in seedlings of Col-0, *igp1*^{AEQ}, *igp3*^{AEQ} and *igp4* treated with 100 µM MLG43, 10 µM CEL3, 50 µM CHI6 or water (mock). Western Blot using α-pTEpY antibody (α-p42/44) for phosphorylated MAPK moieties was performed with samples harvested at 10 and 20 minutes. Mock samples (Mo) corresponding to a 10-minutes treatment with water were included as basal expression controls. Black arrows indicate the positions of phosphorylated MPK6 (top), MPK3 (middle) and MPK4/11 (bottom). α-MPK3 was used as a total protein control to show the loading of each gel. These results are from one representative experiment out of two performed that gave similar results.

Last, we performed qRT-PCR analysis to study the expression of *WRKY53* and *CYP81F2*, two PTI-marker genes upregulated by CHI6 and MLG43 (Mélida *et al.*, 2018, Rebaque *et al.*, 2021) in the *igp* mutants (Figure 4.12). The upregulation of *WRKY53* and *CYP81F2* in response to MLG43 (Figure 4.12 a, d) and CEL3 (Figure 4.12b, e) was partially impaired in *igp1*^{AEQ}, *igp3*^{AEQ} and *igp4* seedlings, compared with Col-0 plants, whereas it was similar in response to CHI6 (Figure 4.12c, f).

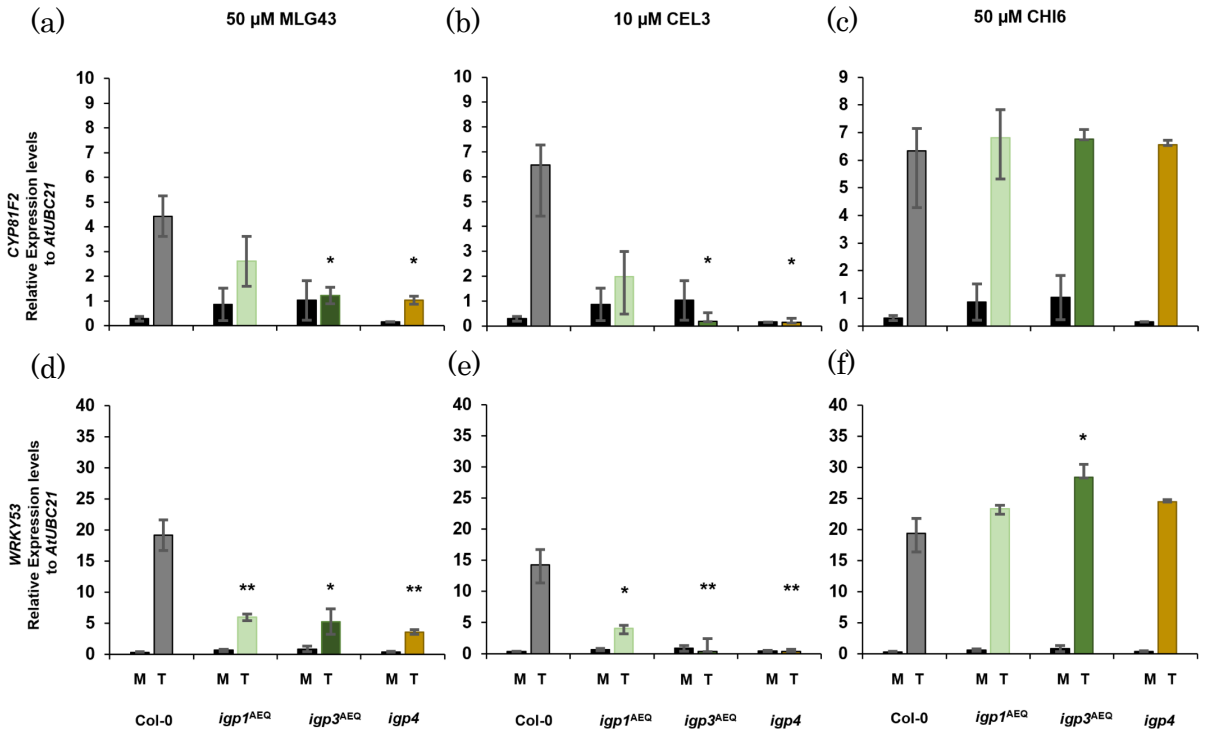

Figure 4.12: qRT-PCR analysis reinforced the role of IGPs in the perception of cellulose- and MLGs-derived oligosaccharides. Expression levels of *CYP81F2* marker gene after (a) 50 µM MLG43, (b) 10 µM CEL3 and (c) 50 µM CHI6 treatments; and *WRKY53* marker gene after (d) 50 µM MLG43, (e) 10 µM CEL3 and (f) 50 µM CHI6 treatments, relative to the housekeeping gene *UBC21* (*AT5G25769*) 30 minutes after mock treatment (M) or the application of the oligosaccharides (T) are shown. Data represent mean ± standard error of three technical replicates out of three independent biological replicates (n = 3). Statistically significant differences between MLG43-, CEL3- or CHI6-treated *igp*s *versus* treated Col-0 according to Student's t-test (*P < 0.05, **0.01 < P > 0.001, ***P < 0.001).

Together, these data support the role of the three LRR-MAL RKs in the perception of cellulose-derived oligosaccharides and, to a lesser extent, in the perception of MLGs-derived oligosaccharides.

4.1.5. Role of LysM-RKs in CEL- and MLGs derived oligosaccharides perception

As previous works reported that MLGs perception in Arabidopsis and rice involved LysM-PRRs, like CERK1, LYK4 and LYK5 (Rebaque *et al.*, 2021, Yang, *et al.*, 2021), we determined ROS production, MPK3/MPK6 phosphorylation and PTI marker genes upregulation upon treatment with MLG43 and CEL3 of seedlings

from Col-0, *cerk1-2* and the *cerk1-2 lyk4 lyk5* triple mutant, which was generated in this work (Figure 4.13). *cerk1-2* and *cerk1-2 lyk4 lyk5* plants displayed similar ROS kinetics and bursts to Col-0 after CEL3 treatment, and only a minor diminution upon MLG43 treatment in comparison to Col-0, whereas this PTI response was greatly impaired after CHI6 treatment (Figure 4.13a, b, c).

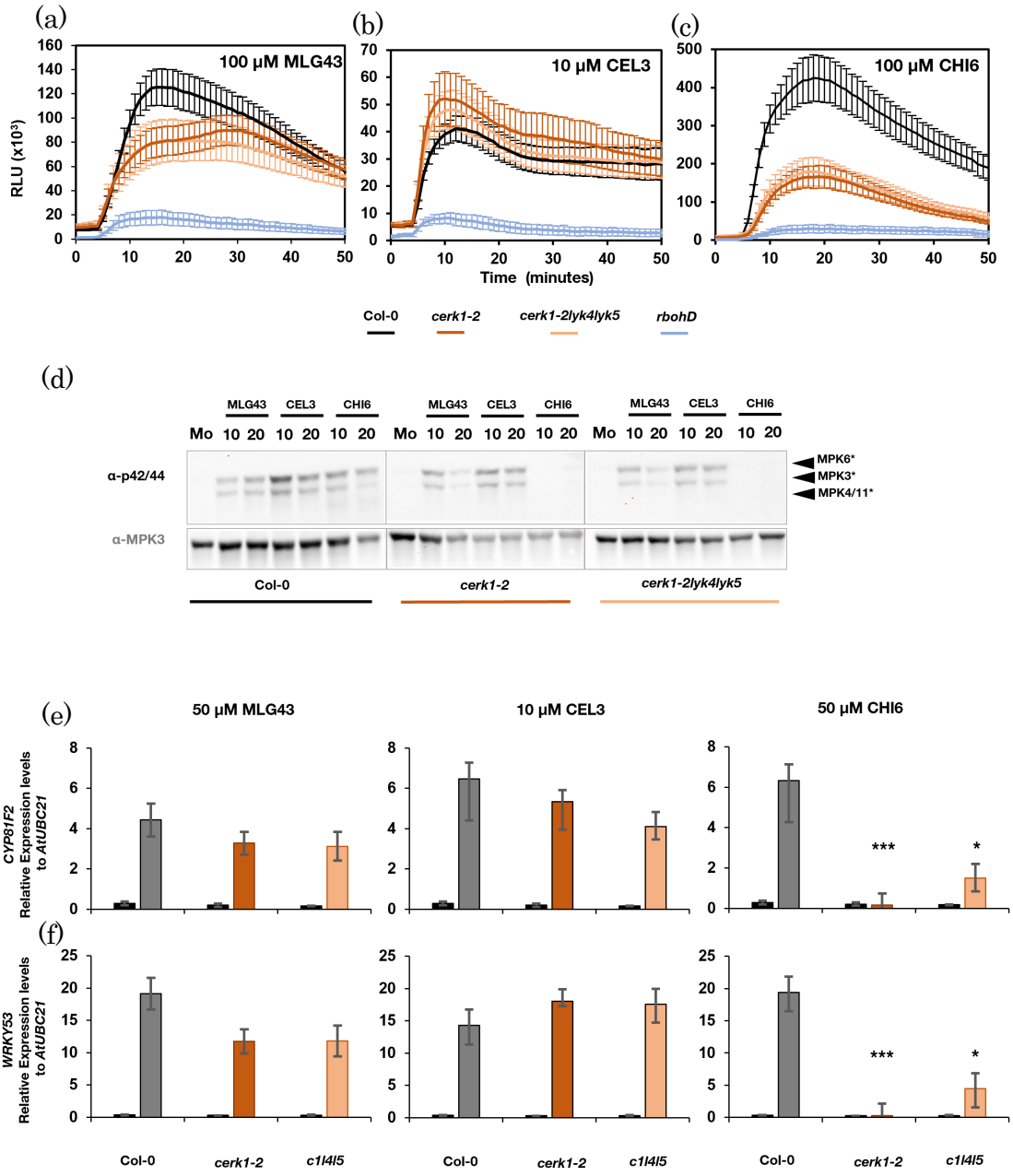

Figure 4.13: Activation of PTI hallmarks by MLG43, CEL3 and CHI6 in LysM-PRR mutants. (a-c) Reactive Oxygen Species (ROS) production was monitored as H_2O_2 production over a period of 50 minutes by luminol-assays, measured as Relative Luminiscence Units (RLUs), in seedlings of the indicated genotypes. Col-0 and *rbohD* were included as controls. Oligosaccharides were added 5 minutes after incubation of the seedling in plates in the Luminometer: (a) 100 µM MLG43; (b) 10 µM CEL3; (c) 100 µM CHI6. Comparison to Col-0 assessed by Student t-test at the time of the Col-

0 peak showed statistically significant differences for *cerk1-2lyk4lyk5* and *cerk1-2* ($P < 0.001$) only in response to CHI6 (c), whereas *rbohD* showed statistically significant differences ($P < 0.001$) in all treatments. Data represent mean ± standard error (n = 24). Data are from one of the three experiments performed that gave similar results. (d) Mitogen-Activated Protein Kinases (MAPK) phosphorylation was analyzed in 12-day-old seedlings of Col-0, *cerk1-2* and *cerk1-2lyk4lyk5* (*c1l4l5*) treated with either 100 µM MLG43, 10 µM CEL3, 50 µM CHI6 or water (mock). Samples were harvested at different time points (10 and 20 minutes). Mock samples (Mo) corresponding to 10 minutes treatment with water were included as basal expression controls. Black arrows indicate the position of phosphorylated MPK6 (top), MPK3 (middle) and MPK4/11 (bottom). α-MPK3 was used as total protein control to show the loading of each gel. These results are from one representative experiment out of the two performed that gave similar results. (e,f) qRT-PCR analysis in 12-days-old seedlings of Col-0, *cerk1-2* and *cerk1-2lyk4lyk5* (*c1l4l5*) genotypes. Expression levels of immune marker genes (e) *CYP81F2* and (f) *WRKY53* relative to housekeeping gene *UBC21* (*AT5G25769*) at 30 min after application of oligosaccharide 100 µM MLG43, 10 µM CEL3, 50 µM CHI6, or water (mock) are shown. Data represent mean ± standard error of three technical replicates out of three independent biological replicates (n = 3). Statistically significant differences between MLG43, CEL3 or CHI6 treated *cerk1-2* and *cerk1-2lyk4lyk5* (c1l4l5) *versus* treated Col-0 seedlings according to Student's t-test (* $P < 0.05$, ** $0.01 < P > 0.001$, *** $P < 0.001$).

Moreover, a slight reduction of the phosphorylation of MPK3/MPK6 in these mutants, compared with Col-0, was observed upon MLG43 and CEL3 treatment, although it was weaker than that observed with CHI6 (Figure 4.13d). Also, the MLG43-mediated upregulation of *WRKY53* and *CYP81F2* was only partially affected in *cerk1-2* and *cerk1-2 lyk4 lyk5* plants, whereas it was not altered upon CEL3 treatment (Figure 4.13e, f). These data indicate that MLG43 perception may involve CERK1, LYK4 and LYK5 LysM RKs, as described previously for MLGs in Arabidopsis and rice (Rebaque *et al.*, 2021; Yang *et al.*, 2021), whereas these RKs have almost no contribution to CEL3 perception.

4.1.6. Developmental phenotypes of *igp* mutants

We assessed the impact of the *igp1–igp4* mutations on plant developmental phenotypes and no significant differences were observed in the rosette and silique size and morphology of *igp1*^{AEQ} and *igp4*^{AEQ} plants in comparison with Col-0^{AEQ} or *cerk1-2*^{AEQ}, whereas *igp2*^{AEQ}/*igp3*^{AEQ} plants have rosettes and siliques slightly smaller than those of Col-0^{AEQ} plants or *cerk1-2*^{AEQ} (Figure 4.14). As *igp2*^{AEQ} and *igp3*^{AEQ} are allelic, we stuck to *igp3*^{AEQ} to characterize its function.

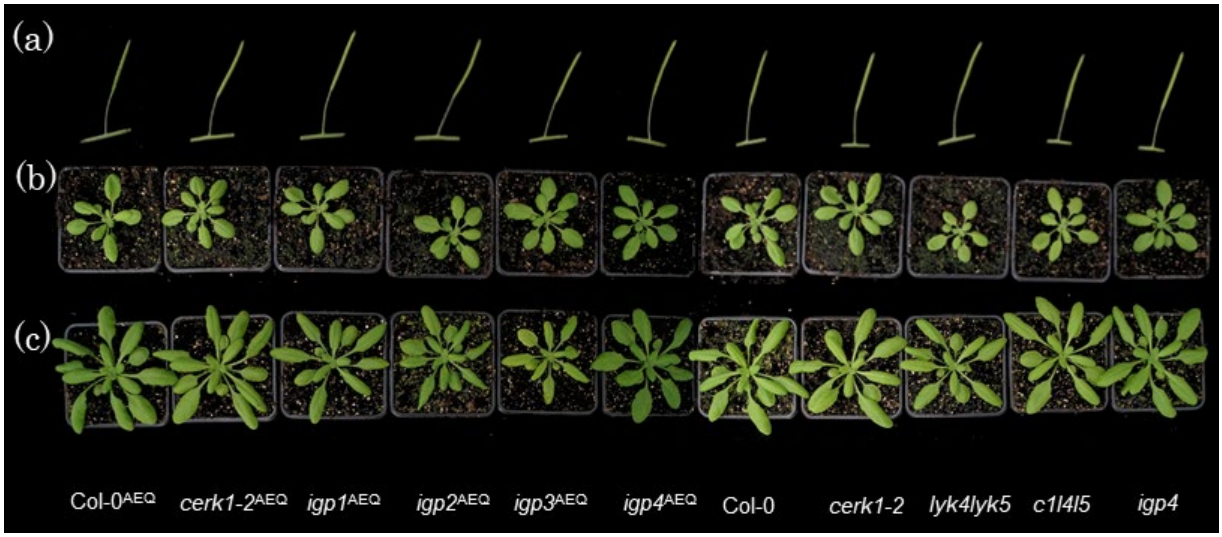

Figure 4.14: Developmental phenotypes of *igp* plants and LysM-PRR mutants. (a) Mature siliques and pedicels from 50-day-old plants of the indicated genotypes. (b,c) Rosettes in (b) 23 day-old plants grown under short-day photoperiod (10:14 hours light:dark), and (c) 28 day-old plants grown long-day photoperiod (14:10 hours light:dark). c1/l4/l5 is the abbreviation of the triple mutant *cerk1-2lyk4lyk5*.

4.1.7. *In silico* 3-D structural models of IGPs/LRR-MAL RKs reveal the importance of *igp1* and *igp2/igp3* point mutations in RKs predicted structure and function

To understand the importance of the identified mutations affecting IGPs, we first did a phylogenetic analysis and then modeled their predicted wild-type structures in comparison with mutated ones. Malectin (MAL) domains like those present in the ECDs of the LRR-MAL RK family have been previously described in animals to bind short glycans, based on the Nuclear Magnetic Resonance (NMR) structure of MAL from *Xenopus laevis* in complexes with maltose and nigerose (Schallus *et al.*, 2010). The MAL domain and MLD are present in at least three families of plant RKs (LRR-MAL, MLD-LRRs and CrRLK1Ls) (Yang, Wang *et al.*, 2021), and the ECDs of several CrRLK1L members, like ANXUR1 (ANX1), ANX2 and FERONIA (FER), have been crystallized, but oligosaccharide ligands have not yet identified in ITC binding experiments (Moussu *et al.*, 2018; Xiao *et al.*, 2019).

Phylogenetic analyses based on sequence conservation of ECDs (MAL and LRR domains) of *A. thaliana* LRR-MAL RK members (represented by IGP1/CORK1/AT1G56145) revealed that the MAL and LRR domains are highly conserved in cruciferous and other dicot species (Figure 4.15). On the other hand,

the ECD domains of IGP1/CORK1, IGP3 and IGP4 are evolutionarily divergent from ANX1 and ANX2 and *Xenopus* sp. MLD domains (Figure 4.15).

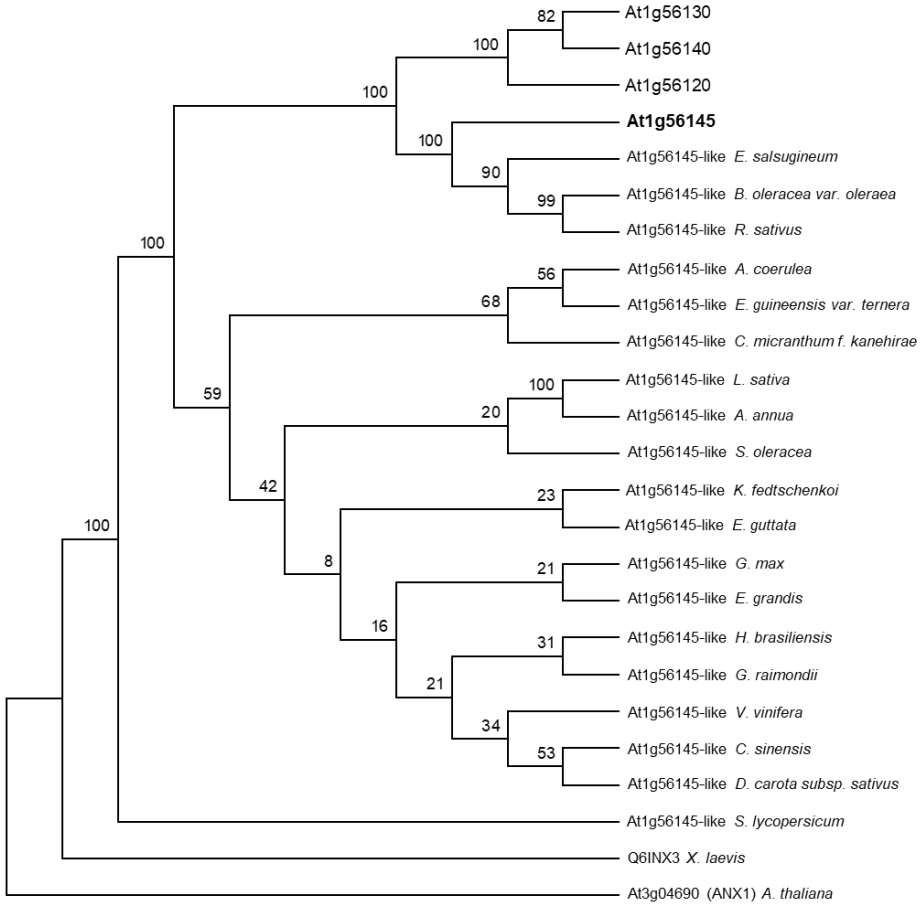

Figure 4.15: Phylogenetic analysis of LRR-MAL RKs in Arabidopsis and other plant species. Phylogenetic tree of the LRR-MAL RKs family members in selected plant species. The LRR-MAL ECD domain of IGP1/AT1G56145 was blasted against Uniprot protein database to retrieve a total of 248 protein ECD sequences that are evolutionarily related to AT1G56145. A representative subset of 25 sequences in different plant species was selected to build up this phylogenetic tree. In addition, the outgroup protein *Arabidopsis thaliana* ANX1, a member of a distinct clade of plant malectin RKs, and the *Xenopus laevis* malectin protein Q6INX3 were included in the tree for comparison. The evolutionary history was inferred using the Minimum Evolution method. Evolutionary analyses were conducted in MEGA6.

By performing the predicted *l*ocal Distance Difference Test (p*l*DDT), we saw that the AlphaFold database displays a spatial arrangement of all domains that does not properly describe the expected organization of these LRR-MAL RKs (Figure 4.16a, b, c). The model structure of IGP4 in the AlphaFold database is correctly

predicted but the spatial organization is not consistent with the extracellular (LRR + MAL) – transmembrane (TM) – intracellular (KD) separation (Figure 4.16d).

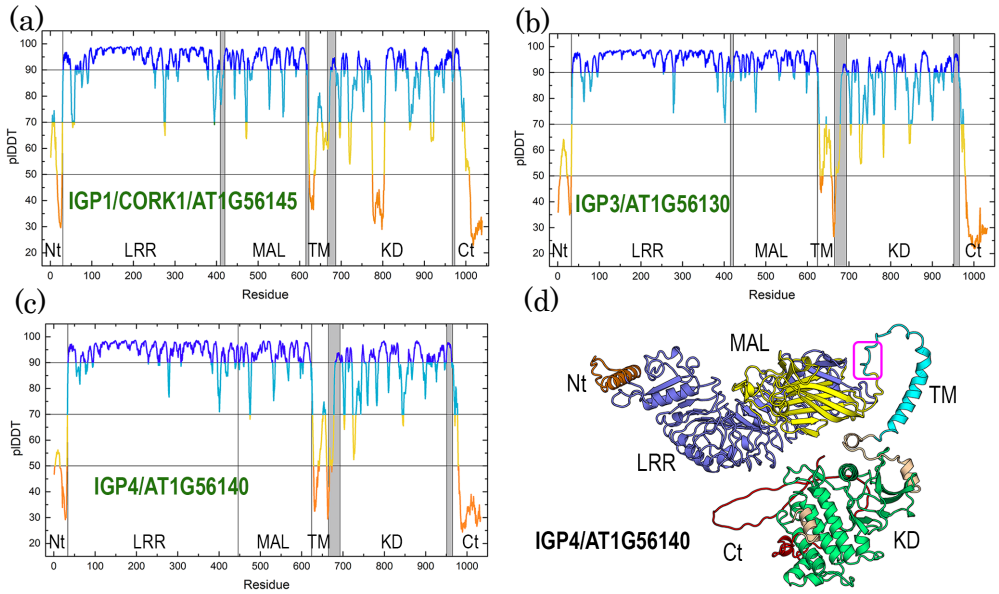

Figure 4.16: AlphaFold predictions for IGP1, IGP3 and IGP4 protein structures. (a) Plot of predicted *l*ocal Distance Difference Test (p*l*DDT) for IGP1/CORK1/AT1G56145. This AlphaFold metric gives a per-residue confidence score between 0 and 100. Horizontal lines and the corresponding colours follow the AlphaFold guidelines to consider the model confidence *very high* (p*l*DDT > 90, blue), *high* (90 > p*l*DDT > 70, light blue), *low* (70 > p*l*DDT > 50, light orange), and very low (p*l*DDT < 50, deep orange). According to AlphaFold, regions with p*l*DDT < 50 may be unstructured in isolation. Vertical lines separate the six domains labelled below. Regions shaded grey correspond to short segments not assigned to any domain. (b) The same plot for IGP3/AT1G56130. (c) The same plot for IGP4/AT1G56140. (d) AlphaFold structure predicted for IGP4/AT1G56140 protein. The structure of the domains is correctly predicted but their spatial organization is not consistent with the extracellular (LRR + MAL) – transmembrane (TM) – intracellular (KD) separation. The short loop region enclosed in the magenta box is the segment used to modify the complete structure to obtain the proper spatial organization.

Therefore, to explore the impact of *igp1* and *igp2/igp3* point mutations in the KD of these RKs, we first obtained models with the correct domain organization (Figure 4.17a). These models provide a complete picture of the proteins to be used as initial geometries for further computational studies. We then used TM-ALIGN (Zhang & Skolnick, 2005) to evaluate the structural similarity of MAL domains from IGP1/CORK1, IGP3 and IGP4 with several entries in the Protein Data Bank (PDB, https://www.rcsb.org) with MAL and MLD domains (five plant RKs from CrRLK1Ls and nine human and bacteria proteins), including the NMR structures of malectin from *Xenopus laevis* in complex with maltose (Schallus *et al.*, 2010), an

apo form and a complex with nigerose (Schallus *et al.*, 2008), and the crystal structure of tandem MLDs from the ANX1/ANX2 ECDs (Moussu *et al.*, 2018) (Figure 4.17a). In all cases, TM-ALIGN scores between 0.623 and 0.710 were found, thus indicating highly similar folds of IGP MAL domains to animal malectin and to plant MLD structures.

Similar structural comparison analyses were performed for the KDs of IGP1/CORK1, IGP3 and IGP4, with some kinase crystals, like MPK6 from Arabidopsis (PDB: 5CI6, Wang *et al.*, 2016; PDB: 6DTL, Putarjunan *et al.*, 2019) (Figure 4.17a). The structural alignment data showed that the IGP1/CORK1 KD is noticeably different from that of the two other RKs because of the extra loop seen in the intracellular part of its complete structure (indicated by an arrow in Figure 4.17a), which is not predictable from IGP protein sequence alignments. Nevertheless, the conformation of side chains of catalytic residues was found to be identical in wild-type and mutant structures, a result worth emphasizing as the mutation positions are near the catalytic site in both IGP1/ CORK1 and IGP3 (Figure 4.17a).

Next, we tested *in silico* the possible structural impact of the single mutations of E906K in IGP1/CORK1 and G773E in IGP2/IGP3 KDs by generating new model structures of the KD of wild-type and mutants with AlphaFold 2 (Figure 4.17b, c). We found that the backbones remained unaltered and that E906K in IGP1 and G773E in IGP2/IGP3 had the effect of increasing the surface patch associated with the mutated position (Figure 4.17b, c). However, the major effect of these single mutations was found in the surface electrostatic potential (Figure 4.17d, e). The region around E906 in wild-type IGP1/CORK1 shows a weakly negative electrostatic character, whereas, in the *igp1* mutant, the E906 negative charge of IGP1/CORK1 is substituted for a K906 positive charge, which gives rise to a strongly positive electrostatic potential in a large area around position 906 (Figure 4.17d).

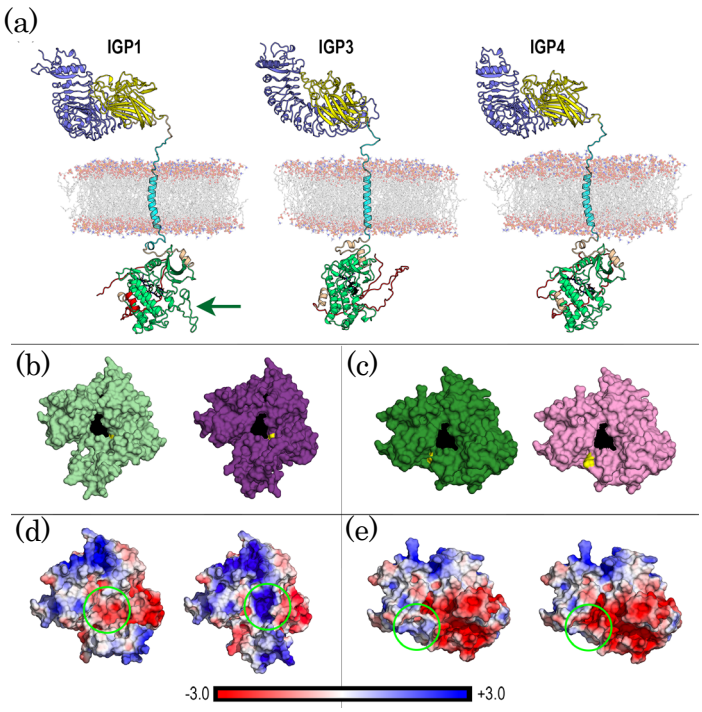

Figure 4.17: "*In silico*" model structures of IGP1/CORK1, IGP3 and IGP4 proteins. (a) Structures obtained upon modification of the AlphaFold models shown in Figure 4.16 to suit the extracellular/membrane/intracellular organization. Domains colored as follows: LRR, slate blue; MAL, yellow; segment containing transmembrane helix, cyan; KD, green with catalytic residues shown as black sticks; C-terminal, red. The bilayer modeled by 256 POPC lipids is shown as sticks for tails and spheres for polar heads. The arrow in IGP1 indicates an extra loop in its KD absent in IGP3 and IGP4. (b) Molecular surface of wild-type (pale green) and E906K mutant (*igp1*, purple) structures of KD of IGP1. Surface patches of the catalytic site and residue 906 are colored black and yellow, respectively. (c). Molecular surface of wild-type (green) and G773E mutant (*igp2/igp3*, pink) structures of KD of IGP3. Surface patches of the catalytic site and residue 773 are colored black and yellow, respectively. (d,e) KD of (d) IGP1 and (e) IGP3 comparing the Poisson-Boltzmann (PB) Electrostatic Potential (EP) mapped onto the protein surface of the Wild-Type (WT) (left) and mutant (right) forms. Green circles indicate surface regions at which the mutations E906K (d, right) and G773E (e, right) provoke a significant electrostatic change in the corresponding WT surfaces of IGP1 (d, left) and IGP3 (e, left). The bar shows the colour code for the PB EP in *kT/e* units (*k*: Boltzmann constant, *T*: absolute temperature, *e*: electron charge unit).

The equivalent region around G773 in wild-type IGP2/IGP3 displays a weakly positive electrostatic character, which becomes strongly negative upon the G773E mutation (Figure 4.17e). It is noted that these electrostatic effects extend over a surface region far larger than that expected from the small, exposed surface areas of residues 906 and 773 (Figure 4.17d, e). These changes in the KD domains of IGP1/CORK1 and IGP2/IGP3 LRR-MAL RKs might explain their loss of functionality.

4.1.8. The ECD of IGP1 directly binds CEL3 and CEL5 but not MLG43

Based on the initial structural models of MAL domains in the three LRR-MAL RKs and their similarities with the MAL domain from *Xenopus* sp. that binds short glycans (Figure 4.17) (Schallus *et al.*, 2010), we tested whether ECDs of these LRR-MAL RKs could be glycan receptors for cellulose- and MLGs-derived oligosaccharides. We expressed the ECDs of IGP1, IGP4 and IGP3 in insect cells and purified them by affinity chromatography (Figure 4.18a, b, c respectively). As the ECD of IGP3 turned out to form aggregates, this ECD was not suitable for further purification steps and was not available for binding experiments (Figure 4.18c).

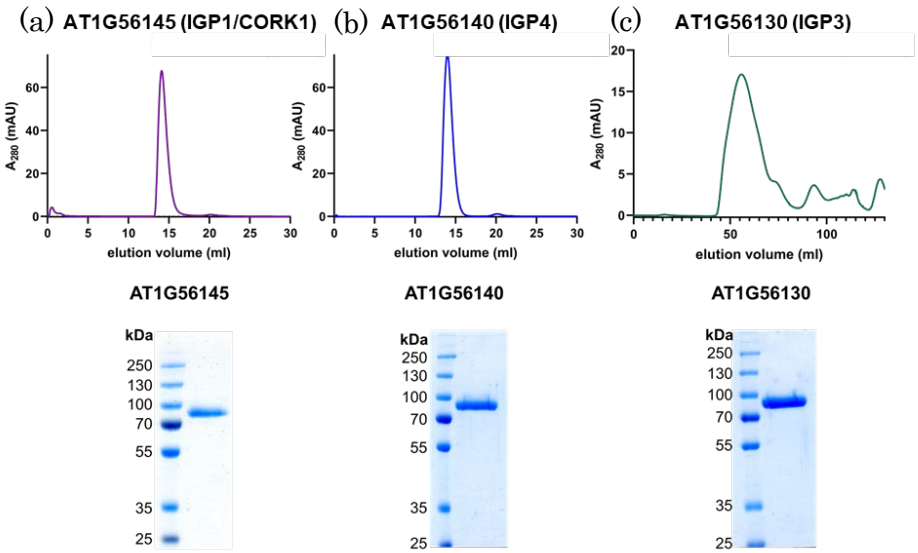

Figure 4.18: Purification of IGP1/CORK1, IGP3 and IGP4 ECDs. Analytical Size Exclusion Chromatography (SEC) and SDS-PAGE of (a) IGP1, (b) IGP4 and (c) IGP3 purified by SEC and used in the Isothermal Titration Calorimetry (ITC) binding assays, except IGP3.

Then, ITC experiments (Sandoval & Santiago, 2020) were carried out to test the binding of MLG43 and CEL3 to IGP1/CORK1 and IGP4 ECDs (Figures 4.19 and 4.20). The ITC results proved the existence of direct interactions between CEL3 and the ECD of IGP1/ CORK1 (Figure 4.19a) (Kd = 1.19 ± 0.03 µM; Figure 4.19b), but not with the ECD of IGP4 (Figure 4.20). Additional ITC experiments showed that none of the ECDs bind, at least directly, to MLG43 (Figures 4.19 and 4.20).

(a)

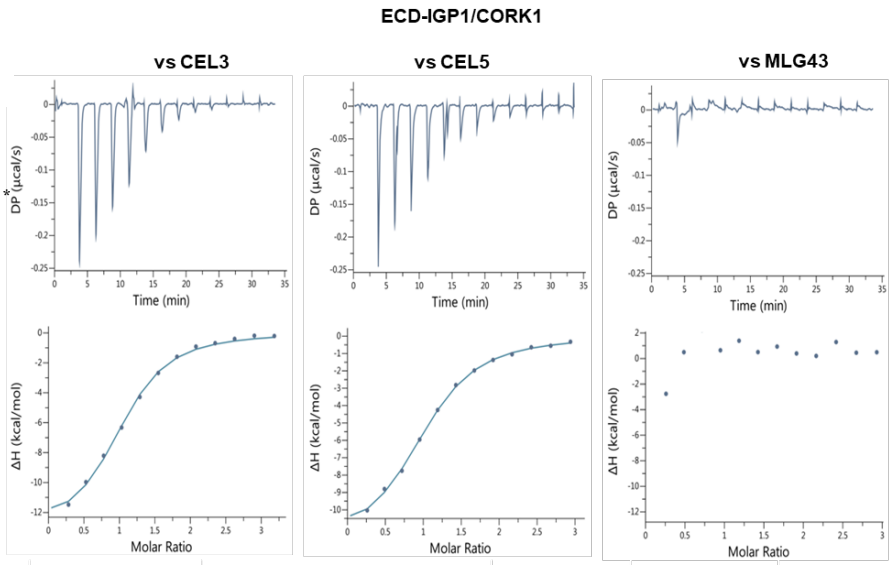

(b)

Ligand (syringe)	Protein (cell)	K_d (µM)	ΔH (kcal/mol)	N
CEL3	AT1G56145(IGP1/CORK1)	1.19 ± 0.03	13.60 ± 0.30	1
CEL5	AT1G56145(IGP1/CORK1)	1.40 ± 0.01	12.50 ± 0.15	1
MLG43	AT1G56145(IGP1/CORK1)	n.d.		

Figure 4.19: The IGP1/CORK1 ectodomain (ECD) directly binds cellulose-derived oligosaccharides (DP>2). (a) Isothermal Titration Calorimetry (ITC) experiments of ECD-IGP1/CORK1 *versus* CEL3, CEL5 and MLG43. (b) ITC summary of ECD-IGP1 *versus* CEL3, CEL5 and MLG43. The binding affinities of ECD-IGP1/CORK1 are reported as K*d* (dissociation constant, in micromoles), *DP** indicates measured power differential between the reference and sample cells to maintain a zero temperature between the cells inside the ITC device, N indicates the reaction stoichiometry (N = 1 for a 1:1 interaction) and ΔH indicates the enthalpy variation. Values indicated in the table are means ± standard deviation of independent experiments (n = 2). n.d., no binding detected.

Similar binding experiments were performed with CEL5 and the ECD of IGP1/CORK1 to determine the specificity of receptor–ligand recognition, and direct binding was also detected (Figure 4.19a) with similar high affinity (K*d* = 1.40 ± 0.01 µM; Figure 4.19b). The binding reactions measured for CEL3 and CEL5 were exothermic, with a single binding site (n = 1) and very similar values of ΔH, indicating that extra sugar subunits in the CEL5 oligomer do not improve the detected binding (Figure 4.19b).

These data support the role of the ectodomain of IGP1 as a receptor for cellulose-derived oligosaccharides and suggest that IGP4 RK might function as an RK required for the sensing complex for cellulose- and MLG- derived oligosaccharides.

(a)

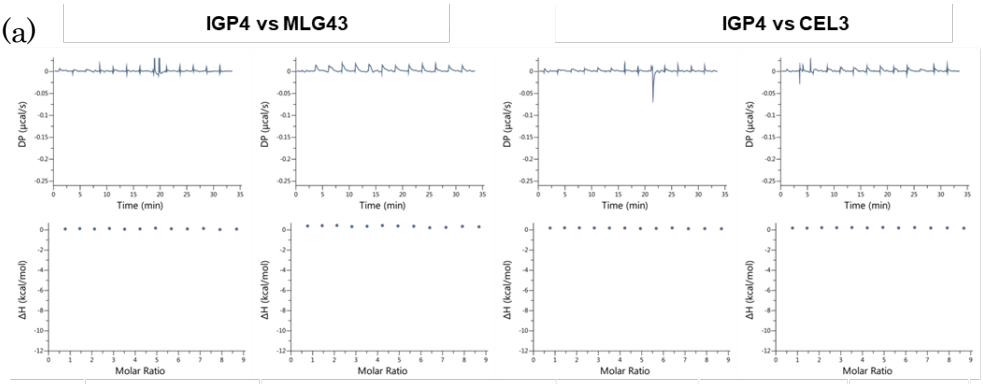

(b)

Ligand (syringe)	Protein (cell)	K_d (µM)	ΔH (kcal/mol)	N
CEL3	AT1G56140(IGP4)	n.d.		
MLG43	AT1G56140(IGP4)	n.d.		

Figure 4.20: The IGP4 ectodomain (ECD) doesn't bind MLG43 either CEL3. (a) Isothermal Titration Calorimetry (ITC) experiments of ECD-IGP4 *versus* MLG43 and CEL3. (b) ITC summary of ECD-IGP4 *versus* CEL3, MLG43. The results are from two independent experiments. n.d., no binding detected.

4.1.9. Constitutive expression of IGP1 protein in *igp1* restores CEL3 perception of this mutant

We tested whether IGP1 overexpression might complement *igp1* mutation and/or increase the sensitivity of wild-type plants to glycans. Therefore, we obtained Col-0 and *igp1*^{AEQ}, *igp3*^{AEQ} and *igp4* mutant lines constitutively expressing IGP1 fused to different tags in its C-terminal region that favours IGP detection by Western Blot (*35S*::*IGP1*-TAG; i.e. Hemagglutinin (HA) and FLAG epitopes, and Green-Fluorescence-Protein (GFP)). For that, we employed pGWB600 vector series carrying a glufosinate-ammonium (BASTA) resistance gene for the selection of positive transgenic lines. Additionally, we express IGP4 and AT1G56120 in Col-0, *igp1*^{AEQ}, *igp2*^{AEQ}, *igp3*^{AEQ} and *igp4* genetic backgrounds as shown in Table 4.3. Unfortunately, the synthesis of IGP3 RK failed in all the attempts we carried out. Only truncated or mutated versions were obtained, therefore, we decided to not proceed further in the analysis of this gene.

Table 4.3: Transgenic constitutive expression and complementation lines, showing the different backgrounds in which the constructs were introduced.

	BACKGROUND				
	igp1^{AEQ}	*igp2*^{AEQ}	*igp3*^{AEQ}	*igp4*	Col-0
CONSTRUCTS	*35S*::*IGP1*-HA				
	35S::*IGP4*-HA				
	35S::*AT1G56120*-HA				
	35S::*IGP1*-FLAG				
	35S::*IGP4*-FLAG				
	35S::*AT1G56120*-FLAG				
	35S::*IGP1*-GFP				
	35S::*IGP4*-GFP				
	35S::*AT1G56120*-GFP				

We used BASTA-selected T_2 lines of the *35S*::*IGP1*-HA lines in Col-0 to check out the protein expression levels, using different protein extraction conditions. For example, we found out that the pH of the extraction buffer was critical to visualize the protein in Western Blots (4,6 for these proteins). Denaturalized Western Blot analysis of protein fractions extracted from the transgenic lines generated allowed the identification of bands with a molecular weight equivalent to the tagged versions of IGP1, being IGP1~115 kDa (Figure 4.21a). Therefore, the obtained transgenic lines expressed our protein of interest and were suitable for further molecular/biochemical characterizations.

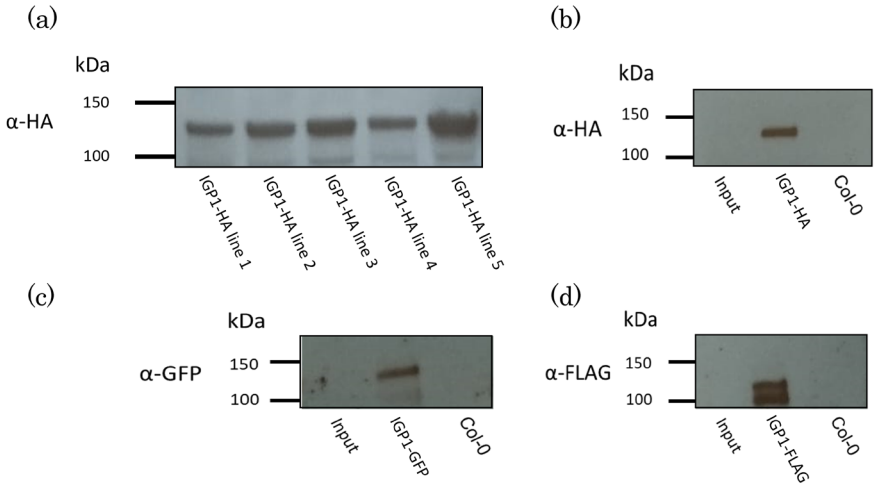

Figure 4.21: IGP1 detection in transgenic lines. The expression of IGP1 was determined by Western Blot. (a) Detection of IGP1-HA (119 kDa) in 5 lines that constitutively express the gene in Col-0 background showing that IGP1 protein can be detected by chemiluminescence. (b) (c) (d) Immunoprecipitation of IGP1 in complementation lines of *igp1*^{AEQ} background. Different antibodies against the proteins tagged to IGP were used for IGP1 detection: (b) HA (119 kDa), (c) GFP (141 kDa) and (d) FLAG (116 kDa).

Similarly, we verified the expression of IGP1 in the *igp1*^{AEQ} mutant background (Figure 4.21 b, c, d). In the present Thesis we have focused in the biochemical and

molecular characterization of IGP1 using the developed transgenic lines. The contribution of additional IGPs in the perception of glycans will be further studied by other members of the group using the transgenics generated in this Thesis. Overall, we obtained stable transgenics lines expressing IGP1 fused to the three selected tags. These lines do not differ phenotypically from Col-0 or *igp1*^{AEQ} mutant (data not shown). Since we already checked that these lines express IGP1 correctly (Figure 4.21b, c, d), they were further characterized analysing different PTI hallmarks such as $_{cyt}Ca^{2+}$ influxes and MAPKs phosphorylation.

Cytoplasmatic Ca^{2+} was measured in the *35S::IGP1-HA igp1*^{AEQ} (Figure 4.22a), *35S*::IGP1-FLAG *igp1*^{AEQ} (Figure 4.22b) and *35S*::IGP1-GFP *igp1*^{AEQ} (Figure 4.22c) after CEL3 treatment. Col-0^{AEQ} and *igp1*^{AEQ} seedlings were used as positive and negative controls, respectively (Figure 4.22).

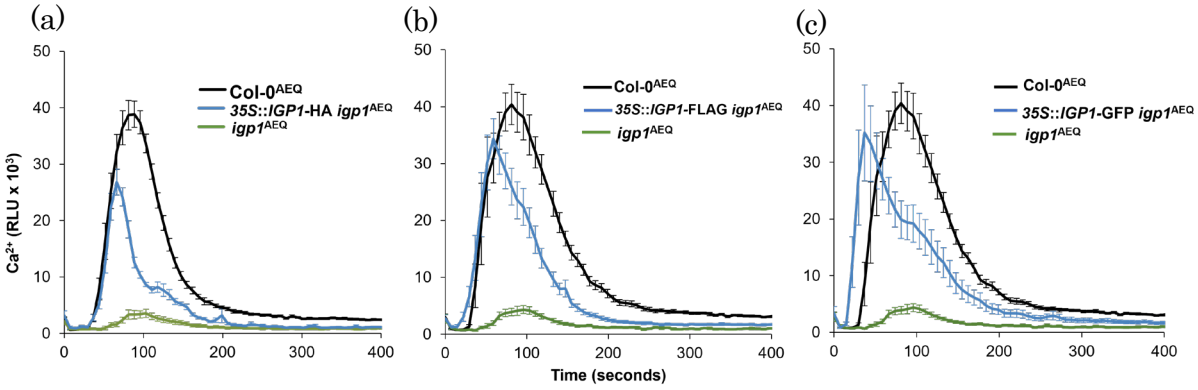

Figure 4.22: IGP1 complementation lines recover calcium response after CEL3 treatment in *igp1*. $_{cyt}Ca^{2+}$ burst measured as Relative Luminescence Units (RLUs) over time in 8-day-old *35S::IGP1 igp1* ^{AEQ} (a) HA tagged, (b) FLAG tagged and (c) GFP tagged T_2 transgenic seedlings and Col-0^{AEQ}, *igp1*^{AEQ} seedlings as controls after 100 µM CEL3 treatment. Data represent the mean ± standard error (n = 4 in the case of Col-0^{AEQ} and *igp1*^{AEQ}; and n = 12 in the case of *35S::IGP1 igp1* ^{AEQ} lines). Data are from one of three experiments performed that gave similar results.

The impairment in $_{cyt}Ca^{2+}$ responses observed in *igp1*^{AEQ} line (Figure 4.22) was almost recovered to wild-type levels in the T_2 *35S::IGP1 igp1*^{AEQ} transgenics. This result is aligned with our previous ITC assays that showed the *in vitro* binding of the ECD domain of IGP1 to cellulose-derived oligosaccharides. Additional evidence of IGP1 requirement for CEL3 perception were also obtained in the MAPKs phosphorylation assays (Figure 4.23). In comparison with the faint phosphorylation bands observed in *igp1*^{AEQ} mutants in response to CEL3, clear phosphorylation events were detected in IGP1 complementation lines (*35S::IGP1*-HA *igp1*^{AEQ}) (Figure 4.23b). Moreover, the constitutive expression of IGP

(*35S::IGP1*-HA Col-0) rendered a stronger phosphorylation in comparison with WT Col-0 plants when seedlings were treated with CEL3 (Figure 4.23a). Altogether, the recovery of the *igp1* mutant phenotype and the binding experiments confirm that IGP1 is the receptor responsible of CEL3 perception.

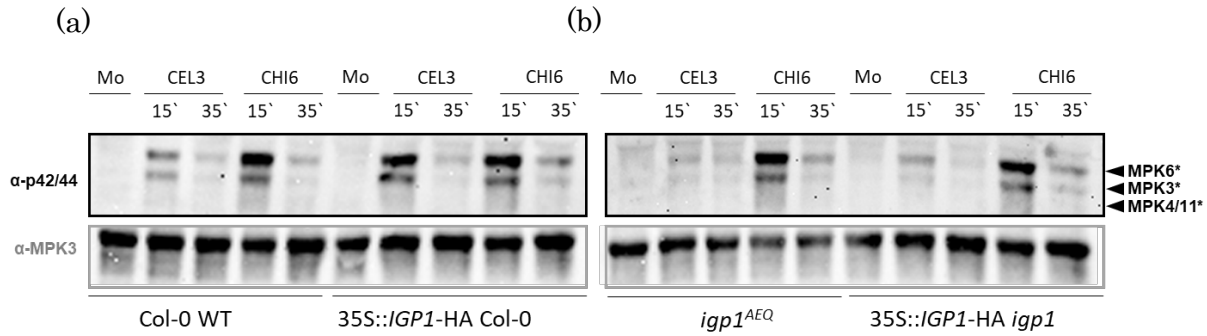

Figure 4.23: MAPKs phosphorylation after CEL3 treatment was stronger in IGP1 overexpression line and partially recovered in the T_2 IGP1 complementation line compared to Col-0. MAPKs phosphorylation was analyzed in seedlings of (a) *35S::IGP1*-HA Col-0 and (b) *35S::IGP1*-HA *igp1*^{AEQ}, using Col-0 and *igp1*^{AEQ} as controls, treated with 10 μM CEL3 or water (mock). Western Blot was performed using α-pTEpY antibody (α-p42/44) for phosphorylated MAPK moieties with samples harvested at 15 and 35 minutes. Mock samples (Mo) corresponding to a 15-minutes treatment with water were included as basal expression controls. Black arrows indicate the positions of phosphorylated MPK6 (top), MPK3 (middle) and MPK4/11 (bottom). α-MPK3 was used as a total protein control to show the loading of each gel. These results are from one representative experiment out of two performed that gave similar results.

We hypothesized that IGP1 and IGP4 have not redundancy function, based on their mutants PTI phenotypes (Figures 4.7, 4.8, 4.10, 4.11, 4.12). To further confirm this lack of redundancy and the relevance of IGP1 in CEL3 perception and downstream PTI activation, we ectopically express IGP4 in *igp1*^{AEQ} mutant and analyzed PTI hallmarks in *35S::IGP4*-FLAG *igp1*^{AEQ} lines (Figure 4.24). Neither $_{cyt}Ca^{2+}$ burst (Figure 4.24a) nor MAPKs phosphorylation (Figure 4.24b) were recovered in *35S::IGP4*-FLAG *igp1*^{AEQ} transgenics, indicating that IGP4 was not able to complement *igp1* mutation.

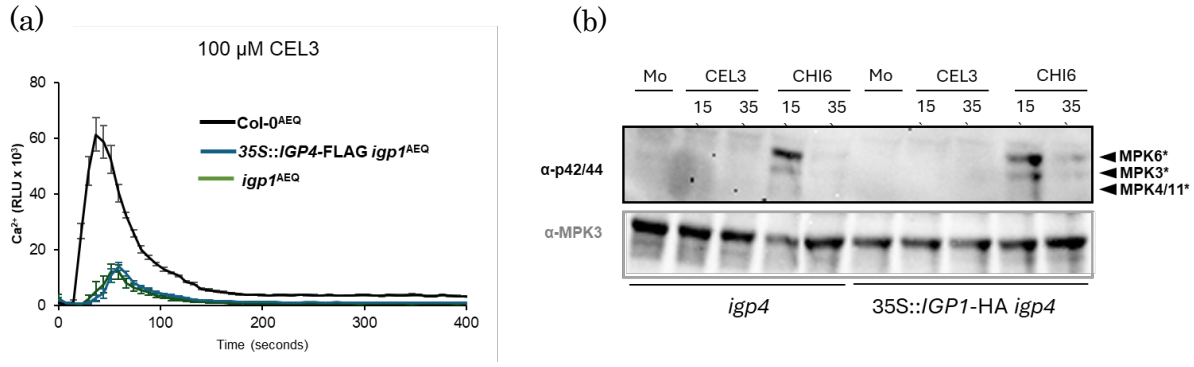

Figure 4.24: IGP4 and IGP1 do not complement *igp1* and *igp4* mutant, respectively. (a) $_{cyt}Ca^{2+}$ burst measured as Relative Luminescence Units (RLUs) over time in 8-day-old *35S::IGP4*-FLAG *igp1*^{AEQ} T_2 transgenic seedlings and Col-0^{AEQ} and *igp1*^{AEQ} seedlings as controls after 100 µM CEL3 treatment. Data represent the mean ± standard error (n = 4 in the case of Col-0^{AEQ} and *igp1*^{AEQ}; and n = 12 in the case of *35S::IGP4*-FLAG *igp1*^{AEQ} line). Data are from one of three experiments performed that gave similar results. (b) MAPKs phosphorylation was analyzed in T_2 seedlings of *35S::IGP1*-HA *igp4*, using *igp4* as control, treated with 10 µM CEL3 or water (mock). Western Blot was performed as described in Figure 4.23. These results are from one representative experiment out of two performed that gave similar results.

Since we confirmed that IGP4 function was not complemented by IGP1 and vice versa (Figure 4.24), but both are needed to activate PTI hallmarks in response to CEL3, we asked whether there is an interaction among them that might explain the lack of response to glycans when only one is missed. For that, we carried out heterologous expression of IGP1 and IGP4 in *Nicotiana benthamiana*, co-infiltrating constructs of both genes carrying different tags that allow pull-down and detection of IGP1 and IGP4 (Table 4.3). 48 hours after infiltration we harvested the infiltrated tissues and performed protein extraction followed by co-immunoprecipitation using affinity beads and finally carried out a Western Blot. As is shown in Figure 4.25 we were able to immunoprecipitate both IGP1 and ERECTA (an LRR fused to HA which was used as a control). However, no interaction between IGP1 and IGP4 was detected in these assays (Figure 4.25). An optimization of infiltration and co-immunoprecipitation (Co-IP) experiments might be required to further address the interaction between IGP1 and IGP4. We cannot exclude the presence of additional molecular components acting as linkers between proteins that might be required and also that pre-treatment of plants with CEL3 might be need for Co-IP. Therefore, more experiments of Co-IP and proteomics analysis are underway to decipher the composition of a putative IGP receptor complex.

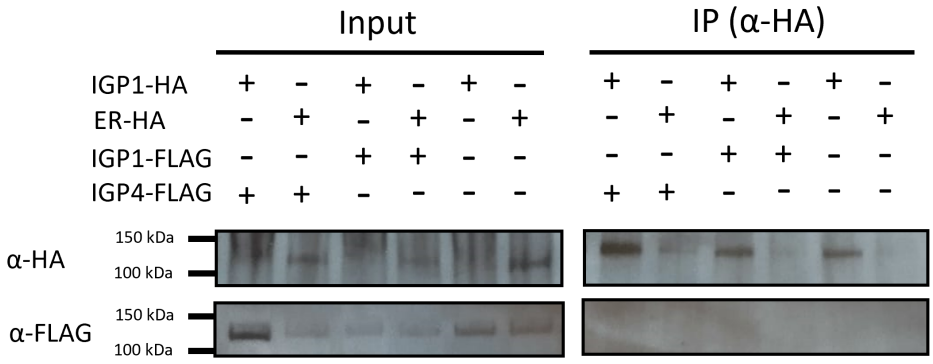

Figure 4.25: IGP1 doesn't interact with IGP4 in Agroinfiltration experiments. Co-IP carried out by infiltration in *N. benthamiana* leaves, where the constructs IGP4-FLAG and IGP1-FLAG were co-infiltrated with IGP1-HA, using ER-HA (ERECTA) as a control. Interaction between the selected proteins where not observed.

To further proof that IGP1 is a membrane-anchored RK, we tested its localization in plant cells since plant PRRs are in the plasma membrane with their ECD in the apoplast to bind cell wall-derived DAMPs. To this aim, we agroinfiltrated *N. benthamiana* leaf with the construct *35S::IGP1*-GFP (Figure 4.26a) and we checked IGP1 localization by confocal microscopy (Leica TCS SP8) (Figure 4.26b). We found that IGP1-GFP was localized in the plasma membrane of the cell, as expected (Figure 4.26b). This result also confirms that *N. benthamiana* leaf agroinfiltration can be used for characterization of IGP1 molecular interactions in a heterologous system.

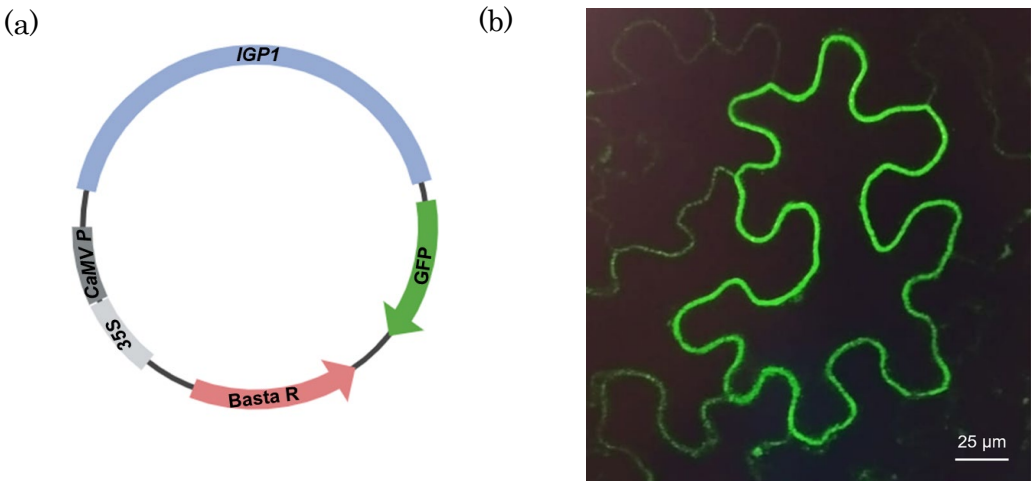

Figure 4.26: Subcellular localization of GFP targeted to IGP1 in the plasma membrane. *35S::IGP1*-GFP construct (a) was infiltrated in a *Nicotiana benthamiana* leaf and visualized by confocal microscopy. (b) IGP1 was visualized in the plasma membrane of the cell.

4.2. Identification of additional *igp* mutants

Our results point to the LRR-MAL RK family as a set of plant proteins involved in the perception of carbohydrate-based DAMPs and MAMPs, as previously suggested (del Hierro *et al.*, 2021). So far, plant RKs described to be involved in glycan perception belong to the LysM, WAK, and CrRLK1 RK families (Bellande *et al.*, 2017; Brutus *et al.*, 2010; Cao *et al.*, 2014; del Hierro *et al.*, 2021; Liu *et al.*, 2012; Liu, Wang *et al.*, 2016; Tang *et al.*, 2017; Wong *et al.*, 2020). The function of most of these proteins in oligosaccharide perception and PTI activation was discovered through the isolation and characterization of Arabidopsis mutants (e.g. *cerk1, lyk4, lyk5, wak1, wak2* and *fer1*). In general, such mutants share redundant functions with additional RKs, and therefore individually they are either unaffected or only partially impaired in PTI responses triggered by specific DAMPs and MAMPs. Accordingly, higher-order RK mutants that overcome redundancy must be analyzed to observe PTI-deficient phenotypes (Brutus *et al.*, 2010; Cao *et al.*, 2014; Dünser *et al.*, 2019; Liu *et al.*, 2012; Liu, Wang *et al.*, 2016; Miya *et al.*, 2007).

Similarly, our genetic screening led to the identification of additional mutants impaired in glycan perception (Tables 4.4 and 4.5). From 6400 individuals screened, 15 additional *igp* mutants (*igp5-igp19*) were affected in MLG43 but not CHI6 perception and 24 had different responses to these glycans (Table 4.4).

Table 4.4: Candidates selected from 6400 screened by their response to MLG43 and CHI6.

	Low response to MLG43	High response to MLG43	Response as control to MLG43
Low response to CHI6	9	0	2
High response to CHI6	0	4	4
Response as control to CHI6	19	5	6357

Table 4.5: Summary of all *igp mutants* selected from our screening perception and the mutations found in those that were sequenced.

MUTANT	GENE	PROTEIN	ALLELISM	MUTATION
igp1^{AEQ}	*AT1G56145*	IGP1	*igp6-9*	*E906K*
igp2^{AEQ}	*AT1G56130*	IGP3	*igp3*	*G773E*
igp3^{AEQ}	*AT1G56130*	IGP3	*igp2*	*G773E*
igp4^{AEQ}	*AT1G56140*	IGP4	*igp5*	*T-DNA (KO)*
igp5^{AEQ}	*AT1G56140*	IGP4	*igp4*	*Stop codon Q461X*
igp6^{AEQ}	*AT1G56145*	IGP1	*igp1*	*E805K*
igp7^{AEQ}	*AT1G56145*	IGP1	*igp1*	*D85N*
igp8^{AEQ}	*AT1G56145*	IGP1	*igp1*	*P207S*
igp9^{AEQ}	*AT1G56145*	IGP1	*igp1*	*E879K/E906K*
igp10^{AEQ}	sequencing ongoing	/	/	/
igp11^{AEQ}	sequencing ongoing	/	/	/
igp12^{AEQ}	sequencing ongoing	/	/	/
igp13^{AEQ}	sequencing ongoing	/	/	/
igp14^{AEQ}	sequencing ongoing	/	/	/
igp15^{AEQ}	sequencing ongoing	/	/	/
igp16^{AEQ}	sequencing ongoing	/	/	/
igp17^{AEQ}	sequencing ongoing	/	/	/
igp18^{AEQ}	sequencing ongoing	/	/	/
igp19^{AEQ}	sequencing ongoing	/	/	/

From these new *igp*s impaired in MLG43 perception, we continue studying *igp5-igp9*, and determined whether they were also impaired in CEL3 perception. As shown in Figure 4.27, $_{cyt}Ca^{2+}$ elevations indicated that *igp5-igp9* were not only impaired in MLG43 but also in CEL3 perception (Figure 4.27 a, c). However, they were not impaired in CHI6 perception (Figure 4.27b). *igp5-igp9* phenotypes resembled *igp1-igp4* phenotypes and indeed sequencing confirmed that *igp5-igp9* mutants were allelic to *igp1* or *igp4* (Table 4.5). These results support the important role of IGP1 and IGP4 in MLGs- and CEL-derived oligosaccharide, specially, of IGP1, since in one single screening we obtained 5 alleles with 5 different mutations in two main Domains (ECD and KD) of IGP1 protein (Figure 4.28). Additional *igp* mutants (*igp10-igp19*) are under sequencing and allelism test to unravel other molecular components of glycan perception.

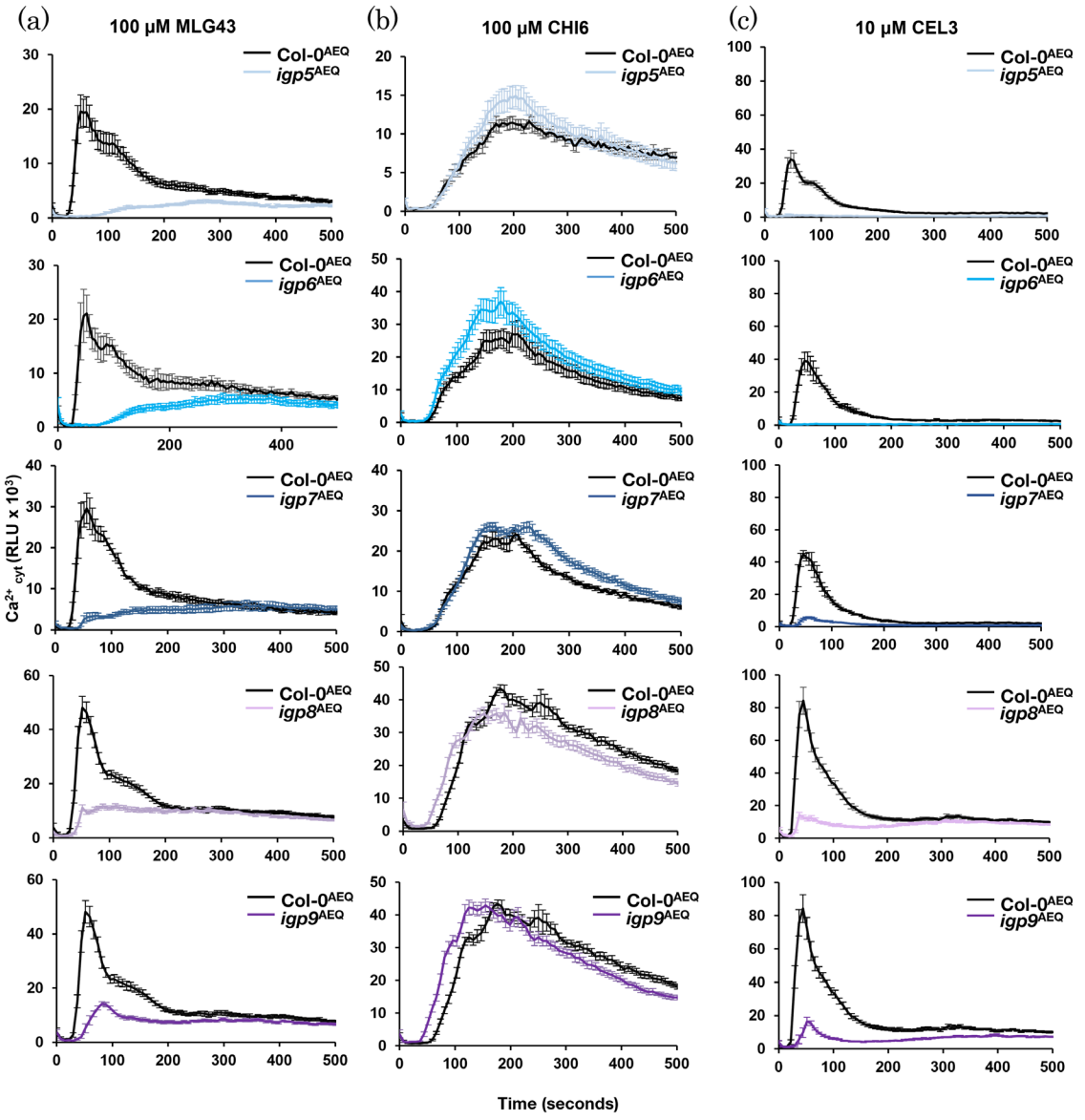

Figure 4.27: Identification of additional *igp* (*igp5*-*igp9*) mutants impaired in MLG43 and CEL3 perception. Calcium burst was measured as Relative Luminescence Units (RLUs) over time in eight-day-old seedlings of Col-0^{AEQ} in comparison with *igp5*^{AEQ}-*igp9*^{AEQ} mutants after treatment with (a) 100 µM of MLG43, (b) 100 µM of CHI6 and (c) 10 µM of CEL3. Data represent the mean ± standard error (n = 3 in the case of Col-0^{AEQ} and n = 12 in the case of *igp*^{AEQ} mutants).

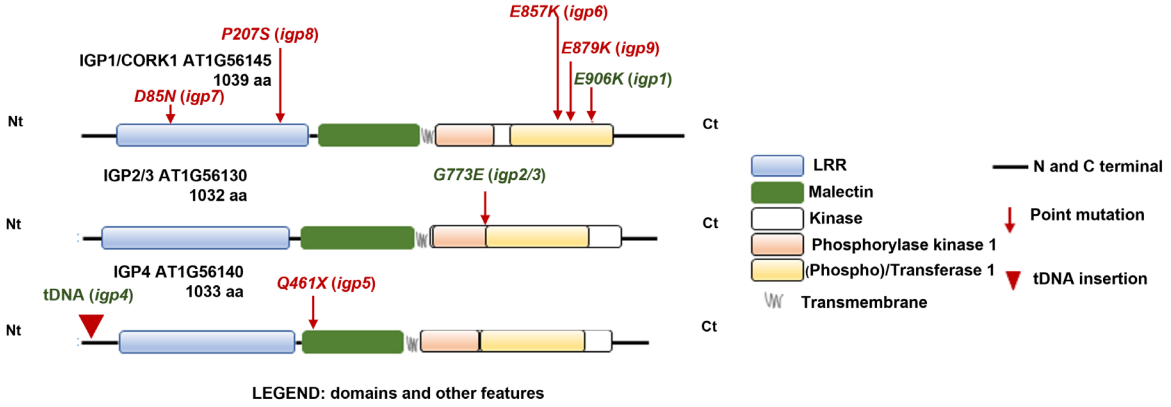

Figure 4.28: Representation of the localization of *igp5*-igp9 mutations. Red arrows indicate the position of the mutations in the coding regions of *igp5*-9^{AEQ}, and the red triangle indicates the insertion of the T-DNA sequence in *igp4*. Leucine-Rich Repeat (LRR; blue), malectin (MAL; green), phosphorylase kinase (orange) and phophotransferase (yellow) of Kinase Domain (KD; white), N- and C-terminal domains (black lines) and Transmembrane Domain (TM; gray).

4.3. IGPs are also required for Arabidopsis immune responses triggered by additional glycans as XYL4 and XA_3XX

Since we demonstrated the importance of the IGPs in the immune responses triggered by several β-glycans (MLG43 and CEL3), we also checked their implication in the perception of additional β–glycans that have been recently described by our group as activators of PTI in plants, for example, XYL4 and XA_3XX (Fernández-Calvo *et al.*, 2024; Mélida *et al.*, 2020). These glycans are derived from hemicelluloses being the main cross-linking elements of cell walls. They are ß-1,4-D-glycans with four xyloses in pyranose form (carrying arabinose decorations in the case of XA_3XX).

First, we checked if XYL4 and XA_3XX shared signalling pathways performing cross -elicitation assays (Figure 4.29). In these experiments, we measured the reduction of $_{cyt}Ca^{2+}$ burst in Col-0^{AEQ} seedlings after sequential application of different glycans (Mélida *et al.*, 2020; Rebaque *et al.*, 2021). Notably, Col-0^{AEQ} seedlings demonstrated strong refractory responses when XYL4-XA_3XX were combined (Figure 4.29c), though the reduction of $_{cyt}Ca^{2+}$ burst was not total after XA_3XX treatment in comparison to the observed in the control XYL4-XYL4 experiment (Figure 4.29e). These results indicate that the perception mechanisms of XYL4 and XA_3XX are very similar.

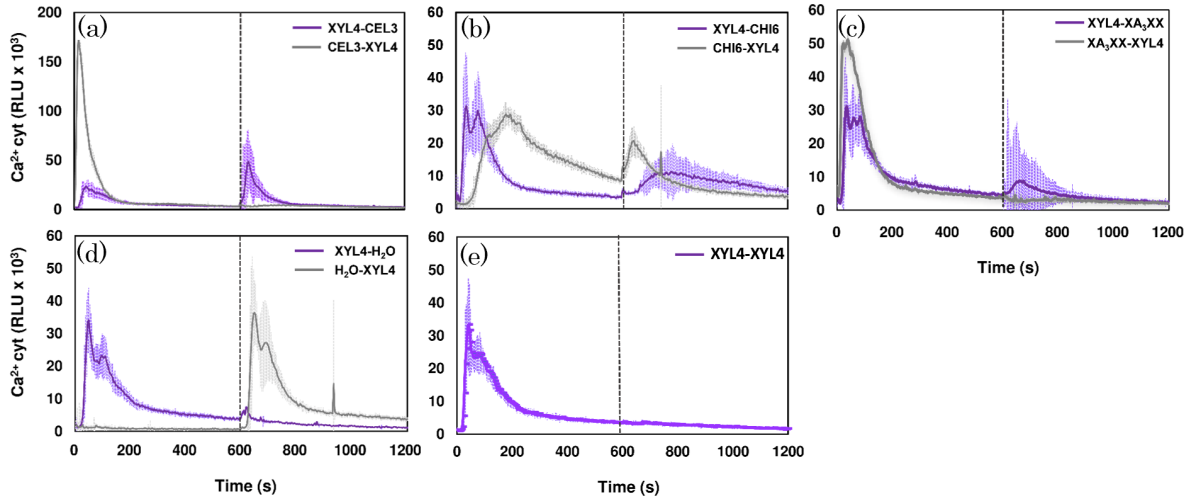

Figure 4.29: Cross-elicitation during the refractory period of calcium burst triggered by XYL4 in combination with CEL3, CHI6 and/or XA_3XX. Cytoplasmatic Ca^{2+} burst (RLU) over time in 8-day-old Col-0^{AEQ} seedlings after sequential treatments with 250 µM XYL4 followed by (a) CEL3, (b) 50 µM CHI6, (c) 250 µM XA_3XX, (d) water, or (e) 250 µM XYL4 and vice versa. (d) and (e) panels represents the negative and positive controls of the experiment, respectively. XYL4 as the first treatment applied is indicated in purple and any other compound and/or water in grey. Pointed

lines indicate the application time of the second elicitor. Data represent the average RLU values of 4 seedlings (n = 4) ± standard deviation.

Remarkably, a strong refractory response was observed in XYL4-CEL3 combination (Figure 4.29a). Still, the intensity of CEL3 $_{cyt}Ca^{2+}$ burst was stronger than that of XYL4 and accordingly sequential application of XYL4-CEL3 did not completely abolish CEL3 triggered $_{cyt}Ca^{2+}$ burst in contrast to CEL3-XYL4 sequential application (Figure 4.29a). Of note, these results suggest that the mechanism of recognition of XYL4 and XA_3XX overlaps with those of CEL3, suggesting that IGPs might participate in the perception of these glycans.

Additionally, a weak but significant refractory response was observed when XYL4 and CHI6 were sequentially applied to Col-0^{AEQ} seedlings (Figure 4.29b), suggesting that the mechanisms of perception of XYL4 and CHI6 are not identical, but might share some LysM-RK components. Together these data indicate that perception of ß-1,4-D-Xyl-based oligosaccharides, as XYL4 and XA_3XX, and oligosaccharides containing ß-1,4-D-glycans bonds, like CEL3 and MLG43, might require similar receptors and/or co-receptors.

4.3.1. PTI hallmarks in response to XYL4 and XA_3XX

To further unravel the implication of the IGPs in the perception mechanisms of XYL4 and XA_3XX in *Arabidopsis thaliana* we performed PTI immunity hallmarks assays with the *igps*^{AEQ} mutants and the two different elicitors (Figure 4.30; Figure 4.31). We monitored early cytoplasmic Ca^{2+} influxes in these mutants upon XYL4 treatment and found that $_{cyt}Ca^{2+}$ influx in *igp3*^{AEQ} and *igp4*^{AEQ} lines was fully impaired upon XYL4 treatment, whereas in *igp1*^{AEQ} plants a significant reduction of the burst was observed in comparison to Col-0^{AEQ} plants (Figure 4.30a). Next, we tested MAPKs phosphorylation by Western Blot in *igp1*^{AEQ}, *igp3*^{AEQ,} and *igp4*^{AEQ} lines and Col-0 ^{AEQ} plants upon XYL4 treatment in comparison with CHI6- and mock-treated plants. We found that MAPKs phosphorylation levels were weaker in the *igp1*^{AEQ}, *igp3*^{AEQ,} and *igp4*^{AEQ} mutants than in Col-0 ^{AEQ} plants upon XYL4 treatment (Figure 4.30b). We also tested the up-regulation of two PTI marker genes (*CYP81F2* and *WRKY53*) upon XYL4 treatment in these *igp* mutants and Col-0 wild-type plants. We found that the up-regulation of such genes was also impaired in *igp* mutants in comparison to Col-0 plants (Figure 4.30c). These data confirm that IGPs are not only required for CEL/MLG43-dependent PTI activation

but also play a role in XYL4 perception, further expanding the function of this novel group of LRR-MAL RKs in the perception of glycans.

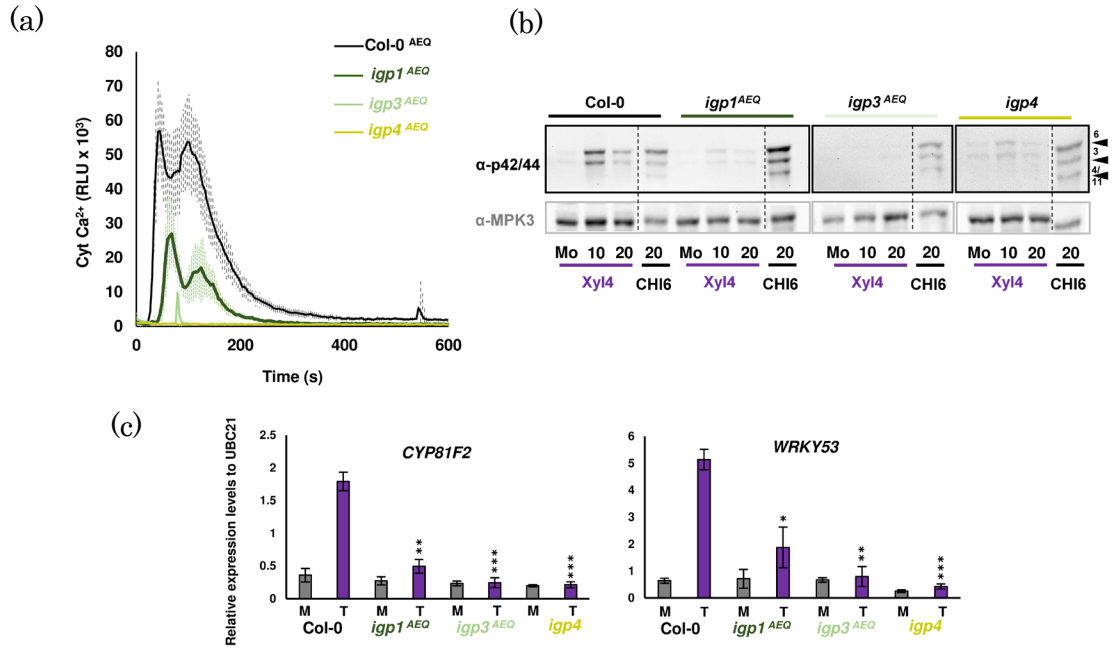

Figure 4.30: *igp* mutants are impaired in XYL4 perception. Determination of PTI hallmarks (a) cytoplasmatic Ca^{2+} influx, (b) phosphorylation of MAPKs, and (c) marker genes up-regulation in *igp* mutants upon XYL4 treatment. Data represent (a) the mean ± standard error (n=8) of cytoplasmatic calcium influx measured as Relative Luminescence Units (RLU) over time in 8-days-old Arabidopsis Col-0^{AEQ} and *igp*s^{AEQ} mutants treated with 250 µM XYL4; (b) a representative Western Blot out of three replicates (dotted lines indicate that bands were cut from the membrane to relocate them in proper order) where seedlings were treated with 250 µM XYL4 and water as mock, harvested at 10 and 20 minutes after treatment application, and (c) the mean ± standard error (n=3) of PTI-related gene expression *CYP81F2* and *WRKY33* measured by qRT-PCR at 30 minutes after 250 µM XYL4 application. Statistically significant differences between compound-treated (T) plants *versus* mock-treated (M, H_2O) were calculated according to Student's t-test (*P < 0.05, **0.01 < P > 0.001, ***P < 0.001).

Concurrently, we performed the same experiments but using XA_3XX as the elicitor (Figure 4.31). We used Col-0^{AEQ}, *igp1*^{AEQ}, *igp3*$^{AEQ.}$ and *igp4*^{AEQ} lines to monitor early cytoplasmic Ca^{2+} influxes in these mutants upon XA_3XX treatment. Notably, $_{cyt}Ca^{2+}$ influxes in XA_3XX-treated *igp1*^{AEQ}, *igp3*^{AEQ}, and *igp4*^{AEQ} seedlings were reduced in comparison to those in Col-0^{AEQ} (Figure 4.31a). These reductions upon XA_3XX were like those observed after treatment of these plants with XYL4, both in signal intensity and in the fact that reduction was higher in *igp3*^{AEQ} and *igp4*^{AEQ} than in *igp1*^{AEQ} (Figure 4.31a). Next, we tested the phosphorylation of MAPKs by Western Blot in *igp1*^{AEQ}, *igp3*^{AEQ}, *igp4,* and Col-0 plants upon XA_3XX treatment. We found that MAPKs phosphorylation levels were also reduced in the *igp1*^{AEQ},

igp3^{AEQ} and *igp4* mutants in comparison to wild-type plants, though this reduction was weaker in *igp1* ^{AEQ} than in *igp3* ^{AEQ} and *igp4* plants (Figure 4.31b).

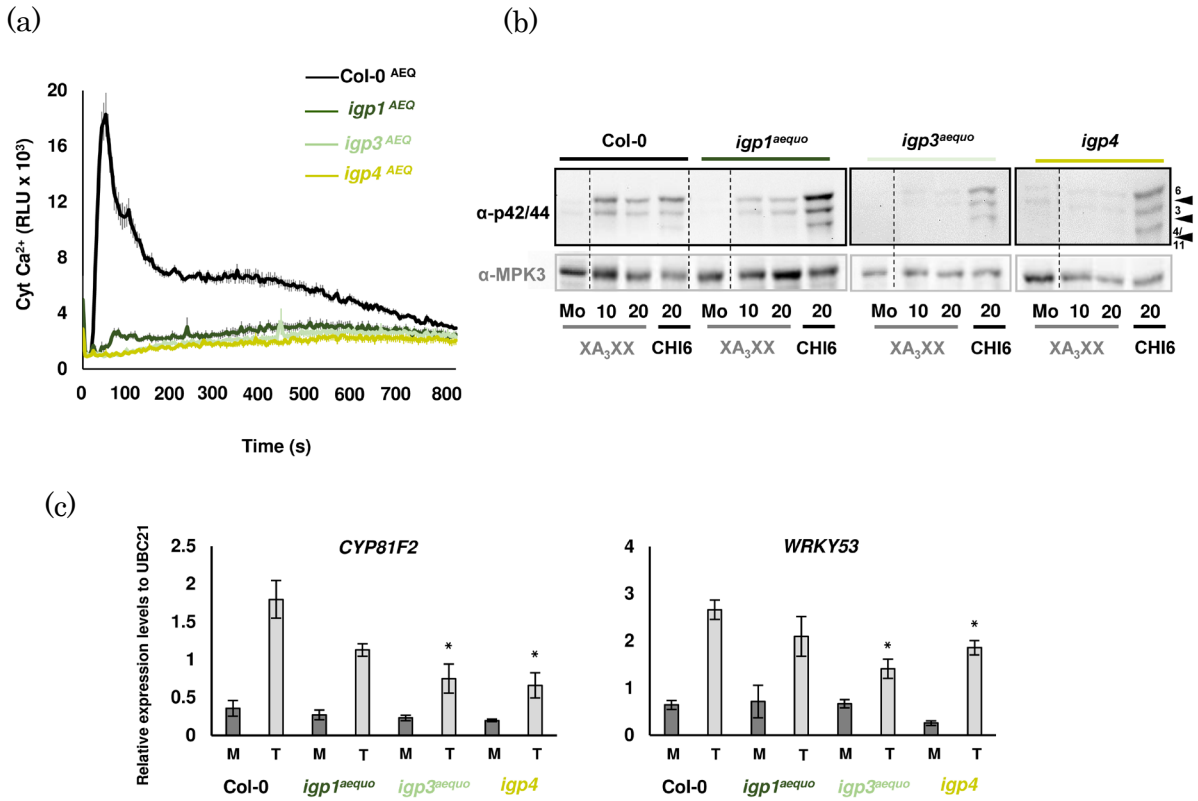

Figure 4.31: *igp* mutants are impaired in XA$_3$XX perception. Determination of PTI hallmarks (a) cytoplasmatic Ca^{2+} influx, (b) phosphorylation of MAPKs, and (c) marker genes up-regulation in *igp* mutants upon XA$_3$XX treatment. Data represent (a) the mean ± standard error (n=8) of cytoplasmatic calcium influx measured as Relative Luminescence Units (RLU) over time in 8-days-old Arabidopsis Col-0^{AEQ} and *igp*s^{AEQ} mutants treated with 250 µM XA$_3$XX; (b) a representative Western Blot out of three replicates (dotted lines indicate that bands were cut from the membrane to relocate them in proper order) where seedlings were treated with 250 µM XA$_3$XX and water as mock, harvested at 10 and 20 minutes after treatment application and (c) the mean ± standard error (n=3) of PTI-related gene expression *CYP81F2* and *WRKY33* measured by qRT-PCR at 30 minutes after 250 µM XA$_3$XX application. Statistically significant differences between compound-treated (T) plants *versus* mock-treated (M, H_2O) were calculated according to Student's t-test (*P < 0.05, **0.01 < P > 0.001, ***P < 0.001).

In agreement with MAPKs phosphorylation levels, we found that the observed up-regulation of PTI marker genes *CYP81F2* and *WRKY53* upon treatment of Col-0 plants with XA$_3$XX was significantly impaired in *igp3*^{AEQ} and *igp4* mutants, whereas such reduction was milder in *igp1*^{AEQ} plants (Figure 4.31c). These data indicate that IGPs also play a function in XA$_3$XX perception in *Arabidopsis thaliana*.

4.3.2. Role of LysM-RKs in XYL4 and XA_3XX perception

Since CERK1, LYK4 and LYK5 may participate in MLG43 perception, and it is also described that OsCERK1 is required for MLGs perception in rice (Rebaque *et al.*, 2021; Yang *et al.*, 2021), we checked if these LysM RKs participates in XYL4 and XA_3XX perception analyzing different PTI immunity hallmarks (Figure 4.32). We used Col-0^{AEQ} and *cerk1-2*^{AEQ} lines to monitor whether early cytoplasmic Ca^{2+} influxes were impaired in *cerk1-2*^{AEQ} upon XYL4 and XA_3XX treatments (Figure 4.32a). Notably, $_{cyt}Ca^{2+}$ influxes in XYL4 and XA_3XX-treated *cerk1-2*^{AEQ} seedlings were similar to those observed in Col-0^{AEQ} plants, whereas CHI6 did not trigger $_{cyt}Ca^{2+}$ influxes in *cerk1-2*^{AEQ} seedlings, as described previously (Mélida *et al.*, 2020) (Figure 4.32a).

cerk1-2 lyk4 lyk5 triple mutant generated in this Thesis was used to test MAPKs phosphorylation upon XYL4 and XA_3XX treatment. As shown in Figure 4.32b, phosphorylation of MAPKs in *cerk1-2 lyk4 lyk5* mutant upon CHI6 treatment was fully impaired, as predicted from the requirement of CERK1, LYK4, and LYK5 for its perception. In contrast, phosphorylation of MAPKs in the LysM triple mutant upon XYL4 or XA_3XX treatment was slightly reduced, but not fully impaired (Figure 4.32b).

Regarding the expression level of the marker genes, *WRKY53* expression in the triple mutant was similar to that of Col-0, but the expression was slightly lower for *CYP81F2*, for both treatments (Figure 4.32c). These results indicate that LysM receptors play a minor function in the perception of xylose-containing glycans in *Arabidopsis thaliana* and also demonstrate that the mechanisms of perception of XYL4/XA_3XX and CHI6 are different.

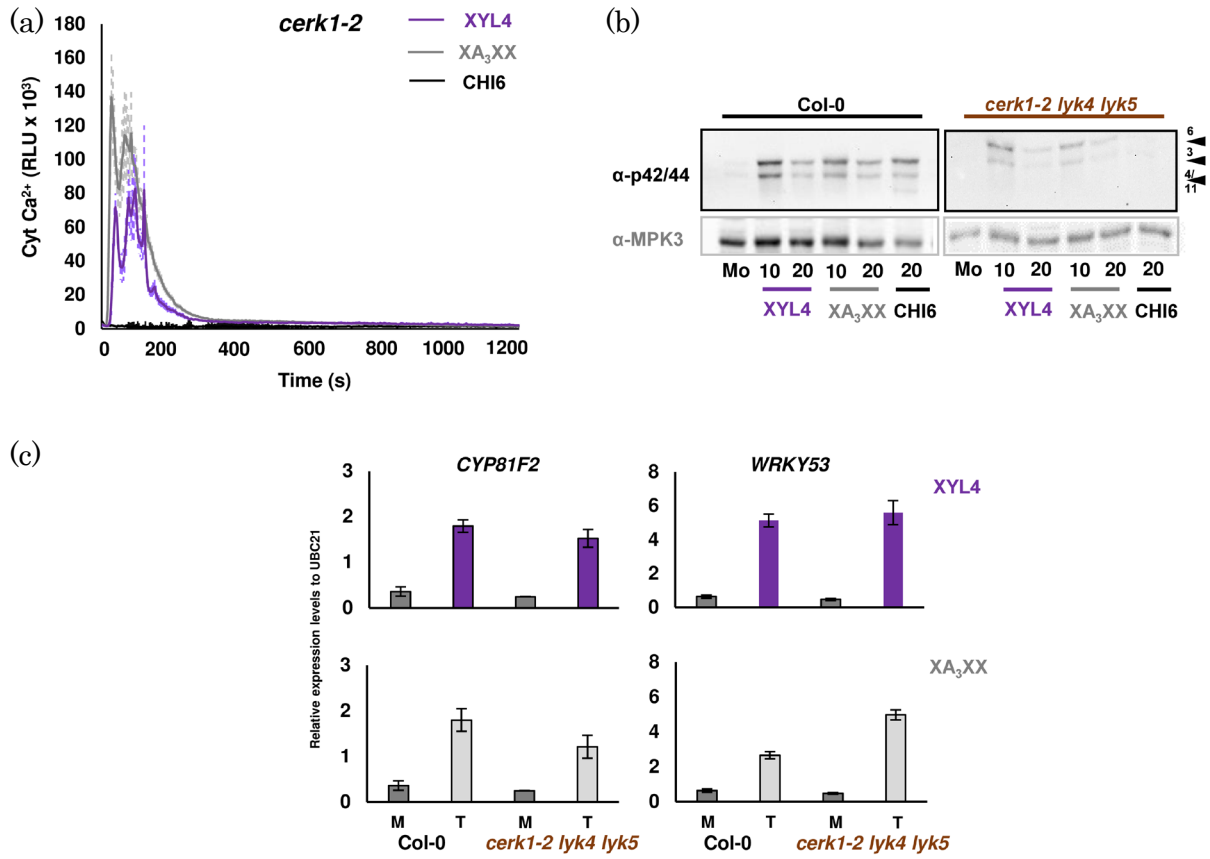

Figure 4.32: LysM RKs have a minor role in XYL4 and XA3XX perception. The activation of immunity hallmarks such as (a) cytoplasmatic Ca $^{2+}$ influx in *cerk1-2*^{AEQ} mutant lines, (b) phosphorylation of MAPKs and (c) marker gene expression in *cerk1-2 lyk4 lyk5* seedlings is partially impaired. Experiments were performed (a) using the mean ± standard error (n=8) of cytoplasmatic calcium influx measured as Relative Luminescence Units (RLU) over time in 8-days-old Arabidopsis Col-0^{AEQ} and *igp*s^{AEQ} mutants treated with 250 µM XYL4 and XA3XX; (b) a representative Western Blot out of three replicates where seedlings were treated with 250 µM XYL4 and XA3XX and water as mock, harvested at 10 and 20 minutes after treatment application and (c) the mean ± standard error (n=3) of PTI-related gene expression *CYP81F2* and *WRKY33* measured by qRT-PCR at 30 minutes after 250 µM XYL4 and XA3XX application. Statistically significant differences between compound-treated (T) plants *versus* mock-treated (M, H_2O) were calculated according to Student's t-test (*P < 0.05, **0.01 < P > 0.001, ***P < 0.001).

5. Discussion

Plant cell walls are very complex and dynamic structures that function as structural elements, providing cell shape and turgor, and protecting the cell content. In recent years, plant cell walls have emerged as an essential component of plant adaptation to biotic and abiotic stresses, and as key regulators of the plant immune system, since the walls are main reservoirs of different glycans/oligosaccharides that trigger immunity (Fernández-Calvo *et al.*, 2024; Mélida *et al.*, 2018; Mélida *et al.*, 2020; Versluys *et al.*, 2022; Voxeur *et al.*, 2019; Wanke *et al.*, 2020; Zang *et al.*, 2019). Cell wall oligosaccharides released during the interaction between pathogens and plants are perceived as DAMPs by PRRs and activate PTI responses. Similarly, other carbohydrate-derived MAMPs from the outmost layers of the pathogens are also perceived as ligands by plant PRRs triggering PTI (Bacete *et al.*, 2018).

Many PRR/peptidic DAMP/MAMP pairs have been elucidated in PTI, like AtPep1 DAMP and bacterial flg22 MAMP peptides, which are directly bound by Arabidopsis PEPR1/2 and FLS2 PRRs, respectively (Bigeard *et al.*, 2015; Boutrot & Zipfel, 2017; Tang *et al.*, 2017). Despite glycans are very abundant molecules in plant and microbial cell walls and out layers, the molecular mechanisms responsible for the perception of glycans in plants are poorly characterized and just a few PRRs and co-PRRs have been described to be involved in these recognition processes. Among these PRRs are members of the LysM RKs, the WAK family as well as CrRLK1 and Lectin-RKs (Dai *et al.*, 2023; Johnson *et al.*, 2018; Kaku *et al.*, 2006; Liu, Yu *et al.*, 2023; Moussu *et al.*, 2023; Yang *et al.*, 2021).

This Thesis has contributed to expand our knowledge of RKs that are involved in the perception of glycans by the plant immune system. Thus, it is described here a group of Arabidopsis RKs – IGP1, IGP3/IGP2 and IGP4 – with LRR-MAL domains in their ECDs, which are required to trigger immune responses mediated by oligosaccharides derived from cellulose (e.g. CEL3– CEL5), MLGs (e.g. MLG43 and MLG34), xylans (e.g. XYL4) and arabinoxylans (e.g. XA_3XX) (Fernandez-Calvo *et al.*, 2024; Martín-Dacal *et al.*, 2023). We also demonstrate that IGP1/CORK1 is a *bona fide* PRR for glycans in plants, and that its ECD binds in ITC experiments CEL3 and CEL5, but not MLG43 (Martín-Dacal *et al.*, 2023).

Our data point to the LRR-MAL RK family as a set of plant proteins involved in the perception of carbohydrate-based DAMPs and MAMPs. So far, the plant RKs

described to be involved in glycan perception belong to the LysM, WAK and CrRLK1 RK families (Bellande *et al.*, 2017; Brutus *et al.*, 2010; Cao *et al.*, 2014; del Hierro *et al.*, 2021; Liu *et al.*, 2012; Liu, Wang *et al.*, 2016; Tang *et al.*, 2022; Wong *et al.*, 2020). The function of most of these proteins in oligosaccharide perception and PTI activation was discovered through the isolation and characterization of Arabidopsis mutants (e.g. *cerk1, lyk4, lyk5, wak1, wak2* and *fer1*).

Similarly, our genetic screening of Col-0^{AEQ} EMS mutagenized population to identify mutants impaired in glycan perception led to the identification of a high number of mutants (*igp1–igp20*) (Table 4.5). *igp1, igp2, igp3*, and *igp4*, that were initially isolated as mutants impaired in MLG43 recognition, have been later proven to be also defective in the perception of cellulose- (CEL3–CEL, xylan- (e.g. XYL4) and arabinoxylan- (e.g. XA_3XX) derived oligosaccharides. These results suggest that the mechanisms of perception of CEL, MLG, xylan and arabinoxylans-derivatives shared some components in Arabidopsis, and this is supported by CEL3/MLG43, XYL4/CEL3 and XYL4/XA_3XX cross-elicitation experiments (Figures 4.9 and 4.29). Despite the similarities between the mechanisms of perception of MLG- and CEL- derived oligosaccharides, some differences might exist among them. For example, we found that LysM RKs (i.e. CERK1, LYK4 and LYK5) have a partial contribution to the perception of MLG43, as described previously (Rebaque *et al.*, 2021; Yang *et al.*, 2021) (Figure 4.13). In contrast, their role in CEL3 perception is residual as only minor differences in PTI activation were observed in *cerk1-2* and *cerk1-2 lyk4 lyk5* triple mutants in comparison with Col-0 plants treated with CEL3 (Figure 4.13). The partial requirement of LysM RKs for MLG perception in Arabidopsis is in line with the described function of rice LysM RK members in the perception of MLG-derived oligosaccharides and immune activation (Yang *et al.*, 2021).

The mechanisms of PTI activation mediated by IGP1, IGP3 and IGP4 LRR-MAL RKs described here differ from that required for pectin and OGs perception involving FER1 and WAK1–WAK5 respectively (Brutus *et al.*, 2010; Dünser *et al.*, 2019; Tang *et al.*, 2022). The mechanism regulated by LRR-MAL RKs also differs from those needed for other MAMPs and DAMPs perception (e.g. flg22 and AtPEP1), since $_{cyt}Ca^{2+}$ burst in *igp1*^{AEQ}–*igp4*^{AEQ} upon treatment with these elicitors was like that of Col-0^{AEQ} plants (Figure 4.7).

Sequencing of *igp1* and *igp2/igp3* mutants revealed point mutations in IGPs KDs that may impact their functionality (Table 4.2). E906K in IGP1 and G773E in IGP3

do not seem to impair the catalytic sites of the kinase domains of these RKs, which are predicted to be almost identical to that of wild-type KDs (Figure 4.17). However, such mutations are predicted to increase the surface patch, resulting in drastic changes in the surface electrostatic potential of the residues around the mutated positions (Figure 4.17). As kinase activity can be altered by mutations at distant residues from the active site (McClendon *et al.*, 2014), we can hypothesize that E906K and G773E mutations might either affect the catalytic activity of the KDs or interfere with the interaction of the RK KDs with other RKs, like true PRRs for other glycans (as MLG43), co-receptors proteins of IGP1 PRR (e.g. IGP2/3 and IGP4) or additional protein partners.

Remarkably, we demonstrate here by ITC binding experiments that the IGP1 ECD, produced in insect cells, binds CEL3 and CEL5 with high affinity ($Kd = 1.19 \pm 0.03\ \mu M$ and $Kd = 1.40 \pm 0.01\ \mu M$, respectively) (Figure 4.19). These results support the function of IGP1/CORK1 as a PRR for cellulose-derived oligosaccharides. The lack of IGP1-ECD binding to MLG43, at least under the *in vitro* conditions of ITC tested, suggests that IGP1 might function as co-receptor for MLG43 perception (Figure 4.19). Similarly, the lack of binding of CEL3 or MLG43 by ECD-IGP4 suggests that this RK might function as co-PRR (Figure 4.20). Since we could not produce IGP3 ECD in insect cells and test its binding capacity in ITC experiments, we do not know the function of IGP3 in this mechanism of perception and downstream activation of PTI responses. Remarkably, IGP1 might be a key element in glycan perception since, besides being the main receptor of cellulose-derived oligosaccharides, we have found in our screening additional alleles with different mutations along IGP1 sequence (*igp6-igp9*) (Table 4.5). Interestingly, those additional mutations located in the ECD are just in the LRR domain, but not in the MAL or transmembrane domains of the protein (Figure 4.28), emphasizing the importance of LRR domain in the functionality of the protein and suggesting that some pocket in this domain might bind CEL3.

A recent article reports that two LRR RKs, STRESS INDUCED FACTOR 2 and 4 (SIF2, AT1G51850; SIF4, AT1G51820), are also required for the immune responses triggered by cellulose-derived oligosaccharides and could also be part of the PRR complex involved in their perception (Zarattini *et al.*, 2021). Also, a poly(A)-specific ribonuclease (AtPARN, AT1G55870) was found to be required for the regulation of the immune responses triggered by CEL3 in Arabidopsis, probably through a mechanism of degradation of the polyA tail from specific mRNAs (Johnson *et al.*, 2018). However, this AtPARN regulatory mechanism of CEL3-mediated responses

acts downstream of CEL3 perception by PRRs at the cell surface described here. Moreover, *sif2* and *sif4* mutants are defective in the synthesis of camalexin upon CEL-oligosaccharides treatment, but do not seem to be impaired in MAPKs phosphorylation and gene expression triggered by these DAMPs (Zarattini *et al.*, 2021).

The mechanisms of perception of MLGs-derived oligosaccharides in Arabidopsis has been partially elucidated in this Thesis with the discovery of IGP1, IGP2/3 and IGP4 (Figure 5.1a). However, direct binding of MLG43 to the ECD of IGP1 and IGP4 has not been proved. In rice, OsCERK1 has been suggested to be the PRR receptor of MLG-derived oligosaccharides (Yang *et al.*, 2021; Figure 5.1b) based on microscale thermophoresis analysis performed with the ECD produced in baculovirus, whereas OsCeBiP, the rice receptor for chitin-derived oligosaccharides, has been proposed to be the MLG co-receptor of CERK1, based on the lack of binding of its ECD to these MLG ligands (Figure 5.1b) (Yang *et al.*, 2021). The K*d* values of ECD–OsCERK1 for MLG43 are in the range of 1–2 μ_M, similar to that found for IGP1 binding to CEL3/CEL5 in this work, and to that of ECD– OsCeBiP for CHI6 (Yang *et al.*, 2021). Of note, the perception of CHI6 is neither altered in *igp1-igp4* nor altered in *igp5-igp9* mutants, further indicating that Arabidopsis IGPs proteins are not required for CHI6 perception (Figures 4.2, 4.11 and 4.27). These data point to separate mechanisms for the perception of CHI6 and the CEL- and MLGs-derived oligosaccharides in Arabidopsis, but also to some differences in the mechanism of perception of CEL3 (independent of CERK1, LYK4 and LYK5, and with IGP1 as a true PRR) and MLG43 (requiring CERK1, LYK4 and LYK5, with the true PRR yet to be determined). Recently, a LEC-RK has been also described to be required for the perception of MLG43 in rice and binding of MLG43 to the full-length protein produced in bacteria has been shown in thermal shift experiments (Figure 5.1b) (Dai *et al.*, 2023). Whether a putative ortholog of LEC-RK in Arabidopsis might be involved in MLG43 perception is unknown, and an *igp* mutant impaired in the rice ortholog gene has not been identified in the set of *igp* mutants sequenced so far.

As we saw that CEL- and MLGs-derived oligosaccharides' perception shared triggering and signalling pathways, we checked if IGPs were implicated in the perception of additional carbohydrates. We found that they are also involved in the activation of PTI responses triggered by xylan-containing oligosaccharides (e.g. XYL4 and XA_3XX) (Figures 4.30 and 4.31). Our data suggest that IGP RKs are central components in the perception and downstream PTI activation triggered by

a diversity of oligosaccharides with different carbohydrate moieties in their composition (glucose, xylans, arabinofucose) and distinct structures, that include, at least CEL3-CEL5, MLG43, XYL4 and XA_3XX (Figure 5.1a). Despite the differential composition and structures of these oligosaccharides, they share some features that might explain their similar mechanisms of perception by IGP1/IGP3/IGP4: i) they are composed of monosaccharides (pentose and hexoses) in pyranose conformation; and ii) they have two units with a ß-1,4-D-linkage, including the anomeric carbon (position 1) that is probably in its reduced form. The differential impairment of PTI response upon XYL4 and XA_3XX observed in *igp4* and *igp3* (fully blocked responses), in comparison to *igp1* (partially impaired) might be explained by the fact that *igp1* is not a loss-of-function mutant, since a similar pattern of impairment of PTI responses has been observed after CEL3 and MLG43 treatments. Whether IGP3 and/or IGP4 might be the bona-fide PRRs for XYL4 and XA_3XX might be addressed with a deeper biochemical characterization and binding assays with their ECDs.

Here we also show that the mechanism of perception of XYL4 and XA_3XX requires partially LysM-RKs, CERK1, LYK5, and LYK4, probably acting as redundant co-receptors. Our data further expand the previously described function of these LysM-RKs as putative co-receptors for MLG43 and ß-1,3-Glc oligosaccharides (e.g. LAM6) (del Hierro *et al.*, 2021; Mélida *et al.*, 2020; Rebaque *et al.*, 2021). The role of LysM RKs in the mechanisms of perception of several glycans in plant-microbe interactions is an emerging topic that deserves further characterization (Yang, Wang, *et al.*, 2021).

Despite the structural diversity of ligands that can be bound by plants ECD-PRRs, most of the best characterised ECD-PRR/ligand pairs at the structural level are LRR-ECD/peptide ones, like FLAGELLIN-SENSITIVE 2 (FLS2)/flg22 (MAMP from bacterial flagellum) (Figure 5.1a), EF-Tu Receptor (EFR)/elf18 (MAMP from bacterial Elongation Factor protein) or PEP RECEPTOR 1 (PEPR1)/PEP1 (phytocytokine peptide; Bartels & Boller, 2015; Boutrot & Zipfel, 2017; Gully *et al.*, 2019; Peng *et al.*, 2018). These LRR-ECD/peptide pairs have been successfully crystalized with the ligand in the binding pocket, and in some cases with the co-PRR included in the crystal structure (e.g. RKs of SOMATIC EMBRYOGENESIS RECEPTOR-LIKE KINASES family, such as BRI1-ASSOCIATED KINASE 1 (BAK1) RK for FLS2, EFR and PEPR1: Boutrot & Zipfel, 2017; Li *et al.*, 2020). In contrast to the numerous peptidic-ECDs structures of RKs determined, the number of crystal structures of PRR/glycan pairs characterized so far is limited to

a few examples: LysM-chitin in PTI and LysM-LCOs/COs in symbiosis (Figure 5.1) (Gysel *et al.*, 2021; Khokhani *et al.*, 2021; Liu *et al.*, 2012) and a recent example of LRR-extensin involving FERONIA RK (Figure 5.1a) (Moussu *et al.*, 2023; Schoenaers *et al.*, 2024). A summary of our current knowledge of perception of glycans by ECD-PRR structures is described in Figure 5.1. A detailed knowledge of the binding mechanisms of glycans (MAMPs/DAMPs) by ECD-PRR structures is needed, as recently remarked in two reviews (Lee & Santiago, 2023; Molina *et al.*, 2024).

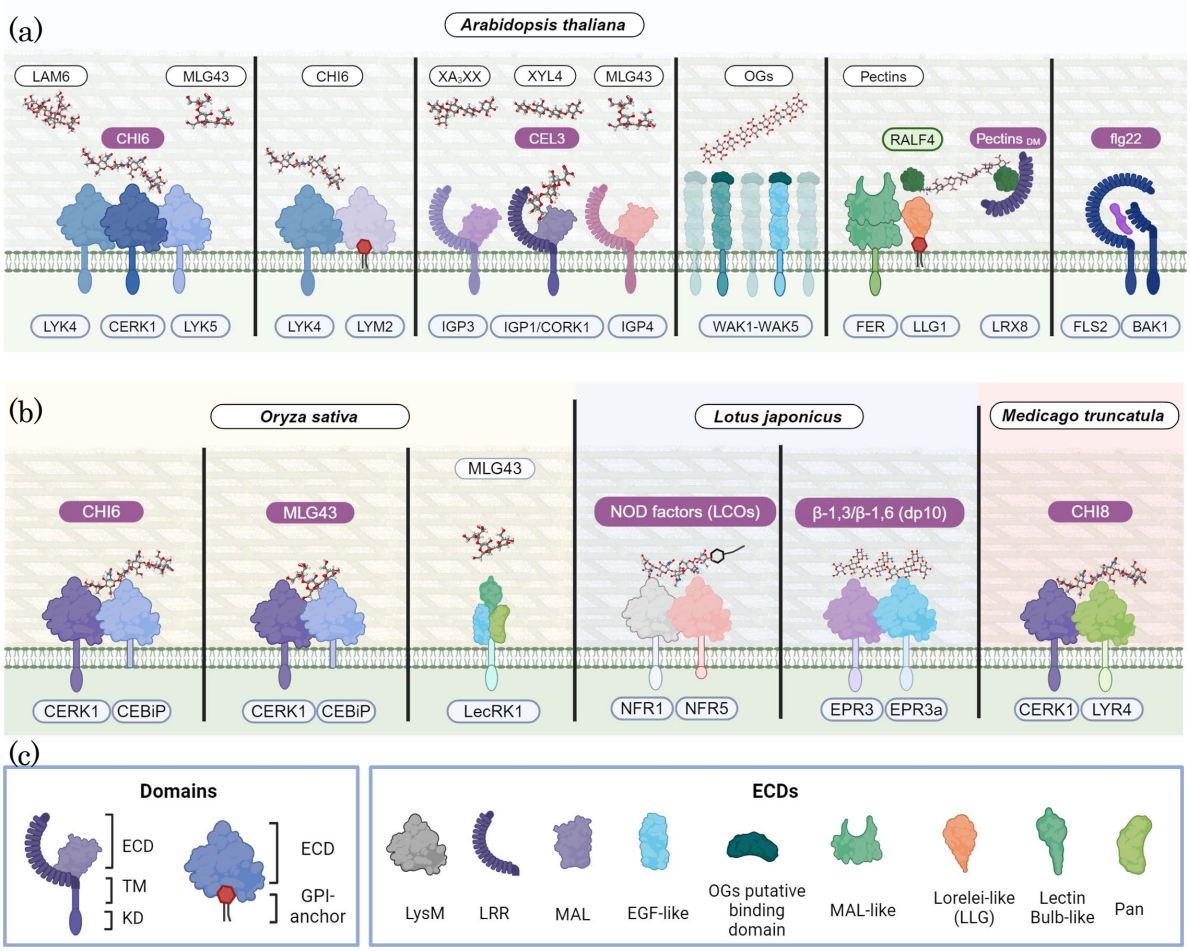

Figure 5.1: Plant receptors involved in the perception of different glycans structures in plant immunity or symbiosis. Updated version of Figure 1.2, including IGPs and their target glycans identified in this Thesis. In panel (a) are shown PRRs and co-PRRs from *Arabidopsis thaliana* and in panel (b) from other plant species, *Oryza sativa*, *Lotus japonicus* and *Medicago trunculata*. Glycan names indicated in purple correspond to DAMPs/MAMPs that have been demonstrated to be bound by the indicated PRRs, protein receptors (e.g., LRX8), or RALF peptides, either by *in vitro* binding experiments or by structural characterization, and are shown in close interaction with the corresponding receptor. The co-PRRs involved in glycan perception are also depicted. Glycans highlighted in white have been shown to require these PRR-co-PRRs complexes to trigger immune/symbiotic responses, but direct binding by PRR has not been demonstrated. FLS2-BAK1-flg22 recognition complex is included for comparison. Overlapping of RK domains indicates that

PRR-coPRR interaction has been demonstrated. The different structures of plant receptors (RK/RP/RPe/g) and the domains in their ECDs represented in panels (a) and (b) are indicated in the inset (c).

The crystal structure of the CERK1-ECD bound to chitin-derived oligosaccharides revealed the structural basis of chitin recognition (Liu *et al.*, 2012; Yang *et al.*, 2021). Other plant ECD-RKs like ANX1, ANX2 and FER1, which harbour two tandem MLDs, have been also purified and crystallized, but their putative glycoligand(s) has not been identified yet (Moussu *et al.*, 2018). Notably, the MLDs of ANX1, ANX2 and FER1 seem to show some differences compared with those MAL domains present in the ECDs of the three IGP RKs identified in this work, which also contain an N-terminal LRR domain (Yang, Wang *et al.*, 2021). We have generated *de novo* structural models for the three LRR-MAL RKs, and these models suggest that IGP1, IGP3 and IGP4 have similar structures, in line with their putative recent evolutionary divergence, although IGP1 has an extra loop in its KD (Figure 4.17). Remarkably, MAL domains of these RKs are structurally very similar to that of the MAL protein of *Xenopus* sp., which is involved in oligosaccharide binding, and to that of plant ANX1/ANX2 from the CrRLK1 family. In recent reports by Tseng *et al.*, (2022), two phenylalanine residues conserved in all Arabidopsis MAL domains, but not in MAL from *Xenopus* sp. (Schallus *et al.*, 2010) are noted as essential for CEL3 perception and PTI activation, but this hypothesis has not been validated through binding experiments. Therefore, we hypothesize that the LRR domain of ECDs in IGP1 might be essential for the formation of the structural pocket involved in the observed CEL3 and CEL5 binding, since all the ECD-mutations identified in *igp1* alleles are in this domain and not in MAL domain (Figure 4.28). Obtaining crystallized structures of CEL3/ECD-IGP1 will contribute to decipher the structural bases of CEL3–CEL5 recognition by LRR-MAL ECD.

On the other hand, IGP1, IGP3 and IGP4 genes are in a cluster in the *A. thaliana* genome, indicating recent duplication events (Yang, Wang *et al.*, 2021). These genes form part of a family of at least 13 members that has not been characterized in detail previously. Some of these members have been involved in plant disease resistance responses (Le *et al.* 2014), brassinosteroids-associated mechanisms (Xu *et al.*, 2014), and promotion of early compatible pollen responses in Arabidopsis pistil (Lee & Goring, 2021). Some of these processes have associated changes in cell wall composition (Lee & Goring, 2021; Rajaraman *et al.*, 2016). This clade of

LRR-MAL RKs seems to be conserved and diversified in dicots and in some monocots, like rice. However, the few relatives RKs found in grasses are structurally dissimilar and phylogenetically distant (Yang, Wang *et al.*, 2021). LRR-MAL RKs have ECDs with 12 LRRs followed by a MAL domain that differs from the MAL-like domain of CrRLK1 ECDs (Yang, Wang, *et al.* 2021). Based on the structural similarity of MAL domains of LRR-MAL RKs with those from mammals and *Xenopus* sp, that bind glycans (Schallus *et al.* 2008), it had been hypothesized that MAL domains of these LRR-MAL RKs could also bind glycans. However, other alternatives for CEL3/CEL5 binding to IGP1 ECD rather than binding to MAL domains might be feasible, like a potential binding pocket comprising the two domains (MAL and LRR) which upon glycan binding induces receptor conformational change and kinase domain activation of IGP1. Also, it should not be excluded that LRR domains could bind glycans based on the heterogenicity of biomolecules that plant LRR domains can bind (e.g. from H_2O_2 to brassinosteroids and peptides) (Bojar *et al.*, 2014; Rhodes *et al.*, 2021; Sun, Li, *et al.*, 2013; Sun, Han, *et al.*, 2013).

Likewise, it should be kept in mind that some other additional RKs from this family might be *bona fide* PRRs for XYL4 and/or XA_3XX. Though some of these LRR-MAL RK members have been involved in pollen migration and fertility (Lee & Santiago, 2023), an alternative function for such PRRs in oligosaccharide perception cannot be discarded, since pollen migration and lateral root formation promote changes in cell wall integrity and composition (Lee & Santiago, 2023; Moussu *et al.*, 2023). Xylans-, arabinoxylans-, MLGs- and cellulose-derived oligosaccharides can also be released upon alteration of plant cell wall integrity triggered by other stresses (e.g. salt or drought) or across plant development (e.g. during cell wall remodeling; Bacete *et al.*, 2022, Gigli-Bisceglia *et al.*, 2022). During these processes plant endogenous enzymes can hydrolase cell wall polysaccharides, as described recently for a *Zea mays* (maize) GH17 licheninase that releases MLG43- derived and other oligosaccharides (Kraemer *et al.*, 2021). The characterization of the role of glycan-mediated responses in these additional processes must be determined to understand their interaction with PTI/disease resistance responses and their impact on plant fitness.

Plants must control the generation and levels of active DAMPs and the exposure to DAMPs and MAMPs that trigger PTI, given their fundamental role in modulating growth-defence trade-offs (Molina *et al.*, 2021; Pontiggia *et al.*, 2020). Long-lasting or intense activation of defensive signaling pathways can generate

hyper-immunity that might cause cell death and plant development alterations (Berry & Argueso, 2022). For example, OGs overaccumulation leads to reduced plant growth and even lethality (Benedetti *et al.*, 2015). In plants, cell wall remodelling is a relevant process that takes place during cell expansion and growth (Delmer *et al.*, 2024), and therefore some mechanisms are needed to fine-tune the turnover/metabolism of cell wall-derived signals during non-pathogenic (e.g. cell expansion) and pathogenic conditions (De Lorenzo & Cervone, 2022).

Until recently, plant mechanisms modulating homeostasis of cell wall-derived danger signals were unknown. Notably, several plant enzymes have been identified that can modify the released DAMPs thereby fine-tuning their eliciting capacity and the amplitude of the defence responses triggered (Benedetti *et al.*, 2018; Locci *et al.*, 2019). The Arabidopsis superfamily of FAD-binding berberine bridge enzyme like (AtBBE-like) has turned out to play relevant functions in the homeostasis of certain DAMPs. Of note, the expression of several *AtBBE-like* genes is up-regulated during infection and upon plant treatment with MAMPs/DAMPs (Figure 5.2) (Benedetti *et al.*, 2018; Costantini *et al.*, 2024; Locci *et al.*, 2019; Mélida *et al.*, 2018; Mélida *et al.*, 2020; Pontiggia *et al.*, 2020). Four OG-oxidases (OGOXs) and one cellodextrin oxidase (CELLOX) from the AtBBE-like family have been found to oxidize the anomeric carbon of some oligosaccharides. OGOXs specifically oxidate the anomeric carbon of OGs with different DP to inactivate them (Benedetti *et al.*, 2018), while CELLOX oxidizes the anomeric carbon of CEL3-CEL6 and some MLGs (e.g. MLG43), but not that of glucose (Figure 5.2) (Locci *et al.*, 2019). The oxidized OGs and CEL-oligos are biologically less active triggering PTI than the reduced ones, probably because PRRs have lower affinity for these modified glycans (Figure 5.2). It has also been described that these oxidized glycans are less accessible to fungal lytic enzymes (PGs and endoglucanases), limiting fungi access to carbon sources (glycans of low DP) that they can use for the energetic catabolism and as building blocks for biosynthetic processes, thus reducing pathogen proliferation (Figure 5.2) (Locci *et al.*, 2019; Zarattini *et al.*, 2021). Interestingly, CEL3, the most active cellulose-derived DAMPs activating PTI (Locci *et al.*, 2019; Martín-Dacal *et al.*, 2023), is the best substrate for CELLOX (Locci *et al.*, 2019), highlighting the fundamental role of these modifying enzymes in the regulation of the activity and homeostasis of cell wall-derived DAMPs (Figure 5.2). It should be noted that oxidation of OGs and CEL-oligos generates H_2O_2, which plays an essential function in the subsequent strengthening of the cell wall and cell signaling mediated through the extracellular H_2O_2 sensor HPCA1

(Scortica *et al.*, 2022; Wu *et al.*, 2020). To further decipher the complex roles of glycans in plants, it is also important to analyse in depth the regulation of the homeostasis of cell wall-derived oligosaccharides.

Also, other key questions exemplified in Figure 5.2 need to be clarified: i) if LRR-MAL RKs are subjected to endocytosis upon glycan perception, as described for other PRRs (Claus *et al.*, 2018; Irani & Russinova, 2009); or ii) if there is upregulation of LRR-MAL RKs gene expression upon glycan perception, among other relevant questions.

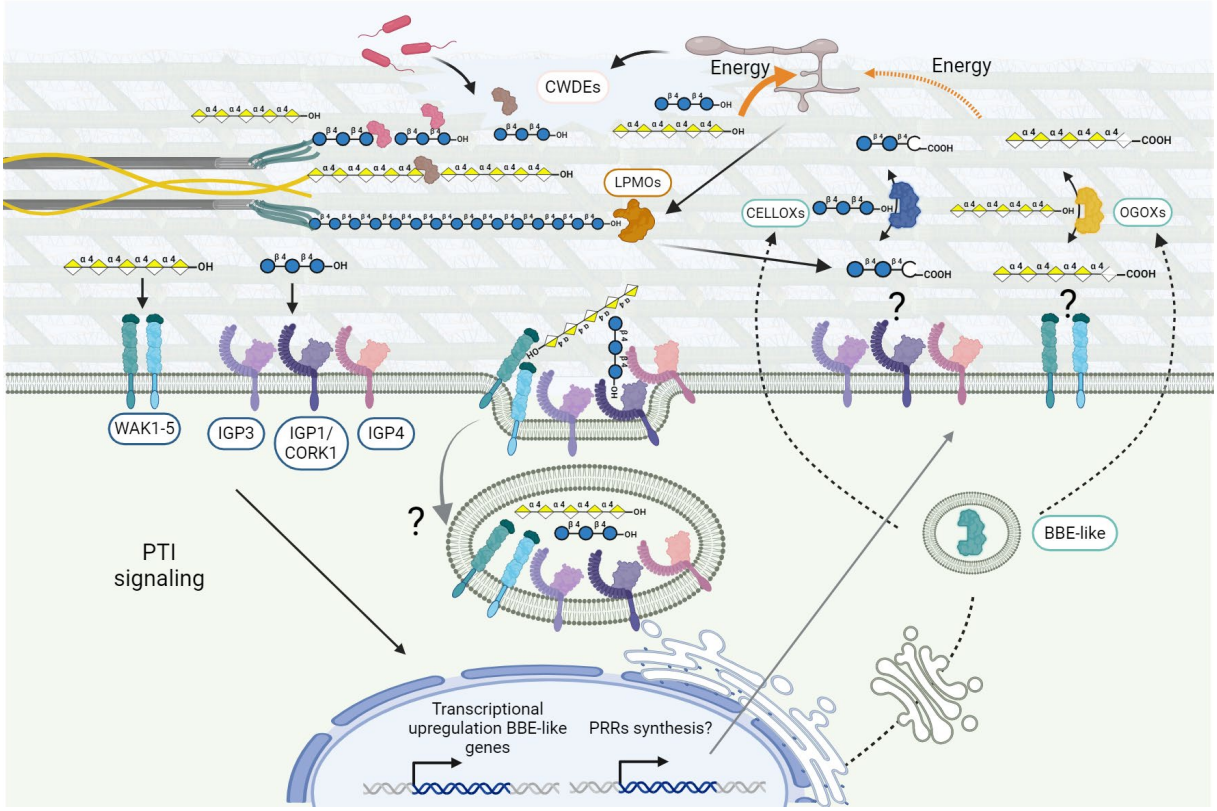

Figure 5.2: Release and homeostasis of cell wall-derived DAMPs triggering immune responses in plants. Cell Wall Degrading Enzymes (CWDEs) secreted by pathogens hydrolyse cell wall polysaccharides (e.g., cellulose and HG) releasing glycans that can be used by pathogens as a source of carbons for their energetic catabolism and/or building blocks for biosynthesis. Some of the released glycans, such as CEL3-CEL5 and OGs, can be perceived as DAMPs by plant PRRs (e.g., IGP1 and WAK RKs, respectively) that might form complexes with some additional RKs functioning as co-PRRs (e.g., IGP3/IGP4 and other WAKs, respectively). The binding of glycan by PRR activates PTI signalling and transcriptional regulation of several immune genes, such as those encoding PRRs and co-PRRs, that might replenish these proteins at the plasma membrane. Pathogens also secrete Lytic Polysaccharide Monooxygenases (LPMOs) that oxidatively cleave cell wall polysaccharides, such as cellulose, releasing C1 carbon oxidized oligosaccharides with lower PTI activity. Whether PRRs/co-PRRs binding glycans are internalized by endocytosis upon ligand binding, as described for some ligand-LRR RK complex (FLS2-BAK1-flg22), is unknown. Genes

encoding BBE-like enzymes are also upregulated upon pathogen infection and DAMP treatment, and BBE proteins (CELLOXs and OGOXs) are secreted to the apoplast to oxidize glycans (e.g., CEL3 and OGs) at the anomeric carbon (-COOH at C1) probably lowering their binding affinity by PRRs. Oxidized oligosaccharides (-COOH at C1) are poor substrates for the energetic catabolism of pathogens hindering their colonization. Question marks indicate open topics that deserve further investigation. The glycan structures were drawn following the SNFG (Symbol Nomenclature for Glycans) (Neelamegham *et al.*, 2019; Varki *et al.*, 2016). IGPs and WAK RK domains are described in Figure 5.1.

On the other hand, *in silico* synthesis of diverse glycan structures using novel chemical methodologies or synthetic biology from microorganisms would be needed, since these pure glycans structures should be used in genetic and functional screenings designed to identify novel DAMPs/MAMPs or to determine ECD-PRRs binding specificities (Chaube *et al.*, 2022). Moreover, genetic screening and the use of genome editing to generate higher order mutants in putative glycan *PRR* gene families might be required to overcome receptor redundancy in plants. Additional studies in the field are necessary to expand our knowledge of plant immunity activation and regulation and will provide new ideas and tools that might be useful to develop more sustainable agriculture practices. It is expected that active glycans will emerge as bio-control compounds that will burst the adaptative response of the plants in a changing environmental adaptation of crops (Melida *et al.*, 2018; Rebaque *et al.*, 2021). Last, the identification of genetic traits impacting cell wall integrity and cell wall-mediated disease resistance (e.g. PRRs and co-PRRs) will contribute to improve crop adaptation to environmental changes. Indeed, several crop disease resistance Quantitative Trait Locis (QTLs) have been shown to encode WAK genes (Huerta *et al.*, 2023; Zuo *et al.*, 2015).

In summary, our results contribute to further understanding the mechanisms of perception of oligosaccharides by the plant immune system and to expand the set of families of PRRs and the ECD structures involved in glycan-based ligand recognition and immune activation in plants. The valuable knowledge and tools generated in this Thesis might be implemented in the future in the form of new biocontrol compounds and genetic traits to increase crop disease resistance technologies and products contributing to develop more sustainable agriculture solutions.

6. Conclusions

1. *igp1, igp2/3* and *igp4* are *Arabidopsis thaliana* mutants altered in three receptor kinases (RKs) – AT1G56145 (IGP1), AT1G56130 (IGP2/IGP3) and AT1G56140 (IGP4) – with Leucine-Rich-Repeat (LRR) and Malectin (MAL) domains in their ectodomains.
2. *igp1, igp2/3* and *igp4* are defective in Pattern Triggered Immunity (PTI) activation mediated by MLG43 and CEL3.
3. XYL4 and XA_3XX perception is also impaired in *igp1, igp2/3* and *igp4* mutants.
4. IGP1, IGP3 and IGP4 RKs are required for the perception of cellulose- (CEL3-CEL5), MLGs- (MLG43, MLG34), xylans- (XYL4), and arabinoxylans- (XA_3XX) derived oligosaccharides in *Arabidopsisis thaliana*
5. There is no functional redundancy between IGP RKs since the lack of one of them affects plants cellulose-, MLGs- and xylose-derived glycans perception.
6. IGP1/CORK1 RK ectodomain binds CEL3 and CEL5 in Isothermal Titration Calorimetry (ITC) experiments, indicating that it is a Pattern Recognition Receptor (PRR) for these glycans. IGP1/CORK1 RK is the first Pattern Recognition Receptor (PRR) described for cellulose, the main component of plant cell walls.
7. IGP2/3 and IGP4 RKs play a role in cellulose-derived glycans perception but probably as co-receptors and/or additional components of the perception complex.
8. IGP1 RK and IGP4 RK ectodomains do not bind MLG43 in Isothermal Titration Calorimetry (ITC) experiments, suggesting that they probably are co-receptors and/or additional components of a receptor complex required for MLG43 perception in *Arabidopsis thaliana.*
9. LysM RKs CERK1, LYK4 and LYK5 are additional components that partially participate in the perception of MLGs-derived oligosaccharides and, to a lesser extent, in XYL4 and XA_3XX perception, but not in the perception of CEL3 and CEL5 glycans.
10. Our results contribute to further understand plant mechanisms of oligosaccharides perception, expanding the group of Pattern Recognition

Receptor (PRR) families and ectodomain structures described in ligand recognition and plants' immune activation.

References

Abarca, A., Franck, C. M., & Zipfel, C. (2021). Family-wide evaluation of RAPID ALKALINIZATION FACTOR peptides. *Plant Physiology*, *187*(2), 996-1010.

Addison, B., Bu, L., Bharadwaj, V., Crowley, M. F., Harman-Ware, A. E., Crowley, M. F., Bomble, Y. J., & Ciesielski, P. N. (2024). Atomistic, macromolecular model of the Populus secondary cell wall informed by solid-state NMR. *Science Advances*, *10*(1), eadi7965.

Afzal, A. J., Wood, A. J., & Lightfoot, D. A. (2008). Plant receptor-like serine threonine kinases: roles in signaling and plant defense. *Molecular Plant-Microbe Interactions*, *21*(5), 507-517.

Albersheim, P., Darvill, A., Roberts, K., Sederoff, R., & Staehelin, A. (2010). *Plant cell walls*. Garland Science.

Albert, I., Böhm, H., Albert, M., Feiler, C. E., Imkampe, J., Wallmeroth, N., Brancato, C., Raaymakers, T. M., Oome, S., Zhang, H., Krol, E., Grefen, C., Gust, A. A., Chai, J., Hedrich, R., Van den Ackervejen, G., & Nürnberger, T. (2015). An RLP23–SOBIR1–BAK1 complex mediates NLP-triggered immunity. *Nature plants, 1*(10), 1-9.

Alonso Baez, L., & Bacete, L. (2023). Cell wall dynamics: novel tools and research questions. *Journal of Experimental Botany*, *74*(21), 6448-6467.

Álvarez-Martínez, I., Ruprecht, C., Senf, D., Wang, H. T., Urbanowicz, B. R., & Pfrengle, F. (2023). Chemo-Enzymatic Synthesis of Long-Chain Oligosaccharides for Studying Xylan-Modifying Enzymes. *Chemistry–A European Journal*, *29*(26), e202203941.

Andrews, S. (2010) FastQC: A Quality Control Tool for High Throughput Sequence Data. https://www.bioinformatics.babraham.ac.uk/projects/fastqc/

Arya, G. C., Sarkar, S., Manasherova, E., Aharoni, A., & Cohen, H. (2021). The plant cuticle: an ancient guardian barrier set against long-standing rivals. *Frontiers in plant science*, *12*, 663165.

Atkinson, N. J., & Urwin, P. E. (2012). The interaction of plant biotic and abiotic stresses: from genes to the field. *Journal of experimental botany*, *63*(10), 3523-3543.

Atmodjo, M. A., Hao, Z., & Mohnen, D. (2013). Evolving views of pectin biosynthesis. *Annual review of plant biology*, *64*, 747-779.

Aziz, A., Gauthier, A., Bézier, A., Poinssot, B., Joubert, J. M., Pugin, A., Heyraud, A., & Baillieul, F. (2007). Elicitor and resistance-inducing activities of β-1, 4 cellodextrins in grapevine, comparison with β-1, 3 glucans and α-1, 4 oligogalacturonides. *Journal of experimental botany*, *58*(6), 1463-1472.

Bacete, L., Mélida, H., López, G., Dabos, P., Tremousaygue, D., Denancé, N., Miedes, E., Bulone, V., Goffner, D., & Molina, A. (2020). Arabidopsis response regulator 6 (ARR6) modulates plant cell-wall composition and disease resistance. *Molecular Plant-Microbe Interactions*, *33*(5), 767-780.

Bacete, L., Mélida, H., Miedes, E., & Molina, A. (2018). Plant cell wall-mediated immunity: cell wall changes trigger disease resistance responses. *The Plant Journal*, *93*(4), 614-636.

Bacete, L., Mélida, H., Pattathil, S., Hahn, M. G., Molina, A., & Miedes, E. (2017). Characterization of plant cell wall damage-associated molecular patterns regulating immune responses. *Plant Pattern Recognition Receptors: Methods and Protocols*, 13-23.

Bacete, L., Schulz, J., Engelsdorf, T., Bartosova, Z., Vaahtera, L., Yan, G., Gerhold, J. M., Tichá, T., Øvstebø, C., Gigli-Bisceglia, N., Joahannessen-Starheim, S., Margueritat, J., Kollist, H., Dehoux, T., McAdam, S. A. M., & Hamann, T. (2022). THESEUS1 modulates cell wall stiffness and abscisic acid production in Arabidopsis thaliana. *Proceedings of the National Academy of Sciences*, *119*(1), e2119258119.

Baez, L. A., Tichá, T., & Hamann, T. (2022). Cell wall integrity regulation across plant species. *Plant Molecular Biology*, *109*(4), 483-504.

Bai, L., Zhang, G., Zhou, Y., Zhang, Z., Wang, W., Du, Y., Wu, Z., & Song, C. P. (2009). Plasma membrane-associated proline-rich extensin-like receptor kinase 4, a novel regulator of Ca2+ signalling, is required for abscisic acid responses in *Arabidopsis thaliana*. *The Plant Journal*, *60*(2), 314-327.

Banik, M., Liu, S., Yu, K., Poysa, V., & Park, S. J. (2007). Molecular TILLING and EcoTILLING: effective tools for mutant gene detection in plants. *Genes Genomes Genomics, 1*(2), 123-132.

Barghahn, S., Arnal, G., Jain, N., Petutschnig, E., Brumer, H., & Lipka, V. (2021). Mixed linkage β-1, 3/1, 4-glucan oligosaccharides induce defense responses in *Hordeum vulgare* and *Arabidopsis thaliana*. *Frontiers in plant science, 12*, 682439.

Bartels, S., & Boller, T. (2015). Quo vadis, Pep? Plant elicitor peptides at the crossroads of immunity, stress, and development. *Journal of experimental botany*, *66*(17), 5183-5193.

Bellande, K., Bono, J. J., Savelli, B., Jamet, E., & Canut, H. (2017). Plant lectins and lectin receptor-like kinases: how do they sense the outside?. *International journal of molecular sciences*, *18*(6), 1164.

Bender, K. W., & Zipfel, C. (2023). Paradigms of receptor kinase signaling in plants. *Biochemical Journal*, *480*(12), 835-854.

Benedetti, M., Pontiggia, D., Raggi, S., Cheng, Z., Scaloni, F., Ferrari, S., Ausubel, F. M., Cervone, F., & De Lorenzo, G. (2015). Plant immunity triggered by engineered in vivo release of oligogalacturonides, damage-associated molecular patterns. *Proceedings of the National Academy of Sciences*, *112*(17), 5533-5538.

Benedetti, M., Verrascina, I., Pontiggia, D., Locci, F., Mattei, B., De Lorenzo, G., & Cervone, F. (2018). Four Arabidopsis berberine bridge enzyme-like proteins are specific oxidases that inactivate the elicitor-active oligogalacturonides. *The Plant Journal*, *94*(2), 260-273.

Berry, H. M., & Argueso, C. T. (2022). More than growth: Phytohormone-regulated transcription factors controlling plant immunity, plant development and plant architecture. *Current Opinion in Plant Biology*, *70*, 102309.

Bethke, G., Thao, A., Xiong, G., Li, B., Soltis, N. E., Hatsugai, N., Hillmer, R. A., Katagiri, F., Kliebenstein, D. J., Pauly, M., & Glazebrook, J. (2016). Pectin biosynthesis is critical for cell wall integrity and immunity in *Arabidopsis thaliana*. *The Plant Cell*, *28*(2), 537-556.

Bhat, A., & Ryu, C. M. (2016). Plant perceptions of extracellular DNA and RNA. *Molecular plant, 9*(7), 956-958.

Bigeard, J., Colcombet, J., & Hirt, H. (2015). Signaling mechanisms in pattern-triggered immunity (PTI). *Molecular plant*, *8*(4), 521-539.

Bisceglia, N.G., Gravino, M., & Savatin, D. V. (2015). Luminol-based assay for detection of immunity elicitor-induced hydrogen peroxide production in *Arabidopsis thaliana* leaves. *Bio-Protocol, 5(24)*, e1685.

Bjornson, M., Pimprikar, P., Nürnberger, T., & Zipfel, C. (2021). The transcriptional landscape of *Arabidopsis thaliana* pattern-triggered immunity. *Nature plants*, *7*(5), 579-586.

Boerjan, W., Ralph, J., & Baucher, M. (2003). Lignin biosynthesis. *Annual review of plant biology*, *54*(1), 519-546.

Böhm, H., Albert, I., Oome, S., Raaymakers, T. M., Van den Ackerveken, G., & Nürnberger, T. (2014). A conserved peptide pattern from a widespread microbial virulence factor triggers pattern-induced immunity in Arabidopsis. *PLoS pathogens, 10*(11), e1004491.

Boisson-Dernier, A., Kessler, S. A., & Grossniklaus, U. (2011). The walls have ears: the role of plant CrRLK1Ls in sensing and transducing extracellular signals. *Journal of experimental botany*, *62*(5), 1581-1591.

Bojar, D., Martinez, J., Santiago, J., Rybin, V., Bayliss, R., & Hothorn, M. (2014). Crystal structures of the phosphorylated BRI 1 kinase domain and implications for brassinosteroid signal initiation. *The Plant Journal*, *78*(1), 31-43.

Bose, J., Rodrigo-Moreno, A., & Shabala, S. (2014). ROS homeostasis in halophytes in the context of salinity stress tolerance. *Journal of experimental botany*, *65*(5), 1241-1257.

Boudsocq, M., Droillard, M. J., Regad, L., & Laurière, C. (2012). Characterization of Arabidopsis calcium-dependent protein kinases: activated or not by calcium?. *Biochemical Journal*, *447*(2), 291-299.

Boudsocq, M., Willmann, M. R., McCormack, M., Lee, H., Shan, L., He, P., Bush, J., Cheng, S. H., & Sheen, J. (2010). Differential innate immune signalling via Ca2+ sensor protein kinases. *Nature*, *464*(7287), 418-422.

Bourne, Y., Abergel, C., Cambillau, C., Frey, M., Rouge, P., & Fontecilla-Camps, J. C. (1990). X-ray crystal structure determination and refinement at 1.9 Å resolution of isolectin I from the seeds of *Lathyrus ochrus*. *Journal of molecular biology*, *214*(2), 571-584.

Boutrot, F., & Zipfel, C. (2017). Function, discovery, and exploitation of plant pattern recognition receptors for broad-spectrum disease resistance. *Annual review of phytopathology*, *55*, 257-286.

Bowman, J. L., Kohchi, T., Yamato, K. T., Jenkins, J., Shu, S., Ishizaki, S. Yamaoka, K., Nishihama, R., Nakamura, Y., Berger, F., Adam, C., Aki, S. S., Althoff, F., Araki, T., Arteaga-Vazquez, M. A., Balasubrmanian, S., Barry, K., Bauer, D., Boehm, C. R., Briginshaw, L., Caballero-Perez, J., Catarino, B., Chen, F., Chiyoda, S., Chovatia, M., Davies, K. M., Delmans, M., Demura, T., Dierschke, T., Dolan, L., Dorantes-Acosta, A. E., Eklund, D. M., Florent, S. N., Flores-Sandoval, E., Fujiyama, A., Fukuzawa, H., Galik,

B., Grimanelli, D., Grimwood, J., Grossniklaus, U., Hamada, T., Haseloff, J., Hetherington, A. J., Higo, A., Hirakawa, Y., Hundley, H. N., Ikeda, Y., Inoue, K., Inoue, S. I., Ishida, S., Jia, Q., Kakita, M., Kanazawa, T., Kawai, Y., Kawashima, T., Kennedy, M., Kinose, K., Kinoshita, T., Kohara, Y., Koide, E., Komatsu, K., Kopischke, S., Kubo, M., Kyozuka, J., Lagercrantz, U., Lin, S. S., Lindquist, E., Lipzen, A. M., Lu, C. W., De Luna, E., Martienssen, R. A., Minamino, N., Mizutani, M., Mochizuki, N., Monte, I., Mosher, R., Nagasaki, H. Nakagami, H., Naramoto, S., Nishitani, K., Ohtani, M., Okamoto, T., Okumura, M., Phillips, J., Pollak, B., Reinders, A., Rövekamp, M., Sano, R., Sawa, S., Schmid, M. W., Shirakawa, M., Solano, R., Spunde, A., Suetsugu, N., Sugano, S., Sugiyama, A., Sun, R., Suzuki, Y., Takenaka, M., Takezawa, D,. Tomogane, H., Tsuzuki, M., Ueda, T., Umeda, M., Ward, J. M., Watanabe, Y., Yazaki, K., Yokoyama, R., Yoshitake, Y., Yotsui, I., Zachgo, S., & Schmutz, J. (2017). Insights into land plant evolution garnered from the *Marchantia polymorpha* genome. *Cell*, *171*(2), 287-304.

Bowman, S. M., & Free, S. J. (2006). The structure and synthesis of the fungal cell wall. *Bioessays*, *28*(8), 799-808.

Bozsoki, Z., Cheng, J., Feng, F., Gysel, K., Vinther, M., Andersen, K. R., Oldroyd, G., Blaise, M., Radutoiu, S., & Stougaard, J. (2017). Receptor-mediated chitin perception in legume roots is functionally separable from Nod factor perception. *Proceedings of the National Academy of Sciences*, *114*(38), E8118-E8127.

Brown, D. M., Goubet, F., Wong, V. W., Goodacre, R., Stephens, E., Dupree, P., & Turner, S. R. (2007). Comparison of five xylan synthesis mutants reveals new insight into the mechanisms of xylan synthesis. *The Plant Journal*, *52*(6), 1154-1168.

Brown, D. M., Zeef, L. A., Ellis, J., Goodacre, R., & Turner, S. R. (2005). Identification of novel genes in Arabidopsis involved in secondary cell wall formation using expression profiling and reverse genetics. *The Plant Cell, 17*(8), 2281-2295.

Brown, G. D. (2006). Dectin-1: a signalling non-TLR pattern-recognition receptor. *Nature Reviews Immunology*, *6*(1), 33-43.

Brutus, A., Sicilia, F., Macone, A., Cervone, F., & De Lorenzo, G. (2010). A domain swap approach reveals a role of the plant wall-associated kinase 1 (WAK1) as a receptor of oligogalacturonides. *Proceedings of the National Academy of Sciences*, *107*(20), 9452-9457.

Buist, G., Steen, A., Kok, J., & Kuipers, O. P. (2008). LysM, a widely distributed protein motif for binding to (peptido) glycans. *Molecular microbiology*, *68*(4), 838-847.

Buratowski, S. (2009). Progression through the RNA polymerase II CTD cycle. *Molecular cell*, *36*(4), 541-546.

Burton, R. A., & Fincher, G. B. (2009). (1, 3; 1, 4)-β-d-glucans in cell walls of the *Poaceae*, lower plants, and fungi: a tale of two linkages. *Molecular plant*, *2*(5), 873-882.

Burton, R. A., Gidley, M. J., & Fincher, G. B. (2010). Heterogeneity in the chemistry, structure and function of plant cell walls. *Nature chemical biology*, *6*(10), 724-732.

Buscaill, P., & van der Hoorn, R. A. (2021). Defeated by the nines: nine extracellular strategies to avoid microbe-associated molecular patterns recognition in plants. *The Plant Cell, 33*(7), 2116-2130.

Busse-Wicher, M., Gomes, T. C., Tryfona, T., Nikolovski, N., Stott, K., Grantham, N. J., Bolam, D. N., Skaf, M. S., & Dupree, P. (2014). The pattern of xylan acetylation suggests xylan may interact with cellulose microfibrils as a twofold helical screw in the secondary plant cell wall of *Arabidopsis thaliana*. *The Plant Journal*, *79*(3), 492-506.

Cao, Y., Liang, Y., Tanaka, K., Nguyen, C. T., Jedrzejczak, R. P., Joachimiak, A., & Stacey, G. (2014). The kinase LYK5 is a major chitin receptor in Arabidopsis and forms a chitin-induced complex with related kinase CERK1. *elife*, *3*, e03766.

Carpita, N. C., & Gibeaut, D. M. (1993). Structural models of primary cell walls in flowering plants: consistency of molecular structure with the physical properties of the walls during growth. *The Plant Journal*, *3*(1), 1-30.

Carpita, N., & McCann, M. (2000). *The Cell Wall in Biochemistry and Molecular Biology of Plants.* Buchanan, BB, Gruissem, W. & Jones, RL, eds. pp. 55-108.

Carpita, N. C., & McCann, M. C. (2020). Redesigning plant cell walls for the biomass-based bioeconomy. *Journal of Biological Chemistry*, *295*(44), 15144-15157.

Chandrasekar, B., Wanke, A., Wawra, S., Saake, P., Mahdi, L., Charura, N., Neidert, M., Poschmann, G., Malisic, M., Thiele, M., Stühler, K., Dama, M., Pauly, M., & Zuccaro, A. (2022). Fungi hijack a ubiquitous plant apoplastic

endoglucanase to release a ROS scavenging ß-glucan decasaccharide to subvert immune responses. *The Plant Cell*, *34*(7), 2765-2784.

Chaube, M. A., Trattnig, N., Lee, D. H., Belkhadir, Y., & Pfrengle, F. (2022). Synthesis of fungal cell wall oligosaccharides and their ability to trigger plant immune responses. *European Journal of Organic Chemistry*, *2022*(27), e202200313.

Chen, P., Shrotri, A., & Fukuoka, A. (2021). Synthesis of cello-oligosaccharides by depolymerization of cellulose: A review. *Applied Catalysis A: General, 621*, 118177.

Chen, T. (2021). Identification and characterization of the LRR repeats in plant LRR-RLKs. *BMC molecular and cell biology*, *22*, 1-16.

Cheval, C., Samwald, S., Johnston, M. G., de Keijzer, J., Breakspear, A., Liu, X., Bellandi, A., Kadota, Y., Zipfel, C., & Faulkner, C. (2020). Chitin perception in plasmodesmata characterizes submembrane immune-signaling specificity in plants. *Proceedings of the National Academy of Sciences*, *117*(17), 9621-9629.

Chinchilla, D., Zipfel, C., Robatzek, S., Kemmerling, B., Nürnberger, T., Jones, J. D., Felix, G., & Boller, T. (2007). A flagellin-induced complex of the receptor FLS2 and BAK1 initiates plant defence. *Nature*, *448*(7152), 497-500.

Chiniquy, D., Underwood, W., Corwin, J., Ryan, A., Szemenyei, H., Lim, C. C., Stonebloom, S. H., Birdseye, D. S., Vogel, J., Kliebenstein, D., Scheller, H. V., & Somerville, S. (2019). PMR 5, an acetylation protein at the intersection of pectin biosynthesis and defense against fungal pathogens. *The Plant Journal*, *100*(5), 1022-1035.

Chowdhury, J., Henderson, M., Schweizer, P., Burton, R. A., Fincher, G. B., & Little, A. (2014). Differential accumulation of callose, arabinoxylan and cellulose in nonpenetrated versus penetrated papillae on leaves of barley infected with *Blumeria graminis* f. sp. *hordei*. *New Phytologist*, *204*(3), 650-660.

Claus, L. A. N., Savatin, D. V., & Russinova, E. (2018). The crossroads of receptor-mediated signaling and endocytosis in plants. *Journal of integrative plant biology*, *60*(9), 827-840.

Claverie, J., Balacey, S., Darblade, B., & Poinssot, B. (2018). The cell wall-derived xyloglucan is a new DAMP triggering plant immunity in *Vitis vinifera* and *Arabidopsis thaliana*. *Frontiers in Plant Science, 9*, 419889.

Clough, S. J., & Bent, A. F. (1998). Floral dip: a simplified method for Agrobacterium - mediated transformation of *Arabidopsis thaliana*. *The plant journal, 16(6)*, 735-743.

Coenen, G. J., Bakx, E. J., Verhoef, R. P., Schols, H. A., & Voragen, A. G. J. (2007). Identification of the connecting linkage between homo-or xylogalacturonan and rhamnogalacturonan type I. *Carbohydrate polymers*, *70*(2), 224-235.

Colcombet, J., & Hirt, H. (2008). Arabidopsis MAPKs: a complex signalling network involved in multiple biological processes. *Biochemical Journal*, *413*(2), 217-226.

Cosgrove, D. J. (2022). Building an extensible cell wall. *Plant Physiology*, *189*(3), 1246-1277.

Cosgrove, D. J. (2023). Structure and growth of plant cell walls. Nature Reviews *Molecular Cell Biology*, 1-19.

Costantini, S., Benedetti, M., Pontiggia, D., Giovannoni, M., Cervone, F., Mattei, B., & De Lorenzo, G. (2024). Berberine bridge enzyme–like oxidases of cellodextrins and mixed-linked ß-glucans control seed coat formation. *Plant Physiology*, *194*(1), 296-313.

Coutinho, P. M., Deleury, E., Davies, G. J., & Henrissat, B. (2003). An evolving hierarchical family classification for glycosyltransferases. *Journal of molecular biology*, *328*(2), 307-317.

Cui, X., Fan, B., Scholz, J., & Chen, Z. (2007). Roles of Arabidopsis cyclin-dependent kinase C complexes in cauliflower mosaic virus infection, plant growth, and development. *The Plant Cell*, *19*(4), 1388-1402.

Dai, Y. S., Liu, D., Guo, W., Liu, Z. X., Zhang, X., Shi, L. L., Zhou, D. M., Wang, L. N., Kang, K., Wang, F. Z., Zhao, S. S., Tan, Y. F., Hu, T., Cheng, W., Li, P., Zhou, Q. M., Yuan, L. Y., Zhang, Z., Chen, Y. Q., Zhang, W. Q., Li, J., Yu, L. J., & Xiao, S. (2023). Poaceae-specific ß-1, 3; 1, 4-d-glucans link jasmonate signalling to OsLecRK1-mediated defence response during rice-brown planthopper interactions. *Plant Biotechnology Journal*, *21*(6), 1286-1300.

Danecek, P., Bonfield, J., Liddle, J., Marshall, J., Ohan, V., Pollard, M., Whitwham, A., Keane, T., McCarthy, S., Davies, R., & Li, H. (2021) Twelve years of SAMtools and BCFtools. *GigaScience, 10*, giab008.

Darvill, J. E., McNeil, M., Darvill, A. G., & Albersheim, P. (1980). Structure of Plant Cell Walls: XI. Glucuronoarabinoxylan, a second hemicellulose in the

primary cell walls of suspension-cultured sycamore cells. *Plant Physiology*, *66*(6), 1135-1139.

Davidsson, P., Broberg, M., Kariola, T., Sipari, N., Pirhonen, M., & Palva, E. T. (2017). Short oligogalacturonides induce pathogen resistance-associated gene expression in *Arabidopsis thaliana*. *BMC plant biology*, *17*, 1-17.

Deeken, R., & Kaldenhoff, R. (1997). Light-repressible receptor protein kinase: a novel photo-regulated gene from *Arabidopsis thaliana*. *Planta*, *202*(4), 479-486.

Decreux, A., & Messiaen, J. (2005). Wall-associated kinase WAK1 interacts with cell wall pectins in a calcium-induced conformation. *Plant and Cell Physiology*, *46*(2), 268-278.

Decreux, A., Thomas, A., Spies, B., Brasseur, R., Van Cutsem, P., & Messiaen, J. (2006). In vitro characterization of the homogalacturonan-binding domain of the wall-associated kinase WAK1 using site-directed mutagenesis. *Phytochemistry*, *67*(11), 1068-1079.

Delannoy-Bruno, O., Desai, C., Castillo, J. J., Couture, G., Barve, R. A., Lombard, V., Henrissat, B., Cheng, J., Han, N., Hayashi, D. K., Meynier, A., Vinoy, S., Lebrilla, C. B., Marion, S., Heath, A. C., Barrat, M. J., & Gordon, J. I. (2022). An approach for evaluating the effects of dietary fiber polysaccharides on the human gut microbiome and plasma proteome. *Proceedings of the National Academy of Sciences*, *119*(20), e2123411119.

Delgado-Cerezo, M., Sánchez-Rodríguez, C., Escudero, V., Miedes, E., Fernández, P. V., Jordá, L., Hernández-Blanco, C., Sánchez-Vallet, A., Bednarek, P., Schulze-Lefert, P., Somerville, S., Estevez, J. M., Persson, S., & Molina, A. (2012). Arabidopsis heterotrimeric G-protein regulates cell wall defense and resistance to necrotrophic fungi. *Molecular plant*, *5*(1), 98-114.

De Lorenzo, G., & Cervone, F. (2022). Plant immunity by damage-associated molecular patterns (DAMPs). *Essays in Biochemistry*, *66*(5), 459-469.

Delormel, T. Y., Avila-Ospina, L., Davanture, M., Zivy, M., Lang, J., Valentin, N., Rayapuram, N., Hirt, H., Colcombet, J., & Boudsocq, M. (2022). *In vivo* identification of putative CPK5 substrates in *Arabidopsis thaliana*. *Plant Science*, *314*, 111121.

DeFalco, T. A., & Zipfel, C. (2021). Molecular mechanisms of early plant pattern-triggered immune signaling. *Molecular Cell*, *81*(17), 3449-3467.

Del Hierro, I., Melida, H., Broyart, C., Santiago, J., & Molina, A. (2021). Computational prediction method to decipher receptor–glycoligand interactions in plant immunity. *The Plant Journal, 105*(6), 1710-1726.

Delmer, D., Dixon, R. A., Keegstra, K., & Mohnen, D. (2024). The plant cell wall—dynamic, strong, and adaptable—is a natural shapeshifter. *The Plant Cell*, koad325.

Denancé, N., Sánchez-Vallet, A., Goffner, D., & Molina, A. (2013). Disease resistance or growth: the role of plant hormones in balancing immune responses and fitness costs. *Frontiers in plant science*, *4*, 44526.

Denness, L., McKenna, J. F., Segonzac, C., Wormit, A., Madhou, P., Bennett, M., Mansfield, J., Zipfel, C., & Hamann, T. (2011). Cell wall damage-induced lignin biosynthesis is regulated by a reactive oxygen species-and jasmonic acid-dependent process in Arabidopsis. *Plant physiology*, *156*(3), 1364-1374.

Denoux, C., Galletti, R., Mammarella, N., Gopalan, S., Werck, D., De Lorenzo, G., Ferrari, S., Ausubel, F., & Dewdney, J. (2008). Activation of defense response pathways by OGs and Flg22 elicitors in Arabidopsis seedlings. *Molecular plant*, *1*(3), 423-445.

Desaki, Y., Kouzai, Y., Ninomiya, Y., Iwase, R., Shimizu, Y., Seko, K., Molinaro, A., Minami, E., Shibuya, N., Kaku, H., & Nishizawa, Y. (2018). Os CERK 1 plays a crucial role in the lipopolysaccharide-induced immune response of rice. *New Phytologist*, *217*(3), 1042-1049.

Dewangan, B. P., Gupta, A., Sah, R. K., Das, S., Kumar, S., Bhattacharjee, S., & Pawar, P. A. M. (2023). Xylobiose treatment triggers a defense-related response and alters cell wall composition. *Plant Molecular Biology*, *113*(6), 383-400.

Dievart, A., Gottin, C., Périn, C., Ranwez, V., & Chantret, N. (2020). Origin and diversity of plant receptor-like kinases. *Annual Review of Plant Biology*, *71*, 131-156.

Dixit, S., Upadhyay, S. K., Singh, H., Sidhu, O. P., Verma, P. C., & K, C. (2013). Enhanced methanol production in plants provides broad spectrum insect resistance. *PLoS One*, *8*(11), e79664.

Dora, S., Terrett, O. M., & Sánchez-Rodríguez, C. (2022). Plant–microbe interactions in the apoplast: Communication at the plant cell wall. *The Plant Cell*, *34*(5), 1532-1550.

Doughari, J. (2015). An overview of plant immunity. *Plant Pathology Microbiology, 6*(11), 10-4172.

Drula, E., Garron, M. L., Dogan, S., Lombard, V., Henrissat, B., & Terrapon, N. (2022). The carbohydrate-active enzyme database: functions and literature. *Nucleic acids research*, *50*(D1), D571-D577.

Dubiella, U., Seybold, H., Durian, G., Komander, E., Lassig, R., Witte, C. P., Schulze, W. X., & Romeis, T. (2013). Calcium-dependent protein kinase/NADPH oxidase activation circuit is required for rapid defense signal propagation. *Proceedings of the National Academy of Sciences*, *110*(21), 8744-8749.

Dünser, K., Gupta, S., Herger, A., Feraru, M. I., Ringli, C., & Kleine-Vehn, J. (2019). Extracellular matrix sensing by FERONIA and Leucine-Rich Repeat Extensins controls vacuolar expansion during cellular elongation in Arabidopsis thaliana. *The EMBO journal*, *38*(7), e100353.

Dziarski, R., & Gupta, D. (2006). The peptidoglycan recognition proteins (PGRPs). *Genome biology*, *7*(8), 232.

Earley, K. W., Haag, J. R., Pontes, O., Opper, K., Juehne, T., Song, K., & Pikaard, C. S. (2006). Gateway - compatible vectors for plant functional genomics and proteomics. *The Plant Journal, 45(4)*, 616-629.

Ebringerová, A., Hromádková, Z., & Heinze, T. (2005). Hemicellulose. *Polysaccharides I: Structure, characterization and use*, 1-67.

Ellis, C., Karafyllidis, I., & Turner, J. G. (2002). Constitutive activation of jasmonate signaling in an Arabidopsis mutant correlates with enhanced resistance to *Erysiphe cichoracearum*, *Pseudomonas syringae*, and *Myzus persicae*. *Molecular Plant-Microbe Interactions*, *15*(10), 1025-1030.

Ellis, C., Karafyllidis, I., Wasternack, C., & Turner, J. G. (2002). The Arabidopsis mutant *cev1* links cell wall signaling to jasmonate and ethylene responses. *The Plant Cell*, *14*(7), 1557-1566.

Engelsdorf, T., & Hamann, T. (2014). An update on receptor-like kinase involvement in the maintenance of plant cell wall integrity. *Annals of botany*, *114*(6), 1339-1347.

Engelsdorf, T., Kjaer, L., Gigli-Bisceglia, N., Vaahtera, L., Bauer, S., Miedes, E., Wormit, A., James, L., Chairam, I., Molina, A., & Hamann, T. (2019). Functional characterization of genes mediating cell wall metabolism and

responses to plant cell wall integrity impairment. *BMC plant biology, 19*, 1-15.

Engelsdorf, T., Will, C., Hofmann, J., Schmitt, C., Merritt, B. B., Rieger, L., Frenger, M. S., Marschall, A., Franke, R. B., Pattathil, S., & Voll, L. M. (2017). Cell wall composition and penetration resistance against the fungal pathogen *Colletotrichum higginsianum* are affected by impaired starch turnover in Arabidopsis mutants. *Journal of Experimental Botany*, *68*(3), 701-713.

Erbs, G., & Newman, M. A. (2012). The role of lipopolysaccharide and peptidoglycan, two glycosylated bacterial microbe‐associated molecular patterns (MAMPs), in plant innate immunity. *Molecular Plant Pathology, 13*(1), 95-104.

Erbs, G., Silipo, A., Aslam, S., De Castro, C., Liparoti, V., Flagiello, A., Pucci, P., Lanzetta, R., Parrilli, M., Molinaro, A., Newman, M. A., & Cooper, R. M. (2008). Peptidoglycan and muropeptides from pathogens Agrobacterium and Xanthomonas elicit plant innate immunity: structure and activity. *Chemistry & biology*, *15*(5), 438-448.

Erwig, L. P., & Gow, N. A. (2016). Interactions of fungal pathogens with phagocytes. *Nature Reviews Microbiology*, *14*(3), 163-176.

Escudero, V., Jordá, L., Sopeña-Torres, S., Melida, H., Miedes, E., Muñoz-Barrios, A., Swami, S., Alexander, D., McKee, L. S., Sánchez-Vallet, A., Bulone, V., Jones, A. M., & Molina, A. (2017). Alteration of cell wall xylan acetylation triggers defense responses that counterbalance the immune deficiencies of plants impaired in the ß-subunit of the heterotrimeric G-protein. *The Plant Journal*, *92*(3), 386-399.

Faik, A., Price, N. J., Raikhel, N. V., & Keegstra, K. (2002). An Arabidopsis gene encoding an α-xylosyltransferase involved in xyloglucan biosynthesis. *Proceedings of the National Academy of Sciences*, *99*(11), 7797-7802.

Farrokhi, N., Burton, R. A., Brownfield, L., Hrmova, M., Wilson, S. M., Bacic, A., & Fincher, G. B. (2006). Plant cell wall biosynthesis: genetic, biochemical and functional genomics approaches to the identification of key genes. *Plant biotechnology journal, 4*(2), 145-167.

Faulkner, C., Petutschnig, E., Benitez-Alfonso, Y., Beck, M., Robatzek, S., Lipka, V., & Maule, A. J. (2013). LYM2-dependent chitin perception limits

molecular flux via plasmodesmata. *Proceedings of the National Academy of Sciences*, *110*(22), 9166-9170.

Felix, G., Duran, J. D., Volko, S., & Boller, T. (1999). Plants have a sensitive perception system for the most conserved domain of bacterial flagellin. *The Plant Journal*, *18*(3), 265-276.

Felsenstein, J. (1985) Confidence limits on phylogenies: an approach using the bootstrap. *Evolution, 39*, 783–791.

Feng, F., Sun, J., Radhakrishnan, G. V., Lee, T., Bozsóki, Z., Fort, S., Gavrin, A., Gysel, K., Thygesen, M. B., Andersen, K. R., Radutoiu, S., Stougaard, J., & Oldroyd, G. E. (2019). A combination of chitooligosaccharide and lipochitooligosaccharide recognition promotes arbuscular mycorrhizal associations in *Medicago truncatula*. *Nature communications*, *10*(1), 5047.

Fernández-Calvo, P., López, G., Martín-Dacal, M., Aitouguinane, M., Carrasco-López, C., González-Bodí, S., Bacete, L., Mélida, H., Sánchez-Vallet, A., & Molina, A. (2024). Leucine rich repeat-malectin receptor kinases IGP1/CORK1, IGP3 and IGP4 are required for arabidopsis immune responses triggered by ß-1, 4-D-Xylo-oligosaccharides from plant cell walls. *The Cell Surface*, *11*, 100124.

Ferrari, S., Galletti, R., Denoux, C., De Lorenzo, G., Ausubel, F. M., & Dewdney, J. (2007). Resistance to *Botrytis cinerea* induced in Arabidopsis by elicitors is independent of salicylic acid, ethylene, or jasmonate signaling but requires PHYTOALEXIN DEFICIENT3. *Plant physiology*, *144*(1), 367-379.

Ferrari, S., Savatin, D. V., Sicilia, F., Gramegna, G., Cervone, F., & Lorenzo, G. D. (2013). Oligogalacturonides: plant damage-associated molecular patterns and regulators of growth and development. *Frontiers in plant science*, *4*, 49.

Fischer, M. H., Yu, N., Gray, G. R., Ralph, J., Anderson, L., & Marlett, J. A. (2004). The gel-forming polysaccharide of psyllium husk (*Plantago ovata* Forsk). *Carbohydrate research*, *339*(11), 2009-2017.

Franck, C. M., Westermann, J., & Boisson-Dernier, A. (2018). Plant malectin-like receptor kinases: from cell wall integrity to immunity and beyond. *Annual Review of Plant Biology*, *69*, 301-328.

Fry, S. C., Aldington, S., Hetherington, P. R., & Aitken, J. (1993). Oligosaccharides as signals and substrates in the plant cell wall. *Plant physiology*, *103*(1), 1.

Fry, S. C., Nesselrode, B. H., Miller, J. G., & Mewburn, B. R. (2008). Mixed-linkage (1→ 3, 1→ 4)-ß-d-glucan is a major hemicellulose of Equisetum (horsetail) cell walls. *New Phytologist*, *179*(1), 104-115.

Galletti, R., Ferrari, S., & De Lorenzo, G. (2011). Arabidopsis MPK3 and MPK6 play different roles in basal and oligogalacturonide-or flagellin-induced resistance against *Botrytis cinerea*. *Plant physiology*, *157*(2), 804-814.

Gámez-Arjona, F. M., Vitale, S., Voxeur, A., Dora, S., Müller, S., Sancho-Andrés, G., Montesinos, J. C., Di Pietro, A., & Sánchez-Rodríguez, C. (2022). Impairment of the cellulose degradation machinery enhances *Fusarium oxysporum* virulence but limits its reproductive fitness. *Science Advances*, *8*(16), eabl9734.

Geoghegan, I., Steinberg, G., & Gurr, S. (2017). The role of the fungal cell wall in the infection of plants. *Trends in microbiology*, *25*(12), 957-967.

Gifford, J. L., Walsh, M. P., & Vogel, H. J. (2007). Structures and metal-ion-binding properties of the Ca2+-binding helix–loop–helix EF-hand motifs. *Biochemical Journal*, *405*(2), 199-221.

Gigli-Bisceglia, N., van Zelm, E., Huo, W., Lamers, J., & Testerink, C. (2022). Arabidopsis root responses to salinity depend on pectin modification and cell wall sensing. *Development*, *149*(12), dev200363.

Gille, S., Hänsel, U., Ziemann, M., & Pauly, M. (2009). Identification of plant cell wall mutants by means of a forward chemical genetic approach using hydrolases. *Proceedings of the National Academy of Sciences, 106*(34), 14699-14704.

Gómez-Gómez, L., & Boller, T. (2000). FLS2: an LRR receptor–like kinase involved in the perception of the bacterial elicitor flagellin in Arabidopsis. *Molecular cell*, *5*(6), 1003-1011.

Goring, D. R. (2023). A new "lock-and-key" system revealed for plant reproductive barriers. *Cell*, *186*(22), 4734-4736.

Guerra, T., Schilling, S., Hake, K., Gorzolka, K., Sylvester, F. P., Conrads, B., Westermann, B., & Romeis, T. (2020). Calcium-dependent protein kinase 5 links calcium signaling with N-hydroxy-l-pipecolic acid-and SARD 1-dependent immune memory in systemic acquired resistance. *New Phytologist*, *225*(1), 310-325.

Guerriero, G., Fugelstad, J., & Bulone, V. (2010). What do we really know about cellulose biosynthesis in higher plants?. *Journal of integrative plant biology*, *52*(2), 161-175.

Gully, K., Pelletier, S., Guillou, M. C., Ferrand, M., Aligon, S., Pokotylo, I., Perrin, A., Vergne, E., Fagard, M., Ruelland, E., Grappin, P., Bucher, E., Renou, J. P., & Aubourg, S. (2019). The SCOOP12 peptide regulates defense response and root elongation in *Arabidopsis thaliana*. *Journal of experimental botany*, *70*(4), 1349-1365.

Gust, A. A., Biswas, R., Lenz, H. D., Rauhut, T., Ranf, S., Kemmerling, B., Götz, F., Lawischnig, E., Lee, J., Felix, G., & Nürnberger, T. (2007). Bacteria-derived peptidoglycans constitute pathogen-associated molecular patterns triggering innate immunity in Arabidopsis. *Journal of Biological Chemistry*, *282*(44), 32338-32348.

Gust, A. A., Pruitt, R., & Nürnberger, T. (2017). Sensing danger: key to activating plant immunity. *Trends in plant science*, *22*(9), 779-791.

Gust, A. A., Willmann, R., Desaki, Y., Grabherr, H. M., & Nürnberger, T. (2012). Plant LysM proteins: modules mediating symbiosis and immunity. *Trends in plant science*, *17*(8), 495-502.

Gysel, K., Laursen, M., Thygesen, M. B., Lironi, D., Bozsóki, Z., Hjuler, C. T., Maolanon, N. N., Cheng, J., Bjørk, P. K., Vinther, M., Madsen, L. H., Rübsam, H., Muszynski, A., Ghodrati, A., Azadi, P., Sullivan, T. J., Ronson, C. W., Jensen, K. J., Blaise, M., Radutoiu, S., Stougaard, J., & Andersen, K. R. (2021). Kinetic proofreading of lipochitooligosaccharides determines signal activation of symbiotic plant receptors. *Proceedings of the National Academy of Sciences*, *118*(44), e2111031118.

Haltom, A. R., & Jafar-Nejad, H. (2015). The multiple roles of epidermal growth factor repeat O-glycans in animal development. *Glycobiology*, *25*(10), 1027-1042.

Hann, C. T., Bequette, C. J., Dombrowski, J. E., & Stratmann, J. W. (2014). Methanol and ethanol modulate responses to danger-and microbe-associated molecular patterns. *Frontiers in Plant Science*, *5*, 108482.

Harris, D., Bulone, V., Ding, S. Y., & DeBolt, S. (2010). Tools for cellulose analysis in plant cell walls. *Plant physiology*, *153*(2), 420-426.

Harris, P. J., & Fincher, G. B. (2009). Distribution, fine structure and function of (1, 3; 1, 4)-β-glucans in the grasses and other taxa. *Chemistry, Biochemistry, and Biology of 1-3 Beta Glucans and Related Polysaccharides*, 621-654.

Hashimoto, Y., Zhang, S., Zhang, S., Chen, Y. R., & Blissard, G. W. (2012). Erratum to: BTI-Tnao38, a new cell line derived from *Trichoplusia ni*, is permissive for AcMNPV infection and produces high levels of recombinant proteins. *BMC biotechnology, 12*, 1-4.

Hatfield, R. D., Rancour, D. M., & Marita, J. M. (2017). Grass cell walls: a story of cross-linking. *Frontiers in plant science*, *7*, 204954.

Have, A. T., Mulder, W., Visser, J., & van Kan, J. A. (1998). The endopolygalacturonase gene Bcpg1 is required for full virulence of *Botrytis cinerea*. *Molecular Plant-Microbe Interactions*, *11*(10), 1009-1016.

Hayashi, T. (1989). Xyloglucans in the primary cell wall. *Annual review of plant biology*, *40*(1), 139-168.

He, J., Kong, M., Qian, Y., Gong, M., Lv, G., & Song, J. (2023). Cellobiose elicits immunity in lettuce conferring resistance to *Botrytis cinerea*. *Journal of Experimental Botany*, *74*(3), 1022-1038.

Hernandez-Blanco, C., Feng, D. X., Hu, J., Sanchez-Vallet, A., Deslandes, L., Llorente, F., Berrocal-Lobo, M., Keller, H., Barlet, X., Sánchez-Rodríguez, C., Anderson, L. K., Somerville, S., Marco, Y., & Molina, A. (2007). Impairment of cellulose synthases required for Arabidopsis secondary cell wall formation enhances disease resistance. *The Plant Cell*, *19*(3), 890-903.

Herold, L., Hua, C., Kohorn, B., Nuernberger, T., DeFalco, T. A., & Zipfel, C. (2024). Arabidopsis WALL-ASSOCIATED KINASES are not required for oligogalacturonide-induced signaling and immunity. *bioRxiv*, 2024-04.

Hervé, C., Serres, J., Dabos, P., Canut, H., Barre, A., Rougé, P., & Lescure, B. (1999). Characterization of the Arabidopsis lecRK-a genes: members of a superfamily encoding putative receptors with an extracellular domain homologous to legume lectins. *Plant Molecular Biology*, *39*, 671-682.

Hok, S., Danchin, E. G., Allasia, V., Panabières, F., Attard, A., & Keller, H. (2011). An Arabidopsis (malectin-like) leucine-rich repeat receptor-like kinase contributes to downy mildew disease. *Plant, cell & environment*, *34*(11), 1944-1957.

Hou, S., Liu, Z., Shen, H., & Wu, D. (2019). Damage-associated molecular pattern-triggered immunity in plants. *Frontiers in plant science*, *10*, 646.

Hou, S., Wang, X., Chen, D., Yang, X., Wang, M., Turrà, D., Di Pietro, A., & Zhang, W. (2014). The secreted peptide PIP1 amplifies immunity through receptor-like kinase 7. *PLoS pathogens*, *10*(9), e1004331.

Hong, Z., Kajiura, H., Su, W., Jin, H., Kimura, A., Fujiyama, K., & Li, J. (2012). Evolutionarily conserved glycan signal to degrade aberrant brassinosteroid receptors in Arabidopsis. *Proceedings of the National Academy of Sciences*, *109*(28), 11437-11442.

Huang, J., Gu, M., Lai, Z., Fan, B., Shi, K., Zhou, Y. H., Yu, J. Q., & Chen, Z. (2010). Functional analysis of the Arabidopsis PAL gene family in plant growth, development, and response to environmental stress. *Plant physiology*, *153*(4), 1526-1538.

Huang, J., Rauscher, S., Nawrocki, G., Ran, T., Feig, M., De Groot, B. L., Grubmüller, H., & MacKerell Jr, A. D. (2017). CHARMM36m: an improved force field for folded and intrinsically disordered proteins. *Nature methods, 14*(1), 71-73.

Huerta, A. I., Sancho-Andrés, G., Montesinos, J. C., Silva-Navas, J., Bassard, S., Pau-Roblot, C., Kesten, C., Schlechter, R., Dora, S., Ayupov, T., Pelloux, J., Santiago, J., & Sánchez-Rodríguez, C. (2023). The WAK-like protein RFO1 acts as a sensor of the pectin methylation status in Arabidopsis cell walls to modulate root growth and defense. *Molecular plant*, *16*(5), 865-881.

Huffaker, A., Pearce, G., Veyrat, N., Erb, M., Turlings, T. C., Sartor, R., Shen, Z., Briggs, S. P., Vaughan, M. M., Alborn, H, T., Teal, P. E. A., & Schmelz, E. A. (2013). Plant elicitor peptides are conserved signals regulating direct and indirect antiherbivore defense. *Proceedings of the National Academy of Sciences, 110*(14), 5707-5712.

Humphrey, T. V., Haasen, K. E., Aldea-Brydges, M. G., Sun, H., Zayed, Y., Indriolo, E., & Goring, D. R. (2015). PERK–KIPK–KCBP signalling negatively regulates root growth in *Arabidopsis thaliana*. *Journal of experimental botany*, *66*(1), 71-83.

Humphrey, W., Dalke, A., & Schulten, K. (1996). VMD: visual molecular dynamics. *Journal of molecular graphics, 14*(1), 33-38.

Huynh, K., & Partch, C. L. (2015). Analysis of protein stability and ligand interactions by thermal shift assay. *Current protocols in protein science, 79(1)*, 28-9.

Hwang, I., Kim, S. Y., Kim, C. S., Park, Y., Tripathi, G. R., Kim, S. K., & Cheong, H. (2010). Over-expression of the IGI1 leading to altered shoot-branching development related to MAX pathway in Arabidopsis. *Plant molecular biology*, *73*, 629-641.

Iizasa, E. I., Mitsutomi, M., & Nagano, Y. (2010). Direct binding of a plant LysM receptor-like kinase, LysM RLK1/CERK1, to chitin in vitro. *Journal of Biological Chemistry*, *285*(5), 2996-3004.

Irani, N. G., & Russinova, E. (2009). Receptor endocytosis and signaling in plants. *Current opinion in plant biology*, *12*(6), 653-659.

Jensen, J. K., Sørensen, S. O., Harholt, J., Geshi, N., Sakuragi, Y., Møller, I., Zandleven, J., Bernal, A. J., Jensen, N. B., Sørensen, C., Pauly, M., Beldman, G., Willats, W. G. T., & Scheller, H. V. (2008). Identification of a xylogalacturonan xylosyltransferase involved in pectin biosynthesis in Arabidopsis. *The Plant Cell*, *20*(5), 1289-1302.

Jeppesen, M. G., Navratil, T., Spremulli, L. L., & Nyborg, J. (2005). Crystal structure of the bovine mitochondrial elongation factor Tu· Ts complex. *Journal of Biological Chemistry*, *280*(6), 5071-5081.

Jia, Z., Cash, M., Darvill, A. G., & York, W. S. (2005). NMR characterization of endogenously O-acetylated oligosaccharides isolated from tomato (*Lycopersicon esculentum*) xyloglucan. *Carbohydrate research*, *340*(11), 1818-1825.

Jo, S., Kim, T., & Im, W. (2007). Automated builder and database of protein/membrane complexes for molecular dynamics simulations. *PloS one, 2(9)*, e880.

Jo, S., Kim, T., Iyer, V. G., & Im, W. (2008). CHARMM‐GUI: a web‐based graphical user interface for CHARMM. *Journal of computational chemistry, 29*(11), 1859-1865.

Johnson, J. M., Thürich, J., Petutschnig, E. K., Altschmied, L., Meichsner, D., Sherameti, I., Dindas, J., Mrozinska, A., Paetz, C., Scholz, S. S., Furch, A. C. U., Lipka, V., Hedrich, R., Schneider, B. Svatos, A., & Oelmüller, R. (2018). A poly (A) ribonuclease controls the cellotriose-based interaction between *Piriformospora indica* and its host Arabidopsis. *Plant physiology*, *176*(3), 2496-2514.

Jones, J. D., & Dangl, J. L. (2006). The plant immune system. *nature*, *444*(7117), 323-329.

Jumper, J., Evans, R., Pritzel, A., Green, T., Figurnov, M., Ronneberger, O., Tunyasuvunakool, K., Bates, R., Žídek, A., Potapenko, A., Bridgland, A., Meyer, C., Kohl, S., Ballard, A., Cowie, A., Romera-Paredes, B., Nikolov, S., Jain, R., Adler, J., Back, T., Petersen, S., Reiman, D., Clancy, E., Zielinski, M., Steinegger, M., Pacholska, M., Berghammer, T., Bodenstein, S., Silver,

D., Vinyals, O., Senior, A., Kavukcuoglu, K., Kohli, P., & Hassabis, D. (2021). Highly accurate protein structure prediction with AlphaFold. *Nature, 596(7873)*, 583-589.

Jurrus, E., Engel, D., Star, K., Monson, K., Brandi, J., Felberg, L. E., Brookes, D., Wilson, L., Chen, J., Liles, K., Chun, M., Li, P., Gohara, D., Dolinsky, T., Konecny, R., Koes, D., Nielsen, J., Head-Gordon, T., Geng, W., Krasny, R., Wei, G., Holst, M., McCammon, J., & Baker, N. A. (2018). Improvements to the APBS biomolecular solvation software suite. *Protein Science, 27*(1), 112-128.

Kadota, Y., Sklenar, J., Derbyshire, P., Stransfeld, L., Asai, S., Ntoukakis, V., Jones, J., Shirasu, K., Menke, F., Jones, A., & Zipfel, C. (2014). Direct regulation of the NADPH oxidase RBOHD by the PRR-associated kinase BIK1 during plant immunity. *Molecular cell*, *54*(1), 43-55.

Kaku, H., Nishizawa, Y., Ishii-Minami, N., Akimoto-Tomiyama, C., Dohmae, N., Takio, K., Minami, E., & Shibuya, N. (2006). Plant cells recognize chitin fragments for defense signaling through a plasma membrane receptor. *Proceedings of the National Academy of Sciences*, *103*(29), 11086-11091.

Kang, X., Kirui, A., Dickwella Widanage, M. C., Mentink-Vigier, F., Cosgrove, D. J., & Wang, T. (2019). Lignin-polysaccharide interactions in plant secondary cell walls revealed by solid-state NMR. *Nature communications*, *10*(1), 347.

Karasov, T. L., Chae, E., Herman, J. J., & Bergelson, J. (2017). Mechanisms to mitigate the trade-off between growth and defense. *The Plant Cell*, *29*(4), 666-680.

Kelly, S. J., Muszyński, A., Kawaharada, Y., Hubber, A. M., Sullivan, J. T., Sandal, N., Carlson, R. W., Stougaard, J., & Ronson, C. W. (2013). Conditional requirement for exopolysaccharide in the *Mesorhizobium–Lotus* symbiosis. *Molecular plant-microbe interactions*, *26*(3), 319-329.

Kelly, S., Hansen, S. B., Rübsam, H., Saake, P., Pedersen, E. B., Gysel, K., Madland, E., Wu, S., Wawra, S., Reid, D., Sullivan, J. T., Blahovska, Z., Vinther, M., Muszynski, A., Azadi, P., Thygesen, M. B., Aachamann, F. L., Ronson, C. W., Zuccaro, A., Andersen, K. R., Radutoiu, S., & Stougaard, J. (2023). A glycan receptor kinase facilitates intracellular accommodation of arbuscular mycorrhiza and symbiotic rhizobia in the legume *Lotus japonicus*. *PLoS Biology*, *21*(5), e3002127.

Khan, A., Shah, S. T., Basit, A., Mohamed, H. I., & Li, Y. (2024). Mitogen-Activated Protein Kinase: A Potent Signaling Protein that Combats Biotic and Abiotic Stress in Plants. *Journal of Plant Growth Regulation*, 1-25.

Khokhani, D., Carrera Carriel, C., Vayla, S., Irving, T. B., Stonoha-Arther, C., Keller, N. P., & Ané, J. M. (2021). Deciphering the chitin code in plant symbiosis, defense, and microbial networks. *Annual Review of Microbiology*, *75*, 583-607.

Kidd, B. N., Cahill, D. M., Manners, J. M., Schenk, P. M., & Kazan, K. (2011, September). Diverse roles of the Mediator complex in plants. In *Seminars in cell & developmental biology* (Vol. 22, No. 7, pp. 741-748). Academic Press.

Kim, E. K., & Choi, E. J. (2010). Pathological roles of MAPK signaling pathways in human diseases. *Biochimica et Biophysica Acta (BBA)-Molecular Basis of Disease*, *1802*(4), 396-405.

Kim, S. J., Bhandari, D. D., Sokoloski, R., & Brandizzi, F. (2023). Immune activation during Pseudomonas infection causes local cell wall remodeling and alters AGP accumulation. *The Plant Journal*, *116*(2), 541-557.

Kim, S. J., Chandrasekar, B., Rea, A. C., Danhof, L., Zemelis-Durfee, S., Thrower, N., Shepard, Z. S., Pauly, M., Brandizzi, F., & Keegstra, K. (2020). The synthesis of xyloglucan, an abundant plant cell wall polysaccharide, requires CSLC function. *Proceedings of the National Academy of Sciences*, *117*(33), 20316-20324.

Kim, S. J., Zemelis-Durfee, S., Jensen, J. K., Wilkerson, C. G., Keegstra, K., & Brandizzi, F. (2018). In the grass species *Brachypodium distachyon*, the production of mixed-linkage (1, 3; 1, 4)-ß-glucan (MLG) occurs in the Golgi apparatus. *The Plant Journal*, *93*(6), 1062-1075.

Kim, Y., Schumaker, K. S., & Zhu, J. K. (2006). EMS mutagenesis of Arabidopsis. *Arabidopsis protocols*, 101-103.

Klarzynski, O., Plesse, B., Joubert, J. M., Yvin, J. C., Kopp, M., Kloareg, B., & Fritig, B. (2000). Linear ß-1, 3 glucans are elicitors of defense responses in tobacco. *Plant physiology*, *124*(3), 1027-1038.

Kloareg, B., Badis, Y., Cock, J. M., & Michel, G. (2021). Role and evolution of the extracellular matrix in the acquisition of complex multicellularity in eukaryotes: a macroalgal perspective. *Genes*, *12*(7), 1059.

Knight, M. R., Campbell, A. K., Smith, S. M., & Trewavas, A. J. (1991). Transgenic plant aequorin reports the effects of touch and cold-shock and elicitors on cytoplasmic calcium. *Nature, 352*(6335), 524-526.

Kohorn, B. D., Johansen, S., Shishido, A., Todorova, T., Martinez, R., Defeo, E., & Obregon, P. (2009). Pectin activation of MAP kinase and gene expression is WAK2 dependent. *The Plant Journal*, *60*(6), 974-982.

Körner, E., von Dahl, C. C., Bonaventure, G., & Baldwin, I. T. (2009). Pectin methylesterase Na PME1 contributes to the emission of methanol during insect herbivory and to the elicitation of defence responses in *Nicotiana attenuata*. *Journal of experimental botany*, *60*(9), 2631-2640.

Kouzai, Y., Nakajima, K., Hayafune, M., Ozawa, K., Kaku, H., Shibuya, N., Minami, E., & Nishizawa, Y. (2014). CEBiP is the major chitin oligomer-binding protein in rice and plays a main role in the perception of chitin oligomers. *Plant molecular biology*, *84*, 519-528.

Kraemer, F. J., Lunde, C., Koch, M., Kuhn, B. M., Ruehl, C., Brown, P. J., Hoffmann, P., Göhre, V., Hake, S., Pauly, M., & Ramírez, V. (2021). A mixed-linkage (1, 3; 1, 4)-β-D-glucan specific hydrolase mediates dark-triggered degradation of this plant cell wall polysaccharide. *Plant Physiology*, *185*(4), 1559-1573.

Kubicek, C. P., Starr, T. L., & Glass, N. L. (2014). Plant cell wall–degrading enzymes and their secretion in plant-pathogenic fungi. *Annual review of phytopathology*, *52*, 427-451.

Kumar, M., Campbell, L., & Turner, S. (2016). Secondary cell walls: biosynthesis and manipulation. *Journal of experimental botany*, *67*(2), 515-531.

Lai, Z., Schluttenhofer, C. M., Bhide, K., Shreve, J., Thimmapuram, J., Lee, S. Y., Yun, D. J., & Mengiste, T. (2014). MED18 interaction with distinct transcription factors regulates multiple plant functions. *Nature communications*, *5*(1), 3064.

Latgé, J. P., & Calderone, R. (2006). The fungal cell wall. In *Growth, Differentiation and Sexuality* (pp. 73-104). Berlin, Heidelberg: Springer Berlin Heidelberg.

Lazaridou, A., & Biliaderis, C. G. (2007). Molecular aspects of cereal β-glucan functionality: Physical properties, technological applications and physiological effects. *Journal of cereal science*, *46*(2), 101-118.

Le, M. H., Cao, Y., Zhang, X. C., & Stacey, G. (2014). LIK1, a CERK1-interacting kinase, regulates plant immune responses in Arabidopsis. *PloS one*, *9*(7), e102245.

Lee, H. K., & Goring, D. R. (2021). Two subgroups of receptor-like kinases promote early compatible pollen responses in the *Arabidopsis thaliana* pistil. *Journal of Experimental Botany*, *72*(4), 1198-1211.

Lee, H. K., & Santiago, J. (2023). Structural insights of cell wall integrity signaling during development and immunity. *Current Opinion in Plant Biology*, 102455.

Lee, S. J., Saravanan, R. S., Damasceno, C. M., Yamane, H., Kim, B. D., & Rose, J. K. (2004). Digging deeper into the plant cell wall proteome. *Plant physiology and Biochemistry*, *42*(12), 979-988.

Lehti-Shiu, M. D., Zou, C., Hanada, K., & Shiu, S. H. (2009). Evolutionary history and stress regulation of plant receptor-like kinase/pelle genes. *Plant physiology*, *150*(1), 12-26.

Leszczuk, A., Kalaitzis, P., Kulik, J., & Zdunek, A. (2023). structure and modifications of arabinogalactan proteins (AGPs). *BMC Plant Biology*, *23*(1), 45.

Li, B., Meng, X., Shan, L., & He, P. (2016). Transcriptional regulation of pattern-triggered immunity in plants. *Cell host & microbe, 19*(5), 641-650.

Li, F., Cheng, C., Cui, F., de Oliveira, M. V., Yu, X., Meng, X., Intorne, A. C., Babilonia, K., Li, M., Li, B., Chen, S., Ma, X., Xiao, S., Zheng, Y., Fei, Z., Metz, R. P., Johnson, C. D., Koiwa, H., Sun, W., Li, Z., Filho, G., Shan, L., & He, P. (2014). Modulation of RNA polymerase II phosphorylation downstream of pathogen perception orchestrates plant immunity. *Cell host & microbe*, *16*(6), 748-758.

Li, H. (2013) Aligning sequence reads, clone sequences and assembly contigs with BWA-MEM. *arXiv*, 1303.3997v2.

Li, L., Li, M., Yu, L., Zhou, Z., Liang, X., Liu, Z., Cai, G., Gao, L., Zhang, X., Wang, Y., Chen, S., & Zhou, J. M. (2014). The FLS2-associated kinase BIK1 directly phosphorylates the NADPH oxidase RbohD to control plant immunity. *Cell host & microbe*, *15*(3), 329-338.

Li, L., Yu, Y., Zhou, Z., & Zhou, J. M. (2016). Plant pattern-recognition receptors controlling innate immunity. *Science China Life Sciences*, *59*, 878-888.

Li, Q., Wang, C., & Mou, Z. (2020). Perception of damaged self in plants. *Plant physiology*, *182*(4), 1545-1565.

Li, X. (2011). Infiltration of *Nicotiana benthamiana* protocol for transient expression via Agrobacterium. *Bio-protocol*, e95-e95.

Liepman, A. H., & Cavalier, D. M. (2012). The cellulose synthase-like A and cellulose synthase-like C families: recent advances and future perspectives. *Frontiers in plant science*, *3*, 109.

Lionetti, V., Fabri, E., De Caroli, M., Hansen, A. R., Willats, W. G., Piro, G., & Bellincampi, D. (2017). Three pectin methylesterase inhibitors protect cell wall integrity for Arabidopsis immunity to Botrytis. *Plant Physiology*, *173*(3), 1844-1863.

Little, A., Schwerdt, J. G., Shirley, N. J., Khor, S. F., Neumann, K., O'Donovan, L. A., Lahnstein, J., Collins, H. M., Henderson, M., Fincher, G. B., & Burton, R. A. (2018). Revised phylogeny of the cellulose synthase gene superfamily: insights into cell wall evolution. *Plant physiology*, *177*(3), 1124-1141.

Liu, C., Yu, H., Voxeur, A., Rao, X., & Dixon, R. A. (2023). FERONIA and wall-associated kinases coordinate defense induced by lignin modification in plant cell walls. *Science Advances*, *9*(10), eadf7714.

Liu, S., Kracher, B., Ziegler, J., Birkenbihl, R. P., & Somssich, I. E. (2015). Negative regulation of ABA signaling by WRKY33 is critical for Arabidopsis immunity towards Botrytis cinerea 2100. *elife*, *4*, e07295.

Liu, S., Wang, J., Han, Z., Gong, X., Zhang, H., & Chai, J. (2016). Molecular mechanism for fungal cell wall recognition by rice chitin receptor OsCEBiP. *Structure*, *24*(7), 1192-1200.

Liu, T., Liu, Z., Song, C., Hu, Y., Han, Z., She, J., Fan, F., Wang, J., Jin, C., Chang, J., Zhou, J. M., & Chai, J. (2012). Chitin-induced dimerization activates a plant immune receptor. *science*, *336*(6085), 1160-1164.

Liu, X., Zhou, Y., Chen, K., Xiao, Z., Liang, X., & Lu, D. (2023). Phosphorylation status of CPK28 affects its ubiquitination and protein stability. *New Phytologist*, *237*(4), 1270-1284.

Liu, Y., & He, C. (2016). Regulation of plant reactive oxygen species (ROS) in stress responses: learning from AtRBOHD. *Plant Cell Reports, 35*, 995-1007.

Liu, Z., Persson, S., & Sánchez-Rodríguez, C. (2015). At the border: the plasma membrane–cell wall continuum. *Journal of Experimental Botany*, *66*(6), 1553-1563.

Locci, F., Benedetti, M., Pontiggia, D., Citterico, M., Caprari, C., Mattei, B., cervone, F., & De Lorenzo, G. (2019). An Arabidopsis berberine bridge enzyme - like protein specifically oxidizes cellulose oligomers and plays a role in immunity. *The Plant Journal, 98*(3), 540-554.

Lombard, V., Golaconda Ramulu, H., Drula, E., Coutinho, P. M., & Henrissat, B. (2014). The carbohydrate-active enzymes database (CAZy) in 2013. *Nucleic acids research*, *42*(D1), D490-D495.

Loris, R. (2002). Principles of structures of animal and plant lectins. *Biochimica et Biophysica Acta (BBA)-General Subjects*, *1572*(2-3), 198-208.

Lorrai, R., & Ferrari, S. (2021). Host cell wall damage during pathogen infection: Mechanisms of perception and role in plant-pathogen interactions. *Plants*, *10*(2), 399.

Lozano-Durán, R., & Zipfel, C. (2015). Trade-off between growth and immunity: role of brassinosteroids. *Trends in plant science*, *20*(1), 12-19.

Luna, E., Pastor, V., Robert, J., Flors, V., Mauch-Mani, B., & Ton, J. (2011). Callose deposition: a multifaceted plant defense response. *Molecular Plant-Microbe Interactions*, *24*(2), 183-193.

Luo, R., Schatz, M., & Salzberg, S. (2017) 16GT: a fast andsensitive variant caller using a 16-genotype probabilistic model. *GigaScience, 6(7)*, 1–4.

Madsen, E. B., Madsen, L. H., Radutoiu, S., Olbryt, M., Rakwalska, M., Szczyglowski, K., Sato, S., Kaneko, T., Tabata, S., Sandal, N., & Stougaard, J. (2003). A receptor kinase gene of the LysM type is involved in legume perception of rhizobial signals. *Nature*, *425*(6958), 637-640.

Man, J., Gallagher, J. P., & Bartlett, M. (2020). Structural evolution drives diversification of the large LRR-RLK gene family. *New phytologist*, *226*(5), 1492-1505.

Manabe, Y., Nafisi, M., Verhertbruggen, Y., Orfila, C., Gille, S., Rautengarten, C., Cherk, C., Marcus, S. E., Somerville, S., Pauly, M., Knox, J. P., Sakuragi, Y., & Scheller, H. V. (2011). Loss-of-function mutation of REDUCED WALL ACETYLATION2 in Arabidopsis leads to reduced cell wall acetylation and increased resistance to *Botrytis cinerea*. *Plant physiology*, *155*(3), 1068-1078.

Mao, G., Meng, X., Liu, Y., Zheng, Z., Chen, Z., & Zhang, S. (2011). Phosphorylation of a WRKY transcription factor by two pathogen-responsive MAPKs drives phytoalexin biosynthesis in Arabidopsis. *The Plant Cell*, *23*(4), 1639-1653.

Marowa, P., Ding, A., & Kong, Y. (2016). Expansins: roles in plant growth and potential applications in crop improvement. *Plant cell reports*, *35*, 949-965.

Martín-Dacal, M., Fernández-Calvo, P., Jiménez-Sandoval, P., Lopez, G., Garrido-Arandía, M., Rebaque, D., del Hierro, I., Berlanga, D. J., Torres, M. A., Kumar, V., Mélida, H., Pacios, L. F., Santiago, J., & Molina, A. (2023). Arabidopsis immune responses triggered by cellulose-and mixed-linked glucan-derived oligosaccharides require a group of leucine-rich repeat malectin receptor kinases. *The Plant Journal*, *113*(4), 833-850.

Matsushima, N., Tanaka, T., Enkhbayar, P., Mikami, T., Taga, M., Yamada, K., & Kuroki, Y. (2007). Comparative sequence analysis of leucine-rich repeats (LRRs) within vertebrate toll-like receptors. *BMC genomics*, *8*, 1-20.

McCallum, C. M., Comai, L., Greene, E. A., & Henikoff, S. (2000). T argeting I nduced L ocal L esions IN G enomes (TILLING) for plant functional genomics. *Plant physiology, 123*(2), 439-442.

McClendon, C. L., Kornev, A. P., Gilson, M. K., & Taylor, S. S. (2014). Dynamic architecture of a protein kinase. *Proceedings of the National Academy of Sciences*, *111*(43), E4623-E4631.

McDonald, C., Inohara, N., & Nuñez, G. (2005). Peptidoglycan signaling in innate immunity and inflammatory disease. *Journal of Biological Chemistry*, *280*(21), 20177-20180.

McNamara, J. T., Morgan, J. L., & Zimmer, J. (2015). A molecular description of cellulose biosynthesis. *Annual review of biochemistry*, *84*, 895-921.

Mélida, H., Bacete, L., Ruprecht, C., Rebaque, D., Del Hierro, I., Lopez, G., Brunner, F., Pfrengle, F., & Molina, A. (2020). Arabinoxylan-oligosaccharides act as damage associated molecular patterns in plants regulating disease resistance. *Frontiers in Plant Science, 11*, 1210.

Mélida, H., Sopeña‐Torres, S., Bacete, L., Garrido‐Arandia, M., Jordá, L., Lopez, G., Muñoz-Barrios, A., Pacios, L. F., & Molina, A. (2018). Non‐branched β‐1, 3‐glucan oligosaccharides trigger immune responses in Arabidopsis. *The Plant Journal, 93*(1), 34-49.

Meng, X., & Zhang, S. (2013). MAPK cascades in plant disease resistance signaling. *Annual review of phytopathology*, *51*, 245-266.

Miedes, E., Vanholme, R., Boerjan, W., & Molina, A. (2014). The role of the secondary cell wall in plant resistance to pathogens. *Frontiers in plant science*, *5*, 100584.

Mirdita, M., Schütze, K., Moriwaki, Y., Heo, L., Ovchinnikov, S., & Steinegger, M. (2022). ColabFold: making protein folding accessible to all. *Nature methods, 19*(6), 679-682.

Mistry, J., Chuguransky, S., Williams, L., Qureshi, M., Salazar, G. A., Sonnhammer, E. L., Tosatto, S., Paladin, L., Raj, S., Richardson, L., Finn, R., & Bateman, A. (2021). Pfam: The protein families database in 2021. *Nucleic acids research, 49(D1)*, D412-D419.

Mithöfer, A., & Mazars, C. (2002). Aequorin-based measurements of intracellular Ca $^{2+}$-signatures in plant cells. *Biological Procedures, 4*, 105-118.

Mittler, R., & Blumwald, E. (2015). The roles of ROS and ABA in systemic acquired acclimation. *The Plant Cell*, *27*(1), 64-70.

Miya, A., Albert, P., Shinya, T., Desaki, Y., Ichimura, K., Shirasu, K., Narusaka, Y., Kawakami, N., Kaku, H., & Shibuya, N. (2007). CERK1, a LysM receptor kinase, is essential for chitin elicitor signaling in Arabidopsis. *Proceedings of the National Academy of Sciences*, *104*(49), 19613-19618.

Mohammad, E., & McFarlane, H. E. (2024). Two roads diverge for cellulose synthase complex trafficking. *Trends in Plant Science*.

Mohnen, D. (2008). Pectin structure and biosynthesis. *Current opinion in plant biology*, *11*(3), 266-277.

Molina, A., Jordá, L., Torres, M. Á., Martín-Dacal, M., Berlanga, D. J., Fernández-Calvo, P., Gómez-Rubio, E. & Martín-Santamaría, S., (2024). Plant cell wall-mediated disease resistance: Current understanding and future perspectives. *Molecular Plant*.

Molina, A., Miedes, E., Bacete, L., Rodríguez, T., Mélida, H., Denancé, N., Sánchez-Vallet, A., Rivière, M. P., López, G., Freydier, A., Barlet, X., Pattathil, S., Hahn, M., & Goffner, D. (2021). Arabidopsis cell wall composition determines disease resistance specificity and fitness. *Proceedings of the National Academy of Sciences*, *118*(5), e2010243118.

Møller, I. M., Jensen, P. E., & Hansson, A. (2007). Oxidative modifications to cellular components in plants. *Annual Review of Plant Biology*, *58*, 459-481.

Monson, R. K., Trowbridge, A. M., Lindroth, R. L., & Lerdau, M. T. (2022). Coordinated resource allocation to plant growth–defense tradeoffs. *New Phytologist*, *233*(3), 1051-1066.

Morales, J., Kadota, Y., Zipfel, C., Molina, A., & Torres, M.A. (2016) The Arabidopsis NADPH oxidases Rboh D and Rboh F display differential expression patterns and contributions during plant immunity. *Journal of Experimental Botany, 67*, 1663–1676.

Morgan, J. L., Strumillo, J., & Zimmer, J. (2013). Crystallographic snapshot of cellulose synthesis and membrane translocation. *Nature*, *493*(7431), 181-186.

Mott, G. A., Thakur, S., Smakowska, E., Wang, P. W., Belkhadir, Y., Desveaux, D., & Guttman, D. S. (2016). Genomic screens identify a new phytobacterial microbe-associated molecular pattern and the cognate Arabidopsis receptor-like kinase that mediates its immune elicitation. *Genome biology, 17*, 1-15.

Moussu, S., Augustin, S., Roman, A.O., Broyart, C., & Santiago, J. (2018) Crystal structures of two tandem malectin-like receptor kinases involved in plant reproduction. *Acta crystallographica Section D, Structural Biology, 74*, 671–680.

Moussu, S., Broyart, C., Santos-Fernandez, G., Augustin, S., Wehrle, S., Grossniklaus, U., & Santiago, J., (2020). Structural basis for recognition of RALF peptides by LRX proteins during pollen tube growth. *Proceedings of the National Academy of Sciences*, *117*(13), 7494-7503.

Moussu, S., Lee, H. K., Haas, K. T., Broyart, C., Rathgeb, U., De Bellis, D., Levasseur, T., Schoenaers, S., Fernandez, G., Grossniklaus, U., Bonnin, E., Hosy, E., Vissenberg, K., Geldner, N., Cathala, B., Höfte, H., & Santiago, J. (2023). Plant cell wall patterning and expansion mediated by protein-peptide-polysaccharide interaction. *Science, 382(6671)*, 719-725.

Murashige, T., & Skoog, F. (1962). A revised medium for rapid growth and bioassays with tobacco tissue cultures. *Physiologia Plantarum, 15*, 473-497.

Nakamura, A., Furuta, H., Maeda, H., NAGAMATsu, Y., & Yoshimoto, A. (2001). Analysis of structural components and molecular construction of soybean soluble polysaccharides by stepwise enzymatic degradation. *Bioscience, biotechnology, and biochemistry*, *65*(10), 2249-2258.

Nakhamchik, A., Zhao, Z., Provart, N. J., Shiu, S. H., Keatley, S. K., Cameron, R. K., & Goring, D. R. (2004). A comprehensive expression analysis of the Arabidopsis proline-rich extensin-like receptor kinase gene family using bioinformatic and experimental approaches. *Plant and Cell Physiology*, *45*(12), 1875-1881.

Naran, R., Chen, G., & Carpita, N. C. (2008). Novel rhamnogalacturonan I and arabinoxylan polysaccharides of flax seed mucilage. *Plant physiology*, *148*(1), 132-141.

Navarro-Gochicoa, M. T., Camut, S., Timmers, A. C., Niebel, A., Hervé, C., Boutet, E., Bono, J. J., Imberty, A., & Cullimore, J. V. (2003). Characterization of four lectin-like receptor kinases expressed in roots of *Medicago truncatula*. Structure, location, regulation of expression, and potential role in the symbiosis with *Sinorhizobium meliloti*. *Plant physiology*, *133*(4), 1893-1910.

Neelamegham, S., Aoki-Kinoshita, K., Bolton, E., Frank, M., Lisacek, F., Lütteke, T., O`Boyle, N., Packer, N. H., Stanley, P., Toukach, P., Varki, A., & Woods, R. J. (2019). Updates to the symbol nomenclature for glycans guidelines. *Glycobiology*, *29*(9), 620-624.

Nei, M., & Kumar, S. (2000) *Molecular evolution and phylogenetics*. USA: Oxford University Press.

Newman, M. A., Dow, J. M., Molinaro, A., & Parrilli, M. (2007). Invited review: priming, induction and modulation of plant defence responses by bacterial lipopolysaccharides. *Journal of endotoxin research*, *13*(2), 69-84.

Newman, M. A., Sundelin, T., Nielsen, J. T., & Erbs, G. (2013). MAMP (microbe-associated molecular pattern) triggered immunity in plants. *Frontiers in plant science, 4*, 139.

Norkunas, K., Harding, R., Dale, J., & Dugdale, B. (2018). Improving agroinfiltration-based transient gene expression in *Nicotiana benthamiana*. *Plant methods, 14*, 1-14.

Ogden, M., Whitcomb, S. J., Khan, G. A., Roessner, U., Hoefgen, R., & Persson, S. (2024). Cellulose biosynthesis inhibitor isoxaben causes nutrient-dependent and tissue-specific Arabidopsis phenotypes. *Plant Physiology*, *194*(2), 612-617.

O'Neill, M. A., Ishii, T., Albersheim, P., & Darvill, A. G. (2004). Rhamnogalacturonan II: structure and function of a borate cross-linked cell wall pectic polysaccharide. *Annual Review of Plant Biology*, *55*, 109-139.

O'Neill, M. A., & York, W. S. (2018). The composition and structure of plant primary cell walls. *Annual Plant Reviews online*, 1-54.

Oome, S., & Van den Ackerveken, G. (2014). Comparative and functional analysis of the widely occurring family of Nep1-like proteins. *Molecular plant-microbe interactions*, *27*(10), 1081-1094.

Park, Y. B., & Cosgrove, D. J. (2012). Changes in cell wall biomechanical properties in the xyloglucan-deficient *xxt1/xxt2* mutant of Arabidopsis. *Plant physiology*, *158*(1), 465-475.

Pawar, P. M. A., Derba-Maceluch, M., Chong, S. L., Gómez, L. D., Miedes, E., Banasiak, A., Ratke, C., Gaertner, C., Mouille, G., McQueen-Mason, S. J., Molina, A., Sellstedt, A., Tenkanen, M., & Mellerowicz, E. J. (2016). Expression of fungal acetyl xylan esterase in *Arabidopsis thaliana* improves saccharification of stem lignocellulose. *Plant biotechnology journal*, *14*(1), 387-397.

Peng, X., Li, S., & Wang, H. (2018). Time bomb for pollen tubes: peptide RALF-mediated signaling. *Molecular Plant*, *11*(4), 518-520.

Peracchi, L. M., Panahabadi, R., Barros-Rios, J., Bartley, L. E., & Sanguinet, K. A. (2024). Grass lignin: biosynthesis, biological roles, and industrial applications. *Frontiers in Plant Science, 15*, 1343097.

Pettersen, E. F., Goddard, T. D., Huang, C. C., Couch, G. S., Greenblatt, D. M., Meng, E. C., & Ferrin, T. E. (2004). UCSF Chimera—a visualization system for exploratory research and analysis. *Journal of computational chemistry*, *25*(13), 1605-1612.

Petutschnig, E. K., Jones, A. M., Serazetdinova, L., Lipka, U., & Lipka, V. (2010). The lysin motif receptor-like kinase (LysM-RLK) CERK1 is a major chitin-binding protein in *Arabidopsis thaliana* and subject to chitin-induced phosphorylation. *Journal of Biological Chemistry*, *285*(37), 28902-28911.

Pfaffl, M. W. (2001). A new mathematical model for relative quantification in real-time RT–PCR. *Nucleic acids research, 29(9)*, e45-e45.

Phillips, J. C., Hardy, D. J., Maia, J. D., Stone, J. E., Ribeiro, J. V., Bernardi, R. C., Buch, C., Fiorin, G., Hénin, J., Jiang, W., McGreevy, R., Melo, M., Radak, B., Skeel, R., Singharoy, A., Wang, Y., Roux, B., Aksimentiev, A., Luthey-Schulten, Z., Kalé, L., Schulten, K., Chipot, C., & Tajkhorshid, E. (2020). Scalable molecular dynamics on CPU and GPU architectures with NAMD. *The Journal of chemical physics*, *153*(4).

Pitzschke, A., & Hirt, H. (2006). Mitogen-activated protein kinases and reactive oxygen species signaling in plants. *Plant physiology*, *141*(2), 351-356.

Poinssot, B., Vandelle, E., Bentéjac, M., Adrian, M., Levis, C., Brygoo, Y., Garin, J., Sicilia, F., Thévenot, P. C., & Pugin, A. (2003). The endopolygalacturonase 1 from *Botrytis cinerea* activates grapevine defense reactions unrelated to its enzymatic activity. *Molecular Plant-Microbe Interactions, 16*(6), 553-564.

Poovaiah, C. R., Nageswara-Rao, M., Soneji, J. R., Baxter, H. L., & Stewart Jr, C. N. (2014). Altered lignin biosynthesis using biotechnology to improve lignocellulosic biofuel feedstocks. *Plant biotechnology journal*, *12*(9), 1163-1173.

Pontiggia, D., Benedetti, M., Costantini, S., De Lorenzo, G., & Cervone, F. (2020). Dampening the DAMPs: how plants maintain the homeostasis of cell wall molecular patterns and avoid hyper-immunity. *Frontiers in Plant Science*, *11*, 613259.

Pring, S., Kato, H., Imano, S., Camagna, M., Tanaka, A., Kimoto, H., Chen, P., Shrotri, A., Kobayashi, H., Fukupka, A., Saito, M., Suzuki, T., Terauchi, R., Sato, I., Chiba, S., & Takemoto, D. (2023). Induction of plant disease resistance by mixed oligosaccharide elicitors prepared from plant cell wall and crustacean shells. *Physiologia Plantarum*, *175*(5), e14052.

Purushotham, P., Ho, R., & Zimmer, J. (2020). Architecture of a catalytically active homotrimeric plant cellulose synthase complex. *Science*, *369*(6507), 1089-1094.

Putarjunan, A., Ruble, J., & Srivastava, A. (2019) Bipartite anchoring of SCREAM enforces stomatal initiation by coupling MAP kinases to SPEECHLESS. *Nature Plants, 5*, 742–754.

Quentin, M., Allasia, V., Pegard, A., Allais, F., Ducrot, P. H., Favery, B., Levis, C., Martinet, S., Masur, C., Ponchet, M., Roby, D., Schlaich, N. L., Jouanin, L., & Keller, H. (2009). Imbalanced lignin biosynthesis promotes the sexual reproduction of homothallic oomycete pathogens. *PLoS pathogens*, *5*(1), e1000264.

Qutob, D., Kemmerling, B., Brunner, F., Kufner, I., Engelhardt, S., Gust, A. A., Luberacki, B., Seitz, H. U., Stahl, D., Rauhut, T., Glawischnig, E., Schween, G., Lacombe, B., Watanabe, N., Lam, E., Schlichting, R., Scheel, D., Nau, K., Dodt, G., Hubert, D., Gijzen, M., & Nürnberger, T. (2006). Phytotoxicity and

innate immune responses induced by Nep1-like proteins. *The Plant Cell*, *18*(12), 3721-3744.

Radutoiu, S., Madsen, L. H., Madsen, E. B., Felle, H. H., Umehara, Y., Grønlund, M., Sato, S., Nakamura, Y., Tabata, S., Sandal, N., & Stougaard, J. (2003). Plant recognition of symbiotic bacteria requires two LysM receptor-like kinases. *Nature*, *425*(6958), 585-592.

Raetz, C. R., & Whitfield, C. (2002). Lipopolysaccharide endotoxins. *Annual review of biochemistry*, *71*(1), 635-700.

Rajaraman, J., Douchkov, D., Hensel, G., Stefanato, F. L., Gordon, A., Ereful, N., Caldararu, O. F., Petrescu, A. J., Kumlehn, J., Boyd, L. A., & Schweizer, P. (2016). An LRR/malectin receptor-like kinase mediates resistance to non-adapted and adapted powdery mildew fungi in barley and wheat. *Frontiers in plant science*, *7*, 1836.

Ramos, B., González-Melendi, P., Sánchez-Vallet, A., Sánchez-Rodríguez, C., López, G., & Molina, A. (2013). Functional genomics tools to decipher the pathogenicity mechanisms of the necrotrophic fungus *P. lectosphaerella* cucumerina in *Arabidopsis thaliana*. *Molecular Plant Pathology*, *14*(1), 44-57.

Ramos, H. C., Rumbo, M., & Sirard, J. C. (2004). Conservation of flagellin detection systems in plants and mammals. *Trends in Microbiology*, *11*(12), 509-517.

Ranf, S., Eschen‐Lippold, L., Pecher, P., Lee, J., & Scheel, D. (2011). Interplay between calcium signalling and early signalling elements during defence responses to microbe‐or damage‐associated molecular patterns. *The Plant Journal, 68*(1), 100-113.

Ranf, S., Grimmer, J., Pöschl, Y., Pecher, P., Chinchilla, D., Scheel, D., & Lee, J. (2012). Defense-related calcium signaling mutants uncovered via a quantitative high-throughput screen in *Arabidopsis thaliana*. *Molecular plant*, *5*(1), 115-130.

Rasmussen, M. W., Roux, M., Petersen, M., & Mundy, J. (2012). MAP kinase cascades in Arabidopsis innate immunity. *Frontiers in plant science*, *3*, 29027.

Rebaque, D., Del Hierro, I., Lopez, G., Bacete, L., Vilaplana, F., Dallabernardina, P., Pfrengle, F., Jordá, L., Sánchez-Vallet, A., Pérez, R., Brunner, F., Molina, A., & Mélida, H. (2021). Cell wall‐derived mixed‐linked β‐1, 3/1, 4

glucans trigger immune responses and disease resistance in plants. *The Plant Journal, 106*(3), 601-615.

Rennie, E. A., & Scheller, H. V. (2014). Xylan biosynthesis. *Current opinion in biotechnology*, *26*, 100-107.

Rhodes, J., Yang, H., Moussu, S., Boutrot, F., Santiago, J., & Zipfel, C. (2021). Perception of a divergent family of phytocytokines by the Arabidopsis receptor kinase MIK2. *Nature Communications, 12*(1), 705.

Ride, J. P., & Barber, M. S. (1990). Purification and characterization of multiple forms of endochitinase from wheat leaves. *Plant Science*, *71*(2), 185-197.

Ridley, B. L., O'Neill, M. A., & Mohnen, D. (2001). Pectins: structure, biosynthesis, and oligogalacturonide-related signaling. *Phytochemistry*, *57*(6), 929-967.

Roudaire, T., Marzari, T., Landry, D., Löffelhardt, B., Gust, A. A., Jermakow, A., Dry, I., Winckler, P., Héloir, M. C., & Poinssot, B. (2023). The grapevine LysM receptor-like kinase VvLYK5-1 recognizes chitin oligomers through its association with VvLYK1-1. *Frontiers in Plant Science*, *14*, 1130782.

Roux, M., Schwessinger, B., Albrecht, C., Chinchilla, D., Jones, A., Holton, N., Malinovsky, F. G., Tör, M., de Vries, S., & Zipfel, C. (2011). The Arabidopsis leucine-rich repeat receptor–like kinases BAK1/SERK3 and BKK1/SERK4 are required for innate immunity to hemibiotrophic and biotrophic pathogens. *The Plant Cell, 23(6)*, 2440-2455.

Rui, Y., & Dinneny, J. R. (2020). A wall with integrity: surveillance and maintenance of the plant cell wall under stress. *New Phytologist*, *225*(4), 1428-1439.

Rzhetsky, A., & Nei, M. (1992) A simple method for estimating and testing minimum-evolution trees. *Molecular Biology and Evolution, 9*, 945.

Sagi, M., & Fluhr, R. (2006). Production of reactive oxygen species by plant NADPH oxidases. *Plant physiology*, *141*(2), 336-340.

Saitou, N., & Nei, M. (1987) The neighbor-joining method: a new method for reconstructing phylogenetic trees. *Molecular Biology and Evolution, 4*, 406–425.

Salvador, P., & Lasserre, T. (2010). *U.S. Patent Application No. 12/675,587*.

Samanta, S., & Thakur, J. K. (2015). Importance of Mediator complex in the regulation and integration of diverse signaling pathways in plants. *Frontiers in plant science*, *6*, 158580.

Sánchez-Vallet, A., Mesters, J. R., & Thomma, B. P. (2015). The battle for chitin recognition in plant-microbe interactions. *FEMS microbiology reviews, 39*(2), 171-183.

Sandoval, P.J., & Santiago, J. (2020) In vitro analytical approaches to study plant ligand-receptor interactions. *Plant Physiology, 182*, 1697–1712.

Sarkar, P., Bosneaga, E., & Auer, M. (2009). Plant cell walls throughout evolution: towards a molecular understanding of their design principles. *Journal of experimental botany*, *60*(13), 3615-3635.

Savatin, D. V., Bisceglia, N. G., Marti, L., Fabbri, C., Cervone, F., & De Lorenzo, G. (2014). The Arabidopsis NUCLEUS-AND PHRAGMOPLAST-LOCALIZED KINASE1-related protein kinases are required for elicitor-induced oxidative burst and immunity. *Plant Physiology*, *165*(3), 1188-1202.

Schallus, T., Fehér, K., Sternberg, U., Rybin, V., & Muhle-Goll, C. (2010) Analysis of the specific interactions between the lectin domain of malectin and diglucosides. *Glycobiology, 20*, 1010–1020.

Schallus, T., Jaeckh, C., Fehér, K., Palma, A. S., Liu, Y., Simpson, J. C., Mackeen, M., Stier, G., Gibson, T. J., Feizi, T., Pieler, T., & Muhle-Goll, C. (2008). Malectin: a novel carbohydrate-binding protein of the endoplasmic reticulum and a candidate player in the early steps of protein N-glycosylation. *Molecular biology of the cell, 19*(8), 3404-3414.

Scheller, H. V., & Ulvskov, P. (2010). Hemicelluloses. *Annual review of plant biology*, *61*, 263-289.

Schoenaers, S., Lee, H. K., Gonneau, M., Faucher, E., Levasseur, T., Akary, E., Claeijs, N., Moussu, S., Broyart, C., Balcerowicz, D., AbdElgawad, H., Bassi, A., Damineli, D. S. C., Costa, A., Feijó, J. A., Moreau, C., Bonnin, E., Cathala, B., Santiago, J., Höfte, H., & Vissenberg, K. (2024). Rapid alkalinization factor 22 has a structural and signalling role in root hair cell wall assembly. *Nature Plants*, 1-18.

Schrödinger, L.L.C. (2020) The PyMOL molecular graphics system, version 2.5. New York, NY: Schrödinger, LLC.

Schulze, B., Mentzel, T., Jehle, A. K., Mueller, K., Beeler, S., Boller, T., Felix, G., & Chinchilla, D. (2010). Rapid heteromerization and phosphorylation of

ligand-activated plant transmembrane receptors and their associated kinase BAK1. *Journal of Biological Chemistry*, *285*(13), 9444-9451.

Scortica, A., Giovannoni, M., Scafati, V., Angelucci, F., Cervone, F., De Lorenzo, G., Benedetti, M., & Mattei, B. (2022). Berberine bridge enzyme-like oligosaccharide oxidases act as enzymatic transducers between microbial glycoside hydrolases and plant peroxidases. *Molecular Plant-Microbe Interactions*, *35*(10), 881-886.

Sechet, J., Frey, A., Effroy-Cuzzi, D., Berger, A., Perreau, F., Cueff, G., Charif, D., Rajjou, L., Mouille, G., North, H. M., & Marion-Poll, A. (2016). Xyloglucan metabolism differentially impacts the cell wall characteristics of the endosperm and embryo during Arabidopsis seed germination. *Plant Physiology*, *170*(3), 1367-1380.

Sherson, S., Gy, I., Medd, J., Schmidt, R., Dean, C., Kreis, M., Lecharny, A., & Cobbett, C. (1999). The arabinose kinase, ARA1, gene of Arabidopsis is a novel member of the galactose kinase gene family. *Plant molecular biology*, *39*, 1003-1012.

Shi, Y., Song, B., Liang, Q., Su, D., Lu, W., Liu, Y., & Li, Z. (2023). Molecular regulatory events of flower and fruit abscission in horticultural plants. *Horticultural Plant Journal*, *9*(5), 867-883.

Shiu, S. H., & Bleecker, A. B. (2001). Plant receptor-like kinase gene family: diversity, function, and signaling. *Science's STKE*, *2001*(113), re22-re22.

Showalter, A. M. (1993). Structure and function of plant cell wall proteins. *The plant cell*, *5*(1), 9.

Silva, N. F., & Goring, D. R. (2002). The proline-rich, extensin-like receptor kinase-1 (PERK1) gene is rapidly induced by wounding. *Plant molecular biology*, *50*, 667-685.

Sinclair, S. A., Larue, C., Bonk, L., Khan, A., Castillo-Michel, H., Stein, R. J., Grolimund, D., Begerow, D., Meumann, U., Haydon, M. H., & Krämer, U. (2017). Etiolated seedling development requires repression of photomorphogenesis by a small cell-wall-derived dark signal. *Current Biology*, *27*(22), 3403-3418.

Smakowska-Luzan, E., Mott, G. A., Parys, K., Stegmann, M., Howton, T. C., Layeghifard, M., Neuhold, J., Lehner, A., Kong, J., Grünwald, K., Weinberger, N., Satbhai, S. B., Mayer, D., Busch, W., Madalinski, M., Stolt-Bergner, P., Provart, N. J., Mukhtar, S., Zipfel, C., Desveaux, D., Guttman,

D. S., & Belkhadir, Y. (2018). An extracellular network of Arabidopsis leucine-rich repeat receptor kinases. *Nature*, *553*(7688), 342-346.

Soejima, Y., Lee, J., Nagata, Y., Mon, H., Iiyama, K., Kitano, H., Matsuyama, M., & Kusakabe, T. (2013). Comparison of signal peptides for efficient protein secretion in the baculovirus-silkworm system. *Open Life Sciences, 8(1)*, 1-7.

Sørensen, I., Pettolino, F. A., Wilson, S. M., Doblin, M. S., Johansen, B., Bacic, A., & Willats, W. G. (2008). Mixed-linkage (1→ 3),(1→ 4)-ß-d-glucan is not unique to the *Poales* and is an abundant component of *Equisetum arvense* cell walls. *The Plant Journal*, *54*(3), 510-521.

Souza, C.A., Li, S., & Lin, A.Z. (2017) Cellulose-derived oligomers act as damage-associated molecular patterns and trigger defense-like responses. *Plant Physiology, 173*, 2383–2398.

Stegmann, M., Monaghan, J., Smakowska-Luzan, E., Rovenich, H., Lehner, A., Holton, N., Belkhadir, Y., & Zipfel, C. (2017). The receptor kinase FER is a RALF-regulated scaffold controlling plant immune signaling. *Science*, *355*(6322), 287-289.

Su, C. (2023). Pectin modifications at the symbiotic interface. *New Phytologist*, *238*(1), 25-32.

Sun, L., Ropartz, D., Cui, L., Shi, H., Ralet, M. C., & Zhou, Y. (2019). Structural characterization of rhamnogalacturonan domains from Panax ginseng CA Meyer. *Carbohydrate polymers*, *203*, 119-127.

Sun, W., Cao, Y., Jansen Labby, K., Bittel, P., Boller, T., & Bent, A. F. (2012). Probing the Arabidopsis flagellin receptor: FLS2-FLS2 association and the contributions of specific domains to signaling function. *The plant cell*, *24*(3), 1096-1113.

Sun, Y., Han, Z., Tang, J., Hu, Z., Chai, C., Zhou, B., & Chai, J. (2013). Structure reveals that BAK1 as a co-receptor recognizes the BRI1-bound brassinolide. *Cell research*, *23*(11), 1326-1329.

Sun, Y., Li, L., Macho, A. P., Han, Z., Hu, Z., Zipfel, C., Zhou, J. M., & Chai, J. (2013). Structural basis for flg22-induced activation of the Arabidopsis FLS2-BAK1 immune complex. *Science*, *342*(6158), 624-628.

Tamura, K., Stecher, G., Peterson, D., Filipski, A., & Kumar, S. (2013) MEGA6: molecular evolutionary genetics analysis version 6.0. *Molecular Biology and Evolution, 30*, 2725–2729.

Tan, L., Eberhard, S., Pattathil, S., Warder, C., Glushka, J., Yuan, C., Hao, Z., Zhu, X., Avci, U., Miller, J. S., Baldwin, D., Pham, C., Orlando, R., Darvill, a., Hahn, M. G., Kieliszewski, M. J., & Mohnen, D. (2013). An Arabidopsis cell wall proteoglycan consists of pectin and arabinoxylan covalently linked to an arabinogalactan protein. *The Plant Cell*, *25*(1), 270-287.

Tanaka, K., & Heil, M. (2021). Damage-associated molecular patterns (DAMPs) in plant innate immunity: applying the danger model and evolutionary perspectives. *Annual review of phytopathology, 59*, 53-75.

Tang, D., Wang, G., & Zhou, J. M. (2017). Receptor kinases in plant-pathogen interactions: more than pattern recognition. *The Plant Cell*, *29*(4), 618-637.

Tang, P., Zhang, Y., Sun, X., Tian, D., Yang, S., & Ding, J. (2010). Disease resistance signature of the leucine-rich repeat receptor-like kinase genes in four plant species. *Plant science*, *179*(4), 399-406.

Tang, W., Lin, W., Zhou, X., Guo, J., Dang, X., Li, B., Lin, D., & Yang, Z. (2022). Mechano-transduction via the pectin-FERONIA complex activates ROP6 GTPase signaling in Arabidopsis pavement cell morphogenesis. *Current Biology*, *32*(3), 508-517.

Tao, H., Miao, H., Chen, L., Wang, M., Xia, C., Zeng, W., Sun, B., Zhang, F., Zhang, S., Li, C., & Wang, Q. (2022). WRKY33-mediated indolic glucosinolate metabolic pathway confers resistance against Alternaria brassicicola in Arabidopsis and Brassica crops. *Journal of integrative plant biology*, *64*(5), 1007-1019.

Tateno, M., Brabham, C., & DeBolt, S. (2016). Cellulose biosynthesis inhibitors–a multifunctional toolbox. *Journal of experimental botany*, *67*(2), 533-542.

Taylor, N. G. (2008). Cellulose biosynthesis and deposition in higher plants. *New phytologist*, *178*(2), 239-252.

Thor, K., Jiang, S., Michard, E., George, J., Scherzer, S., Huang, S., Dindas, J., Derbyshire, P., Leitao, N., DeFalco, T. A., Köster, P., Hunter, K., Kimura, S., Gronnier, J., Stransfeld, L., Kadota, Y., Bücherl, C. A., Charpentier, M., Wrzaczek, M., MacLean, D., Oldroyd, G. E. D., Menke, F. L. H., Roelfsema, M. R. G., Hedrich, R., Feijó, J., & Zipfel, C. (2020). The calcium-permeable channel OSCA1. 3 regulates plant stomatal immunity. *Nature*, *585*(7826), 569-573.

Tian, W., Hou, C., Ren, Z., Wang, C., Zhao, F., Dahlbeck, D., Hu, S., Zhang, L., Niu, Q., Li, L., Staskawicz, B. J., & Luan, S. (2019). A calmodulin-gated calcium

channel links pathogen patterns to plant immunity. *Nature*, *572*(7767), 131-135.

Torres, M. A. (2010). ROS in biotic interactions. *Physiologia plantarum*, *138*(4), 414-429.

Torres, M. A., Dangl, J. L., & Jones, J. D. (2002). Arabidopsis gp91phox homologues AtrbohD and AtrbohF are required for accumulation of reactive oxygen intermediates in the plant defense response. *Proceedings of the National Academy of Sciences*, *99*(1), 517-522.

Torres, M. A., & Dangl, J. L. (2005). Functions of the respiratory burst oxidase in biotic interactions, abiotic stress and development. *Current opinion in plant biology*, *8*(4), 397-403.

Torres, M. A., Morales, J., Sánchez-Rodríguez, C., Molina, A., & Dangl, J. L. (2013). Functional interplay between Arabidopsis NADPH oxidases and heterotrimeric G protein. *Molecular plant-microbe interactions*, *26*(6), 686-694.

Tran, D., Dauphin, A., Meimoun, P., Kadono, T., Nguyen, H. T., Arbelet-Bonnin, D., Zhao, T., Errakhi, R., Lehner, A., Kawano, T., & Bouteau, F. (2018). Methanol induces cytosolic calcium variations, membrane depolarization and ethylene production in arabidopsis and tobacco. *Annals of botany*, *122*(5), 849-860.

Tronchet, M., Balagué, C., Kroj, T., Jouanin, L., & Roby, D. (2010). Cinnamyl alcohol dehydrogenases-C and D, key enzymes in lignin biosynthesis, play an essential role in disease resistance in Arabidopsis. *Molecular plant pathology*, *11*(1), 83-92.

Tseng, Y. H., Scholz, S. S., Fliegmann, J., Krüger, T., Gandhi, A., Furch, A. C., Kniemeyer, O., Brakhage, A. A., & Oelmüller, R. (2022). CORK1, a LRR-malectin receptor kinase, is required for cellooligomer-induced responses in Arabidopsis thaliana. *Cells*, *11*(19), 2960.

Tsuda, K., & Somssich, I. E. (2015). Transcriptional networks in plant immunity. *New Phytologist*, *206*(3), 932-947.

Tunyasuvunakool, K., Adler, J., Wu, Z., Green, T., Zielinski, M., Žídek, A., Brigland, A., Cowie, A., Meyer, C., Laydon, A., Velankar, S., Kleywegt, G., Bateman, A., Evans, R., Pritzel, A., Figurnov, M., Ronneberger, O., Bates, R., Kohl, S., Potapenko, A., Ballard, A., Romera-Paredes, B., Nikolov, S., Jain, R., Clancy, E., Reiman, D., Petersen, S., Senior, A., Kavukcuoglu, K., Birney, E., Kohli, P., Jumper, J., & Hassabis, D. (2021). Highly accurate

protein structure prediction for the human proteome. *Nature, 596(7873)*, 590-596.

Turner, S., & Kumar, M. (2018). Cellulose synthase complex organization and cellulose microfibril structure. *Philosophical Transactions of the Royal Society A: Mathematical, Physical and Engineering Sciences*, *376*(2112), 20170048.

Vaahtera, L., Schulz, J., & Hamann, T. (2019). Cell wall integrity maintenance during plant development and interaction with the environment. *Nature plants*, *5*(9), 924-932.

Vaid, N., Macovei, A., & Tuteja, N. (2013). Knights in action: lectin receptor-like kinases in plant development and stress responses. *Molecular plant*, *6*(5), 1405-1418.

Van Damme, E. J., Lannoo, N., & Peumans, W. J. (2008). Plant lectins. In *Advances in botanical research* (Vol. 48, pp. 107-209). Academic Press.

Vanholme, R., De Meester, B., Ralph, J., & Boerjan, W. (2019). Lignin biosynthesis and its integration into metabolism. *Current opinion in biotechnology*, *56*, 230-239.

Vargas-Rechia, C., Reicher, F., Rita Sierakowski, M., Heyraud, A., Driguez, H., & Liénart, Y. (1998). Xyloglucan octasaccharide XXLGol derived from the seeds of *Hymenaea courbaril* acts as a signaling molecule. *Plant Physiology*, *116*(3), 1013-1021.

Varki, A., Cummings, R. D., Aebi, M., Packer, N. H., Seeberger, P. H., Esko, J. D., Stanley, P., Hart, G., Darvill, A., Kinoshita, T., Prestegard, J. J., Schnaar, R. L., Freeze, H. H., Marth, J. D., Bertozzi, C. R., Etzler, M. E., Frank, M., Vliegenthart, J. F., Lütteke, T., Perez, S., Bolton, E., Rudd, P., Paulson, J., Kanehisa, M., Toukach, P., Aoki-Kinoshita, K. F., Dell, A., Narimatsu, H., York, W., Taniguchi, N., & Kornfeld, S. (2016). Symbol nomenclature for glycans (SNFG). *Glycobiology, 25(12)*, 1323-4.

Versluys, M., Toksoy Öner, E., & Van den Ende, W. (2022). Fructan oligosaccharide priming alters apoplastic sugar dynamics and improves resistance against Botrytis cinerea in chicory. *Journal of Experimental Botany*, *73*(12), 4214-4235.

Vogel, J. (2008). Unique aspects of the grass cell wall. *Current opinion in plant biology*, *11*(3), 301-307.

Vogel, J. P., Raab, T. K., Schiff, C., & Somerville, S. C. (2002). PMR6, a pectate lyase–like gene required for powdery mildew susceptibility in Arabidopsis. *The Plant Cell*, *14*(9), 2095-2106.

Vogel, J. P., Raab, T. K., Somerville, C. R., & Somerville, S. C. (2004). Mutations in PMR5 result in powdery mildew resistance and altered cell wall composition. *The Plant Journal*, *40*(6), 968-978.

Von Dahl, C. C., & Baldwin, I. T. (2007). Deciphering the role of ethylene in plant–herbivore interactions. *Journal of plant growth regulation*, *26*, 201-209.

Voxeur, A., Habrylo, O., Guénin, S., Miart, F., Soulié, M. C., Rihouey, C., Pau-Roblot, C., Domon, J. M., Gutierrez, L., Pelloux, J., Mouille, G., Fagard, M., Höfte, H., & Vernhettes, S. (2019). Oligogalacturonide production upon Arabidopsis thaliana–Botrytis cinerea interaction. *Proceedings of the National Academy of Sciences*, *116*(39), 19743-19752.

Wan, J., He, M., Hou, Q., Zou, L., Yang, Y., Wei, Y., & Chen, X. (2021). Cell wall associated immunity in plants. *Stress Biology*, *1*(1), 3.

Wan, J., Tanaka, K., Zhang, X. C., Son, G. H., Brechenmacher, L., Nguyen, T. H. N., & Stacey, G. (2012). LYK4, a lysin motif receptor-like kinase, is important for chitin signaling and plant innate immunity in Arabidopsis. *Plant physiology*, *160*(1), 396-406.

Wan, J., Zhang, X. C., Neece, D., Ramonell, K. M., Clough, S., Kim, S. Y., Stacey, M., & Stacey, G. (2008). A LysM receptor-like kinase plays a critical role in chitin signaling and fungal resistance in Arabidopsis. *The Plant Cell*, *20*(2), 471-481.

Wang, Y., Kang, Y., Ma, C., Miao, R., Wu, C., Long, Y., Ge, T., Wu, Z., Hou, X., Zhang, J., & Qi, Z. (2017). CNGC2 is a Ca2+ influx channel that prevents accumulation of apoplastic Ca2+ in the leaf. *Plant Physiology*, *173*(2), 1342-1354.

Wang, B., Qin, X., Wu, J., Deng, H., Li, Y., Yang, H., Chen, Z., Liu, G., & Ren, D. (2016). Analysis of crystal structure of Arabidopsis MPK6 and generation of its mutants with higher activity. *Scientific reports, 6*(1), 25646.

Wang, C., & Luan, S. (2024). Calcium homeostasis and signaling in plant immunity. *Current opinion in plant biology, 77*, 102485.

Wang, G., Ellendorff, U., Kemp, B., Mansfield, J. W., Forsyth, A., Mitchell, K., Bastas, K., Liu, C. M., Woods-Tör, A., Zipfel, C., de Wit, P. J. G. M., Jones, J. D. G., Tör, M., & Thomma, B. P. (2008). A genome-wide functional

investigation into the roles of receptor-like proteins in Arabidopsis. *Plant physiology*, *147*(2), 503-517.

Wanke, A., Malisic, M., Wawra, S., & Zuccaro, A. (2021). Unraveling the sugar code: the role of microbial extracellular glycans in plant–microbe interactions. *Journal of Experimental Botany, 72*(1), 15-35.

Wanke, A., Rovenich, H., Schwanke, F., Velte, S., Becker, S., Hehemann, J. H., Wawra, S., & Zuccaro, A. (2020). Plant species-specific recognition of long and short ß-1, 3-linked glucans is mediated by different receptor systems. *The Plant Journal*, *102*(6), 1142-1156.

Wanke, A., van Boerdonk, S., Mahdi, L. K., Wawra, S., Neidert, M., Chandrasekar, B., Saake, P., Saur, I. M. L., Derbyshire, P., Holston, N., Menke, F. L. H., Brands, M., Pauly, M., Acosta, I. F., & Zuccaro, A. (2023). A GH81-type ß-glucan-binding protein enhances colonization by mutualistic fungi in barley. *Current Biology*, *33*(23), 5071-5084.

Waterhouse, A., Bertoni, M., Bienert, S., Studer, G., Tauriello, G., Gumienny, R., Heer, F., de Beer, T., Rempfer, C., Bordoli, L., Lepore, R., & Schwede, T. (2018). SWISS-MODEL: homology modelling of protein structures and complexes. *Nucleic acids research, 46*(W1), W296-W303.

Wawra, S., Fesel, P., Widmer, H., Timm, M., Seibel, J., Leson, L., Kesseler, L., Nostadt, R., Hilbert, M., Langen, G., & Zuccaro, A. (2016). The fungal-specific ß-glucan-binding lectin FGB1 alters cell-wall composition and suppresses glucan-triggered immunity in plants. *Nature Communications, 7*(1), 13188.

Willmann, R., Lajunen, H. M., Erbs, G., Newman, M. A., Kolb, D., Tsuda, K., Katagiri, F., Fliegmann, J., Bono, J. J., Cullimore, J. V., Jehle, A. K., Götz, F., Kulik, A., Molinaro, A., Lipka, V., Gust, A. A., & Nürnberger, T. (2011). Arabidopsis lysin-motif proteins LYM1 LYM3 CERK1 mediate bacterial peptidoglycan sensing and immunity to bacterial infection. *Proceedings of the National Academy of Sciences*, *108*(49), 19824-19829.

Wolf, S. (2022) Cell Wall Signaling in Plant Development and Defense. *Annual Review Plant Biology, 73*, 323-353.

Wolf, S., Mravec, J., Greiner, S., Mouille, G., & Höfte, H. (2012). Plant cell wall homeostasis is mediated by brassinosteroid feedback signaling. *Current Biology*, *22*(18), 1732-1737.

Wong, J. E., Gysel, K., Birkefeldt, T. G., Vinther, M., Muszyński, A., Azadi, P., Laursen, N. S., Sullivan, J. T., Ronson, C. W., Stougaard, J., & Andersen, K.

R. (2020). Structural signatures in EPR3 define a unique class of plant carbohydrate receptors. *Nature Communications*, *11*(1), 3797.

Wormit, A., & Usadel, B. (2018). The multifaceted role of pectin methylesterase inhibitors (PMEIs). *International journal of molecular sciences*, *19*(10), 2878.

Wrzaczek, M., Brosche, M., & Kangasjärvi, J. (2013). ROS signaling loops—production, perception, regulation. *Current opinion in plant biology*, *16*(5), 575-582.

Wu, A. M., Rihouey, C., Seveno, M., Hörnblad, E., Singh, S. K., Matsunaga, T., Ishii, T., Lerouge, P., & Marchant, A. (2009). The Arabidopsis IRX10 and IRX10-LIKE glycosyltransferases are critical for glucuronoxylan biosynthesis during secondary cell wall formation. *The Plant Journal*, *57*(4), 718-731.

Wu, F., Chi, Y., Jiang, Z., Xu, Y., Xie, L., Huang, F., Wan, D., Ni, J., Yuan, F., Wu, X., Zhang, Y., Wang, L., Ye, R., Byeon, B., Wang, W., Zhang, S., Sima, M., Chen, S., Zhu, M., Pei, J., Johnson, D. M., Zhu, S., Cao, X., Pei, C., Zai, Z., Liu, Y., Liu, T., Swift, G. B., Zhang, W., Yu, M., Hu, Z., Siedow, J. N., Chen, X., & Pei, Z. M. (2020). Hydrogen peroxide sensor HPCA1 is an LRR receptor kinase in Arabidopsis. *Nature, 578*(7796), 577-581.

Xiao, Y., Stegmann, M., Han, Z., DeFalco, T. A., Parys, K., Xu, L., Belkhadir, Y., Zipfel, C., & Chai, J. (2019). Mechanisms of RALF peptide perception by a heterotypic receptor complex. *Nature, 572*(7768), 270-274.

Xie, C., Yang, L., & Gai, Y. (2023). MAPKKKs in plants: multidimensional regulators of plant growth and stress responses. *International Journal of Molecular Sciences*, *24*(4), 4117.

Xu, P., Xu, S. L., Li, Z. J., Tang, W., Burlingame, A. L., & Wang, Z. Y. (2014). A brassinosteroid-signaling kinase interacts with multiple receptor-like kinases in Arabidopsis. *Molecular Plant*, *7*(2), 441-444.

Xue, D. X., Li, C. L., Xie, Z. P., & Staehelin, C. (2019). LYK4 is a component of a tripartite chitin receptor complex in Arabidopsis thaliana. *Journal of experimental botany*, *70*(19), 5507-5516.

Yadav, S., & Chattopadhyay, D. (2023). Lignin: the building block of defense responses to stress in plants. *Journal of Plant Growth Regulation, 42*(10), 6652-6666.

Yamaguchi, K., & Kawasaki, T. (2021). Pathogen-and plant-derived peptides trigger plant immunity. *Peptides, 144*, 170611.

Yamaguchi, Y., Huffaker, A., Bryan, A. C., Tax, F. E., & Ryan, C. A. (2010). PEPR2 is a second receptor for the Pep1 and Pep2 peptides and contributes to defense responses in Arabidopsis. *The Plant Cell*, *22*(2), 508-522.

Yamaguchi, Y., Pearce, G., & Ryan, C. A. (2006). The cell surface leucine-rich repeat receptor for At Pep1, an endogenous peptide elicitor in Arabidopsis, is functional in transgenic tobacco cells. *Proceedings of the National Academy of Sciences*, *103*(26), 10104-10109.

Yang, C., Liu, R., Pang, J., Ren, B., Zhou, H., Wang, G., Wang, E., & Liu, J. (2021). Poaceae-specific cell wall-derived oligosaccharides activate plant immunity via OsCERK1 during Magnaporthe oryzae infection in rice. *Nature communications, 12*(1), 2178.

Yang, C., Wang, E., & Liu, J. (2022) CERK1, more than a co-receptor in plant–microbe interactions. *New Phytologist, 234*, 1606–1613.

Yang, H., Wang, D., Guo, L., Pan, H., Yvon, R., Garman, S., Wu, H., & Cheung, A. Y. (2021). Malectin/Malectin-like domain-containing proteins: a repertoire of cell surface molecules with broad functional potential. *The Cell Surface, 7*, 100056.

Yeh, Y. H., Panzeri, D., Kadota, Y., Huang, Y. C., Huang, P. Y., Tao, C. N., Roux, M., Chien, H. C., Chin, T. C., Chu, P. W., Zipfel, C., & Zimmerli, L. (2016). The Arabidopsis malectin-like/LRR-RLK IOS1 is critical for BAK1-dependent and BAK1-independent pattern-triggered immunity. *The Plant Cell*, *28*(7), 1701-1721.

Yong, W., Link, B., O'Malley, R., Tewari, J., Hunter, C. T., Lu, C. A., Li, X., Blleecker, A. B., Koch, K. E., McCann, M. C., McCarty, D. R., Patterson, S. E., Reiter, W. D., Staiger, C., Thomas, S. R., Vermerris, W., & Carpita, N. C. (2005). Genomics of plant cell wall biogenesis. *Planta*, *221*, 747-751.

Yuan, M., Ngou, B. P. M., Ding, P., & Xin, X. F. (2021). PTI-ETI crosstalk: an integrative view of plant immunity. *Current opinion in plant biology*, *62*, 102030.

Zablackis, E., Huang, J., Muller, B., Darvill, A. G., & Albersheim, P. (1995). Characterization of the cell-wall polysaccharides of *Arabidopsis thaliana* leaves. *Plant physiology*, *107*(4), 1129-1138.

Zamil, M. S., & Geitmann, A. (2017). The middle lamella—more than a glue. *Physical Biology*, *14*(1), 015004.

Zang, H., Xie, S., Zhu, B., Yang, X., Gu, C., Hu, B., Gao, T., Chen, Y., & Gao, X. (2019). Mannan oligosaccharides trigger multiple defence responses in rice and tobacco as a novel danger-associated molecular pattern. *Molecular plant pathology*, *20*(8), 1067-1079.

Zarattini, M., Corso, M., Kadowaki, M. A., Monclaro, A., Magri, S., Milanese, I., Jolivet, S., Ortiz de Godoy, M., Hermans, C., Fagard, M., & Cannella, D. (2021). LPMO-oxidized cellulose oligosaccharides evoke immunity in Arabidopsis conferring resistance towards necrotrophic fungus B. cinerea. *Communications biology*, *4*(1), 727.

Zeiner, A., Colina, F. J., Citterico, M., & Wrzaczek, M. (2023). CYSTEINE-RICH RECEPTOR-LIKE PROTEIN KINASES: their evolution, structure, and roles in stress response and development. *Journal of Experimental Botany*, *74*(17), 4910-4927.

Zeković, D. B., Kwiatkowski, S., Vrvić, M. M., Jakovljević, D., & Moran, C. A. (2005). Natural and modified (1→ 3)-β-D-glucans in health promotion and disease alleviation. *Critical reviews in biotechnology*, *25*(4), 205-230.

Zhang, B., Chang, L., Sun, W., Ullah, A., & Yang, X. (2021). Overexpression of an expansin-like gene, GhEXLB2 enhanced drought tolerance in cotton. *Plant Physiology and Biochemistry*, *162*, 468-475.

Zhang, B., Gao, Y., Zhang, L., & Zhou, Y. (2021). The plant cell wall: Biosynthesis, construction, and functions. *Journal of Integrative Plant Biology*, *63*(1), 251-272.

Zhang, L., Kars, I., Essenstam, B., Liebrand, T. W., Wagemakers, L., Elberse, J., Tagkalaki, P., Tjoitang, D., van den Ackerveken, G., & van Kan, J. A. (2014). Fungal endopolygalacturonases are recognized as microbe-associated molecular patterns by the Arabidopsis receptor-like protein RESPONSIVENESS TO BOTRYTIS POLYGALACTURONASES1. *Plant physiology, 164*(1), 352-364.

Zhang, X., Dong, W., Sun, J., Feng, F., Deng, Y., He, Z., Oldroyd, G. E. D., & Wang, E. (2015). The receptor kinase CERK 1 has dual functions in symbiosis and immunity signalling. *The Plant Journal*, *81*(2), 258-267.

Zhang, X., Yang, Z., Wu, D., & Yu, F. (2020). RALF–FERONIA signaling: linking plant immune response with cell growth. *Plant communications*, *1*(4).

Zhang, Y., & Skolnick, J. (2005). TM-align: a protein structure alignment algorithm based on the TM-score. *Nucleic acids research, 33*(7), 2302-2309.

Zhao, W., Ding, L., Liu, J., Zhang, X., Li, S., Zhao, K., Guan, Y., Song, A., Wang, H., Chen, S., Jiang, J., & Chen, F. (2022). Regulation of lignin biosynthesis by an atypical bHLH protein CmHLB in Chrysanthemum. *Journal of Experimental Botany*, *73*(8), 2403-2419.

Zhao, C., Tang, Y., Wang, J., Zeng, Y., Sun, H., Zheng, Z., Su, R., Schneeberger, K., Parker, J. E., & Cui, H. (2021). A mis-regulated cyclic nucleotide-gated channel mediates cytosolic calcium elevation and activates immunity in Arabidopsis. *New Phytologist*, *230*(3), 1078-1094.

Zheng, D., Wang, H., Zhong, H., Ke, W., Hu, H., Sun, M., & Ruan, L. (2021). Elucidation of the Pathogenicity-Associated Regulatory Network in *Xanthomonas oryzae* pv*. oryzae*. *Msystems*, *6*(2), 10-1128.

Zheng, Z., Qamar, S. A., Chen, Z., & Mengiste, T. (2006). Arabidopsis WRKY33 transcription factor is required for resistance to necrotrophic fungal pathogens. *The Plant Journal*, *48*(4), 592-605.

Zipfel, C. (2014). Plant pattern-recognition receptors. *Trends in immunology*, *35*(7), 345-351.

Zipfel, C., Kunze, G., Chinchilla, D., Caniard, A., Jones, J. D., Boller, T., & Felix, G. (2006). Perception of the bacterial PAMP EF-Tu by the receptor EFR restricts Agrobacterium-mediated transformation. *Cell*, *125*(4), 749-760.

Zuo, W., Chao, Q., Zhang, N., Ye, J., Tan, G., Li, B., Xing, Y., Zhang, B., Liu, H., Fengler, K. A., Zhao, J., Zhao, X., Chen, Y., Lai, J., Yan, J., & Xu, M. (2015). A maize wall-associated kinase confers quantitative resistance to head smut. *Nature genetics*, *47*(2), 151-157.

Annexes

A.1: Online data set: includes the genome assembly data for *igp1*^{AEQ}, *igp2*^{AEQ}, *igp3*^{AEQ}, *igp4* and Col-0^{AEQ} and can be retrieved from the NCBI Sequence Read Archive (SRA) under BioProject ID PRJNA864842 and Biosample accessions SAMN30087195, SAMN30087196, SAMN30087197, SAMN30087198 and SAMN30087199.

A.2: Martín-Dacal, M., Fernández-Calvo, P., Jiménez-Sandoval, P., Lopez, G., Garrido-Arandía, M., Rebaque, D., del Hierro, I., Berlanga, D. J., Torres, M. A., Kumar, V., Mélida, H., Pacios, L. F., Santiago, J., & Molina, A. (2023). Arabidopsis immune responses triggered by cellulose-and mixed-linked glucan-derived oligosaccharides require a group of leucine-rich repeat malectin receptor kinases. *The Plant Journal, 113*(4), 833-850.

A.3: Fernández-Calvo, P., López, G., Martín-Dacal, M., Aitouguinane, M., Carrasco-López, C., González-Bodi, S.,Bacete, L., Mélida, H., Sánchez-Vallet, A., & Molina, A. (2024). Leucine rich repeat-malectin receptor kinases IGP1/CORK1, IGP3 and IGP4 are required for arabidopsis immune responses triggered by ß-1, 4-D-Xylo-oligosaccharides from plant cell walls. *The Cell Surface, 100124*.

A.4: Molina, A., Jordá, L., Torres, M. Á., Martín-Dacal, M., Berlanga, D. J., Fernández-Calvo, P.,Gómez-Rubio, E., & Martín-Santamaría, S. (2024). Plant cell wall-mediated disease resistance: Current understanding and future perspectives. *Molecular Plant*.

the plant journal

SEB SOCIETY FOR EXPERIMENTAL BIOLOGY

The Plant Journal (2023) **113,** 833–850 doi: 10.1111/tpj.16088

Arabidopsis immune responses triggered by cellulose- and mixed-linked glucan-derived oligosaccharides require a group of leucine-rich repeat malectin receptor kinases

Marina Martín-Dacal[1,2,†], Patricia Fernández-Calvo[1,2,*,†], Pedro Jiménez-Sandoval[3], Gemma López[1], María Garrido-Arandía[1,2], Diego Rebaque[1,2,‡], Irene del Hierro[1], Diego José Berlanga[1,2], Miguel Ángel Torres[1,2], Varun Kumar[1], Hugo Mélida[1,§], Luis F. Pacios[1,2], Julia Santiago[3] and Antonio Molina[1,2,*]

[1]*Centro de Biotecnología y Genómica de Plantas, Universidad Politécnica de Madrid (UPM) – Instituto Nacional de Investigación y Tecnología Agraria y Alimentaria (INIA/CSIC), Campus de Montegancedo UPM, 28223, Pozuelo de Alarcón, Spain,*

[2]*Departamento de Biotecnología-Biología Vegetal, Escuela Técnica Superior de Ingeniería Agronómica, Alimentaría y de Biosistemas, UPM, 28040, Madrid, Spain,*

[3]*University of Lausanne (UNIL), Biophore Building, Département de Biologie Moléculaire Végétale (DBMV), UNIL Sorge, CH-1015, Lausanne, Switzerland*

Received 28 October 2022; revised 15 December 2022; accepted 21 December 2022; published online 29 December 2022.

*For correspondence (e-mail patricia.fernandez.calvo@upm.es; antonio.molina@upm.es).

†These authors contributed equally to this work.

‡Present address: Division of Glycoscience, School of Biotechnology, Royal Institute of Technology (KTH), Stockholm, Sweden

§Present address: Área de Fisiología Vegetal, Departamento de Ingeniería y Ciencias Agrarias, Universidad de León, León, Spain

SUMMARY

The plant immune system perceives a diversity of carbohydrate ligands from plant and microbial cell walls through the extracellular ectodomains (ECDs) of pattern recognition receptors (PRRs), which activate pattern-triggered immunity (PTI). Among these ligands are oligosaccharides derived from mixed-linked β-1,3/β-1,4-glucans (MLGs; e.g. β-1,4-D-$(Glc)_2$-β-1,3-D-Glc, MLG43) and cellulose (e.g. β-1,4-D-$(Glc)_3$, CEL3). The mechanisms behind carbohydrate perception in plants are poorly characterized except for fungal chitin oligosaccharides (e.g. β-1,4-D-$(GlcNAc)_6$, CHI6), which involve several receptor kinase proteins (RKs) with LysM-ECDs. Here, we describe the isolation and characterization of *Arabidopsis thaliana* mutants impaired in glycan perception (*igp*) that are defective in PTI activation mediated by MLG43 and CEL3, but not by CHI6. *igp1*–*igp4* are altered in three RKs – AT1G56145 (IGP1), AT1G56130 (IGP2/IGP3) and AT1G56140 (IGP4) – with leucine-rich-repeat (LRR) and malectin (MAL) domains in their ECDs. *igp1* harbors point mutation E906K and *igp2* and *igp3* harbor point mutation G773E in their kinase domains, whereas *igp4* is a T-DNA insertional loss-of-function mutant. Notably, isothermal titration calorimetry (ITC) assays with purified ECD-RKs of IGP1 and IGP3 showed that IGP1 binds with high affinity to CEL3 (with dissociation constant K_D = 1.19 ± 0.03 μM) and cellopentaose (K_D = 1.40 ± 0.01 μM), but not to MLG43, supporting its function as a plant PRR for cellulose-derived oligosaccharides. Our data suggest that these LRR-MAL RKs are components of a recognition mechanism for both cellulose- and MLG-derived oligosaccharide perception and downstream PTI activation in Arabidopsis.

Keywords: *Arabidopsis thaliana*, cellulose, mixed-linked glucans (MLGs), immunity, oligosaccharides, pattern recognition receptors (PRRs), leucine-reach repeat/Malectin receptor kinase (LRR-MAL RK).

INTRODUCTION

Plants have evolved a complex immune system that comprises several defense layers and mechanisms for the recognition of pathogens and pests that cooperatively interact to restrict plant infection. One of these layers, known as pattern-triggered immunity (PTI), is based on the recognition of damage- and microbe-associated molecular patterns (DAMPs and MAMPs) derived from plants or microorganisms, respectively, by plasma membrane-resident pattern recognition receptors (PRRs) (Ngou et al., 2022). Upon DAMP/MAMP recognition by ectodomains (ECDs) of PRRs, additional proteins are recruited to form ligand–PRR complexes, triggering the activation of PRR cytoplasmic protein kinase domains (KDs) that initiate phosphorylation and signaling cascades (Boutrot &

Zipfel, 2017; Ngou et al., 2022). Early PTI responses include increases in the cytoplasmic concentration of the second messenger, Ca^{2+}, the production of reactive oxygen species (ROS) by NADPH oxidases (e.g. respiratory burst oxidase homolog protein D, RBOHD), the phosphorylation of mitogen-activated protein kinases (MAPKs) and Ca^{2+}-dependent protein kinases (CPKs), and transcriptional reprogramming that ultimately restrict the colonization of the plant by pathogens or pests (Bigeard et al., 2015; Boutrot & Zipfel, 2017). DAMPs or MAMPs are molecules with different biochemical composition, such as peptides, carbohydrates (oligosaccharides) or fatty acids, among other molecules (Bigeard et al., 2015; Boutrot & Zipfel, 2017; Ngou et al., 2022).

Many PRR/peptidic DAMP/MAMP pairs triggering PTI responses have been elucidated, like AtPep1 DAMP and bacterial flg22 MAMP peptides, which are directly bound by Arabidopsis PEPR1/2 and FLS2 PRRs, respectively (Bigeard et al., 2015; Boutrot & Zipfel, 2017; Tang & Wang, 2017). These PRRs require members of the SOMATIC EMBRYOGENESIS RECEPTOR KINASE (SERK) family, like BAK1, for active complex formation and downstream PTI activation (Bigeard et al., 2015; Boutrot & Zipfel, 2017; Tang & Wang, 2017). FLS2 and PEPR1/2 are receptor kinase (RK) proteins with an ECD harboring leucine-rich repeats (LRRs), a transmembrane domain (TM) and a cytoplasmic serine/threonine KD. Plant PRRs with LRR-ECDs comprise about 50% of RKs (Bellande et al., 2017; del Hierro et al., 2021). The *Arabidopsis thaliana* genome has more than 600 genes encoding members of RKs, receptor-like proteins (RLPs, with ECD and TM but lacking the KD) and receptor proteins (RPs, with ECD but lacking TM), which in some cases are clustered in the same plant genomic region, illustrating their recent evolutionary divergence (del Hierro et al., 2021; Franck et al., 2018; Ngou et al., 2022).

In contrast to the extended knowledge of peptidic DAMP and MAMP perception, our understanding of plant immunity activation by carbohydrate-based DAMPs and MAMPs is scarce. However, carbohydrates are highly abundant molecules in plant and microbial extracellular layers, such as cell walls, and several of them are known to be perceived by the plant immune system and to trigger PTI: oligosaccharides from chitin, e.g. chitohexaose (β-1,4-D-*N*-acetylglucosamine)$_6$ (CHI6), and β-1,3-glucan of fungal/oomycete cell walls, peptidoglycan from bacterial walls, and oligosaccharides derived from plant cell wall polymers, such as cellulose (β-1,4-glucan), mixed-linked glucans (MLGs; β-1,4/β-1,3-glucans), xyloglucan, mannan, xylan and homogalacturonan/pectins (oligogalacturonides or OGs), and from other glycans, such as fructans (Aziz et al., 2007; Claverie et al., 2018; Denoux et al., 2008; Gust et al., 2007; Kaku et al., 2006; Klarzynski et al., 2000; Mélida et al., 2018; Mélida et al., 2020; Versluys et al., 2022; Voxeur et al., 2019; Wanke et al., 2020; Zang et al., 2019). Remarkably, about 50% of RK/RLP/RP from plant genomes have ECDs that are predicted to bind carbohydrate-based ligands and are grouped in different families: lysin motif (LysM), lectins (G-, L- and C-lectins), crinkly-like (CR4L), wall-associated kinases (WAKs), cysteine-rich kinases (CRK/DUF26) and families with malectin (MAL) or malectin-like domains (MLDs) in their ECDs (LRR-MAL, MLD-LRRs and *Catharanthus roseus* receptor-like kinases 1-like, CrRLK1Ls) (Bacete et al., 2018; Bellande et al., 2017; del Hierro et al., 2021). Therefore, oligosaccharide–PRR pairs are expected to play a role in immune activation by carbohydrates in plants (Cosgrove, 2022; Wan et al., 2021).

Cellulose, a linear polymer of β-1,4-glucosyl residues, is present in all plants, most algae, some protists and microbial (bacteria and oomycete) extracellular matrixes or walls, being the most abundant biomolecule on earth (Burton & Fincher, 2009; Kloareg et al., 2021; Morgan et al., 2013). MLGs, consisting of unbranched and unsubstituted chains of β-1,4-glucosyl residues interspersed by β-1,3-linkages, are widely distributed as matrix polysaccharides in the cell walls of plants from the Poaceae family (cereals), but have also been reported in *Equisetum* spp. and other vascular plants (Fry et al., 2008; Sørensen et al., 2008), bryophytes and algae (Popper & Fry, 2003; Salmeán et al., 2017), bacteria (Pérez-Mendoza et al., 2015), and fungi and oomycetes (Fontaine et al., 2000; Pettolino et al., 2009; Rebaque et al., 2021). MLG-derived oligosaccharides, e.g. MLG43 (β-1,4-D-(Glc)$_2$-β-1,3-D-Glc), MLG443 (β-1,4-D-(Glc)$_3$-β-1,3-D-Glc) and MLG34 (β-1,3-D-Glc-β-1,4-D-Glc$_2$), are perceived with different degrees of specificity by the immune system of several plant species, e.g. Arabidopsis, *Capsicum annuum* (pepper), *Hordeum vulgare* (barley), *Oryza sativa* (rice), and *Solanum lycopersicum* (tomato), with MLG43-mediated PTI responses being the best characterized (Barghahn et al., 2021; Rebaque et al., 2021; Yang, Liu, et al., 2021a; Yang, Liu, et al., 2021b). Similarly, cellulose-derived oligosaccharides, e.g. β-1,4-D-(Glc)$_2$ to β-1,4-D-(Glc)$_6$ (cellobiose to cellohexaose or CEL2–CEL6), trigger PTI responses in Arabidopsis, rice and other plant species (Klarzynski et al., 2000; Locci et al., 2019; Rebaque et al., 2021; Souza et al., 2017; Yang, Liu, et al., 2021a; Yang, Liu, et al., 2021b). MLG- and CEL-derived oligosaccharides are self-alert signals (DAMPs) of plant colonization by pathogens, as they can be released from plant cell walls by the activity of microbial endoglucanases, such as cellulases, secreted during plant colonization (Gámez-Arjona et al., 2022; Yang, Liu, et al., 2021b). MLGs can also be perceived as MAMPs by plant species that do not contain them in their cell walls (Barghahn et al., 2021; Rebaque et al., 2021).

The mechanisms of oligosaccharide perception by the mammal immune system through carbohydrate

recognition domains are well documented (Bacete et al., 2018; Cummings et al., 2022; Taylor et al., 2022). In contrast, our understanding of the structural basis of oligosaccharide perception by plant PRRs is limited and mainly restricted to PRRs of the LysM family, e.g. CHITIN ELICITOR RECEPTOR KINASE 1 (CERK1) and LysM motif receptor kinases 4 and 5 (LYK4 and LYK5). Such proteins harbor promiscuous ECDs involved in the activation of PTI mediated by structural diverse ligands, such as CHI6–CHI8, β-1,3-glucan (laminarihexaose, LAM6) and MLGs (MLG43, MLG34 and MLG443) (Cao et al., 2014; Desaki et al., 2018; Liu et al., 2012; Mélida et al., 2018; Miya et al., 2007; Rebaque et al., 2021; Wanke et al., 2020; Willmann et al., 2011; Yang, Liu, et al., 2021b). Immune responses triggered by CHI6, LAM6 and MLG43 are partially impaired in *cerk1* single and *lyk4 lyk5* double mutants (Cao et al., 2014; Liu et al., 2012; Mélida et al., 2018; Rebaque et al., 2021; Shimizu et al., 2010; Yang et al., 2022). However, a direct binding of LAM6 and MLG43 to the *A. thaliana* CERK1 ECD was discarded based on *in silico* structural molecular dynamics simulations and isothermal titration calorimetry (ITC) binding assays (del Hierro et al., 2021). These data suggest that CERK1, LYK4 and LYK5 might function as protein partners in the LAM6 perception system. Notably, rice OsCERK1 seems to be the PPR binding MLG43 and MLG443, whereas OsCeBIP, the rice chitin PRR, is required for the perception of these ligands, but not for their direct binding (Yang, Liu, et al., 2021b). In addition to LysM-PRRs, Arabidopsis WAK receptors (e.g. WAK1 and WAK2) are PRRs required for the perception of OGs, and the CrRLK1L member FERONIA (FER), with two malectin-like domains in its ECD, binds homogalacturonans (Brutus et al., 2010; Tang et al., 2022). Recently, two LRR-RKs have been implicated in PTI activation triggered by CEL-derived oligosaccharides in Arabidopsis (Zarattini et al., 2021), and the CELLO-OLIGOMER RECEPTOR KINASE 1 (CORK1, an LRR-MAL RK) has been described to be required for CEL3 perception and PTI activation in Arabidopsis (Tseng et al., 2022). However, the structural bases of CEL-derived oligosaccharide recognition by these putative PRRs have not yet been elucidated.

We designed genetic screenings in Arabidopsis to identify mutants impaired in glycan (e.g. MLGs) perception (*igp*). We selected several mutants (*igp1*–*igp9*) that are impaired in the perception of both MLG43 and CEL3, but not CHI6. Here we show that *IGP1*, *IGP2/IGP3* and *IGP4* encode three RK members (AT1G56145/CORK1, AT1G56130 and AT1G56140, respectively) with LRR-MAL in their ECDs. We also demonstrate that the ECD of IGP1, previously described as CORK1 (Tseng et al., 2022), binds directly to CEL3 and CEL5 with high affinity, further supporting its function as a plant PRR involved in the perception of cellulose-derived oligosaccharides. These results expand our knowledge of the mechanisms of immune activation by oligosaccharides in plants.

RESULTS

Identification and isolation of Arabidopsis *igp1*–*igp9* mutants

We generated an ethyl methanesulfonate (EMS) mutagenized population of the *A. thaliana* aequorin-based Ca^{2+} sensor line Col-0^{AEQ} (Knight et al., 1991; Mélida et al., 2018; Ranf et al., 2011) to perform a genetic screening aiming to isolate mutants impaired in glycan perception (*igp*; Figure S1). First, we performed a genetic screening to identify *igp* mutants impaired in MLG perception, and we selected for the screening MLG43 trisaccharide as its PTI-mediated responses in Arabidopsis are the best characterized (Barghahn et al., 2021; Rebaque et al., 2021; Yang, Liu, et al., 2021a; Yang, Liu, et al., 2021b). Eight-day-old seedlings (about 6400 individuals) of 13 M_2 EMS-mutagenized Col-0^{AEQ} families were grown in microtiter plates together with the Col-0^{AEQ} control line, treated with 100 μM MLG43, and changes of cytoplasmic Ca^{2+} concentration were then determined in a luminometer (Figure S1). Several mutants (*igp1*^{AEQ}–*igp9*^{AEQ}) that showed a weaker Ca^{2+} burst than that of Col-0^{AEQ} plants were selected for further genetic characterization (backcrosses and allelism tests; Figures 1a and S2; Table S1). To assess the specificity of MLG43 perception impairment in *igp* mutants we also treated *igp* lines with CHI6 (50 μM) and found that it triggered similar Ca^{2+} bursts in the *igp* mutants as those observed in Col-0^{AEQ} plants, whereas *cerk1*^{AEQ} plants were fully impaired in CHI6 perception, as previously reported (Figures 1b and S2; Mélida et al., 2018; Rebaque et al., 2021). These data suggest that the mechanism of perception of CHI6 and MLG43 in Arabidopsis might not be identical, in contrast to what has been described in rice (Yang et al., 2022). No mutations were found in the *Aequorin* gene sequence in *igp1*^{AEQ}–*igp3*^{AEQ} (Online data set), and no differences were observed in endogenous Ca^{2+} levels between the *igp1*^{AEQ}–*igp3*^{AEQ} and Col-0^{AEQ} seedlings, based on Ca^{2+} discharge analyses (Figure S1). These data support that the lower Ca^{2+} bursts observed in MLG43-treated *igp1*^{AEQ}–*igp3*^{AEQ} seedlings were the result of the defective perception of MLG43.

igp1^{AEQ}, *igp2*^{AEQ} and *igp3*^{AEQ} mutants harbor recessive mutations (chi-square test, $0.7 > P > 0.5$, $0.5 > P > 0.3$ and $0.8 > P > 0.7$, respectively; Table S2), and *igp2*^{AEQ} and *igp3*^{AEQ} were allelic (chi-square test, $P > 0.95$; Figure S1; Table S1). Genomic DNA from F_2 progeny of *igp1*^{AEQ}, *igp2*^{AEQ} and *igp3*^{AEQ} backcrosses with Col-0^{AEQ} was sequenced and assembled to identify putative mutations (frequency higher than 0.99 in alignments; Table S2). We found that *igp1*^{AEQ} has a point mutation in the *AT1G56145* gene, encoding an RK with

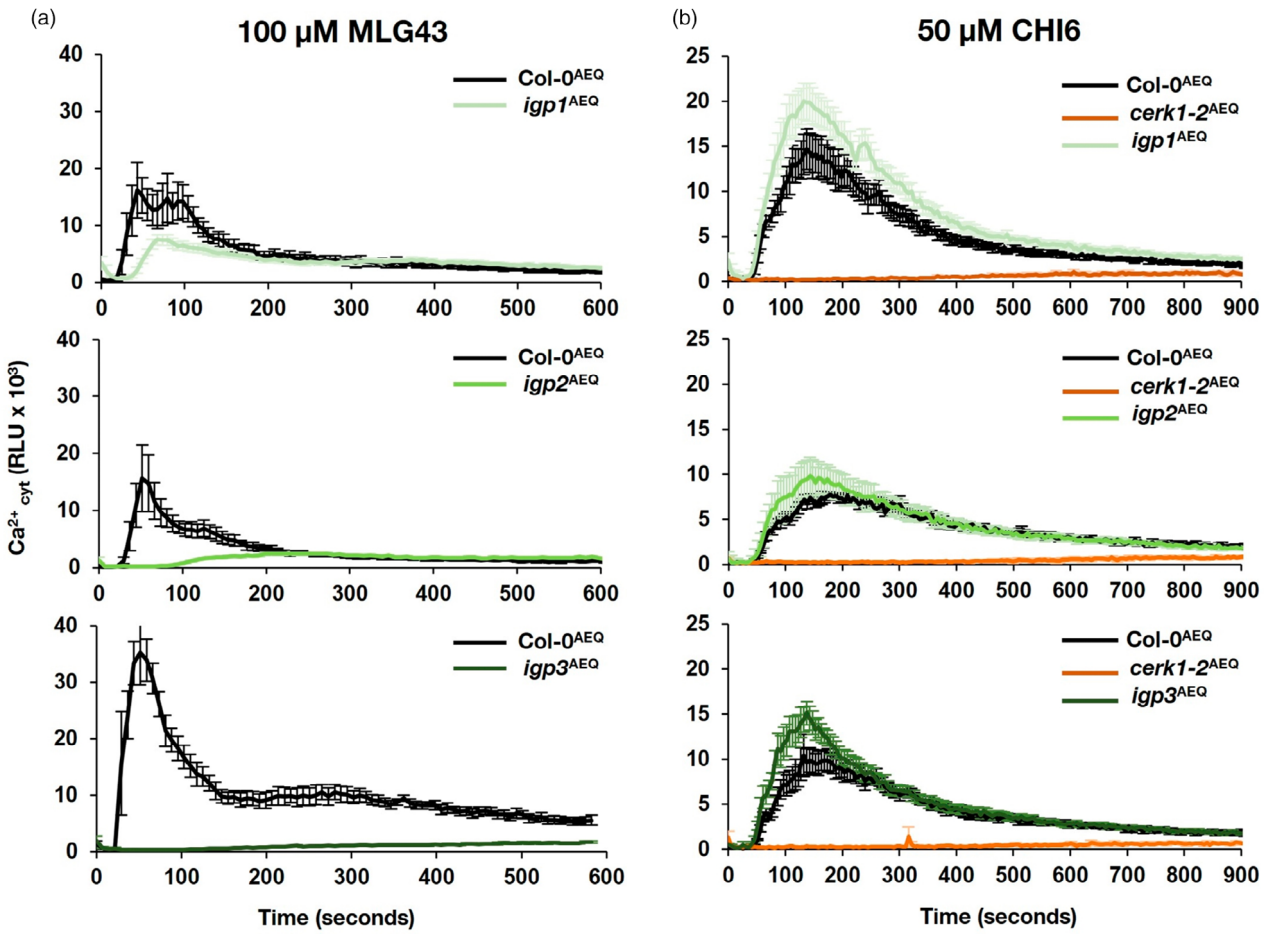

Figure 1. Identification of *Arabidopsis thaliana* mutants impaired in glycan perception (*igp*).
Ca^{2+} burst upon application of (a) 100 µM MLG43 and (b) 50 µM CHI6 was measured as relative luminescence units (RLUs) over time in Col-0^{AEQ} and *igp*^{AEQ} mutants. The *cerk1-2*^{AEQ} line, impaired in CHI6 perception, was included for comparison. Data represent the mean ± standard error ($n = 4$ in Col-0^{AEQ} and *cerk1-2*^{AEQ}; $n = 8$ in *igp*^{AEQ}). Data are from one of the four experiments performed that gave similar results.

an LRR-MAL ECD, which resulted in E906K amino acid change in its KD (Figure 2a). On the other hand, *igp2*^{AEQ} and *igp3*^{AEQ} share the same point mutation in the *AT1G56130* gene, encoding an additional LRR-MAL RK, which resulted in G773E amino acid change in its KD (Figure 2a). Notably, these two LRR-MAL RKs are in a genomic cluster with two additional genes, *AT1G56120* and *AT1G56140*, which encode two additional LRR-MAL RKs (Yang, Wang, et al., 2021). These RKs are members of a specific group of LRR-MAL proteins that comprise at least 13 genes in the *A. thaliana* genome, with *AT1G56120*, *AT1G56130*, *AT1G56140* and *AT1G56145* genes constituting a specific clade of the family (Figure S3; del Hierro et al., 2021). This family has a few characterized members, such as *RFK1* (*AT1G29720*), that promote compatible pollen grain hydration and pollen tube growth (Lee & Goring, 2021), the recently described IGP1/CORK1 protein (Tseng, et al., 2022), and the so-called BRASSINOSTEROID (BR) KINASE (BSK) 3-INTERACTING RLK (BSR) members, which are not well characterized (Yang, Wang, et al., 2021).

Using reverse transcription quantitative real-time polymerase chain reaction (RT-qPCR), we determined that the expression of *AT1G56140*, but not that of *AT1G56120*, *AT1G56130* and *AT1G56145*, was upregulated upon treatment of seedlings with MLG43, CHI6 and other glucans (e.g. CEL3; Figure S3). We then selected T-DNA insertional mutants of *AT1G56120* and *AT1G56140* genes and tested their perception of MLG43 and CHI6 by determining the upregulation of PTI marker genes *WRKY53* and *CYP81F2* using RT-qPCR (Mélida et al., 2018, Rebaque et al., 2021; Figure S3). The expression of these genes was compromised in the *at1g56140* knockout mutant, whereas the expression in the *at1g56120* mutant was very similar to that of Col-0 (Figure S3). Both mutants displayed a similar upregulation of *WRKY53* and *CYP81F2* expression to that of wild-type plants upon CHI6 treatment (Figure S3). To further validate the phenotype of the *at1g56140* mutant,

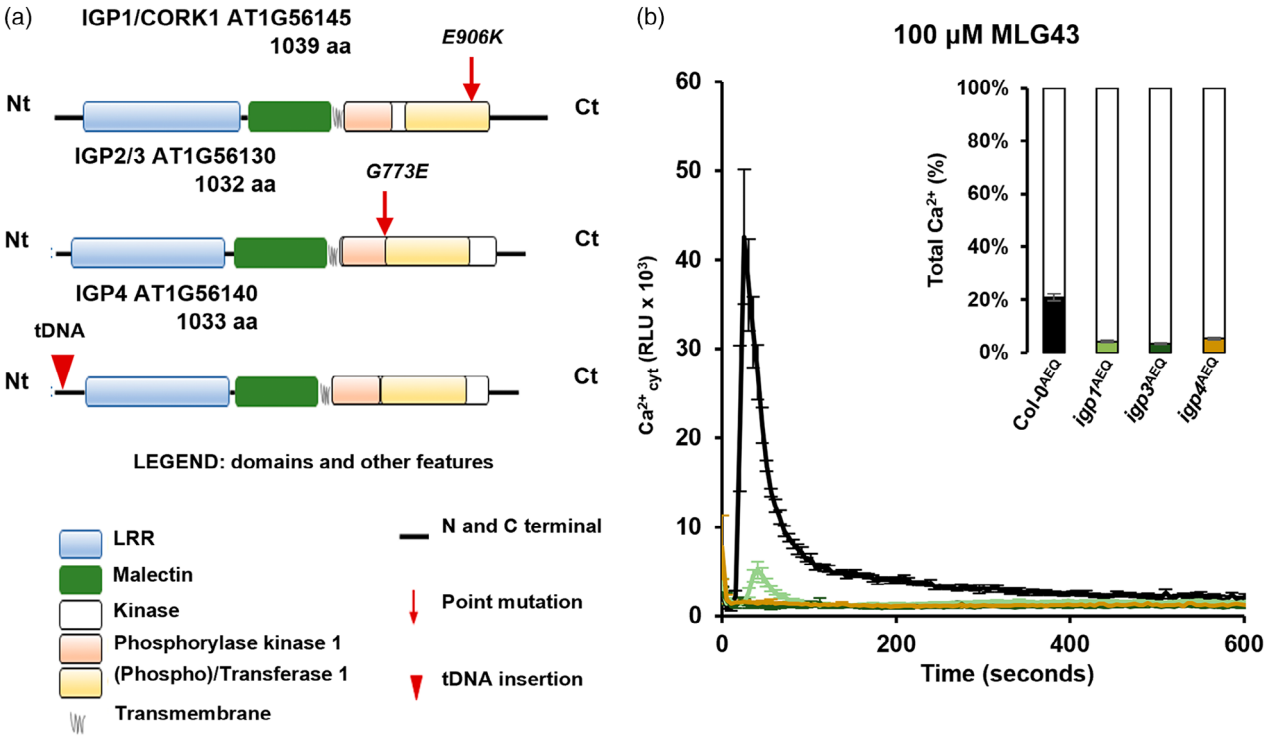

Figure 2. Identification of mutations in *igp1–igp4* mutants.
(a) Representation of IGP1, IGP2/3 and IGP4 domains: leucine-rich repeat (LRR; blue), malectin (MAL; green), phosphorylase kinase (orange) and phophotransferase (yellow) of kinase domain (KD; white), N- and C-terminal domains (black lines) and transmembrane domain (TM; gray). Red arrows indicate the position of the mutations in the coding regions of *igp1*^{AEQ}, *igp2*^{AEQ} and *igp3*^{AEQ}, and the red triangle indicates the insertion of the T-DNA sequence in *igp4* (Online data set). (b) Ca^{2+} burst measured as relative luminescence units (RLUs) over time in Col-0^{AEQ}, *igp1*^{AEQ}, *igp3*^{AEQ} and *igp4/at1g56140*^{AEQ} seedlings upon treatment with 100 µM MLG43. Data represent the mean ± standard error ($n = 4$ in Col-0^{AEQ} and $n = 8$ in *igp*^{AEQ}). Total Ca^{2+} was discharged by the addition of 1 mM $CaCl_2$ to the wells and these values were used for the calculation of the total Ca^{2+} % induced by MLG43 treatment (graph at top right). This is one of three experiments performed that gave similar results.

we crossed this line with Col-0^{AEQ} and the homozygous *at1g56140*^{AEQ} line generated was tested for Ca^{2+} burst upon MLG43 and CHI6 treatment. *at1g56140*^{AEQ} was impaired in MLG43 but not CHI6 perception, like *igp1*^{AEQ}–*igp3*^{AEQ}, and this defective response was not caused by any alteration in the endogenous levels of Ca^{2+}, as revealed by Ca^{2+} discharge experiments. Accordingly, the *at1g56140* mutant was named *igp4* and selected for further analyses to determine the contribution of AT1G56140/IGP4 RK in the regulation of PTI responses mediated by MLG- and CEL-derived oligosaccharides (Figure 2b). We assessed the impact of the *igp1–igp4* mutations on plant developmental phenotypes and no significant differences were observed in the rosette and silique size and morphology of *igp1*^{AEQ} and *igp4*^{AEQ} plants in comparison with Col-0^{AEQ} or *cerk1-2*^{AEQ}, whereas *igp2*^{AEQ}/*igp3*^{AEQ} plants have rosettes and siliques slightly smaller than those of Col-0 plants or *cerk1-2*^{AEQ} (Figure S4). As the last two mutants are allelic, we stuck to *igp3*^{AEQ} to characterize its function across this article. Accordingly, we will refer to *IGP3* and IGP3, when discussing the gene and the encoded protein, respectively, affected in this mutant.

LRR-MAL RKs are also required for the perception of additional cellulose- and MLG-derived oligosaccharides

To assess the specificity of MAMPs and DAMPs that activate the Ca^{2+} response through these LRR-MAL RKs, we measured the Ca^{2+} bursts in *igp1*^{AEQ}, *igp3*^{AEQ}, *igp4*^{AEQ} and Col-0^{AEQ} seedlings after treatment with different DAMPs, i.e. carbohydrate ligands such as CEL3 and OGs (DP10–DP12) and the peptide AtPep1, and the MAMP flg22. Remarkably, the three *igp*^{AEQ} lines were almost fully impaired in CEL3-mediated Ca^{2+} burst activation, suggesting that these RKs are also required for the perception of cellulose-derived oligosaccharides (Figure 3a,b). In contrast, the Ca^{2+} responses induced by flg22, OGs and AtPep1 treatments in the mutants were similar to those observed in Col-0^{AEQ} (Figure 3c–e). The response of *igp5*^{AEQ}–*igp9*^{AEQ} mutants to CEL3 was also impaired (Figure S5), further supporting the hypothesis that the mechanisms of perception of MLG43 and CEL3 in Arabidopsis share some components. As additional cellulose- and MLG-derived oligosaccharides, such as cellobiose (CEL2), cellotetraose (CEL4), cellopentaose (CEL5) and MLG34, trigger PTI in Arabidopsis (Locci

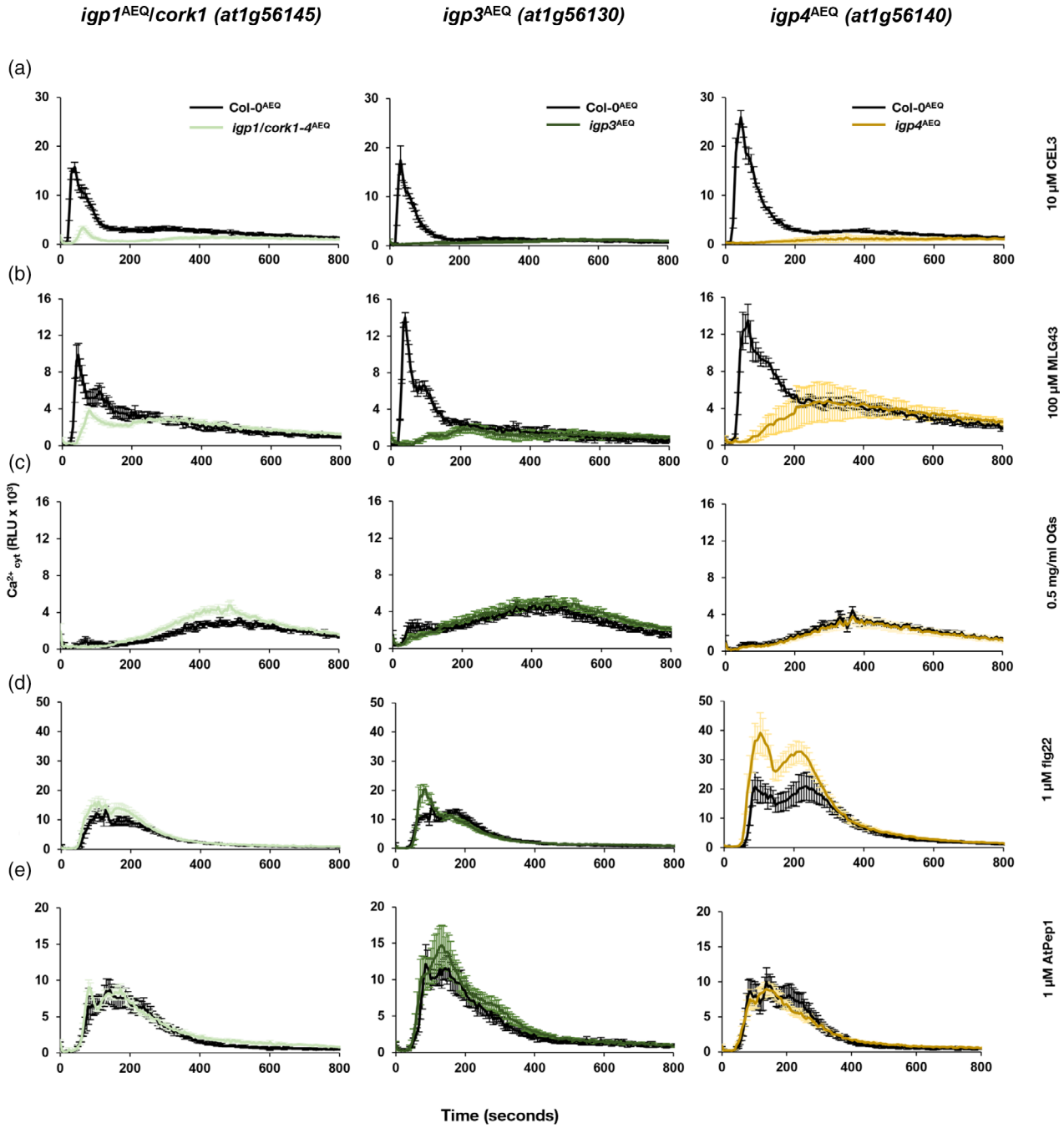

Figure 3. Cytoplasmic calcium burst triggered by CEL3 is impaired in *igp*^{AEQ} mutants.
Ca^{2+} burst measured as relative luminescence units (RLUs) over time in Col-0^{AEQ}, *igp1*^{AEQ}, *igp3*^{AEQ} and *igp4*^{AEQ} seedlings after treatment with: (a) 10 µM CEL3; (b) 100 µM MLG43; (c) 0.5 mg mL^{-1} OGs; (d) 1 µM flg22; and (e) 1 µM AtPep1. Data represent the mean ± standard error (n = 4 in Col-0^{AEQ} and n = 8 in *igp*^{AEQ}). Data are from one of three experiments performed that gave similar results.

et al., 2019; Rebaque et al., 2021; Souza et al., 2017), we also determined the Ca^{2+} burst activated by these glycans in *igp*^{AEQ} mutants and Col-0^{AEQ}. The three mutants showed reduced Ca^{2+} influxes in comparison with Col-0^{AEQ} upon treatment with MLG34, CEL4 and CEL5 (Figure 4b,d,e), indicating that the three LRR-MAL RKs are required for the perception of these cellulose- and MLG-derived oligosaccharides. By contrast, the Ca^{2+} influxes triggered by CEL2 were, under our experimental conditions, very low, even in Col-0^{AEQ} (Figure 4f), suggesting that this disaccharide has low immunogenic activity in Arabidopsis, and that CEL3 is the cellulose-derived oligosaccharide with the lowest degree of poyimerization (DP) perceived through the sensing mechanism involving these RKs (Figure 4c).

To further validate whether the mechanism of perception of cellulose- and MLG-derived oligosaccharides in Arabidopsis share some PRRs and signaling components, we performed cross-elicitation experiments by treating 8-day-old Col-0^{AEQ} seedlings, first with MLG43 or CEL3, and a few minutes later with either CEL3 or MLG43. In Col-0^{AEQ} seedlings first treated with MLG43, Ca^{2+} influxes were not observed upon the second application of CEL3 (MLG43 + CEL3), similarly to what was observed after treatments with CEL3 + CEL3 and MLG43 + MLG43 (Figure S6), indicating that the mechanisms of perception of MLG43 and CEL3 share molecular components in Arabidopsis.

To confirm the role of this group of LRR-MAL receptors as potential RKs for cellulose- and MLG-derived oligosaccharide perception and PTI activation, we first monitored ROS production in *igp1*^{AEQ}, *igp3*^{AEQ}, *igp4*, Col-0 and *rbohD* lines, impaired in DAMP/MAMP-triggered ROS production (Morales et al., 2016), upon treatment with MLG43, CEL3 and CHI6. The ROS burst was partially impaired in the *igp* mutants compared with the Col-0 plants after treatment with MLG43, and was significantly reduced, even to a higher extent, after CEL3 treatment (Figure 5a,b). In both cases, the reduction in ROS was not as noticeable as in *rbohD*. Notably, the ROS burst in *igp* mutants upon treatment with CHI6 and flg22 was not altered in comparison with Col-0 plants (Figure S7), as observed for the Ca^{2+} burst (Figure 3). Next, we tested the phosphorylation of MAP kinases by Western blot. MPK3 and MPK6 phosphorylation triggered by MLG43 and CEL3 was reduced in *igp1*^{AEQ}, *igp3*^{AEQ} and *igp4* plants, compared with Col-0 plants, whereas it responded similarly to Col-0 in response to CHI6 (Figure 5c). MPK4/11 phosphorylation was almost undetectable in either CEL3-treated or MLG43-treated plants, as reported previously (Rebaque et al., 2021). Last, we performed RT-qPCR analysis to study the expression of two PTI-marker genes upregulated by CHI6 and MLG43 (*WRKY53* and *CYP81F2*; Mélida et al., 2018, Rebaque et al., 2021). The upregulation of *WRKY53* and *CYP81F2* in response to MLG43 and CEL3 was partially impaired in *igp1*^{AEQ}, *igp3*^{AEQ} and *igp4* seedlings, compared with Col-0 plants, whereas it was similar in response to CHI6 (Figure 5d,e). Together, these data support the role of the three LRR-MAL RKs in the perception of cellulose-derived oligosaccharides and, to a lesser extent, in the perception of MLG-derived oligosaccharides.

As previous works reported that MLG perception in Arabidopsis and rice involved LysM-PRRs (e.g. CERK1, LYK4 and LYK5 in Arabidopsis; Rebaque et al., 2021, Yang, Liu, et al., 2021a), we determined ROS production, MPK3/MPK6 phosphorylation and PTI marker upregulation upon treatment with MLG43 or CEL3 in seedlings of Col-0, *cerk1-2* and the *cerk1-2 lyk4 lyk5* triple mutant, which was generated in this work (Figure S8). *cerk1-2* and *cerk1-2 lyk4 lyk5* plants displayed similar ROS kinetics and bursts to those of Col-0 after CEL3 treatment, and only a minor diminution upon MLG43 treatment in comparison to Col-0, whereas this PTI response was greatly impaired after CHI6 treatment (Figure S8). Moreover, a slight reduction of the phosphorylation of MPK3/MPK6 in these mutants, compared with Col-0, was observed upon MLG43 and CEL3 treatment, although it was weaker than that observed with CHI6 (Figure S8). Also, the MLG43-mediated upregulation of *WRKY53* and *CYP81F2* was only partially affected in *cerk1-2* and *cerk1-2 lyk4 lyk5* plants, whereas it was not altered upon CEL3 treatment (Figure S8). These data indicate that MLG43 perception may involve CERK1, LYK4 and LYK5 LysM RKs, as described previously for MLGs in Arabidopsis and rice (Rebaque et al., 2021; Yang, Liu, et al., 2021b), whereas these RKs have almost no contribution to CEL3 perception.

Model structures of IGP1, IGP3 and IPG4 proteins point to their function as RKs

Malectin (MAL) domains like those present in the ECDs of the LRR-MAL RK family have been previously described in animals to bind short glycans, based on the NMR structure of MAL from *Xenopus laevis* in complexes with maltose and nigerose (Schallus et al., 2010). The MAL domain and MLD are present in at least three families of plant RKs (LRR-MAL, MLD-LRRs and CrRLK1Ls; Yang, Wang, et al., 2021), and the ECDs of several CrRLK1L members, e.g. ANXUR1 (ANX1), ANX2 and FERONIA (FER), have been crystallized, but no oligosaccharide ligands were identified in ITC binding experiments (Moussu et al., 2018; Xiao et al., 2019). Phylogenetic analyses of MAL domains of *A. thaliana* LRR-MAL RK members (represented by IGP1/CORK1 and AT1G56145) revealed that the MAL domain is highly conserved in cruciferous and other dicot species (Figure S9; Yang, Wang, et al., 2021). On the other hand, the MAL domain of IGP1/CORK1, IGP3 and IGP4 are evolutionarily divergent from ANX1 and ANX2 and *Xenopus* sp. MLD domains (Figure S9; Yang, Wang, et al., 2021).

The model structures of IGP1/CORK1, IGP3 and IGP4 in the AlphaFold database display a spatial arrangement of all domains that does not properly describe the expected organization of these LRR-MAL RKs (Figure S10). Therefore, to explore the impact of *igp1* and *igp2*/*igp3* point mutations in the KD of these RKs, we first obtained models with the correct domain organization, as described in the Experimental procedures. These models provide a complete picture of the proteins to be used as initial geometries for further computational studies (Figure S11). We then used TM-ALIGN (Zhang & Skolnick, 2005) to evaluate the structural similarity of MAL domains from IGP1/CORK1, IGP3 and IGP4 with several entries in the Protein Data Bank (PDB, https://www.rcsb.org) with MAL and MLD domains (five plant RKs from CrRLK1Ls and nine human and

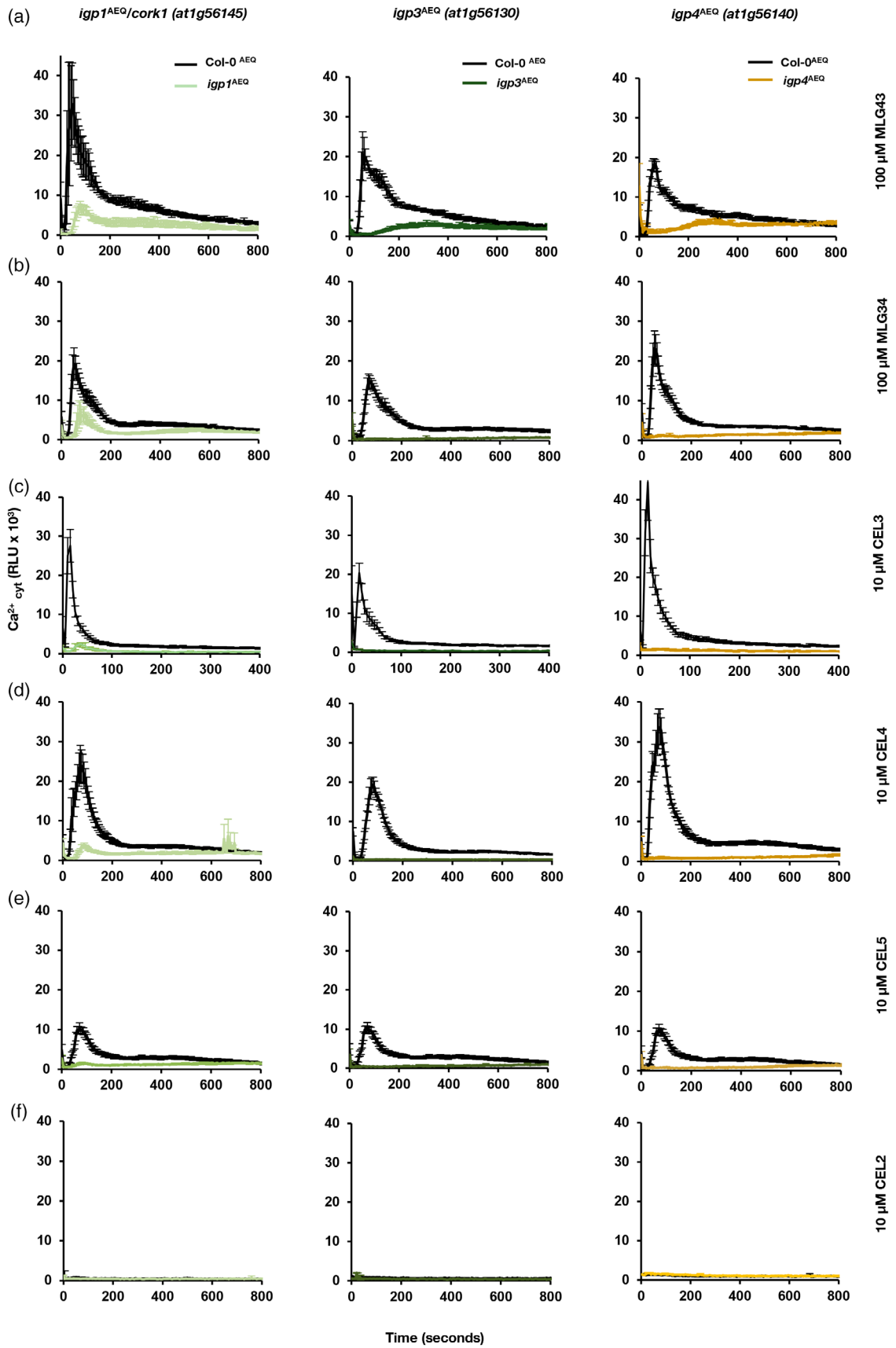

Figure 4. Calcium burst in response to MLG34- and cellulose-derived oligosaccharides is impaired in *igp* mutants.
Ca^{2+} burst measured as relative luminescence units (RLUs) over time in 8-day-old Col-0^{AEQ}, *igp1*^{AEQ}, *igp3*^{AEQ} and *igp4*^{AEQ} seedlings after treatment with: (a) 100 μM MLG43; (b) 100 μM MLG34; (c) 10 μM CEL3; (d) 10 μM CEL4; (e) 10 μM CEL5; and (f) 10 μM CEL2. Data represent the mean ± standard error ($n = 3$ in the case of Col-0^{AEQ} and $n = 12$ in the case of *igp*^{AEQ}). The *x*-axis scale in (c) has been shortened for a better comparison of the enhanced response of seedlings to CEL3. Data are from one of three experiments performed that gave similar results.

bacteria proteins), including the NMR structures of malectin from *Xenopus laevis* in complex with maltose (Schallus et al., 2010), an apo form and a complex with nigerose (Schallus et al., 2008), and the crystal structure of tandem MLDs from the ANX1/ANX2 ECDs (Moussu et al., 2018). In all cases, TM scores between 0.623 and 0.710 were found, thus indicating highly similar folds of IGP MAL domains to animal malectin and to plant MLD structures.

Similar structural comparison analyses were performed for the KDs of IGP1/CORK1, IGP3 and IGP4, with some kinase crystals, like MPK6 from Arabidopsis (5CI6, Wang et al., 2016; 6DTL, Putarjunan et al., 2019). The structural alignment data showed that the IGP1/CORK1 KD is noticeably different from that of the two other RKs because of the extra loop seen in the intracellular part of its complete structure (indicated by an arrow in Figure S11), which is not predictable from IGP protein sequence alignments. Notwithstanding, the conformation of side chains of catalytic residues was found to be identical in wild-type and mutant structures, a result worth emphasizing as the mutation positions are near the catalytic site in both IGP1/CORK1 and IGP3 (Figure S11). Next, we tested *in silico* the possible structural impact of the single mutations of E906K in IGP1/CORK1 and G773E in IGP2/IGP3 KDs by generating new model structures of the KD of wild-type and mutants with AlphaFold 2. We found that the backbones remained unaltered, and that E906K in IGP1 and G773E in IGP2/IGP3 had the effect of increasing the surface patch associated with the mutated position (Figure S11). However, the major effect of these single mutations was found in the surface electrostatic potential (Figure S11). The region around E906 in wild-type IGP1/CORK1 shows a weakly negative electrostatic character, whereas in the *igp1* mutant the E906 negative charge of IGP1/CORK1 is substituted for a K906 positive charge, which gives rise to a strongly positive electrostatic potential in a large area around position 906 (Figure S11). The equivalent region around G773 in wild-type IGP2/IGP3 displays a weakly positive electrostatic character, which becomes strongly negative upon the G773E mutation (Figure S11). It is noted that these electrostatic effects extend over a surface region far larger than that expected from the small, exposed surface areas of residues 906 and 773 (Figure S11). These changes in the KD domains of IGP1/CORK1 and IGP2/IGP3 LRR-MAL RKs might explain their loss of functionality. Additional mutations in the KD of IGP1/CORK1 have been proven recently to impair its kinase activity in phosphorylation experiments performed *in vitro* with CORK1 recombinant proteins (wild-type and mutant versions) expressed in *Escherichia coli* (Tseng, et al., 2022).

The ECD of IGP1/CORK1 directly binds cellulose-derived oligosaccharides CEL3 and CEL5

Based on the initial structural models of MAL domains in the three LRR-MAL RKs and their similarities with the MAL domain from *Xenopus* sp. that binds short glycans (Figure S11; Schallus et al., 2010), we tested whether ECDs of these LRR-MAL RKs could be glycan receptors for cellulose- and MLG-derived oligosaccharides. We expressed the ECDs of IGP1/CORK1, IGP3 and IGP4 in insect cells and purified them by affinity chromatography. As the ECD of IGP3 turned out to form aggregates, this ECD was not suitable for further purification steps and was not available for binding experiments (Figure S12). Then, ITC experiments (Sandoval & Santiago, 2020) were carried out to test the binding of MLG43 and CEL3 to IGP1/CORK1 and IGP4 ECDs. The ITC results proved the existence of direct interactions between CEL3 and the ECD of IGP1/CORK1 (K_D = 1.19 ± 0.03 μM; Figure 6a), but not with the ECD of IGP4 (Figure S12). However, the results obtained with ITC clearly indicated that these ECDs did not bind, at least directly, to MLG43 (Figures 6a,b and S12). Similar binding experiments were performed with CEL5 and the ECD of IGP1/CORK1 to determine the specificity of receptor–ligand recognition, and direct binding was also detected with similar high affinity (K_D = 1.40 ± 0.01 μM; Figure 6a). The binding reactions measured for CEL3 and CEL5 were exothermic, with a single binding site ($n = 1$) and very similar values of ΔH, indicating that extra sugar subunits in the CEL5 oligomer do not improve the detected binding. These data support the role of the ectodomain of IGP1/CORK1 as a receptor for cellulose-derived oligosaccharides and suggest that IGP4 RK might function as an RK required for the sensing complex for cellulose- and MLG-derived oligosaccharides.

DISCUSSION

Plant immunity is activated by a diverse set of ligands (DAMPs and MAMPs) with different biochemical composition and structure. These DAMPs and MAMPs are specifically perceived by diverse sets of ECDs from plant PRRs, triggering the formation of a ligand–PRR complex that involves additional proteins that contribute to the functionality of the recognition complex (Bigeard et al., 2015; Boutrot & Zipfel, 2017; Ngou et al., 2022). Some of the best-characterized DAMPs and MAMPs are oligoglycans from

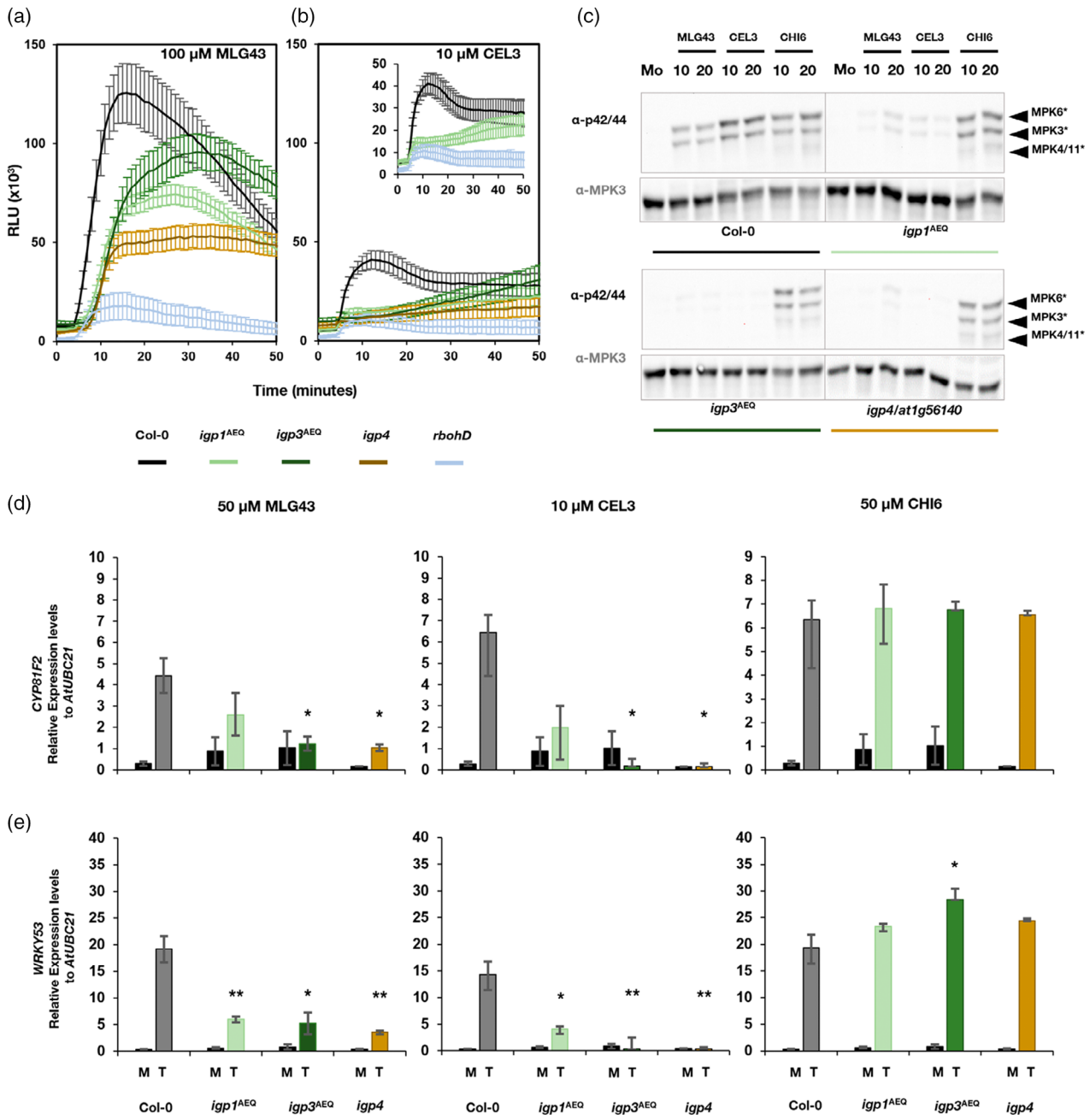

Figure 5. Activation of pattern-triggered immunity (PTI) hallmarks by MLG43, CEL3 and CHI6 in *igp*^{AEQ}.
(a, b) Reactive oxygen species (ROS) production was monitored as H_2O_2 production over a period of 50 min by luminol assays and measured as relative luminescence units (RLUs) in the indicated genotypes; 100 µM MLG43 (a) and 10 µM CEL3 (b) were added 5 min after the transfer to the luminometer of the plate with seedling and luminol reagents. Data represent mean ± standard error ($n = 8$). Comparison with Col-0 assessed by Student's *t*-test ($n = 24$) at the time of the Col-0 peak shows statistically significant differences for *igp1*^{AEQ} and *igp3*^{AEQ} ($P < 0.01$) and *igp4*^{AEQ} ($P < 0.001$) in response to MLG43. Likewise, all three mutants show statistical differences at $P < 0.001$, compared with Col-0, in response to CEL3. *rbohD* plants impaired in ROS production showed statistically significant differences ($P < 0.001$) with both treatments. These results are from one representative experiment out of three performed that gave similar results. The inset in (b) has been included in the graph to allow an easy comparison of the RLU data for *igp1*^{AEQ} and Col-0. (c) Mitogen-activated protein kinase (MAPK) phosphorylation was analyzed in seedlings of Col-0, *igp1*^{AEQ}, *igp3*^{AEQ} and *igp4*^{AEQ} treated with 100 µM MLG43, 10 µM CEL3, 50 µM CHI6 or water (mock). Western blotting using anti-pTEpY antibody (anti-p42/44) for phosphorylated MAPK moieties was performed with samples harvested at 10 and 20 min. Mock samples (Mo) corresponding to a 10-min treatment with water were included as basal expression controls. Black arrows indicate the positions of phosphorylated MPK6 (top), MPK3 (middle) and MPK4/11 (bottom). Anti-MPK3 was used as a total protein control to show the loading of each gel. These results are from one representative experiment out of two performed that gave similar results. (d, e) RT-qPCR analysis in the indicated genotypes. Expression levels of *CYP81F2* (d) and *WRKY53* (e) genes, relative to the housekeeping gene *UBC21* (*AT5G25769*) 30 min after mock treatment (M) or the application of the oligosaccharides (T) are shown. Data represent mean ± standard error of three technical replicates out of three independent biological replicates ($n = 3$). Statistically significant differences between MLG43-, CEL3- or CHI6-treated *igp*^{AEQ} versus treated Col-0 according to Student's *t*-test (*$P < 0.05$, **$0.01 < P > 0.001$, ***$P < 0.001$).

(a)

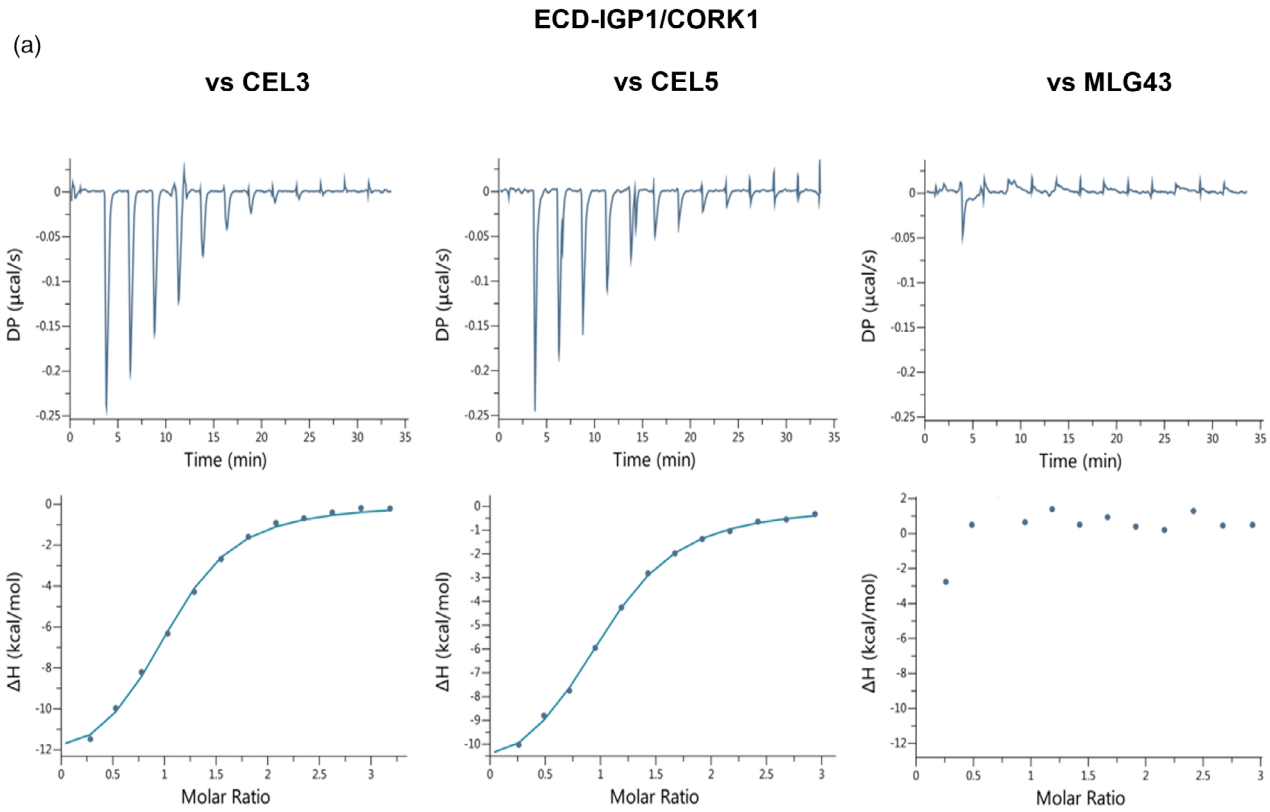

(b)

Ligand (syringe)	Protein (cell)	K_d (µM)	ΔH (kcal/mol)	N
CEL3	AT1G56145 (IGP1/CORK1)	1.19 ± 0.03	13.60 ± 0.30	1
CEL5	AT1G56145 (IGP1/CORK1)	1.40 ± 0.01	12.50 ± 0.15	1
MLG43	AT1G56145 (IGP1/CORK1)	n.d.		
CEL3	AT1G56140 (IGP4)	n.d.		
MLG43	AT1G56140 (IGP4)	n.d.		

Figure 6. The IGP1/CORK1 ectodomain (ECD) directly binds CEL3- and CEL5-derived oligosaccharides.
(a) Isothermal titration calorimetry (ITC) experiments of ECD-IGP1/CORK1 versus CEL3, MLG43 and CEL5. (b) ITC summary of ECD-IGP1 and ECD-IGP4 versus CEL3, MLG43 and CEL5. The binding affinities of ECD-IGP1/CORK1 are reported as K_D (dissociation constant, in micromoles), *DP* indicates measured power differential between the reference and sample cells to maintain a zero temperature between the cells inside the ITC device, *N* indicates the reaction stoichiometry (*N* = 1 for a 1:1 interaction) and Δ*H* indicates the enthalpy variation. Values indicated in the table are means ± SDs of independent experiments (*n* = 2). n.d., no binding detected.

fungal chitin (e.g. CHI6) or plant pectins (e.g. OGs), which are perceived by LysM-PRRs and WAK1/2/FER1-PRRs, respectively (Brutus et al., 2010; Miya et al., 2007; Tang et al., 2022). Several glycan ligands derived from cell walls or extracellular matrixes from plants or microorganisms that trigger immune responses in plants have recently been described (Aziz et al., 2007; Barghahn et al., 2021; Claverie et al., 2018; Denoux et al., 2008; Gust et al., 2007; Kaku et al., 2006; Klarzynski et al., 2000; Mélida et al., 2018; Mélida et al., 2020; Rebaque et al., 2021; Versluys et al., 2022; Voxeur et al., 2019; Wanke et al., 2020; Yang, Liu, et al., 2021a; Yang, Liu, et al., 2021b; Zang et al., 2019). Among them are oligosaccharides derived from β-glucans of plant cell walls, like MLGs (e.g. MLG43, MLG34 and MLG443), or cellulose (e.g. CEL2, CEL3, CEL4, CEL5 and CEL6). Here, we describe a group of *Arabidopsis thaliana* RKs – IGP1, IGP3 and IGP4 – with LRR-MAL domains in their ECDs that are required to trigger immune responses mediated by oligosaccharides derived from cellulose (e.g. CEL3–CEL5) and MLGs (e.g. MLG43 and MLG34) (Figures 1 and 2).

We demonstrate by ITC binding experiments that the IGP1/CORK1 RK is a PRR for cellulose-derived oligosaccharides, further supporting its recently proposed function by Tseng et al. (2022) that identified CORK1/IGP1 in a similar genetic screening to the one performed here. We demonstrate the direct interaction of IGP1/CORK1-ECD with CEL3 and with CEL5 with high affinity (K_D = 1.19 ± 0.03 μM and K_D = 1.40 ± 0.01 μM, respectively), and the absence of binding with MLG43, at least under the *in vitro* conditions of ITC tested (Figures 6 and S12). Our data suggest that the IGP1/CORK1 RK might be a true PRR receptor for CEL3–CEL5 oligosaccharides, and that IGP3 and IGP4 RKs might function in Arabidopsis as components of the PRR complex involved in the perception of these oligosaccharides or the signaling complex activating downstream PTI responses (Figure 5). A recent article reports that two LRR RKs, SIF2 (AT1G51850) and SIF4 (AT1G51820), are also required for the immune responses triggered by cellulose-derived oligosaccharides and could also be part of the PRR complex involved in their perception (Zarattini et al., 2021). Also, a poly(A)-specific ribonuclease (AtPARN, AT1G55870) was found to be required for the regulation of the immune responses triggered by CEL3 in Arabidopsis, probably through a mechanism of degradation of the polyA tail from specific mRNAs (Johnson et al., 2018). However, this AtPARN regulatory mechanism of CEL3-mediated responses acts downstream of CEL3 perception by PRRs at the cell surface described here.

Our results point to the LRR-MAL RK family as a set of plant proteins involved in the perception of carbohydrate-based DAMPs and MAMPs, as previously suggested (del Hierro et al., 2021). So far, the plant RKs described to be involved in glycan perception belong to the LysM, WAK and CrRLK1 RK families (Bellande et al., 2017; Brutus et al., 2010; Cao et al., 2014; del Hierro et al., 2021; Liu et al., 2012; Liu et al., 2016; Tang et al., 2022; Wong et al., 2020). The function of most of these proteins in oligosaccharide perception and PTI activation was discovered through the isolation and characterization of Arabidopsis mutants (e.g. *cerk1*, *lyk4*, *lyk5*, *wak1*, *wak2* and *fer1*). In general, such mutants share redundant functions with additional RKs, and therefore individually they are either unaffected or only partially impaired in PTI responses triggered by specific DAMPs and MAMPs. Accordingly, higher-order RK mutants that overcome redundancy must be analyzed to observe PTI-deficient phenotypes (Brutus et al., 2010; Cao et al., 2014; Dünser et al., 2019; Guo et al., 2018; Liu et al., 2012; Liu et al., 2016; Miya et al., 2007). Similarly, our genetic screening led to the identification of nine mutants impaired in glycan perception (*igp1*–*igp9*), among them *IGP1/CORK1*, *IGP2/IGP3* and *IGP4* have been isolated as mutants impaired in MLG43 recognition, and later proven to also be defective in the perception of cellulose-derived oligosaccharides (CEL3–CEL5; Figures 3 and 4). These results suggest that the mechanisms of perception of CEL- and MLG-derived oligosaccharides overlap in Arabidopsis, and this is supported by CEL3/MLG43 cross-elicitation experiments (Figure S6). However, despite the similarities between the mechanisms of perception of MLG- and CEL-derived oligosaccharides, some differences might exist among them. For example, we found that LysM RKs (i.e. CERK1, LYK4 and LYK5) have a partial contribution in the perception of MLG43 (Figure S8), as described previously (Rebaque et al., 2021). In contrast, their role in CEL3 perception is residual as only minor differences in PTI activation were observed in *cerk1-2* and *cerk1-2 lyk4 lyk5* triple mutants in comparison with Col-0 plants treated with CEL3 (Figure S8). The partial requirement of LysM RKs for MLG perception in Arabidopsis is in line with the described function of rice LysM RK members in the perception of MLG-derived oligosaccharides and immune activation. OsCERK1 has been suggested to be the PRR receptor of MLG-derived oligosaccharides based on microscale thermophoresis analysis performed with the ECD produced in baculovirus, whereas OsCeBiP, the rice receptor for chitin-derived oligosaccharides, has been proposed to be the MLG co-receptor of CERK1, based on the lack of binding of its ECD to these MLG ligands (Yang, Liu, et al., 2021b). The K_D values of ECD–OsCERK1 for MLG43 are in the range of 1–2 μM, similar to that found for IGP1/CORK1 binding to CEL3/CEL5 in this work (Figure 6), and to that of ECD–OsCeBiP for CHI6 (Yang, Liu, et al., 2021b). Of note, the perception of CHI6 is neither altered in *igp1-igp4* nor altered in *igp5-igp9* mutants (Figures 1 and S2), further indicating that Arabidopsis IGP1–IGP9 proteins are not required for CHI6 perception. These data point to separate mechanisms for the perception of CHI6 and the CEL3- and MLG43-derived oligosaccharides in Arabidopsis, but also to some differences in the mechanism of perception of CEL3 (independent of CERK1, LYK4 and LYK5, and with IGP1/CORK1 as a true PRR) and MLG43 (requiring CERK1, LYK4 and LYK5, with the true PRR yet to be determined). The role of LysM RKs in the mechanisms of perception of several glycans and in plant–microbe interactions is an emerging issue (Yang, Wang, et al., 2021). The mechanisms of PTI activation mediated by IGP1, IGP3 and IGP4 LRR-MAL RKs described here also differ from that of pectin and OG perception involving FER1 and WAK1–WAK2 (Brutus et al., 2010; Dünser et al., 2019; Tang et al., 2022), respectively, and that of other MAMPs and DAMPs (e.g. flg22 and AtPEP1), because the Ca^{2+} burst in *igp1*^{AEQ}–*igp4*^{AEQ} upon treatment with these elicitors was similar to that of Col-0^{AEQ} plants (Figure 3c–e). All these data support the specific function of IGP1/CORK1, IGP3 and IGP4 RKs in MLG- and CEL-derived oligosaccharide recognition.

The crystallized structures of ECDs of CERK1- and chitin-derived oligosaccharides revealed the structural

basis of this recognition (Liu et al., 2012; Yang, Liu, et al., 2021b). Other plant ECD-RKs like ANX1, ANX2 and FER1, which harbor two tandem MLDs, have been also purified and crystallized, but their putative glycoligand(s) has not been identified (Moussu et al., 2018). Notably, the MLDs of ANX1, ANX2 and FER1 seem to show some differences compared with those MAL domains present in the ECDs of the three IGP RKs identified in this work, which also contain an N-terminal LRR domain (Figure S11; (Yang et al., 2021)). We have generated *de novo* structural models for the three LRR-MAL RKs, and these models suggest that IGP1/CORK1, IGP3 and IGP4 have similar structures, in line with their putative recent evolutionary divergence (Figure S3), although IGP1/CORK1 has an extra loop in its KD (Figure S11). Remarkably, MAL domains of these RKs are structurally very similar to that of the MAL protein of *Xenopus* sp., which is involved in oligosaccharide binding, and to that of plant ANX1/ANX2 from the CrRLK1 family (Figure S11). In recent reports by Tseng et al. (2022), two Phe residues conserved in all *A. thaliana* MAL domains, but not in MAL from *Xenopus* sp. (Schallus et al., 2010) are noted as essential for CEL3 perception and PTI activation, but this hypothesis has not been validated through binding experiments. Therefore, we hypothesize that the LRR domain of ECDs in IGP1/CORK1 might be essential for the formation of the structural pocket involved in the observed CEL3 and CEL5 binding. Obtaining crystallized structures of CEL3/ECD-IGP1 will contribute to decipher the structural bases of CEL3–CEL5 recognition by LRR-MAL ECD.

We show here that *igp1* and *igp2/igp3* mutants have point mutations in their KDs that may impact their functionality (Figure 2). E906K in IGP1/CORK1 and G773E in IGP3 do not seem to impair the catalytic sites of these RKs, which are predicted to be almost identical to that of wild-type KDs (Figure S11). However, such mutations are predicted to increase the surface patch, resulting in drastic changes on the surface electrostatic potential of the residues around the mutated positions (Figure S11). As kinase activity can be altered by mutations at distant residues from the active site (McClendon et al., 2014), we can hypothesize that E906K and G773E mutations might either affect the catalytic activity of the KDs or interfere with the interaction of the RK KDs with other RKs, like true PRR for MLG43 perception, co-receptors proteins of IGP1/CORK1 PRR (e.g. IGP2/3 and IGP4) or additional protein partners.

The exogenous application of glycans enhanced disease resistance of different plant species to diverse pathogens, acknowledging the relevance of these carbohydrate-based ligands released during plant–microbe interaction in the regulation of plant disease resistance (Mélida et al., 2018; Rebaque et al., 2021). This oligosaccharide-mediated priming effect on PTI and disease resistance has driven the development of sustainable crop protection solutions based on combinations of active glycans (DAMPs and MAMPs; Chaliha et al., 2020, Lemke et al., 2022). The discovery of counterpart receptors for these active glycans in crops would accelerate the selection of the corresponding genes in breeding programs to enhance crop disease resistance. Notably, the *IGP1/CORK1*, *IGP3* and *IGP4* genes are in a cluster in the *A. thaliana* genome, indicating recent duplication events (Yang, Wang, et al., 2021). These genes form part of a family of at least 13 members that has not been characterized in detail previously, except for RFK1, a protein involved in pollen tube growth (Lee & Goring, 2021). This clade of LRR-MAL RKs seems to be conserved and diversified in dicots (Fig. S10) and in some monocots, like rice. However, the few relatives RKs found in grasses are structurally dissimilar and phylogenetically distant (Yang, Wang, et al., 2021).

The MLG- and cellulose-derived oligosaccharides can also be released upon alteration of plant cell wall integrity triggered by other stresses (e.g. salt or drought) or across plant development (e.g. during cell wall remodeling; Bacete et al., 2022, Gigli-Bisceglia et al., 2022). During these processes plant endogenous enzymes can hydrolase cell wall polysaccharides, as described recently for a *Zea mays* (maize) GH17 licheninase that releases MLG43-derived and other oligosaccharides (Kraemer et al., 2021). The characterization of the role of glycan-mediated responses in these additional processes must be determined to understand their interaction with PTI/disease resistance responses and their impact on plant fitness. Also, the regulation of the homeostasis of cell wall-derived oligosaccharides needs to be analyzed in depth. For example, several plant berberine-bridge enzymes control CEL–oligosaccharide homeostasis by oxidating the anomeric carbon of CEL3–CEL6 oligosaccharides, thus reducing both their activity as DAMPs and their preferred use as a carbon source by fungi (Benedetti et al., 2018). In summary, our results contribute to further understanding the mechanisms of perception of oligosaccharides by the plant immune system and to expand the set of families of PRRs and the ECD structures involved in ligand recognition and immune activation in plants.

EXPERIMANTAL PROCEDURES

Biological material and growth conditions

The *A. thaliana* lines used in this study, all in the Columbia-0 (Col-0) background, were Col-0^{AEQ}, carrying the calcium reporter aequorin protein (Knight et al., 1991; Ranf et al., 2011), *cerk1-2*^{AEQ} (Ranf et al., 2011), *rbohD* (Morales et al., 2016) and *igp*^{AEQ}, isolated in this work. The *cerk1-2 lyk4 lyk5* triple mutant was generated by crossing *cerk1-2* and the *lyk4 lyk5* double mutant (Rebaque et al., 2021) and selecting the triple mutants with the oligonucleotides described (Table S3). The *at1g56140* (*igp4*) and the *at1g56120* T-DNA mutants were obtained from NASC (SALK_005808 and SALK_043782, respectively). Plants used for cytoplasmatic Ca^{2+} measurements and ROS were grown in 96-well plates (with one seedling per well), and

for MAPK phosphorylation and gene expression analyses plants were grown in 24-well plates (with approx. 10 seedlings per well). Seedlings were grown under long-day conditions (14 hours of light) at 19–22°C in half-strength liquid MS medium. Plants were also grown in a soil–vermiculite (3:1) mixture under a short-day photoperiod (10 h of light/14 h of dark, 21–20°C) or a long-day photoperiod (14 h of light/10 h of dark, 19–22°C).

Carbohydrates used in the experiments

MLG43 (β-1,4-D-$(Glc)_2$-β-1,3-D-Glc; #O-BGTRIB), MLG34 (β-1,3-D-$(Glc)_2$-β-1,4-D-Glc; #O-BGTRIA), hexaacetyl-chitohexaose (CHI6; β-1,4-D-$(GlcNAc)_6$; #O-CHI6), CEL3 (β-1,4-D-$(Glc)_3$; O-CTR), CEL4 (β-1,4-D-$(Glc)_4$; #O-CTE), CEL5 (β-1,4-D-$(Glc)_5$; #O-CPE) were purchased from Megazyme (https://www.megazyme.com). CEL2 (cellobiose, β-1,4-D-$(Glc)_2$; C7252) came from Sigma-Aldrich (https://www.sigmaaldrich.com). OGs (galacturonan oligosaccharides mixture DP10/DP15; GalAα1–4(GalAα1–4)8_{-13}GalA; GAT114) were from ELICITYL (https://www.elicityl-oligotech.com). Peptides flg22 and AtPEP1 were from EZBiolab (http://www.ezbiolab.com) and Abyntek (https://www.abyntek.com), respectively.

Genetic screening to identify *igp* mutants

Col-0^{AEQ} seeds were mutagenized with 0.3% EMS for 17 h. Seeds were sown in soil–vermiculite (3:1) to obtain next-generation seeds (e.g. M_1 and M_2) (Ranf et al., 2012). M_2 seedlings were grown *in vitro* for 8 days, and cytoplasmic Ca^{2+} influxes were evaluated using a Varioskan Lux Reader luminometer (ThermoFisher Scientific, https://www.thermofisher.com) upon treatment with 100 μM MLG43, as described (Rebaque et al., 2021). Seedlings with low response to MLG43 were transferred to soil (230 putative mutants out of 6400 total seedlings screened), self-crossed and then the Ca^{2+} burst was tested in F_1 seedlings to confirm the impaired response to MLG43. Validated *igp* mutants (*igp1*^{AEQ}–*igp3*^{AEQ} and *igp5*^{AEQ}–*igp9*^{AEQ}, described here, and *igp10*^{AEQ}–*igp20*^{AEQ}, not described here) were selected for further characterization and backcrossed with Col-0^{AEQ}. Total Ca^{2+} discharge was performed by treating seedlings with 1 M $CaCl_2$ and then the Ca^{2+} burst was measured in the luminometer.

Mapping by whole-genome sequencing and SNP analysis

Tissue from 50 individuals of F_2 *igp*^{AEQ} × Col-0^{AEQ} segregating plants with impaired response to MLG43 and from control line Col-0^{AEQ} was harvested and pooled for whole-genome sequencing of gDNA to identify single-nucleotide polymorphisms (SNPs) associated with phenotypes in *igp*^{AEQ}. Sequencing (150-bp paired-end reads) was performed on an Illumina platform (https://www.illumina.com) to reach a coverage of 30 million reads (Andrews, 2010), which were aligned with BWA-MEM 0.7.17 (Macrogen, https://dna.macrogen.com) against the *A. thaliana* TAIR10 genome release (Li, 2013). BAM files were obtained with SAMTOOLS 1.15.1 (http://www.htslib.org). The variant caller 16GT DOCKER IMAGE was employed to obtain VCF files (Danecek et al., 2021; Luo et al., 2017). From these VCF files, chromosome, position, reference, alternate and allelic depth (AD) fields were extracted with BCFTOOLS 1.15.1, and SNPs were subtracted from the resulting files. Frequency was calculated from AD fields as follows: [AD-alternate allele/(AD-alternate allele + AD-reference allele)]. SNPs with frequency values higher than 0.99 were selected for further analyses (Online data set; Table S2).

Determination of PTI responses

Reactive oxygen species (ROS; H_2O_2) production was determined in 10-day-old seedlings after treatment with MAMPs and DAMPs using the luminol assay, as described by Rebaque et al. (2021). MAPK activation was determined in 12-day-old seedlings grown on half-strength liquid MS medium and treated with water (mock) or different oligosaccharides for 0, 10 and 20 mins. Then seedlings were harvested and Western blotting was performed as described previously, with a few modifications (Rebaque et al., 2021). Gene expression analysis was carried out in 12-day-old seedlings grown on half-strength liquid MS medium, and treated with oligosaccharides (i.e. 100 μM MLG43, 10 μM CEL3 or 50 μM CHI6) or water (mock) for 30 min. Then total RNA extraction and RT-qPCR analyses were performed as described by Rebaque et al. (2021). Gene expression and normalization to mock samples were determined using PFAFFL (Pfaffl, 2001). The oligonucleotides used for PCR are described in Table S3.

Phylogenetic analysis

The evolutionary history of IGP proteins was inferred using the minimum evolution (ME) method (Rzhetsky & Nei, 1992). The bootstrap consensus tree inferred from 1000 replicates is taken to represent the evolutionary history of the taxa analyzed (Felsenstein, 1985). Branches corresponding to partitions reproduced in less than 50% bootstrap replicates are collapsed. The percentage of replicate trees in which the associated taxa clustered together in the bootstrap test (1000 replicates) are shown next to the branches (Felsenstein, 1985). The evolutionary distances were computed using the p-distance method (Nei & Kumar, 2000). The ME tree was searched using the close-neighbor-interchange (CNI) algorithm (Nei & Kumar, 2000) at a search level of 1. The neighbor-joining algorithm (Saitou & Nei, 1987) was used to generate the initial tree. The analysis involved 25 amino acid sequences. All ambiguous positions were removed for each sequence pair and a total of 709 positions were present in the final data set. Evolutionary analyses were conducted in MEGA 6 (Tamura et al., 2013).

Structure analyses *in silico*

Model structures of IGP1/CORK1/AT1G56145, IGP3/AT1G56130 and IGP4/AT1G56140 were downloaded from the AlphaFold Protein Structure Database (Tunyasuvunakool & Adler, 2021). They present six identifiable domains: N-terminal containing a signal peptide annotated in PFAM (Mistry et al., 2021), LRR, MAL, TM, KD and the C-terminal tail. The pDDT metric over most of LRR, MAL and KDs is ≥90% (Figure S10) (Jumper et al., 2021). To achieve the proper extracellular/TM/intracellular domain separation, and taking the IGP4 model as the benchmark, we proceeded as follows: (i) torsions were applied to backbone dihedral angles in the segment following MAL (magenta box in Figure S10) with CHIMERA 1.15 (Pettersen et al., 2004); (ii) energy minimization of the extended segment joining the MAL and TM domains was performed with CHIMERA 1.15, keeping all the remaining structure fixed; (iii) the resulting structure was inserted in a pre-equilibrated model of a bilayer composed of 256 phosphatidylcholine (POPC) lipids with a pore of radius 8 Å, downloaded from the CHARMM-GUI archive (Jo et al., 2007), and the protein-bilayer system was parametrized using the CHARMM 3.6 force field (Huang et al., 2017) with CHARMM-GUI (Jo et al., 2008); (iv) the protein bilayer system was solvated with a 16-Å margins solvation box and NaCl 0.150 M salt ions with VMD 1.9.3 (Humphrey et al., 1996), and the whole structure was optimized with 10 000 conjugated gradient minimization steps using NAMD 2.14 (Phillips & Hardy, 2020). The optimized final structure of IGP4 was then used as the input for modeling the corresponding structures of IGP1/CORK1 and IGP3 with SWISS-MODEL (Waterhouse et al., 2018) in 'user template mode'. The structural

comparisons of MAL and KD were analyzed with the TM-Align web server (Zhang & Skolnick, 2005) The structural analysis of mutants IGP1-E906K and IGP3-G773E, and their corresponding wild-type KDs, was addressed by modeling them separately with AlphaFold 2 (Jumper et al., 2021) using ColabFold (Mirdita & Schütze, 2022). Poisson–Boltzmann (PB) electrostatic potentials (EPs) were computed with the Adaptive Poisson Boltzmann Solver, APBS 3.0.0 (Jurrus et al., 2018) through its plug-in in PYMOL 2.5.1 (Schrödinger, 2020), solving the nonlinear PB equation in sequential focusing multigrid mode at 3D grids of $161^3 = 4\,173\,281$ points (approx. 0.5-Å step size), with $T = 298$ K, ionic concentration of 0.150 M (NaCl), and dielectric constants of 4.00 for proteins and 78.54 for water. The PB EP was then mapped onto molecular surfaces computed and rendered with PYMOL 2.5.1 (Schrödinger, 2020).

Protein expression and purification from insect cells

Codon-optimized synthetic genes corresponding to the ectodomains of AT1G56145 (residues 25–630), AT1G56140 (residues 29–636) and AT1G56130 (residues 30–636) from Invitrogen GeneArt were cloned into a modified pFastBac donor vector (Geneva Biotech, https://geneva-biotech.com) harboring the *Drosophila BiP* (Smakowska-Luzan et al., 2018) or the 30K *Bombyx mori* (Soejima et al., 2013) secretion signal peptides, and with a TEV (tobacco etch virus protease) cleavable C-terminal StrepII-9xHis tag. Baculovirus vectors were generated in DH10MultiBac *E. coli* cells (Geneva Biotech). Briefly, virus amplification was carried out in *Spodoptera frugiperda* Sf9 cells (Geneart, Thermo Fisher Scientific) and was used to infect *Trichoplusia ni* Tnao38 cells (Hashimoto et al., 2012) for protein expression. The cells were grown for 1 day at 28°C and for 2 days at 22°C with gentle shaking. The secreted proteins were subjected to tandem affinity purification, using Ni^{2+} (HisTrap excel, equilibrated in 25 mM KPi, pH 7.8, and 500 mM NaCl; GE Healthcare, https://www.gehealthcare.com) and Strep columns (Strep-Tactin Superflow high-capacity; IBA, https://www.iba.de) equilibrated in (25 mM Tris, pH 8.0, 250 mM NaCl, 1 mM EDTA. Affinity tags were removed using His-tagged TEV protease in a 1:50 ratio at 4°C overnight. Separation of cleavage tags and aggregated proteins was performed using size-exclusion chromatography on a Superdex 200 Increase 10/300 GL column (GE Healthcare) equilibrated in 20 mM citric acid, pH 5.0, 150 mM NaCl. Proteins were analyzed for purity and structural integrity by SDS-PAGE.

Analytical size-exclusion (SEC) chromatography

Analytical size-exclusion experiments were performed on a Superdex 200 Increase 10/300 GL column (GE Healthcare) equilibrated in 20 mM citric acid, pH 5.0, 150 mM NaCl. A 400-μg portion of protein (aprox. 6 μM) was injected using a loop of 1 mL, and the sample was eluted with a flow of 0.5 mL min^{-1}. UV absorbance at 280 nm was used to monitor the elution of proteins. The peak fractions were analyzed by SDS-PAGE followed by Coomassie blue staining.

Isothermal titration calorimetry (ITC)

Experiments were performed at 25°C using a MicroCal PEAQ-ITC (Malvern Instruments, https://www.malvernpanalytical.com) with a 200-μL standard cell and a 40-μL titration syringe. Briefly, for ITC experiments in MicroCal PEAQ-ITC, proteins were gel-filtrated into the ITC buffer (20 mM sodium citrate, pH 5.0, 150 mm NaCl). A 3-μL sample of potential ligand (CEL3, CEL5 or MLG43) was injected at a concentration range between 135 and 400 μM into the ITC cell containing ECDs of AT1G56145 or AT1G56140 protein at 9 μM. A total of 13 injections were performed at 150-s intervals with a 500-rpm stirring speed. Dilution heat was corrected using the thermograph of the titration of the ligand into the cell containing only buffer as a control. Experiments were performed in duplicate or triplicate, unless otherwise specified, and data were analyzed using the MICROCAL PEAQ-ITC analysis software provided by the manufacturer. All ITC runs used for data analysis have an N ranging from 0.98 to 1.05. The N values were fitted to 1 in the analysis.

ACCESSION NUMBERS

Genes described in this work are: *IGP1/AT1G56145*; *IGP2/AT1G56130*; *IGP3/AT1G56130*; *IGP4/AT1G56140*; *CERK1/AT3G14840*; *LYK4/AT2G23770*; *LYK5/AT2G33580*; *RBOHD/AT5G47910*.

AUTHOR CONTRIBUTIONS

MM-D performed research and generated data, designed some figures and reviewed the article. PF-C conceived, designed and performed research, generated data, designed some figures and wrote the article. PJS performed research on ECD purification and ITC assays, generated and analyzed the data, designed some figures and reviewed the article. GL performed research and generated data. MG-A designed and performed structural *in silico* analyses, designed some figures and wrote the article. DR performed research, generated data and designed some figures. IDH performed research and assembled *igp* mutant genomes. MAT and DJB performed research, generated reactive oxygen species production and designed some figures. VK performed research, generated data and reviewed the article. HM conceived and designed some experiments, analyzed data, designed some figures and revised the article. LFP conceived, designed and performed structural *in silico* analyses, designed some figures and wrote the article. JS conceived and designed ECD protein production and ITC binding experiments, analyzed the data, designed figures and wrote the article. AM conceived and designed the research, analyzed the data, designed figures and wrote the article.

CONFLICT OF INTEREST

All authors confirm that they have no conflicts of interest associated with this work.

ACKNOWLEDGEMENTS

We thank Dr Sonsoles Martín-Santamaria and Elena Gómez-Rubio (Centro de Investigaciones Biológicas Margarita Salas-CSIC, Spain) for their advice on deciphering the structure of the ECD LRR-MAL. We thank Dr Jose María Jiménez-Gomez and Dr René Toribio (Centro de Biotecnología y Genómica de Plantas (CBGP), Spain) for their kind advice on SNP identification and Western blotting, respectively. This work was supported by grant RTI2018-096975-B-I00 from the Spanish Ministry of Science, Innovation and Universities to AM and grant PID-2021-126006OB-100 from the Spanish Ministry of Science and Innovation to AM. This work has also been financially supported by the 'Severo Ochoa (SO) Programme for Centres of Excellence in R&D' from the Agencia

Estatal de Investigación (AEI) of Spain (grants SEV-2016-0672 (2017-2021) and CEX2020-000999-S (2022-2025) to the CBGP). In the frame of the SO program, HM and PF-C were supported with postdoctoral fellowships. MM-D, DJB and DR were recipients of PhD Fellows PRE2019-088120 and PRE2019-091276 (SEV-2016-0672) from AEI, and IND2017/BIO-7800 from Madrid Regional Government, respectively. Research in the lab of JS was financially supported by the University of Lausanne, the European Research Council (ERC) (grant agreement no. 716358) and the Swiss National Science Foundation (grant no. 310030_204526).

DATA AVAILABILITY STATEMENT

All relevant data can be found within the article and its supporting materials (Online data set; NCBI whole-genome sequence data set). Online data set include the genome assembly data for *igp1*^{AEQ}, *igp2*^{AEQ}, *igp3*^{AEQ}, *igp4* and Col-0^{AEQ} and can be retrieved from the NCBI Sequence Read Archive (SRA) under BioProject ID PRJNA864842 and Biosample accessions SAMN30087195, SAMN30087196, SAMN30087197, SAMN30087198 and SAMN30087199. Materials and data are available upon request to the corresponding authors.

SUPPORTING INFORMATION

Additional Supporting Information may be found in the online version of this article.

Figure S1. Forward genetic screening using Col-0^{AEQ} was used as a tool to discover PRRs and proteins involved in oligosaccharide perception and PTI activation.

Figure S2. Identification of additional *igp* (*igp5*–*igp9*) mutants impaired in MLG43 perception.

Figure S3. LRR-MAL-RK family in *Arabidopsis thaliana* includes additional members such as IGP4/AT1G56140, which is also required for MLG43 perception.

Figure S4. Developmental phenotypes of *igp* plants and LysM-PRR mutants.

Figure S5. Cytoplasmic calcium burst in response to CEL3 is impaired in *igp5*–*igp9* mutants.

Figure S6. Cross-elicitation during the refractory period of calcium burst triggered by MLG43 or CEL3.

Figure S7. ROS production triggered by flg22 and CHI6 in *igp1*–*igp4* mutants.

Figure S8. Activation of PTI hallmarks by MLG43, CEL3 and CHI6 in LysM-PRR mutants.

Figure S9. Phylogenetic analysis of LRR-MAL RKs in Arabidopsis and other plant species.

Figure S10. AlphaFold predictions for IGP1, IGP3 and IGP4 proteins.

Figure S11. Model structures of IGP1/CORK1, IGP3 and IGP4 proteins.

Figure S12. Purification of ECDs of IGP1/CORK1, IGP3 and IGP4 and ITC of IGP1/CORK1 binding of MLG43 and CEL3.

Table S1. Chi-square test statistics for *igp1*^{AEQ}–*igp3*^{AEQ} mutant segregation.

Table S2. Chromosomal localization of SNP mutations in *igp* mutants.

Table S3. Oligonucleotides used in this work.

REFERENCES

Andrews, S. (2010) FastQC: A Quality Control Tool for High Throughput Sequence Data.

Aziz, A., Gauthier, A., Bézier, A., Poinssot, B., Joubert, J.M., Pugin, A. *et al.* (2007) Elicitor and resistance-inducing activities of beta-1,4 cellodextrins in grapevine, comparison with beta-1,3 glucans and alpha-1,4 oligogalacturonides. *Journal of Experimental Botany*, **58**, 1463–1472.

Bacete, L., Mélida, H., Miedes, E. & Molina, A. (2018) Plant cell wall-mediated immunity: cell wall changes trigger disease resistance responses. *The Plant Journal*, **93**, 614–636.

Bacete, L., Schulz, J., Engelsdorf, T., Bartosova, Z., Vaahtera, L., Yan, G. *et al.* (2022) THESEUS1 modulates cell wall stiffness and abscisic acid production in Arabidopsis thaliana. *Proceedings of the National Academy of Sciences of the United States of America*, **119**, e2119258119.

Barghahn, S., Arnal, G., Jain, N., Petutschnig, E., Brumer, H. & Lipka, V. (2021) Mixed linkage β-1,3/1,4-Glucan oligosaccharides induce defense responses in Hordeum vulgare and Arabidopsis thaliana. *Frontiers in Plant Science*, **12**, 682439.

Bellande, K., Bono, J.J., Savelli, B., Jamet, E. & Canut, H. (2017) Plant lectins and lectin receptor-like kinases: how do they sense the outside? *International Journal of Molecular Sciences*, **18**, 1164.

Benedetti, M., Verrascina, I., Pontiggia, D., Locci, F., Mattei, B., De Lorenzo, G. *et al.* (2018) Four Arabidopsis berberine bridge enzyme-like proteins are specific oxidases that inactivate the elicitor-active oligogalacturonides. *The Plant Journal*, **94**, 260–273.

Bigeard, J., Colcombet, J. & Hirt, H. (2015) Signaling mechanisms in pattern-triggered immunity (PTI). *Molecular Plant*, **8**, 521–539.

Boutrot, F. & Zipfel, C. (2017) Function, discovery, and exploitation of plant pattern recognition receptors for broad-Spectrum disease resistance. *Annual Review of Phytopathology*, **55**, 257–286.

Brutus, A., Sicilia, F., Macone, A., Cervone, F. & De Lorenzo, G. (2010) A domain swap approach reveals a role of the plant wall-associated kinase 1 (WAK1) as a receptor of oligogalacturonides. *Proceedings of the National Academy of Sciences*, **107**, 9452–9457.

Burton, R.A. & Fincher, G.B. (2009) (1,3;1,4)-beta-D-glucans in cell walls of the poaceae, lower plants, and fungi: a tale of two linkages. *Molecular Plant*, **2**, 873–882.

Cao, Y., Liang, Y. & Tanaka, K. (2014) The kinase LYK5 is a major chitin receptor in Arabidopsis and forms a chitin-induced complex with related kinase CERK1. *eLife*, **3**, e03766.

Chaliha, C., Field, R.A. & Kalita, E. (2020) Glycans as Plant Defense Priming Agents Against Filamentous Pathogens. In: Mérillon, J.-M. & Ramawat, K.G. (Eds.) *Plant Defence: Biological Control*. Cham: Springer International Publishing, pp. 99–118.

Claverie, J., Balacey, S., Lemaître-Guillier, C., Brulé, D., Chiltz, A., Granet, L. *et al.* (2018) The Cell Wall-derived xyloglucan is a new DAMP triggering plant immunity in Vitis vinifera and Arabidopsis thaliana. *Frontiers in Plant Science*, **9**, 1725.

Cosgrove, D.J. (2022) Building an extensible cell wall. *Plant Physiology*, **189**, 1246–1277.

Cummings, R.D., Schnaar, R.L., Esko, J.D., Woods, R.J., Drickamer, K. & Taylor, M.E. (2022) Chapter 29. Principles of glycan recognition. In: Varki, A., Cummings, R.D. & Esko, J.D., ***et al.*** (Eds.) *Essentials of glycobiology*, 4th edition. Cold Spring Harbor, NY: Cold Spring Harbor Laboratory Press.

Danecek, P., Bonfield, J., Liddle, J., Marshall, J., Ohan, V., Pollard, M. *et al.* (2021) Twelve years of SAMtools and BCFtools. *GigaScience*, **10**, giab008.

del Hierro, I., Mélida, H., Broyart, C., Santiago, J. & Molina, A. (2021) Computational prediction method to decipher receptor–glycoligand interactions in plant immunity. *The Plant Journal*, **105**, 1710–1726.

Denoux, C., Galletti, R., Mammarella, N., Gopalan, S., Werck, D., De Lorenzo, G. *et al.* (2008) Activation of defense response pathways by OGs and Flg22 elicitors in Arabidopsis seedlings. *Molecular Plant*, **1**, 423–445.

Desaki, Y., Kouzai, Y., Ninomiya, Y., Iwase, R., Shimizu, Y., Seko, K. *et al.* (2018) OsCERK1 plays a crucial role in the lipopolysaccharide-induced immune response of rice. *The New Phytologist*, **217**, 1042–1049.

Dünser, K., Gupta, S., Herger, A., Feraru, M.I., Ringli, C. & Kleine-Vehn, J. (2019) Extracellular matrix sensing by FERONIA and leucine-rich repeat Extensins controls vacuolar expansion during cellular elongation in Arabidopsis thaliana. *The EMBO Journal*, **38**, e100353.

Felsenstein, J. (1985) Confidence limits on phylogenies: an approach using the bootstrap. *Evolution*, **39**, 783–791.

Fontaine, T., Simenel, C., Dubreucq, G., Adam, O., Delepierre, M., Lemoine, J. *et al.* (2000) Molecular organization of the alkali-insoluble fraction of aspergillus fumigatus cell wall. *The Journal of Biological Chemistry*, **275**, 27594–27607.

Franck, C., Westermann, J. & Boisson-Dernier, A. (2018) Plant Malectin-like receptor kinases: from Cell Wall integrity to immunity and beyond. *Annual Review of Plant Biology*, **69**, 301–328.

Fry, S.C., Nesselrode, B., Miller, J.G. & Mewburn, B.R. (2008) Mixed-linkage (1→3,1→4)-β-d-glucan is a major hemicellulose ofEquisetum(horsetail) cell walls. *The New Phytologist*, **179**, 104–115.

Gámez-Arjona, F.M., Vitale, S., Voxeur, A., Dora, S., Müller, S., Sancho-Andrés, G. *et al.* (2022) Impairment of the cellulose degradation machinery enhances Fusarium oxysporum virulence but limits its reproductive fitness. *Science. Advances*, **8**, eabl9734.

Gigli-Bisceglia, N., van Zelm, E., Huo, W., Lamers, J. & Testerink, C. (2022) Arabidopsis root responses to salinity depend on pectin modification and cell wall sensing. *Development*, **149**, dev200363.

Guo, H., Nolan, T.M., Song, G., Liu, S., Xie, Z., Chen, J. *et al.* (2018) FERONIA receptor kinase contributes to plant immunity by suppressing Jasmonic acid signaling in Arabidopsis thaliana. *Current Biology*, **28**, 3316–3324.e3316.

Gust, A.A., Biswas, R., Lenz, H.D., Rauhut, T., Ranf, S., Kemmerling, B. *et al.* (2007) Bacteria-derived peptidoglycans constitute pathogen-associated molecular patterns triggering innate immunity in Arabidopsis. *The Journal of Biological Chemistry*, **282**, 32338–32348.

Hashimoto, Y., Zhang, S., Zhang, S., Chen, Y.R. & Blissard, G.W. (2012) Correction: BTI-Tnao38, a new cell line derived from Trichoplusia ni, is permissive for AcMNPV infection and produces high levels of recombinant proteins. *BMC Biotechnology*, **12**, 12.

Huang, J., Rauscher, S., Nawrocki, G., Ran, T. & Feig, M. (2017) CHARMM36m: an improved force field for folded and intrinsically disordered proteins. *Nature Methods*, **14**, 71–73.

Humphrey, W., Dalke, A. & Schulten, K. (1996) VMD: visual molecular dynamics. *Journal of Molecular Graphics*, **14**(33–38), 27–38.

Jo, S., Kim, T. & Im, W. (2007) Automated builder and database of protein/membrane complexes for molecular dynamics simulations. *PLoS One*, **2**, e880.

Jo, S., Kim, T., Iyer, V.G. & Im, W. (2008) CHARMM-GUI: a web-based graphical user interface for CHARMM. *Journal of Computational Chemistry*, **29**, 1859–1865.

Johnson, J.M., Thürich, J., Petutschnig, E.K., Altschmied, L., Meichsner, D., Sherameti, I. *et al.* (2018) A poly(a) ribonuclease controls the Cellotriose-based interaction between Piriformospora indica and its host Arabidopsis. *Plant Physiology*, **176**, 2496–2514.

Jumper, J., Evans, R., Pritzel, A. & Green, T. (2021) Highly accurate protein structure prediction with AlphaFold. *Nature*, **596**, 583–589.

Jurrus, E., Engel, D., Star, K., Monson, K., Brandi, J., Felberg, L.E. *et al.* (2018) Improvements to the APBS biomolecular solvation software suite. *Protein Science*, **27**, 112–128.

Kaku, H., Nishizawa, Y., Ishii-Minami, N., Akimoto-Tomiyama, C., Dohmae, N., Takio, K. *et al.* (2006) Plant cells recognize chitin fragments for defense signaling through a plasma membrane receptor. *Proceedings of the National Academy of Sciences of the United States of America*, **103**, 11086–11091.

Klarzynski, O., Plesse, B., Joubert, J.M., Yvin, J.C., Kopp, M., Kloareg, B. *et al.* (2000) Linear beta-1,3 glucans are elicitors of defense responses in tobacco. *Plant Physiology*, **124**, 1027–1038.

Kloareg, B., Badis, Y., Cock, J.M. & Michel, G. (2021) Role and evolution of the extracellular matrix in the Acquisition of Complex Multicellularity in eukaryotes: a macroalgal perspective. *Genes*, **12**, 1059.

Knight, M.R., Campbell, A.K., Smith, S.M. & Trewavas, A.J. (1991) Transgenic plant aequorin reports the effects of touch and cold-shock and elicitors on cytoplasmic calcium. *Nature*, **352**, 524–526.

Kraemer, F.J., Lunde, C., Koch, M., Kuhn, B.M., Ruehl, C., Brown, P.J. *et al.* (2021) A mixed-linkage (1,3;1,4)-β-D-glucan specific hydrolase mediates dark-triggered degradation of this plant cell wall polysaccharide. *Plant Physiology*, **185**, 1559–1573.

Lee, H.K. & Goring, D.R. (2021) Two subgroups of receptor-like kinases promote early compatible pollen responses in the Arabidopsis thaliana pistil. *Journal of Experimental Botany*, **72**, 1198–1211.

Lemke, P., Jünemann, L. & Moerschbacher, B.M. (2022) Synergistic antimicrobial activities of chitosan mixtures and chitosan-copper combinations. *International Journal of Molecular Sciences*, **23**, 3345.

Li, H. (2013) Aligning sequence reads, clone sequences and assembly contigs with BWA-MEM. *arXiv*, 1303.3997v2.

Liu, S., Wang, J., Han, Z., Gong, X., Zhang, H. & Chai, J. (2016) Molecular mechanism for fungal Cell Wall recognition by Rice chitin receptor OsCEBiP. *Structure*, **24**, 1192–1200.

Liu, T., Liu, Z., Song, C., Hu, Y., Han, Z., She, J. *et al.* (2012) Chitin-induced dimerization activates a plant immune receptor. *Science*, **336**, 1160–1164.

Locci, F., Benedetti, M., Pontiggia, D., Citterico, M., Caprari, C., Mattei, B. *et al.* (2019) An Arabidopsis berberine bridge enzyme-like protein specifically oxidizes cellulose oligomers and plays a role in immunity. *The Plant Journal*, **98**, 540–554.

Luo, R., Schatz, M. & Salzberg, S. (2017) 16GT: a fast andsensitive variant caller using a 16-genotype probabilistic model. *GigaScience*, **6**(7), 1–4.

McClendon, C.L., Kornev, A.P., Gilson, M.K. & Taylor, S.S. (2014) Dynamic architecture of a protein kinase. *Proceedings of the National Academy of Sciences of the United States of America*, **111**, E4623–E4631.

Mélida, H., Bacete, L., Ruprecht, C., Rebaque, D., Del Hierro, I., López, G. *et al.* (2020) Arabinoxylan-oligosaccharides act as damage associated molecular patterns in plants regulating disease resistance. *Frontiers in Plant Science*, **11**, 1210.

Mélida, H., Sopeña-Torres, S., Bacete, L., Garrido-Arandia, M., Jordá, L., López, G. *et al.* (2018) Non-branched β-1,3-glucan oligosaccharides trigger immune responses in Arabidopsis. *The Plant Journal*, **93**, 34–49.

Mirdita, M. & Schütze, K. (2022) ColabFold: making protein folding accessible to all. *Nature Methods*, **19**, 679–682.

Mistry, J., Chuguransky, S., Williams, L., Qureshi, M., Salazar, G.A., Sonnhammer, E.L.L. *et al.* (2021) Pfam: the protein families database in 2021. *Nucleic Acids Research*, **49**, D412–d419.

Miya, A., Albert, P., Shinya, T., Desaki, Y., Ichimura, K., Shirasu, K. *et al.* (2007) CERK1, a Lys M receptor kinase, is essential for chitin elicitor signaling in Arabidopsis. *Proceedings of the National Academy of Sciences of the United States of America*, **104**, 19613–19618.

Morales, J., Kadota, Y., Zipfel, C., Molina, A. & Torres, M.A. (2016) The Arabidopsis NADPH oxidases Rboh D and Rboh F display differential expression patterns and contributions during plant immunity. *Journal of Experimental Botany*, **67**, 1663–1676.

Morgan, J.L., Strumillo, J. & Zimmer, J. (2013) Crystallographic snapshot of cellulose synthesis and membrane translocation. *Nature*, **493**, 181–186.

Moussu, S., Augustin, S., Roman, A.O., Broyart, C. & Santiago, J. (2018) Crystal structures of two tandem malectin-like receptor kinases involved in plant reproduction. *Acta crystallographica Section D, Structural Biology*, **74**, 671–680.

Nei, M. & Kumar, S. (2000) *Molecular evolution and phylogenetics*. USA: Oxford University Press.

Ngou, B.P.M., Ding, P. & Jones, J.D.G. (2022) Thirty years of resistance: zig-Zag through the plant immune system. *The Plant Cell*, **34**, 1447–1478.

Pérez-Mendoza, D., Rodríguez-Carvajal, M., Romero-Jiménez, L., Farias Gde, A., Lloret, J., Gallegos, M.T. *et al.* (2015) Novel mixed-linkage β-glucan activated by c-di-GMP in Sinorhizobium meliloti. *Proceedings of the National Academy of Sciences of the United States of America*, **112**, 757–765.

Pettersen, E.F., Goddard, T.D., Huang, C.C., Couch, G.S., Greenblatt, D.M., Meng, E.C. *et al.* (2004) UCSF chimera?A visualization system for exploratory research and analysis. *Journal of Computational Chemistry*, **25**, 1605–1612.

Pettolino, F., Sasaki, I., Turbic, A., Wilson, S.M., Bacic, A., Hrmova, M. *et al.* (2009) Hyphal cell walls from the plant pathogen Rhynchosporium secalis contain (1,3/1,6)-beta-D-glucans, galacto- and rhamnomannans, (1,3;1,4)-beta-D-glucans and chitin. *The FEBS Journal*, **276**, 3698–3709.

Pfaffl, M.W. (2001) A new mathematical model for relative quantification in real-time RT-PCR. *Nucleic Acids Research*, **29**, e45.

Phillips, J.C. & Hardy, D.J. (2020) Scalable molecular dynamics on CPU and GPU architectures with NAMD. *The Journal of Chemical Physics*, **153**, 44130.

Popper, Z.A. & Fry, S.C. (2003) Primary cell wall composition of bryophytes and charophytes. *Annals of Botany*, **91**, 1–12.

Putarjunan, A., Ruble, J. & Srivastava, A. (2019) Bipartite anchoring of SCREAM enforces stomatal initiation by coupling MAP kinases to SPEECHLESS. *Nature Plants*, **5**, 742–754.

Ranf, S., Eschen-Lippold, L., Pecher, P., Lee, J. & Scheel, D. (2011) Interplay between calcium signalling and early signalling elements during defence responses to microbe- or damage-associated molecular patterns. *The Plant Journal*, **68**, 100–113.

Ranf, S., Grimmer, J., Pöschl, Y., Pecher, P., Chinchilla, D., Scheel, D. *et al.* (2012) Defense-related calcium signaling mutants uncovered via a quantitative high-throughput screen in Arabidopsis thaliana. *Molecular Plant*, **5**, 115–130.

Rebaque, D., del Hierro, I., López, G., Bacete, L., Vilaplana, F., Dallabernardina, P. *et al.* (2021) Cell wall-derived mixed-linked β-1,3/1,4-glucans trigger immune responses and disease resistance in plants. *The Plant Journal*, **106**, 601–615.

Rzhetsky, A. & Nei, M. (1992) A simple method for estimating and testing minimum-evolution trees. *Molecular Biology and Evolution*, **9**, 945.

Saitou, N. & Nei, M. (1987) The neighbor-joining method: a new method for reconstructing phylogenetic trees. *Molecular Biology and Evolution*, **4**, 406–425.

Salmeán, A.A., Duffieux, D., Harholt, J., Qin, F., Michel, G., Czjzek, M. *et al.* (2017) Insoluble (1 → 3), (1 → 4)-β-D-glucan is a component of cell walls in brown algae (Phaeophyceae) and is masked by alginates in tissues. *Scientific Reports*, **7**, 2880.

Sandoval, P.J. & Santiago, J. (2020) In vitro analytical approaches to study plant ligand-receptor interactions. *Plant Physiology*, **182**, 1697–1712.

Schallus, T., Fehér, K., Sternberg, U., Rybin, V. & Muhle-Goll, C. (2010) Analysis of the specific interactions between the lectin domain of malectin and diglucosides. *Glycobiology*, **20**, 1010–1020.

Schallus, T., Jaeckh, C., Fehér, K., Palma, A.S., Liu, Y., Simpson, J.C. *et al.* (2008) Malectin: a novel carbohydrate-binding protein of the endoplasmic reticulum and a candidate player in the early steps of protein N-glycosylation. *Molecular Biology of the Cell*, **19**, 3404–3414.

Schrödinger, L.L.C. (2020) *The PyMOL molecular graphics system, version 2.5*. New York, NY: Schrödinger, LLC.

Shimizu, T., Nakano, T., Takamizawa, D., Desaki, Y., Ishii-Minami, N., Nishizawa, Y. *et al.* (2010) Two LysM receptor molecules, CEBiP and OsCERK1, cooperatively regulate chitin elicitor signaling in rice. *The Plant Journal*, **64**, 204–214.

Smakowska-Luzan, E., Mott, G.A., Parys, K., Stegmann, M., Howton, T.C., Layeghifard, M. *et al.* (2018) An extracellular network of Arabidopsis leucine-rich repeat receptor kinases. *Nature*, **553**, 342–346.

Soejima, Y., Lee, J., Nagata, Y., Mon, H., Iiyama, K., Kitano, H. *et al.* (2013) Comparison of signal peptides for efficient protein secretion in the baculovirus-silkworm system. *Open Life Sciences*, **8**, 1–7.

Sørensen, I., Pettolino, F.A., Wilson, S.M., Doblin, M.S., Johansen, B., Bacic, A. *et al.* (2008) Mixed-linkage (1→3),(1→4)-β-d-glucan is not unique to the Poales and is an abundant component of Equisetum arvense cell walls. *The Plant Journal*, **54**, 510–521.

Souza, C.A., Li, S. & Lin, A.Z. (2017) Cellulose-derived oligomers act as damage-associated molecular patterns and trigger defense-like responses. *Plant Physiology*, **173**, 2383–2398.

Tamura, K., Stecher, G., Peterson, D., Filipski, A. & Kumar, S. (2013) MEGA6: molecular evolutionary genetics analysis version 6.0. *Molecular Biology and Evolution*, **30**, 2725–2729.

Tang, D. & Wang, G. (2017) Receptor kinases in plant-pathogen interactions: more than pattern recognition. *The Plant Cell*, **29**, 618–637.

Tang, W., Lin, W., Zhou, X., Guo, J., Dang, X., Li, B. *et al.* (2022) Mechanotransduction via the pectin-FERONIA complex activates ROP6 GTPase signaling in Arabidopsis pavement cell morphogenesis. *Current Biology*, **32**, 508–517.e503.

Taylor, M., Drickamer, K., Imberty, A., van Kooyk, Y., Schnaar, R., Etzler, M. *et al.* (2022) Discovery and Classification of Glycan-Binding Proteins. In: Varki, A., Cummings, R.D., Esko, J.D. ***et al.*** (Eds.) *Discovery and Classification of Glycan-Binding Proteins*, editors edition. Cold Spring Harbor (NY): Cold Spring Harbor Laboratory Press.

Tseng, Y.-H., Scholz, S.S., Fliegmann, J., Krüger, T., Gandhi, A., Furch, A.C.U. *et al.* (2022) CORK1, a LRR-Malectin receptor kinase, is required for Cellooligomer-induced responses in Arabidopsis thaliana. *Cells*, **11**, 2960.

Tunyasuvunakool, K. & Adler, J. (2021) Highly accurate protein structure prediction for the human proteome. *Nature*, **596**, 590–596.

Versluys, M., Toksoy Öner, E. & Van den Ende, W. (2022) Fructan oligosaccharide priming alters apoplastic sugar dynamics and improves resistance against Botrytis cinerea in chicory. *Journal of Experimental Botany*, **73**, 4214–4235.

Voxeur, A., Habrylo, O., Guénin, S., Miart, F., Soulié, M.C., Rihouey, C. *et al.* (2019) Oligogalacturonide production upon Arabidopsis thaliana-Botrytis cinerea interaction. *Proceedings of the National Academy of Sciences of the United States of America*, **116**, 19743–19752.

Wan, J., He, M., Hou, Q., Zou, L., Yang, Y., Wei, Y. *et al.* (2021) Cell wall associated immunity in plants. *Stress Biology*, **1**, 3.

Wang, B., Qin, X., Wu, J., Deng, H., Li, Y., Yang, H. *et al.* (2016) Analysis of crystal structure of Arabidopsis MPK6 and generation of its mutants with higher activity. *Scientific Reports*, **6**, 25646.

Wanke, A., Rovenich, H., Schwanke, F., Velte, S., Becker, S., Hehemann, J.H. *et al.* (2020) Plant species-specific recognition of long and short β-1,3-linked glucans is mediated by different receptor systems. *The Plant Journal*, **102**, 1142–1156.

Waterhouse, A., Bertoni, M., Bienert, S., Studer, G., Tauriello, G., Gumienny, R. *et al.* (2018) SWISS-MODEL: homology modelling of protein structures and complexes. *Nucleic Acids Research*, **46**, W296–w303.

Willmann, R., Lajunen, H.M., Erbs, G., Newman, M.A., Kolb, D., Tsuda, K. *et al.* (2011) Arabidopsis lysin-motif proteins LYM1 LYM3 CERK1 mediate bacterial peptidoglycan sensing and immunity to bacterial infection. *Proceedings of the National Academy of Sciences of the United States of America*, **108**, 19824–19829.

Wong, J.E.M.M., Gysel, K., Birkefeldt, T.G., Vinther, M., Muszyński, A., Azadi, P. *et al.* (2020) Structural signatures in EPR3 define a unique class of plant carbohydrate receptors. *Nature Communications*, **11**, 3797.

Xiao, Y., Stegmann, M., Han, Z., DeFalco, T.A., Parys, K., Xu, L. *et al.* (2019) Mechanisms of RALF peptide perception by a heterotypic receptor complex. *Nature*, **572**, 270–274.

Yang, C., Liu, R., Pang, J., Ren, B., Zhou, H., Wang, G. *et al.* (2021a) Addendum: Poaceae-specific cell wall-derived oligosaccharides activate plant immunity via OsCERK1 during Magnaporthe oryzae infection in rice. *Nature Communications*, **12**, 3945.

Yang, C., Liu, R., Pang, J., Ren, B., Zhou, H., Wang, G. *et al.* (2021b) Poaceae-specific cell wall-derived oligosaccharides activate plant immunity via OsCERK1 during Magnaporthe oryzae infection in rice. *Nature Communications*, **12**, 2178.

Yang, C., Wang, E. & Liu, J. (2022) CERK1, more than a co-receptor in plant–microbe interactions. *New Phytologist*, **234**, 1606–1613.

Yang, H., Wang, D., Guo, L., Pan, H., Yvon, R., Garman, S. *et al.* (2021) Malectin/Malectin-like domain-containing proteins: a repertoire of cell surface molecules with broad functional potential. *The Cell Surface*, **7**, 100056.

Zang, H., Xie, S., Zhu, B., Yang, X., Gu, C., Hu, B. *et al.* (2019) Mannan oligosaccharides trigger multiple defence responses in rice and tobacco as a novel danger-associated molecular pattern. *Molecular Plant Pathology*, **20**, 1067–1079.

Zarattini, M., Corso, M., Kadowaki, M.A., Monclaro, A., Magri, S., Milanese, I. *et al.* (2021) LPMO-oxidized cellulose oligosaccharides evoke immunity in Arabidopsis conferring resistance towards necrotrophic fungus B. cinerea. *Communications Biology*, **4**, 727.

Zhang, Y. & Skolnick, J. (2005) TM-align: a protein structure alignment algorithm based on the TM-score. *Nucleic Acids Research*, **33**, 2302–2309.

A3

The Cell Surface 11 (2024) 100124

Contents lists available at ScienceDirect

The Cell Surface

journal homepage: www.sciencedirect.com/journal/the-cell-surface

Leucine rich repeat-malectin receptor kinases IGP1/CORK1, IGP3 and IGP4 are required for arabidopsis immune responses triggered by β-1,4-D-Xylo-oligosaccharides from plant cell walls

Patricia Fernández-Calvo [a,1,*], Gemma López [a], Marina Martín-Dacal [a,b], Meriem Aitouguinane [a], Cristian Carrasco-López [a], Sara González-Bodí [a], Laura Bacete [a,b,2], Hugo Mélida [a,3], Andrea Sánchez-Vallet [b], Antonio Molina [a,b,*]

[a] Centro de Biotecnología y Genómica de Plantas, Universidad Politécnica de Madrid (UPM), Instituto Nacional de Investigación y Tecnología Agraria y Alimentaria (INIA/CSIC), Campus de Montegancedo UPM, Pozuelo de Alarcón, Madrid, Spain
[b] Departamento de Biotecnología-Biología Vegetal, Escuela Técnica Superior de Ingeniería Agronómica, Alimentaría y de Biosistemas, UPM, Madrid, Spain

ARTICLE INFO

Keywords:
Arabidopsis thaliana
Cell wall
Disease resistance
Leucine rich repeat-malectin receptor kinases
Pattern triggered immunity
Pseudomonas syringae
Xylans
Xylotetraose

ABSTRACT

Pattern-Triggered Immunity (PTI) in plants is activated upon recognition by Pattern Recognition Receptors (PRRs) of Damage- and Microbe-Associated Molecular Patterns (DAMPs and MAMPs) from plants or microorganisms, respectively. An increasing number of identified DAMPs/MAMPs are carbohydrates from plant cell walls and microbial extracellular layers, which are perceived by plant PRRs, such as LysM and Leucine Rich Repeat-Malectin (LRR-MAL) receptor kinases (RKs). LysM-RKs (e.g. CERK1, LYK4 and LYK5) are needed for recognition of fungal MAMP chitohexaose (β-1,4-D-$(GlcNAc)_6$, CHI6), whereas IGP1/CORK1, IGP3 and IGP4 LRR-MAL RKs are required for perception of β-glucans, like cellotriose (β-1,4-D-$(Glc)_3$, CEL3) and mixed-linked glucans. We have explored the diversity of carbohydrates perceived by *Arabidopsis thaliana* seedlings by determining PTI responses upon treatment with different oligosaccharides and polysaccharides. These analyses revealed that plant oligosaccharides from xylans [β-1,4-D-$(xylose)_4$ (XYL4)], glucuronoxylans and α-1,4-glucans, and polysaccharides from plants and seaweeds activate PTI. Cross-elicitation experiments of XYL4 with other glycans showed that the mechanism of recognition of XYL4 and the DAMP 3^3-α-L-arabinofuranosyl-xylotetraose (XA_3XX) shares some features with that of CEL3 but differs from that of CHI6. Notably, XYL4 and XA_3XX perception is impaired in *igp1/cork1, igp3* and *igp4* mutants, and almost not affected in *cerk1 lyk4 lyk5* triple mutant. XYL4 perception is conserved in different plant species since XYL4 pre-treatment triggers enhanced disease resistance in tomato to *Pseudomonas syringae* pv *tomato* DC3000 and PTI responses in wheat. These results expand the number of glycans triggering plant immunity and support IGP1/CORK1, IGP3 and IGP4 relevance in *Arabidopsis thaliana* glycans perception and PTI activation.

Significance Statement: The characterization of plant immune mechanisms involved in the perception of carbohydrate-based structures recognized as DAMPs/MAMPs is needed to further understand plant disease resistance modulation. We show here that IGP1/CORK1, IGP3 and IGP4 LRR-MAL RKs are required for the perception of carbohydrate-based DAMPs β-1,4-D-$(xylose)_4$ (XYL4) and 3^3-α-L-arabinofuranosyl-xylotetraose (XA_3XX), further expanding the function of these LRR-MAL RKs in plant glycan perception and immune activation.

* Corresponding authors at: Centro de Biotecnología y Genómica de Plantas, Universidad Politécnica de Madrid UPM) - Instituto Nacional de Investigación y Tecnología Agraria y Alimentaria (INIA/CSIC).
E-mail addresses: pfcalvo@mbg.csic.es (P. Fernández-Calvo), antonio.molina@upm.es (A. Molina).
[1] Current address: Misión Biológica de Galicia, Consejo Superior de Investigaciones Científicas (CSIC).
[2] Current address: Umea Plant Science Center, Umea University, Sweden.
[3] Current address: Área de Fisiología Vegetal, Departamento de Ingeniería y Ciencias Agrarias, Universidad de León, León, Spain.

https://doi.org/10.1016/j.tcsw.2024.100124
Received 22 February 2024; Received in revised form 3 April 2024; Accepted 3 April 2024
Available online 4 April 2024

Introduction

Plants have a complex immune system that comprises several layers of defence that function cooperatively to confer broad-spectrum disease resistance to pathogens and pests (Ngou et al., 2022). One of these plant immunity layers is the so-called Pattern-Triggered Immunity (PTI). PTI is based on the recognition of Damage- and Microbe-Associated Molecular Patterns (DAMPs and MAMPs) derived from plants or microorganisms, respectively, by plant plasma membrane-resident Pattern Recognition Receptors (PRRs) (Nguyen et al., 2021) PRRs are modular proteins that harbour an extracellular Ectodomain (ECD) connected to a transmembrane domain (TMD), as it occurs in Receptor-Like proteins (RLPs). Some PRRs (i.e. Receptor Kinases or RKs) can also have, in addition to ECD and TMD, a cytoplasmic kinase domain (KD) (del Hierro et al., 2021). Upon DAMP/MAMP recognition by the specific ECD-PRR, the formation of an active PRR complex with additional co-receptor proteins (e.g., RKs or RLPs) occurs leading to the activation of protein kinase signalling cascades [e.g. involving Mitogen-Activated Protein Kinases (MPKs) or Calcium-Dependent Protein Kinases (CDPKs)], which in turns trigger gene reprogramming and disease resistance responses (Bigeard et al., 2015; Boutrot and Zipfel, 2017). The importance of PTI in plant defence is illustrated by the fact that disease resistance to pathogens is compromised in plants defective in PRRs and/or in their counterpart co-receptors. For example, *Arabidopsis thaliana* mutants impaired either in FLS2 RK, which is the PRR recognizing bacterial flg22 MAMP peptide through its Leucine-Rich Repeats (LRR) ECD, or in its LRR-RK co-receptor BAK1, are more susceptible to bacterial pathogens (Gómez-Gómez and Boller, 2000; Kemmerling et al., 2007). Similarly, *Arabidopsis thaliana* mutants impaired in LysM-RKs CERK1, LYK5 or LYK4, which are required for the perception of chitin oligosaccharides (e.g. β-1,4-D-$(GlcNAc)_{6\text{-}8}$, CHI6-CHI8) from fungal walls, have been described to be slightly more susceptible to fungal pathogens (Miya et al., 2007; Cao et al., 2014). PTI has been shown recently to cooperate in disease resistance with Effector Trigger Immunity (ETI) which is activated upon recognition of effector molecules from pathogens by cytoplasmic plant receptors (Yuan et al., 2021). Some of the pathogens' virulence effectors target PTI components to interfere with plant immune activation and/or to block up/hinder the crosstalk between ETI-PTI defensive responses (Yuan et al., 2021; Ngou et al., 2022).

Many PRR/peptidic DAMP/MAMP pairs triggering PTI have been characterized (Boutrot and Zipfel, 2017; Tang and Wang, 2017; Hou et al., 2019; Tanaka and Heil, 2021). In addition to peptidic ligands, plant PRRs can recognize and bind DAMPs/MAMPs of different biochemical nature like carbohydrates, lipids and other molecules (Boutrot and Zipfel, 2017; Tang and Wang, 2017). The number of carbohydrate-based DAMPs and MAMPs that have been described to be recognized by the plant immune system has increased in the last few years. However, our knowledge of the specific mechanisms of plant defence activation by carbohydrate-based ligands is behind our understanding of peptide ligands (DAMPs/MAMPs) recognition by plant PRRs (Bacete et al., 2018; Lee and Santiago, 2023). Oligosaccharide structures present in plant cell walls and microbial extracellular layers are quite diverse and can be released or modified by the activity of cell wall degrading or modifying enzymes (CWDEs) from microorganisms that target plant wall polysaccharides, or by the activity of plant enzymes that target plant and/or microbial walls/extracellular layers (aKraemer et al., 2021; Chandrasekar et al., 2022). Despite the potential diversity of glycan structures in nature that can be perceived as DAMPs/MAMPs by plants, only a few ones have been characterized so far. Among glycans perceived by plants, and in particular by *Arabidopsis thaliana*, are chitin oligosaccharides (chitohexaose, CHI6), linear β-1,3-glucans (i.e. laminarinhexaose), β-1,3-glucans with β-1,6-glucan branches, and β-1,6-glucan oligosaccharides from fungal/oomycete cell walls and peptidoglycan from bacterial walls (Klarzynski et al., 2000; Kaku et al., 2006; Aziz et al., 2007; Gust et al., 2007; Mélida et al., 2018; Wanke et al., 2020; Chaube et al., 2022). Also, plant immune system perceives oligosaccharides derived from plant cell walls polymers (DAMPs) like cellulose [β-1,4-glucan; β-1,4-D-$(Glc)_{3\text{-}5}$ or CEL3-CEL5], mixed-linked glucans [MLGs: β-1,4-D-$(Glc)_2$-β-1,3-D-Glc (MLG43), β-1,4-D-$(Glc)_3$-β-1,3-D-Glc (MLG443)], xyloglucans, xylans, mannans, arabinoxylans (e.g. 3^3-α-L-arabinofuranosyl-xylotetraose or XA_3XX) and homogalacturonans [e.g. oligogalacturonides (OGs) like $GalA_3$] (Klarzynski et al., 2000; Kaku et al., 2006; Aziz et al., 2007; Galletti et al., 2008; Claverie et al., 2018; Voxeur et al., 2019; Zang et al., 2019; Mélida et al., 2020; Malivert et al., 2021; Rebaque et al., 2021; Moussu et al., 2023; Pring et al., 2023). Moreover, some additional plant sugars that are not present in plant cell walls, like fructans, are perceived by plant cells and trigger signalling responses (Dobrange et al., 2019; Benkeblia, 2020), and some seaweed glycan structures of high molecular weight, like sulfated fucans (fucoidans) and alginates, have been also shown to active defensive responses in some plant species (Klarzynski et al., 2000; Aitouguinane et al., 2020; Aitouguinane et al., 2023; Wang et al., 2023).

In plants, PRR/carbohydrate ligand characterization at the structural level has been mainly restricted to PRRs of the LysM-RK family, which harbour ECDs with three LysM domains and have been involved in the recognition of several DAMPs/MAMPs including chitin oligomers (CHI6-CHI8), peptidoglycans, lipopolysaccharides, and lipochitooligosaccharides (MYC and Nod factors triggering symbiosis). LysM-RKs are also required for the perception of MLGs and β-1,3-glucan oligosaccharides (Miya et al., 2007; Willmann et al., 2011; Liu et al., 2012; Cao et al., 2014; Desaki et al., 2018; Mélida et al., 2018; Wanke et al., 2020). Specifically, β-1,3-glucan hexasaccharide (LAM6), MLG43 and MLG443 are immune-active structures whose recognition depends on *Arabidopsis thaliana* LysM-PRR CERK1 (Chitin Elicitor Receptor Kinase 1) (Mélida et al., 2018; Rebaque et al., 2021). However, direct binding of LAM6 and/or MLG43 to CERK1 ECD has not been either observed in Isothermal Titration Calorimetry (ITC) binding assays performed with purified ECD-CERK1 or predicted using *in silico* structural molecular dynamics simulations (del Hierro et al., 2021). Similarly, rice LysM RKs have been described to be required for the perception and binding of CHI6 and MLGs (e.g. MLG43) (Yang et al., 2021a). In addition to LysM-RKs, some Wall Associated Kinases (WAKs) and Malectin-Like RKs (e.g. FERONIA, FER) have been involved in the activation of adaptative response triggered by pectin-derived oligosaccharides, though a direct binding of the corresponding $GalA_n$ glycans to their ECDs has not been demonstrated (Malivert et al., 2021; Moussu et al., 2023). Recently, Dai and colleagues (2023) reported that the Lectin-RK OsLecRK1 is required to perceive MLGs in rice, and that OsLecRK1 produced in bacteria binds *in vitro* MLGs, but the corresponding ortholog has not been identified in *Arabidopsis thaliana* yet.

In addition to these RKs involved in oligosaccharides perception, several *Arabidopsis thaliana* RKs with Leucine-Rich-Repeat (LRR) and Malectin (MAL) domains in their ECDs have been recently characterized as components of novel recognition mechanisms for both cellulose and MLG-derived oligosaccharides (Tseng et al., 2022; Martín-Dacal et al., 2023). Several *Arabidopsis thaliana* mutants *i*mpaired in *g*lycan *p*erception (*igp; igp1-igp7*) were isolated in genetic screening to identify proteins (e.g. PRRs) required for immune activation triggered by MLG43 and CEL3, but not by CHI6 (Martín-Dacal et al., 2023). *igp1, igp3* and *igp4* were found to be altered in three LRR-MAL RKs [AT1G56145 (IGP1/CORK1 (Cello Oligosaccharide Receptor Kinase 1), AT1G56130 (IGP2/IGP3), and AT1G56140 (IGP4)] (Martín-Dacal et al., 2023). The ECD of IGP1 binds CEL3 and CEL5, but not MLG43 in ITC assays, supporting IGP1′s function as a PRR for cellulose oligosaccharides recognition and probably as a co-receptor for MLG43 perception (Martín-Dacal et al., 2023). LRR-MAL RK family comprises 13 putative members in *Arabidopsis thaliana*, with some of them involved in the regulation of pollen migration and fertility (Bordeleau et al., 2022; Lee and Santiago, 2023; Liu et al., 2024).

The potential diversity of oligosaccharide structures that are present in plant cell walls and extracellular layers of microorganisms is quite high (Wanke et al., 2020). However, only a few structures have been

demonstrated to be recognized as DAMPs/MAMPs by plants. To further characterize novel carbohydrate-based structures (MAMPs or DAMPs) perceived by plants, we tested the ability of different oligosaccharide structures to trigger early PTI responses in *Arabidopsis thaliana*. We show that oligosaccharides derived from plant polysaccharides like xylans, glucuronoxylans, arabinogalactans, and maltose-based glucans are perceived by the *Arabidopsis thaliana* immune system. Notably, we demonstrate that perception of DAMPs containing β-1,4-D-(xylose)$_n$, like XYL4 and XA$_3$XX (Mélida et al., 2020), is impaired in *igp1/cork1, igp3* and *igp4* mutants, further expanding the function of these LRR-MAL RKs beyond β-glucan perception in plants. This work expands the diversity of characterized glycans perceived as DAMPs by plants and supports the relevance of IGP1, IGP3 and IGP4 LRR-MAL RKs in plant immunity.

Material and methods

Biological material and growth conditions

Arabidopsis thaliana lines used in this study were in the Columbia-0 (Col-0) background. The following *Arabidopsis thaliana* plants carrying the calcium reporter aequorin were used for cytoplasmic calcium (cyt Ca^{2+}) measurements: Col-0^{AEQ} (Knight et al., 1991), *cerk1-2*^{AEQ} (Ranf et al., 2012), and *igp1*^{AEQ}, *igp3*^{AEQ} and *igp4*^{AEQ} (Martín-Dacal et al., 2023). The *cerk1-2 lyk4-1 lyk5-1* triple mutant used was previously obtained in the lab (Martín-Dacal et al., 2023). For MAPKs phosphorylation and gene expression analyses Col-0 wild-type (WT) and mutant seedlings were grown in 24-well plates (~10 seedlings per well) under long-day conditions (16 h of light: 8 h of darkness) at 19–21 °C in liquid ½ MS medium with 1 % saccharose. Tomato plants (*Solanum lycopersicum,* Moneymaker) were grown in the greenhouse in a mixture of soil and vermiculite (3:1) at under 14 h of light/10 h of dark at 24–22 °C. Wheat plants (*Triticum aestivum* cultivar Titlis) were grown in greenhouse in soil-vermiculite (3:1) at under 14 h of light/10 h of dark at 24–19 °C.

Carbohydrates and peptides used in the experiments

Hexaacetyl-chitohexaose (CHI6; β-1,4-D-(GlcNAc)$_6$; #O-CHI6), CEL3 (β-1,4-D-(Glc)$_3$; O-CTR), xylobiose (XYL2), xylotriose (XYL3), 2^3–(4-O-Methyl-α-D-Glucuronyl)-xylotetraose (XUXX), α-D-Maltotetraose (MAL4), XA$_3$XX, and 6^3-α-D-Maltotriosyl-maltotriose (MAL3$_2$) were purchased from Megazyme (Wicklow, Ireland). β-1,4-D-Xylotetraose (XYL4) was purchased both from Megazyme (0-XTE) (Wicklow, Ireland) and Cymit Química (Barcelona, Spain). The peptide flg22 was synthesized by Abyntek (Zamudio, Spain). Oligosaccharides/polysaccharides used in the experiments are summarized in Table S1.

β-1,6-D-glucan oligosaccharides were purified from commercial pustulan polysaccharide (InvivoGen #tlrl-pst) as detailed below. Fifty mg of pustulan was added to 25 mL of 0.2 N HCl and incubated at 100 °C for 8 h. Afterwards, hydrolysates were cooled down and neutralized by adding an equal volume of 0.2 N NaOH. Digestion products were desalted and pre-purified using a Sephadex G-10 column (90 cm^3 bed-volume in a 1.5 cm diameter column; Merck) and size-fractionated using a Biogel P2 Extrafine column (140 cm^3 bed-volume in a 1.6 cm diameter column; BioRad). Columns were connected to a Biologic-LP instrument, distilled water was used as the mobile phase and the flow rates were 0.24 mL/min. Purified oligosaccharides were monitored by high-performance liquid chromatography (HPLC). The oligosaccharides were injected into an Agilent 1200 Series HPLC equipped with an Agilent 6130 quadrupole mass spectrometer (MS) and an Agilent 1200 Evaporative Light Scattering Detector (ELSD). The purified oligosaccharides were separated on a graphitized carbon Hypercarb column (150 x 4.6 mm, Thermo Scientific) using a water (including 0.1 % formic acid)-acetonitrile (ACN) gradient. The peaks in the ELSD traces were assigned based on their retention time and the corresponding masses in the MS. For additional MS analyses, a fraction of each oligosaccharide sample was injected directly into an Agilent 1260 Infinity II Series, LC/MSD XT (Single Quadrupol mit ESI-Jetstream-source).

Polysaccharides from different sources were also examined, including alginate from brown algae (Thermo Fisher Scientific; CAS: 9005-38-3; (C6H7O7)a(C6H7O7)bNa; Geel, Belgium), fucoidan from *Undaria pinnatifida* (Sigma-Aldrich; CAS:9072-19-9; Saint Louis, USA) and arabinogalactan from Larch Wood (TCI; CAS: 9036-66-2; [(C5H8O4)(C6H10O5)6]x; Tokyo, Japan). Alginate was applied at 0.5 g/L, fucoidan at 3 g/L, and arabinogalactan at 0.33 g/L.

Aequorin luminescence measurements and cross-elicitation experiments

Arabidopsis thaliana Col-0^{AEQ} 8-day-old seedlings grown in liquid medium were used for cytoplasmic calcium (cyt Ca^{2+}) measurements using the method previously described (Bacete et al., 2017). Negative controls (water = mock) were included in all the experiments. The elevation of cytoplasmic calcium concentration was measured as relative luminescence units (RLU) of aequorin luminescence with a Varioskan Lux Reader (Thermo Scientific) as described previously (Mélida et al., 2018). Cross-elicitation during the refractory period of calcium signaling upon the sequential application of two different compounds (e.g. XYL4-CEL3, XYL4-XA3XX, XYL4-CHI6, and vice versa), as well as XYL4-XYL4 (positive control), and XYL4-water (negative control) were performed as previously described (Rebaque et al., 2021).

Immunoblot analysis of MPKs activation

Twelve-day-old *Arabidopsis thaliana* seedlings from different genotypes grown on liquid MS medium in 24-well plates were treated with water (mock) and different oligosaccharides for 0, 10 and 20 min, and then harvested in liquid nitrogen. Seedlings were homogenized using FastPrep Bead Beating Systems (MP Biomedicals) in extraction buffer (50 mM Tris-HCl pH 7.5, 200 mM NaCl, 1 mM EDTA, 10 mM NaF, 2 mM sodium orthovanadate, 1 mM sodium molybdate, 10 % (v/v) glycerol, 0.1 % (v/v) Tween-20, 1 mM 1,4-dithiothreitol, 1 mM phenylmethylsulfonyl fluoride, and phosphatase inhibitor cocktail P9599 (Sigma)). Total protein extracts were quantified by Bradford assay (Bio-Rad). Equal amounts of proteins were separated on Mini-PROTEAN TGX, 10 %, 10-well, 30 μL (Bio-Rad) gel and transferred to PVDF membranes using Invitrogen™ iBlot™ 2 Gel Transfer Device. Membranes were blocked with Protein-Free (TBS) Blocking Buffer (Thermo Scientific; Pierce) for 2 h at room temperature. Membranes were incubated overnight at 4 °C in TBS containing Phospho-p44/42 MAPK (Erk1/2) (Thr202/Tyr204) antibody (Cell Signaling Technology) (1:1000) or Anti-AtMPK3 (1:2500) (Sigma-Aldrich). The latest was used as an internal control for protein loading. Membranes were cleaned fourth with TBS containing 0.1 % Tween-20 and incubated with horseradish peroxidase-conjugated anti-rabbit antibody (GE-Healthcare) (1:5000) in TBS. Membranes were cleaned again and revealed by ECL Western Blotting Substrate (Thermo Scientific; Pierce) and detected using iBright FL1000 Image System (ThermoFisher Scientific). Finally, the membranes were stained with Ponceau-S Red (Sigma Aldrich) to ensure the presence of proteins in all the lanes. Western experiments were repeated at least twice.

Gene expression analyses

For gene expression analysis (qRT-PCR and RNA sequencing), 12-day-old *Arabidopsis thaliana* seedlings grown on liquid MS medium were treated with oligosaccharides or water (mock) for 30 min. Total RNA was purified with the RNeasy Plant Mini Kit (Qiagen) according to the manufacturer's protocol. qRT-PCR analyses were performed as previously reported (Bacete et al., 2017). *UBC21* (*At5g25760*) expression was used to normalize the transcript level in each reaction. The forward and reverse sequences of the oligonucleotides used to monitor gene expression levels of *WRKY53* (*At4g23810*), *CYP81F2* (*At5g57220*) and *UBC21* (*At5g25760*) are:

WRKY53: 5́-CACCAGAGTCAAACCAGCCATTA-3́/5́-CTTTACCATCATCAAGCCCATCGG-3́;

CYP81F2: 5́-TATTGTCCGCATGGTCACAGG-3́/5́-CCACTGTTGTCATTGATGTCCG-3́;

UBC21: 5́-GCTCTTATCAAAGGACCTTCGG-3́/5́-CGAACTTGAGGAGGTTGCAAAG-3́.

For RNA-seq analyses, samples from three biological replicates for each treatment were sequenced using 50 bp Illumina Hiseq 2500. RNA-seq read data can be retrieved from the NCBI Sequence Read Archive (SRA) under BioProject accession ID PRJNA625401 (BioSample accession SAMN15682114). The initial quality control of sequencing data was evaluated using FastQC (v0.11.9) (Andrews, 2010) and multiqc (v1.7) (Ewels et al., 2016). This data was then used to filter sequences with the Trimmomatic tool (v0.36) (Bolger et al., 2014). For each sample, RNA-seq raw reads (paired-end, 150 bp) were trimmed to remove potential Illumina adaptor contamination, followed by read trimming and clipping of low-quality bases. The remaining reads were aligned to the *Arabidopsis thaliana* TAIR10 reference genome, using the Araport11 annotation (Cheng et al., 2017) with the STAR aligner (v2.5.3a) (Dobin et al., 2013) and specific command-line parameters: –outFilterMultimapNmax 20 –alignSJoverhangMin 8 –alignSJDBoverhangMin 8 –outFilterMismatchNmax 8 –alignIntronMin 35 –alignMatesGapMax 100,000 –alignIntronMax 20,000. HTSeq (v1.99.2) (Anders et al., 2010) was used with the intersection 'union' option to generate the read counts per gene, based on the RNA-seq mapped reads and the Araport11 annotation. Normalization and statistical analyses of differential gene expression were performed with the DESeq2 Bioconductor package in R (Love et al., 2014). Genes were considered differentially expressed (DEGs), as either up or down regulated, if they had a log2-fold change [log2-FC] > 0.58 with an adjusted P value ≤ 0.05. The lists of DEGs generated from DESeq2 were used to perform functional enrichment analysis against the biological process subset of the gene ontology (GO) using the 'enrichGO' function of the R package clusterProfiler (v4.2.2) (Wu et al., 2021). GO terms were considered overrepresented if their False Discovery Rate (FDR) were $\leq$ 0.05. Redundant GO terms were removed using 'simplify' function from clusterProfiler with z score cutoff of 0.5. Figures of enrichment analysis were generated by ggplot2 package (v3.4.4) (Wickham, 2016).

Tomato disease resistance assays

Tomato plants (*S. lycopersicum* Moneymaker) were grown in a greenhouse in soil-vermiculite (3:1) under 14 h of light/10 h of dark at 24–22 °C. The third and fourth leaves of three-week-old plants were sprayed with 2 mL of an XYL4 solution (450 μM) in water containing 0,1% Tween 20 (Sigma) as an adjuvant. The adjuvant solution in water was used as a mock. *Pseudomonas syringae* pv. *tomato* DC3000 infections were performed 48 h after pre-treatments according to (Santamaría-Hernando et al., 2019) Briefly, plants were sprayed with a suspension of the bacterium (10^8 cfu/ml), and two tomato leaf discs were collected from 4 different plants at 0- and 7 days post-infection (dpi). Colony forming units (cfu) per foliar area were determined after plating serial dilutions onto KB plates with rifampicin (25 μg/ml).

Determination of reactive oxygen species (ROS) production in wheat

Disks (12.6 mm2) from second leaves of 14-day-old wheat plants were pre-treated with 100 μL of 150 nM Luminol L-012 (FUJIFILM Wako Pure Chemical Corporation, 120–04891) and 15 μg/mL Peroxidase from horseradish (Sigma-Aldrich, P6782). After 16 h incubation in the dark at 15 °C, 50 μL of 750 μM XYL4, 3 μM flg22 or H_2O (control/mock) were added, and luminescence was measured using Varioskan Lux (Thermo Scientific). Eight leaf discs per treatment were used in each experiment. The experiment was performed three times independently.

Results

A diverse set of oligosaccharides trigger calcium influxes in Arabidopsis thaliana

We used the Aequorin-based cytoplasmic Ca^{2+} (Col-0^{AEQ}) sensor *Arabidopsis thaliana* system (Knight et al., 1991; Martín-Dacal et al., 2023) to expand our knowledge on plant/microbial/seaweed oligosaccharides that are perceived by the plant immune system. We measured early cytoplasmic Ca^{2+} influxes (burst) in Col-0^{AEQ} seedlings upon treatment with different oligo- and polysaccharides. Oligosaccharides tested were molecules derived from plant polysaccharides such as xylans (e.g. β-1,4-D-Xylotetraose or XYL4), glucuronoxylans (2^3–(4-O-Methyl-α-D-Glucuronyl)-xylotetraose or XUXX), and α-1,4-glucans (α-1,4-D-Glc based maltodextrins: α-D-Maltotetraose (MAL4) and 6^3-α-D-Maltotriosyl-maltotriose ($MAL3_2$)). We found that XYL4 and XUXX triggered Ca^{2+} bursts with different kinetics (Fig. 1A). XYL4 promotes a very fast Ca^{2+} burst in Col-0^{AEQ}, whereas the pentasaccharide XUXX triggered a Ca^{2+} burst similar to that of CHI6 (Fig. 1A). MAL4 and $MAL3_2$ also elicited a weak, but reproducible Ca^{2+} burst in Col-0^{AEQ} seedlings (Fig. 1A), indicating that *Arabidopsis thaliana* can perceive α-1,4-glucan-derived oligosaccharides in addition to the previously described β-glucan-derived ones (Mélida et al., 2018; Rebaque et al., 2021; Martín-Dacal et al., 2023).

To validate PTI activity of XYL4, XUXX, MAL4 and $MAL3_2$, we next monitored the phosphorylation levels of the protein kinases MPK3, MPK6, MPK4 and MPK11 and the up-regulation of PTI-associated genes (*CYP81F2* and *WRKY53*) upon treatment of *Arabidopsis thaliana* Col-0 wild-type seedlings with these active glycans. Western-blot assays confirmed MPK3- and MPK6-phosphorylation upon application of XYL4 (250 μM) to Col-0 seedlings, with the maximum phosphorylation levels reached at 20 min post-treatment (Fig. 1B). MPKs phosphorylation triggered by XYL4 was weaker than those observed after treatment with CHI6 included for comparison (Fig. 1B). MPK4/11-phosphorylation was almost not-detectable in XYL4-treated plants, which contrasted with the observed phosphorylation of these MPKs in Col-0 plants upon CHI6 treatment (Fig. 1B). MAL4 triggered MPKs phosphorylation to a similar level than XYL4 (Fig. 1B), whereas XUXX and $MAL3_2$ triggered weaker MPKs phosphorylation than XYL4 (Fig. 1B). Expression of two PTI-marker genes (*WRKY53* and *CYP81F2*), that are up-regulated by several glycans (Mélida et al., 2018), was assessed by qRT-PCR in *Arabidopsis thaliana* Col-0 seedlings 30 min after treatment with these oligosaccharides or with water (mock). Of note, we found that these two genes were up regulated after treatment with the four analysed glycans (Fig. 1C). The level of up-regulation of *WRKY53* and *CYP81F2* upon XYL4 or MAL4 treatment was very similar to those observed after CHI6 treatment (Fig. 1C), whereas XUXX and $MAL3_2$ triggered weaker up-regulation of these marker genes (Fig. 1C), which is in line with the faint phosphorylation of MPK bands observed in Western blot analyses (Fig. 1B). These results further indicated that XUXX and $MAL3_2$ are not very active DAMPs in *Arabidopsis thaliana*.

To expand the list of active oligosaccharides triggering PTI in *Arabidopsis thaliana*, we also measured early cytoplasmic Ca^{2+} influxes (burst) in Col-0^{AEQ} seedlings upon treatment with additional glycans/polysaccharides with distinct composition/structure. We tested the effect on Ca^{2+} influxes of purified β-1,6-D-$(Glc)_{3-4}$ oligosaccharides from bacterial pustulan (Fig. S1A, and different polysaccharides from plants (arabinogalactans) and seaweed (fucoidan and low molecular weight alginates). We purified β-1,6-D-(Glc) oligosaccharides with different Degree of Polymerization [DP: β-1,6-D-$(Glc)_{3-4}$; Fig. S1A] and demonstrated that they triggered weak Ca^{2+} burst and MPK phosphorylation (Fig. S1B, C), further confirming that plants perceive β-1,6 glucan structures (Chaube et al., 2022) in addition to lineal β-1,3 and branched β-1,3/β-1,6 glucans, which are present in laminarin and some fungal cell wall glycans (Mélida et al., 2018; Wanke et al., 2020; Wanke et al., 2023). Moreover, we found that arabinogalactans, fucoidans, and

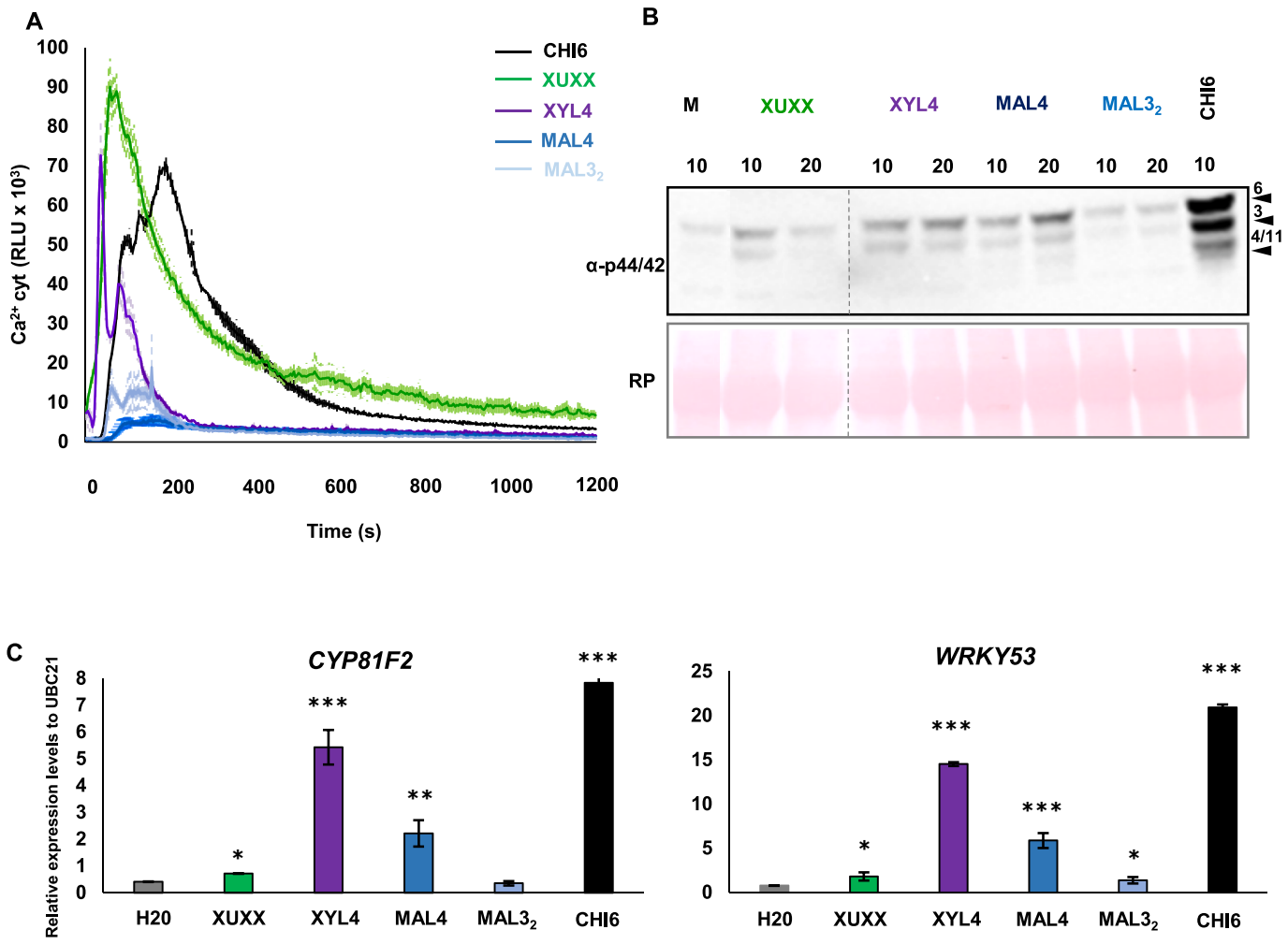

Fig. 1.

Fig. 1. Xylotetraose (XYL4) activates immune hallmarks in *Arabidopsis thaliana*. (A) Cytoplasmic calcium (cyt Ca^{2+}) influx was measured as relative luminescence units (RLU) over time in 8-days-old *Arabidopsis* Col-0 ^{AEQ} (WT) treated with 250 μM of candidate oligosaccharides: 2^3-(4-O-Methyl-α-D-Glucuronyl)-xylotetraose (XUXX), β-1,4-D-Xylotetraose (XYL4), α-D-Maltotetraose (MAL4), 6^3-α-D-Maltotriosyl-maltotriose ($MAL3_2$) and chitin (CHI6, 50 μM). (B) Phosphorylation of mitogen-activated protein kinases (MPKs) analysed by Western-blot (WB) in seedlings treated with the indicated compounds or water (mock) and harvested at 10 and 20 min after treatment application. Dotted lines indicate that bands were cut from the membrane to relocate them in proper order. (C) PTI-related gene expression (*CYP81F2* and *WRKY53*) measured by RT-quantitative PCR at 30 min after compound application. Similarly, water-treated seedlings were analysed as negative controls. Data represent (A) the mean ± error standard (n = 8) of a representative experiment, (B) representative WB out of two independent experiments performed, and (C) the mean ± error standard (n = 3) of three independent experiments. Statistically significant differences between compound-treated plants versus mock-treated (M, H_2O) were calculated according to Student's *t*-test (*P < 0.05, **0.01 < P > 0.001, ***P < 0.001).

alginates induced Ca^{2+} bursts, though these responses were observed only at very high concentrations (mM level) of these compounds (Fig. S2A). Hence our data confirmed the previously described elicitor activity of fucoidans and alginates in different plant species (Klarzynski et al., 2000; Aitouguinane et al., 2020; Aitouguinane et al., 2023; Wang et al., 2023) and highlighted the appropriateness of *Arabidopsis thaliana* as a suitable system to study the mechanisms of perception of these glycans and the PRRs involved in their recognition.

Mechanism of perception of XYL4 share some components with those of CHI6, CEL3 and XA_3XX

Provided that XYL4 triggered a strong and consistent response in Ca^{2+} input, gene expression levels and MAPK phosphorylation, we further determine the specificity of PTI responses triggered by XYL4 and decipher its mechanism of perception by *Arabidopsis thaliana*. We performed cross-elicitation experiments, using Col-0^{AEQ} seedlings, treated with XYL4, CEL3 CHI6, and the DAMP arabinoxylan-derived pentasaccharide XA_3XX previously described (Mélida et al., 2020). In these experiments, we measured Ca^{2+} burst in Col-0^{AEQ} seedlings after the sequential application of different glycans (Mélida et al., 2020; Rebaque

et al., 2021). As shown in control treatment XYL4-XYL4, a total reduction of second Ca^{2+} burst (refractory response) was observed upon the second treatment of plants with XYL4, showing an RLU kinetic that was similar to that of XYL4-H_2O control treatment (Fig. 2A, B). Remarkably, a strong refractory response was observed in the XYL4-CEL3 combination (Fig. 2C), which was similar to that of XYL4-XYL4 treatment (Fig. 2 A). Still, the intensity of CEL3 Ca^{2+} burst is stronger than that of XYL4 and accordingly sequential application of XYL4-CEL3 did not completely abolish CEL3 triggered Ca^{2+} burst in contrast to CEL3-XYL4 sequential application (Fig. 2C). Of note, these results suggest that the mechanisms of recognition of XYL4 overlap with those of CEL3, which involve the recently characterized IGP1/IGP3/IGP4 LRR-MAL RKs (Martín-Dacal et al., 2023). In contrast, a weak refractory response (reduction of Ca^{2+} burst) was observed when XYL4 and CHI6 were sequentially applied to Col-0^{AEQ} seedlings (Fig. 2D), suggesting that the mechanisms of perception of XYL4 and CHI6 are not identical, but might share some LysM-RK components (Fig. 2B). Notably, Col-0^{AEQ} seedlings showed strong refractory responses when XYL4-XA_3XX were combined (Fig. 2E), but the observed reduction of Ca^{2+} burst was not total in comparison to that observed in the control experiments (XYL4-XYL4: Fig. 2A). Additionally, these data indicated that XYL4 shares some receptor components required for XA_3XX perception, that have not been yet identified. Together these data suggest that β-1,4-D-Xyl-based oligosaccharides (i.e. XYL4 and XA_3XX) and oligosaccharides with β-1,4-D-Glc bonds (i.e. CEL3 and MLG43) might share some perception mechanisms.

The mechanism of XYL4 perception in Arabidopsis thaliana depends on IGP1/IGP3/IGP4 LRR-MAL RKs

To further unravel the perception mechanism of XYL4 in *Arabidopsis thaliana* we tested XYL4-mediated cytoplasmic Ca^{2+} burst in *igp1*^{AEQ}, *igp3*^{AEQ} and *igp4*^{AEQ} mutant lines. *igp1*^{AEQ} is impaired in IGP1/CORK1, the probed PRR pair for CEL3/CEL5 DAMPs ((Martín-Dacal et al., 2023). Likewise, *igp3*^{AEQ} and *igp4*^{AEQ} are defective in IGP3 and IGP4 RKs that might function as co-PRRs in CEL3/CEL5 perception. These three LRR-MAL RKs are also required for MLG43 perception (Martín-Dacal et al., 2023). We monitored early cytoplasmic Ca^{2+} influx (burst) in these mutants upon XYL4 treatment and found that Ca^{2+} influx in *igp3*^{AEQ} and *igp4*^{AEQ} lines was fully impaired upon XYL4 treatment, whereas in *igp1*^{AEQ} plants a significant reduction of the burst was observed in comparison to Col-0^{AEQ} plants (Fig. 3A), as observed previously for CEL3 and MLG43 perception (Martín-Dacal et al., 2023). Next, we tested MPKs phosphorylation by western blot in *igp1*^{AEQ}, *igp3*^{AEQ,} and *igp4*^{AEQ} lines and Col-0^{AEQ} plants upon XYL4 treatment in comparison with CHI6- and mock-treated plants. We found that MPKs phosphorylation levels were weaker in the *igp1*^{AEQ}, *igp3*^{AEQ,} and *igp4*^{AEQ} mutants than in Col-0^{AEQ} plants upon XYL4 treatment, whereas phosphorylation triggered by CHI6 was not significantly affected in these *igp* mutants, as reported [Fig. 3B; (Martín-Dacal et al., 2023)]. This prompted us to also test the up-regulation of two PTI marker genes (i.e. *CYP81F2* and *WRKY53*) upon XYL4 treatment in *igp* mutants and Col-0 wild-type plants. We found that up-regulation of such genes was also impaired in *igp* mutants in comparison to Col-0 plants (Fig. 3C). These data confirm that the LRR-MAL RKs (IGP1/CORK1, IGP3, and IGP4), that are required for CEL/MLG43-dependent PTI activation, also play a role in XYL4 perception, further expanding the function of this novel group of LRR-MAL RK in the perception of additional glycans.

XA_3XX perception in Arabidopsis thaliana also depends on IGP1/IGP3/IGP4 LRR-MAL RKs

Refractory experiments suggested similarities between XYL4 and XA_3XX perception mechanisms (Fig. 2C). Additionally, the involvement of IGP1/IGP3/IGP4 RKs in XYL4 recognition by *Arabidopsis thaliana* points to a broader role of such RKs in oligosaccharide perception. Therefore, we questioned whether these RKs might be also involved in XA_3XX recognition by plants. We used Col-0^{AEQ}, *igp1*^{AEQ}, *igp3*^{AEQ,} and *igp4*^{AEQ} lines to monitor early cytoplasmic Ca^{2+} influx in these mutants upon XA_3XX treatment. Notably, Ca^{2+} influxes in XA_3XX-treated *igp1*^{AEQ}, *igp3*^{AEQ}, and *igp4*^{AEQ} seedlings were reduced in comparison to those in Col-0^{AEQ} (Fig. 4A). The reductions observed upon XA_3XX treatment were similar to those observed after treatment of these plants with XYL4, with stronger impairment in *igp3*^{AEQ} and *igp4*^{AEQ} than in *igp1*^{AEQ} (Fig. 3A), as previously described for CEL3 and MLG43 (Martín-Dacal et al., 2023). Next, we tested the phosphorylation of MPKs by western blot in *igp1*^{AEQ}, *igp3*^{AEQ}, *igp4* and Col-0 plants upon XA_3XX treatment. We found that MPKs phosphorylation levels were reduced in the *igp1*^{AEQ}, *igp3*^{AEQ} and *igp4* mutants in comparison to wild-type (Col-0) plants, and that this reduction was weaker in *igp1* ^{AEQ} than in *igp3* ^{AEQ} and *igp4* plants (Fig. 4B). As described previously, MPKs phosphorylation triggered by CHI6 treatment, included as a control, was not impaired in the *igp* mutants (Fig. 4B). In agreement with MPKs phosphorylation levels, we found that the observed up-regulation of PTI marker genes *CYP81F2* and *WRKY53* upon treatment of Col-0 plants with XA_3XX was significantly impaired in *igp3* ^{AEQ} and *igp4* mutants, whereas such reduction was milder in *igp1*^{AEQ} plants (Fig. 4C). These data indicate that IGP1, IGP3 and IGP4 RKs, which are required for PTI activation mediated by CEL/MLG43 (Martín-Dacal et al., 2023)and XYL4 (Figs. 1 and 3), also play a function in XA_3XX perception in *Arabidopsis thaliana*.

Since LRR-MAL RKs are required for the perception of different oligosaccharides, we tested whether the perception of arabinogalactan, fucoidans, and alginates, that trigger PTI responses in *Arabidopsis thaliana* [Fig. S2; (Wang et al., 2023)] was dependent on these LRR-MAL RKs. We used Col-0^{AEQ}, *igp1*^{AEQ} and *igp4*^{AEQ} lines (Martín-Dacal et al., 2023) to monitor early cytoplasmic Ca^{2+} influx and upon treatment with these polysaccharides. We found that Ca^{2+} influxes were not impaired in *igp1*^{AEQ} and *igp4*^{AEQ} lines, further indicating that at least IGP1/CORK1and IGP4 are not required for the perception of these plant/seaweed-derived DAMPs (Fig. S2B). To further corroborate these data, we determined phosphorylation of MPKs by western blot in *igp1*^{AEQ}, *igp4* and Col-0 plants upon treatment with these polysaccharides. We found that MPKs phosphorylation levels were not impaired in the *igp1*^{AEQ} and *igp4* mutants in comparison to wild-type (Col-0) plants, which contrasted with the observed reduction of MPKs phosphorylation observed in mutants treated with CEL3 (Fig. S2C). These data further confirmed that IGP1/CORK1 and IGP4 are not required for the perception of these plant-derived (arabinogalactan) and seaweed-derived (fucoidans and alginates) glycans. Hence additional mechanisms, yet unknown, might be involved in the perception of these polysaccharides by plants.

XYL4 and XA_3XX perception in Arabidopsis thaliana depends partially on CERK1, LYK4 and LYK5 LysM receptors

The refractory experiments between XYL4 and CHI6 suggested that the mechanism of perception of these two glycans might share some components (Fig. 2C). Accordingly, we used Col-0^{AEQ} and *cerk1-2*^{AEQ} lines to monitor whether early cytoplasmic Ca^{2+} influxes were impaired in *cerk1-2*^{AEQ} upon XYL4 and XA_3XX treatments. Notably, XYL4 and XA_3XX triggered Ca^{2+} influxes in *cerk1-2*^{AEQ} seedlings whereas CHI6 did not (Fig. 5A), as described previously (Mélida et al., 2020). Since LysM proteins CERK1, LYK5 and LYK4 play redundant functions in CHI6 perception (Miya et al., 2007; Cao et al., 2014; Mélida et al., 2018), we used *cerk1-2 lyk4-1 lyk5-1* triple mutant to test MPKs phosphorylation upon XYL4 and XA_3XX treatments. As shown in Fig. 5B, phosphorylation of MPKs in *cerk1-2 lyk4-1 lyk5-1* mutant upon CHI6 treatment was fully impaired, as predicted from the requirement of CERK1, LYK4 and LYK5 for its perception (Martín-Dacal et al., 2023). In contrast, phosphorylation of MPKs in the LysM triple mutant upon XYL4 or XA_3XX treatment was only slightly reduced (Fig. 5B) indicating that these receptors play some minor function in the perception of xylose-containing glycans in *Arabidopsis thaliana*. In line with this minor function of LysM-RKs, the up-regulation of the PTI marker genes *CYP81F2* and *WRKY53* in *cerk1-2 lyk4-1 lyk5-1* lines upon XYL4 or XA_3XX treatment was not significantly different from that observed in Col-0 plants (Fig. 5C). These results also

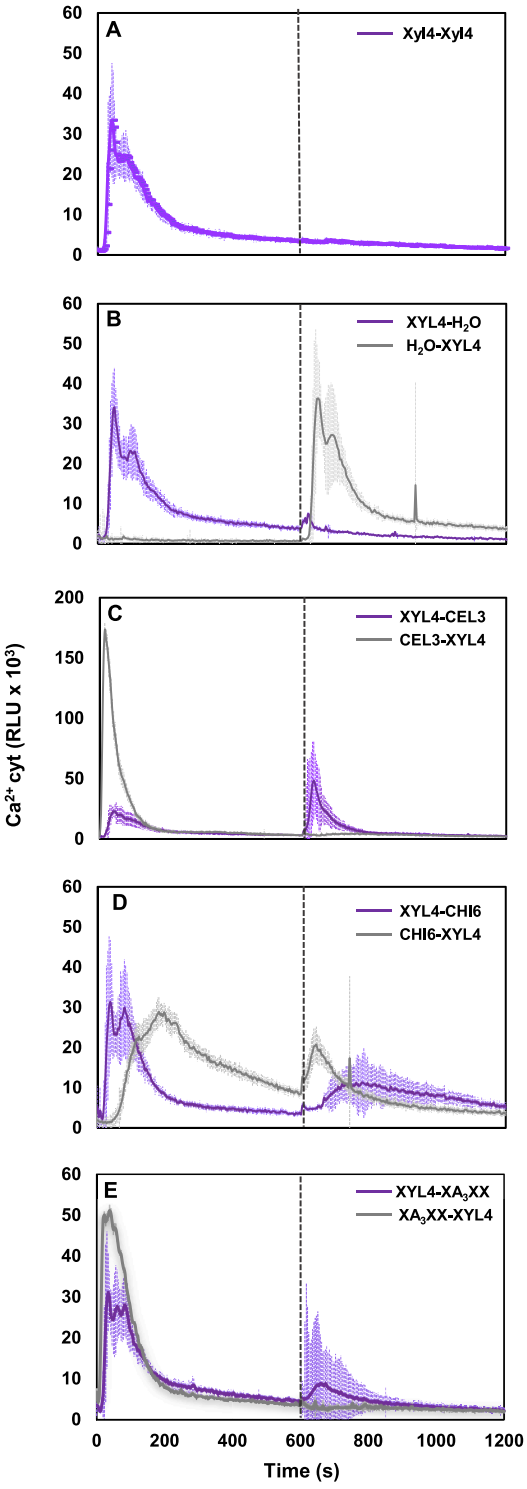

Fig. 2.

(caption on next column)

Fig. 2. Cross-elicitation during the refractory period of calcium burst triggered by XYL4 in combination with CEL3, CHI6, and/or XA_3XX. Cyt Ca^{2+} burst (RLU) over time in 8-day-old Col-0^{AEQ} seedlings after sequential treatments with 250 μM XYL4 followed by 250 μM XYL4 (A), WATER (B), 10 μM CEL3 (C), 50 μM CHI6 (D), or 250 μM XA_3XX (E) and vice versa. A and B panels represent the negative and positive controls of the experiment, respectively. XYL4 as the first treatment applied is indicated in purple and any other compound and/or water added is indicated in grey. Pointed lines indicate the application time of the second glycan/water. Data represent the average RLU values of 4 seedlings (n = 4) ± standard deviation. This is a representative experiment of the two performed that gave similar results. (For interpretation of the references to colour in this figure legend, the reader is referred to the web version of this article.)

demonstrated that the mechanisms of perception of XYL4/XA_3XX and CHI6 are different.

XYL4 triggered defensive responses in different plant species

To further characterize the basis of XYL4-mediated PTI activation, we performed RNA-seq analyses of Col-0 seedlings treated for 30 min with XYL4, CEL3, CHI6 or water (Mock: Fig. 6, Table S2-S3-S4). XYL4 triggered the differential expression of 185 genes (DEGs), most of which (154) were up-regulated (Fig. S6A and Table S2). On the other hand, treatments either with CEL3 or CHI6 resulted in 679 and 581 DEGs, respectively (Table S3 and S4, Fig. 6), most of them up-regulated (562 by CEL3- and 532 by CHI6-treatment). The overlapping of DEGs among the three compounds, as shown in the Venn Diagram (Fig. 6A, B), strongly points to shared molecular components in the signalling mechanisms activated by XYL4 and CEL3/CHI6, as shown above in cross-elicitation experiments (Fig. 2). XYL4 up-regulated genes mainly grouped into gene ontology (GO) terms related to immune system processes, and response to different stimuli, including biotic and abiotic stresses, among other GOs (Fig. 6B). Likewise, similar enriched GOs were found in response to CEL3 and CHI6, which shared DEGs between them and with XYL4 (Fig. S3 and Table S5). Overall, these analyses indicate that the transcriptional reprogramming triggered by XYL4 overlaps partially with that induced by other well-known DAMPs and MAMPs, such as CEL3 and/or CHI6, though with specific DEGs and GOs. The majority of shared DEGs upon XYL4, CEL3 and CHI6 treatment are immune and stress related genes (Table S5) further confirming the function of these glycans in the regulation of plant disease resistance. Among XYL4 specific DEGs some encoded RLPs/RKs and other stress-associated proteins (Table S6). Together these data indicate that the mechanism of XYL4 perception shares some similar components (e.g. RKs) but is not identical to that of CEL3 and/or CHI6, as indicated by the cross-elicitation and genetics experiments (Figs. 2, 3, and 5).

XA_3XX has been shown previously to trigger disease resistance in tomatoes and peppers against bacterial and fungal pathogens, respectively (Mélida et al., 2020). XYL4, like XA_3XX oligosaccharide, can be released from plants cell walls upon pathogen infection by the activity of *endo*-xylanases or arabinoxylanases (e.g., GH11) secreted by these pathogens during colonization, as suggested recently (Mélida et al., 2020; Pring et al., 2023). Therefore, we tested the elicitor activity of XYL4 in three-week-old tomato plants (var. Moneymaker), which were treated by foliar spray with XYL4 two days prior spray-inoculation with the virulent bacterium *Pseudomonas syringae* pv. *tomato* DC3000. Notably, bacterial population, determined as colony forming units (cfu) per leaf area (cm^2), was significantly reduced in the XYL4-pretreated tomato plants at 7 days post inoculation compared to mock-treated plants (Fig. S4). We also tested if xylooligosaccharides (XYL4, XYL3 and XYL2) were perceived by monocot crops (i.e. wheat) by determining the production of reactive oxygen species (ROS), one of the PTI hallmarks in plants, upon treatment of wheat leaf discs with these glycans. As shown in Fig. 7, XYL4 triggered ROS production in wheat leaf discs that was weaker than that induced by MAMP flg22 used as a control MAMP in the experiment. In contrast, XYL2 and XYL3 were not active in

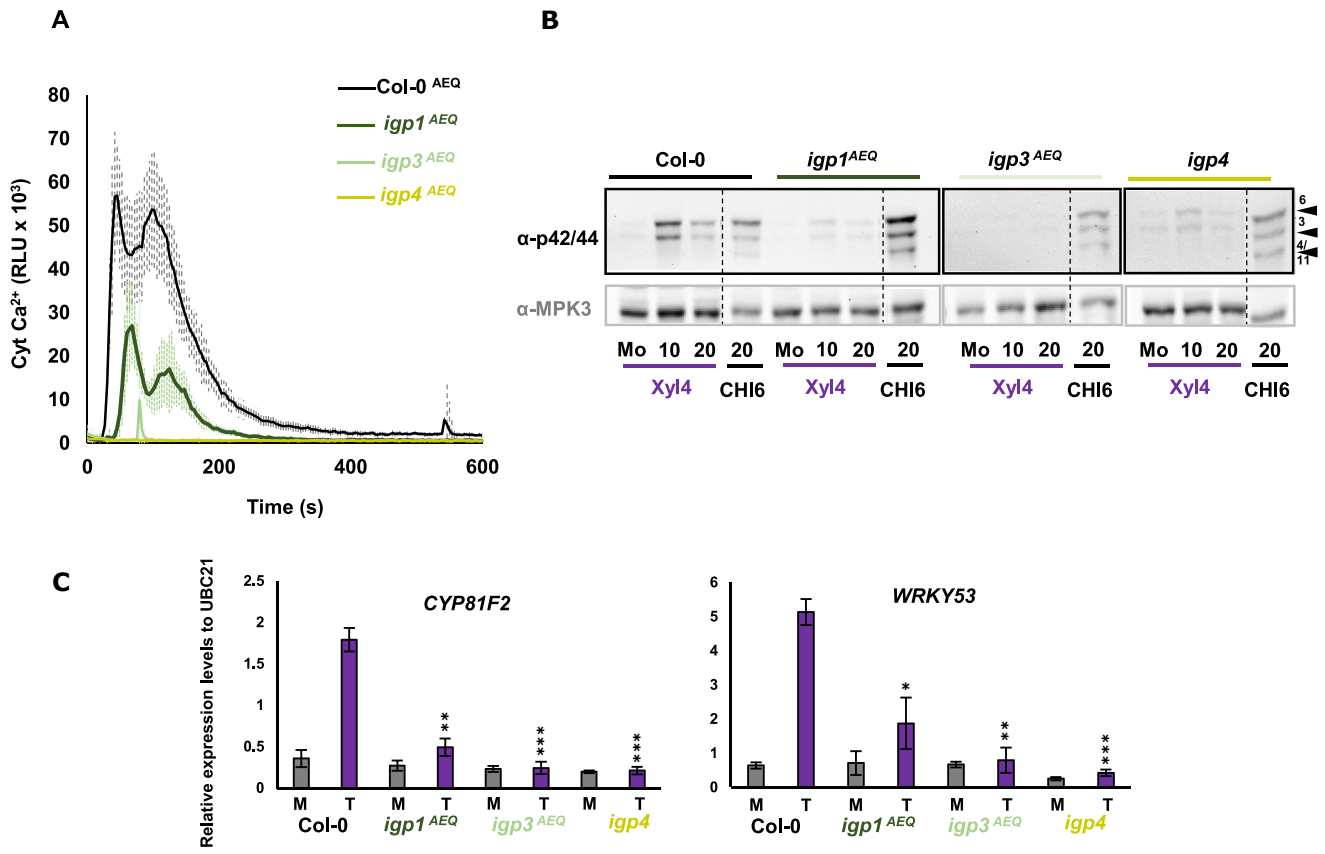

Fig. 3.

Fig. 3. *igp1, igp3 and igp4* mutants are impaired in XYL4 perception. The activation of immunity hallmarks such as cyt Ca^{2+} influx (A), phosphorylation of MPKs (B), and gene expression triggered by 250 μM XYL4 is defective in *igp* mutants tested. Experiments were performed as previously described in Fig. 1. Data represent (A) the mean ± error standard (n = 8) of two independent experiments performed, (B) a representative WB out of three replicates (dotted lines indicate that bands were cut from the membrane to relocate them in proper order), and (C) the mean ± error standard (n = 3) of three independent experiments. Statistically significant differences between compound-treated (T) plants versus mock-treated (M, H_2O) were calculated according to Student's *t*-test (*P < 0.05, **0.01 < P > 0.001, ***P < 0.001).

triggering ROS (Fig. 7). The activation of XYL4-triggered immune responses in *Arabidopsis thaliana*, tomato, and wheat suggests that these species have the receptors required for XYL4 perception and PTI activation and that xylan-derived oligosaccharides might be used for crop protection in tomato and other crops, as reported recently for mixtures of oligosaccharides derived from enzymatic hydrolysis of xylans (Pring et al., 2023).

Discussion

Activation of plant PTI by glycans derived from plant cell walls (DAMPs) and extracellular layers from pathogens (MAMPs) is an essential process to mount an effective disease resistance response during plant microbe-interactions (Bacete et al., 2018; Kongala and Kondreddy, 2023; Lee and Santiago, 2023). The structural diversity of glycans (DAMPs/MAMPs) that can be perceived by plants has been growing in the last years and include linear and branched oligosaccharides (generally of DP 3–10) which are mainly homo-oligosaccharides composed of D-monosaccharides (e.g. Glc, Xyl, Ara, GalA and Man) bound through different types of linkages (e.g. β-1,4, β-1,3, β-1,6 and α-1,4) (Klarzynski et al., 2000; Kaku et al., 2006; Aziz et al., 2007; Galletti et al., 2008; Claverie et al., 2018; Voxeur et al., 2019; Zang et al., 2019; Mélida et al., 2020; Malivert et al., 2021; Rebaque et al., 2021; Moussu et al., 2023; Pring et al., 2023). Also, branched oligosaccharides (e.g. with Ara at position 3 in XA_3XX or β-1,6-D-Glc branches in β-1,3-D-Glc glycans) have been shown to trigger PTI (Mélida et al., 2020; Wanke et al., 2020). These DAMPs/MAMPs can be released from plant cell walls and extracellular surfaces of microorganisms by the activity of CWDEs secreted by pathogens and plants during their interactions (Wanke et al., 2023). Thus, plant and microbial cell walls are rich sources of carbohydrate-based defence signalling molecules (DAMP and MAMPs) that are poorly characterized. Plant pathogens and their hosts have co-evolved an arsenal of CWDEs to break down the opponent's wall during their interactions (Rovenich et al., 2016). The great arsenal of CWDEs from pathogens and plants described (see CAZy database, www.cazy.org; (Drula et al., 2021)) and the huge diversity of polysaccharide structures present in plant walls (Delmer et al., 2024) and microorganism surfaces (Wanke et al., 2023) anticipate that the number of carbohydrate-based DAMPs/MAMPs recognized by plant immune system should grow significantly.

Here we show that *Arabidopsis thaliana* perceives β-1,4-D-XYL_4 further confirming previous results demonstrating that *Arabidopsis*

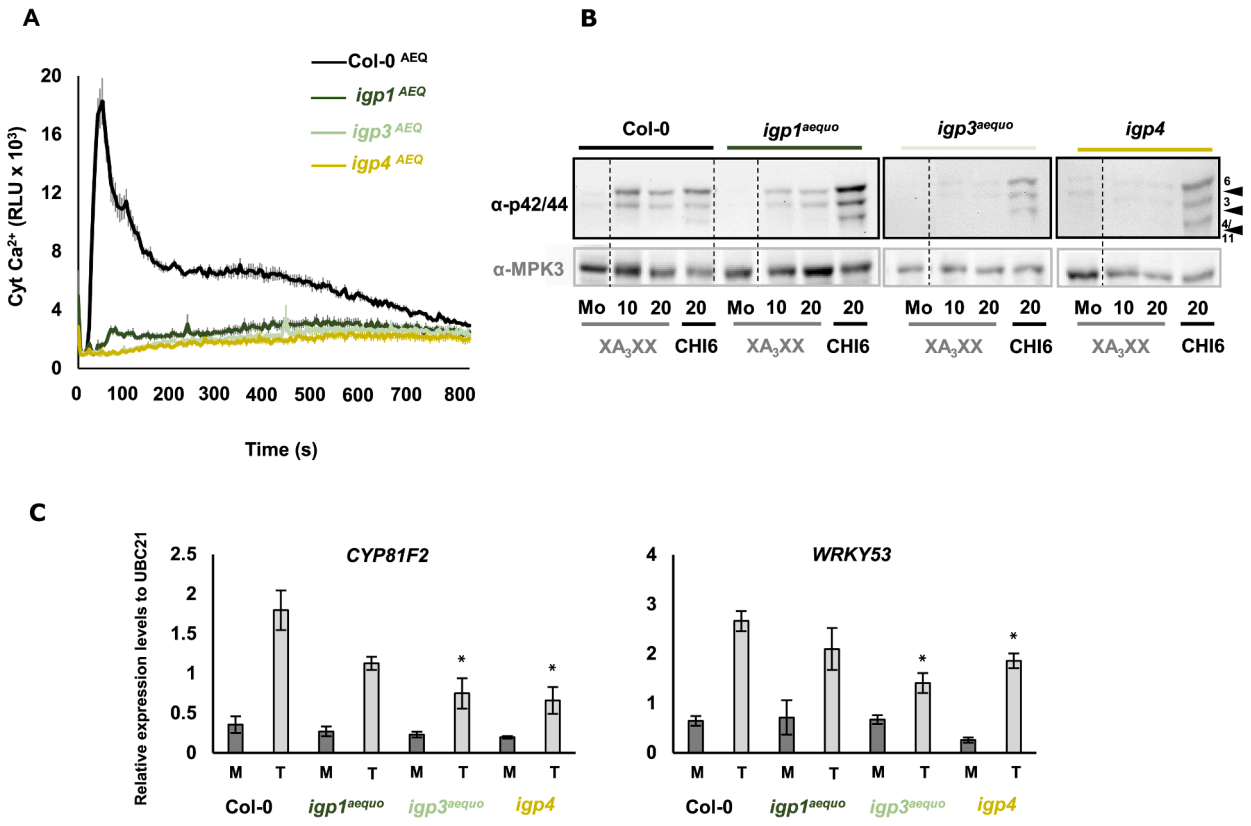

Fig. 4. *igp1, igp3 and igp4* mutants are impaired in XA_3XX perception. The activation of immunity hallmarks such as cyt Ca^{2+} influx (A) and phosphorylation of MPKs (B) is defective in *igp* mutants tested. Experiments were performed as described in Fig. 1. Data represent (A) the mean ± error standard (n = 8) of two independent experiments performed, (B) a representative WB out of three replicates (dotted lines indicate that bands were cut from the membrane to relocate them in proper order), and (C) the mean ± error standard (n = 3) of three independent experiments. Statistically significant differences between compound-treated (T) plants versus mock-treated (M, H2O) were calculated according to Student's *t*-test (*P < 0.05, **0.01 < P > 0.001, ***P < 0.001).

thaliana perceives oligosaccharides mixtures derived from xylan hydrolysis (Pring et al., 2023), including XYL2 disaccharide that triggers defensive-related responses and alteration in cell wall composition in *Arabidopsis thaliana* (Dewangan et al., 2023). We also show that *Arabidopsis thaliana* perceived previously undescribed plant-derived glycans like 2^3–(4-O-Methyl-α-D-Glucuronyl)-xylotetraose (XUXX) and α-glucans (α-1,4-D-Glc based maltodextrins: α-D-Maltotetraose (MAL4) and 6^3-α-D-Maltotriosyl-maltotriose ($MAL3_2$)), as well as polysaccharides mixtures from plants, like arabinogalactans (Fig. 1 and Fig. S2). The perception of XYL4 and XUXX by *Arabidopsis thaliana* immune system, together with the previous description of XA_3XX (Mélida et al., 2020), XYL2, XYL3 and XYL5 as DAMPs (Dewangan et al., 2023; Pring et al., 2023), suggest that linear and branched β-1,4-D-XYL_n oligosaccharides are perceived with different degree of specificity by plant immune systems. Notably, β-1,4-D-XYL_4 oligosaccharides with branching at position 2 show a reduced activity triggering PTI in comparison to XA_3XX which harbours an Ara at position 3 (Mélida et al., 2020). The observation that *Arabidopsis thaliana* recognizes β-1,6-D-Glc oligosaccharides (purified here for the first time from fungal pustulan), as well as fucoidan and low molecular weight-alginates (Figs. S1 and S2) is in line with the previous description of the effect of these compounds eliciting defensive and abiotic stress responses in different plant species (Aitouguinane et al., 2020; Aitouguinane et al., 2023; Liu et al., 2023), and indicates that their mechanisms of perception (e.g. PRRs) are conserved in *Arabidopsis thaliana*. Alginate is mainly composed of two conformational isomer residues, D-mannuronic acid (M) and L-guluronic acid (G), constituting homopolymeric (MM, GG) and heteropolymeric (MG, GM) sequential block structures (Aitouguinane et al., 2020; Aitouguinane et al., 2023). Fucoidans from brown marine algae are polysaccharides that consist predominantly of sulphated L-fucoses (Klarzynski et al., 2000; Wang et al., 2023). Our results and previous data indicate that *Arabidopsis thaliana* perceives glycan structures containing a great diversity of monosaccharides, including at least four different types of acidic monosaccharides (e.g. D-mannuronic acid and L-guluronic acid in alginates; Fig. S2), D-Glucuronyl in XUXX (Fig. 1) and GalA in OGs (Galletti et al., 2008; Voxeur et al., 2019; Liu et al., 2023). Also, *Arabidopsis thaliana* perceives glycan structures containing L-monosaccharides (L-Arabinose in arabinoxylans, L-Fucose in fucoidans and L-guluronic acid (G), in alginates: Fig. S2).

The molecular mechanisms implicated in the perception of glycans in plants are poorly characterized and just a few PRRs and co-PRRs have been described to be involved in these recognition processes. These PRRs characterised so far include LysM RKs (Kaku et al., 2006; Johnson et al., 2018; Yang et al., 2021a), members of the LRR-MAL, WAK, Malectin-like and Lectin RKs (Dai et al., 2023; Martín-Dacal et al., 2023; Moussu et al., 2023; Liu et al., 2024). However, with a few exceptions direct binding of glycans to ECDs of these RKs has not been demonstrated yet (Cao et al., 2014; Martín-Dacal et al., 2023). Here we showed that IGP1/CORK1, IGP3 and IGP4 proteins from LRR-MAL RK family, which are required for CEL3 and MLG43 perception and downstream PTI activation (Martín-Dacal et al., 2023), are also needed for the activation of immune responses triggered by XYL4 and XA_3XX, but not of other complex glycan structures, like fucoidan, alginates and arabinogalactans (Fig. 2 and Fig. S2). These results corroborate the relevance of this new family of LRR-MAL RKs as PRR/co-PRR in the activation of PTI in *Arabidopsis thaliana* and probably in other plant species (see Fig. 8).

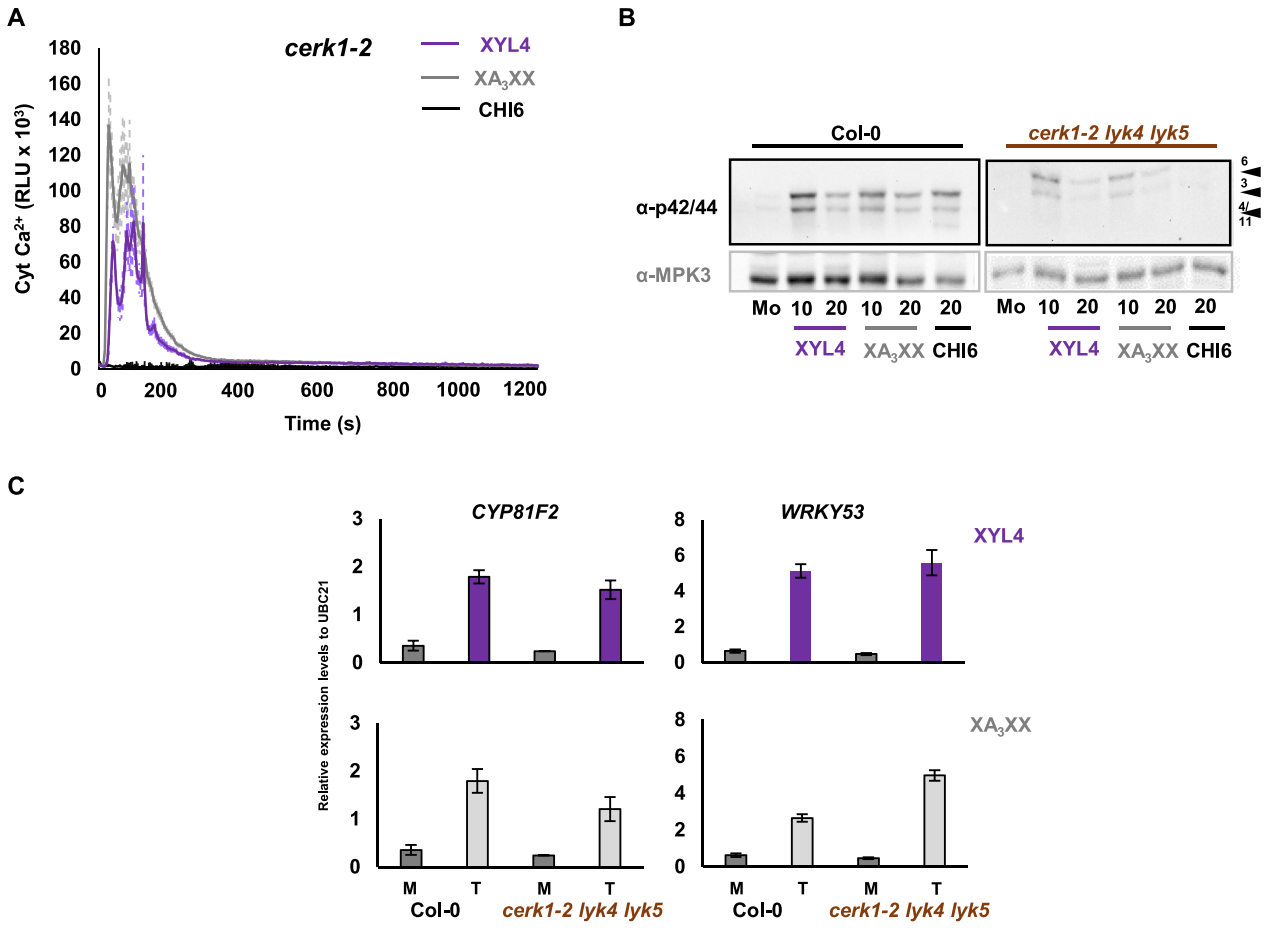

Fig. 5.

Fig. 5. CERK1, LYK4, and LYK5 LysM RKs have a minor role in XYL4 and XA_3XX perception. The activation of immunity hallmarks such as cyt Ca^{2+} influx (A) in *cerk1-2*^{AEQ} mutant line, and phosphorylation of MPKs (B) and gene marker expression (C) in *cerk1-2 lyk4 lyk5* triple mutant line are partially impaired after treatment with 450 μM of XYL4 or XA_3XX. Experiments were performed as previously described in Fig. 1. Data represent (A) the mean ± error standard (n = 8) of two independent experiments performed, (B) a representative WB out of three replicates (dotted lines indicate that bands were cut from the membrane to relocate them in proper order), and (C) the mean ± error standard (n = 3) of three independent experiments. Statistically significant differences between compound-treated (T) plants versus mock-treated (M, H_2O) were calculated according to Student's *t*-test (*P < 0.05, **0.01 < P > 0.001, ***P < 0.001).

Our data suggests that IGP RKs are central components in activation of immune responses (e.g. transcriptional upregulation of genes) triggered by a diversity of glycans with different carbohydrate moieties in their composition (Glc, Xyl, Ara) and distinct structures, that include, at least CEL3-CEL5, XYL4 and XA_3XX, as well as MLG43(Martín-Dacal et al., 2023)). These DAMPs can be released from plant cell wall polysaccharides by the action of microbial CWDEs (Fig. 8). Despite the differential composition and structures of these glycans, they share some features that might explain their similar mechanisms of perception by IGP1/IGP3/IGP4: i) they are composed of monosaccharides (pentose and hexoses) in pyranose conformation; and ii) they have two units bound with a β-1,4-D-linkage, including the anomeric carbon (position 1) that is probably in its reduced form. The differential impairment of PTI response upon XYL4 and XA_3XX observed in *igp4-1* and *igp3-1* (fully blocked responses), in comparison to *igp1-1* (partially impaired), might be explained by the fact that *igp1* is not a loss-of-function mutant, since a similar pattern of impairment of PTI responses has been observed after CEL3 and MLG43 treatment (Martín-Dacal et al., 2023). Whether IGP1/CORK1, IGP3 and IGP4 might be the *bona-fide* PRRs for XYL4 and XA_3XX require additional characterization and binding assays with their ECDs. Likewise, LRR-MAL RK family comprises 13 members in *Arabidopsis thaliana* and it cannot be excluded that some other additional RKs might be the *bona fide* PRRs for XYL4 and/or XA_3XX (Yang et al., 2021a; Martín-Dacal et al., 2023). Notably, LRR-MAL RK family members are present in all the plant species, including monocots, like wheat and rice, though the orthologs of IGP1/CORK1, IGP3 and IGP4 in other plant species have not been functionally characterized (Yang et al., 2021b; Martin-Dacal et al., 2023). Though some of these LRR-MAL RK members have been involved in pollen migration and fertility (Lee et al., 2024), an alternative function for such PRRs in oligosaccharide perception cannot be discarded, since pollen migration and lateral root formation promote changes in cell wall integrity and composition (Moussu et al., 2023; Lee et al., 2024). Despite the relevance of LRR-MAL RKs in glycan perception and PTI activation, additional, uncharacterized mechanisms for oligosaccharide recognition should exist in *Arabidopsis thaliana*, because the perception of glycans present in arabinogalactan proteins and seaweed glycans triggering defensive responses (i.e., fucoidan and alginates) is not altered in *igp1/cork1* and *igp4* mutants (Fig. S2).

Here we also showed that the mechanisms of perception of XYL4 and XA_3XX might require the LysM-RKs CERK1, LYK5 and LYK4, probably

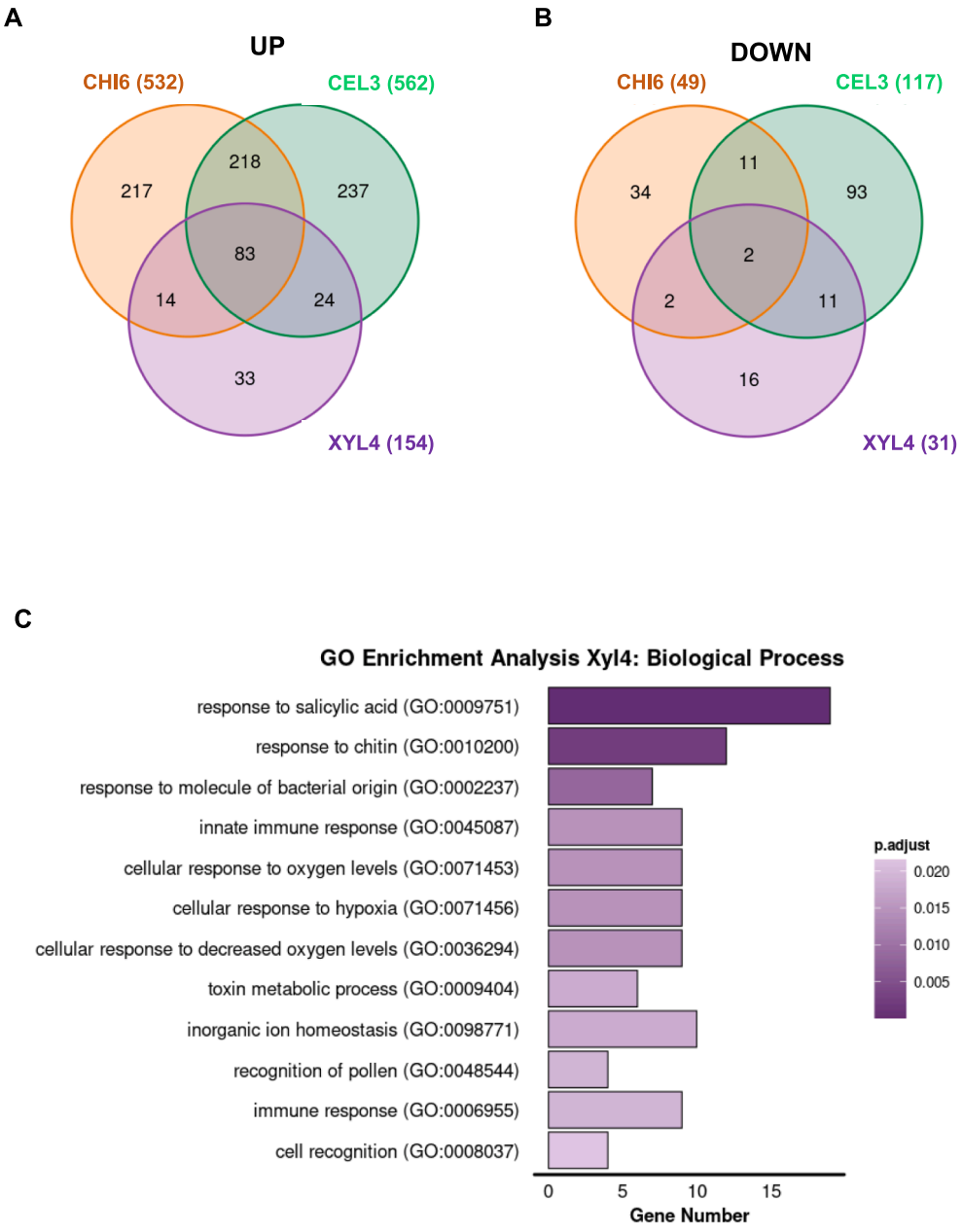

Fig. 6.

Fig. 6. XYL4 triggers the differential regulation of immunity-associated genes in *Arabidopsis thaliana*. (A)Venn diagrams of the number of the differentially expressed genes (DEGs) up-regulated (left) and down-regulated (right) upon treatment of *Arabidopsis thaliana* Col-0 seedlings with either XYL4 (250 μM), CEL3 (50 μM) or CHI6 (50 μM). The total number of DEGs is indicated with the glycan and the overlapped genes are shown in the circles. (B) GO enrichment analysis of biological process among the up DEGs upon treatment with XYL4. See material and methods for additional details.

acting as redundant co-receptors. These LysM-RKs, which are required for CHI6 perception and PTI activation (Fig. 8), have been shown to function as putative co-receptors for MLG43 and β-1,3-Glc oligosaccharides (e.g. LAM6) (Mélida et al., 2018; del Hierro et al., 2021; Rebaque et al., 2021). Notably, perception of CHI6, that can be released from fungal cell wall by the action of plant CWDEs, does not requires IGP1/CORK1, IGP3 or IGP4 RKs, indicating that these sets of receptors (LysM-RKs and LRR-MAL RKs) control different PTI signalling pathways (Fig. 8). PTI responses triggered by CHI6 and XYL4 are shown here to activate transcriptional responses that share over 80 % of the up-regulated genes, further demonstrating a very high gene reprogramming overlap upon treatment with these glyco-ligands (Figs. 6 and 8). These data are in line with previous transcriptomic analyses comparing *Arabidopsis thaliana* responsive genes to single-linked β-1,3- (DAMP/MAMP) and β-1,4-glucans (DAMPs) and chitin (MAMP) that revealed that a significant percentage of DEGs were common between glucans

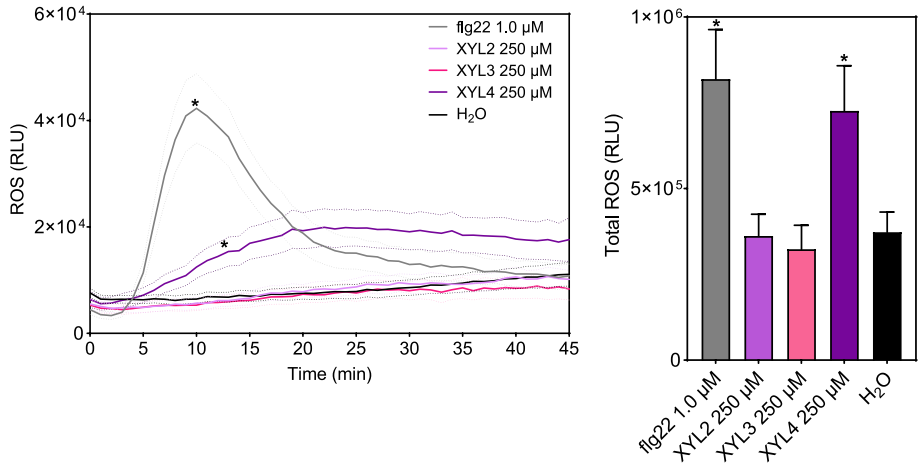

Fig. 7.

Fig. 7. XYL4 activates ROS production in wheat·H_2O_2 accumulation in wheat leaves of cultivar Titlis upon treatment with 250 μM of XYL2, XYL3, or XYL4·H_2O_2 levels were estimated by measuring for 45 min the relative luminescence units (RLU) using the luminol-20 assay. The peptide flg22 (1 μM) and H_2O were used as positive and negative controls, respectively. The total ROS production is displayed on the right side of the panel. The standard error of the mean (n = 8) is shown. Asterisks (*) indicate significant differences (*$p < 0.05$) with the negative control according to the Kruskal-Wallis test. This is one of the three experiments performed with similar results.

and chitin treatments (Souza et al., 2017; Johnson et al., 2018; Mélida et al., 2018).

As previously described for XA_3XX (Mélida et al., 2020), we show here that XYL4 is perceived by different plant species (tomato and wheat) and that pre-treatment of these species with XYL4 triggers PTI responses (i.e. in wheat; Fig. 7) and crop protection (i.e. in tomato; Fig. 4S). These data support that LRR-MAL RK orthologs of IGP1/CORK1, IGP3 and IGP4 are present in other plant species, including wheat and tomato, that deserve further characterization (Yang et al., 2021b; Martin-Dacal et al., 2023). These data are also in line with the recent demonstration of the activity of mixtures of oligosaccharides from xylan hydrolysis on crop protection (Dewangan et al., 2023; Pring et al., 2023). Similarly, several studies have reported the use of alginate in agriculture to stimulate plant growth and development (Liu et al., 2023) and to induce plant resistance mechanisms, but the molecular bases of these responses have not been determined (Klarzynski et al., 2000; Aitouguinane et al., 2020; Aitouguinane et al., 2023; Wang et al., 2023). Together these results confirm the potential of glycans to activate PTI and to develop biological products that boost crop natural defence against pathogens, contributing to replacing chemical pesticides and implementing more sustainable agriculture practices. In the last years, several glycan-based agrobiological products have been successfully developed to be used in agriculture (e.g. products based on cell walls/extracts of brown Seaweed, laminarin, or chitin). However, the identification of active glycans in these complex mixtures and the determination of their mechanism of perception (e.g. identification of PRRs) by crops is essential to further expand a glycańs science-based technology in agriculture.

Funding and Acknowledgements

This work was supported by grants RTI2018-096975-B-I00 to AM funded by Spanish Ministry of Science, Innovation and Universities, and by grant PID2021-126006OB-I00 to AM, funded by MCIN/AEI/ https://doi.org/10.13039/501100011033 and by "ERDF A way of making Europe". This work was also supported by ĹOreal-FWIS Spanish edition 2019 grant to PF-C "*Inmunidad por azúcares en plantas*". PF-C, HM and CCL have been financially supported by the "Severo Ochoa Program for Centres of Excellence in R&D (grant SEV-2016-0672 and CEX2020-000999-S (2022-2025)) funded by MCIN/AEI/ https://doi.org/10.13039/501100011033. MA was a postdoctoral fellow supported by PID2021-126006OB-I00. MM-D was the recipient of PhD fellow (PRE2019-08812). ASV was a recipient of the RYC2018-025530-I grant from the Spanish Ministry of Science, Innovation, and Universities. SG-B was supported by PTA2021-020636-I, funded by the Spanish Ministry of Science and Innovation (MCIN/AEI/https://dx.https://doi.org/10.13039/501100011033) and the European Social Fund Plus (FSE+).

We thank Lucia Jordá and Miguel Ángel Torres for the critical reading of the manuscript and suggestions provided.

CRediT authorship contribution statement

Patricia Fernández-Calvo: Writing – original draft, Validation, Supervision, Investigation, Funding acquisition, Formal analysis, Data curation, Conceptualization. **Gemma López:** Methodology, Investigation, Formal analysis. **Marina Martín-Dacal:** Validation, Methodology, Investigation, Formal analysis, Data curation. **Meriem Aitouguinane:** Validation, Methodology, Investigation, Formal analysis. **Cristian Carrasco-López:** Writing – original draft, Validation, Methodology, Investigation, Formal analysis. **Sara González-Bodí:** Writing – original draft, Software, Methodology, Investigation, Formal analysis, Data curation. **Laura Bacete:** Methodology, Investigation, Formal analysis. **Hugo Mélida:** Writing – original draft, Validation, Supervision, Methodology, Investigation, Formal analysis, Conceptualization. **Andrea Sánchez-Vallet:** Writing – original draft, Investigation, Formal analysis, Conceptualization. **Antonio Molina:** Writing – original draft, Validation, Supervision, Project administration, Methodology, Investigation, Funding acquisition, Formal analysis, Data curation, Conceptualization.

Declaration of competing interest

The authors declare the following financial interests/personal relationships which may be considered as potential competing interests: Antonio Molina reports financial support was provided by Spanish Research Agency. Patricia Fernandez-Calvo reports financial support

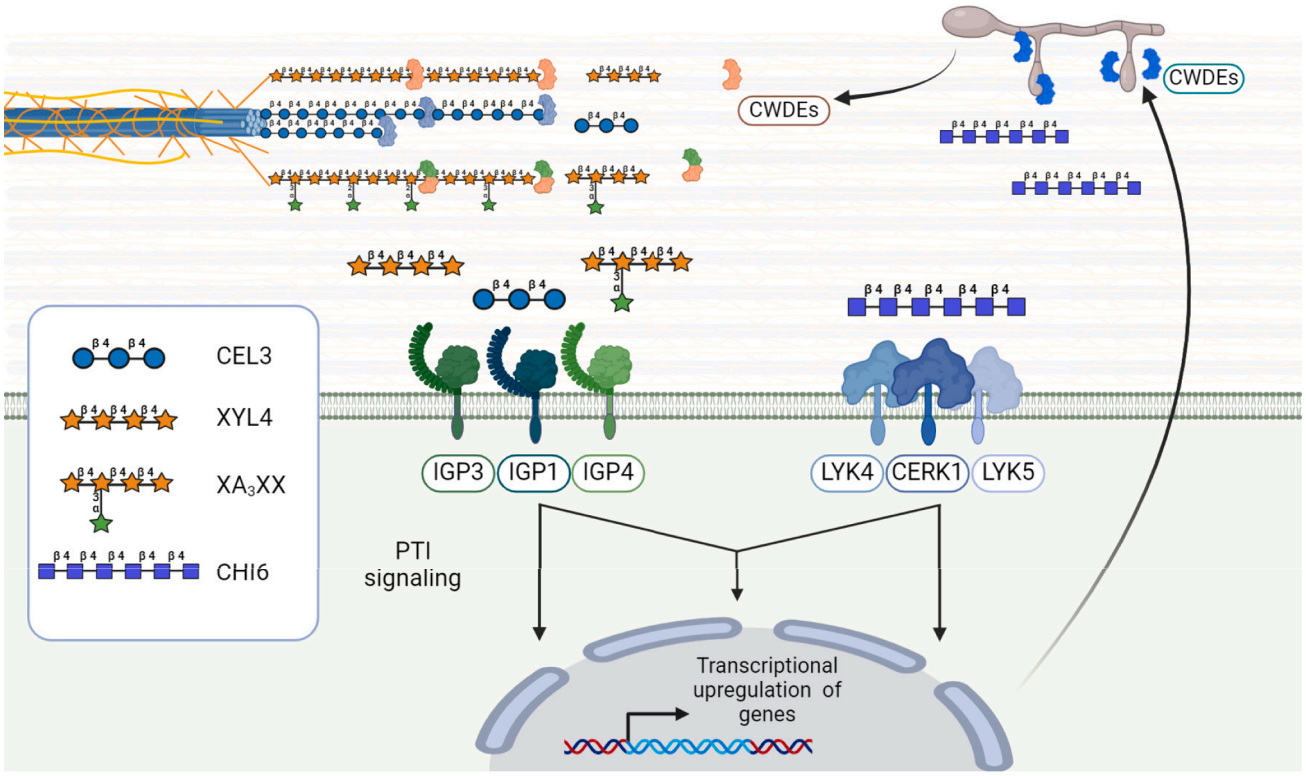

Fig. 8.

Fig. 8. Model of IGPs function in the perception of glycans with different composition. Fungi secretes CWDEs that hydrolyse plant cell wall polysaccharides (cellulose, xylans and arabinoxylans) releasing DAMPs like XYL4, XA_3XX or CEL3 that are perceived through LRR-MAL RKs (IGP1/CORK1, IGP3 and IGP4) triggering PTI and transcriptional upregulation of genes. Plants can secrete CWDEs that hydrolyse chitin from fungal cell walls releasing CHI6 MAMPs that is perceived through LysM-RKs (CERK1, LYK5 and LYK4) triggering PTI responses, which overlap with some PTI responses triggered by IGPs RKs.

was provided by L óreal Spain. Patricia Fernandez-Calvo reports was provided by Spanish Research Agency. Hugo Melida reports financial support was provided by Spanish Research Agency. Marina Martin-Dacal reports financial support was provided by Spanish Research Agency. Cristian Carrasco-Lopez reports financial support was provided by Spanish Research Agency. Sara Gonzalez-Bodi reports financial support was provided by Spanish Research Agency. If there are other authors, they declare that they have no known competing financial interests or personal relationships that could have appeared to influence the work reported in this paper.

Appendix A. Supplementary data

Supplementary data to this article can be found online at https://doi.org/10.1016/j.tcsw.2024.100124.

References

Aitouguinane, M., Bouissil, S., Mouhoub, A., Rchid, H., Fendri, I., Abdelkafi, S., Ould El-Hadj, M.D., Boual, Z., Dubessay, P., Gardarin, C., Michaud, P., El Alaoui-Talibi, Z., El Modafar, C., Pierre, G., Delattre, C., 2020. Induction of natural defenses in tomato seedlings by using alginate and oligoalginates derivatives Extracted from moroccan Brown algae. Mar. Drugs 18, 521.

Aitouguinane, M., El Alaoui-Talibi, Z., Rchid, H., Fendri, I., Abdelkafi, S., El-Hadj, M.D. O., Boual, Z., Le Cerf, D., Rihouey, C., Gardarin, C., Dubessay, P., Michaud, P., Pierre, G., Delattre, C., El Modafar, C., 2023. Elicitor activity of low-Molecular-weight alginates obtained by oxidative degradation of alginates Extracted from Sargassum muticum and Cystoseira myriophylloides. Mar. Drugs 21.

Anders S, Pyl PT, Huber W (2010) HTSeq: Analysing high-throughput sequencing data with Python.

Andrews, S., 2010. FastQC: A Quality Control Tool for High Throughput Sequence Data. In.

Aziz, A., Gauthier, A., Bézier, A., Poinssot, B., Joubert, J.M., Pugin, A., Heyraud, A., Baillieul, F., 2007. Elicitor and resistance-inducing activities of beta-1,4 cellodextrins in grapevine, comparison with beta-1,3 glucans and alpha-1,4 oligogalacturonides. J. Exp. Bot. 58, 1463–1472.

Bacete, L., Mélida, H., Pattathil, S., Hahn, M.G., Molina, A., Miedes, E., 2017. Characterization of plant Cell Wall damage-associated Molecular patterns regulating immune responses. Methods Mol. Biol. 1578, 13–23.

Bacete, L., Mélida, H., Miedes, E., Molina, A., 2018. Plant cell wall-mediated immunity: cell wall changes trigger disease resistance responses. Plant J. 93, 614–636.

Benkeblia, N., 2020. Potato glycoalkaloids: occurrence, biological activities and extraction for biovalorisation – a review. Int. J. Food Sci. Technol. 55, 8.

Bigeard, J., Colcombet, J., Hirt, H., 2015. Signaling mechanisms in pattern-triggered immunity (PTI). Mol. Plant 8, 521–539.

Bolger, A., Marc, L., Bjoern, U., 2014. Trimmomatic: a flexible trimmer for illumina sequence data. Bioinformatics 30.

Bordeleau, S.J., Canales Sanchez, L.E., Goring, D.R., 2022. Finding new Arabidopsis receptor kinases that regulate compatible pollen-pistil interactions. Front. Plant Sci. 13.

Boutrot, F., Zipfel, C., 2017. Function, discovery, and exploitation of plant pattern recognition receptors for broad-Spectrum disease resistance. Annu. Rev. Phytopathol. 55, 257–286.

Cao, Y., Liang, Y., Tanaka, K., 2014. The kinase LYK5 is a major chitin receptor in Arabidopsis and forms a chitin-induced complex with related kinase CERK1. Elife 3.

Chandrasekar, B., Wanke, A., Wawra, S., Saake, P., Mahdi, L., Charura, N., Neidert, M., Poschmann, G., Malisic, M., Thiele, M., Stühler, K., Dama, M., Pauly, M., Zuccaro, A., 2022. Fungi hijack a ubiquitous plant apoplastic endoglucanase to release a ROS scavenging β-glucan decasaccharide to subvert immune responses. Plant Cell 34, 19.

Cheng, C.Y., Krishnakumar, V., Chan, A.P., Thibaud-Nissen, F., Schobel, S., Town, C.D., 2017. Araport11: a complete reannotation of the Arabidopsis thaliana reference genome. Plant J. 89, 789–804.
Claverie, J., Balacey, S., Lemaitre-Guillier, C., Brule, D., Chiltz, A., Granet, L., Noirot, E., Daire, X., Darblade, B., Heloir, M.C., Poinssot, B., 2018. The Cell Wall-derived xyloglucan is a new DAMP triggering plant immunity in Vitis vinifera and Arabidopsis thaliana. Front. Plant Sci. 9, 1725.
Dai, Y.-S., Liu, D., Guo, W., Liu, Z.-X., Zhang, X., Shi, L.-L., Zhou, D.-M., Wang, L.-N., Kang, K., Wang, F.-Z., Zhao, S.-S., Tan, Y.-F., Hu, T., Chen, W., Li, P., Zhou, Q.-M., Yuan, L.-Y., Zhang, Z., Chen, Y.-Q., Zhang, W.-Q., Li, J., Yu, L.-J., Xiao, S., 2023. Poaceae-specific β-1,3;1,4-d-glucans link jasmonate signalling to OsLecRK1-mediated defence response during rice-brown planthopper interactions. Plant Biotechnol. J. 21, 1286–1300.
del Hierro, I., Mélida, H., Broyart, C., Santiago, J., Molina, A., 2021. Computational prediction method to decipher receptor–glycoligand interactions in plant immunity. Plant J. 105, 1710–1726.
Delmer, D., Dixon, R.A., Keegstra, K., Mohnen, D., 2024. The plant cell wall—dynamic, strong, and adaptable—is a natural shapeshifter. Plant Cell. https://doi.org/10.1093/pcell/koad325.
Desaki, Y., Kouzai, Y., Ninomiya, Y., Iwase, R., Shimizu, Y., Seko, K., Molinaro, A., Minami, E., Shibuya, N., Kaku, H., Nishizawa, Y., 2018. OsCERK1 plays a crucial role in the lipopolysaccharide-induced immune response of rice. New Phytol. 217, 1042–1049.
Dewangan, B.P., Gupta, A., Sah, R.K., Das, S., Kumar, S., Bhattacharjee, S., Pawar, P.-A.-M., 2023. Xylobiose treatment triggers a defense-related response and alters cell wall composition. Plant Mol. Biol. 113, 383–400.
Dobin, A., Davis, C.A., Schlesinger, F., Drenkow, J., Zaleski, C., Jha, S., Batut, P., Chaisson, M., Gingeras, T.R., 2013. STAR: ultrafast universal RNA-seq aligner. Bioinformatics 29, 15–21.
Dobrange, E., Peshev, D., Loedolff, B., Van den Ende, W., 2019. Fructans as immunomodulatory and antiviral agents: the case of echinacea. Biomolecules 9.
Drula, E., Garron, M.-L., Dogan, S., Lombard, V., Henrissat, B., Terrapon, N., 2021. The carbohydrate-active enzyme database: functions and literature. Nucleic Acids Res. 50, D571–D577.
Ewels, P., Magnusson, M., Lundin, S., Kaller, M., 2016. MultiQC: summarize analysis results for multiple tools and samples in a single report. Bioinformatics 32, 3047–3048.
Galletti, R., Denoux, C., Gambetta, S., Dewdney, J., Ausubel, F.M., De Lorenzo, G., Ferrari, S., 2008. The AtrbohD-mediated oxidative burst elicited by oligogalacturonides in Arabidopsis is dispensable for the activation of defense responses effective against Botrytis cinerea. Plant Physiol. 148, 1695–1706.
Gómez-Gómez, L., Boller, T., 2000. FLS2: an LRR receptor-like kinase involved in the perception of the bacterial elicitor flagellin in Arabidopsis. Mol. Cell 5, 1003–1011.
Gust, A.A., Biswas, R., Lenz, H.D., Rauhut, T., Ranf, S., Kemmerling, B., Götz, F., Glawischnig, E., Lee, J., Felix, G., Nürnberger, T., 2007. Bacteria-derived peptidoglycans constitute pathogen-associated molecular patterns triggering innate immunity in Arabidopsis. J. Biol. Chem. 282, 32338–32348.
Hou, S., Liu, Z., Shen, H., Wu, D., 2019. Damage-associated Molecular pattern-triggered immunity in plants. Front. Plant Sci. 22, 646.
Johnson, J.M., Thürich, J., Petutschnig, E.K., Altschmied, L., Meichsner, D., Sherameti, I., Dindas, J., Mrozinska, A., Paetz, C., Scholz, S.S., Furch, A.C.U., Lipka, V., Hedrich, R., Schneider, B., Svatoš, A., Oelmüller, R., 2018. A poly(a) ribonuclease controls the cellotriose-based Interaction between piriformospora indica and its host Arabidopsis. Plant Physiol. 176, 2496–2514.
Kaku, H., Nishizawa, Y., Ishii-Minami, N., Akimoto-Tomiyama, C., Dohmae, N., Takio, K., Minami, E., Shibuya, N., 2006. Plant cells recognize chitin fragments for defense signaling through a plasma membrane receptor. PNAS 103, 11086–11091.
Kemmerling, B., Schwedt, A., Rodriguez, P., Mazzotta, S., Frank, M., Qamar, S.A., Mengiste, T., Betsuyaku, S., Parker, J.E., Müssig, C., Thomma, B.P., Albrecht, C., de Vries, S.C., Hirt, H.T.N., 2007. The BRI1-associated kinase 1, BAK1, has a brassinolide-independent role in plant cell-death control. Curr. Biol. 17.
Klarzynski, O., Plesse, B., Joubert, J.M., Yvin, J.C., Kopp, M., Kloareg, B., Fritig, B., 2000. Linear beta-1,3 glucans are elicitors of defense responses in tobacco. Plant Physiol. 124, 1027–1038.
Knight, M.R., Campbell, A.K., Smith, S.M., Trewavas, A.J., 1991. Transgenic plant aequorin reports the effects of touch and cold-shock and elicitors on cytoplasmic calcium. Nature 352, 524–526.
Kongala, S.I., Kondreddy, A., 2023. A review on plant and pathogen derived carbohydrates, oligosaccharides and their role in plant's immunity. Carbohydrate Polymer Technologies and Applications 6, 100330.
Kraemer, F.J., Lunde, C., Koch, M., Kuhn, B.M., Ruehl, C., Brown, P.J., Hoffmann, P., Göhre, V., Hake, S., Pauly, M., Ramírez, V., 2021. A mixed-linkage (1,3;1,4)-β-D-glucan specific hydrolase mediates dark-triggered degradation of this plant cell wall polysaccharide. Plant Physiol. 185, 1559–1573.
Lee, H.K., Canales Sanchez, L.E., Bordeleau, S.J., Goring, D.R., 2024. Arabidopsis leucine-rich repeat malectin receptor–like kinases regulate pollen–stigma interactions. Plant Physiol.
Lee, H.K., Santiago, J., 2023. Structural insights of cell wall integrity signaling during development and immunity. Curr. Opin. Plant Biol. 76, 102455.
Liu, J., Li, W., Wu, G., Ali, K., 2024. An update on evolutionary, structural, and functional studies of receptor-like kinases in plants. Front. Plant Sci. 15.
Liu, T., Liu, Z., Song, C., Hu, Y., Han, Z., She, J., Fan, F., Wang, J., Jin, C., Chang, J., Zhou, J.M., Chai, J., 2012. Chitin-induced dimerization activates a plant immune receptor. Science 336, 1160–1164.
Liu, S., Wang, Q., Shao, Z., Liu, Q., He, Y., Ren, D., Yang, H., Li, X., 2023. Purification and Characterization of the enzyme fucoidanase from cobetia amphilecti utilizing fucoidan from Undaria pinnatifida. Foods 12, 1555.
Love, M., Wolfgang, H., Simon, A., 2014. Moderated estimation of fold change and dispersion for RNA-seq data with DESeq2. Genome Biol. 15.
Ma, Chaube, Trattnig, N., Lee, D.H., Belkhadir, Y., Pfrengle, F., 2022. Synthesis of Fungal Cell Wall Oligosaccharides and Their Ability to Trigger Plant Immune Responses. Eur. J. Org. Chem. e202200313.
Malivert, A., Erguvan, O., Chevallier, A., Dehem, A., Friaud, R., Liu, M., Martin, M., Peyraud, T., Hamant, O., Verger, S., 2021. FERONIA and microtubules independently contribute to mechanical integrity in the Arabidopsis shoot. PLoS Biol. 19, e3001454.
Martín-Dacal, M., Fernández-Calvo, P., Jiménez-Sandoval, P., López, G., Garrido-Arandía, M., Rebaque, D., del Hierro, I., Berlanga, D.J., Torres, M.Á., Kumar, V., Mélida, H., Pacios, L.F., Santiago, J., Molina, A., 2023. Arabidopsis immune responses triggered by cellulose- and mixed-linked glucan-derived oligosaccharides require a group of leucine-rich repeat malectin receptor kinases. Plant J. 113, 833–850.
Mélida, H., Sopeña-Torres, S., Bacete, L., Garrido-Arandia, M., Jordá, L., López, G., Muñoz-Barrios, A., Pacios, L.F., Molina, A., 2018. Non-branched β-1,3-glucan oligosaccharides trigger immune responses in Arabidopsis. Plant J. 93, 34–49.
Mélida, H., Bacete, L., Ruprecht, C., Rebaque, D., Del Hierro, I., López, G., Brunner, F., Pfrengle, F., Molina, A., 2020. Arabinoxylan-Oligosaccharides act as damage associated Molecular patterns in plants regulating disease resistance. Front. Plant Sci. 11, 1210.
Miya, A., Albert, P., Shinya, T., Desaki, Y., Ichimura, K., Shirasu, K., Narusaka, Y., Kawakami, N., Kaku, H., Shibuya, N., 2007. CERK1, a LysM receptor kinase, is essential for chitin elicitor signaling in Arabidopsis. PNAS 104, 19613–19618.
Moussu, S., Lee, H.K., Haas, K.T., Broyart, C., Rathgeb, U., De Bellis, D., Levasseur, T., Schoenaers, S., Fernandez, G.S., Grossniklaus, U., Bonnin, E., Hosy, E., Vissenberg, K., Geldner, N., Cathala, B., Höfte, H., Santiago, J., 2023. Plant cell wall patterning and expansion mediated by protein-peptide-polysaccharide interaction. Science 382, 719–725.
Ngou, B.P.M., Ding, P., Jones, J.D.G., 2022. Thirty years of resistance: zig-zag through the plant immune system. Plant Cell 34, 1447–1478.
Nguyen, Q.M., Iswanto, A.B.B., Son, G.H., Kim, S.H., 2021. Recent advances in effector-triggered immunity in plants: new pieces in the puzzle create a different Paradigm. Int. J. Mol. Sci. 22.
Pring, S., Kato, H., Imano, S., Camagna, M., Tanaka, A., Kimoto, H., Chen, P., Shrotri, A., Kobayashi, H., Fukuoka, A., Saito, M., Suzuki, T., Terauchi, R., Sato, I., Chiba, S., Takemoto, D., 2023. Induction of plant disease resistance by mixed oligosaccharide elicitors prepared from plant cell wall and crustacean shells. Physiol. Plant. 175, e14052.
Ranf, S., Grimmer, J., Pöschl, Y., Pecher, P., Chinchilla, D., Scheel, D., Lee, J., 2012. Defense-related calcium signaling mutants uncovered via a quantitative high-throughput screen in Arabidopsis thaliana. Mol. Plant 5, 115–130.
Rebaque, D., del Hierro, I., López, G., Bacete, L., Vilaplana, F., Dallabernardina, P., Pfrengle, F., Jordá, L., Sánchez-Vallet, A., Pérez, R., Brunner, F., Molina, A., Mélida, H., 2021. Cell wall-derived mixed-linked β-1,3/1,4-glucans trigger immune responses and disease resistance in plants. Plant J. 106, 601–615.
Rovenich, H., Zuccaro, A., Thomma, B.P., 2016. Convergent Evolution of Filamentous Microbes towards Evasion of Glycan-Triggered Immunity 212, 896–901.
Santamaría-Hernando, S., Senovilla, M., González-Mula, A., Martínez-García, P.M., Nebreda, S., Rodríguez-Palenzuela, P., López-Solanilla, E., Rodríguez-Herva, J.J., 2019. The Pseudomonas syringae pv. tomato DC3000 PSPTO_0820 multidrug transporter is involved in resistance to plant antimicrobials and bacterial survival during tomato plant infection. PLoS One 14, e0218815.
Souza, C.A., Li, S., Lin, A.Z., 2017. Cellulose-derived Oligomers act as damage-associated Molecular patterns and trigger defense-like responses. Plant Physiol. 173, 2383–2398.
Tanaka, K., Heil, M., 2021. Damage-associated Molecular patterns (DAMPs) in plant innate immunity: applying the danger model and Evolutionary perspectives. Annu. Rev. Phytopathol. 59, 18.
Tang, D., Wang, G., 2017. Receptor kinases in plant-pathogen Interactions: more than pattern recognition. Plant Cell 29, 618–637.
Tseng, Y.-H., Scholz, S.S., Fliegmann, J., Krüger, T., Gandhi, A., Furch, A.C.U., Kniemeyer, O., Brakhage, A.A., Oelmüller, R., 2022. CORK1, a LRR-malectin receptor kinase, is required for Cellooligomer-induced responses in Arabidopsis thaliana. Cells 11, 2960.
Voxeur, A., Habrylo, O., Guénin, S., Miart, F., Soulié, M.C., Rihouey, C., Pau-Roblot, C., Domon, J.M., Gutierrez, L., Pelloux, J., 2019. Oligogalacturonide production upon Arabidopsis thaliana-Botrytis cinerea interaction. PNAS 116, 19743–19752.
Wang, M., Veeraperumal, S., Zhong, S., Cheong, K.L., 2023. Fucoidan-derived functional Oligosaccharides: recent developments, preparation, and potential applications. Foods 12.
Wanke, A., Rovenich, H., Schwanke, F., Velte, S., Becker, S., Hehemann, J.H., Wawra, S., Zuccaro, A., 2020. Plant species-specific recognition of long and short β-1,3-linked glucans is mediated by different receptor systems. Plant J. 102, 1142–1156.
Wanke, A., van Boerdonk, S., Mahdi, L.K., Wawra, S., Neidert, M., Chandrasekar, B., Saake, P., Saur, I.M.L., Derbyshire, P., Holton, N., Menke, F.L.H., Brands, M., Pauly, M., Acosta, I.F., Zipfel, C., Zuccaro, A., 2023. A GH81-type β-glucan-binding protein enhances colonization by mutualistic fungi in barley. Curr. Biol. 33, 5071–5084.e5077.
Wickham H (2016) ggplot2 Elegant Graphics for Data Analysis. In S link, ed, Springer International Publishing, Ed Second Edition.

Willmann, R., Lajunen, H.M., Erbs, G., Newman, M.A., Kolb, D., Tsuda, K., Katagiri, F., Fliegmann, J., Bono, J.J., Cullimore, J.V., Jehle, A.K., Götz, F., Kulik, A., Molinaro, A., Lipka, V., Gust, A.A., Nürnberger, T., 2011. Arabidopsis lysin-motif proteins LYM1 LYM3 CERK1 mediate bacterial peptidoglycan sensing and immunity to bacterial infection. PNAS 108, 19824–19829.

Wu, T., Hu, E., Xu, S., Chen, M., Guo, P., Dai, Z., Feng, T., Zhou, L., Tang, W., Zhan, L., Fu, X., Liu, S., Bo, X., Yu, G., 2021. clusterProfiler 4.0: a universal enrichment tool for interpreting omics data. Innovation (Camb.) 2, 100141.

Yang, C., Liu, R., Pang, J., Ren, B., Zhou, H., Wang, G., Wang, E., Liu, J., 2021a. Poaceae-specific cell wall-derived oligosaccharides activate plant immunity via OsCERK1 during magnaporthe oryzae infection in rice. Nat. Commun. 12, 2178.

Yang, H., Wang, D., Guo, L., Pan, H., Yvon, R., Garman, S., Wu, H.-M., Cheung, A.Y., 2021b. Malectin/Malectin-like domain-containing proteins: a repertoire of cell surface molecules with broad functional potential. Cell Surface 7, 100056.

Yuan, M., Ngou, B.P.M., Ding, P., Xin, X.F., 2021. PTI-ETI crosstalk: an integrative view of plant immunity. Curr. Opin. Plant Biol. 62, 102030.

Zang, H., Xie, S., Zhu, B., Yang, X., Gu, C., Hu, B., Gao, T., Chen, Y., Gao, X., 2019. Mannan oligosaccharides trigger multiple defence responses in rice and tobacco as a novel danger-associated molecular pattern. Mol. Plant Pathol 20, 1067–1079.

Molecular Plant
Review article

CellPress
Partner Journal

Plant cell wall-mediated disease resistance: Current understanding and future perspectives

Antonio Molina[1,2,*], Lucía Jordá[1,2,*], Miguel Ángel Torres[1,2], Marina Martín-Dacal[1,2], Diego José Berlanga[1,2], Patricia Fernández-Calvo[1,4], Elena Gómez-Rubio[3] and Sonsoles Martín-Santamaría[3]

[1]Centro de Biotecnología y Genómica de Plantas, Universidad Politécnica de Madrid (UPM) - Instituto Nacional de Investigación y Tecnología Agraria y Alimentaria (INIA/CSIC), Campus de Montegancedo UPM, Pozuelo de Alarcón (Madrid), Spain

[2]Departamento de Biotecnología-Biología Vegetal, Escuela Técnica Superior de Ingeniería Agronómica, Alimentaría y de Biosistemas, UPM, Madrid, Spain

[3]Centro de Investigaciones Biológicas Margarita Salas, Consejo Superior de Investigaciones Científicas (CSIC), Ramiro de Maeztu 9, 28040 Madrid, Spain

[4]Present address: Misión Biológica de Galicia, Consejo Superior de Investigaciones Científicas (CSIC), Campus de Montegancedo UPM, Pozuelo de Alarcón (Madrid), Spain

***Correspondence: Antonio Molina (antonio.molina@upm.es), Lucía Jordá (lucia.jorda@upm.es)**

https://doi.org/10.1016/j.molp.2024.04.003

ABSTRACT

Beyond their function as structural barriers, plant cell walls are essential elements for the adaptation of plants to environmental conditions. Cell walls are dynamic structures whose composition and integrity can be altered in response to environmental challenges and developmental cues. These wall changes are perceived by plant sensors/receptors to trigger adaptative responses during development and upon stress perception. Plant cell wall damage caused by pathogen infection, wounding, or other stresses leads to the release of wall molecules, such as carbohydrates (glycans), that function as damage-associated molecular patterns (DAMPs). DAMPs are perceived by the extracellular ectodomains (ECDs) of pattern recognition receptors (PRRs) to activate pattern-triggered immunity (PTI) and disease resistance. Similarly, glycans released from the walls and extracellular layers of microorganisms interacting with plants are recognized as microbe-associated molecular patterns (MAMPs) by specific ECD-PRRs triggering PTI responses. The number of oligosaccharides DAMPs/MAMPs identified that are perceived by plants has increased in recent years. However, the structural mechanisms underlying glycan recognition by plant PRRs remain limited. Currently, this knowledge is mainly focused on receptors of the LysM-PRR family, which are involved in the perception of various molecules, such as chitooligosaccharides from fungi and lipo-chitooligosaccharides (i.e., Nod/MYC factors from bacteria and mycorrhiza, respectively) that trigger differential physiological responses. Nevertheless, additional families of plant PRRs have recently been implicated in oligosaccharide/polysaccharide recognition. These include receptor kinases (RKs) with leucine-rich repeat and Malectin domains in their ECDs (LRR-MAL RKs), *Catharanthus roseus* RECEPTOR-LIKE KINASE 1-LIKE group (CrRLK1L) with Malectin-like domains in their ECDs, as well as wall-associated kinases, lectin-RKs, and LRR-extensins. The characterization of structural basis of glycans recognition by these new plant receptors will shed light on their similarities with those of mammalians involved in glycan perception. The gained knowledge holds the potential to facilitate the development of sustainable, glycan-based crop protection solutions.

Key words: *Arabidopsis thaliana*, cell wall, damage-associated molecular patterns, DAMPs, disease resistance, glycans, oligosaccharides, pattern-triggered immunity, PTI, pattern recognition receptor, PRRs

Molina A., Jordá L., Torres M.Á., Martín-Dacal M., Berlanga D.J., Fernández-Calvo P., Gómez-Rubio E., and Martín-Santamaría S. (2024). Plant cell wall-mediated disease resistance: Current understanding and future perspectives. Mol. Plant. **17**, 699–724.

Published by the Molecular Plant Shanghai Editorial Office in association with Cell Press, an imprint of Elsevier Inc., on behalf of CSPB and CEMPS, CAS.

Plants are under continuous biotic stresses caused by their exposure to microbial populations, pathogens, and pests. Despite the diversity of biotic and other environmental challenges to which plants are exposed, they can reprogram their physiological processes to respond to these conditions. This ability of plants is facilitated by a variety of complex and efficient mechanisms of adaptation, which include diverse molecular monitoring systems that perceive stresses-derived signals and trigger specific adaptative responses (Engelsdorf and Hamann, 2014; Wolf, 2022; Alonso Baez and Bacete, 2023; Bender and Zipfel, 2023). Among these adaptative responses is the activation of disease resistance to pathogens, which is costly because implies the allocation to defense of resources (e.g., signaling components and antimicrobial molecules) and this might compromise plants' development, reproduction, and offspring (Denancé et al., 2013; Lozano-Durán and Zipfel, 2015; Karasov et al., 2017; Monson et al., 2022). Thus, activation of plant disease resistance mechanisms against pathogens and pests is tightly regulated and includes cell autonomous monitoring systems to perceive pathogen infection and specific mechanisms to fine-tune the intensity and duration of the responses (Lozano-Durán and Zipfel, 2015; Wolf, 2022; Bender and Zipfel, 2023).

One of these plant monitoring systems is the cell wall that surrounds all plant cells. Cell walls are dynamic structures that provide mechanical support, orchestrate cell growth, and influence cell differentiation and fate, thereby shaping the overall architectural structure of the plant (Yong et al., 2005; Zhang et al., 2021b, 2021c; Wolf, 2022; Delmer et al., 2024). Plant cell walls have relevant functions as safeguards against both biotic and abiotic stresses that can alter wall composition and structure, and accordingly cell wall integrity (CWI) (Miedes et al., 2014; Benedetti et al., 2018; Gigli-Bisceglia and Testerink, 2021; Molina et al., 2021; Baez et al., 2022; Gigli-Bisceglia et al., 2022; Wolf, 2022). CWI alterations occur during plant-microbe interactions since plant walls represent physical barriers that pathogens must overcome and break down by the action of cell wall degrading modifying enzymes (CWDEs) secreted by microorganisms (Zheng et al., 2021). Upon CWI alterations, activation of the signaling process takes place through different sets of receptors/sensors that trigger specific adaptative responses, including the *de novo* synthesis or the modification of wall components, as well as plant cell wall remodeling (Feng et al., 2018; Bacete and Hamann, 2020; Zhao et al., 2021; Bacete et al., 2022; Gigli-Bisceglia et al., 2022; Wolf, 2022). Modifications of plant CWI by exogenous chemical treatments (e.g., by using inhibitors of polysaccharide synthesis) or genetically, by impairing or overexpressing cell wall-related genes in some species (e.g., *Arabidopsis thaliana*), have contributed to understand the impact of some plant cell wall modifications on plant development, but also on disease resistance phenotypes (Denness et al., 2011; Miedes et al., 2014; Tateno et al., 2016; Ogden et al., 2023).

In addition to the cell wall monitoring system, plants have evolutionary acquired the capacity to detect conserved pathogen-derived ("non-self") ligands, known as microbe-associated molecular patterns (MAMPs), by plasma membrane-anchored pattern-recognition receptors (PRRs), which are mainly receptor kinases (RKs) and receptor-like proteins (RPs) (Bender and Zipfel, 2023). These types of receptors can also perceive "plant-self"-derived damage-associated molecular patterns (DAMPs), which are released or synthesized upon plant tissue damage/infection by pathogens (De Lorenzo and Cervone, 2022). MAMP/DAMP recognition by PRRs activate pattern-triggered immunity (PTI) and disease resistance responses. Plant immune system also recognizes microbial effectors (Avr proteins, not conserved between microbial strains) through intracellular receptors that might be encoded by resistance genes (R), activating effector-triggered immunity (ETI) (Li et al., 2016; Boutrot and Zipfel, 2017; DeFalco and Zipfel, 2021). PTI and ETI have recently been shown to function cooperatively in disease resistance (Yuan et al., 2021).

Plant cell walls: Biochemically diverse structures that are not just physical barriers

Pathogens attempting to colonize plant tissues must overcome plant cell wall barriers, which are sometimes reinforced with a cuticle composed of hydrophobic compounds (Arya et al., 2021). All plant cells are surrounded by a primary cell wall (PCW), whereas those cells that have completed their cellular expansion or reinforced their walls for functional specialization, such as xylem cells, have also secondary cell walls (SCWs) (Carpita and McCann, 2020). Plant cell walls are mainly composed of carbohydrate-based polymers (cellulose, pectins, and hemicelluloses) integrated by different monosaccharide moieties (e.g., glucose, xylose, arabinose, galacturonic acid, and rhamnose) bound by diverse types of linkages. These linkages determine the linearity or degree of branching of the polysaccharides. Moreover, glycan moieties of the polysaccharides can have different biochemical decorations (acetylations, esterifications, methylations, aminations, etc.), undergo modifications (oxidation or reduction), or be bound to ions/cations (e.g., calcium, boron), making the structure of cell wall polysaccharides extremely diverse and complex (Burton et al., 2010; Carpita and McCann, 2020; Delmer et al., 2024). Moreover, polysaccharide structures can be modified through linkages established among them and with other cell wall components such as proteins, lignin, and suberin (Delmer et al., 2024). Plant cell walls of eudicots and monocots exhibit substantial variations in the composition and structure of PCWs (type I in eudicots and type II in grasses) and SCWs, that we are still far from characterizing, although significant progresses have been done in the last years (Zhang et al., 2021b; Cosgrove, 2024; Addison et al., 2024; Delmer et al., 2024).

PCW of eudicots (type I) mainly consist of cellulose arrays composed of β-1,4-D-glucan chains (Carpita and Gibeaut, 1993). These chains are synthesized at the plasma membrane by cellulose synthase (CESA) complexes and are subsequently assembled into semi-crystalline microfibrils (Pear et al., 1996; Burton et al., 2010; Turner et al., 2018). These microfibrils gain stability through their interaction with other β-1,4 backbones, mainly xyloglucans (XyG), that are the main hemicelluloses in type I PCW. XyG, that have a complex array of side chain substitutions, are synthesized at the Golgi apparatus by cellulose synthase-like proteins from 'glycosyltransferase 2 family and are transported to the plasma membrane via vesicle trafficking (Kim et al., 2020). The interaction points between cellulose-hemicelluloses determine the biomechanical properties of the

cell wall and serve as target for expansins and other proteins for cell wall remodeling and cell expansion (Park and Cosgrove, 2012; Zhang et al., 2021a). These arrays of fibers are embedded in a matrix of pectins, primarily comprising α-1,4-D-galacturonic acid (GalA) chains that form the structural backbones of homogalacturonans (HG). HG are decorated with diverse sugar branches in rhamnogalacturonan I and rhamnogalacturonan II polymers (Atmodjo et al., 2013). HG are synthesized in the Golgi and secreted in acetylated and methyl-esterified forms (at the carboxylic residue) into the apoplast. Here, they undergo deacetylation by pectin acetyl esterases and/or demethylation by cell wall pectin methylesterases (Pelloux et al., 2007; Sinclair et al., 2020; Delmer et al., 2024). The demethylated regions of HG can bind Ca^{2+} ions, leading to the formation of "egg-box" structures that contribute to form gels and stabilize the cell wall (Zdunek et al., 2021). In addition, pectin methylesterase inhibitors regulate pectin methylesterase activity, loosening the pectin matrix to control cell adhesion and cell expansion (Wormit and Usadel, 2018; Coculo and Lionetti 2022). HG demethylation can also affect the biomechanical properties of the cell wall by rendering pectin susceptible to enzymatic depolymerization by pectin lyases and polygalacturonases (PGs) (De Lorenzo and Cervone, 2022; Cosgrove, 2024). Besides these glycan polymers, highly glycosylated arabinogalactan proteins (AGPs) are covalently linked to hemicelluloses and pectins (Tan et al., 2013). These AGPs influence cell adhesion during growth and development by establishing glycosylphosphatidyl-inositol (GPI) links with the plasma membrane (Leszczuk et al., 2023).

The composition of the type II PCW of grasses differs from that of dicots (type I) in the class and relative abundance of non-cellulosic polysaccharides, proteins and phenolic compounds (Carpita and Gibeaut, 1993; Vogel, 2008). PCW of grasses is mainly composed of a structural framework of cellulose fibers interconnected with arabinoxylans and glucuronoarabinoxylans. Pectins and proteins are less prominent than in dicots, and their structural role is carried out by unbranched and unsubstituted chains of mixed-linked β-1,3/β-1,4-glucans (MLGs) (Vogel, 2008). Moreover, these walls are characterized by the presence of significant quantities of phenylpropanoid molecules including lignin, ferulic acid and *p*-coumaric acid, and suberin in some cells, that are crosslinked to polysaccharides to provide rigidity and mechanical strength to cell walls (Hatfield et al., 2016).

SCWs are composed of robust matrixes primarily consisting of cellulose microfibrils, intertwined with various hemicelluloses, particularly xylans and glucomannans, and mannans (Sarkar et al., 2009; Kumar et al., 2016; Delmer et al., 2024). This structural framework is further strengthened by crosslinking with lignin, resulting in a rigid and impermeable barrier that imparts durability to plant cells (Kang et al., 2019). There is considerable variability in the fine structures of primary or secondary wall polymers (e.g., degree of xylan and pectin acetylation or pectin methylation) within a given phylogenetic group of plants, and even a plant species. Moreover, cell wall composition and structure vary significantly between different tissues (e.g., leaves vs. roots) and even between one cell and its adjacent cells. All these chemical differences have an obvious impact on the three-dimensional architectures and physicochemical properties of plant walls, and on the diversity of wall structures found in plants. We are still far from getting a detailed characterization of wall composition and structure at the cellular level, and *in vivo* mechanical and biochemical properties of cell wall, although some technological progress might contribute to decipher this key question in plant biology (Alonso Baez and Bacete, 2023). Among these emerging non-destructive tools enabling simultaneous *in vivo* visualization of many cell wall features are Brillouin microscopy, multi-target optical nanoscopy, and Raman spectroscopy (Haas et al., 2020; Mateu et al., 2020; Bacete et al., 2022), and some technologies such as metabolic click chemistry labeling for imaging of cell wall polysaccharides in living cells, or proximity labeling to identify proteins that are physically close to wall bait proteins (Herburger et al., 2022; Kumar et al., 2022; Morel et al., 2022; Ropitaux et al., 2022).

The heterogeneity of plants walls is also reflected in the diverse mechanisms that pathogens have evolved to breach them, like the secretion of diverse CWDEs, such as cellulases, PGs, or xylanases. CWDEs represent a significant portion of the encoded proteins of plant-pathogenic fungal genomes, further indicating their relevance for breaching and modifying the walls and suggesting that microbial CWDEs' repertoire might determine plant-microbe specificity and colonization (Kubicek et al., 2014). The arsenal of CWDEs of microbes is quite diverse and is classified into different groups in the carbohydrate-active enzyme (CAZYme) database (http://www.cazy.org; Drula et al., 2022). CWDEs can either hydrolyze/break down linkages between glycan moieties, add/release groups to glycan moieties, or modify wall glycans/polysaccharides through oxidation or reduction. This diversity of activities of microbial CWDEs illustrates the complexity of plant wall structures that microorganisms must encounter and degrade to get into the cell or to release free glycans that they might use as energy source or building blocks for the biosynthesis of new biomolecules of the microorganisms. The diversity of CWDE activities existing in nature has recently expanded with the identification of human/animal microbiomes that can degrade walls and oligosaccharides from plant biomass during digestion (Delannoy-Bruno et al., 2022). The observed expansions in the number of genes within specific CAZYme and peptidase families in the genomes of plant pathogens, compared with non-phytopathogenic microbial genomes, further corroborates the contribution of CWDEs to plant pathogens colonization capacities (Drula et al., 2022; Dort et al., 2023).

Modification of cell wall integrity/composition influences plant disease resistance

Cell wall modifications caused by pathogens during plant cell colonization can be perceived by plant cell wall monitoring systems to trigger defensive responses. Accordingly, mutations affecting plant genes encoding functions related with the synthesis of cell wall components might cause wall modifications that can be perceived by plant monitoring systems and have an impact on plant disease resistance outcome (Miedes et al., 2014; Bacete et al., 2018). These phenotypic alterations have been particularly documented in *Arabidopsis thaliana* (Arabidopsis) mutants impaired in cell wall-related genes and supports the relevant role of this extracellular matrix on plant immunity (Bacete et al., 2018; Molina et al., 2021). For example, mutants impaired in CESA complexes required for

the synthesis of cellulose are usually associated to specific enhanced disease resistance phenotypes. Arabidopsis *cev1* and *rsw* mutants, affected in *CESA3* and *CESA1* genes, respectively, required for PCW cellulose biosynthesis, display enhanced resistance to several biotrophic powdery mildew fungi such as *Golovinomyces cichoracearum*, *G. orontii*, and *Oidium lycopersicum* (Ellis et al., 2002a, 2002b), but did not display altered susceptibility to the necrotrophic fungus *Plectosphaerella cucumerina* or the soil-borne bacterium *Ralstonia solanacearum* (Hernández-Blanco et al., 2007). In contrast, Arabidopsis *irx5-1/irx3-1/irx1-6* mutants, affected, respectively, in *CESA4/CESA7/CESA8* required for SCW cellulose biosynthesis, are more resistant than wild-type plants to *P. cucumerina*, *R. solanacearum*, and the necrotrophic fungus *Botrytis cinerea*, among other pathogens (Hernández-Blanco et al., 2007; Molina et al., 2021). Similarly, mutations in CESA complex-associated proteins involved in cellulose deposition also alter cell wall properties and have an impact on immunity. For example, Arabidopsis plants impaired in the endoglucanase *KORRIGAN* (*KOR1*) show a reduction in the rate of cellulose deposition and enhanced colonization by the bacterium *Pseudomonas syringae*, but restricted invasion by *B. cinerea* (López-Cruz et al., 2014). This mutant, as well as plants defective in other components of the CESA complex such as *CHITINASE-LIKE1* (*CTL1*) and the GPI-anchored plant-specific *COBRA* protein, display less growth of the vascular pathogens *Fusarium oxysporum* and *R. solanacearum* in comparison with wild-type plants (Menna et al., 2021). Thus, alteration in the cellulose framework usually results in significant modifications of plant disease responses to different pathogens.

Alteration of the biosynthesis and/or structure of wall pectins (e.g., degree of methyl-esterification and acetylation) also affect pathogen resistance (Bethke et al., 2016). Mutants with enhanced or reduced pectin content show altered disease resistance against different pathogens. For example, Arabidopsis *powdery mildew-resistant* (*pmr*) mutants, impaired either in a pectin acetyltransferase that transfers acetyl groups to GalA (*pmr5*; Chiniquy et al., 2019) or in a pectate lyase–like protein (*pmr6-1*; Vogel et al., 2002), exhibit cell walls with increased total pectins and enhanced resistance to powdery mildew fungi (*G. cichoracearum* and *Erysiphe orontii*) (Vogel et al., 2002, 2004) and the hemibiotrophic fungus *Colletotricum higginsianum* (Engelsdorf et al., 2017), whereas they are highly susceptible to *B. cinerea* (Wang et al., 2017; Chiniquy et al., 2019) and are unaffected in their resistance to *P. cucumerina* (Hernández-Blanco et al., 2007; Molina et al., 2021). Similarly, Arabidopsis *gae1 gae6* double mutant that is impaired in genes encoding glucuronate 4-epimerases required for pectin precursor UDP-D-GalA biosynthesis and displays strong reduction in GalA, total uronic acids, and pectin in its cell walls, is slightly more susceptible to *P. syringae* pv. *maculicola* ES4326 bacterium and shows enhanced susceptibility to *B. cinerea* isolates (Bethke et al., 2016). In contrast, Arabidopsis plants expressing constitutively a fungal PG that degrades HG, as well as loss-of-function mutants for *QUASIMODO2* (*QUA2*) gene, encoding a pectin methyltransferase relevant for HG biosynthesis, show reduced growth and almost complete resistance to *B. cinerea*, probably explained in this case by the accumulation of reactive oxygen species observed in the mutant in comparison with wild-type plants (Du et al., 2020; Lorrai et al., 2021).

Immunity-related phenotypes have been also documented for some plant mutants with reduced content and/or structural alterations in composition of hemicelluloses (Bacete et al., 2018). For example, mutants in the Arabidopsis xylosidase *XYL1*, which affects XyG structure, and in GPI-linked *IRX6/COBL4* and vacuolar H^+-ATPase Arabidopsis *DE-ETIOLATED 3* (*DET3*), which have increased xylose content, display enhanced resistance to *P. cucumerina* (Delgado-Cerezo et al., 2012). Moreover, mutations affecting side chains of hemicelluloses (e.g., degree of acetylations) also influence disease resistance (Pogorelko et al., 2013), as it has been observed in REDUCED WALL ACETYLATION 2 (RWA2) mutant impaired in an O-acetyltransferase that shows an overall reduction of acetylation on several polymers and enhanced resistance to the biotrophic oomycete *Hyaloperonospora arabidopsidis* and *B. cinerea* fungus, but not to *P. syringae* and *P. cucumerina* (Manabe et al., 2011; Pawar et al., 2016). In contrast, mutations in the plant-specific polysaccharide O-acetyltransferase ESKIMO1 (ESK1), involved in xylan acetylation, show enhanced resistance to *P. cucumerina* but not to the biotrophic pathogens tested (Escudero et al., 2017).

In addition to the cell wall structural polymers, callose, a β-1,3-D-glucan that can be found in several locations within a plant, has been described to play a major role in both development and plant defense processes. Callose is deposited between the plasma membrane and the cell wall, forming papillae at sites where fungal penetration occurs, effectively hindering pathogen intrusion (Voigt, 2014; Wang et al., 2021). Induction of plant callose deposition at the cell wall upon pathogen infection relies on several plant callose synthase enzymes, such as GLUCAN SYNTASE-LIKE 5 (GSL5)/POWDERY MILDEW RESISTANT 4 (PMR4). Depletion of callose in Arabidopsis *gsl5/pmr4* mutant leads to contrasting outcomes in terms of immunity, since *gls5/pmr4* exhibits enhanced resistance to various powdery mildew fungal species, *P. syringae* and *H. arabidopsidis* (Jacobs et al., 2003; Flors et al., 2008). On the other hand, *gls5/pmr4* displays increased susceptibility to the grass powdery mildew fungus *Blumeria graminis* and the necrotrophic fungus *Alternaria brassicicola* (Nishimura et al., 2003; Flors et al., 2008). These data support the role of callose deposition in preventing fungal penetration at papillae (Ellinger et al., 2013). Furthermore, callose also inhibits pathogen spread through its accumulation at plasmodesmata and other plant tissues, as shown in callose-degrading β-1,3-glucanase (AtBG_paps) mutants that have reduced virus spread (Zavaliev et al., 2013).

Alteration (biosynthesis or modification) of complex cell wall components like AGPs also leads to modification in plant disease resistance. Loss-of-function mutants of ARABINOXYLAN PECTIN ARABINOGALACTAN PROTEIN 1 (APAP1), an AGP that is covalently attached to pectin and hemicellulose (Tan et al., 2013), displays increased susceptibility to *P. syringae* (Kim et al., 2023). Conversely, mutants in arabinokinase1 protein (*ara1*), which cannot metabolize exogenously added arabinose (Sherson et al., 1999), display enhanced resistance to this pathogen (Kim et al., 2023). Also, alteration of the cell wall lignin content leads to susceptibility phenotypes (reviewed by Miedes et al., 2014). Arabidopsis mutants in lignin biosynthetic genes encoding phenylalanine ammonia-lyase (Huang et al., 2010), caffeic acid o-methyltransferase

(Quentin et al., 2009), and cinnamyl alcohol dehydrogenase (Tronchet et al., 2010) displaying reduced lignin deposition are more susceptible to various bacterial and fungal pathogens (Miedes et al., 2014). Of note, Arabidopsis lines with similar lignin contents, but strikingly different lignin compositions resulting from the overexpression or loss of function of the enzyme ferulate/coniferaldehyde 5-hydroxylase (F5H) exhibit differential transcriptional expression of defense genes (Gallego-Giraldo et al., 2018). Similarly, Arabidopsis *ccr1-3* mutant in cinnamoyl CoA reductase (CCR) protein shows reduced lignin content and differential resistance to pathogens (Gallego-Giraldo et al., 2018; Liu et al. 2023a, 2023c). Also, overexpression of genes of the ligno-suberin pathway in tomato enhances resistance to *R. solanacearum* by restricting its movement (Kashyap et al., 2022). This is likely because these phenolic compounds function as a physical barrier that restricts pathogen from the infection site and hinders its further spread through vascular tissues (Lee et al., 2019).

Interestingly, some loss of function lines with alterations in PTI signaling components (e.g., heterotrimeric G-protein complex and some PRRs, such as ERECTA RK) exhibit changes in their cell wall structure, linking the activation of immune pathways to cell wall remodeling (Sánchez-Rodríguez et al., 2009; Delgado-Cerezo et al., 2012). In addition, mutants in signaling pathways mediated by hormones, such as *arr6* plants, which are impaired in ARABIDOPSIS RESPONSE REGULATOR 6 (ARR6) involved in cytokinin signaling regulation, show important alterations in cell wall composition and display differential resistance patterns, being more resistant than wild-type plants to *P. cucumerina* but more susceptible to *R. solanacearum* (Bacete et al., 2020). Similarly, mutants in components of abscisic acid (ABA) pathway show alterations in their cell walls and differential resistance to pathogens (Delgado-Cerezo et al., 2012; Sánchez-Vallet et al., 2012). In summary, all these data clearly illustrate the relevance of plant cell walls in disease resistance patterns. However, with some exceptions (Molina et al., 2021), correlations between specific wall structure content/modifications and disease resistance phenotypes have not been established yet. In these few examples, complex and diverse defensive mechanisms are proposed to explain the disease resistance phenotype observed (Bacete et al., 2018; Molina et al., 2021).

From cell wall alterations to immune signaling activation

Mutants impaired in cell wall-associated genes or transgenic lines overexpressing this group of genes are generally affected in the structure/composition of their cell walls in comparison with wild-type plants. These modifications might compromise or facilitate the degradability of the wall barrier by pathogen CWDEs, or/and might lead to the activation of some plant immune pathways contributing to disease resistance, thus explaining the genotype-specific disease resistance phenotypes observed in these plants. In a screening of Arabidopsis cell wall mutants performed to determine the specific contribution of plant cell walls to disease resistance against pathogens with different parasitic styles, a significant set of cell wall mutants were found to be affected in disease resistance to at least one of the pathogens tested (Molina et al., 2021). These genotypes exhibit a high diversity of wall compositions (Molina et al., 2021), as revealed by glycome profiling performed with a set of monoclonal antibodies that detect specific wall carbohydrate moieties (Ruprecht et al., 2017). Mathematical modeling of glycome profiling data of these Arabidopsis wall mutants led to the identification of specific correlations between the amount of specific wall carbohydrate moieties in the wall fractions of these Arabidopsis genotypes and their disease resistance phenotypes to specific pathogens. These analyses demonstrated that some of the observed phenotypes in the Arabidopsis mutants tested could be linked to specific cell wall composition/structure alterations, such as the correlation found between the level of fucosylated xyloglucans in wall extracted fractions of a set of Arabidopsis genotypes and their degree of resistance to *P. cucumerina* (Molina et al., 2021). These data might suggest that the disease resistance phenotypes observed in these genotypes were just due to changes in their wall barriers that are not overcome by pathogens. However, pectin-enriched cell wall fractions extracted chemically from the walls of such mutants (e.g., *arr6* and *irx10*) triggered in Arabidopsis wild-type plants enhanced PTI hallmarks (e.g., calcium burst) compared with those observed after treatment with wild-type plant wall fractions, suggesting that fractions of these mutants contain DAMPs (i.e., oligosaccharides) that are either absent or present at lower concentrations in wild-type plant wall fractions (Molina et al., 2021). Similarly, glycans (DAMPs) extracted with water from cell walls of Arabidopsis lignin mutant *ccr1-3* were shown to be enriched in a galacturonic acid trisaccharide ($GalA_3$) and other DAMPs that trigger upregulation of defensive genes in wild-type plants (Gallego-Giraldo et al., 2018; Liu et al., 2023c). These *ccr1-3* DAMPs probably are released from glucuronic acid-containing xylan oligosaccharides that are enriched in these mutants. This release of DAMPs seems to be impaired in mutants in the MLL-RK FERONIA (FER). Notably, such wall fractions do not trigger immune responses in mutant plants impaired in five wall-associated RKs (WAK1–WAK5) (Liu et al., 2023a). These examples demonstrate that plant cell wall modifications by impairing the expression of cell wall-related genes can lead to the release of wall DAMPs that trigger PTI and disease resistance responses.

Differential modulation of canonical immune pathways has been also suggested previously to account for the immune phenotypes displayed by many plant cell wall mutants (Bacete et al., 2018; Wolf, 2022). For example, Arabidopsis mutants affected in cellulose and pectin synthesis show constitutive activation of defensive pathways regulated by hormones, such as jasmonic acid (JA), ethylene (ET), ABA, or salicylic acid (SA). Indeed, *cev1* displays constitutive activation of JA and ET signaling, and JA signaling was shown to be concomitant to its enhanced resistance phenotypes (Ellis et al., 2002a). Also, immunity phenotypes in the endo-1,4-β-glucanase mutant *kor1* are linked to increases in JA and SA signaling and callose deposition (López-Cruz et al., 2014). On the other hand, enhanced resistance to vascular pathogens *F. oxysporum* and *R. solanacearum* displayed by several Arabidopsis mutants in PCW-CESA complex-associated proteins depends on constitutive activation of ET rather than JA signaling (Menna et al., 2021). By contrast, enhanced immunity phenotypes caused by the disruption of SCW *CESA8/IRX1* and *CESA4/IRX5* genes are dependent on the accumulation of antimicrobial compounds and ABA signaling rather than JA/ET or SA pathways (Hernández-Blanco et al., 2007). Also, the altered immunity of *esk1* plants seems to depend primarily on the accumulation of

antimicrobial peptides and tryptophan-derived secondary metabolites (Escudero et al., 2017). Interestingly, callose depletion in the *gsl5/pmr4* mutant imbalances hormone signaling with a hyperactivation of SA pathway that is concurrent with downregulation of JA signaling (Nishimura et al., 2003; Flors et al., 2008). Whether constitutive activation of these canonical defensive pathways in the indicated cell wall mutants occurs through either wall-derived DAMPs or uncharacterized signaling molecules is unknown and deserves further investigation.

Remarkably, alteration of immunity displayed by cell wall mutants is not always mediated by canonical signaling pathways, since enhanced disease resistance phenotypes of some Arabidopsis cell wall mutants cannot be explained by upregulation of canonical PTI or the expression patterns of phytohormone-related (SA, JA, ET, and ABA) marker genes (Molina et al., 2021). Similarly, other reports describing the transcriptomic profiling of plant cell wall mutants revealed the differential constitutive regulation of non-canonical defensive genes in these plants in comparison with wild-type ones (Gallego-Giraldo et al., 2018). For example, *pmr5*- and *pmr6*-mediated resistance has been proposed to depend on the activation of alternative forms of defense (Vogel et al., 2002, 2004). Additional studies suggest that immunity phenotypes of some mutants impaired in hemicellulose synthesis involve alternative pathways such as brassinosteroid- and strigolactone-mediated signaling (Ramírez and Pauly, 2019). Together these data provide strong evidence for the significant role of plant cell walls in immunity modulation, suggesting that in some cases immune responses could be triggered by uncharacterized wall-derived DAMPs. However, we cannot exclude that other mechanisms of disease resistance activation (no-DAMP dependent) might contribute to the observed phenotypes of some of these cell wall mutants.

From cell walls to wall-derived DAMPs/MAMPs triggering immune responses

During plant-microbe interaction coevolution, pathogens have acquired a wide range of mechanisms to breach plant cell walls, including an arsenal of CAZymes, which specifically hydrolyze or modify different cell wall components to break down wall structural barriers (Drula et al., 2022). The activity of these enzymes on plant cell wall polysaccharides leads to the release of active glycans triggering PTI, further confirming plant cell walls as vast sources of DAMPs that have not been characterized in detail (Mélida et al., 2020; Rebaque et al., 2021; Pring et al., 2023). In recent years, numerous studies have uncovered novel plant cell wall bioactive fragments (DAMPs) as well as new glycan-derived MAMPs that are relevant to plant immunity (Table 1). DAMPs include fragments of β-1,4-D-glucosyl cellulose-derived products or cellodextrins with a degree of polymerization (DP) from two to nine moieties of glucose (e.g., β-1,4-D-$(Glc)_{3-5}$ or CEL3-CEL5) (Aziz et al., 2007; Souza et al., 2017; Johnson et al., 2018; Locci et al., 2019), and oligogalacturonides (OGs), which are α-1,4-D-GalA oligomers generated by the action of plant or pathogen PGs on the pectin HG (Benedetti et al., 2015; Voxeur et al., 2019). Also, β-1,4-linked hemicellulose-derived DAMPs have been identified, including those derived from XyG (β-1,4-D-glucan backbone with xylosyl [Xyl (X)]-, galactosyl-, and fucosyl-type branching, mainly with a DP of 7), mannans (β-1,4-D-$(Man)_{2-6}$) released by the action of endo-1,4-β-mannosidases, arabinoxylan-derived oligosaccharides (such as the pentasaccharide 3^3-α-L-arabinofuranosylxylotetraose or XA_3XX) and xylan-based oligosaccharides (β-1,4-D-$(Xyl)_{2-6}$), which are released by the action of endo-xylanases (Table 1) (Zang et al., 2019; Mélida et al., 2020; Pring et al., 2023; Fernández-Calvo et al., 2024). The diversity of plant and seaweed oligosaccharides/polysaccharides that can be perceived by plants have expanded recently by showing that also glucuronoxylans, α-1,4-D-glucans and different polysaccharides from plants and seaweeds activate PTI reponses in Arabidopsis (Fernández-Calvo et al., 2024).

Interestingly, other carbohydrate-based molecular patterns represent a group of glycans that can be classified as DAMPs and MAMPs, since they can be released from both microbial and plant walls. This group includes the non-branched 1,3-β-D-$(Glc)_{6-12}$ glycans, such as laminarinhexaose (LAM6; 1,3-β-D-$(Glc)_6$), that are present in 1,3-β-D glucans of fungal cell walls and in plant callose, and can be released upon pathogen degradation of plant callose or degradation of fungal cell walls by plant CWDEs (Table 1). In addition, unbranched MLGs, such as β-1,4-D-$(Glc)_2$-β-1,3-D-Glc (MLG43), are present in some groups of plants (e.g., grasses or *Equisetum* sp.), but also in oomycetes and microbial cell walls (Table 1) (Chowdhury et al., 2014; Mélida et al., 2018; Barghahn et al., 2021; Rebaque et al., 2021; Martín-Dacal et al., 2023). DAMPs can also be generated through the action of inherent plant CWDEs and might accumulate in the extracellular matrix where they are perceived alongside microbial MAMPs by plant PRRs activating PTI (Bender and Zipfel, 2023). Since plant genomes encode several hundreds of CAZymes that can potentially target plant cell wall polysaccharides during plant development and in response to different stresses (Drula et al., 2022), the contribution of these plant enzymes to the release of DAMPs needs further investigation.

Cell walls and extracellular outer layers of microorganisms are also a source of carbohydrate-based ligands perceived as MAMPs (reviewed by Wanke et al., 2021). The best characterized carbohydrate-based MAMPs are oligosaccharides derived from fungal chitin (chitooligosaccharides [Cos], such as β-1,4-D-$(GlcNAc)_{6-8}$ or CHI6-CHI8] (Table 1). However, bacterial compounds derived from lipopolysaccharide and peptidoglycan, and 1,6-β-D-glucans, have been described to trigger immune responses in different plant species (Table 1) (Khokhani et al., 2021; Chaube et al., 2022). In addition, 1,3-β-D-Glc oligosaccharides with 1,6-β-D-Glc branches can also trigger immunity in plants (Table 1) (Wanke et al., 2020, 2023). Notably, some complex exopolysaccharides from endophytic fungi, as well as lipo-chitooligosaccharid from symbiotic bacteria (Nod factor) and from arbuscular mycorrhizal fungi (MYC factors), are also perceived by plants. However, these molecules activate symbiotic processes, instead of immune responses, through recognition mechanisms involving mainly RKs with lysin motif (LysM) ECDs (Khokhani et al., 2021; Chandrasekar et al., 2022; Kelly et al., 2023).

The relevance of some of the above-described glycans in activating plant disease resistance is supported by the fact that pre-treatments of plants (Arabidopsis and different crops) with these DAMPs boost plant defense responses by triggering signaling cascades that generate a profound transcriptomic

Glycan	Representative oligosaccharide(s) DAMP/MAMP	Source	PRR[a] (co-PRR)[b]	PTI in plants	Reference
Cellulose	CEL2-CEL9: β-1,4-D-$(Glc)_{2-9}$	plants oomycetes	IGP1/CORK1 (IGP3, IGP4)	Arabidopsis, tomato, lettuce	Aziz et al. (2007) Souza et al. (2017) Johnson et al. (2018) Zarattini et al. (2021) Martín-Dacal et al. (2023) He et al. (2023)
Mixed-linked β-1,3/1,4-glucans (MLGs)	MLG43: D-cellobiosyl-(1,3)-β-D-Glc MLG34/MLG443	plants (monocots) *Equisetum* sp. oomycetes	(IGP1/CORK1, IGP3, IGP4) OsLECRK1/OsCERK1 (OsCeBIP)	Arabidopsis, rice, barley, tomato, pepper	Rebaque et al. (2021), Yang et al. (2021a), 2021b Barghahn et al. (2021) Dai et al. (2023)
Homogalacturonan (HG)	oligogalacturonides (OGs): α-1,4-D-$(GalA)_{9-15}$ $GalA_3$: α-1,4-D-$(GalA)_3$	plants	LRX8-RALF4 (FER/LLGs) LRX1-RALF22 (FER/LLGs) (WAK1-WAK5) (RFO1/WAKL10, FER)[c]	Arabidopsis, tomato, grapevine, and several plant species	Benedetti et al. (2015) Voxeur et al. (2019) Liu et al. (2023a) Moussu et al. (2023) Huerta et al. (2023) Schoenaers et al., 2024
Arabinoxylans	XA_3XX: 3^3-α-L-arabinofuranosylxylotetraose	plants	(IGP1/CORK1, IGP3, IGP4)	Arabidopsis, tomato, pepper	Mélida et al., 2020 Fernández-Calvo et al. (2024)
Xylans	β-1,4-D-$(Xyl)_{2-5}$	plants	(IGP1/CORK1, IGP3, IGP4)	Arabidopsis, tomato, wheat	Dewangan et al., 2023 Pring et al. (2023) Fernández-Calvo et al. (2024)
Mannans	β-1,4-D-$(Man)_{2-6}$	plants	nd	Rice, tobacco	Zang et al. (2019)
Xyloglucans	Heptamaloxyloglucan	plants	nd	Arabidopsis, grapevine, wheat, soybean	Claverie et al. (2018)
Linear β-1,3-D-glucans	LAM6: 1,3- β-D-$(Glc)_6$ LAMINARIN: β-1,3-D-$(Glc)_{>10}$	plants fungi oomycetes	(CERK1, LYK4, LYK5)	Arabidopsis, barley, *Brachypodium distachyon* *Nicotiana benthamiana*[d]	Mélida et al., 2018 Wanke et al. (2020)
Branched β-1,3-D-glucans	β-1,3-D-$(Glc)_n$/β-1,6-D-Glc_n branched (decasaccharide)	fungi oomycetes	LjEPR3/LjEPR3a (CERK1)	*Lotus japonica*, Arabidopsis, rice, barley, tobacco	Kelly et al. (2023) Wanke et al. (2020), 2023
Chitin	CHI6-CHI8: β-1,4-D-$(GlcNAc)_{6-8}$ COs: chitin-oligosaccharides	fungi insects	LYK5, LYK4 (CERK1) OsCEBIP (OsCERK1) (MtCERK1, MtLYR4) (LjCERK6) (VvLYK5-1, VvLYK1-1)	grapevine, and several plant species	Cao et al. (2014)·Liu et al., 2012, 2016 Xue et al. (2019) Khokhani et al. (2021) Roudaire et al. (2023)
β-1,6-D-Glucans	β-1,6-D-$(Glc)_{2-9}$	fungi	(CERK1)	Arabidopsis	Chaube et al. (2022) Fernández-Calvo et al. (2024)

Table 1. Glycan structures that induce PTI responses in plants.

[a]PRR has been identified by direct ECD/PRR-glycan binding assays (e.g., ITC, thermophoresis, crystal structure determined). Os, Mt, Lj, and Vv indicate the names of the plant species. The rest of the PRRs and co-PRRs indicated are from *Arabidopsis thaliana*.

[b]co-PRR has been identified genetically or not direct binding to DAMP/MAMP has been determined.

[c]Direct binding to DAMP/MAMP has been shown, but proof of the PRR function deserves further characterization.

[d]*Nicotiana benthamiana* only perceives long β-1,3-D-glucans (LAMINARIN).

reprogramming of plant cells, at local and systemic levels (Table 1) (Souza et al., 2017; Johnson et al., 2018; Mélida et al., 2020; Gamir et al., 2021; Rebaque et al., 2021; He et al., 2023). For example, exogenous application of OGs to Arabidopsis, tomato and grapevine plants confers disease resistance against *B. cinerea* (Aziz et al., 2004; Ferrari et al., 2007; Gamir et al., 2021). Moreover, expression of PGs and PG-inhibiting proteins (PGIPs) in Arabidopsis plants leads to OGs accumulation in the apoplast and increased resistance to *B. cinerea* and bacterial pathogens (Benedetti et al., 2015; Xiao et al., 2024). Also, treatment with xyloglucans induce phytoalexin synthesis in soybean and protect grapevine and Arabidopsis from *B. cinerea*, and wheat kernels from *Fusarium culmorum* (Claverie et al., 2018). Similarly, XA_3XX and MLG-derived glycans (e.g., MLG43) protect tomato and pepper plants against *P. syringae* and the fungus *Sclerotinia sclerotiorum*, respectively (Mélida et al., 2020; Rebaque et al., 2021), XYL_4 confers enhanced resistance in tomato against *P. syringae* (Fernández-Calvo et al., 2024), and MLGs protect rice from *Magnaporthe oryzae* infection (Yang et al., 2021a). Pre-treatment of tobacco and rice plants with oligomannans (DP 2-6) provide enhanced resistance to the oomycete *Phytophthora nicotianae* and the bacteria *Xanthomonas oryzae*, respectively (Zang et al., 2019). Of note, some chitin-based mixtures and seaweed extracts enriched in β-glucans are commercial products with recognized effectiveness in crop protection, further corroborating the role of glycan-based elicitors in plant immunity and the potential of glycan-based technologies in sustainable agriculture (Bacete et al., 2018; Malerba and Cerana, 2019). The immune responses triggered by these DAMPs/MAMPs conferring enhanced resistance to pathogens show clear overlapping, but it seems that they do not activate exactly the same downstream molecular signaling events/responses, such as reactive oxygen species (ROS) production with different intensity, transcriptional responses, or metabolites accumulation (Claverie et al., 2018; Mélida et al., 2018; Rebaque et al., 2021). An in depth characterization of specific downstream signaling components involved in glycan-mediated responses is needed.

Despite the progress in the characterization of DAMPs and MAMPs, we are just starting to determine glycan structures that might be perceived by plants. The diversity and complexity of glycan ligands that can be potentially recognized as DAMPs/MAMPs by plants is illustrated by the following facts: (1) over 20 different monosaccharides can form the backbone and/or ramifications building blocks of wall polysaccharides, (2) these carbohydrate moieties can be bound through a high number of different glycosidic linkages, (3) monosaccharides can have different biochemical decorations (i.e., acetylation, methylation, amination, etc.), and (4) glycans can differ in their DP, although DAMP/MAMPs identified so far have a narrow DP range from 2 to 12, and the majority are linear glycans (Latgé and Calderone, 2002; Mélida et al., 2013; Srivastava and Kapoor, 2017). Thus, a great variety of uncharacterized DAMPs/MAMPs can be generated from plant cell wall and microbial extracellular layer polymers by the action of CAZYmes from plants and microbes released or secreted during disease progression (Guzha et al., 2022; Kim et al., 2023). Novel methodologies are needed to identify *in vivo* pathogen-driven cell wall modifications and to purify the released DAMPs, although some progress has been done recently (Voxeur et al., 2019; Haas et al., 2020; Voxeur and Höfte, 2020; Morel et al., 2022; Ropitaux et al., 2022). Since most of the putative glycans that can be released from plant walls and function as DAMPs have not been purified or chemically synthesized, the full diversity of oligosaccharides that PRRs might perceive remains unexplored.

Homeostasis of DAMPs/MAMPs determines amplitude of plant immune responses

Long-lasting or intense activation of defensive signaling pathways can generate hyper-immunity that might cause cell death and plant development alterations (Berry and Argueso, 2022). For example, OG overaccumulation leads to reduced plant growth and even lethality (Benedetti et al., 2015). Accordingly, plants must control the generation and levels of active DAMPs and the exposure to DAMPs and MAMPs that trigger PTI, given their fundamental role modulating growth-defense trade-offs (Pontiggia et al., 2020; Molina et al., 2021). In plants, cell wall remodeling is a relevant process that takes place during cell expansion and growth (Delmer et al., 2024), and therefore some mechanisms are needed to fine-tune the turnover/metabolism of cell wall-derived signals during non-pathogenic (e.g., cell expansion) and pathogenic conditions (De Lorenzo and Cervone, 2022). Until recently, plant mechanisms modulating homeostasis of cell wall-derived danger signals were unknown. Notably, several plant enzymes have recently been identified that are able to modify the released DAMPs thereby fine-tuning their eliciting capacity and the amplitude of the defense responses triggered (Benedetti et al., 2018; Locci et al., 2019). The Arabidopsis superfamily of FAD-binding berberine bridge enzyme such as (AtBBE-like) has turned out to play relevant functions in the homeostasis of certain DAMPs. Of note, the expression of several *AtBBE-like* genes has been shown to be upregulated during infection and upon plant treatment with MAMPs/DAMPs (Benedetti et al., 2018; Mélida et al., 2018, 2020; Locci et al., 2019; Pontiggia et al., 2020; Costantini et al., 2023). Four OG-oxidases (OGOXs) and one cellodextrin oxidase (CELLOX) from the AtBBE-like family have been found to oxidize the anomeric carbon of some oligosaccharides. OGOXs specifically oxidate the anomeric carbon of OGs with different DP to inactivate them (Benedetti et al., 2018), while CELLOX oxidizes the anomeric carbon of CEL3-CEL6 and some MLGs (e.g., MLG43), but not that of glucose (Locci et al., 2019). The oxidized OGs and CEL-oligos are biologically less active at triggering PTI than the reduced ones, probably because PRRs have lower affinity for these modified glycans (Figure 1). It has also been described that these oxidized glycans are less accessible to fungal lytic enzymes (PGs and endoglucanases), limiting fungi access to carbon sources (glycans of low DP) that they can use for the energetic catabolism and as building blocks for biosynthetic processes, thus reducing pathogen proliferation (Figure 1) (Locci et al., 2019; Zarattini et al., 2021). Interestingly, CEL3, the most powerful cellulose-derived DAMPs activating PTI (Locci et al., 2019; Martín-Dacal et al., 2023), is the best substrate for CELLOX (Locci et al., 2019), highlighting the fundamental role of these modifying enzymes in the regulation of the activity and homeostasis of cell wall-derived DAMPs (Figure 1). It should be noted that oxidation of OGs and CEL-oligos generates H_2O_2, which plays an essential function in the subsequent strengthening of the cell wall and in cell signaling mediated through the extracellular H_2O_2

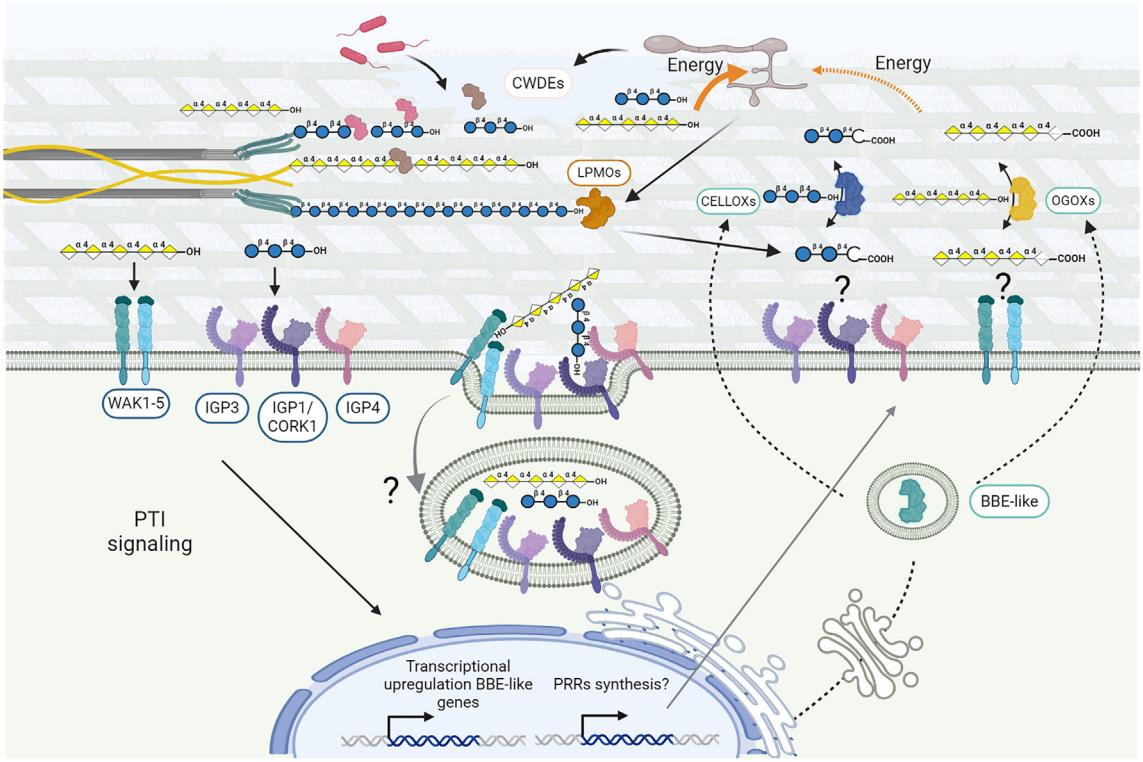

Figure 1. Release and homeostasis of cell wall-derived DAMPs triggering immune responses in plants.
CWDEs secreted by pathogens hydrolyze cell wall polysaccharides (e.g., cellulose and HG) releasing glycans that can be used by pathogens as source of carbons for their energetic catabolism and/or building blocks for biosynthesis. Some of the released glycans, such as CEL3-CEL5 and OGs, can be perceived as DAMPs by plant PRRs (e.g., IGP1/CORK1 and WAK RKs, respectively) that might form complexes with some additional RKs functioning as co-PRRs (e.g., IGP3/IGP4 and other WAKs, respectively; see Figure 2). Binding of glycan by PRR activate PTI signaling and transcriptional regulation of several immune genes, such as those encoding PRRs and co-PRRs, that might replenish these proteins at the plasma membrane. Pathogens also secrete lytic polysaccharide monooxygenases (LPMOs) that oxidatively cleave cell wall polysaccharides, such as cellulose, releasing C1 oxidized oligosaccharides with lower PTI activity. Whether PRRs/co-PRRs binding glycans are internalized by endocytosis upon ligand binding, as described for some ligand-LRR RK complex (FLS2-BAK1-flg22) is unknown. Genes encoding BBE-like enzymes are also upregulated upon pathogen infection and DAMP treatment, and BBE proteins (CELLOXs and OGOXs) are secreted to the apoplast to oxidize glycans (e.g., CEL3 and OGs) at the anomeric carbon (-COOH at C1) probably lowering their binding affinity by PRRs. Oxidized oligosaccharides (-COOH at C1) are poor substrates for energetic catabolism of pathogens hindering their colonization. Question marks indicate open topics that deserve further investigation. The glycan structures were drawn using the code described by Cheng et al. (2017). IGPs and WAK RK domains are described in Figure 2.

sensor HPCA1 (Wu et al., 2020; Scortica et al., 2022). AtBBE8 has been proposed to oxidize some wall-derived oligosaccharides in Arabidopsis guard cells in response to infection by *P. syringae* and the human pathogen *Salmonella enterica*, although its activity on oligosaccharides has not yet been proven (Rodrigues Oblessuc et al., 2019).

Several carbohydrate oxidase BBE-like enzymes have also been identified in other plant species such as the cellobiose oxidase in *Physcomitrella patens* (PpCBOX), which oxidizes CEL2 and lactose but not glucose nor CEL3, and the hexose oxidase from the red algae *Chondrus crispus* and the oxidases from *Helianthus annus* (HaCHOX) and *Lactuca sativa* (LsCHOX), which are able to oxidize glucose, as well as CEL-derived oligomers (Custers et al., 2004). Given the large number of members of the BBE-like family in plant genomes, it cannot be ruled out that these and other oxidases might be involved in the modification of other cell wall-derived eliciting molecules, constituting a battery of enzymes to cope with alterations of cell wall during pathogen infection or developmental processes, such as cell wall expansion or seed formation (Locci et al., 2019; Scortica et al., 2022). An in-depth biochemical characterization of these families of enzymes that affect DAMPs homeostasis is necessary to determine extracellular conditions (e.g., redox state or pH at apoplast) that influence their activity.

Remarkably, oligosaccharide oxidases are not exclusive to plants. They are also present in the genomes of pathogens and saprotrophs that encode a wide repertoire of enzymes capable of modifying and reducing the eliciting activity of DAMPs/MAMPs by selectively oxidizing oligosaccharides at the C1 position (Pontiggia et al., 2020). Some of the best characterized oxidases are fungal glucooligosaccharide oxidases (GOOX-T1 and GOOX-VN) from *Sarocladium strictum* (previously known as *Acremonium strictum*), which exhibit high catalytic activity on substrates such as cello-oligosaccharides (particularly CEL3) and xylo-oligosaccharides (Fan et al., 2000; Foumani et al., 2011). GOOX-T1 crystal structure revealed that its active site contains a relatively open groove for carbohydrate binding compared with other carbohydrate oxidases that

preferentially act on monosaccharides. This difference could explain why these fungal oxidases display a strong substrate preference toward oligosaccharides (Huang et al., 2005). A xylo-oligosaccharide oxidase (XylO) from the thermophilic fungus *Myceliophthora thermophila* was also reported to oxidize xylotetraose, xylotriose, xylobiose, lactose, cellobiose, and D-xylose (Ferrari et al., 2016). And a chito-oligosaccharide oxidase from *Fusarium graminearum* has been identified (Heuts et al., 2008). In addition to these oxidases, microorganisms secrete during plant colonization lytic polysaccharide monooxygenases, which are powerful redox enzymes that oxidatively cleave recalcitrant polysaccharides, such as cellulose, releasing oligosaccharides with C1 oxidized that show lower PTI activity than oligosaccharides released by the action of cellulases (Figure 1) (Zarattini et al., 2021).

During plant colonization, pathogens should control the release of cell wall-derived signals (DAMPs) to weakness or delay PTI activation. It has been shown that changes in the expression patterns of certain fungal CWDEs in genetically modified microbial lead to unexpected virulence phenotypes that contrast with those of wild-type strains (Yang et al., 2021a; Dora et al., 2022; Gámez-Arjona et al., 2022). For example, overexpression of some fungal CWDEs upregulated during plant colonization resulted in fungal strains that were less virulent than the corresponding wild-type ones, probably due to enhanced release of DAMPs and strong activation of PTI that hinder fungal colonization (Yang et al., 2021a; Dora et al., 2022; Gámez-Arjona et al., 2022). This observation further supports that the balance between plant cell wall degradation during pathogen colonization and the perception by PRRs of DAMPs derived from CWDE activity might determine the progression of colonization and disease resistance outcome (Figure 1).

Pathogens also secrete a battery of virulence factors to undermine host defense responses by decreasing the amount of MAMPs (modification or degradation) available for plant perception (Sánchez-Vallet et al., 2015). During infection, microorganisms are exposed to the activity of plant CWDEs that can hydrolyze microbial surfaces at the contact point with the plant cells. As a result of the activity of host CWDEs (e.g., chitinases and glucanases secreted into the apoplast), many fungal oligosaccharides (MAMPs) derived from main fungal wall polysaccharide components, such as chitin or β-1,3-glucans, are released on the pathogen-host interface (Geoghegan et al., 2017; Wanke et al., 2021; Dora et al., 2022). Chitin is one of the main targets for biochemical modification of phytopathogenic fungi to counteract the plant immune response (Khokhani et al., 2021). Several fungi have chitin deacetylases that deacetylate chitin to generate chitosan, a less active MAMP (Xu et al., 2020; Dai et al., 2021; Rizzi et al., 2021; Gámez-Arjona et al., 2022; Xiao et al., 2023). Hydrolysis of chitin oligosaccharides is also a strategy of some pathogens, such as the fungus *M. oryzae*, which expresses a chitinase (MoChia1), to hydrolyze chitin oligomers into monomeric GlcNAc (Yang et al., 2021a). Also, some fungi secrete several β-1,3-glucanosyltransferases (GH72) and exo-β-1,3-glucanase (Ebg1) to suppresses β-1,3-glucan-triggered plant immunity (Samalova et al., 2017; Yang et al., 2019; Liu et al., 2023b). These enzymes are relevant for fungal cell wall remodeling and integrity as well as for pathogen virulence. Notably, some primary structures of these fungal enzymes are recognized by plants as MAMPs. To counteract this recognition, fungi employ a camouflage strategy by secreting proteins, such as EF1α of *M. oryzae* that hijacks Ebg1 in the apoplast to prevent activation of plant cell immune responses by these enzymes (Liu et al., 2023b). Also, it has been reported that certain exopolysaccharides and polysaccharides from fungal walls contain a well-defined β-1,3/β-1,6-decasaccharide released by the action of host CWDEs that does not trigger immunity and can scavenge reactive oxygen species, functioning as a fungal counter-defensive strategy to subvert host immunity (Chandrasekar et al., 2022; Kelly et al., 2023). Last, many fungal pathogens secrete LysM domain-containing effector proteins during host colonization to deregulate chitin-induced plant immunity and successfully establish infection. Such effectors cooperate to form a composite groove with ultra-high (picomolar) chitin-binding affinity that outcompetes plant PRRs for binding to chitin (Tian et al., 2022).

Some plant enzymes can also contribute to the homeostasis of microbial MAMPs as has been described recently (Wanke et al., 2023). In barley, two members of the plant glycoside hydrolase family 81-type glucan-binding protein (GBP1 and GBP2) are β-glucan interactors. Mutation of *GBP1* and *GBP2* genes led to decreased colonization of barley by beneficial root endophytes (e.g., *Serendipita indica*) and arbuscular mycorrhizal fungi (e.g., *Rhizophagus irregularis*), but also by fungal pathogens such as *Bipolaris sorokiniana* and *Blumeria hordei*. This reduced colonization was associated to an enhanced PTI responses of barley cells, implying that GBP1 is involved in the degradation of active β-glucan MAMPs from the fungi and suggesting that the degradation of these MAMPs is critical for the establishment of symbiotic associations with beneficial fungi (Wanke et al., 2023).

Plant receptors for glycan perception and activation of immune responses

Plant perception of DAMPs/MAMPs occurs through different types of receptor proteins that function as PRRs activating PTI responses. Characterized PRRs belong to three main classes of proteins: RKs and RPs with ECDs attached to the plasma membrane by a transmembrane domain, and receptor-proteins that lack transmembrane domain and whose ECDs are either attached to the plasma membrane by a GPI-anchor (RPg) or are extracellular proteins (RPe) (Bellande et al., 2017; Del Hierro et al., 2021). The number of RK/RP/RPg/e proteins in plant genomes is larger than the PRR counterparts in animal genomes (Bacete et al., 2018), supporting the relevance of these receptors in plant development and adaptation to environmental challenges. These receptor proteins comprise more than 600 members in Arabidopsis and, in general, represent 2%–3% of genes of plant genomes. Most of these receptors are found in genomic clusters, indicative of rapid evolution by duplication and gene shuffling (Shiu and Bleecker, 2003; Fritz-Laylin et al., 2005; Lehti-Shiu et al., 2009; Gish and Clark, 2011; Li et al., 2016; Franck et al., 2018; Del Hierro et al., 2021; Yang et al., 2021b; Ortiz-Morea et al., 2022). RKs are the most numerous receptors and can be subdivided into nearly 60 subfamilies that are already present in liverworts and mosses, suggesting that during land plant evolution RK diversity was acquired early (Lehti-Shiu et al., 2009; Bowman et al., 2017;

Dievart et al., 2020), which is in line with the relatively few domain-gain events detected for RKs through evolution (Lehti-Shiu et al., 2009; Man et al., 2020). Plant RK/RP/RPg/e are classified into different types based on their ECD predicted structures, the most abundant receptors being those with leucin-rich repeat (LRR) domains in their ECDs. Other types of described structural domains in receptors ECDs are: LysM (generally containing 3 LysM domains), lectin domains (LEC with either G, L, or C type domains), Malectin (MAL), LRR-MAL, MAL-like domains (MLL) (present in *Cr*RLK1L), proline-rich extensin-like domain (in PERKs and extracellular proteins such as extensins), epidermal growth factor-like domain (in wall-associated kinases [WAKs] and WAK-like receptors) and not well characterized domains present in CRinkly-like (CR4L), pathogenic-related Thaumatin-like (ThaumatinL/PR5), and cysteine-rich receptor kinases (CRK/DUF26) (Del Hierro et al., 2021; Zeiner et al., 2023). Some *in silico* analyses indicate that more than half of the plant receptors might potentially bind glycoligands based on ECD similarities found with carbohydrate binding domains from microorganism or carbohydrate receptor domains (CRD) from mammals (Del Hierro et al., 2021). However, only in a few cases have crystal structures of ECDs been obtained, and most of these crystals do not contain the ligand in the binding pocket.

ECDs of plant receptors show high-affinity recognition for different type of ligands: (1) signaling peptides and hormones functioning as developmental cues (Santiago et al., 2013, 2016; Stegmann et al., 2017; Tang et al., 2017), (2) MAMPs from different biochemical nature (peptides, glycans, lipids, etc.), and (3) diverse types of DAMPs, such as glycans and nucleotides, or phytocytokine peptides that trigger PTI or other physiological responses (Boutrot and Zipfel, 2017; Li et al., 2020; Hou et al., 2021). Upon MAMP/DAMP recognition by ECD-PRRs, formation of protein complexes with other RKs and RPs (co-receptors or co-PRRs) takes place and signaling is initiated by the kinase activity of some RKs forming part of the complex (Bender and Zipfel, 2023). Plant RKs typically exhibit serine/threonine kinase specificity, contrasting with the tyrosine specificity of animal receptor tyrosine kinases involved in activation of innate immune responses (Shiu et al., 2004; Greeff et al., 2012). Early downstream signaling events includes cytoplasmic calcium burst, production of ROS by NADPH oxidases (e.g., RBOH proteins), phosphorylation of mitogen-activated protein kinases) and calcium-dependent protein kinases, and gene transcriptional regulation, among other molecular responses (Greeff et al., 2012; Dangl et al., 2013; Bender and Zipfel, 2023). All these downstream processes activated upon ligand recognition by ECD-PRR have been described in several recent articles and are not described here (Saijo et al., 2018; DeFalco and Zipfel, 2021; Ngou et al., 2022; Bender and Zipfel, 2023).

Despite the structural diversity of ligands that can be bound by plant ECD-PRRs, most of the best-characterized ECD-PRR/ligand pairs at the structural level are LRR-ECD/peptide ones, such as FLAGELLIN-SENSITIVE 2 (FLS2)/flg22 (MAMP from bacterial flagellum), EF-Tu RECEPTOR (EFR)/elf18 (MAMP from bacterial elongation factor protein), or PEP1 RECEPTOR 1 (PEPR1)/PEP1 (phytocytokine peptide) (Bartels and Boller, 2015; Boutrot and Zipfel, 2017; Gully et al., 2019; Peng et al., 2018). These LRR-ECD/peptide pairs have been successfully crystalized with the ligand in the binding pocket, and in some cases with the co-PRR included in the crystal structure (e.g., RKs of SOMATIC EMBRYOGENESIS RECEPTOR-LIKE KINASES family, such as BRI1-ASSOCIATED KINASE 1 [BAK1] RK for FLS2, EFR, and PEPR1: Boutrot and Zipfel, 2017; Li et al., 2020; see Figure 2). In contrast to the numerous peptidic-ECD structures of RKs determined, the number of crystal structures of PRR/glycan pairs characterized so far is limited to a few examples: LysM-chitin in PTI and LysM-LCOs/COs in symbiosis (Liu et al., 2012; Gysel et al., 2021; Khokhani et al., 2021) and a recent example of LRR-extensin involving FERONIA RK (Moussu et al., 2023; Schoenaers et al., 2024). A detailed knowledge of the binding mechanisms of glycans (MAMPs/DAMPs) by ECD-PRR structures is needed (Lee and Santiago, 2023).

LysM receptors: A versatile group of proteins with differential functions in plant-microbe interactions

LysM-PRRs are involved in the direct binding of several ligands such as COs (such as CHI6-CHI8) and LCOs, and are also required for the activation of signaling triggered by other carbohydrate-based ligands such as peptidoglycans, β-1,3-D-glucans, lipopolysaccharides, and MLGs in Arabidopsis and other plant species (Table 1 and Figure 2) (Miya et al., 2007; Willmann et al., 2011; Desaki et al., 2018; Mélida et al., 2018; Yang et al., 2021a; Rebaque et al., 2021). Arabidopsis LysM-PRRs subclass has 10 members, 5 of them are RKs (CHITIN ELICITOR RECEPTOR KINASE 1 [CERK1]/LYK1 [LysM RECEPTOR KINASE], LYK2, LYK3, LYK4, and LYK5), 2 RPs (At5g62150 and At4g25433), and 3 putative RPg/e (LysM DOMAIN CONTAINING PROTEIN 1 [LYM1], LYM2, and LYM3) (Faulkner et al., 2013; Bellande et al., 2017). In the Arabidopsis plasma membrane, LYK5 perceive chitin oligomers (CHI6–CHI8), after which CERK1 associates with it to activate immune signaling (Figure 2 and Table 1) (Petutschnig et al., 2010; Liu et al., 2012; Wan et al., 2012; Cao et al., 2014). LYK4 can additionally associate with CERK1 in a chitin-dependent manner, but this association requires LYK5 (Figure 2) (Xue et al., 2019). Since, the kinase domains of LYK4 and LYK5 have negligible activity *in vitro* (Wan et al., 2012; Cao et al., 2014), it has been suggested that the active kinase of CERK1 initiates signaling upon recruitment of LYK4/LYK5. However, in plasmodesmata, LYM2 forms a complex with LYK4 upon chitin perception in a CERK1-independent mechanism (Figure 2; Faulkner et al., 2013; Cheval et al., 2020). CERK1 is also involved in the perception of bacterial peptidoglycans, with the contribution of LYM1 and LYM3 members, but the exact structure from peptidoglycan recognized by these receptors is unknown (Willmann et al., 2011; Gust et al., 2017). Recent results with single and double LysM Arabidopsis mutants have demonstrated that CERK1, LYK4, and LYK5 also participate in the perception of 1,3-β-glucans, such as LAM6, and MLGs (Figure 2 and Table 1) (Mélida et al., 2018; Wanke et al., 2020). However, Arabidopsis CERK1-ECD and LYK5-ECDs do not bind LAM6 in isothermal titration calorimetry (ITC) analyses and might not bind MLGs based on *in silico* molecular dynamics prediction of ECD-MLGs (Del Hierro et al., 2021), further suggesting that CERK1 and LYK5 would play a function as co-PRRs in LAM6 and MLG perception (Figure 2 and Table 1). Arabidopsis LYK2 has been also shown to be required for chitin perception and to induce resistance against *B. cinerea*

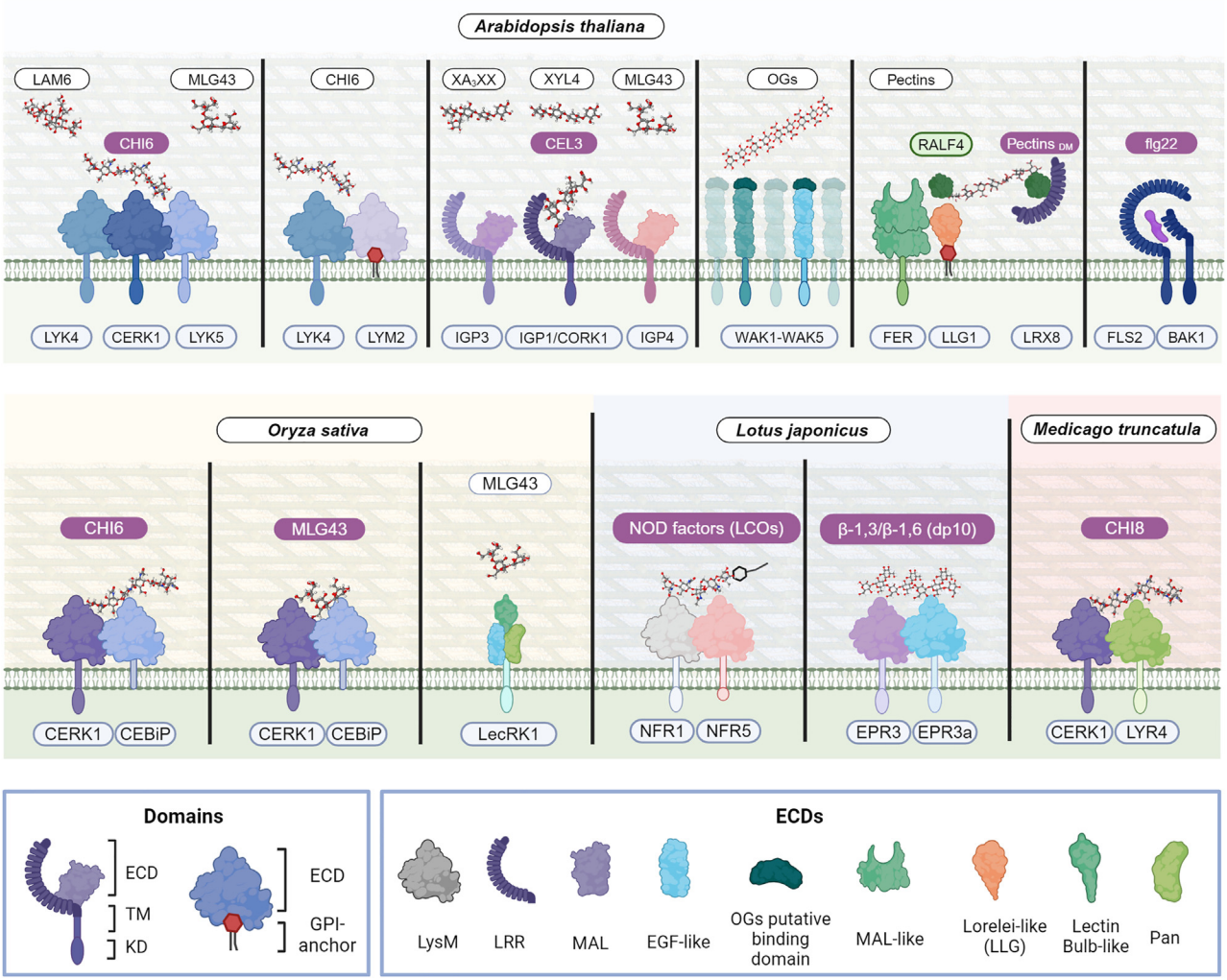

Figure 2. Plant receptors involved in the perception of different glycan structures in plant immunity or symbiosis.
Representation of receptors (PRRs) and co-receptors (co-PRRs) from *Arabidopsis thaliana* (top) and from other plant species (bottom) described to be required for different glycan perception. Glycan names indicated in purple correspond to DAMPs/MAMPs that have been demonstrated to be bound by the indicated PRRs, protein receptors (e.g., LRX8), or RALF peptides, either by *in vitro* binding experiments or by structural characterization, and are shown in close interaction with the corresponding receptor. The co-PRRs involved in glycan perception are also depicted. Glycans highlighted in white have been shown to require these PRR-co-PRRs complexes to trigger immune/symbiotic responses, but direct binding by PRR has not been demonstrated. FLS2-BAK1-flg22 recognition complex is included for comparison. Overlapping of RK domains indicates that PRR-coPRR interaction has been demonstrated. The different structures of plant receptors (RK/RP/RPe/g) and the domains in their ECDs are indicated in the inset and described in the main text. The crystal structure PDBs of AtCERK1, OsCEBiP, FER, and EPR3 ECDs and LRX8 are indicated in the text. MtLYK3 and MtNFP from *M. truncatula* are the corresponding pair/orthologs of LjNFR1 and LjNFR5 from *L. japonicus* shown in the figure. The structures of glycans represented have been obtained from different sources. FLS2-BAK1-flg22 recognition complex is included for comparison.

and *P. syringae* triggered by non-carbohydrate MAMPs, such as flg22 (Giovannoni et al., 2021).

In rice (*Oryza sativa*) chitin is perceived by the LysM-RP CHITIN ELICITOR BINDING PROTEIN (OsCEBiP), but immune signaling is activated by recruitment of OsCERK1 (Figure 2 and Table 1) (Shimizu et al., 2010; Kouzai et al., 2014; Takagi et al., 2022). Notably, OsCERK1, but not OsCEBiP, seems to bind MLGs (MLG43 and MLG443) based on microscale thermophoresis (MST) assays, but crystal structures of this complex have not been obtained (Yang et al., 2021a). OsCEBiP and OsCERK1 form a protein complex in rice protoplast upon treatment with MLGs, as previously shown for chitin (Figure 2) (Yang et al., 2021a). In grapevine, LysM RK VvLYK5-1 recognizes chitin oligomers through its association with VvLYK1-1 (Roudaire et al., 2023). Together these data demonstrate the relevance of LysM-ECDs in perception of glycan-based MAMPs/DAMPs.

The crystal structure of Arabidopsis CERK1 ECD (PDB: 4EBZ) is one of the few glycan-ECD pair structures characterized so far (Liu et al., 2012). In the crystal structure of CERK1, CHI6–CHI8 is bound in the LysM2 pocket, and this binding allows the carbonyl oxygen of the N-acetyl moieties to form hydrogen bonds with the backbone amide nitrogens of the main chain stabilizing the binding. The lack of N-acetyl moieties in chitosan (deacetylated chitin) explains its lower immunogenic activity in

comparison with chitin (Liu et al., 2012). The crystal structures of rice OsCEBiP (PDB: 5JCE) (Liu et al., 2012, 2016) and of the fungal chitin-binding protein Ecp6 (PDB: 4B8V), which binds chitin oligosaccharide (Sánchez-Vallet et al., 2013), further support the relevance of LysM2 in CHI6-CHI8 binding.

Intriguingly, LysM receptors participate in both symbiotic and immune signaling in some plant species (e.g., legumes and rice) through distinct LysM receptor complexes, recognizing chitin from fungal cell walls or LCOs produced by mycorrhiza fungi (MYC factors) and bacteria (Nod factors) (Madsen et al., 2003; Radutoiu et al., 2003; Zhang et al., 2015; Khokhani et al., 2021). In *Medicago truncatula*, MtCERK1 (also known as MtLYK9) and MtLYR4 form a receptor complex to directly bind CHI8 triggering immune responses, but they seem to be also needed to initiate symbiotic responses (Figure 2 and Table 1) (Bozsoki et al., 2017; Feng et al., 2019). In *Lotus japonicus*, LjCERK6 (the ortholog of MtCERK1) participates in chitin-induced immune signaling (Figure 2 and Table 1). In contrast, LCOs are perceived at the plasma membrane by a pair of LysM-RKs: in *L. japonicus* are Nod Factor Receptor 1 (LjNFR1) and Nod Factor Receptor 1 (LjNFR5), and in *M. truncatula* are Nod Factor Perception Protein (MtNFP) and MtLYK3 (Figure 2) (Madsen et al., 2011; Bozsoki et al., 2017; Murakami et al., 2018). Each receptor pair is composed of an RK with an active kinase domain (LYK), such as LjNFR1 or MtLYK3, and one RK with an inactive kinase domain (LYR), such as LjNFR5 or MtNFP (Figure 2) (Madsen et al., 2011; Bozsoki et al., 2017; Murakami et al., 2018). Upon LCO binding, these receptors complex with an LRR-RK (e.g., SYMBIOSIS RECEPTOR KINASE in *L. japonicum* [LjSYMRK]/DOES NOT MAKE INFECTION PROTEIN 2 in *M. truncatula* [MtDMI2]), which likely acts as a co-receptor and initiates signal transduction in the common symbiosis pathway (Endre et al., 2002; Stracke et al., 2002; Yoshida and Parniske, 2005). Results obtained in *M. truncatula nfp cerk1* double mutant, impaired in both LCO and CO perception, indicated that a combination of fungal chitin and LCOs triggers the plant signal transduction through a common symbiosis pathway (Feng et al., 2019). Of note, chimeric receptor analysis and structural comparisons of LysM-RKs involved in symbiosis and immunity indicate that the outermost of the three LysM domains, LysM1, is the primary determinant of chitin oligosaccharide binding in LjCERK6 and LCO binding in LjNFR1 (Broghammer et al., 2012; Bozsoki et al., 2020; Rübsam et al., 2023), which contrast with the function of LysM2 in AtLYK5 binding of CHI6.

Another member of the LysM-RK family in *L. japonica* is EPR3 (EXOPOLYSACCHARIDE RECEPTOR 3) involved in the perception of bacterial carbohydrate-based exopolysaccharides (EPS). Perception of EPS occurs downstream of primary LCO (Nod factor) signaling and is required for the formation of nitrogen-fixing nodules (Kelly et al., 2013). The structure of the EPR3 ectodomain was resolved (PBD: 6QUP), revealing that it represents a unique class of plant RKs with a distinctive modular ectodomain arrangement (Wong et al., 2020). *In vitro*, the EPR3 ectodomain binds EPS from several rhizobial species, including micro-symbionts unable to nodulate in *Lotus* sp., suggesting that the receptor may have a broader role in monitoring glycans from various root-associated microbes (Wong et al., 2020). Recently, the *L. japonica* glycan RK EPR3a, which is closely related to the EPS receptor EPR3, has been also characterized (Kelly et al., 2023). Fungal infection and intracellular arbuscule formation are reduced in *epr3a* mutants, such as previously described in *epr3* plants (Wong et al., 2020; Kelly et al., 2023). EPR3a ectodomain binds *in vitro* cell wall glucans in affinity gel electrophoresis assays, and exopolysaccharide binding is detected in MST assays with affinities comparable with those observed for EPR3 (Kelly et al., 2023). Notably, both EPR3a and EPR3 bind a well-defined β-1,3/β-1,6-decasaccharide derived from exopolysaccharides of endophytic and pathogenic fungi (Figure 2 and Table 1). The presence of *EPR3a* and *EPR3* genes in both eudicot and monocot plant genomes suggest a conserved function of these RKs in glycan perception (Kelly et al., 2023).

WAKs: A group of receptors involved in triggering pectin-mediated immune responses

OGs, originated from the HG component of wall pectins, are the proposed ligands for WAK RKs that have epidermal growth factor (EGF)-like domains in their ECDs (Liu et al., 2023a). However, the EGF-like domain, which is also present in mammalian receptors, is found exclusively in extracellular proteins or regions of transmembrane proteins, and functions primarily in mediating protein–protein interactions (Haltom and Jafar-Nejad, 2015). OG perception by WAKs has been implicated directly in immunity and is also speculated to function during symbiotic interactions (Rui and Dinneny, 2020; Su, 2023). The N-terminal part of WAK1 ECD has been proposed to act as a putative OG-binding domain since it associates with demethylesterified pectin or polygalacturonic acid, with a clear preference for pectate in the Ca^{2+} crosslinked configuration (Figure 2). In contrast, EGF-like repeats have not been demonstrated to participate in binding pectins (Decreux and Messiaen, 2005; Decreux et al., 2006; Kohorn et al., 2009). WAK ECDs appear to bind shorter fragments of HG and OGs, but not monomeric GalA or other types of pectins (Kohorn et al., 2009). Recently, an Arabidopsis *wak1/wak5* quintuple mutant impaired in WAK1–WAK5 receptors was shown to be impaired in the perception of cell wall extracts of *ccr1* that contain several OG-derived DAMPs such as $GalA_3$, suggesting that these WAKs are likely redundantly involved in perceiving *ccr1*-wall DAMPs and $GalA_3$ (Liu et al., 2023a). Recombinant ECD of WAK1 fused to glutathione S-transferase was expressed in *Escherichia coli* was found to bind $GalA_3$ *in vitro* (i.e., in protein gel blot analysis and enzyme-linked immunosorbent assay) (Liu et al., 2023a). However, *in vivo* and/or direct binding assays (e.g., ITC) would be needed to further confirm WAK/$GalA_3$ binding. Likewise, WAK-like (WAKL) protein RESISTANCE TO FUSARIUM OXYSPORUM 1 (RFO1) has been proposed recently to function as sensor of the pectin methylation status in Arabidopsis cell walls to modulate root growth and defense (Huerta et al., 2023). However, the crystal structure of WAK1–WAK5 or WAKL/RFO1 ECD have not been obtained and the potential pocket(s) of WAK/WAKL ECDs involved in the binding of OGs (e.g., $GalA_3$) are unknown. Moreover, *wak1/wak5* quintuple mutant was shown to be impaired in PTI triggered by CHI6 and flg22, suggesting a role for these WAKs beyond OG perception (Kohorn et al., 2021). Clarifying the role of WAK and WAKL RKs in the control of CWI and PTI responses is needed since they are essential components in plant disease resistance. Indeed, several crop disease resistance QTLs have been shown to encode WAK genes (Zuo et al., 2015;

Dmochowska-Boguta et al., 2020; Huerta et al., 2023; Zhang et al., 2023).

CrRLK1 receptors: Regulation of cell wall integrity and immune responses

CrRLK1 proteins, harboring tandem MLL domains in their ECDs (Yang et al., 2021b), have been involved in the regulation of multiple immune responses and development processes, such as pollen tube germination, which is associated with cell wall remodeling (Lee and Goring, 2021; Goring, 2023). However, the molecular mechanism employed by CrRLKs to modulate immunity and development through perception of cell wall components have not been revealed until recently. Several ECDs of CrRLK1, such as ANXUR 1 (ANX1), ANX2, and FER, have been crystalized (PDB: 6FIG, 6A5C, and 6A5E, respectively) (Moussu et al., 2018; Xiao et al., 2019). In some cases, these ECDs (e.g., FER) have been shown to bind pectin *in vitro* (Lin et al., 2022), but crystal structures of ECDs bound to pectins or OGs have not been obtained yet. Instead, some of these ECD-CrRLK1 structures have been shown to bind RAPID ALKALINIZATION FACTOR (RALF) peptides (Moussu et al., 2020). Therefore, it was unclear if pectin binding by these ECDs was direct or indirect (Lee and Santiago, 2023). Recently, this question has been solved by showing that the apoplastic LRR extensin LRX8 protein interacts with RALF4 peptide forming a complex that specifically interacts with demethylesterified pectins in a charge-dependent manner through RALF4's polycationic surface (Moussu et al., 2023). Notably, RALF4 has a dual structural and signaling role by assembling extracellular wall polymers in a complex that involves LRX8, FER, and LORELEI/LORELEI-LIKE GPI-ANCHORED PROTEINS (LLGs) (Figure 2 and Table 1). This complex regulates CWI during pollen growth in Arabidopsis (Moussu et al., 2023). A similar type of complex has been found in root growth involving LRX1, RALF22, FER, and LLGs (Schoenaers et al., 2024). Based on these recent data it seems that the MLL domains of ANX1/ANX2/FER/BUPS1 (BUDDHA'S PAPER SEAL 1) ECDs might not directly bind glycans in contrast to what has been reported for MAL domains from animals, such as X*enopus* sp., for which MAL domain-glycan crystal structures (PDB: 2k46) were obtained (Schallus et al., 2008). Notably, FER was also identified in a genetic screening performed to identify suppressors of constitutive defensive gene activation of Arabidopsis *ccr1-3* mutant. *fer* loss-of-function mutants are affected in cell wall remodeling and *fer ccr1-3* double mutant is impaired in in the release of *ccr1-3*-specific DAMPs (Liu et al., 2023a). Additional analyses might be required to clarify the putative function of FER in sensing the initial wall damage in *ccr1-3* plants, and the potential involvement of FER in perception of wall polysaccharides should not be excluded.

LRR-MAL RKs: Novel players in glycan perception and immune response activation

Two recent parallel studies have identified Arabidopsis LRR-MAL RK family members as new players in the perception of cellulose-derived oligosaccharide (CEL3–CEL5) and in the activation of immune responses. The ECD of the CELLO-OLIGOMER RECEPTOR KINASE 1 (CORK1)/IMPAIRED IN GLYCAN PERCEPTION 1 (IGP1) RK (At1g56145) has been convincingly demonstrated to directly bind CEL3 and CEL5 in ITC assays and to be necessary to trigger immune responses upon CEL-derived oligosaccharide binding (Figure 2 and Table 1) (Tseng et al., 2022; Martín-Dacal et al., 2023). The ECDs of LRR-MAL RKs are composed of 12 LRR domains followed by a MAL domain that differs from the MLL domain of CrRLK1 ECDs (Yang et al., 2021b). Some members of LRR-MAL RKs, which encompasses 13 genes in Arabidopsis (Yang et al., 2021b), have been related to plant disease resistance (Le et al., 2014), but also to plant reproduction and fertility by promoting early compatible pollen responses in pistil (Lee and Goring, 2021), or to brassinosteroid-associated responses (Xu et al., 2014). Some of these processes are associated with changes in cell wall composition (Rajaraman et al., 2016; Lee and Goring, 2021). MAL domains present in mammal and *Xenopus* sp. proteins bind glycans and are structurally similar to MAL domains of LRR-MAL RKs (Schallus et al., 2008). Therefore, it had been hypothesized that plant MAL domains of LRR-MAL RKs might bind glycans. However, other alternatives for CEL3/CEL5 binding to IGP1/CORK1 ECD rather than binding to MAL domains might be feasible, such as a potential binding pocket comprising the two domains (MAL and LRR), which upon glycan binding induces receptor conformational change and kinase domain activation of IGP1/CORK1. Also, it should not be excluded that LRR domains might bind glycans based on the heterogenicity of biomolecules that plant LRR domains can bind (e.g., brassinosteroids and peptides) (Sun et al., 2013a; Sun et al., 2013b; Bojar et al., 2014; Rhodes et al., 2021).

Besides CORK1/IGP1, two additional members of the LRR-MAL RK family (IGP3/At1g56130 and IGP4/At1g56140) were identified in the Arabidopsis genetic screening performed to identify mutants impaired in glycan (*igp*) perception. All the *igp* mutants described so far (*igp1/igp3/igp4*) are impaired in both CEL3/CEL5 and MLG43 perception, but not in CHI6 or OG recognition (Figures 1 and 2 and Table 1) (Martín-Dacal et al., 2023). Since IGP1 and IGP4 were not able to bind MLG43 in ITC experiments, and IGP4 does not bind CEL-derived oligosaccharides (Martín-Dacal et al., 2023), we speculate that IGP1 and IGP4 might function as co-PRRs in the perception of MLG43 and CEL3, respectively (Figures 1 and 2 and Table 1). This group of LRR-MAL RKs have been recently shown to be involved in activation of PTI responses triggered by other glycans, such as the DAMPs XYL4 and XA_3XXX, further demonstrating its relevance in glycan-mediated PTI activation (Figure 2) (Fernández-Calvo et al., 2024). Getting the crystal structure of IGP1 and the other IGPs will clarify the function of this novel RK family in glycan perception and plant PTI activation. Also, the functional characterization of the rest of the family members will contribute to clarify whether LRR-MAL RKs perceive a diversity of carbohydrate-based DAMPs/MAMPs.

Lectin RKs: Less explored plant receptors with possible roles in immune response

LEC domains in plant receptors have been involved in the carbohydrate binding activity of proteins from fungal species. G, L, and C lectin domains have been identified in the ECDs of plant RKs, but until recently few information was available on their binding activity. The rice LECTIN RECEPTOR KINASE1 (OsLecRK1), but not the OsLecRK2, have been shown to bind different MLGs but not CEL4 in MST assays (Figure 2 and Table 1) (Dai et al., 2023). These assays were performed with recombinant purified MBP-OsLecRK1-His and MBP-OsLecRK2-His produced in bacteria (Dai et al., 2023). Since OsCERK1 and

OsCEBiP have been also involved in MLG perception in rice (Yang et al., 2021a), it would be interesting to test the homo- or heterodimerization of OsLecRK1and OsLysM RKs. The potential interaction between OsCERK1 and OsLecRK1 might explain the mechanism of MLG perception in cereals and might help to clarify the putative role of Arabidopsis LecRK1 ortholog in MLG perception. Additional characterization of LEC RKs, including crystal structures of ECDs, will be required to clarify the relevance of this ECD in glycan perception and immune activation in plants.

LRR-RKs involved in cell wall integrity regulation: Looking for carbohydrate ligands and regulatory mechanisms

Several other Arabidopsis RKs have been involved in the regulation of CWI responses or developmental/adaptation to stress processes that might involve either CWI alterations and/or glycan-based DAMPs. For example, a recent study revealed that the LRR-RK STRUBBELIG (SUB) participates in the response to cellulose biosynthesis inhibition independently from THESEUS 1 (THE1) RK and LRR-RK MALE DISCOVERER 1-INTERACTING RECEPTOR LIKE KINASE 2 (MIK2) (Chaudhary et al., 2021). This study also suggests that SUB activity might be regulated by the cell wall, since cellulose synthesis inhibition can phenocopy misspecification of epidermal cell fate and alteration of ovule morphology observed in *sub* mutants (Chaudhary et al., 2020). MIK2 LRR-RK is also involved in regulating abiotic and biotic stress (Hou et al., 2021) and is needed for disease resistance to *F. oxysporum* vascular fungus (Van der Does et al., 2017), suggesting that MIK2 is an integrator of development and stress. However, the ligands for the ECD-MIK2 domain described so far are RALF peptides and not glycans (Hou et al., 2021; Rhodes et al., 2021). Also, the receptor protein RLP44 has been involved in cell wall state regulation through brassinosteroid signaling (Wolf et al., 2014). Like in the case of MIK2 and SUB-RK, ECD-RLP44 binding (direct or indirect) of cell wall-derived glycans (pectins) has not been demonstrated. Additional LRR-RKs, such as the Arabidopsis STRESS-INDUCED FACTOR 2 and 4 (SIF2, SIF4), have been shown to be required, together with BAK1 and THE1, for PTI activation mediated by cellulose oligosaccharides derived from the activity of fungal lytic polysaccharide monooxygenases (Zarattini et al., 2021). Similarly, FEI1 and FEI2 LRR-RKs have been described to regulate together with the extracellular glycoprotein FASCICLIN-LIKE ARABINOGALACTAN PROTEIN 4 (FLA4), a signaling pathway that acts in response to environmental conditions to modulate cell wall structure in response to various growth regulators (Seifert, 2021). Whether these LRR-RKs that have been described to be involved in CWI regulation would bind directly wall polysaccharides or glycans (DAMPs) needs to be determined at the structural level.

Perception of glycans by mammal protein receptors: Lessons to characterize plant PRR-glycan perception

Since the number of elucidated 3D structures, either by X-ray crystallography or NMR, of ECDs from plant RKs with bound glycans is very short, we might learn from receptor/glycan binding properties of 3D structures from CRD from mammalian receptors. Glycan-binding proteins are found in all living organisms, but in mammals they have been well studied due to their significant roles in cell trafficking, cell adhesion, immunity, and infection, and the 3D structures of many receptor/glycan complexes have been characterized at the structural level. One of the most important groups of mammalian glycan receptors are lectins, which selectively recognize a wide variety of glycans, and that are grouped in some main types: C-type lectins, galectins, selectins, and siglecs (Varki et al., 2022). They regulate pathogen recognition (e.g., dendritic cell-specific intercellular adhesion molecule-3-grabbing non-integrin [DC-SIGN]), but also are involved in other functions such as cell adhesion (e.g., selectins, DC-SIGN, and galectins), intracellular trafficking (e.g., galectins), and glycoprotein clearance and turnover (e.g., mannose receptors) (Fuchsberger et al., 2023). Glycan-binding receptors embedded in the plasma membranes of mammalian cells can initiate or inhibit signaling in several different ways. However, in mammals, unlike plants, there are no examples of receptors binding glycans in which a cell surface CRD is linked in a single transmembrane polypeptide to a kinase domain on the cytoplasmic side of the membrane (Taylor and Drickamer, 2014). In contrast, there are multiple examples of receptor polypeptides that contain extracellular CRDs and intracellular motifs that serve as targets and anchoring points for soluble cytoplasmic kinases and phosphatases. Some of the best studied examples are the immunotyrosine inhibitory motifs in the cytoplasmic domains of many of the siglecs such as CD22 (Siglec 2) on B lymphocytes (Macauley et al., 2014).

Mammal lectins are specialized in the recognition of particular glycans, and their CRDs are characterized by exposed binding sites with one aromatic residue, such as Trp or Tyr, to establish CH-π interactions with the sugar CH groups, and polar residues, such as Arg, His, Gln/Asn, and Glu/Asp, to establish complex H-bond networks to anchor the glycan (Varki et al., 2022). The molecular pattern recognized by galectins are β-galactosides, while DC-SIGN, an innate immune C-type lectin receptor, recognizes mannose and fucose glycans, siglecs bind sialic acids, and selectins bind surface glycans containing Lewis blood group family-related structures such as sialyl Lewisx (SLe^x) and sialyl Lewisa (SLe^a) oligosaccharides (Varki et al., 2022).

Galectin-3 (hGal-3), a lectin of biomedical interest in histo blood group antigens A and B determination, have been shown through a combination of structural and computational techniques to bind these rigid natural antigens. Restriction of the conformational flexibility by the branched fucose (Fuc) residue of the ligands modulates the thermodynamics and kinetics of the hGal-3 binding process, illustrating the importance of glycan flexibility for CRD binding (Gimeno et al., 2019). DC-SIGN immune receptor recognizes carbohydrate-based MAMPs of various bacteria, fungi, viruses, and protozoa. The structural bases for selective recognition of oligosaccharides by DC-SIGN and DC-SIGNR were stablished more than 20 years ago once the crystal complex of DC-SIGN and GlcNAc2Man3 was obtained (PDB: 1k9i) (Feinberg et al., 2001). This characterization contributed to the determination of the structural mechanisms for distinct ligand-binding and targeting properties of the receptors DC-SIGN and DC-SIGNR (Guo et al., 2004), such as the crystal structure of the DC-SIGN carbohydrate recognition domain complexed with Man4 (PDB: 1sl4). DC-SIGN also binds the pentamannoside epitope within the complex structure of *Candida albicans* mannan (Krylov et al., 2023), consisting of α-(1→2)-linked mannose chains with one inner α-(1→3)-linked unit. Despite all this progress in recognition

of glycans by mammal receptors, one main difference with plant ECD-PRRs is that, in general, the structural complexity of glycans perceived by mammal CRDs is higher than the known DAMPs/MAMPs perceived by plants. Therefore, it might be difficult to correlate mammalian CRD/glycan binding mechanisms with glycan binding by plant ECD-PRRs, although some of this mammalian CRD knowledge can be incorporated to optimize *in silico* molecular dynamics simulations of glycan-receptors in plants.

Open questions in plant immunity mediated by plant cell walls

Although significant progress has been made in the characterization of the function of plant cell wall on plant disease resistance and in the mechanisms of immunity triggered by carbohydrate-based DAMPs/MAMPs, there are still several fundamental questions that need to be addressed. Among these question we can remark the following: (1) What is the biochemical composition of active DAMPs released from plant cell walls upon plant infection by pathogens? (2) Are glycans released from plant cell walls upon alteration of CWI caused by other biological processes, such as abiotic stresses or development? (3) If this is the case, are these glycans identical to DAMPs released upon pathogen infection and do they trigger signaling responses (e.g., PTI)? (4) What are the main domains (ECDs) of plant receptors involved in the perception of glycans (DAMPs/MAMPs)? (5) What are the binding pockets of these plant ECDs-receptors involved in glycans recognition? (6) What are the co-receptors (co-PRRs) involved in the formation of the glycan–PRR complex required for downstream PTI activation apart from those already determined for CHI6-LysM-RK and RALF-LRX complexes characterized so far? (7) How do plants regulate the homeostasis of released glycans from plant cell walls? (8) How do plants distinguish glycans released from plant cell walls during the development process/abiotic stresses from those generated during pathogen infection by the activity of CWDEs (see Figure 1)? (9) Are the PRRs/co-PRRs exposed to endocytosis, like other PRRs (e.g., FLS2), upon glycan binding (see Figure 1)? (10) Would it be possible to perform reliable *in silico* structural predictions of glycan/ECD-PRR recognition using molecular dynamics tools based on AlphaFold protein structural progress (Jumper et al., 2021; Varadi and Velankar, 2023) and knowledge gained in the characterization of mammalian CRD/glycan pairs and plant ECD-glycan crystal structures? To answer these and additional questions, progress in 3D ECD-receptor determination and glycan binding pocket identification will be required (Lee and Santiago, 2023). Also, *in silico* synthesis of diverse glycan structures using novel chemical methodologies would be needed, since these pure structures should be employed in genetic and functional screenings designed to identify novel DAMP/MAMP receptors, co-receptors, and downstream signaling components, and to determine ECD-PRR binding specificities (Chaube et al., 2022). Moreover, genetic screening and the use of genome editing to generate high-order (multiple) mutants in putative glycan *PRR* gene families will be required to overcome receptor redundancy in plants. These required efforts will contribute to identify glycan/receptor pairs that can allow the development of novel sustainable agriculture solution for crop protection by treating plants, harboring the appropriate PRRs, with cell wall-derived glycans (pure or mixtures of ligands) that might trigger adaptative responses to biotic stresses and probably to abiotic stresses. Last, the identification of genetic traits impacting on CWI and cell wall-mediated disease resistance (e.g., PRRs and co-PRRs) will contribute to improve crop adaptation to environmental changes.

FUNDING

This work was supported by grant PID2021-126006OB-I00 to A.M. and L.J., and grant PID20220-113588RB-I00 to S.M.-S. funded by MCIN/AEI/10.13039/501100011033 and by ERDF A way of making Europe. D.J.B. was supported by PRE2019-091276 and P.F.-C. by post-doctoral fellowships financially supported by the Severo Ochoa Program for Centres of Excellence in R&D (grants SEV-2016-0672 and CEX2020-000999-S) funded by MCIN/AEI/10.13039/501100011033. M.M.-D. was recipient of PhD fellow (PRE2019-08812) funded by MCIN/AEI/10.13039/501100011033. E.G.-R. was supported by Autonomous Region of Madrid fellowship (S2017/BMD-3673) and the European Commission – Next Generation EU (Regulation EU2020/2094) through CSIC's Global Health Platform PTI Salud Global. We acknowledge the significant contributions of a lot of researchers to the progresses of this field, which we have not been able to cite properly due to space limitations. These additional contributions are cited in recent reviews.

AUTHOR CONTRIBUTIONS

A.M., L.J., M.A.T., and S.M.-S. wrote and edited the article. P.F.-C., E.G.-R., M.M.-D., and D.J.B. reviewed and edited the article. M.M.-D. and D.J.B. designed the figures and P.F.- C. prepared the table.

ACKNOWLEDGMENTS

No conflict of interest declared.

Received: February 12, 2024
Revised: April 3, 2024
Accepted: April 5, 2024
Published: April 9, 2024

REFERENCES

Addison, B., Bu, L., Bharadwaj, V., Crowley, M.F., Harman-Ware, A.E., Crowley, M.F., Bomble, Y.J., and Ciesielski, P.N. (2024). Atomistic, macromolecular model of the populus secondary cell wall informed by solid-state NMR. Sci. Adv. **10**, eadi7965. https://doi.org/10.1126/sciadv.adi7965.

Alonso Baez, L., and Bacete, L. (2023). Cell wall dynamics: novel tools and research questions. J. Exp. Bot. **74**:6448–6467. https://doi.org/10.1093/jxb/erad310.

Arya, G.C., Sarkar, S., Manasherova, E., Aharoni, A., and Cohen, H. (2021). The plant cuticle: an ancient guardian barrier set against long-s rivals. Front. Plant Sci. **12**, 663165. https://doi.org/10.3389/fpls.2021.663165.

Atmodjo, M.A., Hao, Z., and Mohnen, D. (2013). Evolving views of pectin biosynthesis. Annu. Rev. Plant Biol. **64**:747–779. https://doi.org/10.1146/annurev-arplant-042811-105534.

Aziz, A., Heyraud, A., and Lambert, B. (2004). Oligogalacturonide signal transduction, induction of defense-related responses and protection of grapevine against Botrytis cinerea. Planta **218**:767–774. https://doi.org/10.1007/s00425-003-1153-x.

Aziz, A., Gauthier, A., Bézier, A., Poinssot, B., Joubert, J.M., Pugin, A., Heyraud, A., and Baillieul, F. (2007). Elicitor and resistance-inducing activities of beta-1,4 cellodextrins in grapevine, comparison with beta-1,3 glucans and alpha-1,4 oligogalacturonides. J. Exp. Bot. **58**:1463–1472. https://doi.org/10.1093/jxb/erm008.

Bacete, L., and Hamann, T. (2020). The role of mechanoperception in plant cell wall integrity maintenance. Plants **9**:574. https://doi.org/10.3390/plants9050574.

Bacete, L., Mélida, H., Miedes, E., and Molina, A. (2018). Plant cell wall-mediated immunity: cell wall changes trigger disease resistance responses. Plant J. **93**:614–636. https://doi.org/10.1111/tpj.13807.

Bacete, L., Mélida, H., López, G., Dabos, P., Tremousaygue, D., Denancé, N., Miedes, E., Bulone, V., Goffner, D., and Molina, A. (2020). Response regulator 6 (ARR6) modulates plant cell-wall composition and disease resistance. Mol. Plant Microbe Interact. **33**:767–780. https://doi.org/10.1094/MPMI-12-19-0341-R.

Bacete, L., Schulz, J., Engelsdorf, T., Bartosova, Z., Vaahtera, L., Yan, G., Gerhold, J.M., Tichá, T., Øvstebø, C., Gigli-Bisceglia, N., et al. (2022). THESEUS1 modulates cell wall stiffness and abscisic acid production in Arabidopsis thaliana. Proc. Natl. Acad. Sci. USA **119**, e2119258119. https://doi.org/10.1073/pnas.2119258119.

Baez, L.A., Tichá, T., and Hamann, T. (2022). Cell wall integrity regulation across plant species. Plant Mol. Biol. **109**:483–504. https://doi.org/10.1007/s11103-022-01284-7.

Barghahn, S., Arnal, G., Jain, N., Petutschnig, E., Brumer, H., and Lipka, V. (2021). Mixed linkage β-1,3/1,4-glucan oligosaccharides induce defense responses in Hordeum vulgare and Arabidopsis thaliana. Front. Plant Sci. **12**, 682439. https://doi.org/10.3389/fpls.2021.682439.

Bartels, S., and Boller, T. (2015). Quo vadis, Pep? Plant elicitor peptides at the crossroads of immunity, stress, and development. J. Exp. Bot. **66**:5183–5193. https://doi.org/10.1093/jxb/erv180.

Bellande, K., Bono, J.J., Savelli, B., Jamet, E., and Canut, H. (2017). Plant lectins and lectin receptor-like kinases: how do they sense the outside? Int. J. Mol. Sci. **18**, 1164.

Bender, K.W., and Zipfel, C. (2023). Paradigms of receptor kinase signaling in plants. Biochem. J. **480**:835–854. https://doi.org/10.1042/BCJ20220372.

Benedetti, M., Pontiggia, D., Raggi, S., Cheng, Z., Scaloni, F., Ferrari, S., Ausubel, F.M., Cervone, F., and De Lorenzo, G. (2015). Plant immunity triggered by engineered *in vivo* release of oligogalacturonides, damage-associated molecular patterns. Proc. Natl. Acad. Sci. USA **112**:5533–5538. https://doi.org/10.1073/pnas.1504154112.

Benedetti, M., Verrascina, I., Pontiggia, D., Locci, F., Mattei, B., De Lorenzo, G., and Cervone, F. (2018). Four Arabidopsis berberine bridge enzyme-like proteins are specific oxidases that inactivate the elicitor-active oligogalacturonides. Plant J. **94**:260–273. https://doi.org/10.1111/tpj.13852.

Berry, H.M., and Argueso, C.T. (2022). More than growth: phytohormone-regulated transcription factors controlling plant immunity, plant development and plant architecture. Curr. Opin. Plant Biol. **70**, 102309. https://doi.org/10.1016/j.pbi.2022.102309.

Bethke, G., Thao, A., Xiong, G., Li, B., Soltis, N.E., Hatsugai, N., Hillmer, R.A., Katagiri, F., Kliebenstein, D.J., Pauly, M., et al. (2016). Pectin biosynthesis is critical for cell wall integrity and immunity in Arabidopsis thaliana. Plant Cell **28**:537–556. https://doi.org/10.1105/tpc.15.00404.

Bojar, D., Martinez, J., Santiago, J., Rybin, V., Bayliss, R., and Hothorn, M. (2014). Crystal structures of the phosphorylated BRI1 kinase domain and implications for brassinosteroid signal initiation. Plant J. **78**:31–43. https://doi.org/10.1111/tpj.12445.

Boutrot, F., and Zipfel, C. (2017). Function, discovery, and exploitation of plantpattern recognition receptors for broad-spectrum disease resistance. Annu. Rev. Phytopathol. **55**:257–286. https://doi.org/10.1146/annurev-phyto-080614-120106.

Bowman, J.L., Kohchi, T., Yamato, K.T., Jenkins, J., Shu, S., Ishizaki, K., Yamaoka, S., Nishihama, R., Nakamura, Y., Berger, F., et al. (2017). Insights into land plant evolution garnered from the Marchantia polymorpha Genome. Cell **171**:287–304.e15. https://doi.org/10.1016/j.cell.2017.09.030.

Bozsoki, Z., Cheng, J., Feng, F., Gysel, K., Vinther, M., Andersen, K.R., Oldroyd, G., Blaise, M., Radutoiu, S., and Stougaard, J. (2017). Receptor-mediated chitin perception in legume roots is functionally separable from Nod factor perception. Proc. Natl. Acad. Sci. USA **114**:E8118–E8127. https://doi.org/10.1073/pnas.1706795114.

Bozsoki, Z., Gysel, K., Hansen, S.B., Lironi, D., Krönauer, C., Feng, F., de Jong, N., Vinther, M., Kamble, M., Thygesen, M.B., et al. (2020). Ligand-recognizing motifs in plant LysM receptors are major determinants of specificity. Science **369**:663–670. https://doi.org/10.1126/science.abb3377.

Broghammer, A., Krusell, L., Blaise, M., Sauer, J., Sullivan, J.T., Maolanon, N., Vinther, M., Lorentzen, A., Madsen, E.B., Jensen, K.J., et al. (2012). Legume receptors perceive the rhizobial lipochitin oligosaccharide signal molecules by direct binding. Proc. Natl. Acad. Sci. USA **109**:13859–13864. https://doi.org/10.1073/pnas.1205171109.

Burton, R.A., Gidley, M.J., and Fincher, G.B. (2010). Heterogeneity in the chemistry, structure and function of plant cell walls. Nat. Chem. Biol. **6**:724–732. https://doi.org/10.1038/nchembio.439.

Cao, Y., Liang, Y., Tanaka, K., Nguyen, C.T., Jedrzejczak, R.P., Joachimiak, A., and Stacey, G. (2014). The kinase LYK5 is a major chitin receptor in Arabidopsis and forms a chitin-induced complex with related kinase CERK1. Elife **3**.

Carpita, N.C., and Gibeaut, D.M. (1993). Structural models of primary cell walls in flowering plants: consistency of molecular structure with the physical properties of the walls during growth. Plant J. **3**:1–30. https://doi.org/10.1111/j.1365-313x.1993.tb00007.x.

Carpita, N.C., and McCann, M.C. (2020). Redesigning plant cell walls for the biomass-based bioeconomy. J. Biol. Chem. **295**:15144–15157. https://doi.org/10.1074/jbc.REV120.014561.

Chandrasekar, B., Wanke, A., Wawra, S., Saake, P., Mahdi, L., Charura, N., Neidert, M., Poschmann, G., Malisic, M., Thiele, M., et al. (2022). Fungi hijack a ubiquitous plant apoplastic endoglucanase to release a ROS scavenging β-glucan decasaccharide to subvert immune responses. Plant Cell **34**:2765–2784. https://doi.org/10.1093/plcell/koac114.

Chaube, M.A., Trattnig, N., Lee, D.H., Belkhadir, Y., and Pfrengle, F. (2022). Synthesis of fungal cell wall oligosaccharides and their ability to trigger plant immune responses. Eur. J. Org Chem. **2022**, e202200313. https://doi.org/10.1002/ejoc.202200313.

Chaudhary, A., Chen, X., Gao, J., Leśniewska, B., Hammerl, R., Dawid, C., and Schneitz, K. (2020). The Arabidopsis receptor kinase STRUBBELIG regulates the response to cellulose deficiency. PLoS Genet. **16**, e1008433. https://doi.org/10.1371/journal.pgen.1008433.

Chaudhary, A., Chen, X., Leśniewska, B., Boikine, R., Gao, J., Wolf, S., and Schneitz, K. (2021). Cell wall damage attenuates root hair patterning and tissue morphogenesis mediated by the receptor kinase STRUBBELIG. Development **148**:dev199425. https://doi.org/10.1242/dev.199425.

Cheng, K., Zhou, Y., and Neelamegham, S. (2017). DrawGlycan-SNFG: a robust tool to render glycans and glycopeptides with fragmentation information. Glycobiology **27**:200–205. https://doi.org/10.1093/glycob/cww115.

Cheval, C., Samwald, S., Johnston, M.G., de Keijzer, J., Breakspear, A., Liu, X., Bellandi, A., Kadota, Y., Zipfel, C., and Faulkner, C. (2020). Chitin perception in plasmodesmata characterizes submembrane immune-signaling specificity in plants. Proc. Natl. Acad. Sci. USA **117**:9621–9629. https://doi.org/10.1073/pnas.1907799117.

Chiniquy, D., Underwood, W., Corwin, J., Ryan, A., Szemenyei, H., Lim, C.C., Stonebloom, S.H., Birdseye, D.S., Vogel, J., Kliebenstein, D., et al. (2019). PMR5, an acetylation protein at the intersection of pectin biosynthesis and defense against fungal pathogens. Plant J. **100**:1022–1035. https://doi.org/10.1111/tpj.14497.

Chowdhury, J., Henderson, M., Schweizer, P., Burton, R.A., Fincher, G.B., and Little, A. (2014). Differential accumulation of callose, arabinoxylan and cellulose in nonpenetrated versus penetrated papillae on leaves of barley infected with *Blumeria graminis* f. sp. hordei. New Phytol. **204**:650–660. https://doi.org/10.1111/nph.12974.

Claverie, J., Balacey, S., Lemaître-Guillier, C., Brulé, D., Chiltz, A., Granet, L., Noirot, E., Daire, X., Darblade, B., Héloir, M.C., et al. (2018). The cell wall-derived xis a new DAMP triggering plant immunity in *Vitis vinifera* and *Arabidopsis thaliana*. Front. Plant Sci. **9**:1725. https://doi.org/10.3389/fpls.2018.01725.

Coculo, D., and Lionetti, V. (2022). The plant invertase/pectin methylesterase inhibitor superfamily. Front. Plant Sci. **13**, 863892. https://doi.org/10.3389/fpls.2022.863892.

Cosgrove, D.J. (2024). Structure and growth of plant cell walls. Nat. Rev. Mol. Cell Biol. **25**:340–358. https://doi.org/10.1038/s41580-023-00691-y.

Costantini, S., Benedetti, M., Pontiggia, D., Giovannoni, M., Cervone, F., Mattei, B., and De Lorenzo, G. (2023). Berberine bridge enzyme-like oxidases of cellodextrins and mixed-linked β-glucans control seed coat formation. Plant Physiol. **194**:296–313. https://doi.org/10.1093/plphys/kiad457.

Custers, J.H.H.V., Harrison, S.J., Sela-Buurlage, M.B., van Deventer, E., Lageweg, W., Howe, P.W., van der Meijs, P.J., Ponstein, A.S., Simons, B.H., Melchers, L.S., et al. (2004). Isolation and characterisation of a class of carbohydrate oxidases from higher plants, with a role in active defence. Plant J. **39**:147–160. https://doi.org/10.1111/j.1365-313X.2004.02117.x.

Dai, M.D., Wu, M., Li, Y., Su, Z.Z., Lin, F.C., and Liu, X.H. (2021). The chitin deacetylase PoCda7 is involved in the pathogenicity of *Pyricularia oryzae*. Microbiol. Res. **248**, 126749. https://doi.org/10.1016/j.micres.2021.126749.

Dai, Y.S., Liu, D., Guo, W., Liu, Z.X., Zhang, X., Shi, L.L., Zhou, D.M., Wang, L.N., Kang, K., Wang, F.Z., et al. (2023). Poaceae-specific β-1,3;1,4-d-glucans link jasmonate signalling to OsLecRK1-mediated defence response during rice-brown planthopper interactions. Plant Biotechnol. J. **21**:1286–1300. https://doi.org/10.1111/pbi.14038.

Dangl, J.L., Horvath, D.M., and Staskawicz, B.J. (2013). Pivoting the plant immune system from dissection to deployment. Science **341**:746–751. https://doi.org/10.1126/science.1236011.

De Lorenzo, G., and Cervone, F. (2022). Plant immunity by damage-associated molecular patterns (DAMPs). Essays Biochem. **66**:459–469. https://doi.org/10.1042/EBC20210087.

Decreux, A., and Messiaen, J. (2005). Wall-associated kinase WAK1 interacts with cell wall pectins in a calcium-induced conformation. Plant Cell Physiol. **46**:268–278. https://doi.org/10.1093/pcp/pci026.

Decreux, A., Thomas, A., Spies, B., Brasseur, R., Van Cutsem, P., and Messiaen, J. (2006). In vitro characterization of the homogalacturonan-binding domain of the wall-associated kinase WAK1 using site-directed mutagenesis. Phytochemistry **67**:1068–1079. https://doi.org/10.1016/j.phytochem.2006.03.009.

DeFalco, T.A., and Zipfel, C. (2021). Molecular mechanisms of early plant pattern-triggered immune signaling. Mol. Cell **81**:4346. https://doi.org/10.1016/j.molcel.2021.09.028.

Del Hierro, I., Mélida, H., Broyart, C., Santiago, J., and Molina, A. (2021). Computational prediction method to decipher receptor-glycoligand interactions in plant immunity. Plant J. **105**:1710–1726. https://doi.org/10.1111/tpj.15133.

Delannoy-Bruno, O., Desai, C., Castillo, J.J., Couture, G., Barve, R.A., Lombard, V., Henrissat, B., Cheng, J., Han, N., Hayashi, D.K., et al. (2022). An approach for evaluating the effects of dietary fiber polysaccharides on the human gut microbiome and plasma proteome. Proc. Natl. Acad. Sci. USA **119**, e2123411119. https://doi.org/10.1073/pnas.2123411119.

Delgado-Cerezo, M., Sánchez-Rodríguez, C., Escudero, V., Miedes, E., Fernández, P.V., Jordá, L., Hernández-Blanco, C., Sánchez-Vallet, A., Bednarek, P., Schulze-Lefert, P., et al. (2012). Arabidopsis heterotrimeric G-protein regulates cell wall defense and resistance to necrotrophic fungi. Mol. Plant **5**:98–114. https://doi.org/10.1093/mp/ssr082.

Delmer, D., Dixon, R.A., Keegstra, K., and Mohnen, D. (2024). The plant cell wall—dynamic, strong, and adaptable—is a natural shapeshifter. Plant Cell, koad325. https://doi.org/10.1093/plcell/koad325.

Denancé, N., Sánchez-Vallet, A., Goffner, D., and Molina, A. (2013). Disease resistance or growth: the role of plant hormones in balancing immune responses and fitness costs. Front. Plant Sci. **4**:155. https://doi.org/10.3389/fpls.2013.00155.

Denness, L., McKenna, J.F., Segonzac, C., Wormit, A., Madhou, P., Bennett, M., Mansfield, J., Zipfel, C., and Hamann, T. (2011). Cell wall damage-induced lignin biosynthesis is regulated by a reactive oxygen species- and jasmonic acid-dependent process in Arabidopsis. Plant Physiol. **156**:1364–1374. https://doi.org/10.1104/pp.111.175737.

Desaki, Y., Kouzai, Y., Ninomiya, Y., Iwase, R., Shimizu, Y., Seko, K., Molinaro, A., Minami, E., Shibuya, N., Kaku, H., et al. (2018). OsCERK1 plays a crucial role in the lipopolysaccharide-induced immune response of rice. New Phytol. **217**:1042–1049. https://doi.org/10.1111/nph.14941.

Dewangan, B.P., Gupta, A., Sah, R.K., Das, S., Kumar, S., and Bhattacharjee, S. (2023). Xylobiose treatment triggers a defense-related response and alters cell wall composition. Plant Mol. Biol. **113**:383–400.

Dievart, A., Gottin, C., Périn, C., Ranwez, V., and Chantret, N. (2020). Origin and diversity of plant receptor-like kinases. Annu. Rev. Plant Biol. **71**:131–156. https://doi.org/10.1146/annurev-arplant-073019-025927.

Dmochowska-Boguta, M., Kloc, Y., Zielezinski, A., Werecki, P., Nadolska- Orczyk, A., Karlowski, W.M., and Orczyk, W. (2020). TaWAK6 encoding wall associated kinase is involved in wheat resistance to leaf rust similar to adult plant resistance. PLoS One **15**, e0227713.

Dora, S., Terrett, O.M., and Sánchez-Rodríguez, C. (2022). Plant-microbe interactions in the apoplast: communication at the plant cell wall. Plant Cell **34**:1532–1550. https://doi.org/10.1093/plcell/koac040.

Dort, E.N., Layne, E., Feau, N., Butyaev, A., Henrissat, B., Martin, F.M., Haridas, S., Salamov, A., Grigoriev, I.V., Blanchette, M., et al. (2023). Large-scale genomic analyses with machine learning uncover predictive patterns associated with fungal phytopathogenic lifestyles and traits. Sci. Rep. **13**, 17203. https://doi.org/10.1038/s41598-023-44005-w.

Drula, E., Garron, M.L., Dogan, S., Lombard, V., Henrissat, B., and Terrapon, N. (2022). The carbohydrate-active enzyme database: functions and literature. Nucleic Acids Res. **50**:D571–D577. https://doi.org/10.1093/nar/gkab1045.

Du, J., Kirui, A., Huang, S., Wang, L., Barnes, W.J., Kiemle, S.N., Zheng, Y., Rui, Y., Ruan, M., Qi, S., et al. (2020). Mutations in the pectin methyltransferase QUASIMODO2 influence cellulose biosynthesis and wall iin Arabidopsis. Plant Cell **32**:3576–3597. https://doi.org/10.1105/tpc.20.00252.

Ellinger, D., Naumann, M., Falter, C., Zwikowics, C., Jamrow, T., Manisseri, C., Somerville, S.C., and Voigt, C.A. (2013). Elevated early callose deposition results in complete penetration resistance to powdery mildew in Arabidopsis. Plant Physiol. **161**:1433–1444. https://doi.org/10.1104/pp.112.211011.

Ellis, C., Karafyllidis, I., and Turner, J.G. (2002a). Constitutive activation of jasmonate signaling in an Arabidopsis mutant correlates with enhanced resistance to *Erysiphe cichoracearum, Pseudomonas syringae*, and *Myzus persicae*. Mol. Plant Microbe Interact. **15**:1025–1030. https://doi.org/10.1094/MPMI.2002.15.10.1025.

Ellis, C., Karafyllidis, I., Wasternack, C., and Turner, J.G. (2002b). The Arabidopsis mutant *cev1* links cell wall signaling to jasmonate and ethylene responses. Plant Cell **14**:1557–1566.

Endre, G., Kereszt, A., Kevei, Z., Mihacea, S., Kaló, P., and Kiss, G.B. (2002). A receptor kinase gene regulating symbiotic nodule development. Nature **417**:962–966. https://doi.org/10.1038/nature00842.

Engelsdorf, T., and Hamann, T. (2014). An update on receptor-like kinase involvement in the maintenance of plant cell wall integrity. Ann. Bot. **114**:1339–1347. https://doi.org/10.1093/aob/mcu043.

Engelsdorf, T., Will, C., Hofmann, J., Schmitt, C., Merritt, B.B., Rieger, L., Frenger, M.S., Marschall, A., Franke, R.B., Pattathil, S., et al. (2017). Cell wall composition and penetration resistance against the fungal pathogen *Colletotrichum higginsianum* are affected by impaired starch turnover in Arabidopsis mutants. J. Exp. Bot. **68**:701–713. https://doi.org/10.1093/jxb/erw434.

Escudero, V., Jordá, L., Sopeña-Torres, S., Mélida, H., Miedes, E., Muñoz-Barrios, A., Swami, S., Alexander, D., McKee, L.S., Sánchez-Vallet, A., et al. (2017). Alteration of cell wall xylan acetylation triggers defense responses that counterbalance the immune deficiencies of plants impaired in the β-subunit of the heterotrimeric G-protein. Plant J. **92**:386–399. https://doi.org/10.1111/tpj.13660.

Fan, Z., Oguntimein, G.B., and Reilly, P.J. (2000). Characterization of kinetics and thermostability of *Acremonium strictum* glucooligosaccharide oxidase. Biotechnol. Bioeng. **68**:231–237. https://doi.org/10.1002/(sici)1097-0290(20000420)68:2<231::aid-bit12>3.0.co;2-d.

Faulkner, C., Petutschnig, E., Benitez-Alfonso, Y., Beck, M., Robatzek, S., Lipka, V., and Maule, A.J. (2013). LYM2-dependent chitin perception limits molecular flux via plasmodesmata. Proc. Natl. Acad. Sci. USA **110**:9166–9170. https://doi.org/10.1073/pnas.1203458110.

Feinberg, H., Mitchell, D.A., Drickamer, K., and Weis, W.I. (2001). Structural basis for selective recognition of oligosaccharides by DC-SIGN and DC-SIGNR. Science **294**:2163–2166. https://doi.org/10.1126/science.1066371.

Feng, W., Kita, D., Peaucelle, A., Cartwright, H.N., Doan, V., Duan, Q., Liu, M.C., Maman, J., Steinhorst, L., Schmitz-Thom, I., et al. (2018). The FERONIA receptor kinase maintains cell-wall integrity during salt stress through Ca^{2+} signaling. Curr. Biol. **28**:666–675.e5. https://doi.org/10.1016/j.cub.2018.01.023.

Feng, F., Sun, J., Radhakrishnan, G.V., Lee, T., Bozsóki, Z., Fort, S., Gavrin, A., Gysel, K., Thygesen, M.B., Andersen, K.R., et al. (2019). A combination of chitooligosaccharide and lipochitooligosaccharide recognition promotes arbuscular mycorrhizal associations in Medicago truncatula. Nat. Commun. **10**:5047. https://doi.org/10.1038/s41467-019-12999-5.

Fernández-Calvo, P., López, G., Martín-Dacal, M., et al. (2024). Leucine Rich Repeat-Malectin receptor kinases IGP1/CORK1, IGP3 and IGP4 are required for Arabidopsis immune responses triggered by β-1,4-D-Xylo-oligosaccharides from plant cell walls. The Cell Surface **11**, 100124. https://doi.org/10.1016/j.tcsw.2024.100124.

Ferrari, A.R., Rozeboom, H.J., Dobruchowska, J.M., van Leeuwen, S.S., Vugts, A.S.C., Koetsier, M.J., Visser, J., and Fraaije, M.W. (2016). Discovery of a xylooligosaccharide oxidase from *Myceliophthora thermophila* C1. J. Biol. Chem. **291**:23709–23718. https://doi.org/10.1074/jbc.M116.741173.

Ferrari, S., Galletti, R., Denoux, C., De Lorenzo, G., Ausubel, F.M., and Dewdney, J. (2007). Resistance to *Botrytis cinerea* induced in Arabidopsis by elicitors is independent of salicylic acid, ethylene, or jasmonate signaling but requires PHYTOALEXIN DEFICIENT3. Plant Physiol. **144**:367–379. https://doi.org/10.1104/pp.107.095596.

Flors, V., Ton, J., van Doorn, R., Jakab, G., García-Agustín, P., and Mauch-Mani, B. (2008). Interplay between JA, SA and ABA signalling during basal and induced resistance against *Pseudomonas syringae* and *Alternaria brassicicola*. Plant J. **54**:81–92. https://doi.org/10.1111/j.1365-313X.2007.03397.x.

Foumani, M., Vuong, T.V., and Master, E.R. (2011). Altered substrate specificity of the gluco-oligosaccharide oxidase from *Acremonium strictum*. Biotechnol. Bioeng. **108**:2261–2269. https://doi.org/10.1002/bit.23149.

Franck, C.M., Westermann, J., and Boisson-Dernier, A. (2018). Plant malectin-like receptor kinases: from cell wall integrity to immunity and beyond. Annu. Rev. Plant Biol. **69**:301–328. https://doi.org/10.1146/annurev-arplant-042817-040557.

Fritz-Laylin, L.K., Krishnamurthy, N., Tör, M., Sjölander, K.V., and Jones, J.D.G. (2005). Phylogenomic analysis of the receptor-like proteins of rice and Arabidopsis. Plant Physiol. **138**:611–623. https://doi.org/10.1104/pp.104.054452.

Fuchsberger, F.F., Kim, D., Baranova, N., Vrban, H., Kagelmacher, M., Wawrzinek, R., and Rademacher, C. (2023). Information transfer in mammalian glycan-based communication. Elife **12**, e69415. https://doi.org/10.7554/eLife.69415.

Gallego-Giraldo, L., Posé, S., Pattathil, S., Peralta, A.G., Hahn, M.G., Ayre, B.G., Sunuwar, J., Hernandez, J., Patel, M., Shah, J., et al. (2018). Elicitors and defense gene induction in plants with altered lignin compositions. New Phytol. **219**:1235–1251. https://doi.org/10.1111/nph.15258.

Gámez-Arjona, F.M., Vitale, S., Voxeur, A., Dora, S., Müller, S., Sancho-Andrés, G., Montesinos, J.C., Di Pietro, A., and Sánchez-Rodríguez, C. (2022). Impairment of the cellulose degradation machinery enhances *Fusarium oxysporum* virulence but limits its reproductive fitness. Sci. Adv. **8**:eabl9734. https://doi.org/10.1126/sciadv.abl9734.

Gamir, J., Minchev, Z., Berrio, E., García, J.M., De Lorenzo, G., and Pozo, M.J. (2021). Roots drive oligogalacturonide-induced systemic immunity in tomato. Plant Cell Environ. **44**:275–289. https://doi.org/10.1111/pce.13917.

Geoghegan, I., Steinberg, G., and Gurr, S. (2017). The role of the fungal cell wall in the infection of plants. Trends Microbiol. **25**:957–967. https://doi.org/10.1016/j.tim.2017.05.015.

Gigli-Bisceglia, N., and Testerink, C. (2021). Fighting salt or enemies: shared perception and signaling strategies. Curr. Opin. Plant Biol. **64**, 102120. https://doi.org/10.1016/j.pbi.2021.102120.

Gigli-Bisceglia, N., van Zelm, E., Huo, W., Lamers, J., and Testerink, C. (2022). Arabidopsis root responses to salinity depend on pectin modification and cell wall sensing. Development **149**, dev200363. https://doi.org/10.1242/dev.200363.

Gimeno, A., Delgado, S., Valverde, P., Bertuzzi, S., Berbís, M.A., Echavarren, J., Lacetera, A., Martín-Santamaría, S., Surolia, A., Cañada, F.J., et al. (2019). Minimizing the entropy penalty for ligand binding: lessons from the molecular recognition of the histo blood-group antigens by human galectin-3. Angew. Chem., Int. Ed. Engl. **58**:7268–7272. https://doi.org/10.1002/anie.201900723.

Giovannoni, M., Lironi, D., Marti, L., Paparella, C., Vecchi, V., Gust, A.A., De Lorenzo, G., Nürnberger, T., and Ferrari, S. (2021). The Arabidopsis thaliana LysM-containing Receptor-Like Kinase 2 is required for elicitor-induced resistance to pathogens. Plant Cell Environ. **44**:3545–3562. https://doi.org/10.1111/pce.14192.

Gish, L.A., and Clark, S.E. (2011). The RLK/Pelle family of kinases. Plant J. **66**:117–127. https://doi.org/10.1111/j.1365-313X.2011.04518.x.

Goring, D.R. (2023). A new "lock-and-key" system revealed for plant reproductive barriers. Cell **186**:4734–4736. https://doi.org/10.1016/j.cell.2023.09.005.

Greeff, C., Roux, M., Mundy, J., and Petersen, M. (2012). Receptor-like kinase complexes in plant innate immunity. Front. Plant Sci. **3**:209. https://doi.org/10.3389/fpls.2012.00209.

Gully, K., Pelletier, S., Guillou, M.C., Ferrand, M., Aligon, S., Pokotylo, I., Perrin, A., Vergne, E., Fagard, M., Ruelland, E., et al. (2019). The SCOOP12 peptide regulates defense response and root elongation in *Arabidopsis thaliana*. J. Exp. Bot. **70**:1349–1365. https://doi.org/10.1093/jxb/ery454.

Guo, Y., Feinberg, H., Conroy, E., Mitchell, D.A., Alvarez, R., Blixt, O., Taylor, M.E., Weis, W.I., and Drickamer, K. (2004). Structural basis for distinct ligand-binding and targeting properties of the receptors DC-SIGN and DC-SIGNR. Nat. Struct. Mol. Biol. **11**:591–598. https://doi.org/10.1038/nsmb784.

Gust, A.A., Pruitt, R., and Nürnberger, T. (2017). Sensing danger: key to activating plant immunity. Trends Plant Sci. **22**:779–791. https://doi.org/10.1016/j.tplants.2017.07.005.

Guzha, A., McGee, R., Scholz, P., Hartken, D., Lüdke, D., Bauer, K., Wenig, M., Zienkiewicz, K., Herrfurth, C., Feussner, I., et al. (2022). Cell wall-localized BETA-XYLOSIDASE4 contributes to immunity of Arabidopsis against *Botrytis cinerea*. Plant Physiol. **189**:1794–1813. https://doi.org/10.1093/plphys/kiac165.

Gysel, K., Laursen, M., Thygesen, M.B., Lironi, D., Bozsóki, Z., Hjuler, C.T., Maolanon, N.N., Cheng, J., Bjørk, P.K., Vinther, M., et al. (2021). Kinetic proofreading of lipochitooligosaccharides determines signal activation of symbiotic plant receptors. Proc. Natl. Acad. Sci. USA **118**, 2111031118.

Haas, K.T., Wightman, R., Meyerowitz, E.M., and Peaucelle, A. (2020). Pectin homogalacturonan nanofilament expansion drives morphogenesis in plant epidermal cells. Science **367**:1003–1007. https://doi.org/10.1126/science.aaz5103.

Haltom, A.R., and Jafar-Nejad, H. (2015). The multiple roles of epidermal growth factor repeat O-glycans in animal development. Glycobiology **25**:1027–1042. https://doi.org/10.1093/glycob/cwv052.

Hatfield, R.D., Rancour, D.M., and Marita, J.M. (2016). Grass cell walls: a story of cross-linking. Front. Plant Sci. **7**:2056. https://doi.org/10.3389/fpls.2016.02056.

He, J., Kong, M., Qian, Y., Gong, M., Lv, G., and Song, J. (2023). Cellobiose elicits immunity in lettuce conferring resistance to *Botrytis cinerea*. J. Exp. Bot. **74**:1022–1038. https://doi.org/10.1093/jxb/erac448.

Herburger, K., Schoenaers, S., Vissenberg, K., and Mravec, J. (2022). Shank-localized cell wall growth contributes to Arabidopsis root hair elongation. Nat. Plants **8**:1222–1232. https://doi.org/10.1038/s41477-022-01259-y.

Hernández-Blanco, C., Feng, D.X., Hu, J., Sánchez-Vallet, A., Deslandes, L., Llorente, F., Berrocal-Lobo, M., Keller, H., Barlet, X., Sánchez-Rodríguez, C., et al. (2007). Impairment of cellulose synthases required for Arabidopsis secondary cell wall formation enhances disease resistance. Plant Cell **19**:890–903. https://doi.org/10.1105/tpc.106.048058.

Heuts, D.P.H.M., Winter, R.T., Damsma, G.E., Janssen, D.B., and Fraaije, M.W. (2008). The role of double covalent flavin binding in chito-oligosaccharide oxidase from Fusarium graminearum. Biochem. J. **413**:175–183. https://doi.org/10.1042/BJ20071591.

Hou, S., Liu, D., Huang, S., Luo, D., Liu, Z., Xiang, Q., Wang, P., Mu, R., Han, Z., Chen, S., et al. (2021). The Arabidopsis MIK2 receptor elicits immunity by sensing a conserved signature from phytocytokines and microbes. Nat. Commun. **12**:5494. https://doi.org/10.1038/s41467-021-25580-w.

Huang, C.H., Lai, W.L., Lee, M.H., Chen, C.J., Vasella, A., Tsai, Y.C., and Liaw, S.H. (2005). Crystal structure of glucooligosaccharide oxidase from *Acremonium strictum*: a novel flavinylation of 6-S-cysteinyl, 8alpha-N1-histidyl FAD. J. Biol. Chem. **280**:38831–38838. https://doi.org/10.1074/jbc.M506078200.

Huang, J., Gu, M., Lai, Z., Fan, B., Shi, K., Zhou, Y.H., Yu, J.Q., and Chen, Z. (2010). Functional analysis of the Arabidopsis PAL gene family in plant growth, development, and response to environmental stress. Plant Physiol. **153**:1526–1538. https://doi.org/10.1104/pp.110.157370.

Huerta, A.I., Sancho-Andrés, G., Montesinos, J.C., Silva-Navas, J., Bassard, S., Pau-Roblot, C., Kesten, C., Schlechter, R., Dora, S., Ayupov, T., et al. (2023). The WAK-like protein RFO1 acts as a sensor of the pectin methylation status in Arabidopsis cell walls to modulate root growth and defense. Mol. Plant **16**:865–881. https://doi.org/10.1016/j.molp.2023.03.015.

Jacobs, A.K., Lipka, V., Burton, R.A., Panstruga, R., Strizhov, N., Schulze-Lefert, P., and Fincher, G.B. (2003). An Arabidopsis callose synthase, GSL5, is required for wound and papillary callose formation. Plant Cell **15**:2503–2513. https://doi.org/10.1105/tpc.016097.

Johnson, J.M., Thürich, J., Petutschnig, E.K., Altschmied, L., Meichsner, D., Sherameti, I., Dindas, J., Mrozinska, A., Paetz, C., Scholz, S.S., et al. (2018). A poly(A) ribonuclease controls the cellotriose-based interaction between *Piriformospora indica* and its host Arabidopsis. Plant Physiol. **176**:2496–2514. https://doi.org/10.1104/pp.17.01423.

Jumper, J., Evans, R., Pritzel, A., Green, T., Figurnov, M., Ronneberger, O., Tunyasuvunakool, K., Bates, R., Žídek, A., Potapenko, A., et al. (2021). Highly accurate protein structure prediction with AlphaFold. Nature **596**:583–589. https://doi.org/10.1038/s41586-021-03819-2.

Kang, X., Kirui, A., Dickwella Widanage, M.C., Mentink-Vigier, F., Cosgrove, D.J., and Wang, T. (2019). Lignin-polysaccharide interactions in plant secondary cell walls revealed by solid-state NMR. Nat. Commun. **10**:347. https://doi.org/10.1038/s41467-018-08252-0.

Karasov, T.L., Chae, E., Herman, J.J., and Bergelson, J. (2017). Mechanisms to mitigate the trade-off between growth and defense. Plant Cell **29**:666–680. https://doi.org/10.1105/tpc.16.00931.

Kashyap, A., Jiménez-Jiménez, Á.L., Zhang, W., Capellades, M., Srinivasan, S., Laromaine, A., Serra, O., Figueras, M., Rencoret, J., Gutiérrez, A., et al. (2022). Induced ligno-suberin vascular coating and tyramine-derived hydroxycinnamic acid amides restrict *Ralstonia solanacearum* colonization in resistant tomato. New Phytol. **234**:1411–1429. https://doi.org/10.1111/nph.17982.

Kelly, S., Hansen, S.B., Rübsam, H., Saake, P., Pedersen, E.B., Gysel, K., Madland, E., Wu, S., Wawra, S., Reid, D., et al. (2023). A glycan receptor kinase facilitates intracellular accommodation of arbuscular mycorrhiza and symbiotic rhizobia in the legume *Lotus japonicus*. PLoS Biol. **21**, e3002127. https://doi.org/10.1371/journal.pbio.3002127.

Kelly, S.J., Muszyński, A., Kawaharada, Y., Hubber, A.M., Sullivan, J.T., Sandal, N., Carlson, R.W., Stougaard, J., and Ronson, C.W. (2013). Conditional requirement for exopolysaccharide in the Mesorhizobium-Lotus symbiosis. Mol. Plant Microbe Interact. **26**:319–329. https://doi.org/10.1094/MPMI-09-12-0227-R.

Khokhani, D., Carrera Carriel, C., Vayla, S., Irving, T.B., Stonoha-Arther, C., Keller, N.P., and Ané, J.M. (2021). Deciphering the chitin code in plant symbiosis, defense, and microbial networks. Annu.

Rev. Microbiol. **75**:583–607. https://doi.org/10.1146/annurev-micro-051921-114809.

Kim, S.J., Bhandari, D.D., Sokoloski, R., and Brandizzi, F. (2023). Immune activation during Pseudomonas infection causes local cell wall remodeling and alters AGP accumulation. Plant J. **116**:541–557. https://doi.org/10.1111/tpj.16393.

Kim, S.J., Chandrasekar, B., Rea, A.C., Danhof, L., Zemelis-Durfee, S., Thrower, N., Shepard, Z.S., Pauly, M., Brandizzi, F., and Keegstra, K. (2020). The synthesis of xyloglucan, an abundant plant cell wall polysaccharide, requires CSLC function. Proc. Natl. Acad. Sci. USA **117**:20316–20324. https://doi.org/10.1073/pnas.2007245117.

Kohorn, B.D., Greed, B.E., Mouille, G., Verger, S., and Kohorn, S.L. (2021). Effects of Arabidopsis wall associated kinase mutations on ESMERALDA1 and elicitor induced ROS. PLoS One **16**, e0251922. https://doi.org/10.1371/journal.pone.0251922.

Kohorn, B.D., Johansen, S., Shishido, A., Todorova, T., Martinez, R., Defeo, E., and Obregon, P. (2009). Pectin activation of MAP kinase and gene expression is WAK2 dependent. Plant J. **60**:974–982. https://doi.org/10.1111/j.1365-313X.2009.04016.x.

Kouzai, Y., Nakajima, K., Hayafune, M., Ozawa, K., Kaku, H., Shibuya, N., Minami, E., and Nishizawa, Y. (2014). CEBiP is the major chitin oligomer-binding protein in rice and plays a main role in the perception of chitin oligomers. Plant Mol. Biol. **84**:519–528. https://doi.org/10.1007/s11103-013-0149-6.

Krylov, V.B., Gómez-Redondo, M., Solovev, A.S., Yashunsky, D.V., Brown, A.J.P., Stappers, M.H.T., Gow, N.A.R., Ardá, A., Jiménez-Barbero, J., and Nifantiev, N.E. (2023). Identification of a new DC-SIGN binding pentamannoside epitope within the complex structure of. Cell Surf. **10**, 100109. https://doi.org/10.1016/j.tcsw.2023.100109.

Kubicek, C.P., Starr, T.L., and Glass, N.L. (2014). Plant cell wall-degrading enzymes and their secretion in plant-pathogenic fungi. Annu. Rev. Phytopathol. **52**:427–451. https://doi.org/10.1146/annurev-phyto-102313-045831.

Kumar, M., Campbell, L., and Turner, S. (2016). Secondary cell walls: biosynthesis and manipulation. J. Exp. Bot. **67**:515–531. https://doi.org/10.1093/jxb/erv533.

Kumar, M., Carr, P., and Turner, S.R. (2022). An atlas of Arabidopsis protein S-acylation reveals its widespread role in plant cell organization and function. Nat. Plants **8**:670–681. https://doi.org/10.1038/s41477-022-01164-4.

Latgé, J.P., and Calderone, R. (2002). Host-microbe interactions: fungi invasive human fungal opportunistic infections. Curr. Opin. Microbiol. **5**:355–358. https://doi.org/10.1016/s1369-5274(02)00343-0.

Le, M.H., Cao, Y., Zhang, X.C., and Stacey, G. (2014). LIK1, a CERK1-interacting kinase, regulates plant immune responses in Arabidopsis. PLoS One **9**, e102245. https://doi.org/10.1371/journal.pone.0102245.

Lee, H.K., and Goring, D.R. (2021). Two subgroups of receptor-like kinases promote early compatible pollen responses in the Arabidopsis thaliana pistil. J. Exp. Bot. **72**:1198–1211. https://doi.org/10.1093/jxb/eraa496.

Lee, H.K., and Santiago, J. (2023). Structural insights of cell wall integrity signaling during development and immunity. Curr. Opin. Plant Biol. **76**, 102455. https://doi.org/10.1016/j.pbi.2023.102455.

Lee, M.H., Jeon, H.S., Kim, S.H., Chung, J.H., Roppolo, D., Lee, H.J., Cho, H.J., Tobimatsu, Y., Ralph, J., and Park, O.K. (2019). Lignin-based barrier restricts pathogens to the infection site and confers resistance in plants. EMBO J. **38**, e101948. https://doi.org/10.15252/embj.2019101948.

Lehti-Shiu, M.D., Zou, C., Hanada, K., and Shiu, S.H. (2009). Evolutionary history and stress regulation of plant receptor-like kinase/pelle genes. Plant Physiol. **150**:12–26. https://doi.org/10.1104/pp.108.134353.

Leszczuk, A., Kalaitzis, P., Kulik, J., and Zdunek, A. (2023). Review: structure and modifications of arabinogalactan proteins (AGPs). BMC Plant Biol. **23**:45. https://doi.org/10.1186/s12870-023-04066-5.

Li, L., Yu, Y., Zhou, Z., and Zhou, J.M. (2016). Plant pattern-recognition receptors controlling innate immunity. Sci. China Life Sci. **59**:878–888. https://doi.org/10.1007/s11427-016-0115-2.

Li, Q., Wang, C., and Mou, Z. (2020). Perception of damaged self in plants. Plant Physiol. **182**:1545–1565. https://doi.org/10.1104/pp.19.01242.

Lin, W., Tang, W., Pan, X., Huang, A., Gao, X., Anderson, C.T., and Yang, Z. (2022). Arabidopsis pavement cell morphogenesis requires FERONIA binding to pectin for activation of ROP GTPase signaling. Curr. Biol. **32**:497–507.e4. https://doi.org/10.1016/j.cub.2021.11.030.

Liu, C., Yu, H., Voxeur, A., Rao, X., and Dixon, R.A. (2023a). FERONIA and wall-associated kinases coordinate defense induced by lignin modification in plant cell walls. Sci. Adv. **9**, eadf7714. https://doi.org/10.1126/sciadv.adf7714.

Liu, H., Lu, X., Li, M., Lun, Z., Yan, X., Yin, C., Yuan, G., Wang, X., Liu, N., Liu, D., et al. (2023b). Plant immunity suppression by an exo-β-1,3-glucanase and an elongation factor 1α of the rice blast fungus. Nat. Commun. **14**:5491. https://doi.org/10.1038/s41467-023-41175-z.

Liu, M., Liu, H., Zhang, J., Li, C., Li, Y., Yang, G., Xia, T., Huang, H., Xu, Y., Kong, W., et al. (2023c). Knockout of CAFFEOYL-COA 3-O-METHYLTRANSFERASE 6/6L enhances the S/G ratio of lignin monomers and disease resistance in Nicotiana tabacum. Front. Plant Sci. **14**, 1216702. https://doi.org/10.3389/fpls.2023.1216702.

Liu, S., Wang, J., Han, Z., Gong, X., Zhang, H., and Chai, J. (2016). Molecular mechanism for fungal cell wall recognition by rice chitin receptor OsCEBiP. Structure **24**:1192–1200. https://doi.org/10.1016/j.str.2016.04.014.

Liu, T., Liu, Z., Song, C., Hu, Y., Han, Z., She, J., Fan, F., Wang, J., Jin, C., Chang, J., et al. (2012). Chitin-induced dimerization activates a plant immune receptor. Science **336**:1160–1164. https://doi.org/10.1126/science.1218867.

Locci, F., Benedetti, M., Pontiggia, D., Citterico, M., Caprari, C., Mattei, B., Cervone, F., and De Lorenzo, G. (2019). An Arabidopsis berberine bridge enzyme-like protein specifically oxidizes cellulose oligomers and plays a role in immunity. Plant J. **98**:540–554. https://doi.org/10.1111/tpj.14237.

López-Cruz, J., Finiti, I., Fernández-Crespo, E., Crespo-Salvador, O., García-Agustín, P., and González-Bosch, C. (2014). Absence of endo-1,4-β-glucanase KOR1 alters the jasmonate-dependent defence response to Pseudomonas syringae in Arabidopsis. J. Plant Physiol. **171**:1524–1532. https://doi.org/10.1016/j.jplph.2014.07.006.

Lorrai, R., Francocci, F., Gully, K., Martens, H.J., De Lorenzo, G., Nawrath, C., and Ferrari, S. (2021). Impaired cuticle functionality and robust resistance to *Botrytis cinerea* in Arabidopsis thaliana plants with altered homogalacturonan integrity are dependent on the class III peroxidase AtPRX71. Front. Plant Sci. **12**, 696955. https://doi.org/10.3389/fpls.2021.696955.

Lozano-Durán, R., and Zipfel, C. (2015). Trade-off between growth and immunity: role of brassinosteroids. Trends Plant Sci. **20**:12–19. https://doi.org/10.1016/j.tplants.2014.09.003.

Macauley, M.S., Crocker, P.R., and Paulson, J.C. (2014). Siglec-mediated regulation of immune cell function in disease. Nat. Rev. Immunol. **14**:653–666. https://doi.org/10.1038/nri3737.

Madsen, E.B., Antolín-Llovera, M., Grossmann, C., Ye, J., Vieweg, S., Broghammer, A., Krusell, L., Radutoiu, S., Jensen, O.N., Stougaard, J., et al. (2011). Autophosphorylation is essential for the in vivo function of the *Lotus japonicus* Nod factor receptor 1 and receptor-mediated signalling in cooperation with Nod factor

receptor 5. Plant J. **65**:404–417. https://doi.org/10.1111/j.1365-313X.2010.04431.x.

Madsen, E.B., Madsen, L.H., Radutoiu, S., Olbryt, M., Rakwalska, M., Szczyglowski, K., Sato, S., Kaneko, T., Tabata, S., Sandal, N., et al. (2003). A receptor kinase gene of the LysM type is involved in legume perception of rhizobial signals. Nature **425**:637–640. https://doi.org/10.1038/nature02045.

Malerba, M., and Cerana, R. (2019). Recent applications of chitin- and chitosan-based polymers in plants. Polymers **11**:839. https://doi.org/10.3390/polym11050839.

Man, J., Gallagher, J.P., and Bartlett, M. (2020). Structural evolution drives diversification of the large LRR-RLK gene family. New Phytol. **226**:1492–1505. https://doi.org/10.1111/nph.16455.

Manabe, Y., Nafisi, M., Verhertbruggen, Y., Orfila, C., Gille, S., Rautengarten, C., Cherk, C., Marcus, S.E., Somerville, S., Pauly, M., et al. (2011). Loss-of-function mutation of REDUCED WALL ACETYLATION2 in Arabidopsis leads to reduced cell wall acetylation and increased resistance to *Botrytis cinerea*. Plant Physiol. **155**:1068–1078. https://doi.org/10.1104/pp.110.168989.

Martín-Dacal, M., Fernández-Calvo, P., Jiménez-Sandoval, P., López, G., Garrido-Arandía, M., Rebaque, D., Del Hierro, I., Berlanga, D.J., Torres, M.Á., Kumar, V., et al. (2023). Arabidopsis immune responses triggered by cellulose- and mixed-linked glucan-derived oligosaccharides require a group of leucine-rich repeat malectin receptor kinases. Plant J. **113**:833–850. https://doi.org/10.1111/tpj.16088.

Mateu, B.P., Bock, P., and Gierlinger, N. (2020). Raman imaging of plant cell walls. Methods Mol. Biol. **2149**:251–295. https://doi.org/10.1007/978-1-0716-0621-6_15.

Mélida, H., Bacete, L., Ruprecht, C., Rebaque, D., Del Hierro, I., López, G., Brunner, F., Pfrengle, F., and Molina, A. (2020). Arabinoxylan-oligosaccharides act as damage associated molecular patterns in plants regulating disease resistance. Front. Plant Sci. **11**:1210. https://doi.org/10.3389/fpls.2020.01210.

Mélida, H., Sandoval-Sierra, J.V., Diéguez-Uribeondo, J., and Bulone, V. (2013). Analyses of extracellular carbohydrates in oomycetes unveil the existence of three different cell wall types. Eukaryot. Cell **12**:194–203. https://doi.org/10.1128/EC.00288-12.

Mélida, H., Sopeña-Torres, S., Bacete, L., Garrido-Arandia, M., Jordá, L., López, G., Muñoz-Barrios, A., Pacios, L.F., and Molina, A. (2018). Non-branched β-1,3-glucan oligosaccharides trigger immune responses in Arabidopsis. Plant J. **93**:34–49. https://doi.org/10.1111/tpj.13755.

Menna, A., Dora, S., Sancho-Andrés, G., Kashyap, A., Meena, M.K., Sklodowski, K., Gasperini, D., Coll, N.S., and Sánchez-Rodríguez, C. (2021). A primary cell wall cellulose-dependent defense mechanism against vascular pathogens revealed by time-resolved dual transcriptomics. BMC Biol. **19**:161. https://doi.org/10.1186/s12915-021-01100-6.

Miedes, E., Vanholme, R., Boerjan, W., and Molina, A. (2014). The role of the secondary cell wall in plant resistance to pathogens. Front. Plant Sci. **5**:358. https://doi.org/10.3389/fpls.2014.00358.

Miya, A., Albert, P., Shinya, T., Desaki, Y., Ichimura, K., Shirasu, K., Narusaka, Y., Kawakami, N., Kaku, H., and Shibuya, N. (2007). CERK1, a LysM receptor kinase, is essential for chitin elicitor signaling in Arabidopsis. Proc. Natl. Acad. Sci. USA **104**:19613–19618. https://doi.org/10.1073/pnas.0705147104.

Molina, A., Miedes, E., Bacete, L., Rodríguez, T., Mélida, H., Denancé, N., Sánchez-Vallet, A., Rivière, M.P., López, G., Freydier, A., et al. (2021). cell wall composition determines disease resistance specificity and fitness. Proc. Natl. Acad. Sci. USA **118**. https://doi.org/10.1073/pnas.2010243118.

Monson, R.K., Trowbridge, A.M., Lindroth, R.L., and Lerdau, M.T. (2022). Coordinated resource allocation to plant growth-defense tradeoffs. New Phytol. **233**:1051–1066. https://doi.org/10.1111/nph.17773.

Morel, O., Lion, C., Neutelings, G., Stefanov, J., Baldacci-Cresp, F., Simon, C., Biot, C., Hawkins, S., and Spriet, C. (2022). REPRISAL: mapping lignification dynamics using chemistry, data segmentation, and ratiometric analysis. Plant Physiol. **188**:816–830. https://doi.org/10.1093/plphys/kiab490.

Moussu, S., Augustin, S., Roman, A.O., Broyart, C., and Santiago, J. (2018). Crystal structures of two tandem malectin-like receptor kinases involved in plant reproduction. Acta Crystallogr. D Struct. Biol. **74**:671–680. https://doi.org/10.1107/S205979831800774X.

Moussu, S., Broyart, C., Santos-Fernandez, G., Augustin, S., Wehrle, S., Grossniklaus, U., and Santiago, J. (2020). Structural basis for recognition of RALF peptides by LRX proteins during pollen tube growth. Proc. Natl. Acad. Sci. USA **117**:7494–7503. https://doi.org/10.1073/pnas.2000100117.

Moussu, S., Lee, H.K., Haas, K.T., Broyart, C., Rathgeb, U., De Bellis, D., Levasseur, T., Schoenaers, S., Fernandez, G.S., Grossniklaus, U., et al. (2023). Plant cell wall patterning and expansion mediated by protein-peptide-polysaccharide interaction. Science **382**:719–725. https://doi.org/10.1126/science.adi4720.

Murakami, E., Cheng, J., Gysel, K., Bozsoki, Z., Kawaharada, Y., Hjuler, C.T., Sørensen, K.K., Tao, K., Kelly, S., Venice, F., et al. (2018). Epidermal LysM receptor ensures robust symbiotic signalling in. Elife **7**:e33506. https://doi.org/10.7554/eLife.33506.

Ngou, B.P.M., Ding, P., and Jones, J.D.G. (2022). Thirty years of resistance: Zig-zag through the plant immune system. Plant Cell **34**:1447–1478. https://doi.org/10.1093/plcell/koac041.

Nishimura, M.T., Stein, M., Hou, B.H., Vogel, J.P., Edwards, H., and Somerville, S.C. (2003). Loss of a callose synthase results in salicylic acid-dependent disease resistance. Science **301**:969–972. https://doi.org/10.1126/science.1086716.

Ogden, M., Whitcomb, S.J., Khan, G.A., Roessner, U., Hoefgen, R., and Persson, S. (2023). Cellulose biosynthesis inhibitor isoxaben causes nutrient-dependent and tissue-specific Arabidopsis phenotypes. Plant Physiol. **194**:612–617. https://doi.org/10.1093/plphys/kiad538.

Ortiz-Morea, F.A., Liu, J., Shan, L., and He, P. (2022). Malectin-like receptor kinases as protector deities in plant immunity. Nat. Plants **8**:27–37. https://doi.org/10.1038/s41477-021-01028-3.

Park, Y.B., and Cosgrove, D.J. (2012). Changes in cell wall biomechanical properties in the xyloglucan-deficient *xxt1/xxt2* mutant of Arabidopsis. Plant Physiol. **158**:465–475. https://doi.org/10.1104/pp.111.189779.

Pawar, P.M.A., Derba-Maceluch, M., Chong, S.L., Gómez, L.D., Miedes, E., Banasiak, A., Ratke, C., Gaertner, C., Mouille, G., McQueen-Mason, S.J., et al. (2016). Expression of fungal acetyl xylan esterase in *Arabidopsis thaliana* improves saccharification of stem lignocellulose. Plant Biotechnol. J. **14**:387–397. https://doi.org/10.1111/pbi.12393.

Pear, J.R., Kawagoe, Y., Schreckengost, W.E., Delmer, D.P., and Stalker, D.M. (1996). Higher plants contain homologs of the bacterial celA genes encoding the catalytic subunit of cellulose synthase. Proc. Natl. Acad. Sci. USA **93**:12637–12642. https://doi.org/10.1073/pnas.93.22.12637.

Pelloux, J., Rustérucci, C., and Mellerowicz, E.J. (2007). New insights into pectin methylesterase structure and function. Trends Plant Sci. **12**:267–277. https://doi.org/10.1016/j.tplants.2007.04.001.

Peng, X., Li, S., and Wang, H. (2018). Time bomb for pollen tubes: peptide RALF-mediated signaling. Mol. Plant **11**:518–520. https://doi.org/10.1016/j.molp.2018.02.010.

Petutschnig, E.K., Jones, A.M.E., Serazetdinova, L., Lipka, U., and Lipka, V. (2010). The lysin motif receptor-like kinase (LysM-RLK) CERK1 is a major chitin-binding protein in *Arabidopsis thaliana* and subject to chitin-induced phosphorylation. J. Biol. Chem. **285**:28902–28911. https://doi.org/10.1074/jbc.M110.116657.

Pogorelko, G., Lionetti, V., Fursova, O., Sundaram, R.M., Qi, M., Whitham, S.A., Bogdanove, A.J., Bellincampi, D., and Zabotina, O.A. (2013). Arabidopsis and *Brachypodium distachyon* transgenic plants expressing *Aspergillus nidulans* acetylesterases have decreased degree of polysaccharide acetylation and increased resistance to pathogens. Plant Physiol. **162**:9–23. https://doi.org/10.1104/pp.113.214460.

Pontiggia, D., Benedetti, M., Costantini, S., De Lorenzo, G., and Cervone, F. (2020). Dampening the DAMPs: How plants maintain the homeostasis of cell wall molecular patterns and avoid hyper-Immunity. Front. Plant Sci. **11**, 613259. https://doi.org/10.3389/fpls.2020.613259.

Pring, S., Kato, H., Imano, S., Camagna, M., Tanaka, A., Kimoto, H., Chen, P., Shrotri, A., Kobayashi, H., Fukuoka, A., et al. (2023). Induction of plant disease resistance by mixed oligosaccharide elicitors prepared from plant cell wall and crustacean shells. Physiol. Plant. **175**, e14052. https://doi.org/10.1111/ppl.14052.

Quentin, M., Allasia, V., Pegard, A., Allais, F., Ducrot, P.H., Favery, B., Levis, C., Martinet, S., Masur, C., Ponchet, M., et al. (2009). Imbalanced lignin biosynthesis promotes the sexual reproduction of homothallic oomycete pathogens. PLoS Pathog. **5**, e1000264. https://doi.org/10.1371/journal.ppat.1000264.

Radutoiu, S., Madsen, L.H., Madsen, E.B., Felle, H.H., Umehara, Y., Grønlund, M., Sato, S., Nakamura, Y., Tabata, S., Sandal, N., et al. (2003). Plant recognition of symbiotic bacteria requires two LysM receptor-like kinases. Nature **425**:585–592. https://doi.org/10.1038/nature02039.

Rajaraman, J., Douchkov, D., Hensel, G., Stefanato, F.L., Gordon, A., Ereful, N., Caldararu, O.F., Petrescu, A.J., Kumlehn, J., Boyd, L.A., et al. (2016). An LRR/Malectin receptor-like kinase mediates resistance to non-adapted and adapted powdery mildew fungi in barley and wheat. Front. Plant Sci. **7**:1836. https://doi.org/10.3389/fpls.2016.01836.

Ramírez, V., and Pauly, M. (2019). Genetic dissection of cell wall defects and the strigolactone pathway in Arabidopsis. Plant Direct **3**, e00149. https://doi.org/10.1002/pld3.149.

Rebaque, D., Del Hierro, I., López, G., Bacete, L., Vilaplana, F., Dallabernardina, P., Pfrengle, F., Jordá, L., Sánchez-Vallet, A., Pérez, R., et al. (2021). Cell wall-derived mixed-linked β-1,3/1,4-glucans trigger immune responses and disease resistance in plants. Plant J. **106**:601–615. https://doi.org/10.1111/tpj.15185.

Rhodes, J., Yang, H., Moussu, S., Boutrot, F., Santiago, J., and Zipfel, C. (2021). Perception of a divergent family of phytocytokines by the Arabidopsis receptor kinase MIK2. Nat. Commun. **12**:705. https://doi.org/10.1038/s41467-021-20932-y.

Rizzi, Y.S., Happel, P., Lenz, S., Urs, M.J., Bonin, M., Cord-Landwehr, S., Singh, R., Moerschbacher, B.M., and Kahmann, R. (2021). Chitosan and chitin deacetylase activity are necessary for development and virulence of *Ustilago maydis*. mBio **12**:e03419-20. https://doi.org/10.1128/mBio.03419-20.

Rodrigues Oblessuc, P., Vaz Bisneta, M., and Melotto, M. (2019). Common and unique Arabidopsis proteins involved in stomatal susceptibility to *Salmonella enterica* and *Pseudomonas syringae*. FEMS Microbiol. Lett. **366**:fnz197. https://doi.org/10.1093/femsle/fnz197.

Ropitaux, M., Hays, Q., Baron, A., Fourmois, L., Boulogne, I., Vauzeilles, B., Lerouge, P., Mollet, J.C., and Lehner, A. (2022). Dynamic imaging of cell wall polysaccharides by metabolic click-mediated labeling of pectins in living elongating cells. Plant J. **110**:916–924. https://doi.org/10.1111/tpj.15706.

Roudaire, T., Marzari, T., Landry, D., Löffelhardt, B., Gust, A.A., Jermakow, A., Dry, I., Winckler, P., Héloir, M.C., and Poinssot, B. (2023). The grapevine LysM receptor-like kinase VvLYK5-1 recognizes chitin oligomers through its association with VvLYK1-1. Front. Plant Sci. **14**, 1130782. https://doi.org/10.3389/fpls.2023.1130782.

Rübsam, H., Krönauer, C., Abel, N.B., Ji, H., Lironi, D., Hansen, S.B., Nadzieja, M., Kolte, M.V., Abel, D., de Jong, N., et al. (2023). Nanobody-driven signaling reveals the core receptor complex in root nodule symbiosis. Science **379**:272–277. https://doi.org/10.1126/science.ade9204.

Rui, Y., and Dinneny, J.R. (2020). A wall with integrity: surveillance and maintenance of the plant cell wall under stress. New Phytol. **225**:1428–1439. https://doi.org/10.1111/nph.16166.

Ruprecht, C., Bartetzko, M.P., Senf, D., Dallabernadina, P., Boos, I., Andersen, M.C.F., Kotake, T., Knox, J.P., Hahn, M.G., Clausen, M.H., et al. (2017). A synthetic glycan microarray enables epitope mapping of plant cell wall glycan-directed antibodies. Plant Physiol. **175**:1094–1104. https://doi.org/10.1104/pp.17.00737.

Saijo, Y., Loo, E.P.I., and Yasuda, S. (2018). Pattern recognition receptors and signaling in plant-microbe interactions. Plant J. **93**:592–613. https://doi.org/10.1111/tpj.13808.

Samalova, M., Mélida, H., Vilaplana, F., Bulone, V., Soanes, D.M., Talbot, N.J., and Gurr, S.J. (2017). The β-1,3-glucanosyltransferases (Gels) affect the structure of the rice blast fungal cell wall during appressorium-mediated plant infection. Cell Microbiol. **19**. https://doi.org/10.1111/cmi.12659.

Sánchez-Rodríguez, C., Estévez, J.M., Llorente, F., Hernández-Blanco, C., Jordá, L., Pagán, I., Berrocal, M., Marco, Y., Somerville, S., and Molina, A. (2009). The ERECTA receptor-like kinase regulates cell wall-mediated resistance to pathogens in *Arabidopsis thaliana*. Mol. Plant Microbe Interact. **22**:953–963. https://doi.org/10.1094/MPMI-22-8-0953.

Sánchez-Vallet, A., Mesters, J.R., and Thomma, B.P.H.J. (2015). The battle for chitin recognition in plant-microbe interactions. FEMS Microbiol. Rev. **39**:171–183. https://doi.org/10.1093/femsre/fuu003.

Sánchez-Vallet, A., López, G., Ramos, B., Delgado-Cerezo, M., Riviere, M.P., Llorente, F., Fernández, P.V., Miedes, E., Estevez, J.M., Grant, M., et al. (2012). Disruption of abscisic acid signaling constitutively activates Arabidopsis resistance to the necrotrophic fungus *Plectosphaerella cucumerina*. Plant Physiol. **160**:2109–2124. https://doi.org/10.1104/pp.112.200154.

Sánchez-Vallet, A., Saleem-Batcha, R., Kombrink, A., Hansen, G., Valkenburg, D.J., Thomma, B.P.H.J., and Mesters, J.R. (2013). Fungal effector Ecp6 outcompetes host immune receptor for chitin binding through intrachain LysM dimerization. Elife **2**, e00790. https://doi.org/10.7554/eLife.00790.

Santiago, J., Brandt, B., Wildhagen, M., Hohmann, U., Hothorn, L.A., Butenko, M.A., and Hothorn, M. (2016). Mechanistic insight into a peptide hormone signaling complex mediating floral organ abscission. Elife **5**:e15075. https://doi.org/10.7554/eLife.15075.

Santiago, J., Henzler, C., and Hothorn, M. (2013). Molecular mechanism for plant steroid receptor activation by somatic embryogenesis co-receptor kinases. Science **341**:889–892. https://doi.org/10.1126/science.1242468.

Sarkar, P., Bosneaga, E., and Auer, M. (2009). Plant cell walls throughout evolution: towards a molecular understanding of their design principles. J. Exp. Bot. **60**:3615–3635. https://doi.org/10.1093/jxb/erp245.

Schoenaers, S., Lee, H.K., Fehér, K., Faucher, E., Levasseur, T., Akary, E., Claeijs, N., Moussu, S., Broyart, C., Balcerowicz, D., AbdElgawad, H., and Vissenberg, K. (2008). Malectin: a novel carbohydrate-binding protein of the endoplasmic reticulum and a candidate player in the early steps of protein N-glycosylation. Mol Biol Cell **19**:3404–3414. https://doi.org/10.1091/mbc.e08-04-0354.

Schoenaers, S., Damineli, D.S.C., Costa, A., Feijó, J.A., Moreau, C., Bonnin, E., Cathala, B., Santiago, J., Höfte, H., Balcerowicz, D., et al. (2024). Rapid alkalinization factor 22 has a structural and signalling role in root hair cell wall assembly 10:494–511. https://doi.org/10.1038/s41477-024-01637-8.

Scortica, A., Giovannoni, M., Scafati, V., Angelucci, F., Cervone, F., De Lorenzo, G., Benedetti, M., and Mattei, B. (2022). Berberine bridge enzyme-like oligosaccharide oxidases act as enzymatic transducers between microbial glycoside hydrolases and plant peroxidases. Mol. Plant Microbe Interact. **35**:881–886. https://doi.org/10.1094/MPMI-05-22-0113-TA.

Seifert, G.J. (2021). The FLA4-FEI pathway: a unique and mysterious signaling module related to cell wall structure and stress signaling. Genes **12**:145. https://doi.org/10.3390/genes12020145.

Sherson, S., Gy, I., Medd, J., Schmidt, R., Dean, C., Kreis, M., Lecharny, A., and Cobbett, C. (1999). The arabinose kinase, ARA1, gene of Arabidopsis is a novel member of the galactose kinase gene family. Plant Mol. Biol. **39**:1003–1012. https://doi.org/10.1023/a:1006181908753.

Shimizu, T., Nakano, T., Takamizawa, D., Desaki, Y., Ishii-Minami, N., Nishizawa, Y., Minami, E., Okada, K., Yamane, H., Kaku, H., et al. (2010). Two LysM receptor molecules, CEBiP and OsCERK1, cooperatively regulate chitin elicitor signaling in rice. Plant J. **64**:204–214. https://doi.org/10.1111/j.1365-313X.2010.04324.x.

Shiu, S.H., and Bleecker, A.B. (2003). Expansion of the receptor-like kinase/Pelle gene family and receptor-like proteins in Arabidopsis. Plant Physiol. **132**:530–543. https://doi.org/10.1104/pp.103.021964.

Shiu, S.H., Karlowski, W.M., Pan, R., Tzeng, Y.H., Mayer, K.F.X., and Li, W.H. (2004). Comparative analysis of the receptor-like kinase family in Arabidopsis and rice. Plant Cell **16**:1220–1234. https://doi.org/10.1105/tpc.020834 tpc.020834.

Sinclair, S.A., Gille, S., Pauly, M., and Krämer, U. (2020). Regulation of acetylation of plant cell wall components is complex and responds to external stimuli. Plant Signal. Behav. **15**, 1687185. https://doi.org/10.1080/15592324.2019.1687185.

Souza, C.d.A., Li, S., Lin, A.Z., Boutrot, F., Grossmann, G., Zipfel, C., and Somerville, S.C. (2017). Cellulose-derived oligomers act as damage-associated molecular patterns and trigger defense-like responses. Plant Physiol. **173**:2383–2398. https://doi.org/10.1104/pp.16.01680.

Srivastava, P.K., and Kapoor, M. (2017). Production, properties, and applications of endo-β-mannanases. Biotechnol. Adv. **35**:1–19. https://doi.org/10.1016/j.biotechadv.2016.11.001.

Stegmann, M., Monaghan, J., Smakowska-Luzan, E., Rovenich, H., Lehner, A., Holton, N., Belkhadir, Y., and Zipfel, C. (2017). The receptor kinase FER is a RALF-regulated scaffold controlling plant immune signaling. Science **355**:287–289. https://doi.org/10.1126/science.aal2541.

Stracke, S., Kistner, C., Yoshida, S., Mulder, L., Sato, S., Kaneko, T., Tabata, S., Sandal, N., Stougaard, J., Szczyglowski, K., et al. (2002). A plant receptor-like kinase required for both bacterial and fungal symbiosis. Nature **417**:959–962. https://doi.org/10.1038/nature00841.

Su, C. (2023). Pectin modifications at the symbiotic interface. New Phytol. **238**:25–32. https://doi.org/10.1111/nph.18705.

Sun, Y., Han, Z., Tang, J., Hu, Z., Chai, C., Zhou, B., and Chai, J. (2013a). Structure reveals that BAK1 as a co-receptor recognizes the BRI1-bound brassinolide. Cell Res. **23**:1326–1329. https://doi.org/10.1038/cr.2013.131.

Sun, Y., Li, L., Macho, A.P., Han, Z., Hu, Z., Zipfel, C., Zhou, J.M., and Chai, J. (2013b). Structural basis for flg22-induced activation of the Arabidopsis FLS2-BAK1 immune complex. Science **342**:624–628. https://doi.org/10.1126/science.1243825 science.1243825.

Takagi, M., Hotamori, K., Naito, K., Matsukawa, S., Egusa, M., Nishizawa, Y., Kanno, Y., Seo, M., Ifuku, S., Mine, A., et al. (2022). Chitin-induced systemic disease resistance in rice requires both OsCERK1 and OsCEBiP and is mediated. Front. Plant Sci. **13**, 1064628. https://doi.org/10.3389/fpls.2022.1064628.

Tan, L., Eberhard, S., Pattathil, S., Warder, C., Glushka, J., Yuan, C., Hao, Z., Zhu, X., Avci, U., Miller, J.S., et al. (2013). An Arabidopsis cell wall proteoglycan consists of pectin and arabinoxylan covalently linked to an arabinogalactan protein. Plant Cell **25**:270–287. https://doi.org/10.1105/tpc.112.107334.

Tang, D., Wang, G., and Zhou, J.M. (2017). Receptor kinases in plant-pathogen interactions: more than pattern recognition. Plant Cell **29**:618–637. https://doi.org/10.1105/tpc.16.00891.

Tateno, M., Brabham, C., and DeBolt, S. (2016). Cellulose biosynthesis inhibitors - a multifunctional toolbox. J. Exp. Bot. **67**:533–542. https://doi.org/10.1093/jxb/erv489.

Taylor, M.E., and Drickamer, K. (2014). Convergent and divergent mechanisms of sugar recognition across kingdoms. Curr. Opin. Struct. Biol. **28**:14–22. https://doi.org/10.1016/j.sbi.2014.07.003.

Tian, H., Fiorin, G.L., Kombrink, A., Mesters, J.R., and Thomma, B.P.H.J. (2022). Fungal dual-domain LysM effectors undergo chitin-induced intermolecular, and not intramolecular, dimerization. Plant Physiol. **190**:2033–2044. https://doi.org/10.1093/plphys/kiac391.

Tronchet, M., Balagué, C., Kroj, T., Jouanin, L., and Roby, D. (2010). Cinnamyl alcohol dehydrogenases-C and D, key enzymes in lignin biosynthesis, play an essential role in disease resistance in Arabidopsis. Mol. Plant Pathol. **11**:83–92. https://doi.org/10.1111/j.1364-3703.2009.00578.x.

Tseng, Y.H., Scholz, S.S., Fliegmann, J., Krüger, T., Gandhi, A., Furch, A.C.U., Kniemeyer, O., Brakhage, A.A., and Oelmüller, R. (2022). CORK1, a LRR-Malectin receptor kinase, is required for cellooligomer-induced responses in *Arabidopsis thaliana*. Cells **11**:2960. https://doi.org/10.3390/cells11192960.

Turner, S., Boutrot, F., Breda, A.S., Hardtke, C.S., Molina, A., Rep, M., Testerink, C., Mouille, G., Höfte, H., Hamann, T., and Zipfel, C. (2018). Cellulose synthase complex organization and cellulose microfibril structure. PLoS Genet. **376**, e1006832. https://doi.org/10.1098/rsta.2017.0048.

Van der Does, D., Rhodes, J., McKenna, J.F., Vernhettes, S., Koevoets, I., Tintor, N., Veerabagu, M., Miedes, E., Segonzac, C., and Roux, M. (2017). The Arabidopsis leucine-rich repeat receptor kinase MIK2/LRR-KISS connects cell wall integrity sensing, root growth and response to abiotic and biotic stresses 13, e1006832. https://doi.org/10.1371/journal.pgen.1006832.

Varadi, M., and Velankar, S. (2023). The impact of AlphaFold Protein Structure Database on the fields of life sciences. Proteomics **23**, e2200128. https://doi.org/10.1002/pmic.202200128.

Varki, A., Cummings, R.D., Esko, J.D., Stanley, P., Hart, G.W., Aebi, M., Mohnen, D., Kinoshita, T., Packer, N.H., Prestegard, J.H., et al. (2022). Essentials of glycobiology. NBK579947.

Vogel, J. (2008). Unique aspects of the grass cell wall. Curr. Opin. Plant Biol. **11**:301–307. https://doi.org/10.1016/j.pbi.2008.03.002.

Vogel, J.P., Raab, T.K., Schiff, C., and Somerville, S.C. (2002). PMR6, a pectate lyase-like gene required for powdery mildew susceptibility in

Arabidopsis. Plant Cell **14**:2095–2106. https://doi.org/10.1105/tpc.003509.

Vogel, J.P., Raab, T.K., Somerville, C.R., and Somerville, S.C. (2004). Mutations in PMR5 result in powdery mildew resistance and altered cell wall composition. Plant J. **40**:968–978. https://doi.org/10.1111/j.1365-313X.2004.02264.x.

Voigt, C.A. (2014). Callose-mediated resistance to pathogenic intruders in plant defense-related papillae. Front. Plant Sci. **5**:168. https://doi.org/10.3389/fpls.2014.00168.

Voxeur, A., and Höfte, H. (2020). Pectin-derived immune elicitors in response to lignin modification in plants. Proc. Natl. Acad. Sci. USA **117**:4442–4444. https://doi.org/10.1073/pnas.2000509117.

Voxeur, A., Habrylo, O., Guénin, S., Miart, F., Soulié, M.C., Rihouey, C., Pau-Roblot, C., Domon, J.M., Gutierrez, L., Pelloux, J., et al. (2019). Oligogalacturonide production upon *Arabidopsis thaliana-Botrytis cinerea* interaction. Proc. Natl. Acad. Sci. USA **116**:19743–19752. https://doi.org/10.1073/pnas.1900317116.

Wan, J., Tanaka, K., Zhang, X.C., Son, G.H., Brechenmacher, L., Nguyen, T.H.N., and Stacey, G. (2012). LYK4, a lysin motif receptor-like kinase, is important for chitin signaling and plant innate immunity in Arabidopsis. Plant Physiol. **160**:396–406. https://doi.org/10.1104/pp.112.201699.

Wang, M., Weiberg, A., Dellota, E., Yamane, D., and Jin, H. (2017). Botrytis small RNA Bc-siR37 suppresses plant defense genes by cross-kingdom RNAi. RNA Biol. **14**:421–428. https://doi.org/10.1080/15476286.2017.1291112.

Wang, Y., Li, X., Fan, B., Zhu, C., and Chen, Z. (2021). Regulation and function of defense-related callose deposition in plants. Int. J. Mol. Sci. **22**, 2393.

Wanke, A., Malisic, M., Wawra, S., and Zuccaro, A. (2021). Unraveling the sugar code: the role of microbial extracellular glycans in plant-microbe interactions. J. Exp. Bot. **72**:15–35. https://doi.org/10.1093/jxb/eraa414.

Wanke, A., Rovenich, H., Schwanke, F., Velte, S., Becker, S., Hehemann, J.H., Wawra, S., and Zuccaro, A. (2020). Plant species-specific recognition of long and short β-1,3-linked glucans is mediated by different receptor systems. Plant J. **102**:1142–1156. https://doi.org/10.1111/tpj.14688.

Wanke, A., van Boerdonk, S., Mahdi, L.K., Wawra, S., Neidert, M., Chandrasekar, B., Saake, P., Saur, I.M.L., Derbyshire, P., Holton, N., et al. (2023). A GH81-type β-glucan-binding protein enhances colonization by mutualistic fungi in barley. Curr. Biol. **33**:5071–5084.e5077. https://doi.org/10.1016/j.cub.2023.10.048.

Willmann, R., Lajunen, H.M., Erbs, G., Newman, M.A., Kolb, D., Tsuda, K., Katagiri, F., Fliegmann, J., Bono, J.J., Cullimore, J.V., et al. (2011). Arabidopsis lysin-motif proteins LYM1 LYM3 CERK1 mediate bacterial peptidoglycan sensing and immunity to bacterial infection. Proc. Natl. Acad. Sci. USA **108**:19824–19829. https://doi.org/10.1073/pnas.1112862108.

Wolf, S. (2022). Cell wall signaling in plant development and defense. Annu. Rev. Plant Biol. **73**:323–353. https://doi.org/10.1146/annurev-arplant-102820-095312.

Wolf, S., van der Does, D., Ladwig, F., Sticht, C., Kolbeck, A., Schürholz, A.K., Augustin, S., Keinath, N., Rausch, T., Greiner, S., et al. (2014). A receptor-like protein mediates the response to pectin modification by activating brassinosteroid signaling. Proc. Natl. Acad. Sci. USA **111**:15261–15266. https://doi.org/10.1073/pnas.1322979111 1322979111 [pii].

Wong, J.E.M.M., Gysel, K., Birkefeldt, T.G., Vinther, M., Muszyński, A., Azadi, P., Laursen, N.S., Sullivan, J.T., Ronson, C.W., Stougaard, J., et al. (2020). Structural signatures in EPR3 define a unique class of plant carbohydrate receptors. Nat. Commun. **11**:3797. https://doi.org/10.1038/s41467-020-17568-9.

Wormit, A., and Usadel, B. (2018). The multifaceted role of pectin methylesterase inhibitors (PMEIs). Int. J. Mol. Sci. **19**, 2878.

Wu, F., Chi, Y., Jiang, Z., Xu, Y., Xie, L., Huang, F., Wan, D., Ni, J., Yuan, F., Wu, X., et al. (2020). Hydrogen peroxide sensor HPCA1 is an LRR receptor kinase in Arabidopsis. Nature **578**:577–581. https://doi.org/10.1038/s41586-020-2032-3.

Xiao, M., Chen, D., Liu, S., Chen, A., Fang, A., Tian, B., Yu, Y., Bi, C., Kang, Z., and Yang, Y. (2023). A chitin deacetylase PsCDA2 from *Puccinia striiformis* f. sp. *tritici* confers disease pathogenicity by suppressing chitin-triggered immunity in wheat. Mol. Plant Pathol. **24**:1467–1479. https://doi.org/10.1111/mpp.13381.

Xiao, Y., Sun, G., Yu, Q., Gao, T., Zhu, Q., Wang, R., Huang, S., Han, Z., Cervone, F., Yin, H., et al. (2024). A plant mechanism of hijacking pathogen virulence factors to trigger innate immunity. Science **383**:732–739. https://doi.org/10.1126/science.adj9529.

Xiao, Y., Stegmann, M., Han, Z., DeFalco, T.A., Parys, K., Xu, L., Belkhadir, Y., Zipfel, C., and Chai, J. (2019). Mechanisms of RALF peptide perception by a heterotypic receptor complex. Nature **572**:270–274. https://doi.org/10.1038/s41586-019-1409-7.

Xu, P., Xu, S.L., Li, Z.J., Tang, W., Burlingame, A.L., and Wang, Z.Y. (2014). A brassinosteroid-signaling kinase interacts with multiple receptor-like kinases in Arabidopsis. Mol. Plant **7**:441–444. https://doi.org/10.1093/mp/sst105.

Xu, Q., Wang, J., Zhao, J., Xu, J., Sun, S., Zhang, H., Wu, J., Tang, C., Kang, Z., and Wang, X. (2020). A polysaccharide deacetylase from *Puccinia striiformis* f. sp. *tritici* is an important pathogenicity gene that suppresses plant immunity. Plant Biotechnol. J. **18**:1830–1842. https://doi.org/10.1111/pbi.13345.

Xue, D.X., Li, C.L., Xie, Z.P., and Staehelin, C. (2019). LYK4 is a component of a tripartite chitin receptor complex in *Arabidopsis thaliana*. J. Exp. Bot. **70**:5507–5516. https://doi.org/10.1093/jxb/erz313.

Yang, C., Liu, R., Pang, J., Ren, B., Zhou, H., Wang, G., Wang, E., and Liu, J. (2021a). Poaceae-specific cell wall-derived oligosaccharides activate plant immunity via OsCERK1 during *Magnaporthe oryzae* infection in rice. Nat. Commun. **12**:2178. https://doi.org/10.1038/s41467-021-22456-x.

Yang, C., Yu, Y., Huang, J., Meng, F., Pang, J., Zhao, Q., Islam, M.A., Xu, N., Tian, Y., and Liu, J. (2019). Binding of the *Magnaporthe oryzae* chitinase MoChia1 by a rice tetratricopeptide repeat protein allows free chitin to trigger immune responses. Plant Cell **31**:172–188. https://doi.org/10.1105/tpc.18.00382.

Yang, H., Wang, D., Guo, L., Pan, H., Yvon, R., Garman, S., Wu, H.M., and Cheung, A.Y. (2021b). Malectin/Malectin-like domain-containing proteins: a repertoire of cell surface molecules with broad functional potential. Cell Surf. **7**, 100056. https://doi.org/10.1016/j.tcsw.2021.100056.

Yong, W., Link, B., O'Malley, R., Tewari, J., Hunter, C.T., Lu, C.A., Li, X., Bleecker, A.B., Koch, K.E., McCann, M.C., et al. (2005). Genomics of plant cell wall biogenesis. Planta **221**:747–751. https://doi.org/10.1007/s00425-005-1563-z.

Yoshida, S., and Parniske, M. (2005). Regulation of plant symbiosis receptor kinase through serine and threonine phosphorylation. J. Biol. Chem. **280**:9203–9209. https://doi.org/10.1074/jbc.M411665200.

Yuan, M., Ngou, B.P.M., Ding, P., and Xin, X.F. (2021). PTI-ETI crosstalk: an integrative view of plant immunity. Curr. Opin. Plant Biol. **62**, 102030. https://doi.org/10.1016/j.pbi.2021.102030.

Zang, H., Xie, S., Zhu, B., Yang, X., Gu, C., Hu, B., Gao, T., Chen, Y., and Gao, X. (2019). Mannan oligosaccharides trigger multiple defence responses in rice and tobacco as a novel danger-associated

molecular pattern. Mol. Plant Pathol. **20**:1067–1079. https://doi.org/10.1111/mpp.12811.

Zarattini, M., Corso, M., Kadowaki, M.A., Monclaro, A., Magri, S., Milanese, I., Jolivet, S., de Godoy, M.O., Hermans, C., Fagard, M., et al. (2021). LPMO-oxidized cellulose oligosaccharides evoke immunity in Arabidopsis conferring resistance towards necrotrophic fungus *B. cinerea*. Commun. Biol. **4**:727. https://doi.org/10.1038/s42003-021-02226-7.

Zavaliev, R., Levy, A., Gera, A., and Epel, B.L. (2013). Subcellular dynamics and role of Arabidopsis β-1,3-glucanases in cell-to-cell movement of tobamoviruses. Mol. Plant Microbe Interact. **26**:1016–1030. https://doi.org/10.1094/MPMI-03-13-0062-R.

Zdunek, A., Pieczywek, P.M., and Cybulska, J. (2021). The primary, secondary, and structures of higher levels of pectin polysaccharides. Compr. Rev. Food Sci. Food Saf. **20**:1101–1117. https://doi.org/10.1111/1541-4337.12689.

Zeiner, A., Colina, F.J., Citterico, M., and Wrzaczek, M. (2023). CYSTEINE-RICH RECEPTOR-LIKE PROTEIN KINASES: their evolution, structure, and roles in stress response and development. J. Exp. Bot. **74**:4910–4927. https://doi.org/10.1093/jxb/erad236.

Zhang, B., Chang, L., Sun, W., Ullah, A., and Yang, X. (2021a). Overexpression of an expansin-like gene, GhEXLB2 enhanced drought tolerance in cotton. Plant Physiol. Biochem. **162**:468–475. https://doi.org/10.1016/j.plaphy.2021.03.018.

Zhang, B., Gao, Y., Zhang, L., and Zhou, Y. (2021b). The plant cell wall: biosynthesis, construction, and functions. J. Integr. Plant Biol. **63**:251–272. https://doi.org/10.1111/jipb.13055.

Zhang, B., Su, T., Xin, X., Li, P., Wang, J., Wang, W., Yu, Y., Zhao, X., Zhang, D., Li, D., et al. (2023). Wall-associated kinase BrWAK1 confers resistance to downy mildew in *Brassica rapa*. Plant Biotechnol. J. **21**:2125–2139.

Zhang, X., Dong, W., Sun, J., Feng, F., Deng, Y., He, Z., Oldroyd, G.E.D., and Wang, E. (2015). The receptor kinase CERK1 has dual functions in symbiosis and immunity signalling. Plant J. **81**:258–267. https://doi.org/10.1111/tpj.12723.

Zhang, Y., Yu, J., Wang, X., Durachko, D.M., Zhang, S., and Cosgrove, D.J. (2021c). Molecular insights into the complex mechanics of plant epidermal cell walls. Science **372**:706–711. https://doi.org/10.1126/science.abf2824.

Zhao, C., Jiang, W., Zayed, O., Liu, X., Tang, K., Nie, W., Li, Y., Xie, S., Li, Y., Long, T., et al. (2021). The LRXs-RALFs-FER module controls plant growth and salt stress responses by modulating multiple plant hormones. Natl. Sci. Rev. **8**, nwaa149. https://doi.org/10.1093/nsr/nwaa149.

Zheng, D., Wang, H., Zhong, H., Ke, W., Hu, H., Sun, M., and Ruan, L. (2021). Elucidation of the pathogenicity-associated regulatory network in *Xanthomonas oryzae* pv. *oryzae*. mSystems **6**:e00789-20. https://doi.org/10.1128/mSystems.00789-20.

Zuo, W., Chao, Q., Zhang, N., Ye, J., Tan, G., Li, B., Xing, Y., Zhang, B., Liu, H., Fengler, K.A., et al. (2015). A maize wall-associated kinase confers quantitative resistance to head smut. Nat. Genet. **47**:151–157.